

**Development of Novel Inhibitors of  
Carbohydrate-Processing Targets Involved in  
*Mycobacterium tuberculosis* Cell Wall  
Biosynthesis**



By

**Ben Whitehurst**

Department of Pure and Applied Chemistry, University of Strathclyde

New Chemical Entity Molecular Discovery, GlaxoSmithKline

**March 2016**



# Declaration

This thesis is the result of the author's original research. It has been composed by the author and has not been previously submitted for examination which has led to the award of a degree.

The copyright of this thesis belongs to GSK in accordance with the author's contract of engagement with GSK under the terms of the United Kingdom Copyright Acts. Due acknowledgement must always be made of the use of any material contained in, or derived from, this thesis.

Signed:

Date:

# Acknowledgements

First and foremost, I would like to thank my industrial supervisor Dr. Rob Young for his continual guidance, encouragement, support and teaching that he has offered consistently throughout my PhD. The time you have invested in my development has really paid off, and I truly don't think that I would have the level of understanding I do for medicinal chemistry without your help. Friday morning "Coffee and Pastry" sessions in particular were a great initiative, and I'm pretty sure this is the forum in which I've learnt most (and heard the most anecdotes....!). I would also like to thank you for all your feedback on my written work over the years.

I would like to thank my academic supervisor Dr. Glenn Burley for his guidance and input into my work throughout my PhD, but especially for the time I spent within his group whilst on secondment at the University of Strathclyde. The group meetings with beers and crisps are definitely the best I've been to! Again, I would also like to thank you for your feedback on this manuscript.

Thanks are also due to my colleagues in the GSK hit-to-lead group, who have helped to make my time at GSK very enjoyable. Alan, you've had the pleasure of working next to me for 3 years, which I have enjoyed a lot. You've been a great help during this time (which I appreciate hugely), and we always have a good laugh in the bay, whether it's about your amusingly upper class pastimes or simply saying "tschüß". Justyna and Suzanne, you guys have been really good friends over the last year, and I'm glad you both joined our lab (not least because you come to lunch with me!). Tony, Ian, Jenny, Martin, Lisa, Washio, Steve, Mythily, Andy, Guy, Derek, Jayshree and Pam, you have all been good friends too, helpful in the lab, and most importantly, tea-time companions. I'd like to thank the IP students Greg, Monya, Venla, Lucy, Elle, Stephen, Simon, Anthony, Andrew, Jake, Laura and Danielle for being some really good mates whilst you were on placement – I can barely see through my fumehood sash for all the messages (nice or otherwise) that you left me over the years.

Thanks also go to the rest of my PhD cohort: Aymeric, Nat, Rob, JT, Sam and Craig. We've had a lot of good times together and I know we'll keep up as mates after we're done. I'm still holding you all to our celebratory night at Stevenage's finest establishment Chicagos when we've all passed our vivas.

I would also like to thank all of the following, who each contributed to my PhD, intellectually or otherwise: Olivia Paisley, Sebastian Lamping, Clémence Mdi, Sara De Ornellas, Monica Cacho-Izquierdo, Julia Castro-Pichel, Ana Guardia-Alvarez, Laura Vela-Glez Del Peral, Michelle Pemberton, Christopher Stubbs, Chun-wa Chung, Margarete Neu, Onkar Singh, Ian Wall, Joaquin Rullas-Trincado, Alan Hill, Stephen Brough. In particular, special thanks go to Archie Argyrou, Pete Craggs, Sean Lynn and Bill Leavens.

# Abstract

Tuberculosis (TB) remains one of the world's most lethal infectious diseases. The emergence and increasing prevalence of drug-resistant strains of *Mycobacterium tuberculosis* (*M.tb*) highlights the urgent need for new antitubercular medicines. Decaprenylphosphoryl- $\beta$ -D-ribose 2'-epimerase 1 (DprE1) and *N*-acetylglucosamine-1-phosphate uridylyltransferase (GlmU) are two recently characterised carbohydrate-processing enzymes essential for *M.tb* cell wall biosynthesis, both of which have promising potential as targets for new TB therapies. This thesis describes efforts to identify inhibitors of DprE1 and GlmU as possible new drug candidates for the treatment of TB, or as tool compounds to help develop a wider understanding of these novel targets.

Chapters 1-3 introduce TB, physicochemical properties and their application in drug discovery, and DprE1 respectively. Chapters 4-6 detail hit-to-lead investigations around two compounds identified in a DprE1 high throughput screening (HTS) campaign. Hit validation was performed first, then each hit was expanded into a lead series, delineating structure-activity-relationships and identifying exemplars that displayed both high potency at DprE1 and against *M.tb* *in vitro* (with demonstrable engagement at DprE1). An overall aspiration was to identify DprE1 inhibitors that had high potential to succeed as new medicines for TB; as such, physicochemical properties were at the forefront of the molecular design strategy in these Chapters. Chapter 7 details the design, synthesis and biological evaluation of DprE1 inhibitors based on the natural substrate of the enzyme. This work focussed on investigating whether such ribose-based structures could provide a hydrophilic start-point from which to develop potent DprE1 inhibitors. These substrate analogues were also used as tool compounds to probe interactions between DprE1 and small molecule inhibitors, and to provide insight into the nature of the enzyme-catalysed reaction.

Chapter 8 of this thesis introduces the second *M.tb* target, GlmU. Chapter 9 outlines the design and synthesis of a small set of GlmU acetyltransferase inhibitors based on the substrate of the enzyme. In the absence of any quality literature *M.tb* GlmU inhibitors, this work provided chemical matter to help establish the recently developed GSK *M.tb* GlmU acetyltransferase enzyme assay.

Finally, Chapter 10 reflects on the work presented in this thesis, and offers some perspectives for the future of tuberculosis drug discovery.

# Abbreviations

#Ar	number of aromatic rings
'932-amine.HCl	(4-benzylpiperidin-1-yl)(piperidin-4-yl)methanone hydrochloride
$\mu$ wave	microwave
9-BBN	9-borabicyclo[3.3.1]nonane
Ac	acetate
AcCoA	acetyl coenzyme A
ADME(T)	absorption, distribution, metabolism, excretion, (toxicity)
AFU	arbitrary fluorescence units
AG	arabinogalactan
Alloc	allyloxycarbonyl
ATP	adenosine triphosphate
Bn	benzyl
Boc	<i>tert</i> -butoxycarbonyl
BTZ	benzothiazinone antitubercular drug class
Bz	benzoyl
CD38	cluster of differentiation 38
CFU	colony forming units
Chrom Log P / D <sub>pH</sub>	Chromatographic Log P / D <sub>pH</sub>
Cl <sub>int</sub>	intrinsic clearance
CLND	chemi-luminescent nitrogen detection method for solubility measurement
cLog P	calculated Log P
CMR	calculated molar refraction
COMU	(1-Cyano-2-ethoxy-2-oxoethylideneaminoxy)dimethylamino-morpholino-carbenium hexafluorophosphate

CYP	cytochrome P450
d.e.	diastereomeric excess
DABAL-Me <sub>3</sub>	bis(trimethylaluminum)-1,4-diazabicyclo[2.2.2]octane adduct
DABCO	1,4-diazabicyclo[2.2.2]octane
DAP	(meso)diaminopimelic acid
DCM	dichloromethane
DIBAL-H	diisobutylaluminium hydride
DIC	<i>N,N'</i> -diisopropylcarbodiimide
DIPEA	<i>N,N</i> -diisopropylethylamine
DMAP	4-dimethylaminopyridine
DMF	dimethylformamide
DPA	decaprenylphosphoryl- $\beta$ -D-arabinose
dppf	1,1'-ferrocenediyl-bis(diphenylphosphine)
DPR	decaprenylphosphoryl- $\beta$ -D-ribose
DprE1	decaprenylphosphoryl- $\beta$ -D-ribose 2'-epimerase 1
DPX	ketone product of DprE1-mediated oxidation of DPR
e.e.	enantiomeric excess
F%	oral bioavailability
FAD	flavin adenine dinucleotide (oxidised form)
FADH	flavin adenine dinucleotide (reduced form)
FBDD	fragment-based drug discovery
FDA	Food and Drug Administration (US federal agency)
FPR	farnesylphosphoryl- $\beta$ -D-ribose
GGRP	geranylgeranylphosphoryl- $\beta$ -D-ribose
GlcN-1-P	glucosamine-1-phosphate
GlcNAc	<i>N</i> -acetylglucosamine

GlcNAc-1-P	<i>N</i> -acetylglucosamine-1-phosphate
GlmU	<i>N</i> -acetylglucosamine-1-phosphate uridylyltransferase
GSK	GlaxoSmithKline
h	human
HAC	heavy atom count (count of non-hydrogen atoms)
HATU	1-[bis(dimethylamino)methylene]-1 <i>H</i> -1,2,3-triazolo[4,5- <i>b</i> ]pyridinium 3-oxid hexafluorophosphate
HBA	hydrogen bond acceptor
HBD	hydrogen bond donor
hERG	human Ether-à-go-go Related Gene (potassium ion channel)
HIV	human immunodeficiency virus
HTS	high-throughput screening
HWE	Horner-Wadsworth-Emmons reaction
IC <sub>50</sub>	half maximal inhibitory concentration
InhA	enoyl acyl carrier protein reductase
<i>K</i> <sub>d</sub>	dissociation constant
LCMS	liquid chromatography-mass spectrometry
LDA	lithium diisopropylamide
LE	Ligand Efficiency
LLE <sub>AT</sub>	Astex Lipophilic Ligand Efficiency
m	mouse
<i>m</i>	<i>meta</i>
<i>M.smeg</i>	<i>Mycobacterium smegmatis</i>
<i>M.tb</i>	<i>Mycobacterium tuberculosis</i>
MDR	multi drug-resistant
MIC	minimum inhibitory concentration
MOA	mechanism of action

MOE	Molecular Operating Environment software
Ms	mesyl (methanesulfonyl)
MS	molecular sieves
MurNAc	<i>N</i> -acetylmuramic acid
MurNGlyc	<i>N</i> -glycolylmuramic acid
MW	molecular weight
NAD <sup>+</sup>	nicotinamide adenine dinucleotide (oxidised form)
NADH	nicotinamide adenine dinucleotide (reduced form)
NMR	nuclear magnetic resonance
NOE	nuclear Overhauser effect
<i>o</i>	<i>ortho</i>
OE	over-expression
<i>p</i>	<i>para</i>
PAINS	pan-assay interference compounds
PAMPA	parallel artificial membrane permeation assay
P <sub>app</sub>	apparent permeability
PBP	penicillin binding protein
PD	pharmacodynamics
PFI	Property Forecast Index
PG	peptidoglycan <i>or</i> protecting group
pIC <sub>50</sub>	-log(half maximal inhibitory concentration)
PK	pharmacokinetics
PMB	<i>para</i> -methoxy benzyl
PP <sub>i</sub>	pyrophosphate (P <sub>2</sub> O <sub>7</sub> <sup>4-</sup> )
PPPR	pentaprenylphosphoryl-β-D-ribose
pyr.	pyridine

QSAR	quantitative structure-activity relationship
Red-Al	sodium bis(2-methoxyethoxy)aluminiumhydride
<i>RFpIC</i> <sub>50</sub>	<i>pIC</i> <sub>50</sub> derived from the RapidFire™ mass spectrometry assay
RT	room temperature
SAR	structure-activity relationship
<i>S</i> <sub>N</sub> Ar	nucleophilic aromatic substitution
SPR	structure-property relationship
SSS	sub-structure search
T.B.L.	tight binding limit
TB	tuberculosis
TBAF	tetra- <i>n</i> -butylammonium fluoride
TBS	<i>tert</i> -butyldimethylsilyl
TBSOTf	<i>tert</i> -butyldimethylsilyl trifluoromethanesulfonate
TFA	trifluoroacetic acid
THF	tetrahydrofuran
THIQ	tetrahydroisoquinoline
<i>T</i> <sub>m</sub>	melting temperature
TMSBr	bromotrimethylsilane
TPSA	topological polar surface area
UDP	uridine diphosphate
UDP-GlcNAc	uridine diphosphate <i>N</i> -acetylglucosamine
UDP-MurNAc	uridine diphosphate <i>N</i> -acetylmuramic acid
UTP	uridine triphosphate
WHO	World Health Organisation
XDR	extensively drug-resistant

Proteogenic amino acid abbreviations:

<b>Full name</b>	<b>Abbreviation</b>
Alanine	Ala
Arginine	Arg
Asparagine	Asn
Aspartic acid	Asp
Cysteine	Cys
Glutamic acid	Glu
Glutamine	Gln
Glycine	Gly
Histidine	His
Isoleucine	Ile
Leucine	Leu
Lysine	Lys
Methionine	Met
Phenylalanine	Phe
Proline	Pro
Serine	Ser
Threonine	Thr
Tryptophan	Trp
Tyrosine	Tyr
Valine	Val

# Table of Contents

Declaration.....	3
Acknowledgements.....	4
Abstract.....	6
Abbreviations.....	7
<b>1. Tuberculosis.....</b>	<b>18</b>
1.1 Epidemiology, Pathogenesis and Treatment .....	18
1.2 Tuberculosis Drug Discovery .....	23
1.3 Targeting Mycobacterial Cell Wall Biosynthesis for Tuberculosis Chemotherapy .....	24
1.4 Thesis Overview .....	27
<b>2. Physicochemical Properties in Drug Discovery .....</b>	<b>28</b>
2.1 What Are Physicochemical Properties and Why Are They Important For Drug Discovery?.....	28
2.2 A New Era of Property-Guided Drug Discovery .....	30
2.3 Poor Physicochemical Properties Cause Attrition .....	31
2.4 Physicochemical and Structural Properties Most Pertinent to Drug Discovery .....	32
2.4.1 Lipophilicity .....	32
2.4.2 Number of Aromatic Rings and Molecular Flatness .....	33
2.4.3 Acid/Base Strength.....	33
2.4.4 Solubility.....	34
2.4.5 Molecular Weight .....	34
2.5 The Impact of Physicochemical Properties on ADMET and Other Developability Parameters.....	34
2.5.1 Permeability .....	35
2.5.2 Intrinsic Clearance.....	36
2.5.3 Cytochrome P450 Inhibition .....	37
2.5.4 Cardiac Ion Channel Blocking Activity.....	37
2.5.5 Promiscuity .....	37
2.6 The Use of Metrics and Predictive Tools in Modern Drug Discovery .....	38
2.6.1 The Property Forecast Index.....	38
2.6.2 Ligand Efficiency Metrics .....	39

2.7 Physicochemical Properties and Lead-Compound Profiles in Hit-to-Lead Drug Discovery.....	41
2.8 Physicochemical Properties in Tuberculosis Drug Design.....	43
2.9 Application of Physicochemical Properties in this Thesis .....	43
<b>3. Decaprenylphosphoryl-<math>\beta</math>-D-Ribose 2'-Epimerase 1 .....</b>	<b>44</b>
3.1 The Role of DprE1 in the Biosynthesis of Arabinogalactan.....	44
3.2 DprE1 as a Drug Target: Published Inhibitors .....	46
3.3 Structure of DprE1 .....	49
3.4 Research Goals.....	51
<b>4. The GSK High-Throughput Screen Against DprE1 .....</b>	<b>52</b>
4.1 Introduction to the HTS Screen and Hit Selection .....	52
4.2 Assays Used in the DprE1 HTS Campaign.....	53
4.2.1 The Fluorescence Assay .....	53
4.2.2 The RapidFire™ Assay.....	53
4.2.3 The Diaphorase Fluorescence-Interference Assay.....	54
4.2.4 Assay Tight Binding Concentration .....	55
4.2.5 Minimum Inhibitory Concentration (MIC) Assays.....	55
4.2.6 X-Ray Crystallography .....	55
4.3 Research Goals and the Targeted Lead-Compound Profile for the DprE1 Programme .....	56
<b>5. Hit-to-Lead Work Around GSK'295 .....</b>	<b>57</b>
5.1 Overview of <b>GSK'295</b> .....	57
5.2 Project Aims .....	59
5.3 Design of ' <b>295/932</b> Cross-Over Compounds.....	59
5.4 Synthesis of Crossover Compounds <b>5.3-5.8</b> .....	60
5.5 Biological & Physicochemical Evaluation of Analogues <b>5.3-5.8</b> .....	65
5.6 <i>In Vitro</i> Profiling of 2-Amino Pyrimidine <b>5.3a</b> and Pyrimidin-2(1 <i>H</i> )-one <b>5.6a</b> .....	71
5.7 <i>In Vivo</i> Evaluation of Pyrimidin-2(1 <i>H</i> )-one <b>5.6a</b> .....	73
5.8 Improving the Permeability and <i>In Vitro</i> Metabolic Stability of Pyrimidin-2(1 <i>H</i> )-one <b>5.6a</b> .....	75
5.8.1 Strategy to Improve the Permeability of <b>5.6a</b> .....	75
5.8.2 Strategy to Improve the <i>In Vitro</i> Metabolic Stability of <b>5.6a</b> .....	76
5.8.3 Design of Pyrimidin-2(1 <i>H</i> )-one Analogues <b>5.32a-e</b> .....	76

5.8.4 Synthesis of Pyrimidin-2(1 <i>H</i> )-one Analogues <b>5.32a-e</b> .....	77
5.8.5 Biological, Physicochemical and ADMET Evaluation of Pyrimidin-2(1 <i>H</i> )-ones <b>5.32a-e</b> .....	79
5.9 Conclusions .....	83
5.10 Future Work .....	84
<b>6. Hit-to-Lead Work Around GSK'896</b> .....	87
6.1 Overview of <b>GSK'896</b> .....	87
6.1.1 Medicinal Chemistry Profiling of <b>GSK'896</b> .....	88
6.2 Project Aims .....	90
6.3 SAR Insights from Analysis of the HTS Data and Sub-Structure Searching of the GSK Compound Collection .....	90
6.3.1 SAR Data Evident in the DprE1 HTS Output .....	91
6.3.2 Screening of Compounds Available in the GSK Collection .....	92
6.4 Design, Synthesis and SAR of New Analogues of <b>GSK'896</b> .....	94
6.4.1 Generalised Retrosynthetic Disconnections of <b>GSK'896</b> and Related Analogues	94
6.4.2 Fragmentation of the HTS Hit <b>GSK'896</b> .....	95
6.4.3 Variation of the Amino Acid Linker of <b>GSK'896</b> .....	97
6.4.4 Variation of the Aminobenzodioxane Motif of <b>GSK'896</b> .....	104
6.4.5 Variation of the C-Terminal Aniline of <b>GSK'896</b> .....	108
6.5 Aminobenzodioxane-Phenyl-Propanamides SAR Overview .....	118
6.6 Conclusions .....	119
6.7 Future Work .....	121
<b>7. Substrate Analogues as Inhibitors of DprE1 and Tool Compounds for Chemical Biology</b> .....	122
7.1 Project Aims .....	123
7.2 Design of Substrate Analogues <b>7.1-7.3</b> as Potential DprE1 Inhibitors .....	124
7.2.1 Design of the C2-Modified Ribose Cores for Series <b>7.1-7.3</b> .....	124
7.2.2 Selection of Substituents for Series <b>7.1-7.3</b> .....	124
7.3 Synthesis of the 2-Methyl-1-Phosphoryl- $\beta$ -D-Ribofuranoses <b>7.1</b> .....	125
7.3.1 Synthetic Approaches Towards Ribosyl-1-Phosphates .....	125
7.3.2 Synthesis of Analogues <b>7.1a-j</b> .....	128
7.4 Synthesis of the 2,2-Difluororibophosphonates <b>7.2</b> .....	133
7.4.1 Synthetic Approaches towards Ribosyl-1-Phosphonates .....	133

7.4.2 Synthesis of Analogues <b>7.2a-f</b> .....	135
7.5 Synthesis of the Acyclic Sugar-Phosphonates <b>7.3</b> .....	136
7.6 Evaluation of the Substrate Analogues <b>7.1-7.3</b> as Inhibitors of DprE1.....	137
7.7 DprE1 Substrate Analogues as Tools for Chemical Biology .....	140
7.7.1 Thermal Shift Experiments Show that Binding of Substrate Analogues <b>7.1g-j</b> Correlates with Prenyl Substituent Length and Geometric Isomerism .....	141
7.7.2 Substrate Turnover is Not a Binding Pre-requisite for Small Molecule Inhibitors that Bind to DprE1 Only in the Presence of Oxidisable Substrate .....	144
7.8 Conclusions .....	146
7.9 Future Work .....	147
<b>8. N-Acetylglucosamine-1-Phosphate Uridyltransferase</b> .....	149
8.1 Structure and Biosynthesis of Peptidoglycan .....	149
8.2 Drugs Targeting Peptidoglycan Biosynthesis .....	151
8.3 GlmU Catalyses the Formation of UDP-GlcNAc .....	152
8.3.1 Structural Basis for <i>M.tb</i> GlmU Acetyltransferase activity .....	154
8.3.2 Structural Basis for <i>M.tb</i> GlmU Uridyltransferase activity.....	155
8.3.3 Reported Inhibitors of Bacterial and <i>M.tb</i> GlmU .....	156
8.4 Research Aims.....	157
<b>9. Glucosamine-1-Phosphate Analogues as Inhibitors of <i>M.tb</i> GlmU Acetyltransferase Activity</b> .....	158
9.1 Project Aims .....	158
9.2 Design of GlcN-1-P Analogues <b>9.1a-g</b> as Potential Inhibitors of the GlmU Acetyltransferase Activity .....	158
9.3 Synthesis of <i>N</i> -functionalised GlcN-1-P Analogues <b>9.1a-g</b> .....	161
9.3 Biological Evaluation of GlcN-1-P Analogues <b>9.1a-g</b> .....	166
9.4 Conclusions .....	170
9.5 Future Work .....	170
<b>10. Perspectives and Future Directions</b> .....	174
10.1 A Combined Phenotypic/Target-Based Approach to Tuberculosis Drug Discovery	174
10.2 Relationship Between Lipophilicity and Antimycobacterial Activity .....	176
10.3 Modified Carbohydrates as Scaffolds for Interrupting <i>M.tb</i> Cell Wall Biosynthesis	177
<b>11. Experimental</b> .....	179
11.1 General Experimental .....	179
11.2 Synthesis of Compounds in Chapter 5 .....	183

11.3 Synthesis of Compounds in Chapter 6 .....	205
11.4 Synthesis of Compounds in Chapter 7 .....	242
11.5 Synthesis of Compounds in Chapter 9 .....	272
<b>12. References</b> .....	<b>287</b>
<b>13. Appendix</b> .....	<b>301</b>
A1. The GlnU Acetyltransferase Assay.....	301
A2. Representative NMR Spectra.....	301

# 1. Tuberculosis

## 1.1 Epidemiology, Pathogenesis and Treatment

Tuberculosis (TB) is one of the world's most lethal infectious diseases, second only to the human immunodeficiency virus (HIV).<sup>1</sup> The World Health Organisation (WHO) estimates 9 million people develop active TB every year, with an annual death toll of 1.5 million.<sup>2</sup> Whilst a decline in TB prevalence was observed over the past century<sup>3</sup> (mostly in industrialized nations), antibiotic resistance<sup>4</sup> and the emergence of HIV<sup>5</sup> have led to a resurgent TB pandemic that was declared a "global emergency" by the WHO.<sup>6</sup> New antitubercular medicines are urgently needed to overcome these modern-day challenges.

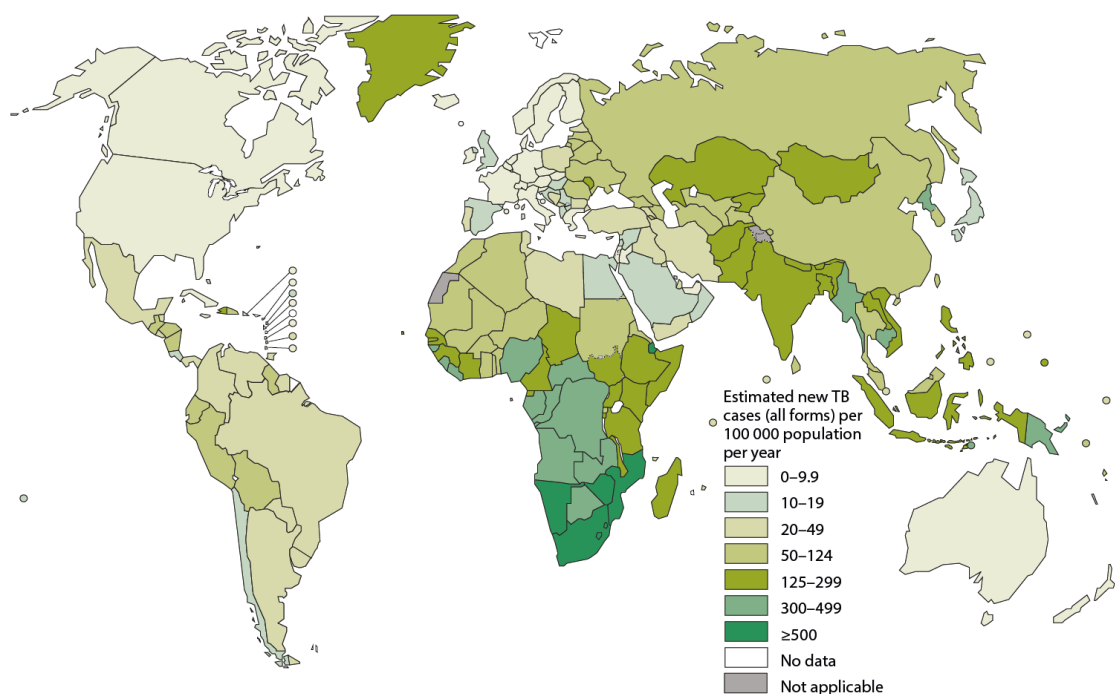


**Figure 1.1.** Estimated worldwide TB incidence rates in 2013.<sup>2</sup> Figure reproduced from the World Health Organisation Global Tuberculosis Report 2014, with permission from the WHO.

TB is a communicable airborne disease caused by the pathogenic organism *Mycobacterium tuberculosis* (*M.tb*). The infection primarily occurs in the lungs (pulmonary TB), resulting in coughing and expectoration of blood and sputum, but can also infiltrate other sites (extrapulmonary TB), such as lymph nodes, joints, and the nervous system.<sup>7</sup> Progression of the disease often follows a relatively well-defined sequence,<sup>8</sup> as shown in Figure 1.2<sup>9</sup>

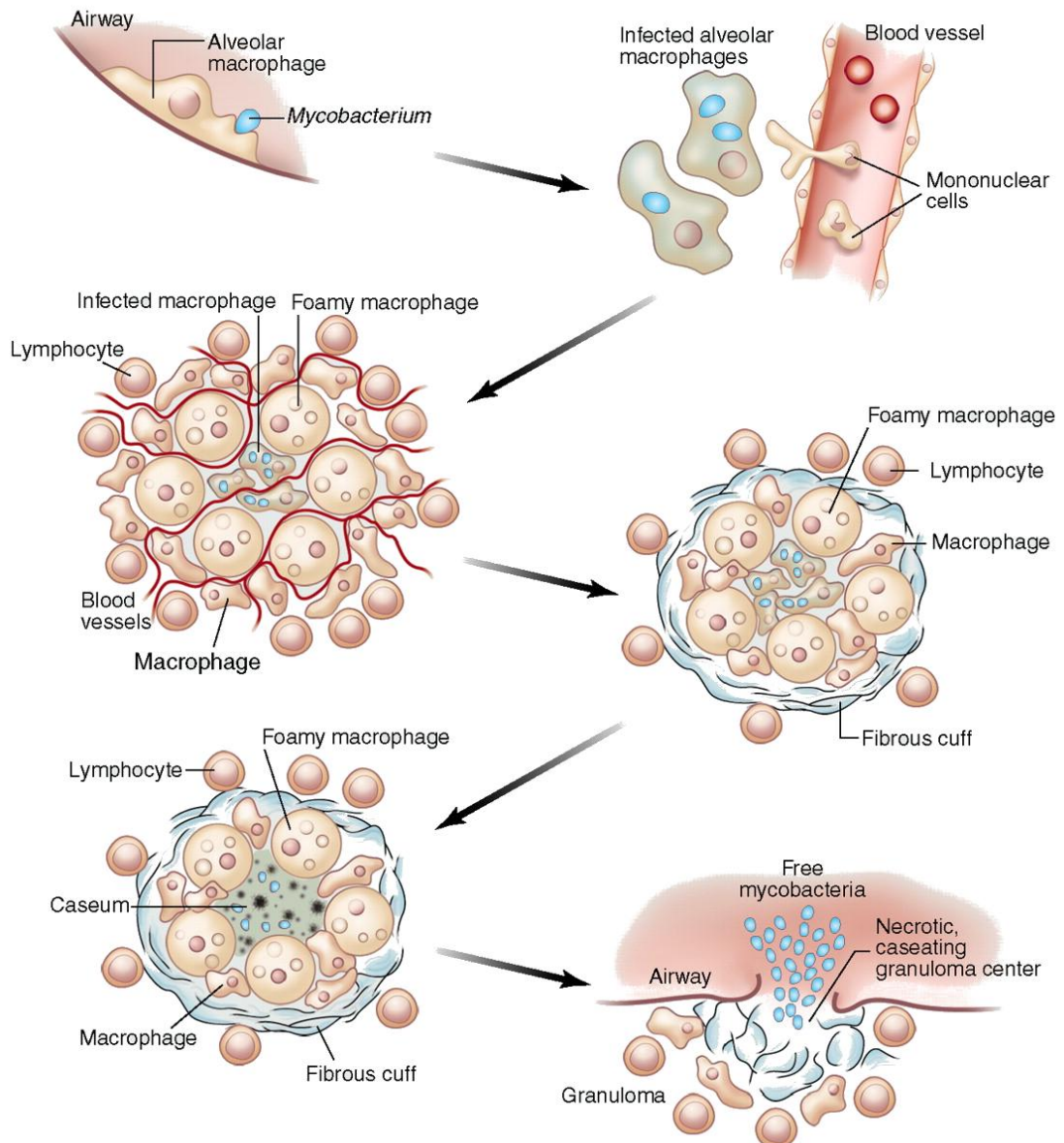


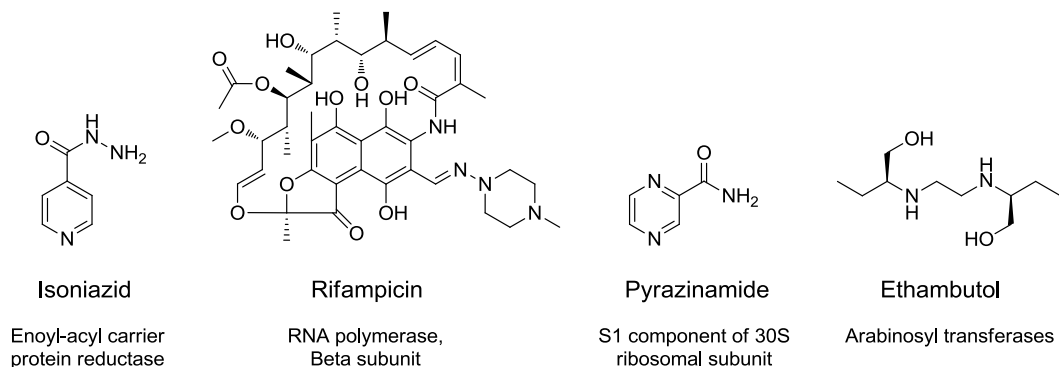
**Figure 1.2.** The tuberculosis disease cycle. Fibrous cuffs form around the infected macrophages, forming granulomas. The material within necrotises to form the caseum, which is released into the airways with *M.tb* bacilli when the granulomas rupture.<sup>9</sup> Figure reproduced from Science, **2010**, 328 (5980), 852-856, with permission from AAAS.

After inhalation of *M.tb*, the bacilli are engulfed by pulmonary macrophages in the airways prompting a proinflammatory response that leads to the recruitment other immune cells, such as neutrophils and lymphocytes. The aggregation of these cells around the infected macrophages results in the formation of walled-off structures termed granulomas, which can act to prevent spread of the infection. Most people are able to control the initial

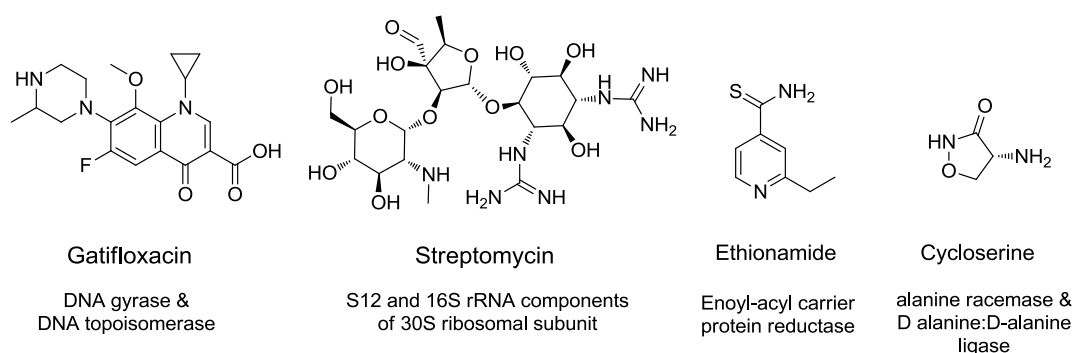
infection through this immune response and remain asymptomatic. It is estimated that one third of the world's population carries latent TB and only 5-10% of infected individuals develop active TB.<sup>10</sup> If the immune system of the host becomes compromised (typically in old-age or due to HIV co-infection), the granulomas weaken and rupture, releasing the necrotising centre (termed the caseum) and infectious *M.tb* bacteria into the airways. This leads to a productive cough which ultimately facilitates the spread of the disease. Death occurs as a result of overwhelming bacterial burden or chronic respiratory failure.<sup>11</sup>

The current standard of care for drug-susceptible TB is a six month regimen of four antibiotics that was introduced over 40 years ago. These so-called "first-line" antituberculars comprise isoniazid (INH), rifampicin (RIF), pyrazinamide (PZA) and ethambutol (EMB) (Fig. 1.3a). All four drugs are administered together for the first two months of treatment, followed by a further four months of isoniazid and rifampicin treatment. Isoniazid exhibits a high early bactericidal activity and acts to quickly eradicate the active replicators in the first two days of treatment, killing up to 95% of organisms present.<sup>12</sup> The bacteriostatic ethambutol is also important for inhibiting bacterial growth of the active replicators during the early stages of chemotherapy.<sup>13</sup> Rifampicin is particularly effective at killing sporadically active *M.tb* bacilli, providing bactericidal activity after the days where isoniazid is most active.<sup>12</sup> Finally, pyrazinamide preferentially kills the non-replicating bacilli of low metabolic activity.<sup>14</sup> The molecular targets of these drugs are indicated in Figure 1.3a.

**(a) First-line antituberculars**



**(b) Example second-line antituberculars**



**(c) Example Third-line antituberculars**

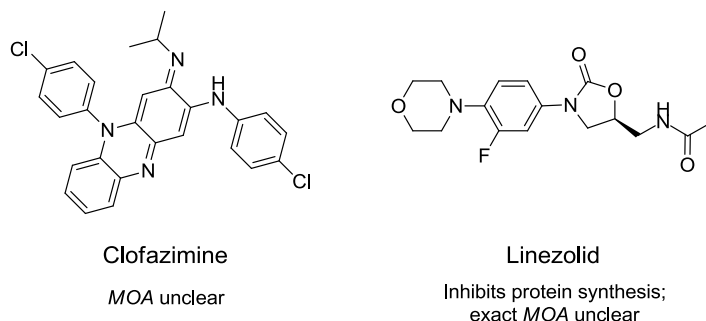


**Figure 1.3.** (a) First-line antituberculars. (b) Examples of second-line antituberculars. (c) Examples of third-line antituberculars. The molecular target of each drug is indicated where known. *MOA* = mechanism of action.

When prosecuted as a course of directly-observed treatment in a hospital setting, this quadruple drug therapy is highly effective at curing drug-susceptible TB (>95% cure rate).<sup>15</sup> In countries with over-burdened resource-limited health systems however, direct observation is often not possible and lack of patient compliance limits success of the treatment. Ultimately this has led to the emergence of drug resistant strains of *M.tb* that

are much more challenging to treat effectively. Multi drug-resistant (MDR) strains of *M.tb* are defined as those that are resistant to at least isoniazid and rifampicin.<sup>4</sup> The WHO estimated 480,000 new cases of MDR-TB occurred world-wide in 2013, representing 3.5% of all reported TB cases that year.<sup>2</sup> Treatment of MDR-TB requires at least two years of medication with less effective “second-line” antituberculars, such as fluoroquinolone and aminoglycoside antibiotics (Fig. 1.3b). Extensively drug-resistant (XDR) isolates of *M.tb* have recently emerged, which show additional resistance to the two main second-line drug classes.<sup>4</sup> Treatment options for XDR-TB are thus seriously limited, requiring expensive, poorly efficacious and poorly tolerable “third-line” drugs (Fig. 1.3c).<sup>16</sup> One African study describing XDR-TB, in which the majority of patients were co-infected with HIV, showed a very high mortality rate (98%), with death occurring on average 16 days after diagnosis.<sup>17</sup>

The second major present-day challenge for the treatment of TB is that of HIV co-infection.<sup>5</sup> The emergence of HIV had a significant impact on TB prevalence due to the inability of a weakened immune system to suppress the onset of tuberculosis, either from nascent TB infection or reactivation of latent TB. The WHO suggested that approximately 25% of TB deaths in 2013 were of HIV-positive individuals.<sup>2</sup> Furthermore, TB is now the leading cause of death amongst people living with HIV, causing a quarter of all HIV-related deaths.<sup>18</sup> A major issue with the treatment of co-infected individuals is that of drug-drug interactions between antituberculars and antiretroviral therapies for HIV.<sup>15</sup> First-line rifampicin is a particularly potent inducer of cytochrome P450 3A4, the action of which markedly reduces concentrations of the concomitantly administered antiretrovirals, such as protease inhibitor indinavir.<sup>15</sup>

The discovery of novel medicines to treat TB is clearly of great importance in today’s global health landscape. Despite this, only two new medicines have been approved since the introduction of the quadruple drug regimen in the 1970’s (Fig. 1.4). Bedaquiline (an *M.tb* ATP synthase inhibitor) was approved by the FDA in 2012 for the treatment of MDR-TB in adults, encouragingly showing equipotent activity against both actively replicating and dormant *M.tb* bacilli.<sup>19</sup> Bedaquiline however, has a potential to induce cardiac arrhythmia; an increased mortality rate was observed during Phase II of clinical trials.<sup>20</sup> The second new medicine, delamanid,<sup>21</sup> was conditionally approved by the European Medicine Agency in 2014 for the treatment of MDR-TB in adults,<sup>22</sup> and only limited information is known about

possible adverse effects. Whilst bedaquiline and delamanid do provide treatment options for MDR-TB infected individuals, the risks from taking these new drugs are high.

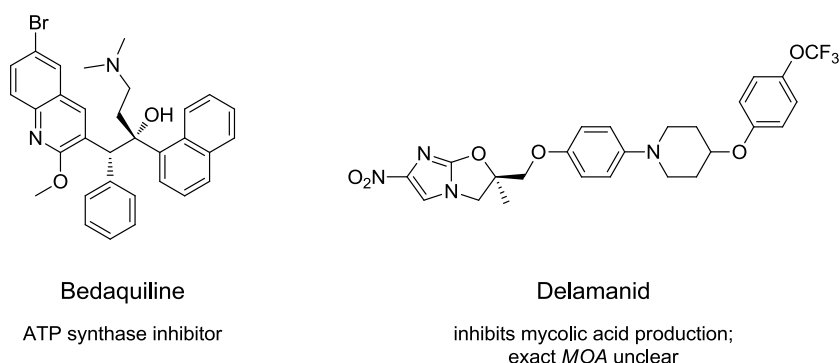


**Figure 1.4** Bedaquiline and delamanid are the only new TB medicines to have been approved in over 40 years.

The above paragraphs highlight the main issues with the current treatment options for drug-susceptible and drug-resistant TB: treatment duration is lengthy, and many of the medicines have a poor safety profile. New TB drugs thus need to be highly efficacious and safe, whilst acting to reduce the duration of treatment relative to the current standard of care.

## 1.2 Tuberculosis Drug Discovery

Drug discovery for tuberculosis poses some significant challenges that are unique to the disease.<sup>23,24</sup> One particular difficulty is that the vast and complex lipid-rich mycobacterial cell wall (Sect. 1.3) presents a significant permeation barrier to small-molecule drugs. The properties which impart permeability across the mycobacterial cell wall remain unclear, as does the extent to which passage is governed by active or passive transport.<sup>25</sup> Further to this, mycobacteria possess a number of active efflux pumps that transport many xenobiotics out of the cell.<sup>25</sup> The combination of these characteristics ultimately leads to poor and unpredictable translation of potency from target-based enzymatic assays to cell-based assays. A molecule that is highly potent against a particular *M.tb* enzyme will not be successful if it is unable to access the target *via* passage across the cell wall. As a result, antitubercular drug discovery programmes have classically adopted a phenotypic whole-cell screening approach, which facilitates the identification of chemotypes inherently capable of crossing the mycobacterial cell wall (or at least capable of accessing the target which they engage).<sup>26,27</sup> Notably, all current TB drugs were discovered using cell-based screening

assays. The archetypal phenotypic assay used in TB drug discovery involves determination of a minimum inhibitory concentration (MIC), defined as the “concentration of an agent that inhibits the growth of 99% of a standardized inoculum of a laboratory strain of *M.tb*”,<sup>24</sup> typically *M.tb* H37Rv.

The main disadvantage of a phenotypic approach can be the difficulty associated with optimising hits without knowledge of the molecular target, and so without the benefit of structure-based drug design<sup>28</sup> (although recent advance in *M.tb* genomics and proteomics can aid the “de-orphaning” of such hits<sup>26</sup>). An alternative protocol for the identification of new TB drugs is a target-based approach, made possible largely by the transcription of the *M.tb* genome in 1998.<sup>29</sup> This method benefits from the possibility of using structure-based drug discovery to guide optimisation of physicochemical property and potency parameters of the hits. The major disadvantage however, remains the poor translation of potency between enzyme and whole-cell activity, and failure to capitalize on target-based drug discovery for tuberculosis is well documented in the literature.<sup>27,30</sup>

### **1.3 Targeting Mycobacterial Cell Wall Biosynthesis for Tuberculosis Chemotherapy**

Targeting mycobacterial cell wall metabolism has represented an important strategy for TB chemotherapy. Firstly, the cell wall is essential for the survival, growth and virulence of the bacteria. Secondly, many of the enzymes involved in the biosynthetic pathways do not have human homologues, negating any issues of mechanism-based toxicity to the host. Indeed, several of the antitubercular drugs currently in use target cell wall metabolism (*vide infra*).

The composition of the mycobacterial cell wall is unique, and comprises three covalently linked constituents (Fig. 1.5), which from the cell membrane to the exterior surface are:

- the *peptidoglycan layer* (PG; Sect. 8.1), a heavily cross-linked polymer that provides a rigid layer enabling the cell to withstand osmotic pressure, as well as a scaffold for other extra-cellular structures;
- the *arabinogalactan layer* (AG; Sect. 3.1), a viscous hydrophilic polysaccharide consisting of a galacto-furanose domain and three arabino-furanose domains, the function of which is to act as a covalent tether between the PG and the mycolic acid layer;

- the *mycolic acid layer*, a monolayer of lipophilic acyl chains that acts as a highly impermeable outer layer, and facilitates intercalation of a variety of non-covalently bound acyl lipids that form the outermost layer, termed the capsule.

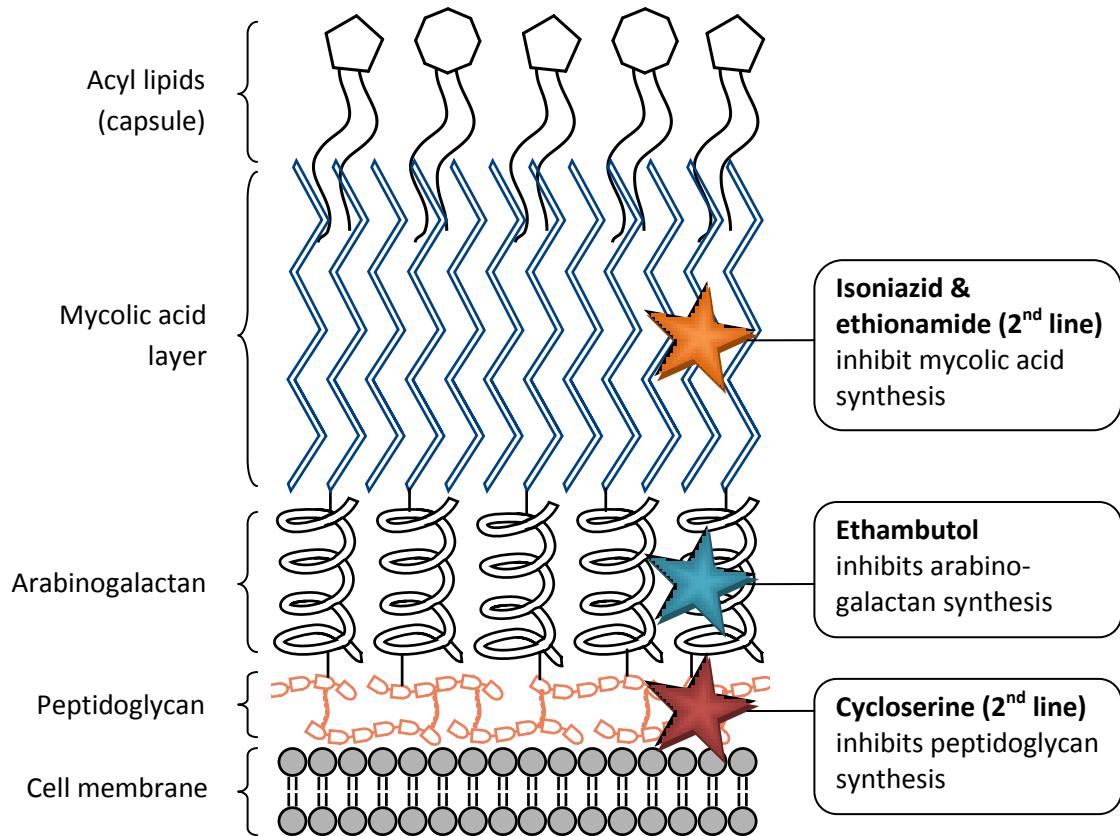
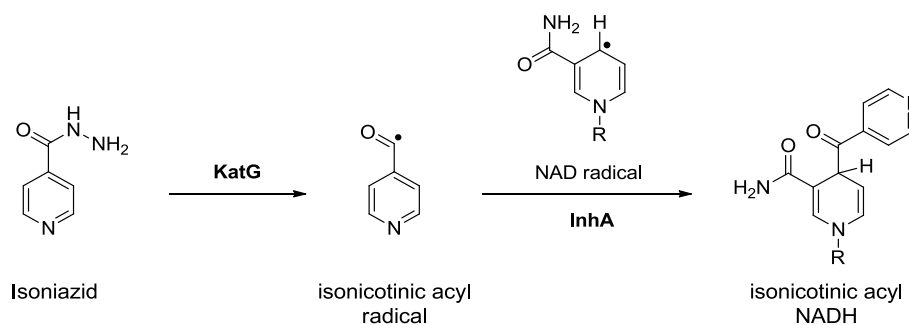


**Figure 1.5.** Schematic of the mycobacterial cell wall, which comprises a peptidoglycan (PG) layer, an arabinogalactan (AG) layer and a mycolic acid layer. These components are flanked by the cell membrane and the outermost layer, the capsule. Collectively, these structures are termed the cell envelope. Current TB drugs that are known to inhibit cell wall metabolism are indicated (see Fig. 1.3 for structures).

Of the TB drugs in regular therapeutic use, four are known to target cell wall biosynthesis (Fig. 1.5). The primary target of isoniazid is the mycolic acid synthesis pathway. Isoniazid is a pro-drug that requires activation by KatG (*M.tb* catalase peroxidase), generating the isonicotinic acyl radical (Scheme 1.1).<sup>31</sup> This radical reacts with the NADH cofactor of *M.tb* enoyl acyl carrier protein reductase (InhA) to afford isonicotinic acyl NADH, which is a potent inhibitor of InhA.<sup>31</sup> Inhibition of InhA interrupts the process required to elongate growing fatty acids that yields the mycolic acids of the cell wall.<sup>31</sup> Second-line ethionamide

is structurally related to isoniazid (Fig. 1.3b), and is also a pro-drug (activated by EtaA, an *M.tb* monooxygenase) that inhibits InhA similarly to isoniazid.<sup>32</sup>



**Scheme 1.1.** The formation of the InhA inhibitor isonicotinic acyl NADH, from the pro-drug isoniazid.<sup>31</sup> The isonicotinic acyl radical likely reacts with the NAD• radical form of the NADH cofactor of InhA.<sup>31</sup>

Ethambutol interferes with AG biosynthesis by inhibiting arabinosyl transferases encoded for by the *embB*, *embA* and *embC* genes, which are responsible for the polymerisation of arabinose into the arabinan of the AG layer<sup>33</sup> (and the lipopolysaccharides lipoarabinomannan, LAM, and mannose-capped lipoarabinomannan, ManLam, found in the capsule<sup>13</sup>).

Finally, cycloserine interrupts PG synthesis by targeting two enzymes: alanine racemase (Alr) and D-alanine:D-alanine ligase (Ddl).<sup>34</sup> In the first two committed steps of bacterial PG synthesis, Alr converts L-alanine to D-alanine, which then acts as a substrate for Ddl to give D-alanyl-D-alanine, which plays a key role in the cross-linking step of PG construction. Inhibition by cycloserine thus acts to prevent transpeptidation of PG monomers.

Whilst there are numerous enzymes involved in *M.tb* cell wall synthesis, only very few have been targeted for TB chemotherapy. In fact, the exact roles of many of the enzymes implicated in *M.tb* cell wall biosynthetic pathways are yet to be elucidated.<sup>29,35</sup> These enzymes, if proven essential to mycobacterial viability, represent an extensive repository of uninvestigated molecular targets for novel TB drugs. Two such enzymes, whose structure and function in *M.tb* cell wall biosynthesis have recently been elucidated, are decaprenylphosphoryl- $\beta$ -D-ribose 2'-epimerase 1 (DprE1; Chapt. 3) and *N*-acetylglucosamine-1-phosphate uridylyltransferase (GlmU; Chapt. 8). DprE1 and GlmU are both essential enzymes implicated in AG and PG biosynthesis respectively, and represent promising novel TB drug targets.

## 1.4 Thesis Overview

In this thesis, efforts to identify potential drug candidates and tool compounds for the *M.tb* targets DprE1 and GlmU are described. These targets are introduced in Chapters 3 and 8 respectively. The enzyme biochemistries, their roles in *M.tb* cell wall biosynthesis, and previously disclosed inhibitors are discussed.

Chapters 4-6 document the work undertaken to confirm two hits discovered in a GSK DprE1 high-throughput screening campaign, and the subsequent efforts performed to develop these hits into lead series. The overall goal was to identify DprE1 lead molecule inhibitors that had high potential to succeed as new medicines for TB. Consequently, physicochemical properties were at the forefront of the molecular design strategy in this body of work (Chapter 2 introduces the concepts of physicochemical property-guided drug design). Furthermore, Chapter 7 describes work to identify inhibitors of DprE1 based on the ribose substrate of the enzyme, affording tool molecules to facilitate chemical biology experiments that provided insight into the characteristic behaviour of DprE1. Chapter 9 of this thesis describes the identification of GlmU inhibitors based on the glucosamine-1-phosphate substrate of this enzyme. Finally, Chapter 10 reflects on the work presented in this thesis, and offers some perspectives for the future of tuberculosis drug discovery.

## 2. Physicochemical Properties in Drug Discovery

Over the past decade, medicinal chemists have become increasingly aware of the relationship between the likelihood of experimental molecules becoming drugs, and the physicochemical properties of the molecules themselves. Today, it is understood that for a molecule to succeed as a drug, it is imperative to identify candidates that are both efficacious and in good property space. The following Sections introduce the contemporary concepts behind this understanding.

### 2.1 What Are Physicochemical Properties and Why Are They Important For Drug Discovery?

How a molecule behaves within a biological system is fundamental to the science of drug discovery. Prior to engaging with the targeted site (e.g. an enzyme), a drug molecule has many biological environments and obstacles to navigate. For example, the compound in question must be soluble in the aqueous intestinal fluid (assuming oral administration), be capable of crossing the gastrointestinal tract and entering the blood stream, and must not be rapidly metabolised, amongst many other factors (Fig. 2.1a). Physicochemical properties are important in drug discovery because they define the intrinsic behavioural characteristics of a molecule within the surrounding biological environment, influencing how a molecule responds to these biological hurdles. Importantly, physicochemical properties are determined by the structure of the molecules themselves, so medicinal chemists are able to modulate behaviour of a molecule within a biological system through structural modification (Fig. 2.1b).

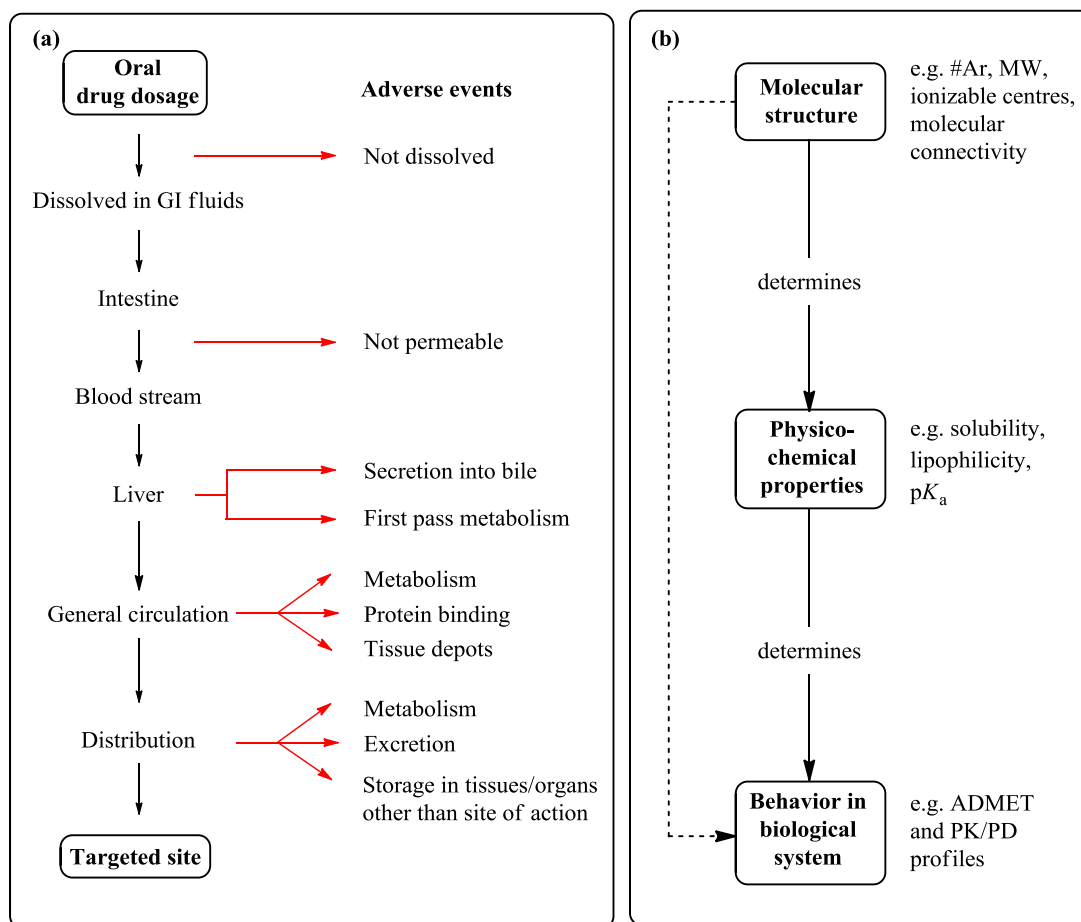


**Figure 2.1.** (a) The route of a drug from oral administration to the targeted site. The red arrows indicate factors that reduce the amount of drug that reaches the target. Figure adapted from “On Medicinal Chemistry”.<sup>36</sup> (b) The interrelation between the structure and physicochemical properties of a molecule with its behaviour in a biological system.

The drug discovery process places many selection criteria on the experimental molecules being pursued as medicines. It is recognised that most molecules that successfully reach the market possess favourable physicochemical properties: “drug-like” properties broadly define the average property space in which the successful drugs reside. Lipinski and co-workers<sup>37</sup> were amongst the first to comment on this with the advent of the “Rule of Five”, illustrating that good drug absorption is more likely when restraints were placed on the size, lipophilicity, and hydrogen bonding character of molecules (Table 2.1).

**Table 2.1.** Lipinski's Rule of 5.<sup>37</sup> The rule refers to the likelihood of a drug molecule exhibiting good oral bioavailability. It predicts poor absorption and permeation when two or more parameters are out of range.

Structural feature	Limit
Molecular Weight	≤500 Da
cLog P	≤5
Hydrogen Bond Donors	≤5
Hydrogen Bond Acceptors	≤10

Following Lipinski's seminal work,<sup>37</sup> efforts to define drug-like property space have investigated many descriptors that influence a molecule's ADMET profile (absorption, distribution, metabolism, excretion and toxicity). These analyses have also examined the trends between certain physicochemical properties and clinical successes or failures. This has led to a contemporary picture of drug-like physicochemical properties that is much more stringent than Lipinski's Rule of 5. One such publication by Gleeson<sup>38</sup> demonstrated that molecules are more likely to have favourable ADMET profiles when cLog P < 4 and molecular weight < 400. An analysis by Hughes and co-workers reported that a reduced likelihood of *in vivo* toxic events was found for less lipophilic and more polar compounds, with cLog P < 3 and topological polar surface area (TPSA) > 75.<sup>39</sup> Leeson and Springthorpe showed that promiscuity (defined as the number of off-target hits at >30% inhibition, at a concentration of 10 μM) was less likely when cLog P < 3 and more likely when cLog P > 4.<sup>40</sup>

## 2.2 A New Era of Property-Guided Drug Discovery

The desire to identify highly potent compounds has always been a key driver in drug discovery campaigns. Classically, chemistry teams have optimised compounds by determining Structure-Activity-Relationships (SAR), focussing heavily on modifications that deliver an increase in biological activity. However, the physicochemical properties associated with tractable potency gains, namely increased lipophilicity and molecular weight, are diametrically opposed to those required for favourable ADMET profiles.<sup>41</sup> Hann suggested that this obsession with high potency is detrimental to the "health" of experimental molecules, leading to excessively large and lipophilic molecules, for which he coined the term "molecular obesity".<sup>42</sup> Whilst this pursuit of potency may result in the

identification of good ligands for the target (probe molecules), it is unlikely to yield successful drugs. The challenge is often to find the compromising “sweet spot”, in which potency is maintained whilst properties are controlled such that favourable ADMET and PK/PD profiles are achieved.<sup>43</sup>

This realisation has led to a paradigm shift into a new era of property-based drug design.<sup>44</sup> Today, a much greater emphasis is placed on the concomitant optimisation of potency *and* physicochemical properties in SAR and SPR (Structure-Property-Relationship) delineation. This holistic approach thus ought to ensure the identification of potent molecules that also exist in good drug-like property space (Fig. 2.2). Whilst some marketed drugs do occupy the extremes about the normal distribution,<sup>45</sup> it would appear that experimental molecules are more likely to become successful medicines when they possess drug-like physicochemical properties.

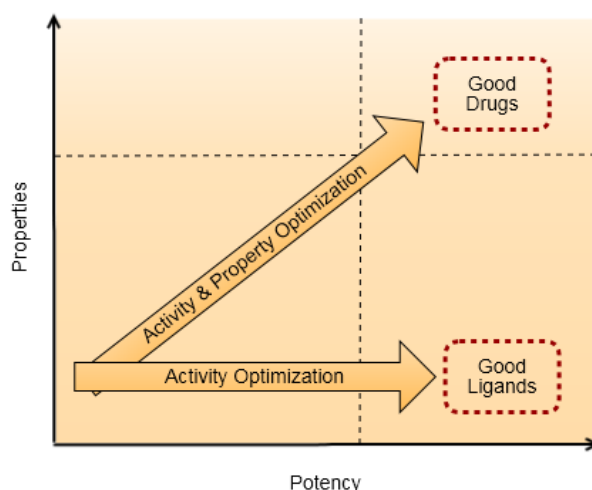


**Figure 2.2.** Optimisation of potency alone whilst ignoring physicochemical properties is likely to yield active compounds which exist in sub-optimal property space. Simultaneous optimisation of potency and properties will likely lead to the identification of potent, drug-like molecules.

### 2.3 Poor Physicochemical Properties Cause Attrition

A recent analysis alleged that only 4-7% of drug candidate molecules succeed as marketed drugs.<sup>46</sup> This represents a considerable loss of invested time and money that is not sustainable. Some of the major causative factors associated with attrition are *biology related* failures, such as lack of efficacy at the target, and mechanism-based toxicity. Attrition due to these failures is likely to be reduced by accumulating the strongest possible

evidence for proof of the biological mechanism to enhance target validation. However, much of the attrition results due to *compound-related* failures, such as the possession of undesirable DMPK, ADME and safety profiles, and off-target toxicity. Specifically, these are shortcomings engendered largely by the physicochemical properties of the compounds themselves: drug candidates with sub-optimal physicochemical property profiles are at an elevated risk of attrition. Therefore, to reduce the risk of attrition, and to maximise the chances of success, striving to achieve good physicochemical properties is integral to contemporary drug design.

## 2.4 Physicochemical and Structural Properties Most Pertinent to Drug Discovery

The physicochemical and structural properties most pertinent to contemporary drug discovery are lipophilicity, molecular size, acid/base strength ( $pK_a$ ), solubility and number of aromatic rings.

### 2.4.1 Lipophilicity

Arguably the single most important physicochemical property is lipophilicity, as potency and most ADMET, pharmacokinetic (PK) and pharmacodynamic (PD) parameters can be related to lipophilicity in some way.<sup>47</sup> Lipophilicity describes the propensity for a molecule to reside in a hydrophobic environment rather than an aqueous one, whilst hydrophilicity refers to the reverse preference. To varying degrees, both lipophilic and hydrophilic character is required to achieve favourable ADMET and PK/PD profiles. For example, solubility in aqueous media is enhanced by hydrophilicity, whilst passive diffusion requires lipophilicity to facilitate permeation from the aqueous intestinal fluid into the lipophilic cell membrane.

Classically, lipophilicity is quantified by  $\text{Log } P$  and  $\text{Log } D_{pH}$ , which describe the ratio of concentrations of a compound partitioned between octanol and water ( $\text{Log } P$ ) or an aqueous buffer ( $\text{Log } D_{pH}$ ).  $\text{Log } P$  expresses the *intrinsic* lipophilicity, measuring the lipophilicity of neutral molecules, and is constant for any particular molecule.<sup>48</sup>  $\text{Log } D_{pH}$  expresses the *effective* lipophilicity, representing the lipophilicity of all present species partitioned between the octanol and aqueous buffer phases (charged and neutral).  $\text{Log } D_{pH}$  is not a constant and depends on the pH and the  $pK_a$  values of the ionisable centres.<sup>48</sup>

Whilst Log P and Log D<sub>pH</sub> measurements are obtained *via* a “shake flask” method,<sup>49</sup> the GSK standard for lipophilicity measurement employs reversed phase chromatography.<sup>50</sup> Chromatographic Log P and chromatographic Log D<sub>pH</sub> (Chrom Log P and Chrom Log D<sub>pH</sub> respectively) measurements are used routinely at GSK (and throughout this thesis). These chromatographic measurements provide improved accuracy over a broader lipophilicity range relative to conventional shake-flask methods, irrespective of solubility class.<sup>51</sup>

The effect of lipophilicity has been the subject of many a review, and excessive lipophilicity has been linked to attrition.<sup>52</sup> Waring suggested that the optimum lipophilicity range in which favourable ADMET parameters are likely is  $\sim 1 < \text{Log D} < 3$ .<sup>47</sup> However, Corwin Hansch (1987) perhaps offered the best advice: “drugs should be made as hydrophilic as possible without loss of efficacy”.<sup>53</sup>

#### **2.4.2 Number of Aromatic Rings and Molecular Flatness**

Ritchie and MacDonald identified that the simple count of aromatic rings profoundly influences ADMET parameters such as solubility, hERG activity and CYP inhibition.<sup>54</sup> They reported that the fewer aromatic rings present, the greater the likelihood of favourable ADMET profiles. A second publication by the same authors detailed that the incorporation of heteroaromatics is generally less detrimental than that of carboaromatics due to the reduced lipophilicity of the former.<sup>55</sup> They concluded that the number of aromatic rings should be kept to a minimum regardless of type. Lovering *et al.* provided an alternative view, identifying that a low proportion of sp<sup>3</sup> centres in drug candidates correlated with a less favourable prognosis during development, demonstrating links with poor solubility, promiscuity and CYP inhibition.<sup>56,57</sup>

#### **2.4.3 Acid/Base Strength**

The vast majority of marketed drugs contain an ionisable centre; approximately 75% are basic, 20% are acidic and only 5% are non-ionizable.<sup>58</sup> Ionic charge has a considerable influence on the polarity of molecules, and can both positively and negatively impact on ADMET parameters. For example, whilst charge improves aqueous solubility, it hinders permeability<sup>59</sup> and increases risk of high serum protein binding (acids)<sup>60</sup> and hERG activity (bases).<sup>61</sup>

#### 2.4.4 Solubility

Aqueous solubility is a desirable attribute for a drug candidate, as a free aqueous fraction of the compound is necessary for interaction with the target. Furthermore, solubility is a prerequisite to intestinal absorption, the first of the biological hurdles on the oral administration route (Fig. 2.1a). Poor solubility will likely result in low systemic exposure and poor oral bioavailability. As mentioned above, aqueous solubility is intrinsically influenced by lipophilicity and aromatic ring count (or molecular planarity).<sup>51</sup> Hydrophilic molecules are more likely to be water-soluble than more lipophilic congeners, and flat, highly aromatic molecules are likely to be poorly soluble due to large energetic barriers to solvation. For ionisable compounds, aqueous solubility is also determined by the extent of ionization, which itself is influenced by  $pK_a$  and pH. This is particularly pertinent to oral absorption as the pHs of the various biological environments encountered after oral administration change on transit through the gastrointestinal tract. For example, the pH of the (fasted) stomach is 1-2.5; the pH of the duodenum is 6.1-7.4.<sup>48</sup>

#### 2.4.5 Molecular Weight

Wenlock *et al.* reported that the mean molecular weight of oral drug candidates decreases at each stage of development, converging to the average molecular weight of marketed oral drugs (345 Da).<sup>52</sup> The analysis suggested a greater likelihood of overall success when the molecular weight is similar to that of marketed drugs, which is much lower than the 500 Da suggested by Lipinski.<sup>37</sup> The link between excessive molecular weight and preclinical demise may originate from the associated general rise in lipophilicity as mass is added, or that larger molecules are more likely to contain metabolic soft-spots or toxic pharmacophores.<sup>52</sup>

### 2.5 The Impact of Physicochemical Properties on ADMET and Other Developability Parameters

ADMET experiments are *in vitro* predictive models that indicate how molecules are likely to behave *in vivo*. Optimizing molecules against ADMET parameters thus increases the chance of favourable *in vivo* behaviour. The following paragraphs introduce some key ADMET assays and concepts which are widely employed in drug discovery programmes, and how certain physicochemical properties influence their outcomes.

## 2.5.1 Permeability

Permeability describes the rate at which a molecule travels through a membrane. Passage across biological membranes is necessary for many processes prior to target engagement, such as absorption in the gastrointestinal tract and penetration into cells. Whilst some authors argue that permeation is wholly protein-mediated,<sup>62</sup> it is likely that both active transport and passive diffusion mechanisms are operative.<sup>63</sup> Optimizing molecules for passive diffusion, often using parallel artificial membrane permeation assays (PAMPA), is therefore a productive pursuit.

Once a molecule has dissolved, permeability is governed principally by three physicochemical properties:  $pK_a$ , lipophilicity and molecular size. Neutral molecules are the predominant form that undergo passive transport, and are much more permeable than their charged forms.<sup>59</sup> Passive transport is linked to lipophilicity through a bilinear relationship.<sup>64,65</sup> Lipophilic character is required to partition into a lipid-rich membrane from the surrounding aqueous environment, whilst hydrophilic character permits diffusion out into the aqueous environment on the other side. Kubinyi showed that for a set of oral drugs, artificial membrane flux increased linearly as  $\text{Log } D_{7.4}$  tended to 2, and decreased similarly as  $\text{Log } D_{7.4}$  increased further (Fig. 2.3).<sup>64</sup> Waring later suggested that the size of a molecule impacts permeability in concert with lipophilicity, reporting that larger molecules need to be more lipophilic to achieve good permeability (Table 2.2).<sup>66</sup>

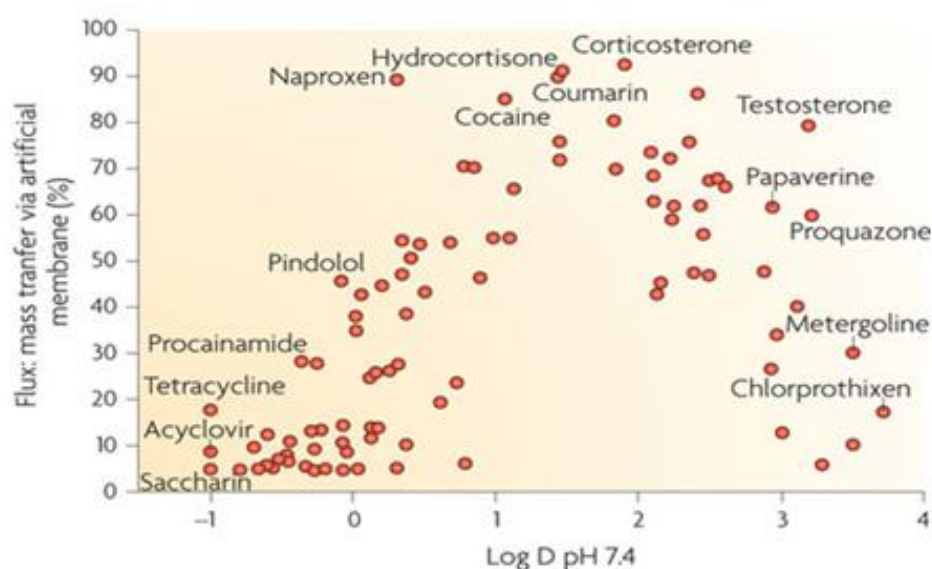


**Figure 2.3.** The bilinear relationship between  $\text{Log } D_{7.4}$  and permeability as described by Kubinyi.<sup>64</sup> Figure reproduced from *Nat. Rev. Drug Discov.* **2010**, 9 (8), 597-614, with permission from Macmillan Publishers Ltd.

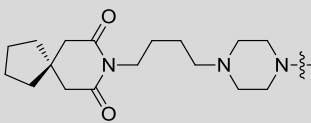
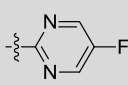
**Table 2.2.** Permeability rules developed by Waring, defining Log D limits required to achieve >50% chance of high permeability for a particular molecular weight band.<sup>66</sup>

MW range	Log D
<300	>0.5
300-350	>1.1
350-400	>1.7
400-450	>3.1
450-500	>3.4
>500	>4.5

## 2.5.2 Intrinsic Clearance

Intrinsic clearance ( $Cl_{int}$ ) assays test the *in vitro* metabolic stability of a compound; high *in vitro* clearance is an indicator of likely rapid *in vivo* clearance and poor oral exposure. These assays measure the rate of disappearance of a molecule in cell preparations such as hepatocytes or liver microsomes, indicating the propensity of a molecule to act as a substrate for any of the metabolic enzymes present in the preparation (of which CYP enzymes are a major component). Intrinsic clearance correlates with hydrophobicity,<sup>65,67</sup> where in general, more lipophilic molecules undergo rapid metabolism. Strategies to improve metabolic stability include reducing lipophilicity and blocking structural sites susceptible to metabolism (e.g. Table 2.3).

**Table 2.3.** Buspirone **2.1** is metabolized *in vivo* primarily by CYP3A4. *in vitro* metabolic stability was greatly improved by blocking the circled site prone to aromatic hydroxylation.<sup>68</sup>

		
	<b>2.1</b>	<b>2.2</b>
Target $pIC_{50}$	7.6	7.2
CYP3A4 $t_{1/2}$ (mins)	4.6	52.3

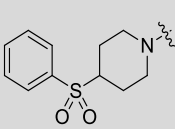
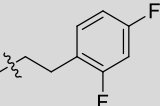
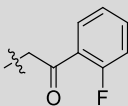
### 2.5.3 Cytochrome P450 Inhibition

Inhibition of particular cytochrome P450 enzymes (CYPs) can cause drug-drug interactions, whereby the inhibiting action of one drug affects the metabolism of another, which may cause adverse or toxic effects. Lipophilicity is known to be the major influence on CYP inhibition, where CYP potency is either linear or bilinear with increasing lipophilicity, depending on the CYP isoform.<sup>69</sup> An increase in molecular size and the number of aromatic rings are also known to correlate with CYP inhibition.<sup>65</sup>

### 2.5.4 Cardiac Ion Channel Blocking Activity

Activity at the hERG potassium ion channel (the alpha subunit of which is encoded for by hERG, the Human Ether-à-go-go Related Gene) is used as an important marker for cardiovascular safety.<sup>61</sup> hERG blocking slows cardiac cell repolarisation, prolonging the QT interval of the heart's electrical cycle, which may trigger the fatal Torsades de Pointes arrhythmia.<sup>70</sup> SAR studies have revealed that an increased risk of hERG activity correlates with lipophilicity, aromaticity, and possession of basic amines.<sup>61,65,71</sup> Flat, lipophilic, positively charged molecules thus pose the greatest risk. Property-guided drug design has been successfully employed to mitigate hERG risk, largely through control of lipophilicity and attenuation of  $pK_a$ <sup>61</sup> (e.g. Table 2.4).

**Table 2.4.** Less lipophilic and less basic 5-HT<sub>2A</sub> receptor antagonist **2.4** is a weaker hERG inhibitor than **2.3**.<sup>72</sup>

			
		<b>2.3</b>	<b>2.4</b>
Target $pIC_{50}$		9.5	8.6
hERG $pIC_{50}$		6.0	5.2
cLog P		2.9	2.2
$pK_a$		7.5	5.3

### 2.5.5 Promiscuity

Promiscuity is the propensity to show activity at multiple receptors or enzymes in addition to the targeted site, which may lead to adverse and toxic effects. Promiscuity is assessed by

screening molecules against a diverse panel of targets relevant to human physiology and measuring for activity.<sup>73</sup> Off-target activity is strongly linked with lipophilicity<sup>40</sup>: protein binding sites are mostly hydrophobic in nature, so lipophilic molecules have a greater chance of recognition through non-specific lipophilic interactions. Other studies investigating promiscuity have shown a correlation with aromatic ring count<sup>65</sup> and  $pK_a$  (basic molecules<sup>40</sup>), but molecular weight appears to have little impact.<sup>48</sup>

## 2.6 The Use of Metrics and Predictive Tools in Modern Drug Discovery

Identifying molecules that have an increased chance of progressing through to a marketed drug represents the current challenge for medicinal chemists. Molecules must be optimised to display favourable ADMET and PK/PD profiles to justify selection as a candidate drug. To direct molecules towards attractive candidates, metrics and predictive tools have become increasingly popular. One such predictive tool used frequently within GSK is the Property Forecast Index (PFI; Sect. 2.6.1).<sup>51,65</sup> Analyses relating physicochemical properties of a molecule to the potency at the desired target are also valuable appraisals in drug discovery.<sup>74</sup> Ligand efficiency metrics (Sect. 2.6.2) are now commonly used to address how efficiently a molecule of a given size<sup>75</sup> and lipophilicity<sup>40,76</sup> engages with the target. Whilst there is some opposition to their use,<sup>77</sup> metrics and predictive tools do provide useful guidance towards the design of molecules with good drug-like physicochemical properties.

### 2.6.1 The Property Forecast Index

Young and Hill identified that the summation of lipophilicity (Chrom Log  $D_{7.4}$ ) and aromatic ring count (#Ar) provides an enhanced predictor of certain developability parameters (Equation 2.1).<sup>51,65</sup> They illustrated that an improved chance of high aqueous solubility, reduced intrinsic clearance and reduced CYP inhibition is likely when  $PFI < 7$  (Table 2.5). Chromatographic measurements of lipophilicity indicate permeability is a bilinear process; accordingly an improved chance of favourable permeability is observed when  $6 < PFI < 8$ . Some developability parameters, notably hERG inhibition and promiscuity, showed clearer probability differentiation with Chrom Log P, rather than Chrom Log  $D_{7.4}$ .  $iPFI$  is the summation of Chrom Log P and aromatic ring count (Equation 2.2). Again, a significantly

improved likelihood of reduced hERG inhibition and promiscuity is apparent for  $iPFI < 7$  (Table 2.5).

$$\text{Property Forecast Index (PFI)} = \text{Chrom Log } D_{7,4} + \#\text{Ar} \quad \text{Equation 2.1}$$

$$iPFI = \text{Chrom Log } P + \#\text{Ar} \quad \text{Equation 2.2}$$

The authors suggested that a  $PFI/iPFI$  below the threshold value of 7 would likely indicate a more favourable developability profile (based on the parameters indicated in Table 2.5). They concluded that for any particular series of molecules, a value of  $PFI/iPFI < 5$  would appear desirable, provided that permeability was not adversely effected.

**Table 2.5.**<sup>65</sup> Percentages of compounds achieving defined target values in the various developability assays categorised by PFI or  $iPFI$  bins.<sup>a</sup>

Assay / target value	PFI								
	< 3	3-4	4-5	5-6	6-7	7-8	8-9	9-10	>10
Solubility > 200 $\mu\text{M}$	89	83	72	58	33	13	5	3	2
2C9 $\text{pIC}_{50} < 5$	97	90	83	68	48	32	23	22	38
2C19 $\text{pIC}_{50} < 5$	97	95	91	82	67	52	42	42	56
3A4 $\text{pIC}_{50} < 5$	92	83	80	75	67	60	58	61	66
$\text{Cl}_{\text{int}} < 3 \text{ mL/min/kg}$	79	76	68	61	54	42	41	39	52
$\text{Papp} > 200 \text{ nm/s}$	20	30	46	65	74	77	65	50	33
	$iPFI$								
	< 3	3-4	4-5	5-6	6-7	7-8	8-9	9-10	>10
hERG $\text{pIC}_{50} < 5$	86	93	88	70	54	36	29	21	11
Promiscuity <5 hits with $\text{pIC}_{50} < 5$	85	78	74	65	49	30	20	13	7

<sup>a</sup> Key: Colours indicate the % chance of achieving benchmark value in that PFI bin: green,  $\geq 67\%$ ; orange, 34–67%; and red,  $< 33\%$ . All values are measured data. 2C9, 2C19 and 3A4 are different isoforms of cytochrome P450 enzymes;  $\text{Cl}_{\text{int}}$ , intrinsic clearance;  $\text{Papp}$ , apparent permeability (PAMPA).

## 2.6.2 Ligand Efficiency Metrics

Ligand Efficiency (LE, Equation 2.3) quantifies free energy of binding (approximated by  $\text{IC}_{50}$ ) with respect to molecular size, defined by the non-hydrogen heavy atom count (HAC).<sup>75</sup> Empirical analysis has shown that LE values of  $\geq 0.3$  ( $\text{kcal mol}^{-1}$  / heavy atom) are indicative of efficient interactions in which the atoms present are effectively contributing to the

binding mode (although the value for many drugs is higher).<sup>74</sup> A low LE (<0.3) is indicative of suboptimal binding efficiency, where some atoms are not involved in key interactions.

$$LE = -\Delta G / HAC$$

$$LE = -\Delta RT \ln(K_d) / HAC$$

$$LE \approx -\Delta RT \ln(IC_{50}) / HAC$$

**Equation 2.3**

Ligand efficiency measures that correct for lipophilicity-enhanced potency have also been developed. Molecules that bind efficiently to the desired target through a hydrophilic scaffold are at reduced risk of lipophilicity-driven adverse consequences. A ligand efficiency metric developed at Astex Therapeutics is Astex Lipophilic Ligand Efficiency (LLE<sub>AT</sub>, Equation 2.4).<sup>76</sup> Here,  $\Delta G^*$  (Equation 2.5) is the modified free energy change where the free energy attributed to non-specific lipophilic binding ( $\Delta G_{lipo}$ ) has been subtracted.  $P$  is the octanol/water partition coefficient. LLE<sub>AT</sub> is normalised for HAC and so exists on the same scale as LE and has the same target of  $\geq 0.3$ . If the LLE<sub>AT</sub> is significantly reduced relative to LE, this likely indicates that lipophilic contact plays an important role in binding affinity.

$$LLE_{AT} = 0.11 - (\Delta G^* / HAC)$$

**Equation 2.4**

$$\Delta G^* = \Delta G - \Delta G_{lipo} \approx RT \ln(IC_{50}) + RT \ln(P)$$

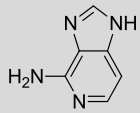
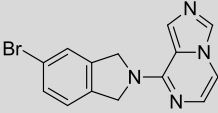
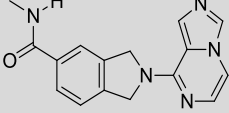
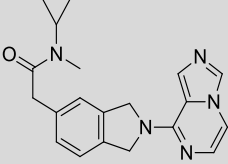
**Equation 2.5**

Generally, it is suggested that both LE and LLE<sub>AT</sub> ought be kept above the desired threshold value of 0.3 during optimisation.<sup>76</sup> This consideration will direct synthetic efforts towards smaller and less lipophilic, but potent compounds, and is especially useful during hit-to-lead activities,<sup>74</sup> including fragment based drug discovery<sup>78</sup> (FBDD). Ligand efficient hits are likely to be chosen for optimization over those equipotent hits with low LE values. Successful optimisation of the hits will then ideally maintain good (or enhanced) LE to provide ligand efficient lead compounds.<sup>79</sup>

Table 2.6 exemplifies the use of ligand efficiency metrics in practice during an FBDD campaign to identify leads against human CD38.<sup>80</sup> Whilst the fragment hit **2.5** was inactive (binding was confirmed by crystallography and two orthogonal biophysical assays), fragment-elaborated bromo-**2.6** was highly potent and ligand efficient. The LLE<sub>AT</sub> was significantly reduced relative to the LE however, reflecting the lipophilic nature of **2.6** (PFI = 7.3). Property guided SAR expansion identified less lipophilic amide **2.7**, which maintained

potency and had a very attractive  $LLE_{AT}$ , implying efficient binding *via* a non-lipophilic scaffold. Further exploration yielded lead-compound **2.8**, with a very favourable potency-property profile, indicated by high ligand efficiencies and attractive PFI.

**Table 2.6.** Bromo-**2.6** had a reduced  $LLE_{AT}$  relative to LE, reflecting non-specific lipophilic interactions likely mediated through the hydrophobic bromine atom. Replacement with polar functionality in amide **2.7** led to an improvement in  $LLE_{AT}$ , indicating productive contact mediated through a non-lipophilic moiety.<sup>a</sup>

				
	<b>Hit 2.5</b>	<b>2.6</b>	<b>2.7</b>	<b>Lead 2.8</b>
<b>pIC<sub>50</sub></b>	<4.0	6.8	6.8	7.3
<b>HAC</b>	10	19	22	26
<b>PFI</b>	1.0	7.3	4.1	5.7
<b>LE</b>	-	0.49	0.42	0.39
<b><math>LLE_{AT}</math></b>	-	0.40	0.49	0.42

<sup>a</sup> Key: HAC, heavy atom count.

## 2.7 Physicochemical Properties and Lead-Compound Profiles in Hit-to-Lead Drug Discovery

As discussed in the previous Sections, a drug candidate will have an improved chance of success if it exists in drug-like physicochemical property space. To facilitate the identification of candidates with attractive properties, an emphasis on the monitoring and control of physicochemical properties is encouraged from the earliest stages of discovery. The hit-to-lead process is the first stage of a discovery campaign in which medicinal chemists begin to establish the potential of molecules against the chosen target. The role of the hit-to-lead chemist is to develop hits identified in a screening campaign into a lead series, with demonstrable SAR, highlighting potent and ligand efficient exemplars. Importantly the leads must exist in good physicochemical property space that facilitates the ensuing lead-optimisation investigations, which often add mass and lipophilicity to the molecules.<sup>81</sup>

Within GSK, the “quality” of any particular lead molecule is judged against the metrics and developability parameters introduced in the preceding Sections. Table 2.7 outlines the criteria that are used to assess lead molecules.<sup>82</sup> Whilst individual hit-to-lead campaigns may have specific requirements, Table 2.7 represents a guide that is generally applicable to most hit-to-lead chemistry activities. To compliment these guidelines, project-specific targeted potency-property profiles are often defined at the outset of a hit-to-lead campaign. For example, the desired lead profile may be <100 nM potency, and PFI <6.

**Table 2.7.** Desirable threshold values for a variety of parameters used to assess the quality of lead compounds. The most attractive leads (and most likely to be successful) are those that adhere to the limits indicated. These numbers do not represent a hard cut-off, rather a guide to indicate the preferable limits for each parameter.<sup>a</sup>

Parameter	Target Threshold Values
<b>pIC<sub>50</sub>, cell potency, selectivity</b>	<i>Determined by project team</i>
LE	≥ 0.3
LLE <sub>AT</sub>	≥ 0.3
PFI	≤ 6
Chrom Log D <sub>7.4</sub>	≤ 4
CLND solubility (μM)	≥ 200
hERG pIC <sub>50</sub>	≤ 4
Cl <sub>int</sub> (mL/min/g tissue)	≤ 3
P <sub>app</sub> (nm/sec)	≥ 100
P450 (3A4) pIC <sub>50</sub>	≤ 4
Secondary Pharmacology <sup>b</sup>	None

<sup>a</sup> Key: LE, ligand efficiency; LLE<sub>AT</sub>, Astex lipophilic ligand efficiency; PFI, property forecast index; CLND, chemiluminescent nitrogen detection method for solubility measurement; Cl<sub>int</sub>, intrinsic clearance (liver microsomes); P<sub>app</sub>, apparent permeability (PAMPA). <sup>b</sup> Activity against a focussed set of targets designed to give a high throughput read-out of off-target risks.<sup>73</sup>

## 2.8 Physicochemical Properties in Tuberculosis Drug Design

Antibacterials in general are known to occupy unique physicochemical property space.<sup>83</sup> Andries *et al.* performed an analysis of TB drugs in an attempt to identify the region of physicochemical property space most relevant to TB chemotherapy.<sup>10</sup> They reported that TB drugs do not fall into one defined region of space, but rather they occupy a very broad area, including: small and polar molecules (e.g. isoniazid, pyrazinamide, ethionamide); large, complex and polar molecules (natural products such as rifampicin and aminoglycosides); small, reactive covalent binders (isoniazid, pyrazinamide, ethionamide); and highly lipophilic molecules (bedaquiline, clofazimine) (Fig. 1.3). It is generally believed that MIC (and therefore permeation across the *M.tb* cell wall) improves within a series as lipophilicity increases,<sup>27</sup> and so the fact that small polar molecules can be effective antituberculars appears paradoxical. It is likely that these drugs enter the *M.tb* cell through porins that facilitate entry of polar nutrients.<sup>84</sup> In general however, the properties required for passage across the mycobacterial cell wall are not known, and this presents a significant challenge to TB drug discovery.

Whilst there is no evident physicochemical property trend amongst the current TB drugs, pursuing drug-like physicochemical property space is likely to maximise the chance of developing successful oral medicines for TB. One particular challenge for TB drug development is maintaining a low MIC whilst reducing lipophilicity, perhaps suggesting that the best starting points are those molecules that already possess both a good MIC and an attractive physicochemical property profile.

## 2.9 Application of Physicochemical Properties in this Thesis

The concepts and hypotheses presented above were applied to the work performed in this thesis, especially in Chapters 4-6 which document efforts to identify lead series from two high-throughput screening hits. It is important to focus on physicochemical properties from this early stage of drug discovery to ensure the delivery of attractive lead series suitable for progression into later stages of drug discovery. As such, it was envisioned that property-focused drug discovery would form the basis of the investigations presented within these Chapters.

### 3. Decaprenylphosphoryl- $\beta$ -D-Ribose 2'-Epimerase 1

Decaprenylphosphoryl- $\beta$ -D-ribose 2'-epimerase 1 (DprE1) has recently emerged as a promising new TB drug target.<sup>85,86</sup> Importantly, DprE1 is a highly validated target, verified by the progression of one particular DprE1 inhibitor (**PBTZ169**, Fig. 3.2) through pre-clinical trials.<sup>87</sup> DprE1 plays an essential role in the synthesis of the mycobacterial cell wall component arabinogalactan (AG), and is vital for *M.tb* survival.

#### 3.1 The Role of DprE1 in the Biosynthesis of Arabinogalactan

AG functions to covalently tether the peptidoglycan (PG) and mycolic acid layers of the mycobacterial cell wall, and is required for cell viability (Sect. 1.3).<sup>88</sup> Figure 3.1 displays a current structural model of AG.<sup>89</sup> The polysaccharide comprises alternating  $\beta$ -(1,5), $\beta$ -(1,6) galactofuranose chains (red), which are linked to the PG layer through a rhamnose-*N*-acetylglucosamine linker (black). Arabinan chains (blue) emanate from the galactofuranose, and consist of linear domains terminated with branched hexa-arabinose motifs (Ara<sub>6</sub>), which themselves are capped with mycolic acids.<sup>89</sup>

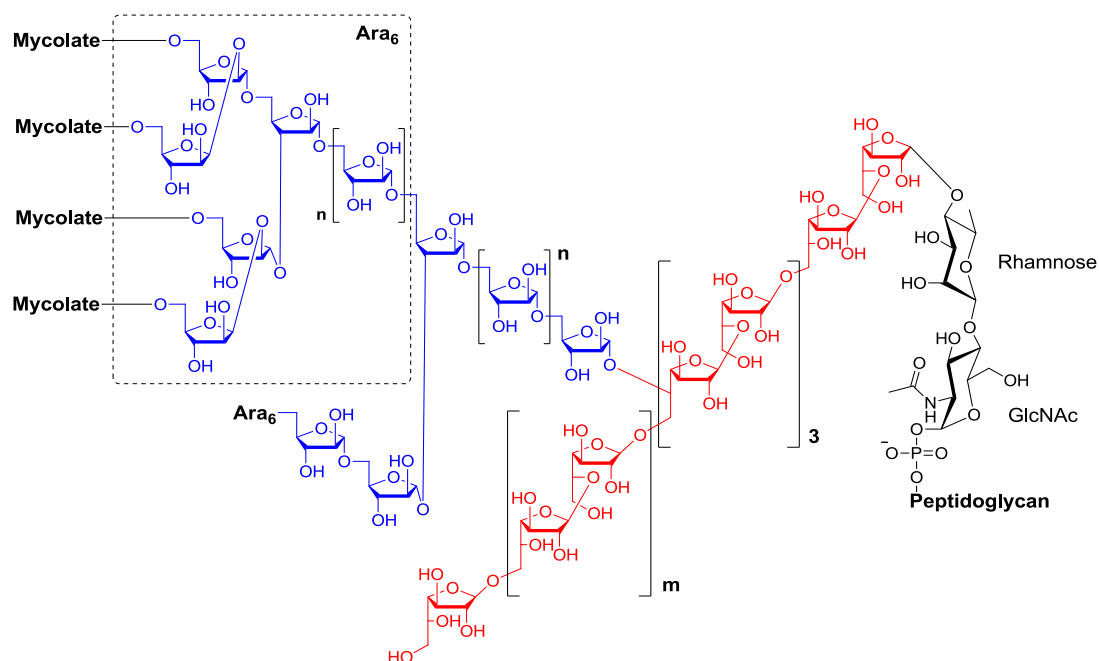


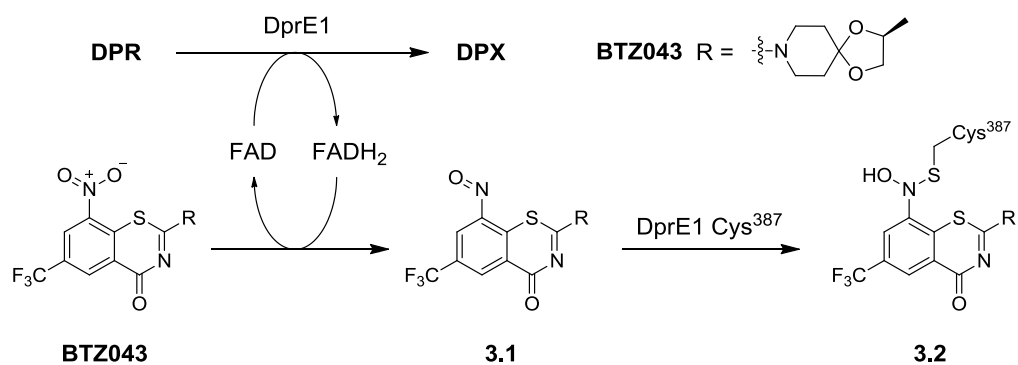
**Figure 3.1.** A current structural model of *M.tb* arabinogalactan.<sup>89</sup> GlcNAc = *N*-acetylglucosamine. Blue = arabinan, red = galactofuranose, black = rhamnose-*N*-acetylglucosamine linker.



to the most dramatic effect on growth arrest when compared to the knock-down mutants of the other enzymes involved in **DPA** biosynthesis. Furthermore, Besra *et al.*<sup>95</sup> identified that inhibition of DprE1 causes cell death not only *via* the prevention of **DPA** synthesis, but also through lack of recycling of decaprenyl phosphate (the mycobacterial lipid carrier for cell wall sugar monomers) and sequestration of this lipid within **DPR**. Together, these findings demonstrate that the DprE1-catalysed oxidation of **DPR** is a particularly vulnerable process in the biogenesis of the mycobacterial cell wall, and has led some authors to refer to DprE1 as a “magic drug-target” for TB.<sup>86</sup> In contrast, DprE2 shows less promise as a therapeutic drug target. Evidence for redundancy of the DprE2-promoted reduction has been reported in the corresponding ortholog of *Corynebacterium glutamicum*.<sup>96</sup>

### 3.2 DprE1 as a Drug Target: Published Inhibitors

DprE1 was identified through the action of a particular class of antimycobacterial agents, the benzothiazinones (BTZs), which demonstrated high potency towards mycobacteria.<sup>85,97</sup> Notably, nitro-containing **BTZ043** (Scheme 3.2) exhibited an extremely potent MIC of 2.3 nM against *M.tb* H37Rv, and displayed comparable MICs against MDR- and XDR-TB strains. Whilst being highly potent against replicating mycobacteria, **BTZ043** was inactive against non-replicating bacilli,<sup>85</sup> likely indicating the inhibition of a target involved in active metabolism. Genetic and biochemical experiments subsequently identified the genes *MSMEG\_6382* and *dprE1* in spontaneous BTZ-resistant mutants, revealing DprE1 as the site of action.<sup>85</sup> It was later discovered<sup>98,99</sup> that the nitro-containing BTZs (e.g. **BTZ043**) are suicide inhibitors of DprE1, as shown in Scheme 3.2. The reduced form of the DprE1 cofactor is oxidised to FAD with concomitant conversion of the nitro-**BTZ043** into the electrophilic nitroso-BTZ **3.1**. This reactive intermediate **3.1** is then trapped by the nucleophilic thiol of an active site cysteine (Cys<sup>387</sup> in *M.tb*), thus irreversibly inactivating the enzyme (and providing rationale for the very low MIC). A crystal structure of the covalent semi-mercaptal adduct **3.2** supports this mode of action.<sup>93</sup>



**Scheme 3.2.** BTZs are suicide inhibitors of DprE1. Reduction of the BTZ nitro group to the nitroso **3.1** is followed by near-quantitative nucleophilic trapping by the active site residue Cys<sup>387</sup>.

Development of **BTZ043** led to the discovery of the second-generation pre-clinical candidate **PBTZ169** (Fig. 3.2), which exhibits even greater efficacy and antimycobacterial activity (MIC < 0.4 nM), and reduced cytotoxicity relative to **BTZ043**.<sup>15,87</sup> Other classes of nitroaromatic inhibitors have since been identified that have the same covalent mechanism of action as **BTZ043**, such as **BT17**,<sup>100</sup> **VI-9376**,<sup>101</sup> **DNB1**<sup>102</sup> and **CT319**<sup>98</sup> (Fig. 3.2), although all are less potent than **BTZ043** and **PBTZ169**.

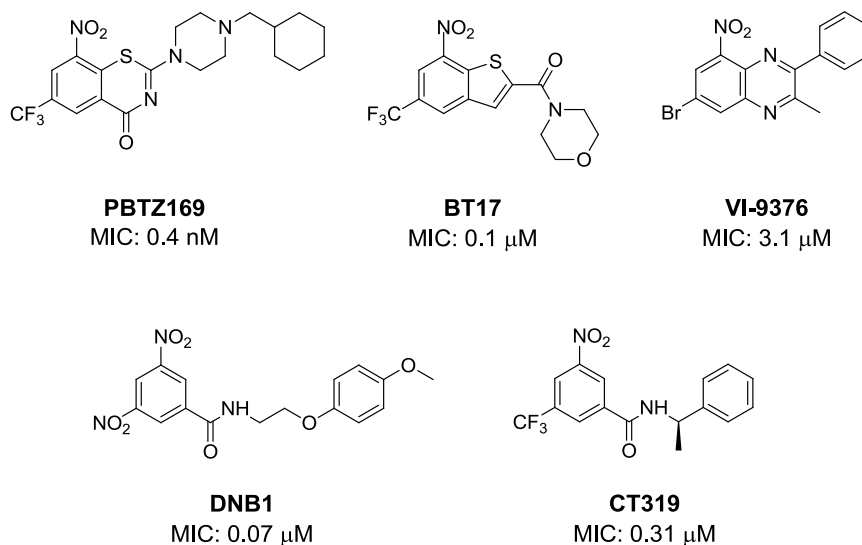


**Figure 3.2.** Nitro-containing covalent DprE1 inhibitors **PBTZ169**,<sup>87</sup> **BT17**,<sup>100</sup> **VI-9376**,<sup>101</sup> **DNB1**<sup>102</sup> and **CT319**.<sup>98</sup>

Despite the fact that benzothiazinone **PBTZ169** has been selected as a pre-clinical candidate, the presence of the nitro group in the compounds above presents a risk. Nitro aromatics are well-known to be reduced *in vivo* by numerous processes, affording potentially carcinogenic intermediates.<sup>103</sup> Additionally, *M.tb* expresses the enzyme NfnB,

which is capable of reducing (and therefore inactivating) such nitro-containing aromatics,<sup>104</sup> causing issues for chronic therapy.

Neres *et al.* identified that replacement of the BTZ 8-nitro group with a pyrrole moiety afforded non-covalent inhibitors of DprE1 (e.g. **PyrBTZ01**, Fig. 3.3) that displayed potent bactericidal activity against *M.tb* H37Rv.<sup>105</sup> However, despite displaying favourable ADMET and PK profiles, **PyrBTZ01** and the other 8-pyrrole BTZ analogues displayed no *in vivo* efficacy in a murine model of TB (covalent inhibitors **BTZ043** and **PBTZ169** had identical PK profiles to **PyrBTZ01** and were efficacious *in vivo*).

Recently, AstraZeneca disclosed three novel series of non-covalent, nitro-free DprE1 inhibitors, the 1,4-azaindoles,<sup>106</sup> aminoquinolones,<sup>107</sup> and pyrazolopyridones,<sup>108</sup> represented by exemplar compounds **3.3a-b**, **3.4** and **3.5** respectively (Fig. 3.3). The most advanced series, the 1,4-azaindoles, demonstrated potent antimycobacterial activity against replicating drug susceptible- and drug resistant-TB strains, and were shown to be bactericidal.<sup>106</sup> The main short-coming of this series was high metabolic clearance, especially in mice (likely driven by relatively high lipophilicity). This was an important factor considering the murine model of TB is typically used to explore *in vivo* efficacy. When administered with a pan-inhibitor of CYP isoforms however, **3.3a** did show good *in vivo* efficacy in acute and chronic murine TB models, thus demonstrating the potential of non-covalent DprE1 inhibitors. Lead-optimized<sup>109</sup> 1,4-azaindole **3.3b** has since been shortlisted as a potential clinical candidate.<sup>110</sup> Neres *et al.* later published another series of structurally disparate non-covalent DprE1 inhibitors, the 2-carboxyquinoxalines, such as **Ty38c** (Fig. 3.3).<sup>111</sup> Whilst **Ty38c** showed potent bactericidal activity, it was discovered that *M.tb* expresses a protein that oxidatively decarboxylates the inhibitor to give a DprE1-inactive derivative. Another published bactericidal non-covalent DprE1 inhibitor is **TCA1** (Fig. 3.3).<sup>112</sup> Unlike all the other reported DprE1 inhibitors, **TCA1** possessed bactericidal activity towards non-replicating bacteria, as well as active replicators. **TCA1** was found to additionally inhibit the mycobacterial enzyme MoeW, which is thought to be involved in molybdenum cofactor biosynthesis.<sup>112</sup> The authors suggested inhibition of this second target was the likely reason for the activity against metabolically inactive bacilli.<sup>112</sup>

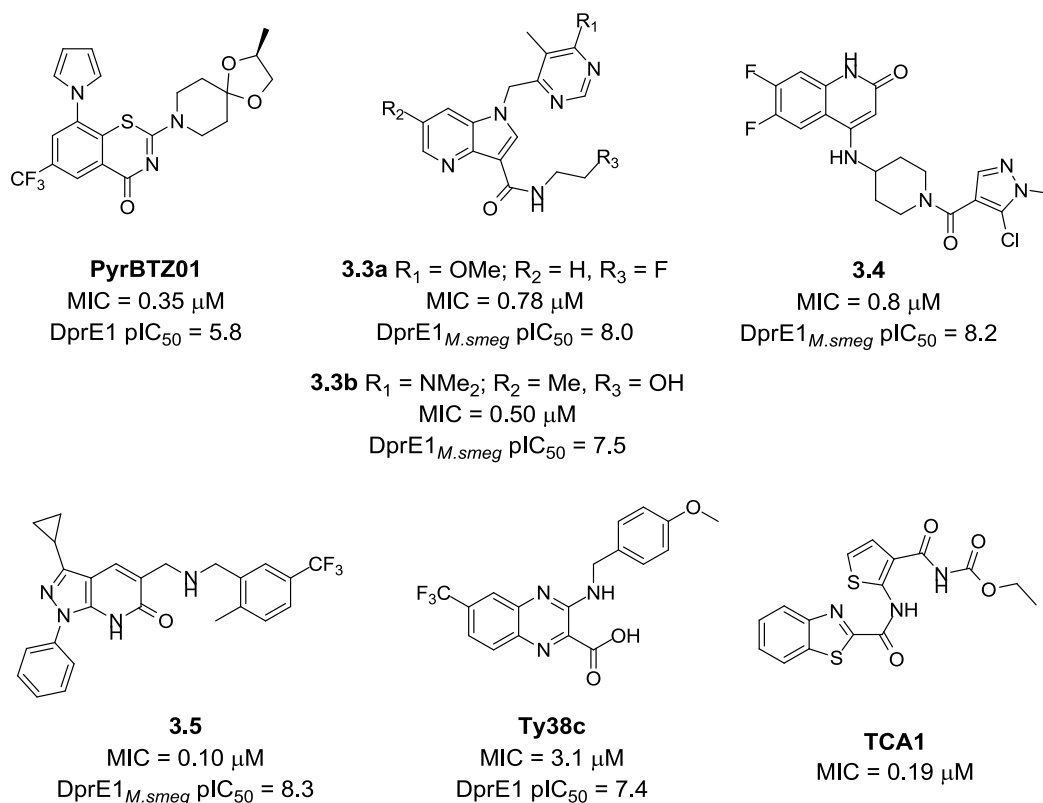


**Figure 3.3.** Published non-covalent inhibitors of DprE1 **PyrBTZ01**,<sup>105</sup> **3.3a-b**,<sup>106,109</sup> **3.4**,<sup>107</sup> **3.5**,<sup>108</sup> **Tyc38c**<sup>111</sup> and **TCA1**.<sup>112</sup> The enzyme activities quoted for **3.3-3.5** were measured against the *M.smeg* DprE1 ortholog MSMEG\_6382.

It appears that DprE1, along with other membrane-bound *M.tb* proteins, may be a particularly druggable TB target.<sup>27,111</sup> Notably, the published inhibitors of DprE1 are structurally unrelated and are broadly chemically diverse (not including the aromatic nitro functionality of the covalent inhibitors). It has been suggested this is due to the presence of highly functionalized residues in the active site.<sup>108</sup> This druggability is likely to be very beneficial in the search for novel TB medicines acting *via* this mechanism of action.

### 3.3 Structure of DprE1

DprE1 is a flavin-containing enzyme, comprising a flavin-binding domain and a substrate-binding domain. The non-covalently bound prosthetic group spans the flavin-binding domain, with the isoalloxazine tri-cycle projecting across the interface between the two domains in the active site cavity<sup>113</sup> (Fig. 3.4a). Site directed mutagenesis<sup>93</sup> of the *M.smeg* DprE1 ortholog (MSMEG\_6382) revealed that the active site residues Gln<sup>343</sup> and Cys<sup>394</sup> (Gln<sup>336</sup> and Cys<sup>387</sup> in *M.tb*) were important for catalytic efficiency. However, the key residue

necessary for the oxidation of **DPR** to **DPX** was found to be the lysine Lys<sup>425</sup> (Lys<sup>418</sup> in *M.tb*), as the Lys<sup>425</sup>Ala mutant was functionally inactive. This lysine residue likely interacts with the **DPR** C2-hydroxyl group, perhaps facilitating deprotonation prior to oxidation.<sup>93</sup> This hypothesis was consistent with the positioning of this critical lysine in DprE1, which is poised directly in front of the flavin moiety (Fig. 3.4b).

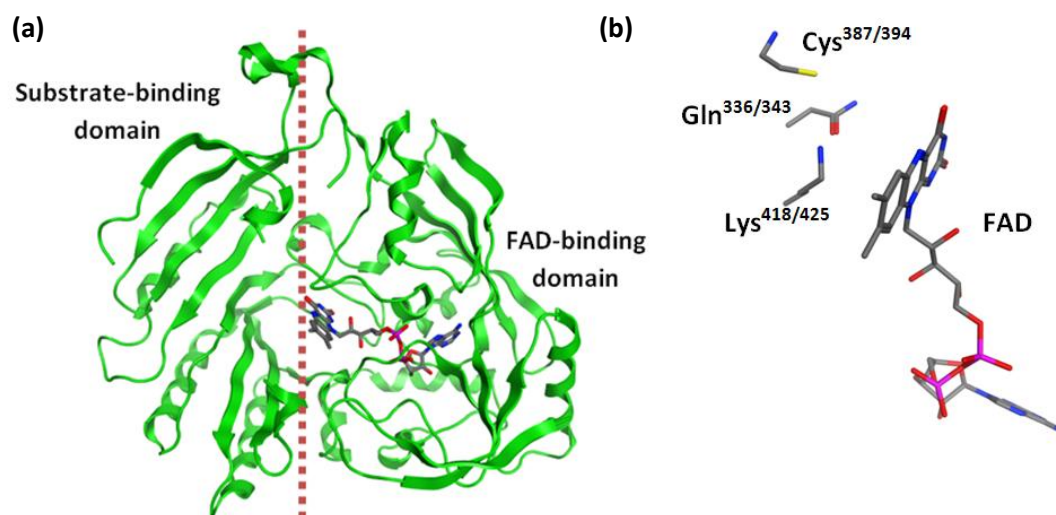


**Figure 3.4.** (a) The crystal structure of native *M.tb* DprE1 defining the two-domain topology common amongst flavoenzymes.<sup>113</sup> (b) The spatial orientation of the important DprE1 residues relative to the FAD cofactor. The two residue numbers refer first to *M.tb* DprE1, then to the *M.smeg* ortholog.

A notable structural feature of DprE1 is the presence of two flexible loop regions on the protein surface (residues 269-297 and 316-330 in *M.tb*), which, depending on the crystallographic conditions, have been observed to be ordered or disordered.<sup>93,113</sup> When both loops are disordered, the active site of DprE1 is open and highly accessible, but when either of the two loops is ordered, the active site is shielded and inaccessible. Figure 3.5 depicts two *M.smeg* crystal structures.<sup>93</sup> The active site of the un-liganded enzyme is blocked as a result of the ordering of residues 323-329 (Fig. 3.5a). In contrast, the flexible loops are displaced by the acetal moiety of the covalent ligand in the **BTZ043**-bound crystal, and the active site is wide open (Fig. 3.5b). A crystal structure of the non-covalently bound **CT319** has also been obtained (in *M.tb* DprE1), in which the active site is shielded through ordering of one of the loops.<sup>113</sup> The flexibility of these loop regions may be important for the functioning of DprE1, perhaps facilitating shuttling between active and inactive forms of the native enzyme, where the active site is either open or inaccessible respectively. It is believed that DprE1 and DprE2 form a membrane-associated complex<sup>92,93,114</sup> (substantiated

by the likelihood that the lipid chain of **DPR** is embedded in the membrane), and that perhaps the activating conformational change occurs on complex formation. The subsequent accessibility of the active site may then facilitate sequestration of **DPR**, or indeed a small-molecule inhibitor.

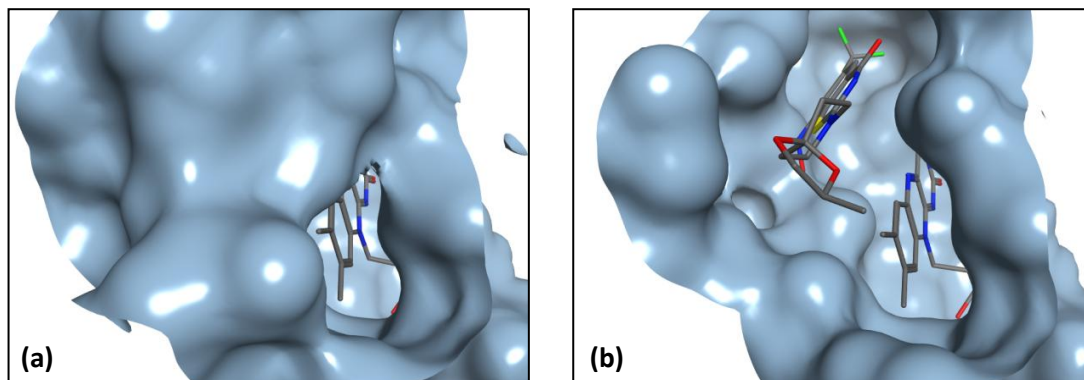


**Figure 3.5.** (a) The native DprE1 ortholog of *M.smeg*. The active site is restricted by the ordering of a flexible loop (the FAD co-factor is visible).<sup>93</sup> (b) *M.smeg* DprE1 liganded with **BTZ043**. The acetal moiety of **BTZ043** displaces the flexible loops leaving the active site wide open.<sup>93</sup>

### 3.4 Research Goals

DprE1 is a highly validated drug target for tuberculosis and suitable inhibitor molecules have exciting potential as new antitubercular medicines. As such, efforts to identify multiple new DprE1 lead series were envisioned. Specifically, the development of two hits from the GSK DprE1 HTS campaign was planned, with a particular focus on delivering potent lead molecules in favourable physicochemical property space. It was anticipated that these lead series would have potential to be further optimised towards novel medicines for tuberculosis.

In addition to the work to identify novel DprE1 inhibitors from the GSK HTS campaign, studies to identify potential inhibitors of DprE1 based on the enzyme substrate were also planned. It was hoped that these molecules would act as DprE1 inhibitors and provide tool compounds with which to further the understanding of DprE1 biology.

## 4. The GSK High-Throughput Screen Against DprE1

### 4.1 Introduction to the HTS Screen and Hit Selection

The GSK DprE1 high-throughput screening (HTS) campaign evaluated approximately 1.8 million compounds using a fluorescence-based biochemical assay (Sect. 4.2.1; all assays and triaging of the HTS data were performed by other individuals within GSK). After triaging the hits, 3986 compounds were progressed to dose-response analysis in the fluorescence assay, such that  $pIC_{50}$  values could be determined and the hits could be ranked on potency and ligand efficiency (Fig. 4.1). An orthogonal mass spectrometry-based assay (the RapidFire™ assay, Sect. 4.2.2) was then used to reconfirm (or dismiss) the potency data from the fluorescence assay. Hit-to-lead efforts were subsequently initiated on two hits of interest: **GSK'295** (Chapt. 5) and **GSK'896** (Chapt. 6). The reasons for selecting each hit are detailed in the respective Chapters.

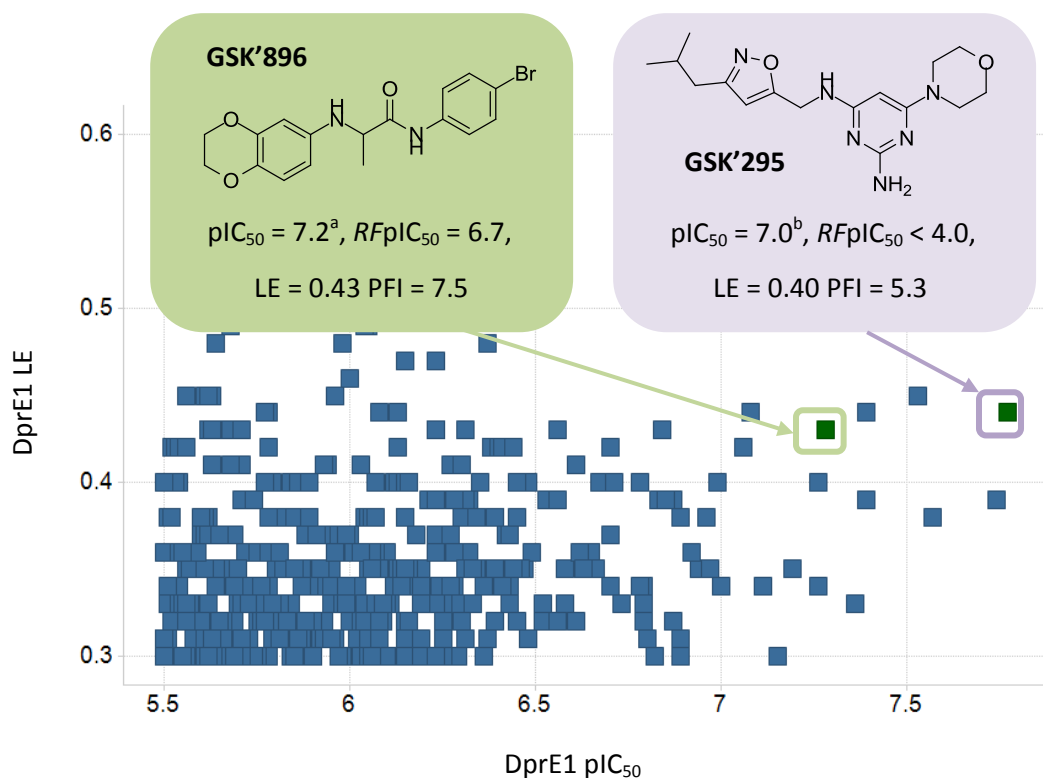


**Figure 4.1.**  $pIC_{50}$  plotted against ligand efficiency for the 3986 hits. Hits with  $pIC_{50} < 5.5$  and  $LE < 0.3$  are not shown. Two hits of interest are highlighted: **GSK'295** and **GSK'896**.  $RFpIC_{50} = \text{RapidFire}^{\text{TM}} pIC_{50}$ . <sup>a</sup> **GSK'896** is shown to have a  $pIC_{50}$  of 7.3 in the plot; after re-testing the mean value fell to 7.2 <sup>b</sup> **GSK'295** is shown to have a  $pIC_{50}$  of 7.7 in the plot; after re-testing the mean value fell to 7.0.

## 4.2 Assays Used in the DprE1 HTS Campaign

### 4.2.1 The Fluorescence Assay

The primary screening assay used to test compounds for DprE1 inhibitory activity was the redox-coupled, fluorescence-based assay depicted in Figure 4.2 (refer to Chapter 3 for a review of the enzymatic function and catalytic cycle of DprE1). Synthetically tractable substrate surrogate *E*-GGPR (*trans*-geranylgeranylphosphoryl- $\beta$ -D-ribose) was used in place of DPR. Inhibition of DprE1 led to a dose-dependent reduction of the resorufin fluorescence signal, which was used to derive pIC<sub>50</sub> values. This assay was developed by Argyrides Argyrou and performed by Laura Vela-Glez Del Peral and Ana Isabel Sanz-Fraile at GSK.

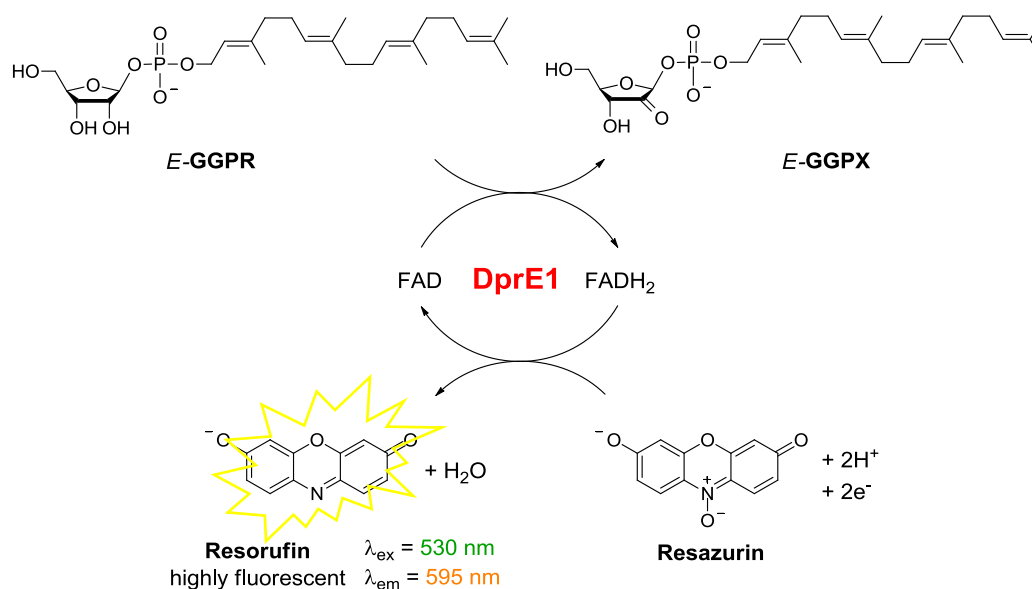


**Figure 4.2.** The biochemistry underlying the fluorescence-based primary biochemical assay. *E*-GGPR = *trans*-geranylgeranylphosphoryl- $\beta$ -D-ribose.

### 4.2.2 The RapidFire™ Assay

Quantitative mass-spectroscopic monitoring of the ratio of *E*-GGPR to *E*-GGPX facilitated measurement of DprE1 inhibition (the biochemistry underlying this assay is illustrated in Fig. 4.3). This assay was used to corroborate (or dismiss) activity observed in the fluorescence biochemical assay. The RapidFire™ assay was developed and performed by Michelle Pemberton at GSK.

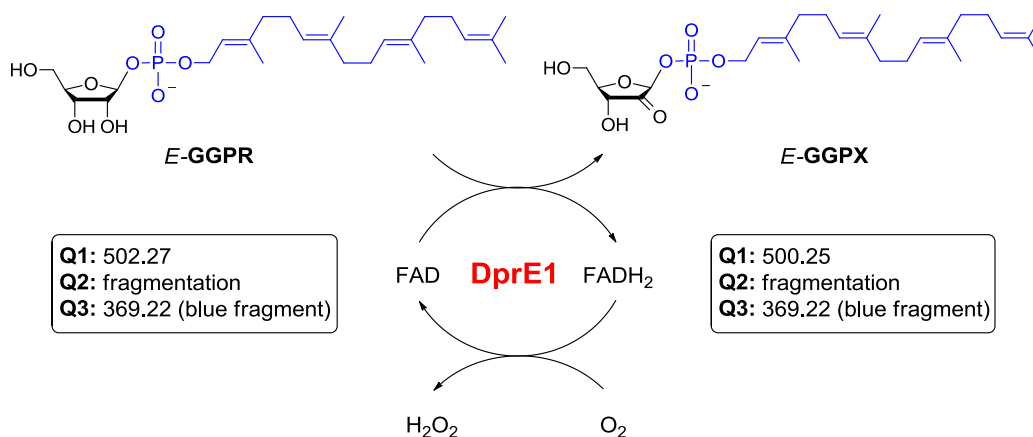


**Figure 4.3.** The biochemistry underlying the mass-spectrometry-based assay (RapidFire™ assay). Q = quadrupole. *E-GGPR* = *trans*-geranylgeranylphosphoryl-β-D-ribose.

### 4.2.3 The Diaphorase Fluorescence-Interference Assay

As part of the triaging process, the DprE1 HTS hits were tested in a counter-screen assay to identify false positive activity associated with redox activity or fluorescence interference. This resorufin-coupled fluorescence assay monitored the diaphorase-mediated conversion of NADH into NAD<sup>+</sup> (Fig. 4.4 illustrates the biochemistry). DprE1 HTS hits that showed activity in the diaphorase assay (causing a measurable change in fluorescence output) were flagged as fluorescence interferers or redox-cyclers, and were not pursued further. This assay was developed by Argyrides Argyrou and performed by Laura Vela-Glez Del Peral and Ana Isabel Sanz-Fraile at GSK.

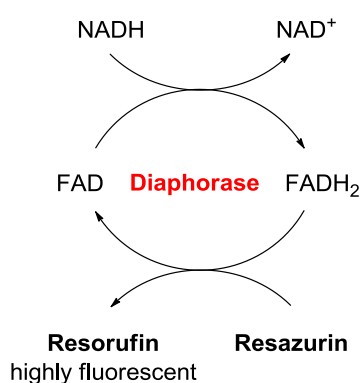


**Figure 4.4.** The Biochemistry of the diaphorase-fluorescence interference assay.

#### 4.2.4 Assay Tight Binding Concentration

Conventional assays use the Michaelis-Menten model for enzyme kinetics,<sup>115</sup> which makes the assumption that the free concentration of inhibitor is equal to the total concentration of inhibitor. If the inhibitor is a particularly tight binder, then the binding of the ligand will sufficiently deplete the concentration of free ligand, invalidating this assumption. This manifests itself in an inability to accurately determine the potency of inhibitors above the tight binding concentration of the assay, which was  $\sim 0.05 \mu\text{M}$  ( $\text{pIC}_{50} = 7.3$ ) for both DprE1 assays. Activities below  $0.05 \mu\text{M}$  ( $\text{pIC}_{50} \geq 7.3$ ) were therefore interpreted with this limitation in mind (an asterisk denotes  $\text{pIC}_{50}$  values at or above this tight-binding regime through-out this thesis). Whilst the tight binding limit may be increased by reducing the concentration of enzyme used, this was not possible for the GSK DprE1 assays, which were insufficiently sensitive at lower enzyme concentrations.

#### 4.2.5 Minimum Inhibitory Concentration (MIC) Assays

A minimum inhibitory concentration (MIC) is defined as the “concentration of an agent that inhibits the growth of 99% of a standardized inoculum of a laboratory strain of *M.tb*”.<sup>24</sup> MICs against *M.tb* H37Rv were determined for the majority of compounds in Chapters 5 and 6. Additionally, selected inhibitors were screened against a strain of *M.tb* over-expressing DprE1 to confirm (or dismiss) DprE1 inhibition as the primary mechanism of action. A significant increase in MIC in the DprE1 over-expressor (OE) assay relative to the H37Rv MIC indicated engagement at DprE1.

#### 4.2.6 X-Ray Crystallography

X-ray crystallography can be highly beneficial to medicinal chemistry programmes, facilitating rational structure-based drug design.<sup>116</sup> Several liganded structures of DprE1 were attained at GSK, however none were relevant to the work presented herein. Consequently, X-ray crystallographic data could not be used to guide compound design.

### 4.3 Research Goals and the Targeted Lead-Compound Profile for the DprE1 Programme

The focus of the work presented in the following two Chapters was to perform hit-to-lead investigations around the two hit molecules highlighted in Figure 4.1: **GSK'295** (Chapt. 5) and **GSK'896** (Chapt. 6). The aim of these investigations was to validate the hits and subsequently develop them into two lead series, demonstrating both structure-activity and structure-property relationships, whilst identifying key exemplars that satisfied the targeted lead-compound profile. The DprE1-programme targeted lead-compound profile was defined as follows:

- High potency at DprE1 ( $pIC_{50} > 7$ );
- Potent MIC ( $< 5 \mu\text{M}$ ), with DprE1 as the proven mechanism of action;
- Good physicochemical property profile (modelled by  $PFI < 7$ );
- Attractive ADMET profile (fulfilling the parameters introduced in Sect. 2.5);
- Positive *in vivo* evaluation (significant reduction of bacterial burden *in vivo*).

The targeted programme potency-property profile was defined as  $pIC_{50} > 7$ ,  $PFI < 7$ .

## 5. Hit-to-Lead Work Around GSK'295

### 5.1 Overview of GSK'295

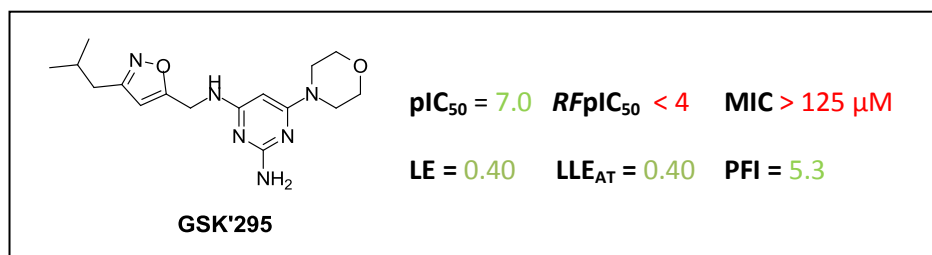


Figure 5.1. Potency and physicochemical property profile for GSK'295.

Figure 5.1 highlights the potency and physicochemical property profile for GSK'295. This HTS hit was of interest as it shared some common structural features with a potent series of cell-active DprE1 inhibitors previously discovered within GSK (Fig. 5.2). GSK'710 was identified in a TB whole-cell screening campaign,<sup>117</sup> and was later confirmed as a DprE1 inhibitor.<sup>118</sup> Physicochemical property-guided optimisation of GSK'710 led to the discovery of lead compound GSK'932, which had similar potency, an improved MIC, and improved property profile relative to GSK'710.<sup>119</sup> Notably, GSK'932 contained a morpholinopyrimidine motif similar to the 2-amino morpholinopyrimidine scaffold present in GSK'295. Fragmentation of GSK'932 showed that the morpholinopyrimidine fragment 5.1 was an efficient binder at DprE1 ( $LE = 0.31$ ). Importantly, GSK'710, GSK'932 and fragment 5.1 all showed DprE1 inhibitory activity in the fluorescence and RapidFire™ assays. GSK'295 however, demonstrated high activity in the fluorescence assay but was inactive in the RapidFire™ assay (Fig. 5.1). Validation of this HTS hit was therefore a priority.

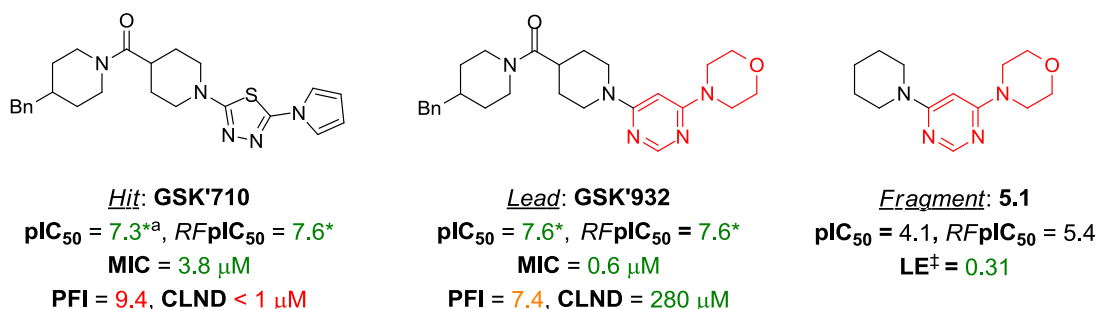
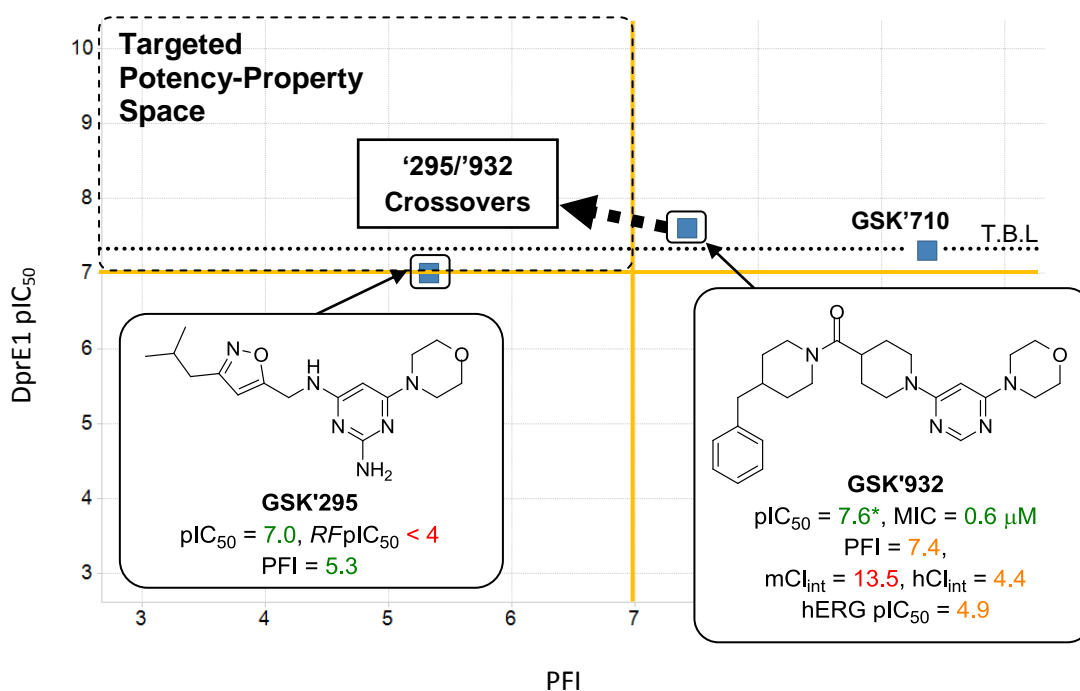


Figure 5.2. Hit-to-lead work around GSK'710 led to the discovery of GSK'932. Morpholinopyrimidine fragment 5.1 was found to be a highly efficient binder at DprE1. <sup>†</sup> LE calculated from fluorescence assay  $pIC_{50}$ . <sup>a</sup> Compound tested as  $pIC_{50} < 4$  in 2 of the 51 test occasions. \* Denotes activity at or above the tight binding limit.





**Figure 5.4.** Plot of potency vs. PFI for **GSK'295**, **GSK'932** and **GSK'710**. The likely position of **'295/932** crossover compounds with retained activity is indicated. T.B.L. = tight binding limit.  $Cl_{int}$  = intrinsic clearance (liver microsomes); h, human; m, mouse. \* Denotes activity at or above the tight binding limit.

## 5.2 Project Aims

The aims of this work were as follows:

- validate **GSK'295** as a genuine DprE1 inhibitor or confirm false positive activity;
- synthesise a small set of **'295/932** cross-over compounds designed to reduce PFI relative to **GSK'932**;
- Identify cross-over analogues that are highly potent against DprE1, exhibit potent MICs, and have an improved ADMET profile relative to **GSK'932**;
- Evaluate the antitubercular properties of such compounds *in vivo*.

## 5.3 Design of '295/932 Cross-Over Compounds

In order to address the aims above, the synthesis of a small set of related **'295/932** cross-over analogues was proposed (Fig. 5.5), including amino-pyrimidines **5.3**, the fragment equivalents **5.4**, and the (2*H*)-pyrimidine equivalent of hit **GSK'295**, **5.5**. The less lipophilic pyrimidinone congeners **5.6-5.8** were also targeted to explore an alternative scaffold that had improved properties whilst retaining the additional hydrogen bond acceptor. Where

depicted in Figure 5.5, regioisomers of each heteroaromatic compound were also targeted to generate SAR.

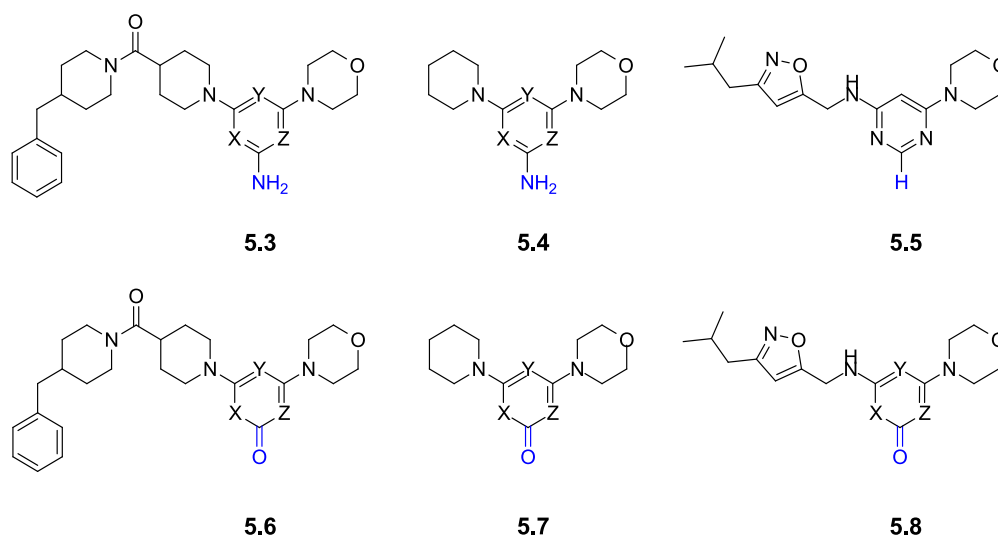
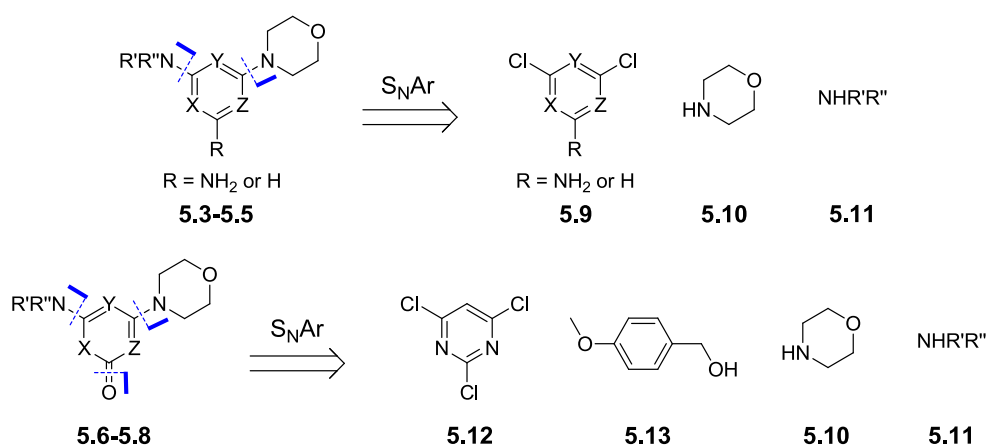


**Figure 5.5.** '295/'932 cross-over compounds designed to test the validity of hit **GSK'295**. X, Y, Z = CH or N/NH, such that the heterocycle is a pyrimidine or pyrimidinone.

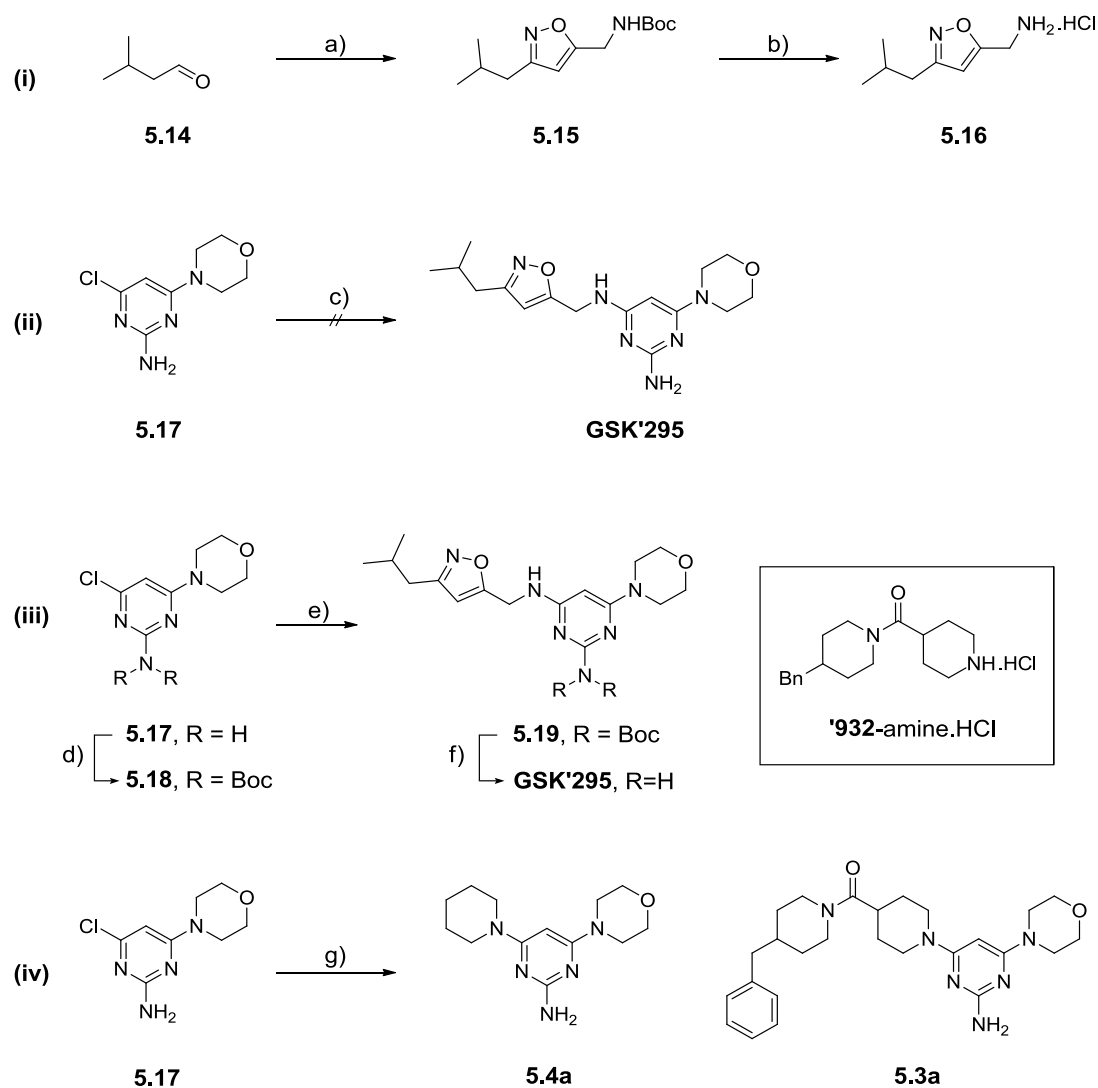
## 5.4 Synthesis of Crossover Compounds 5.3-5.8

Generalised retrosynthetic strategies for the synthesis of the planned targets are outlined in Scheme 5.1.  $S_NAr$  disconnections of aminopyrimidines **5.3-5.4** or pyrimidine **5.5** at the central aromatic moiety yielded the di-chloro heteroaryl **5.9**, morpholine **5.10** and amine **5.11**. Three  $S_NAr$  disconnections<sup>121</sup> of pyrimidinones **5.6-5.8** gave trichloropyrimidine **5.12**, *p*-methoxybenzyl alcohol **5.13**, and amines **5.10** and **5.11**.



**Scheme 5.1** Retrosynthetic strategies for the cross-over compounds **5.3-5.8**. X,Y,Z = CH or N/NH, such that the heterocycle is a pyrimidine or pyrimidinone.

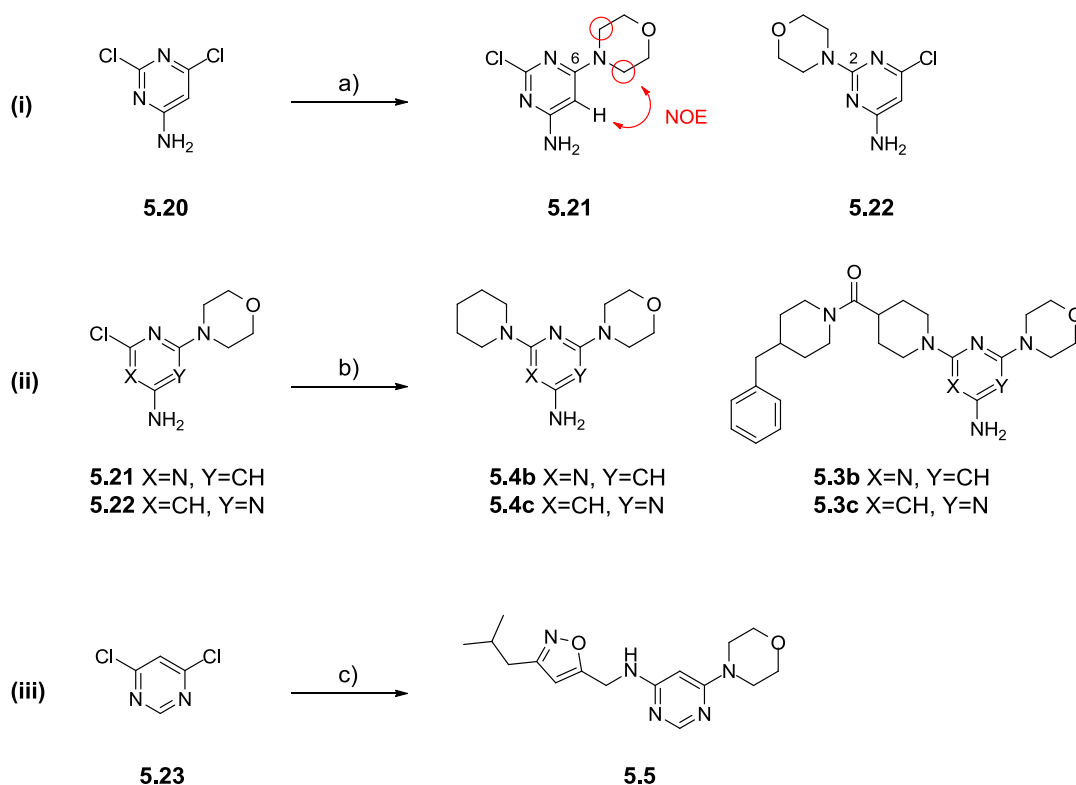
Chemistry initiated with the re-synthesis of the HTS hit to facilitate screening of a new sample of **GSK'295** for hit validation (Scheme 5.2). A one-pot Cu(I)-catalysed isoxazole formation<sup>122</sup> afforded *N*-Boc-methylamino-isoxazole **5.15** in 59% yield from isovaleraldehyde **5.14** (Scheme 5.2i). *N*-Boc deprotection with HCl then revealed the amine **5.16** as the hydrochloride salt. Subsequent efforts to couple amine **5.16** and commercially available 4-chloro-6-morpholinopyrimidin-2-amine **5.17** in a microwave-assisted S<sub>N</sub>Ar reaction as planned were unsuccessful: the reaction did not proceed, presumably due to the particularly electron-rich nature of the pyrimidine **5.17** (Scheme 5.2ii). Converting **5.17** into *bis*-Boc amino pyrimidine **5.18** facilitated a Buchwald amination<sup>123</sup> between the aryl chloride **5.18** and amine **5.16** (Scheme 5.2iii); biaryl phosphane ligand XPhos was used to promote reactivity<sup>124</sup> of the metal towards unactivated aryl chloride **5.18**. Deprotection of the coupled product **5.19** under acidic conditions yielded **GSK'295**. The S<sub>N</sub>Ar reactions between chloropyrimidine **5.17** and secondary amines piperidine and (4-benzylpiperidin-1-yl)(piperidin-4-yl)methanone hydrochloride (available in-house, herein referred to as '932-amine.HCl) proceeded smoothly due to the increased nucleophilicity of the secondary amine coupling partners (Scheme 5.2iv). These reactions afforded the corresponding fragment **5.4a** and **GSK'932**-crossover analogue **5.3a** in good yields.



**Scheme 5.2.** a) i)  $\text{NH}_2\text{OH}\cdot\text{HCl}$ ,  $\text{NaOH}$ ,  $\text{H}_2\text{O}/t\text{BuOH}$ , ii) Chloramine-T,  $\text{Cu}(\text{II})\text{SO}_4\cdot 5\text{H}_2\text{O}$ ,  $\text{Cu}(0)$  turnings, *N*-Boc propargylamine, pH 6, 59%. b)  $\text{HCl}$  (4 M), 1,4-dioxane, 93%. c) **5.16**, DIPEA, EtOH,  $150^\circ\text{C}$ ,  $\mu\text{wave}$ . d)  $\text{NaH}$ ,  $\text{Boc}_2\text{O}$ , DMF, 86%. e)  $\text{Pd}_2(\text{dba})_3$ , XPhos, **5.16**,  $\text{Cs}_2\text{CO}_3$ , DMF,  $100^\circ\text{C}$ ,  $\mu\text{wave}$ , 13%. f)  $\text{HCl}$  (4 M), 1,4-dioxane, 76%. g) piperidine OR '932-amine.HCl, DIPEA, EtOH,  $150^\circ\text{C}$ ,  $\mu\text{wave}$ , **5.4a** = 90%; **5.3a** = 74%.

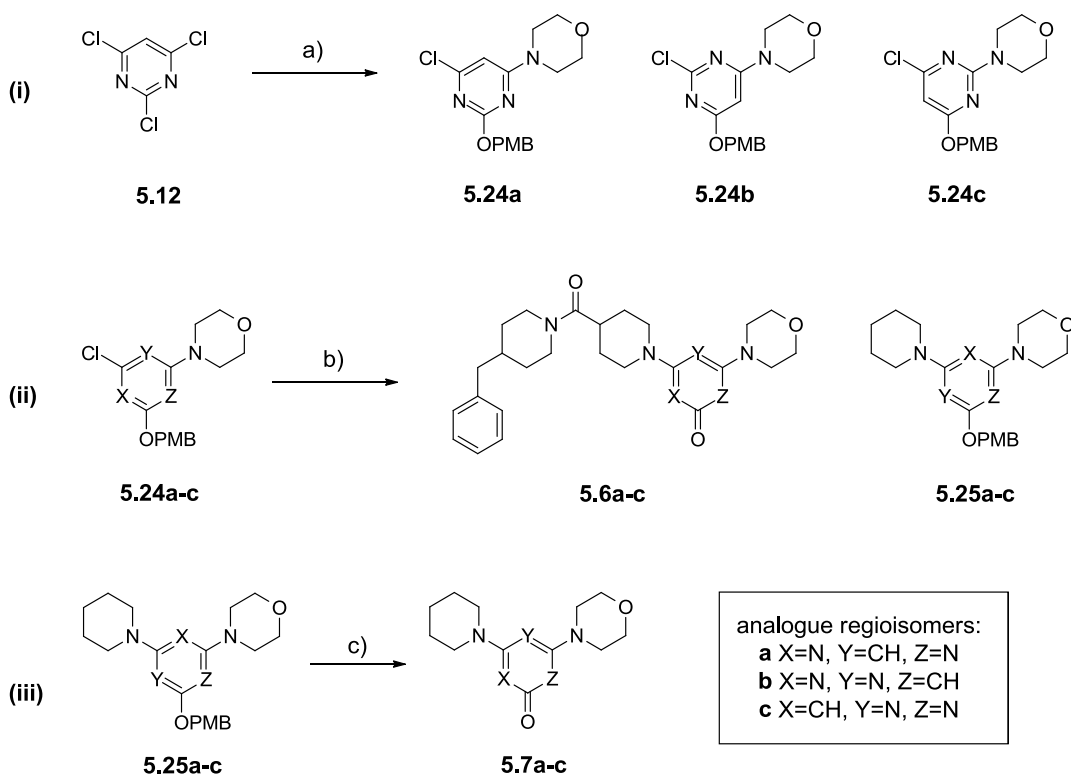
Synthesis of the aminopyrimidine regioisomers **5.3b-c** and **5.4b-c** began with an  $\text{S}_{\text{N}}\text{Ar}$  reaction between 2,6-dichloropyrimidin-4-amine **5.20** and morpholine, which was highly regioselective for substitution at the 2-position as confirmed by NOE experiments (Scheme 5.3i; Appendix A2). After chromatographic separation, 6-morpholinopyrimidine **5.21** and 2-morpholinopyrimidine **5.22** were obtained in 7% yield and 75% yield respectively. Ensuing  $\text{S}_{\text{N}}\text{Ar}$  reactions with the appropriate amine (piperidine or '932-amine.HCl) yielded fragment regioisomers **5.4b** and **5.4c**, and '932-crossover regioisomers **5.3b** and **5.3c** (Scheme 5.3ii; the fragments **5.4b** and **5.4c** were unstable, for example they decomposed in  $\text{CDCl}_3$ , and

were not pursued further). Additionally, one-pot sequential  $S_NAr$  reactions between 4,6-dichloropyrimidine **5.23** and firstly the aminomethyl isoxazole **5.16**, followed by morpholine, yielded the (2*H*)-pyrimidine analogue of **GSK'295**, **5.5** in 63% (Scheme 5.3iii).



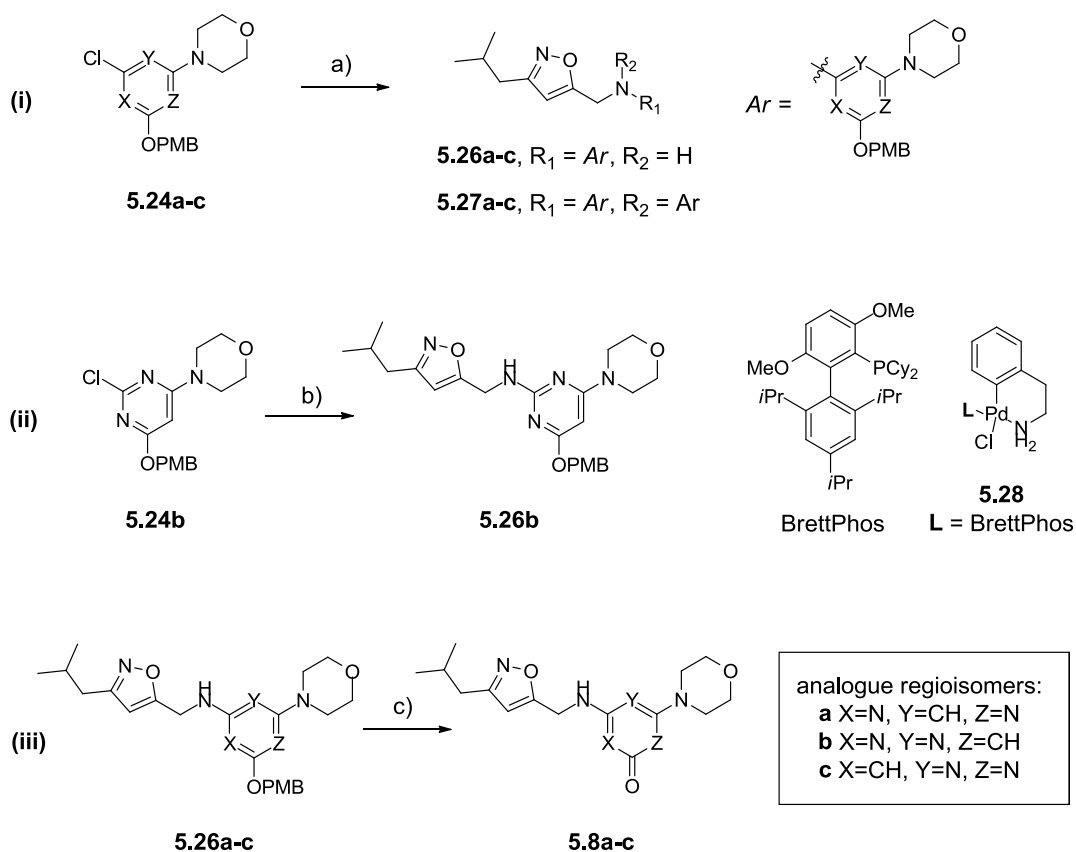
**Scheme 5.3** a) Morpholine, DIPEA, EtOH, 150 °C,  $\mu$ wave, **5.21** = 7%, **5.22** = 75%. b) **5.21** or **5.22**, piperidine OR '932-amine.HCl, DIPEA, EtOH, 150 °C,  $\mu$ wave, **5.4b** & **5.4c** decomposed when dissolved in  $CDCl_3$ , **5.3b** = 35%, **5.3c** = 46%. c) **5.16**, DIPEA, EtOH 150 °C,  $\mu$ wave, then morpholine, 150 °C,  $\mu$ wave, 63%.

Syntheses of all the pyrimidinone congeners **5.6-5.8** were achieved *via* regioisomeric intermediates **5.24a-c**<sup>121</sup> (Scheme 5.4i). Arylation of *p*-methoxybenzylalcohol with 2,4,6-trichloropyrimidine **5.12** followed by an  $S_NAr$  reaction with morpholine gave the regioisomers **5.24a-c** after chromatographic separation. Microwave assisted  $S_NAr$  reactions between **5.24a**, **5.24b** or **5.24c** and piperidine or '932-amine.HCl were then performed (Scheme 5.4ii). The piperidine-substituted intermediates **5.25a-c** were isolated in good yields, but reaction with '932-amine.HCl unexpectedly led to *O*-deprotection to give the appropriately substituted pyrimidinones **5.6a-c**. PMB cleavage of the piperidine-substituted **5.25a-c** with TFA gave final fragment-pyrimidinones **5.7a-c** (Scheme 5.4iii).



**Scheme 5.4.** a) 4-methoxybenzyl alcohol,  $\text{Cs}_2\text{CO}_3$ , MeCN, then morpholine. **5.24a** = 21%, **5.24b** = 6%, **5.24c** = 40%. b) piperidine OR '932-amine.HCl, DIPEA, EtOH, 150 °C,  $\mu\text{wave}$ , **5.6a-c** = 41-81%; **5.25a-c** = 71-93%. c) TFA, DCM (1:1), **5.7a-c** = 66-89%.

Finally, unoptimised Buchwald aminations between **5.24a**, **5.24b** or **5.24c** and aminomethyl isoxazole **5.16** in the presence of  $\text{Pd}_2(\text{dba})_3$ , XPhos and caesium carbonate afforded intermediates **5.26a-c** in 18-28% yields (Scheme 5.5i). LCMS analysis indicated that diarylation of the amine **5.16** had also occurred in each of these reactions to give *bis*-aryl products **5.27a-c** (not isolated), accounting for the low yields of monoarylation products **5.26a-c**. The monoarylation of primary amines is known to be a challenging transformation, although ligands and precatalysts that promote high selectivity for monoarylation over diarylation are available (e.g. BrettPhos<sup>125</sup> and Pd-PEPPSI-IPent<sup>Cl</sup> <sup>126</sup>). Indeed, when aryl halide **5.24b** was reacted with primary amine **5.16** in the presence of BrettPhos and a BrettPhos-palladium precatalyst **5.28** (Scheme 5.5ii),<sup>125</sup> monoarylation product **5.26b** was afforded in 50%, and LCMS of the reaction mixture showed formation of the diarylation product **5.27b** was suppressed relative to when Xphos and  $\text{Pd}_2(\text{dba})_3$  were used. Cleavage of the PMB protecting groups in **5.26a-c** with TFA gave the final compounds **5.8a-c** (Scheme 5.5iii).



**Scheme 5.5.** a)  $\text{Pd}_2(\text{dba})_3$ , XPhos, **5.16**,  $\text{Cs}_2\text{CO}_3$ , DMF,  $100^\circ\text{C}$ ,  $\mu\text{wave}$ , 18-28% for **5.26a-c** (diarylation products **5.27a-c** were not isolated). b) BrettPhos-Pd precatalyst **5.28**, BrettPhos, **5.16**,  $t\text{BuONa}$ , 1,4-dioxane,  $100^\circ\text{C}$ ,  $\mu\text{wave}$ , 50%. c) TFA, DCM 1:1, 47-50%.

## 5.5 Biological & Physicochemical Evaluation of Analogues 5.3-5.8

On completion of the synthesis of compounds **5.3-5.8**, biochemical potency and physicochemical property parameters were assayed. Table 5.1 reports these data.

**Table 5.1.** Potency, ligand efficiency and physicochemical data for **GSK'295**, **GSK'932** and compounds **5.3-5.8**.

No.	R <sub>1</sub>	Heterocycle	pIC <sub>50</sub> <sup>a</sup> (RFpIC <sub>50</sub> <sup>b</sup> )	LE, LLE <sub>AT</sub> <sup>c</sup>	PFI
<b>GSK'295</b>			7.0 (<4.0)	0.40, 0.40	5.3
<b>5.5</b>			4.0 (<4.0)	0.24, 0.24	5.7
<b>5.8a</b>			4.3 (4.6)	0.25, 0.37	4.0
<b>5.8b</b>			<4.0 (<4.0)	-, -	4.7
<b>5.8c</b>			<4.0 (<4.0)	-, -	4.6
<b>5.1</b>			4.1 (5.4)	0.31, 0.31	4.6
<b>5.4a</b>			4.3 (<4.0)	0.31, 0.31	4.2
<b>5.7a</b>			4.5 (<4.0)	0.32, 0.47	2.2
<b>5.7b</b>			<4.0 (<4.0)	-, -	3.2
<b>5.7c</b>			<4.0 (<4.0)	-, -	3.4

Table 5.1 continued overleaf

Table 5.1 continued from overleaf

No.	R <sub>1</sub>	Heterocycle	pIC <sub>50</sub> <sup>a</sup> (RFpIC <sub>50</sub> <sup>b</sup> )	LE, LLE <sub>AT</sub> <sup>c</sup>	PFI
GSK'932			7.6* (7.6*)	0.32, 0.34	7.4
5.3a			7.3* (7.8*)	0.29, 0.32	7.1
5.3b			6.4 (5.9)	0.26, 0.28	7.4
5.3c			7.3* (7.3*)	0.29, 0.32	7.6
5.6a			7.4* (7.9*)	0.30, 0.40	5.6
5.6b			7.0 (7.7*)	0.28, 0.35	6.5
5.6c			7.1 (7.5*)	0.29, 0.36	6.2

<sup>a</sup> pIC<sub>50</sub> measured in the DprE1 fluorescence assay. <sup>b</sup> pIC<sub>50</sub> measured in the DprE1 RapidFire™ assay. <sup>c</sup> Ligand efficiency values are calculated from the fluorescence assay data. \* Denotes activity at or above the tight binding limit.

The re-synthesized HTS hit **GSK'295** maintained a pIC<sub>50</sub> of 7.0 in the fluorescence assay and registered inactive in the RapidFire™ assay, reaffirming the discrepancy between the two assays for this compound. The related (2*H*)-pyrimidine analogue **5.5** was inactive in both

the fluorescence assay and the RapidFire™ assay. Furthermore, the pyrimidinone congeners **5.8a-c** which retained the additional hydrogen bond acceptor capacity of **GSK'295** were either inactive in both assays (**5.8b** and **5.8c**) or only weakly active in both assays (**5.8a**). These observations indicated that HTS hit **GSK'295** was probably a false positive, as it is unlikely that such minor structural modifications would cause such large losses in activity. It was interesting to compare the replacement of the aminomethyl isoxazole component of **GSK'295** with the '932-amine functionality (4-benzylpiperidin-1-yl)(piperidin-4-yl)methanone), which afforded highly potent DprE1 inhibitor **5.3a** that was active in both the fluorescence and RapidFire™ assays (*vide infra*). However, replacement of the core 2-aminopyrimidine motif of **GSK'295** with (2*H*)-pyrimidine (the core motif of **GSK'932**) led to a complete loss of activity in **5.5**. Together, these data suggest that the false positive activity of **GSK'295** was a whole-molecule effect, and not necessarily due to the aminomethyl isoxazole motif alone. Whilst the cause of the false positive activity was not fully investigated, **GSK'295** showed no activity in the diaphorase assay (Sect. 4.2.3), precluding the likelihood of fluorescence interference or redox-activity. Other possible causes of false positive activity include covalent modification of the protein, compound instability and metal complexation.<sup>127</sup>

The fragment compounds **5.4a** and **5.7a** were equipotent with the '932-fragment **5.1** in the fluorescence assay, but were too weakly active to show potency in the RapidFire™ assay. Pyrimidin-2(1*H*)-one **5.7a** was particularly lipophilic ligand efficient ( $LLE_{AT} = 0.47$ ), suggesting this fragment was making highly productive binding contacts through a non-lipophilic motif. This result highlighted the potential benefit of scaffold-hopping from the pyrimidine core of **GSK'932** (**5.1**  $LLE_{AT} = 0.3$ ) to a pyrimidin-2(1*H*)-one structure.

The crossover compounds **5.3a-c** and **5.6a-c** showed particularly encouraging results. All the synthesised molecules in this set exhibited high potency against DprE1 in the fluorescence assay, and all maintained activity in the RapidFire™ assay. Encouragingly, the aminopyrimidines **5.3a** and **5.3c** and pyrimidin-2(1*H*)-one **5.6a** were active at or above the tight binding limit. Additionally, the less lipophilic pyrimidinones **5.6a-c** occupied much improved physicochemical property space as predicted, signified by reduced PFI values.

The antimycobacterial activity of several compounds was next assessed; the data are shown in Table 5.2. **GSK'932** had an MIC of 0.6  $\mu$ M, and remains one of the most potent antimycobacterial compounds in the series. **5.3a** and **5.6a** also showed good whole-cell

activity, possessing MICs of 3.5 and 3.0  $\mu\text{M}$  respectively. This was particularly noteworthy for the less lipophilic pyrimidinone **5.6a**, as improvement of MIC tends to correlate with increased lipophilicity within a series.<sup>27</sup> DprE1 was the confirmed mechanism of action for **5.3a** and **5.6a**, indicated by 43- and 63- fold increases in MIC against the *M.tb* DprE1 over-expressor strain. Other aminopyrimidine and pyrimidinone regioisomers displayed weaker MICs compared to **5.3a** and **5.6a**, generally reflecting weaker DprE1 potency (for example, **5.6b** and **5.6c** were active below the tight binding limit).

Together, the above results confirmed that the aminopyrimidine moiety could be incorporated into the **GSK'932** structure whilst maintaining high enzymatic and whole-cell potency, and in the case of the pyrimidinone congeners, high potency was achieved with a concomitant improvement in physicochemical properties. This was a highly encouraging result as the pyrimidinones **5.6a-c** now satisfied the programme's targeted potency/property criteria ( $\text{pIC}_{50} > 7$ ,  $\text{PFI} < 7$ ).

**Table 5.2.** Enzymatic potency and MIC data for compounds **GSK'932**, **5.3a**, **5.3c**, and **5.6a-c**.

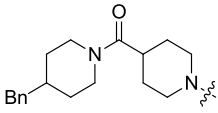
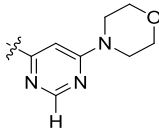
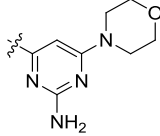
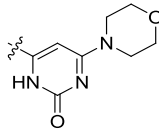
No.	R <sub>1</sub>	Heterocycle	pIC <sub>50</sub> <sup>a</sup>	MIC (μM), <sup>b</sup> [OE shift] <sup>c</sup>
<b>GSK'932</b>			7.6*	0.6 [>53]
<b>5.6a</b>			7.4*	3.0 [63]
<b>5.3a</b>			7.3*	3.5 [43]
<b>5.6b</b>			7.0	12.0
<b>5.6c</b>			7.1	16.0
<b>5.3c</b>			7.3*	24.0

<sup>a</sup> pIC<sub>50</sub> measured in the DprE1 fluorescence assay. <sup>b</sup> MIC against *M.tb* H37Rv. <sup>c</sup> Fold-difference in MIC between the H37Rv MIC and the MIC recorded against the DprE1 over-expressor (OE) strain. \* Denotes activity at or above the tight binding limit.

## 5.6 *In Vitro* Profiling of 2-Amino Pyrimidine 5.3a and Pyrimidin-2(1H)-one 5.6a

Based on the highly encouraging results above, 2-amino pyrimidine **5.3a** and pyrimidin-2(1H)-one **5.6a** were progressed for further profiling. Table 5.3 displays the physicochemical and ADMET data for **5.3a**, **5.6a** and **GSK'932**.

**Table 5.3** Physicochemical and *in vitro* ADMET data for **GSK'932**, **5.3a**, and **5.6a**.<sup>a</sup>

	 <b>GSK'932</b>	 <b>5.3a</b>	 <b>5.6a</b>
PFI	7.4	7.1	5.6
Chrom Log D <sub>7.4</sub>	5.4	5.1	3.6
Molecular Weight (Da)	449	464	465
CLND solubility (μM)	280	303	≥370
Measured pK <sub>a</sub>	5.2 <sup>b</sup>	6.4 <sup>b</sup>	5.2 <sup>b</sup> , 11.2 <sup>c</sup>
hERG pIC <sub>50</sub>	4.9	5.2 <sup>d</sup>	<4.3
hCl <sub>int</sub> (ml/min/g)	4.4	3.4	<0.5
mCl <sub>int</sub> (ml/min/g)	13.5	11.6	4.9
P <sub>app</sub> (nm/sec)	485	360	<3.0
P450 (3A4) pIC <sub>50</sub>	4.8	ND	<4.4
2° pharmacology <sup>e</sup>	Minor flags	ND	Clean profile

<sup>a</sup>Key: Green = good; orange = moderate; red = poor. PFI = Chrom Log D<sub>7.4</sub> + #Ar; CLND, chemi-luminescent nitrogen detection method for solubility measurement; Cl<sub>int</sub>, intrinsic clearance (liver microsomes); h, human; m, mouse; P<sub>app</sub>, apparent permeability (PAMPA); ND, not determined. <sup>b</sup> Basic pK<sub>a</sub>. <sup>c</sup> Acidic pK<sub>a</sub>. <sup>d</sup> Compound failed to fit a curve in 1 out of 6 test occasions. <sup>e</sup> Activity against a focussed set of targets designed to give a high throughput read-out of off-target risks.<sup>73</sup>

The modest decrease in lipophilicity of 2-amino pyrimidine **5.3a** (Chrom Log  $D_{7.4}$  = 5.1) relative to **GSK'923** (Chrom Log  $D_{7.4}$  = 5.4) resulted only in marginal improvement of *in vitro* metabolic stability over **GSK'932**, and hERG activity remained similar. In contrast, the ADMET profile of the much less lipophilic pyrimidinone **5.6a** (Chrom Log  $D_{7.4}$  = 3.6) was greatly improved over **GSK'932**. No measurable activity at hERG or CYP34A was observed and **5.6a** exhibited a clean secondary pharmacology profile. Importantly, **5.6a** demonstrated much improved metabolic stability to mouse liver microsomes compared to **GSK'932**, which was significant as the murine model of TB is most commonly used for *in vivo* efficacy studies (Sect. 5.7). **5.6a** also showed very low *in vitro* clearance against human liver microsomes; values of  $\leq 3$  mL/min/g are regarded as good indicators of favourable *in vivo* clearance and oral exposure (Table 2.7).

Unfortunately, the relatively hydrophilic pyrimidinone **5.6a** suffered a loss of permeability in the parallel artificial membrane permeation assay (PAMPA; passive transport shows a bilinear correlation with lipophilicity; Sect. 2.5.1). It is possible that for its large size (MW = 465), **5.6a** was insufficiently lipophilic to permit favourable permeation. Waring suggested that as the molecular weight of a compound increases, the required lipophilicity (Log D) needed to achieve favourable permeability increases (Table 2.2).<sup>66</sup> Related comparisons within GSK reported similar findings, showing that as the size of a molecule increases (modelled by CMR, the calculated molar refraction), an increase in Log D is required to achieve good oral bioavailability (F%),<sup>48,128</sup> which is a surrogate for good permeation. Figure 5.6 plots Chrom Log  $D_{7.4}$  against CMR for a set of molecules with measured oral bioavailability across a range of size and lipophilicity, onto which **GSK'932**, **5.3a** and **5.6a** are superimposed. This analysis suggested that whilst **GSK'932** and **5.3a** were sufficiently lipophilic to have a good chance of showing favourable permeability, pyrimidinone **5.6a** was not. Interestingly, whilst **5.6a** was poorly permeable in the parallel artificial membrane permeation assay, this compound exhibited a potent MIC (3.0  $\mu$ M), suggesting that PAMPA is not a good indicator of transit across the mycobacterial cell wall.

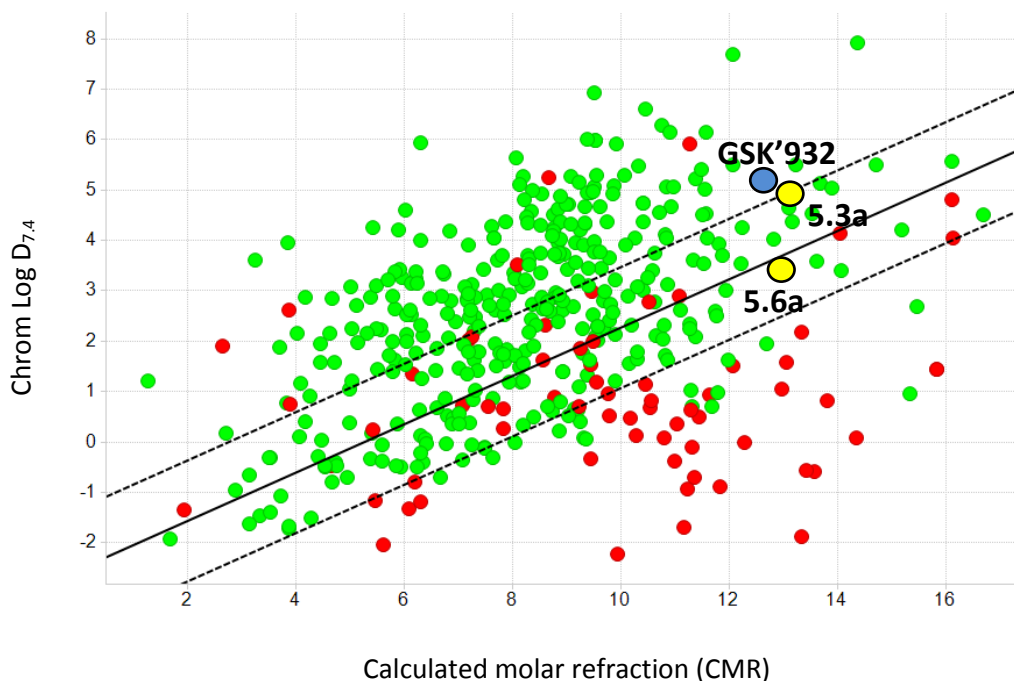


**Figure 5.6.** Plot of calculated Chrom Log  $D_{7,4}$  versus calculated molar refraction (CMR) for a training set of molecules.<sup>48,128</sup> Green spots have  $F\% > 30\%$ ; red spots have  $F\% < 30\%$ . The solid line represents a discriminator for likely good or bad permeability; the upper and lower dotted lines indicate cut-offs for greater certainty of good or poor permeability respectively. **GSK'932** (blue), **5.3a** and **5.6a** (yellow) are superimposed, using measured Chrom Log  $D_{7,4}$  values.

## 5.7 *In Vivo* Evaluation of Pyrimidin-2(1*H*)-one **5.6a**

The *in vivo* efficacy of pyrimidinone **5.6a** was examined in an acute murine model for TB<sup>129</sup> (a standardised assay designed to facilitate rapid evaluation of the therapeutic-efficacy of compounds against actively replicating *M.tb* in the lungs of mice). Pyrimidinone **5.6a** was orally administered once daily (dose = 30 mg/kg) for 8 days after infection with *M.tb* H37Rv; on the 9<sup>th</sup> day the mice were sacrificed and the lung bacterial load was assessed. Disease progression was monitored (in the context of bacterial replication) by counting the number of colony forming units (CFU).

Treatment: uid, po, 8 days (days 1-8 after infection)

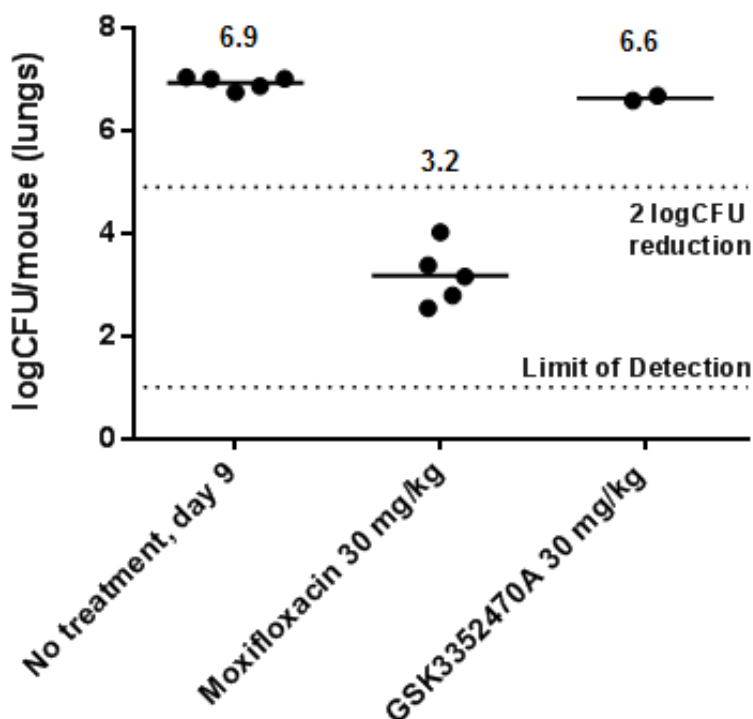


**Figure 5.7.** *In vivo* efficacy evaluation of pyrimidinone **5.6a** in an acute murine model of TB<sup>129</sup> (**GSK3352470A** = **5.6a**). Each dot represents data for one mouse. Figures over the dots show the mean value of logCFU. A 0.3 log unit reduction in CFU was observed for **5.6a**. In contrast, second-line fluoroquinolone moxifloxacin effected a 3.7 log unit reduction in CFU. CFU = colony forming units. uid = *uni in die* (once daily). po = *per os* (oral administration).

Despite high enzymatic potency and a good MIC, no statistically significant decrease in logCFU (relative to the control mice) was seen after dosing the infected animals with **5.6a**. Subsequent DMPK analysis indicated low exposure due to poor oral bioavailability. This result was consistent with the *in vitro* data for **5.6a** that indicated poor permeability ( $P_{app} < 3$  nm/sec) and moderate clearance ( $mCl_{int} = 4.9$  ml/min/g, liver microsomes), each of which could potentially limit oral bioavailability and *in vivo* efficacy.

## 5.8 Improving the Permeability and *In Vitro* Metabolic Stability of Pyrimidin-2(1*H*)-one 5.6a

Pyrimidinone **5.6a** demonstrated no evidence of *in vivo* efficacy in the acute murine model of TB. Poor permeability and only moderate metabolic stability towards mouse liver microsomes were cited as possible causes. Analogues of **5.6a** with both improved permeability and *in vitro* clearance were therefore targeted.

### 5.8.1 Strategy to Improve the Permeability of 5.6a

It was predicted that, as pyrimidinone **5.6a** was perhaps too hydrophilic to show good permeability, designing analogues of **5.6a** with increased lipophilicity may enhance permeability. The key challenge however, was to install adequate lipophilicity to engender good permeability without adversely affecting other ADMET parameters. Analysis of a plot of lipophilicity against permeability for **5.6a**, **5.3a**, **GSK'932** and its analogues (Fig. 5.8) revealed that no examples within the limits  $3.6 > \text{Chrom Log } D_{7.4} \leq 5$  (or  $5.6 > \text{PFI} \leq 7$ ) had been synthesised, so a strategy to address this was pursued.

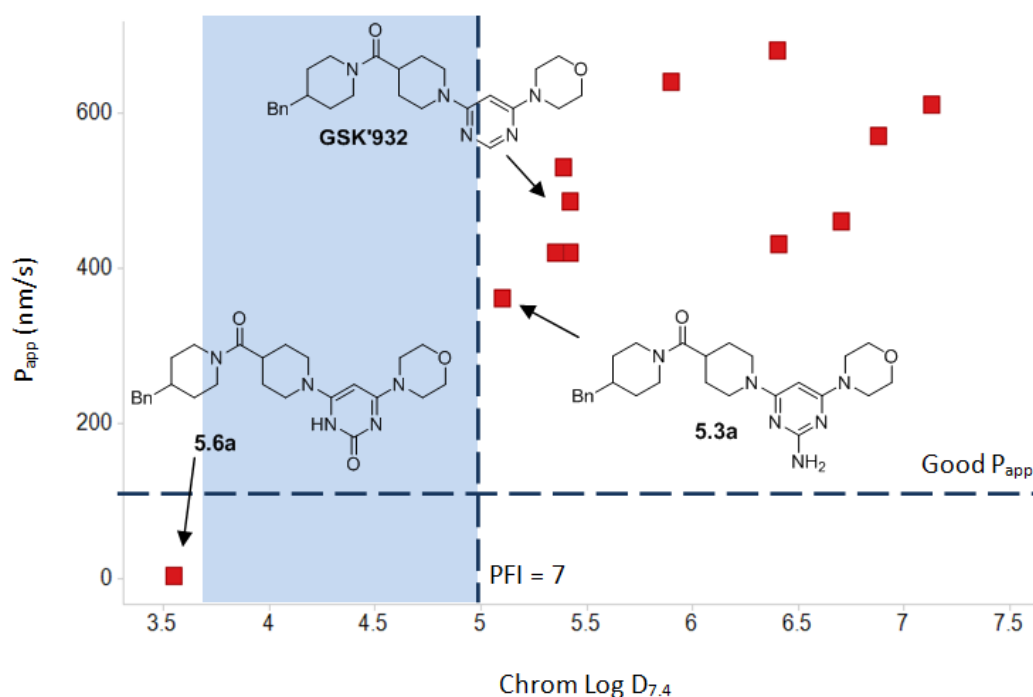


**Figure 5.8.** A plot of Chrom Log  $D_{7.4}$  vs. PAMPA apparent permeability ( $P_{app}$ ) for **5.6a**, **5.3a**, **GSK'932** and its analogues. The blue box indicates the area of unexplored lipophilicity space.

### 5.8.2 Strategy to Improve the *In Vitro* Metabolic Stability of 5.6a

The major pathway for metabolism of xenobiotics is by hydroxylation.<sup>49</sup> Two strategies are often pursued to reduce or prevent susceptibility to these transformations: reducing lipophilicity or blocking the site of metabolism (Sect.2.5.2). MetaSite<sup>130,131</sup> (computational software that predicts locations most susceptible to cytochrome- and monooxygenase-mediated metabolism) identified that the *para* position of the distal phenyl ring in **5.6a** was likely a major site of metabolism (Fig. 5.9). Consequently, blocking of this site was pursued as a strategy to improve the *in vitro* stability of **5.6a** to mouse liver microsomes.

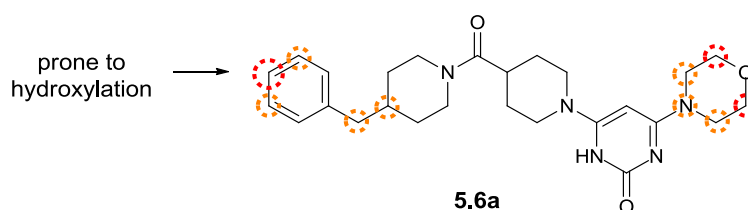


**Figure 5.9.** MetaSite<sup>130</sup> predicted sites of cytochrome- and monooxygenase- mediated metabolism of **5.6a**. The sites predicted to be most susceptible to metabolism are circled. Colour key: red = high probability; orange = moderate probability.

### 5.8.3 Design of Pyrimidin-2(1H)-one Analogues 5.32a-e

Substitution of the **GSK'932** distal phenyl ring was known to be well tolerated, and such compounds were generally active at or above the tight binding limit (Fig. 5.10a). Consequently, this moiety was selected as a structural handle with which to investigate the effect of lipophilicity gain on *in vitro* permeability of the pyrimidin-2(1H)-one series. Furthermore, substitution at the *para* position would block the predicted aromatic hydroxylation and likely improve *in vitro* metabolic stability. To this end, an in-house Chrom Log  $D_{7.4}$  calculator<sup>120</sup> was used to design five *para*-substituted analogues **5.32a-e** within the targeted lipophilicity range ( $3.6 > \text{Chrom Log } D_{7.4} \leq 5$ ; Fig. 5.10b). On comparison of the calculated and measured Chrom Log  $D_{7.4}$  data for **5.6a** (Fig. 5.10b) and other pyrimidin-2(1H)-ones (data not shown), it was apparent that the calculated values were consistently offset by approximately +0.5. This discrepancy was compensated for in the design of **5.32a-e**. Each of the designed analogues **5.32a-e** was predicted to be sufficiently lipophilic to forecast good permeability (*cf.* the Chrom Log  $D_{7.4}$  vs. CMR analysis, Fig. 5.6).

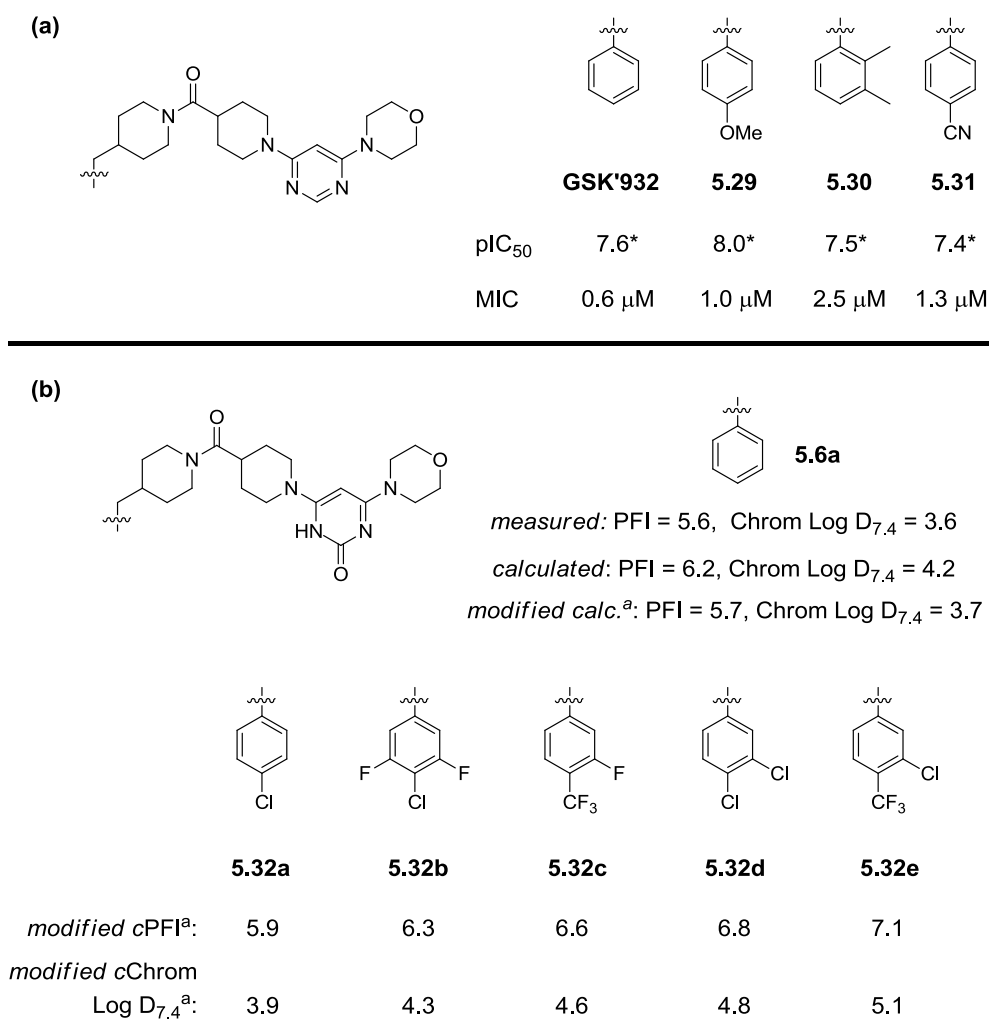
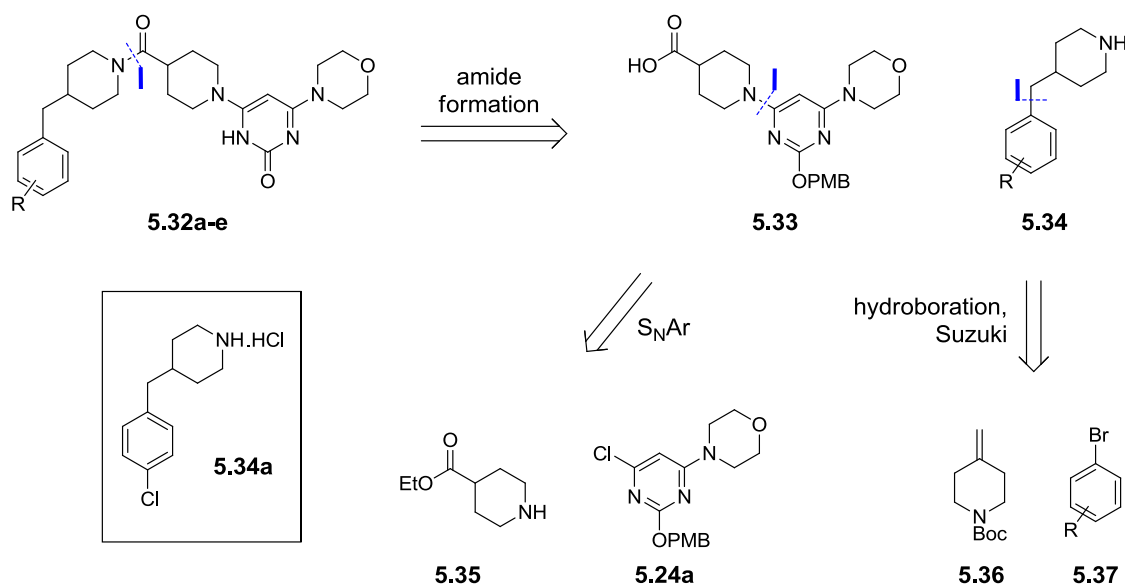


**Figure 5.10.** (a) GSK'932 analogues with substituted phenyl rings (synthesised by others within GSK). (b) Increasingly lipophilic analogues of pyrimidin-2(1H)-one **5.6a** were designed using an in-house Chrom Log D<sub>7.4</sub> calculator.<sup>120</sup> cPFI = calculated PFI; cChrom Log D<sub>7.4</sub> = calculated Chrom Log D<sub>7.4</sub>.<sup>a</sup> 0.5 was subtracted from the calculated values to compensate for the discrepancy between measured and calculated Chrom Log D<sub>7.4</sub> values for pyrimidin-2(1H)-ones. \* Denotes activity at or above the tight binding limit.

#### 5.8.4 Synthesis of Pyrimidin-2(1H)-one Analogues 5.32a-e

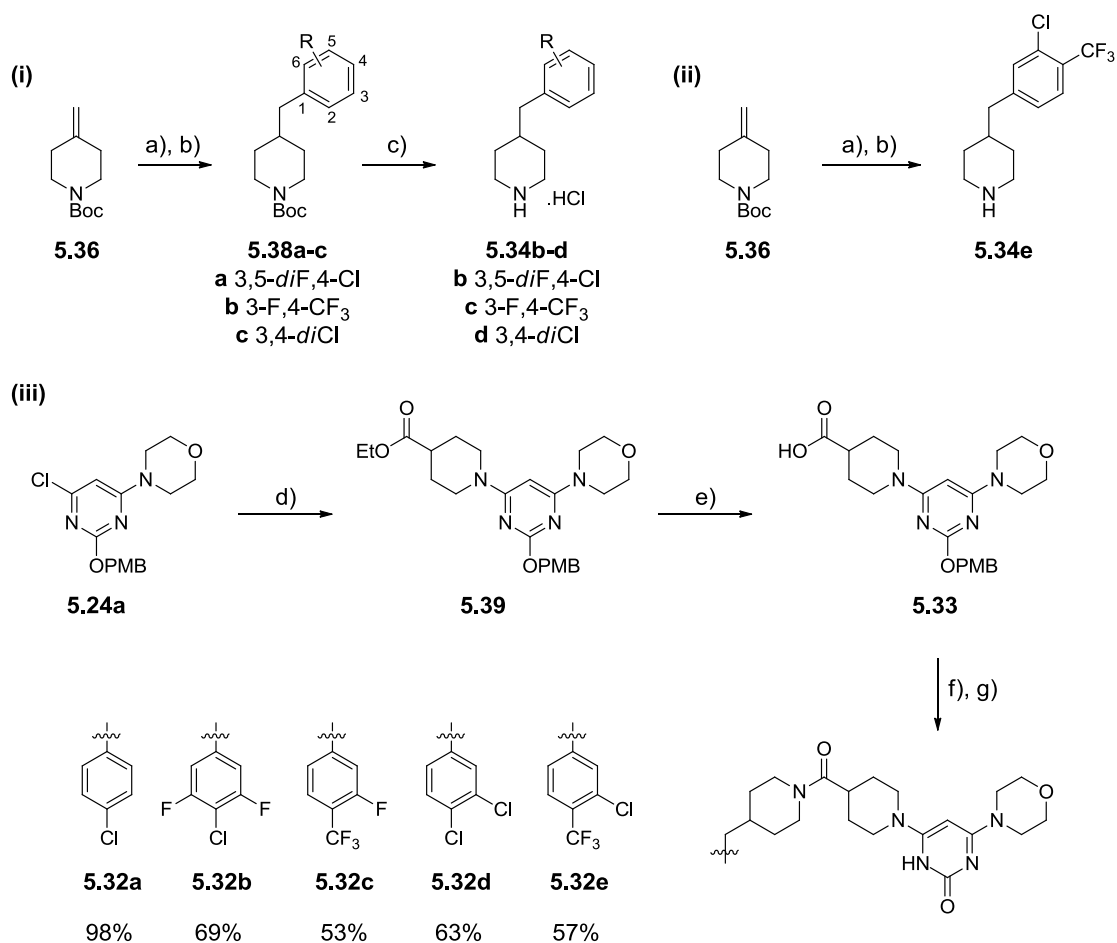
A new disconnection strategy was required for the synthesis of analogues **5.32a-e** to allow for variation of the distal phenyl ring. Disconnection at the amide of **5.32** afforded acid **5.33** and substituted 4-benzyl piperidines **5.34** (Scheme 5.6). Acid **5.33** was accessible from pyrimidine **5.24a**, and piperidines **5.34** were accessible from methylene piperidine **5.36** via a reported hydroboration-Suzuki protocol.<sup>132</sup> The piperidine **5.34a** required for the preparation of chloro-substituted **5.32a** was commercially available and did not require synthesis.



**Scheme 5.6.** Retrosynthetic strategy for the syntheses of pyrimidin-2(1H)-one analogues **5.32a-e**. Chloro-**5.34a** was commercially available and did not require synthesis.

Following the reported Suzuki procedure for the synthesis of 4-benzyl piperidines,<sup>132</sup> hydroboration of *N*-Boc 4-methylene piperidine **5.36** with either 9-BBN (0.5 M in THF) or 9-BBN dimer, followed by palladium-catalysed arylation with an aryl bromide **5.37** afforded the *N*-Boc-4-benzyl piperidines **5.38a-c** (Scheme 5.7i), or the deprotected 4-benzyl piperidine in the case of the 3-Cl,4-CF<sub>3</sub> analogue **5.34e** (Scheme 5.7ii). *N*-Boc piperidines **5.38a-c** were deprotected by treatment with HCl to afford piperidine salts **5.34b-d** (Scheme 5.7i)

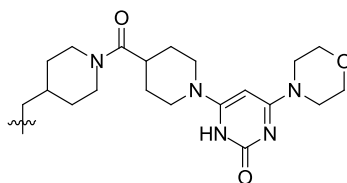
Carboxylic acid **5.33** was synthesised *via* an  $S_NAr$  reaction between chloropyrimidine **5.24a** and ethyl isonipecotate **5.35**, followed by hydrolysis of intermediate ester **5.39** (Scheme 5.7iii). Amide coupling between acid **5.33** and the substituted 4-benzyl piperidines **5.34a-e**, followed by PMB removal with TFA afforded pyrimidin-2(1H)-ones **5.32a-e** in 53-98% yields over the two steps.

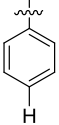
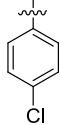
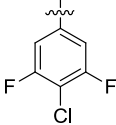
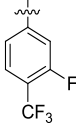
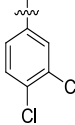
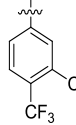


**Scheme 5.7.** a) 9-BBN (0.5 M in THF) or 9-BBN dimer, THF. b) substituted aryl bromide **5.37**, PdCl<sub>2</sub>dppf, K<sub>2</sub>CO<sub>3</sub>, DMF, H<sub>2</sub>O, 18% yield for **5.34e**. c) 4 M HCl, 1,4-dioxane, 15-57% yield over 2 steps for **5.34b-d**. d) ethyl isonipecotate **5.35**, DIPEA, EtOH,  $\mu$ wave, 87%. e) LiOH.H<sub>2</sub>O, 1,4-dioxane, H<sub>2</sub>O, 88%. f) HATU, DIPEA, DMF, then **5.34a-e**. g) TFA, DCM; yields over the two steps f) and g) for **5.32a-e** are indicated in the scheme.

### 5.8.5 Biological, Physicochemical and ADMET Evaluation of Pyrimidin-2(1H)-ones **5.32a-e**

On completion of the synthesis of the set of compounds **5.32a-e**, potency, physicochemical property, intrinsic clearance and compound permeability were assayed. Table 5.4 reports these data.

**Table 5.4.** Potency, physicochemical and ADME data for compounds **5.6a** and **5.32a-e**.<sup>a</sup>

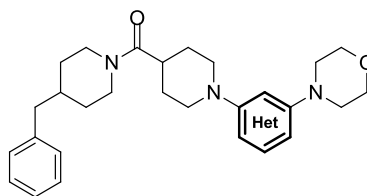
Phenyl Substitution	 H	 Cl	 F, Cl	 CF <sub>3</sub> , F	 Cl, Cl	 Cl, CF <sub>3</sub>
	<b>5.6a</b>	<b>5.32a</b>	<b>5.32b</b>	<b>5.32c</b>	<b>5.32d</b>	<b>5.32e</b>
pIC <sub>50</sub> <sup>b</sup>	7.4*	7.3*	7.7*	7.8*	7.9*	8.2*
MIC (μM) <sup>c</sup>	3.0	2.5	1.3	2.5	0.8	1.3
PFI <sup>d</sup>	5.6	6.4 (5.9)	6.5 (6.3)	6.6 (6.6)	7.0 (6.8)	7.1 (7.1)
Chrom Log D <sub>7.4</sub> <sup>d</sup>	3.6	4.4 (3.9)	4.5 (4.3)	4.6 (4.6)	5.0 (4.8)	5.1 (5.1)
MW (Da)	465	500	535	551	534	568
CLND (μM)	≥370	≥188	276	213	117	105
hCl <sub>int</sub> (ml/min/g)	<0.5	1.2	0.5	0.6	0.8	1.0
mCl <sub>int</sub> (ml/min/g)	4.9	1.2	0.7	1.0	1.4	0.9
P <sub>app</sub> (nm/sec)	<3	<10	23	19	12	18

<sup>a</sup> Key: Green = good; orange = moderate; red = poor. PFI = Chrom Log D<sub>7.4</sub> + #Ar; Mw, molecular weight; CLND, chemi-luminescent nitrogen detection method for solubility measurement; Cl<sub>int</sub>, intrinsic clearance (liver microsomes); h, human; m, mouse; P<sub>app</sub>, apparent permeability (PAMPA). <sup>b</sup> pIC<sub>50</sub> measured in the DprE1 fluorescence assay. <sup>c</sup> MIC against *M.tb* H37Rv. <sup>d</sup> Modified calculated values (from Fig. 5.10b) are shown in parentheses. \* Denotes activity at or above the tight binding limit.

Each of the new analogues **5.32a-e** were highly potent DprE1 inhibitors (active at or above the tight binding limit), and encouragingly showed comparable MICs relative to **5.6a**. With the exception of *p*-chloro **5.32a**, which was rather more lipophilic than predicted by the Chrom Log D<sub>7.4</sub> calculations, the lipophilicities of the other pyrimidinone analogues **5.32b-e** were predicted accurately, providing increasingly lipophilic congeners within the range 4.4 ≥ Chrom Log D<sub>7.4</sub> ≤ 5.1. Solubility was reduced for the most lipophilic compounds

**5.32d-e**, but all analogues displayed low *in vitro* metabolic stability towards both human and mouse microsomes as predicted. Whilst *p*-chloro **5.32a** was poorly permeable in the parallel artificial membrane permeation assay, the more lipophilic analogues **5.32b-e** did show improved permeability over **5.6a**, albeit a modest improvement (permeability within the range  $10 < P_{app} \text{ (nm/sec)} < 100$  is considered moderate). Notably, analogues **5.32b** and **5.32c** possessed the most favourable profiles, demonstrating very good MICs, greater than a 6-fold improvement in permeability over **5.6a**, improved stability towards mouse liver microsomes relative to **5.6a**, and high aqueous solubility. Analogues **5.32b** and **5.32c** therefore represented improved candidates with which to further investigate *in vivo* efficacy of the pyrimidin-2(1*H*)-one series.

At this point it was interesting to consider other physicochemical properties that affect permeability, as the data in Table 5.4 indicated that lipophilicity was not a dominant influence on the permeability of analogues bearing the pyrimidin-2(1*H*)-one motif (**5.6a** and **5.32a-e**). Firstly, the most lipophilic analogues **5.32d** and **5.32e** (Chrom Log  $D_{7.4} = 5.0$  and  $5.1$ ) were at least 20-fold less permeable than the similarly lipophilic (2*H*)-pyrimidine **GSK'932** (Chrom Log  $D_{7.4} = 5.4$ ) and 2-amino pyrimidine **5.3a** (Chrom Log  $D_{7.4} = 5.1$ ; Table 5.3). Secondly, permeability did not track with lipophilicity across the analogues **5.32a-e**, and the maximum permeability achieved was 23 nm/sec for moderately lipophilic **5.32b**. Other properties purported to impact passive permeability are  $pK_a$  (ionisation), topological polar surface area (TPSA) and hydrogen bond donor and acceptor count.<sup>133</sup> Whilst ionisation hinders permeability through depletion of the uncharged form of the molecule (Sect. 2.5.1), TPSA and hydrogen bonding influence the energetic requirement for desolvation of the solute (a prerequisite to permeation). Improved passive permeability generally correlates with reduced TPSA and reduced hydrogen bonding capacity.<sup>133</sup> Table 5.5 compares  $pK_a$ , TPSA and hydrogen bond donor/acceptor counts for (2*H*)-pyrimidine **GSK'932**, 2-amino pyrimidine **5.3a**, pyrimidin-2(1*H*)-one **5.6a**, and pyrimidin-4(3*H*)-ones **5.6b** and **5.6c**.

**Table 5.5.** Permeability and physicochemical property data for compounds **GSK'932**, **5.3a**, **5.6a-c**<sup>a</sup>

Heterocycle	 <b>GSK'932</b>	 <b>5.3a</b>	 <b>5.6a</b>	 <b>5.6b</b>	 <b>5.6c</b>
$P_{app}$ (nm/sec)	485	360	< 3	67	88
Measured $pK_a$	5.2 <sup>b</sup>	6.4 <sup>b</sup>	5.2 <sup>b</sup> , 11.2 <sup>c</sup>	2.8 <sup>b</sup> , 10.4 <sup>c</sup>	3.0 <sup>b</sup> , 10.2 <sup>c</sup>
TPSA <sup>d</sup>	62	89	82	82	82
HBD count	0	2	1	1	1
HBA count	7	8	8	8	8

<sup>a</sup> Key: Green = good; orange = moderate; red = poor.  $P_{app}$ , apparent permeability (PAMPA); TPSA, topological polar surface area; HBD, hydrogen-bond donor; HBA, hydrogen bond acceptor. <sup>b</sup> basic  $pK_a$ . <sup>c</sup> acidic  $pK_a$ . <sup>d</sup> TPSA was calculated using the Daylight TPSA calculator.<sup>134</sup>

At the neutral pH (7.4) of the parallel artificial membrane permeation assay, pyrimidinone **5.6a** would exist predominantly as the uncharged form so it is unlikely that ionization impeded permeability. Pyrimidin-2(1H)-one **5.6a** also had an identical TPSA and the same number of hydrogen bond donors and acceptors to pyrimidin-4(3H)-ones **5.6b** and **5.6c**, which both exhibited much better permeability than **5.6a**. Furthermore, permeable **5.3a** had a higher TPSA than poorly permeable **5.6a**.

Whilst it was not possible to attribute the limited permeability of the pyrimidin-2(1H)-ones **5.6a** and **5.32a-e** to any one of the parameters in Table 5.5 alone, it appeared that when embedded within the **GSK'932** structure, the pyrimidin-2(1H)-one chemotype inherently led to reduced permeability relative to other closely related heteroaromatic isomers and congeners (it is important to note however, that poor permeability is not an inherent shortcoming of pyrimidin-2(1H)-ones in general). One plausible explanation may be that once solubilised, the specific arrangement of heteroatoms present in the pyrimidin-2(1H)-ones **5.6a** and **5.32a-e** creates an extensive water network that increases

the energetic barrier to desolvation, and therefore permeability. Irrespective of the permeability limits however, increasing lipophilicity of **5.6a** did provide multiple analogues that were significantly more permeable than **5.6a**, with a greater chance of favourable absorption, oral bioavailability and *in vivo* efficacy relative to **5.6a**.

## 5.9 Conclusions

Following up on the discrepancy between the potency data from the fluorescence and RapidFire™ assays, the HTS hit **GSK'295** was rapidly identified as a false positive. It was concluded that this was a whole-molecule effect, rather than a result of any particular motif within the HTS hit. Although the HTS hit was a false positive, incorporation of the 2-amino pyrimidine motif of **GSK'295** into the **GSK'932** scaffold led to the highly potent and validated DprE1 inhibitor **5.3a** (Fig.5.11). Furthermore, replacement with the congeneric pyrimidin-2(1*H*)-one motif afforded highly potent **5.6a**, which was in particularly favourable physicochemical property space. Consequently, **5.6a** had a much improved ADMET profile relative to **GSK'932**.

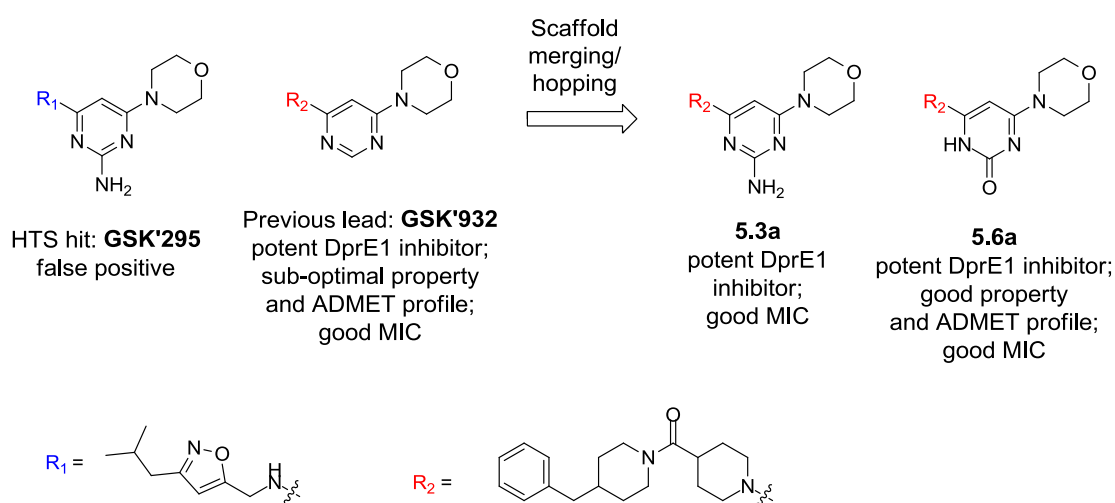


**Figure 5.11.** Merging the core scaffolds of **GSK'295** and **GSK'932** gave highly potent DprE1 inhibitor **5.3a**. The pyrimidin-2(1*H*)-one congener **5.6a** was also highly potent and existed in very good property space.

In spite of all the positive attributes of pyrimidinone **5.6a**, this analogue showed no evidence of *in vivo* efficacy when tested in an acute murine model for TB. One shortcoming of pyrimidin-2(1*H*)-one **5.6a** was its poor permeability, which was cited as a likely cause for low oral exposure and the lack of *in vivo* efficacy. It was likely that **5.6a** was too hydrophilic to be adequately permeable, so analogues of **5.6a** with increasingly lipophilic character

were designed and synthesised. This work led to the identification of two highly potent analogues, pyrimidin-2(1*H*)-ones **5.32b** and **5.32c**, that exhibited improved permeability over **5.6a** with a concurrent improvement in metabolic stability towards mouse liver microsomes (Fig. 5.12). In summary, the combination of these merits mean that analogues **5.32b** and **5.32c** represent improved lead-molecules with which to further investigate *in vivo* efficacy. This series now continues to be investigated in a DprE1 lead-optimisation programme elsewhere within GSK, and the *in vivo* evaluation of **5.32b** is scheduled.

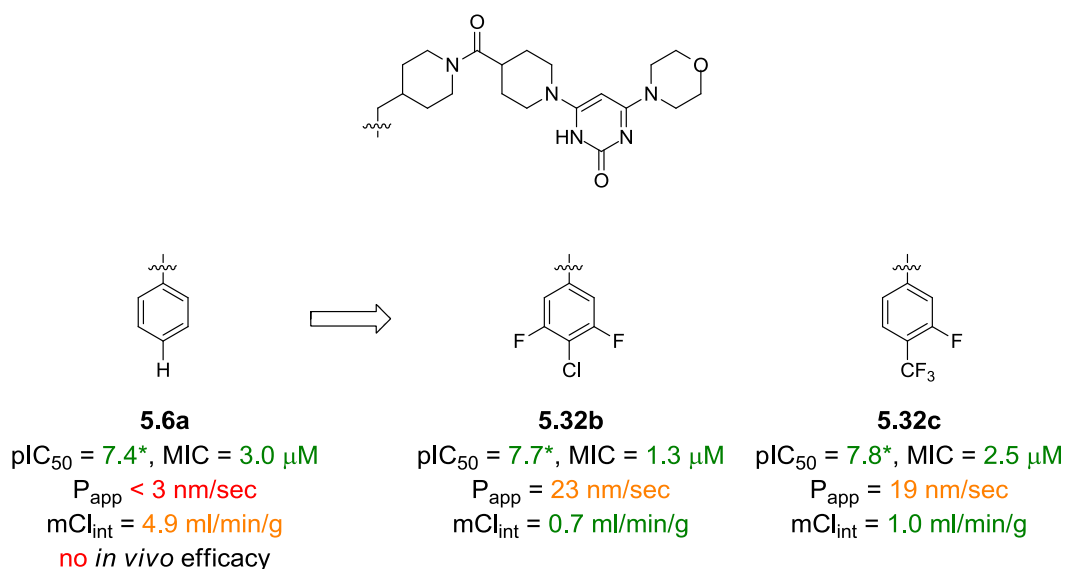


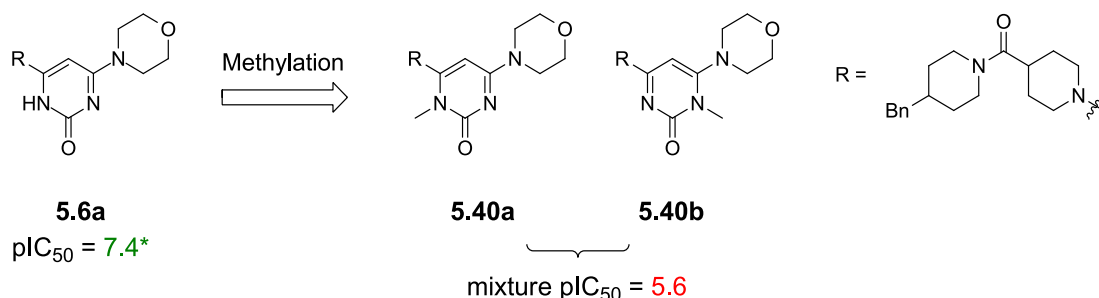
**Figure 5.12.** Optimisation of **5.6a** led to the identification of pyrimidin-2(1*H*)-one analogues **5.32b** and **5.32c** that were highly potent and had improved ADME profiles, notably improved permeability and improved intrinsic clearance against mouse liver microsomes. \* Denotes activity at or above the tight binding limit.

## 5.10 Future Work

The *in vivo* efficacy of analogues **5.32b** and **5.32c** will be tested in the acute murine model of TB. Both analogues have a greater chance of displaying improved *in vivo* efficacy relative to **5.6a** as these new compounds had a lower MIC, were more permeable and showed improved murine metabolic stability *in vitro*. In parallel, other strategies to improve the *in vitro* permeability of the pyrimidin-2(1*H*)-one series could be investigated.

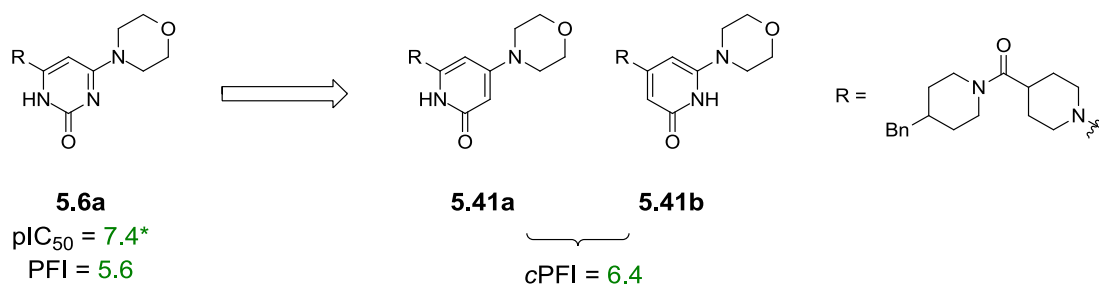
One such effort to improve permeability of the pyrimidin-2(1*H*)-one **5.6a** has since been explored. Methylation of the pyrimidinone core was pursued as a strategy to reduce the polarity of the molecule with the simultaneous removal of a hydrogen bond donor (Fig. 5.13; performed elsewhere within GSK). Unfortunately, the methylated analogues were

only accessible as a mixture of geometric isomers **5.40a** and **5.40b**. This mixture had a  $pIC_{50}$  of 5.6 however, demonstrating that pyrimidinone methylation reduced activity at DprE1 and therefore was not a suitable strategy to improve permeability (the permeability of this mixture was not determined).



**Figure 5.13.** Methylation of the pyrimidin-2(1H)-one core of **5.6a** was not a suitable strategy for improving permeability as it led to a large reduction in DprE1 activity. \* Denotes activity at or above the tight binding limit.

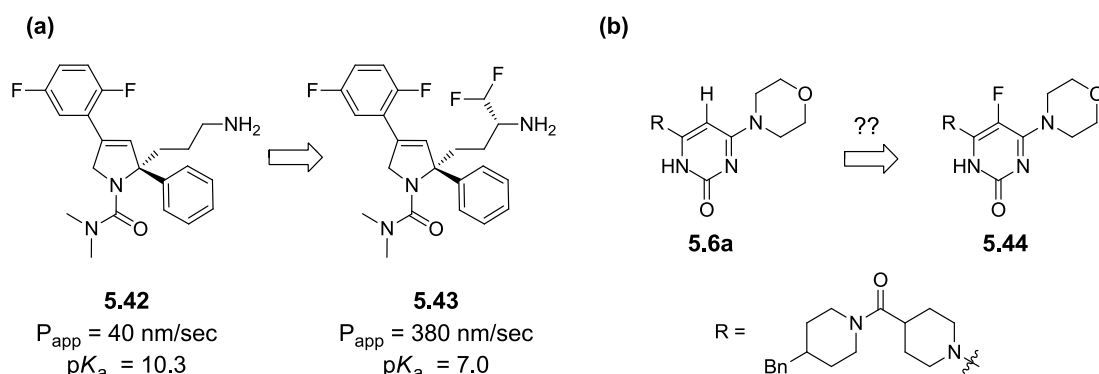
Another strategy to investigate is the replacement of the pyrimidin-2(1H)-one core of **5.6a** with a pyridone motif (Fig. 5.14), as removal of a heteroatom is likely to improve passive permeability.<sup>133</sup> Pyridones **5.41a** and **5.41b** are predicted to remain in better property space than **GSK'932** (calculated PFI = 6.4), so are likely to retain favourable ADMET profiles in addition to improved permeability.<sup>65</sup>



**Figure 5.14.** Pyridones **5.41a-b** have fewer heteroatoms than pyrimidinone **5.6a**. Replacement of the pyrimidin-2(1H)-one core with a pyridone congener may therefore improve permeability. cPFI = calculated PFI. \* Denotes activity at or above the tight binding limit.

Finally, it may be possible to enhance the permeability of the pyrimidin-2(1H)-ones through attenuation of the pyrimidinone hydrogen bonding basicity and/or acidity. These properties influence the strength of the interactions between the solvate and the aqueous solvent, which in turn influences permeability.<sup>133</sup> Cox *et al.*<sup>135</sup> demonstrated that the  $\alpha$ -difluoromethylation of amine **5.42** led to a 9-fold increase in passive permeability for the less basic amine **5.43** (Fig. 5.15a). Similarly, fluorination of **5.6a** would likely reduce the

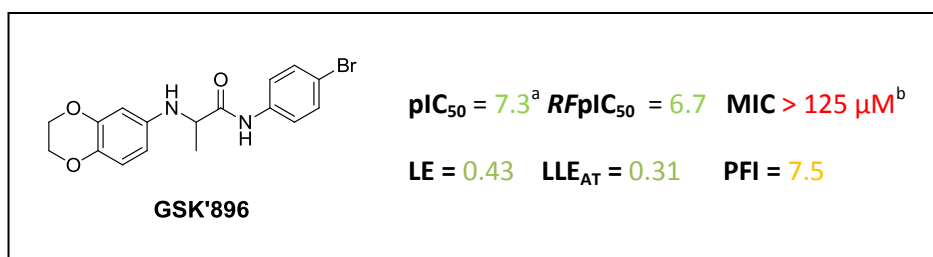
hydrogen bonding basicity of the pyrimidinone **5.44** (Fig. 5.15b), which may improve permeability (provided the increase in hydrogen bonding acidity of the *N*-H was not prevailing).



**Figure 5.15.** (a) Cox *et al.* greatly enhanced the passive permeability of compound **5.42** through modulation of the amine hydrogen bonding basicity.<sup>135</sup> Less basic  $\alpha$ -difluoromethylated **5.43** was much more permeable than **5.42**. (b) Fluorination of pyrimidin-2(1*H*)-one **5.6a** may provide a more permeable analogue **5.44** through attenuation of hydrogen bonding basicity of the pyrimidinone.

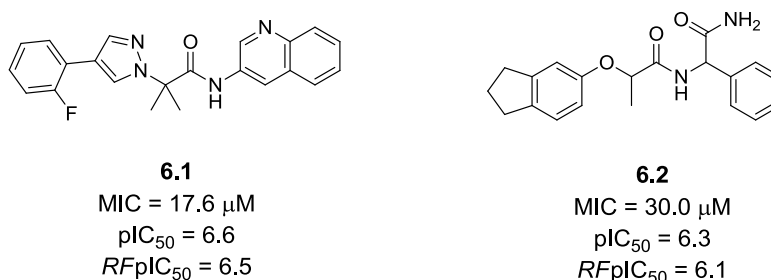
## 6. Hit-to-Lead Work Around GSK'896

### 6.1 Overview of GSK'896



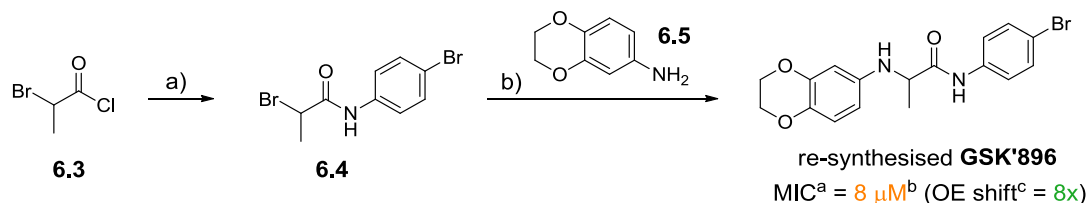
**Figure 6.1.** The potency and physicochemical property profile for **GSK'896** after the DprE1 high-throughput screen. <sup>a</sup>After re-testing the mean  $pIC_{50}$  value fell to 7.2. <sup>b</sup>**GSK'896** was later shown to have an MIC of 8  $\mu M$  (*vide infra*).

Figure 6.1 highlights the potency and physicochemical property profile for **GSK'896**. This HTS hit was attractive as it showed reproducible, potent activity against DprE1 in both the fluorescence and RapidFire™ assays, and was highly ligand efficient ( $LE \gg 0.3$ ). Furthermore, analysis of the 3986 HTS active compounds revealed that the benzodioxane substructure of **GSK'896** was a frequently occurring motif: 69 hits with  $pIC_{50} > 4.0$  contained this functionality. In spite of these positive attributes, concern arose after no antimycobacterial activity was apparent when **GSK'896** was tested from a stock solution ( $MIC > 125 \mu M$ ). However, multiple structurally related compounds identified in a GSK tuberculosis whole-cell screening assay did possess an MIC, and showed activity against DprE1 in both the fluorescence and RapidFire™ assays (Fig. 6.2). The re-synthesis and re-testing of a new sample of the HTS hit **GSK'896** was therefore prioritised.



**Figure 6.2.** Compounds **6.1** and **6.2** were identified in a GSK TB whole-cell screening assay, and were later shown to be active against DprE1 in both the fluorescence and RapidFire™ assays.  $RFpIC_{50} = \text{RapidFire}^{\text{TM}} pIC_{50}$ .

The re-synthesis of **GSK'896** was performed as follows (Scheme 6.1): condensation of 2-bromopropanoyl chloride **6.3** with *p*-bromoaniline afforded amide **6.4** in 97% yield. Subsequent nucleophilic displacement of the bromide **6.4** by 2,3-dihydrobenzo[*b*][1,4]dioxin-6-amine **6.5** afforded **GSK'896** in 63% yield.



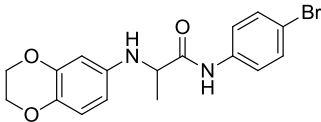
**Scheme 6.1.** a) *p*-bromoaniline, NaHCO<sub>3</sub>, DCM, 0 °C → RT, 97% b) NEt<sub>3</sub>, DMF, 80 °C,  $\mu$ wave, 63%. <sup>a</sup> MIC value against *M.tb* H37Rv. <sup>b</sup> Compound tested inactive (MIC > 125 µM) in 1 out of 5 test occasions. <sup>c</sup> Fold-difference in MIC between the H37Rv MIC and the MIC recorded against the DprE1 over-expressor (OE) strain.

Gratifyingly, the re-made sample maintained activity in the enzymatic assays, and now **GSK'896** did show a highly encouraging MIC of 8 µM. Additionally, cellular engagement at DprE1 was confirmed when the re-synthesised hit was tested against an *M.tb* strain over-expressing DprE1: an 8-fold increase in MIC was observed. Together, these results encouraged a programme of hit-to-lead investigations around **GSK'896**.

### 6.1.1 Medicinal Chemistry Profiling of GSK'896

Whilst **GSK'896** was highly potent against DprE1, this HTS hit lay outside of the programme targeted property space (Sect. 4.3). **GSK'896** was characterised by a high PFI of 7.5, and excessive lipophilicity for a molecule of relatively low heavy atom count (23 heavy atoms). Table 6.1 displays the physicochemical profile and some ADMET parameters for **GSK'896**. hERG activity, solubility and permeability of the HTS hit **GSK'896** were favourable, but the *in vitro* metabolic stability of **GSK'896** was poor.

**Table 6.1.** Physicochemical and ADMET profile for the HTS hit **GSK'896**.<sup>a</sup>



**GSK'896**

PFI	7.5
Chrom Log D <sub>7.4</sub>	5.5
CLND solubility (μM)	214
hERG pIC <sub>50</sub>	<4.3
hCl <sub>int</sub> (ml/min/g)	13.2
mCl <sub>int</sub> (ml/min/g)	23.5
P <sub>app</sub> (nm/sec)	580

<sup>a</sup> Key: Green = good; orange = moderate; red = poor. PFI = Chrom Log D<sub>7.4</sub> + #Ar; CLND, chemi-luminescent nitrogen detection method for solubility measurement; Cl<sub>int</sub>, intrinsic clearance (liver microsomes); h, human; m, mouse; P<sub>app</sub>, apparent permeability (PAMPA).

Three structural features within **GSK'896** were raised as potential toxicity risks: the two anilines and the aminobenzodioxane motif. Whilst anilines are treated with caution as many are mutagenic,<sup>136</sup> oxidative bioactivation of the aminobenzodioxane motif could potentially afford the corresponding reactive catechol **6.6**, *o*-benzoquinone **6.7** or quinone-immine **6.8** (Fig. 6.3), posing further risk of unwanted biological activity (e.g. through time-dependant P450 inhibition or redox cycling).<sup>137-140</sup> NAPQI for example, is a highly toxic quinone imine by-product resulting from the metabolism of paracetamol<sup>141</sup> (Fig.6.3b).

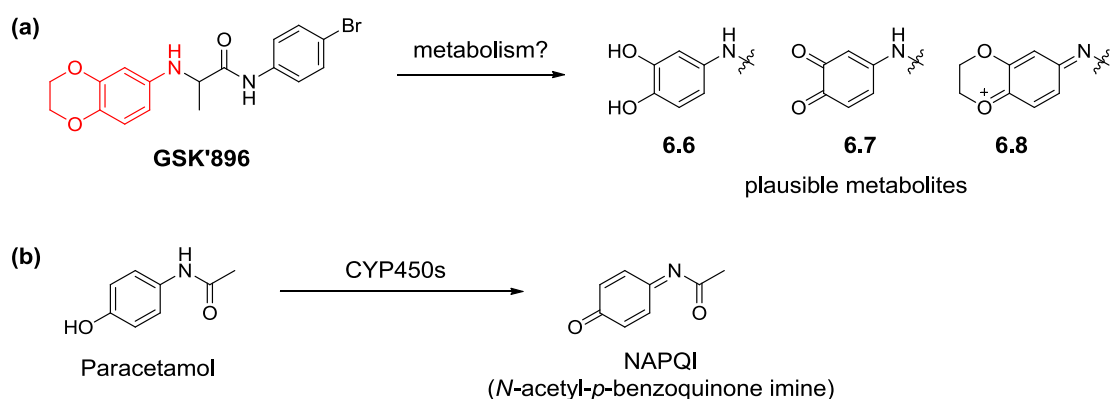


**Figure 6.3.** (a) Oxidative bioactivation of **GSK'896** may produce reactive metabolites such as a catechol **6.6**, *o*-benzoquinone **6.7** or quinone-immine **6.8**. (b) NAPQI is a toxic quinone imine metabolite of paracetamol.

## 6.2 Project Aims

The aim of this work was to establish a novel lead series of DprE1 inhibitors based on the HTS hit **GSK'896**, identifying exemplar compounds that were potent in the enzymatic assays, had a potent MIC, and were in good physicochemical property space, such that the programme targeted activity-property profile was satisfied ( $pIC_{50} > 7$ ,  $PFI < 7$ ). To achieve this, an extensive SAR analysis around **GSK'896** was planned and executed, with a key focus on identifying:

- i) structural modifications that improved enzymatic potency and/or MIC;
- ii) modifications that engendered improved physicochemical properties relative to **GSK'896** (that would likely promote an improved ADMET profile), whilst maintaining or improving potency;
- iii) structural replacements for the aniline and aminobenzodioxane motifs.

## 6.3 SAR Insights from Analysis of the HTS Data and Sub-Structure Searching of the GSK Compound Collection

The SAR investigation began with the analysis of the HTS data (Sect. 6.3.1) followed by the screening of related compounds available in the GSK compound collection (Sect. 6.3.2). Following these exercises, new analogues were designed to specifically address the project aims (Sect. 6.4).

### 6.3.1 SAR Data Evident in the DprE1 HTS Output

An analysis of the 3986 HTS hits revealed some early SAR information (Fig. 6.4).

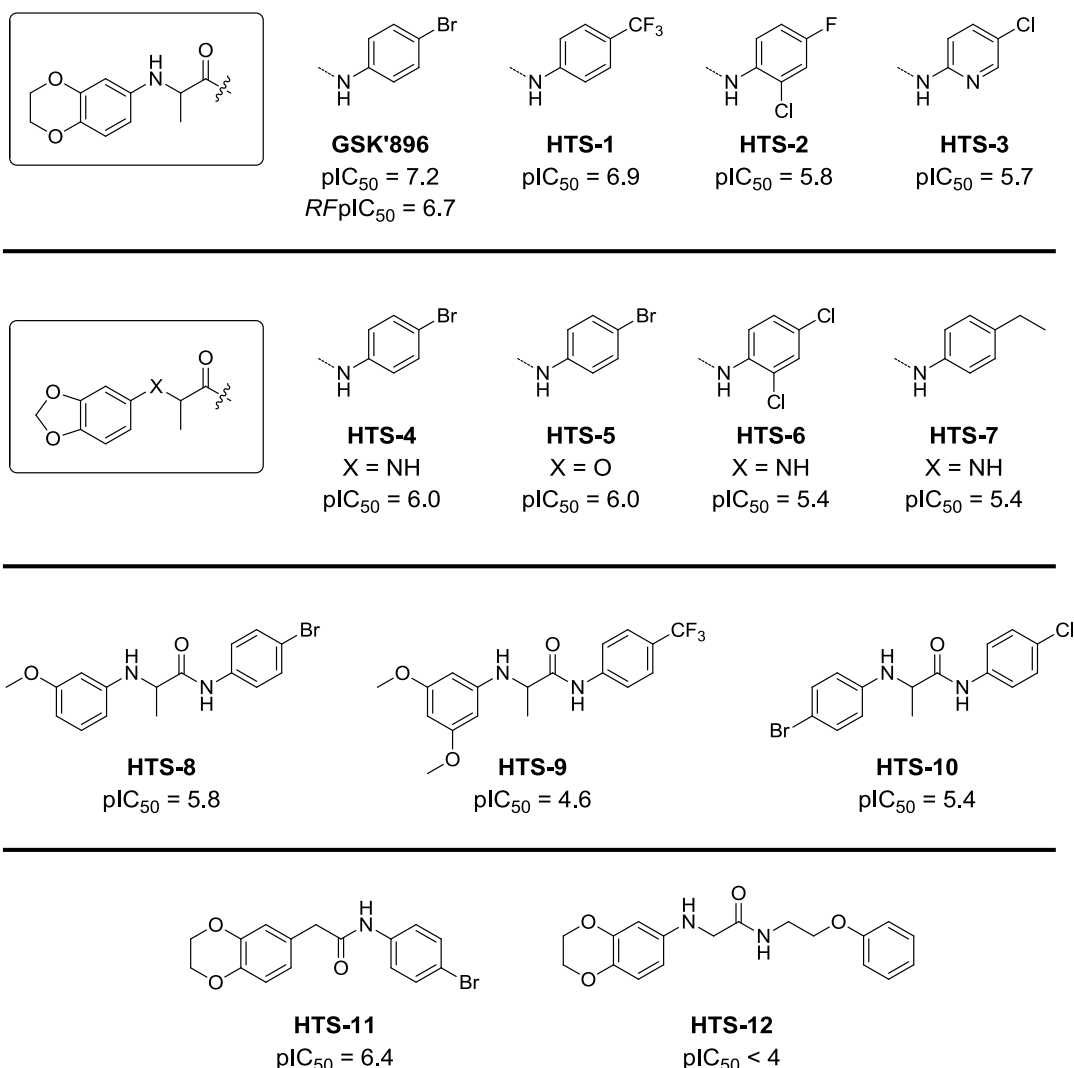


**Figure 6.4.** A selection of representative compounds from the 3986 HTS hits, illustrating some of the general SAR trends.

The main trends evident in this data were summarised as follows:

- A small decrease in potency was observed on replacing the *p*-bromoaniline of **GSK'896** for the *p*-trifluoromethyl derivative of **HTS-1**;
- A substantial loss in potency was observed when the benzodioxane motif was replaced with the smaller benzo[*d*][1,3]dioxole structure (**GSK'896** vs. **HTS-4**);
- The *O*-linked benzodioxole **HTS-5** was equipotent with the *N*-linked equivalent **HTS-4**;

- Replacement of the benzodioxane motif of **GSK'896** with other methoxy-substituted or halogenated aromatics led to a reduction in potency (e.g. **HTS-8**, **HTS-9**, **HTS-10**);
- Molecules with shorter (e.g. **HTS-11**) and longer (e.g. **HTS-12**) linkers were less active than alanine-linked **GSK'896**.

An important observation here was the comparison between the *N*-linked and *O*-linked benzodioxoles **HTS-4** and **HTS-5**. The data indicated that exchange of this aniline for an aromatic ether was tolerated, revealing a possible strategy for replacement of the corresponding aniline in **GSK'896**.

### 6.3.2 Screening of Compounds Available in the GSK Collection

In order to generate additional SAR data prior to the synthesis of new compounds, a sub-structure search (SSS) of the GSK compound collection was conducted. Figure 6.5 illustrates the search criteria used. In all searches the benzodioxane motif was kept constant, based on the observation that this moiety was a frequently occurring motif in the HTS. A set of 40 molecules was constructed and submitted for potency profiling against DprE1. Figure 6.6 depicts representative compounds.

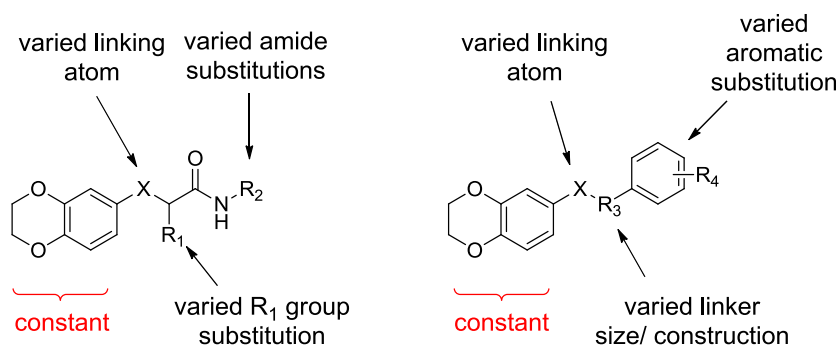


**Figure 6.5.** Sub-structure search criteria. The benzodioxane motif was kept constant in all the searches performed.

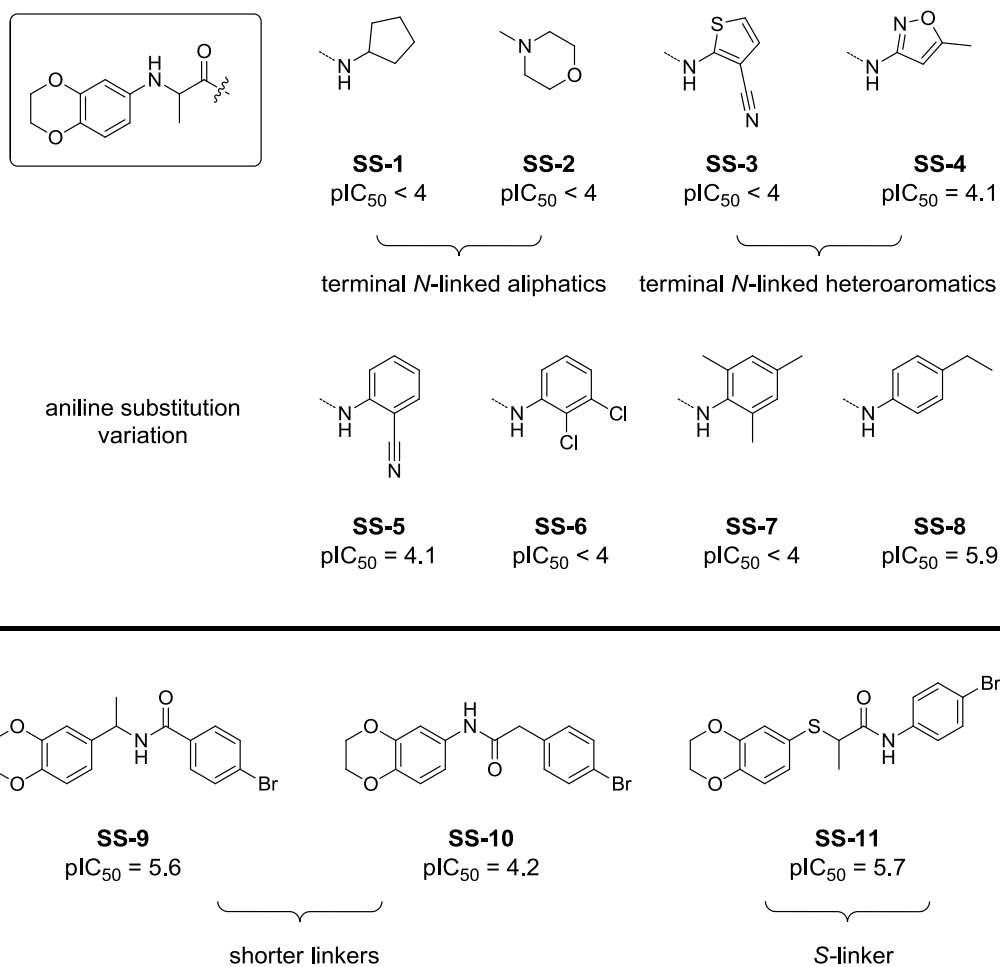


**Figure 6.6.** A selection of representative compounds from the sub-structure searching exercise.

The main SAR trends evident from the sub-structure search were as follows:

- A significant reduction in potency was observed when the *p*-bromoaniline of **GSK'896** was replaced with either small *N*-linked aliphatic moieties (e.g. **SS-1**, **SS-2**) or small *N*-linked heteroaromatics (e.g. **SS-3**, **SS-4**);
- *Para* substitution of this aniline increased potency (**GSK'896**, **SS-8**), whereas *ortho* and *meta* substitution did not appear beneficial (**SS-5**, **SS-6**, **SS-7**);
- Shortening the length of the linker (e.g. **SS-9**, **SS-10**) was not favourable;
- A significant reduction in potency was observed when the aminobenzodioxane motif of **GSK'896** was replaced with the sulphur equivalent (**SS-11**).

## 6.4 Design, Synthesis and SAR of New Analogues of GSK'896

Whilst mining of the HTS data and the sub-structure searching of the GSK compound collection did provide some insight into the structure-activity relationships around **GSK'896**, clear gaps in these data were apparent. As such, new compounds were designed to further explore the SAR, and to specifically address the project aims. In the absence of a crystal structure of DprE1 liganded with **GSK'896** or related compounds, SAR was delineated *via* systematic single-point changes to **GSK'896**. Figure 6.7 outlines the considerations for new compound design.

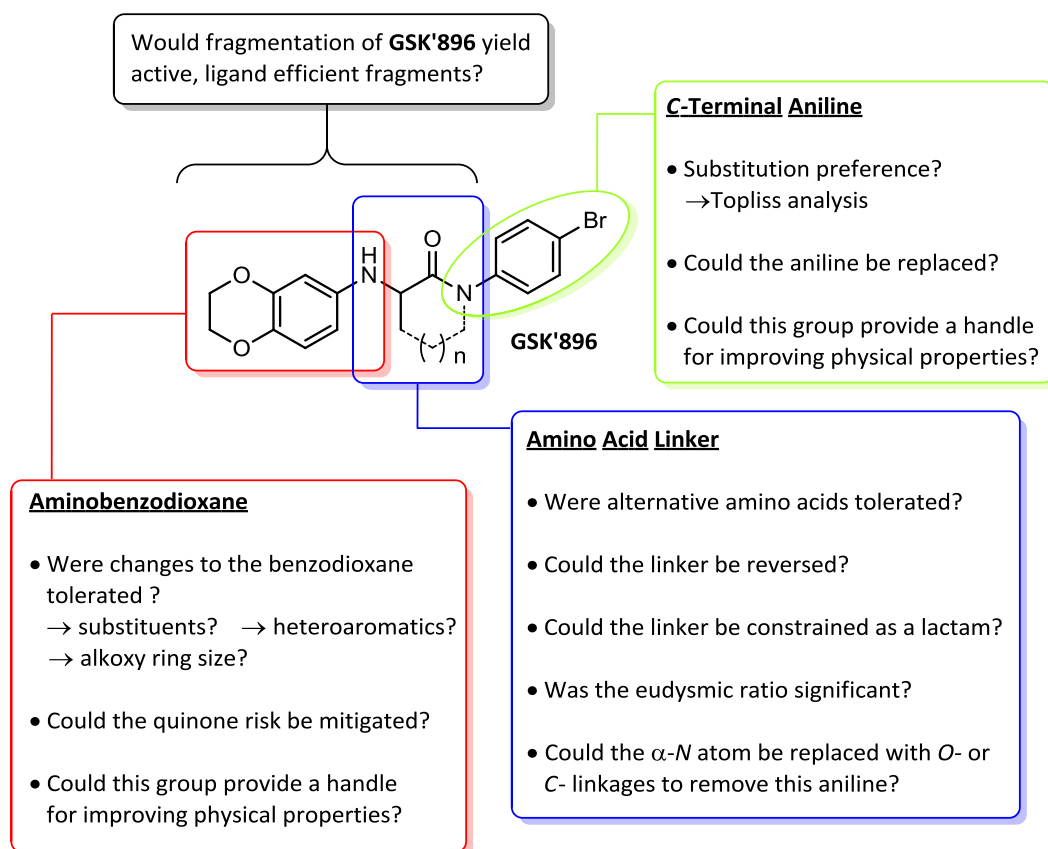
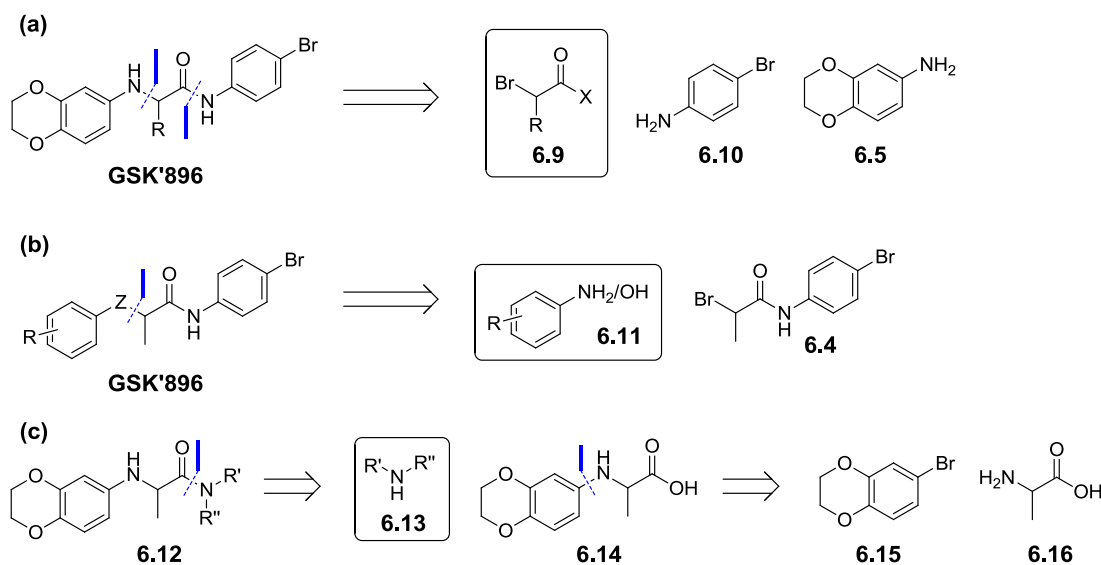


Figure 6.7. Design considerations for new analogues of **GSK'896** to investigate the SAR of the series.

### 6.4.1 Generalised Retrosynthetic Disconnections of **GSK'896** and Related Analogues

To achieve the synthesis of analogues of **GSK'896**, the following disconnections were envisioned to facilitate variation of a) the amino acid linker, b) the aminobenzodioxane motif, and c) the C-terminal aniline (Scheme 6.2).

- a) Disconnection at both the aminobenzodioxane and the amide bond would facilitate sequential addition of *p*-bromoaniline **6.10** and aminobenzodioxane **6.5** onto  $\alpha$ -bromo acid **6.9** (X = Br, Cl or OH), with varying substitution;
- b) Disconnection at the amino acid alpha position would facilitate the alkylation of varied anilines or phenols **6.11** with  $\alpha$ -bromo amide **6.4**.
- c) Amide bond disconnection of **6.12** would allow condensation of varied amines **6.13** with acid **6.14**. Disconnection of this acid **6.14** utilising a metal-mediated amination afforded bromobenzodioxane **6.15** and DL-alanine **6.16**.

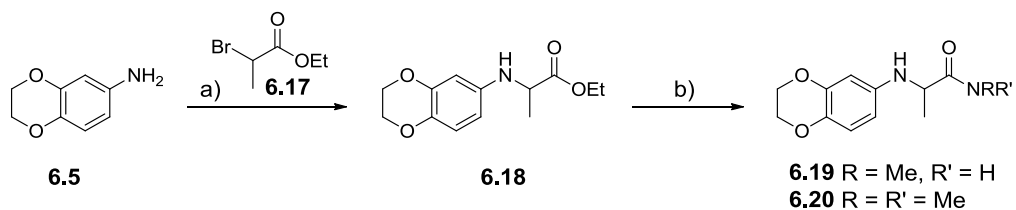


**Scheme 6.2.** Retrosynthetic analyses for the analogues of **GSK'896** with varied a) amino acid linker b) aminobenzodioxane motif, and c) C-terminal aniline. The varied component is outlined in each scheme.

### 6.4.2 Fragmentation of the HTS Hit **GSK'896**

In the absence of X-ray crystallography, it was postulated that the screening of pertinent fragments of **GSK'896** could indicate the relative contributions to binding to DprE1. If a fragment were to remain highly ligand efficient, this would indicate that **GSK'896** was binding efficiently through that scaffold. To this end, *N*-methyl and *N,N'*-dimethyl amides **6.19** and **6.20** were synthesised. It transpired that the carboxylic acid **6.14** proposed in the retrosynthetic disconnection (Scheme 6.2, disconnection route c) was unstable to isolation (*vide infra*; Sect. 6.4.3.1), so an alternative route to the amides **6.19** and **6.20** was pursued (Scheme 6.3). Ethyl 2-bromopropanoate **6.17** was condensed with aminobenzodioxane **6.5** to yield intermediate ester **6.18**. Aluminium mediated aminolysis of this ester **6.18** using

the DABCO adduct of trimethylaluminium<sup>142</sup> (DABAL-Me<sub>3</sub>) afforded amides **6.19** and **6.20**. The data for these compounds are presented in Table 6.2.



**Scheme 6.3.** a) K<sub>2</sub>CO<sub>3</sub>, MeCN, reflux, 73%. b) methylamine or dimethylamine, DABAL-Me<sub>3</sub>, THF, 50 °C, then **6.18**, 90 °C. **6.19** = 62%, **6.20** = 46%.

**Table 6.2** Potency, ligand efficiency and physicochemical data for fragments **6.19** and **6.20**.

No.	R	pIC <sub>50</sub> <sup>a</sup>	LE, LLE <sub>AT</sub>	PFI	MIC (μM)
<b>GSK'896</b>		7.2	0.43, 0.31	7.5	8.0 <sup>b</sup>
<b>6.19</b>		4.5	0.36, 0.40	2.6	>125
<b>6.20</b>		4.4	0.34, 0.34	3.2	>125

<sup>a</sup> pIC<sub>50</sub> measured in the DprE1 fluorescence assay. <sup>b</sup> Compound tested inactive (MIC > 125 μM) in 1 out of 5 test occasions.

Replacement of the C-terminal aniline with small aliphatic groups in **6.19** and **6.20** led to a large reduction in activity, consistent with the observations made during the sub-structure search of the GSK compound collection (Sect. 6.3.2). Both **6.19** and **6.20** were active however, and both were highly ligand efficient, indicating that the aminobenzodioxane propanamide component of **GSK'896** was likely an important contributor to the binding affinity of this HTS hit. This result was corroborated by the fact that the benzodioxane functionality was a frequently occurring motif in the HTS screen. These data also revealed that the amide N-H probably did not participate as a hydrogen bond donor as *N,N'*-dimethyl **6.20** was equipotent with the secondary carboxamide **6.19**.

### 6.4.3 Variation of the Amino Acid Linker of GSK'896

**GSK'896** was racemic so chiral synthesis was an early target to understand which stereoisomer was the more active. A variety of analogues linked by alternative amino acids were also targeted to identify how much space for growth was available in this position. These included the glycine-,  $\alpha$ -methylalanine-,  $\alpha$ -ethylglycine-, valine- and reverse alanine-linked derivatives **6.21-6.25**. Further to this, analogues were synthesised in which the aminobenzodioxane *N*-H was replaced with an *N*-methylated linkage (**6.26**), a methylene linkage (**6.27**), or an *O*-linkage (**6.28**), the latter two targeted to investigate replacement of this aniline moiety. Finally,  $\gamma$ -lactam **6.29** and  $\delta$ -lactam **6.30** allowed the investigation of the effect of conformational restraint on the activity in this series. Whilst modification of the linker unit provided little opportunity to modulate physicochemical properties, the suggested analogues **6.21-6.30** were deemed important for understanding SAR.

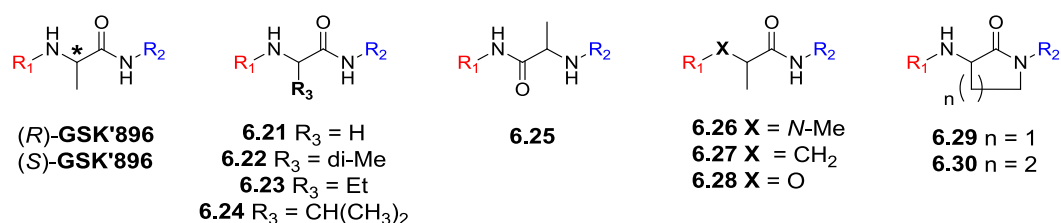
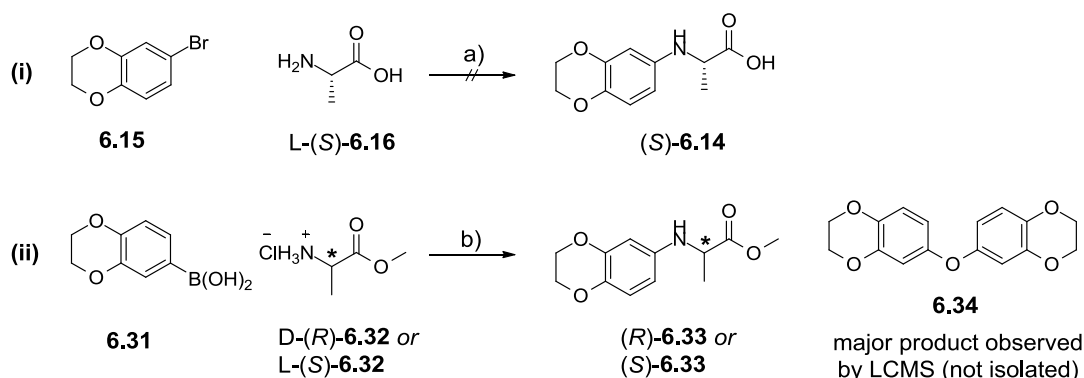


**Figure 6.8.** Analogues of **GSK'896** designed to incorporate alternative linker functionalities.  $R_1$  = benzodioxane.  $R_2$  = *p*-bromoaniline.

#### 6.4.3.1 Synthesis of GSK'896 Analogues with Varied Linkers

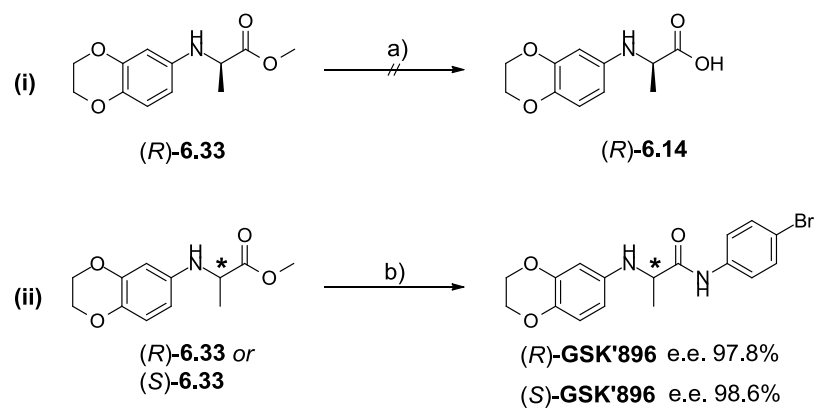
Chemistry initiated with the chiral syntheses of (*R*)-**GSK'896** and (*S*)-**GSK'896**. Following the general disconnection *c* (Scheme 6.2), a substrate-accelerated copper-catalysed Ullman coupling reaction<sup>143,144</sup> between L-alanine (*S*)-**6.16** and aryl halide **6.15** was first investigated (Scheme 6.4i). Conventional heating at 90 °C for 48 hours<sup>143</sup> afforded no product by LCMS analysis. Heating to 140 °C under microwave irradiation<sup>144</sup> led to appreciable conversion to the desired acid (*S*)-**6.14** observed by LCMS, but the compound decomposed upon attempted isolation. This observation was consistent with reports that the Ullman coupling products of an amino acid and aryl halide with *para*-electron donating groups (e.g. OMe,  $\text{NH}_2$ ) have been unstable to isolation.<sup>143,145</sup> In order to investigate the stability of the desired carboxylic acid **6.14**, synthesis of the corresponding ester **6.33** was performed to facilitate preparation of the acid **6.14** *via* simple ester hydrolysis. A copper-mediated Chan-Lam

coupling<sup>146</sup> between boronic acid **6.31** and D-alanine methylester (*R*)-**6.32** was successful, affording the desired ester (*R*)-**6.33** in 15% yield (Scheme 6.4ii). An analogous reaction with L-alanine methylester (*S*)-**6.32** afforded (*S*)-**6.33** in 14% yield. The low yields were consistent with Lam's findings<sup>146</sup> that amino acid esters with small R-groups (e.g. alanine) gave much poorer yields relative to those with larger substituents. Lam reasoned that the low solubility of amino acid esters with small R-groups led to an increase in the competing conversion of the boronic acid to the corresponding phenol, accompanied by subsequent *O*-arylation. Indeed, ether-linked **6.34** was observed by LCMS to be the major product, despite the use of molecular sieves.



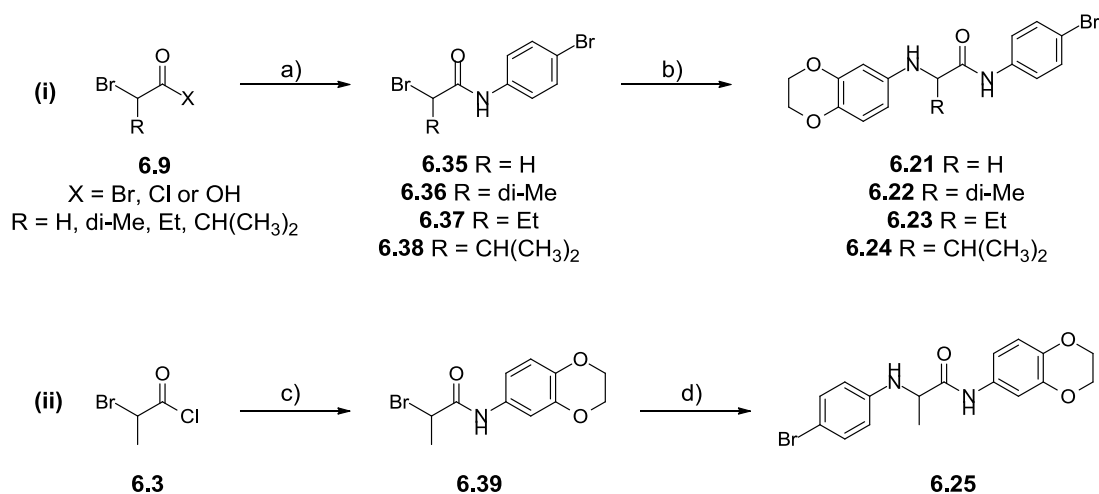
**Scheme 6.4.** a) CuI (10 mol%), K<sub>2</sub>CO<sub>3</sub>, DMF, 140 °C  $\mu$ wave, product (*S*)-**6.14** decomposed on attempted isolation.  
b) Cu(OAc)<sub>2</sub> (1.1 eq), NEt<sub>3</sub>, 4Å MS, DCM, RT, (*R*)-**6.33** = 15%, (*S*)-**6.33** = 14%.

Hydrolysis of ester (*R*)-**6.33** cleanly led to acid (*R*)-**6.14** (100% conversion by LCMS), but attempted isolation under acidic conditions again resulted in complete degradation of the product (*R*)-**6.14** (Scheme 6.5i). In order to avoid the unstable carboxylic acid intermediates **6.14**, aluminium-mediated aminolysis of the stable esters **6.33** was investigated (Scheme 6.5ii). This approach proved successful: treatment of either (*R*)-**6.33** or (*S*)-**6.33** with trimethylaluminum and *p*-bromoaniline furnished the respective amides (*R*)-**GSK'896** and (*S*)-**GSK'896** in high yields. Chiral HPLC confirmed high maintenance of enantiomeric excess (>97%) over the two synthetic steps from the D- or L-alanine methyl esters **6.32**.



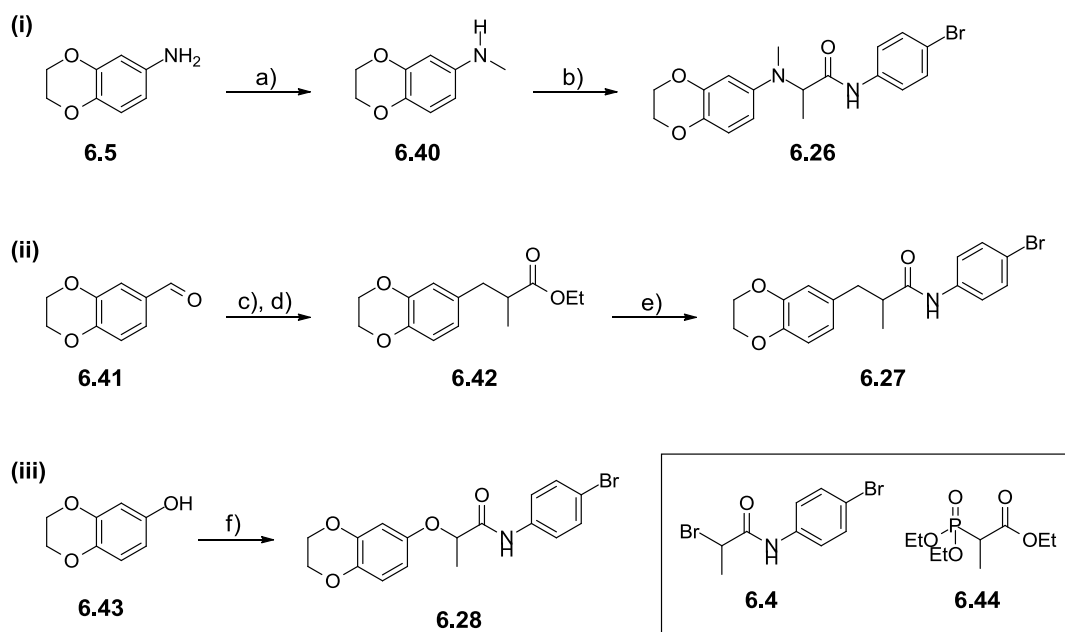
**Scheme 6.5.** a) LiOH, THF, H<sub>2</sub>O, product (R)-6.14 decomposed upon attempted isolation. b) AlMe<sub>3</sub>, *p*-bromoaniline, DCM, then (R)-6.33 or (S)-6.33, (R)-GSK'896 = 75%, (S)-GSK'896 = 73%.

Syntheses of compounds **6.21-6.24** were prosecuted according to disconnection *a* (Scheme 6.2), first by condensation of *p*-bromoaniline with the appropriate  $\alpha$ -bromo acid **6.9**, affording the  $\alpha$ -bromo amides **6.35-6.38** (Scheme 6.6i). Alkylation of 2,3-dihydrobenzo[*b*][1,4]dioxin-6-amine **6.5** with bromides **6.35-6.38** subsequently furnished final compounds **6.21-6.24**. Reverse-linked **6.25** was synthesised in the same manner, but the order of reaction with each aniline was switched (Scheme 6.6ii).



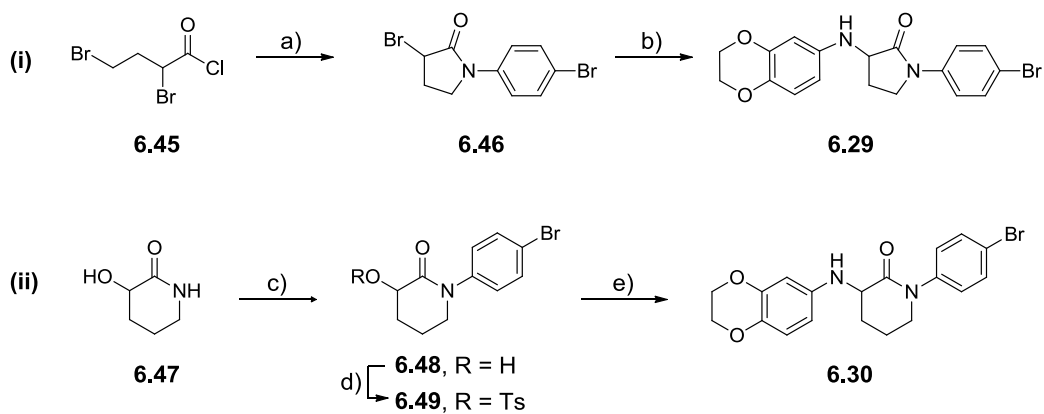
**Scheme 6.6.** a) acid bromide or acid chloride, *p*-bromoaniline, NaHCO<sub>3</sub>, DCM, 0 °C → RT, 72 – 100% yield, OR for **6.38**, 2-bromo-3-methylbutanoic acid, *p*-bromoaniline, DMAP (10 mol%), DIC, DCM, 76%. b) 2,3-dihydrobenzo[*b*][1,4]dioxin-6-amine **6.5**, K<sub>2</sub>CO<sub>3</sub>, MeCN, 90 °C, 58-62% yield; for **6.22**: 2,3-dihydrobenzo[*b*][1,4]dioxin-6-amine **6.5**, NaH, THF, then **6.36**, 57%. c) 2,3-dihydrobenzo[*b*][1,4]dioxin-6-amine **6.5**, NaHCO<sub>3</sub>, DCM, 0 °C → RT, 100%. d) *p*-bromoaniline, K<sub>2</sub>CO<sub>3</sub>, MeCN, 90 °C, 32%.

Synthesis of the *N*-methylated **6.26** began with the generation of *N*-methyl aminobenzodioxane **6.40** *via* a reductive amination reaction between aniline **6.5** and paraformaldehyde. Reaction of **6.40** with  $\alpha$ -halo amide **6.4** furnished final compound **6.26** (Scheme 6.7i). Carbon-linked **6.27** was synthesised from commercial aldehyde **6.41** *via* a Horner-Wadsworth-Emmons reaction with phosphonate **6.44**, hydrogenation of the resulting alkene, and an aluminium-mediated aminolysis<sup>142</sup> of the ester **6.42** (Scheme 6.7ii). Ether-linked **6.28** was prepared *via* an  $S_N2$  displacement of bromide **6.4** by commercial phenol **6.43** (Scheme 6.7iii).



**Scheme 6.7.** a)  $(\text{CH}_2\text{O})_n$ , NaOH, MeOH, RT, then  $\text{NaBH}_4$ , 40 °C, 93%. b) **6.4**,  $\text{K}_2\text{CO}_3$ , MeCN, 90 °C, 49%. c) **6.44**, NaH, THF, 0 °C, then **6.41**, 0 °C  $\rightarrow$  RT, 100%. d) Pd/C,  $\text{H}_2$ , EtOH, 100%. e) *p*-bromoaniline, DABAL-Me<sub>3</sub>, THF, 50 °C, then **6.42**, 90 °C, 83%. f)  $\text{K}_2\text{CO}_3$ , MeCN, 90 °C, 66%.

Preparation of  $\gamma$ -lactam **6.29** initiated with the alkylation of *p*-bromoaniline with 2,4-dibromobutyryl chloride **6.45** in the presence of sodium phosphate, which gave the intermediate  $\alpha,\gamma$ -dibromo amide (not isolated; Scheme 6.8i). Subsequent addition of the stronger base potassium carbonate promoted a 5-*exo*-tet cyclization, affording pyrrolidinone **6.46** in good yield. Condensation with 2,3-dihydrobenzo[*b*][1,4]dioxin-6-amine **6.5** furnished the target derivative **6.29**.  $\delta$ -lactam analogue **6.30** was prepared in three steps *via* a Buchwald amination between hydroxypiperidinone **6.47** and 1-bromo-4-iodobenzene, followed by tosylation of the alcohol and subsequent  $S_N2$  displacement with aniline **6.5** (Scheme 6.8ii).

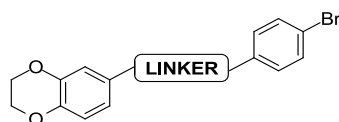


**Scheme 6.8.** a) *p*-bromoaniline, Na<sub>3</sub>PO<sub>4</sub>, MeCN, 0 °C → RT, then K<sub>2</sub>CO<sub>3</sub>, 68%. b) 2,3-dihydrobenzo[*b*][1,4]dioxin-6-amine **6.5**, K<sub>2</sub>CO<sub>3</sub>, MeCN, 90 °C, 67%. c) 1-bromo-4-iodobenzene, Cs<sub>2</sub>CO<sub>3</sub>, XantPhos (15 mol%), Pd(OAc)<sub>2</sub> (6 mol%), 1,4-dioxane, 100 °C,  $\mu$ wave, 40%. d) TsCl, DABCO, DCM, 0 °C → RT, 73%. e) 3-dihydrobenzo[*b*][1,4]dioxin-6-amine **6.5**, K<sub>2</sub>CO<sub>3</sub>, MeCN, 90 °C, 62%.

#### 6.4.3.2 Biological and Physicochemical Evaluation of (*R*)-GSK'896, (*S*)-GSK'896 and 6.21-6.30

Table 6.3 displays potency, ligand efficiency and physicochemical property data for (*R*)-GSK'896, (*S*)-GSK'896 and 6.21-6.30.

**Table 6.3.** Potency and physicochemical data for compounds (*R*)-GSK'896, (*S*)-GSK'896 and 6.21-6.30.



No.	Linker	pIC <sub>50</sub> <sup>a</sup> [RFpIC <sub>50</sub> ] <sup>b</sup>	LE, LLE <sub>AT</sub> <sup>c</sup>	PFI	MIC (μM)
GSK'896		7.2 [6.7]	0.43, 0.31	7.5	8.0 <sup>d</sup>
( <i>R</i> )-GSK'896		6.6 [6.6]	0.39, 0.27	7.5	6.5
( <i>S</i> )-GSK'896		6.0	0.36, 0.24	7.5	12.8
6.21		6.7	0.42, 0.30	7.1	15.8
6.22		6.9	0.39, 0.26	8.3	4.0
6.23		5.4	0.31, 0.17	8.0	62.0
6.24		4.4	0.24, 0.09	8.6	>125
6.25		4.2 <sup>e</sup>	0.24, 0.12	7.3	125
6.26		7.2	0.41, 0.26	8.7	2.5
6.27		5.7	0.34, 0.17	8.2	109.5
6.28		6.7	0.40, 0.26	8.2	12.0
6.29		4.5	0.26, 0.13	8.0	>125
6.30		4.2	0.23, 0.08	7.8	109.5

<sup>a</sup> pIC<sub>50</sub> measured in the DprE1 fluorescence assay. <sup>b</sup> pIC<sub>50</sub> measured in the DprE1 RapidFire™ assay. <sup>c</sup> Ligand efficiency values are calculated from the fluorescence assay data. <sup>d</sup> Compound tested inactive (MIC > 125 μM) in 1 out of 5 test occasions. <sup>e</sup> Compound tested as pIC<sub>50</sub> < 4 in 2 out of 4 test occasions.

The (*R*)-enantiomer (*R*)-**GSK'896** was the more potent stereoisomer, matching the activity of the racemate **GSK'896** in the RapidFire™ assay ( $RFpIC_{50} = 6.6$  vs. 6.7). Consistently, (*R*)-**GSK'896** exhibited an MIC (6.5  $\mu$ M) similar to racemic **GSK'896** (8.0  $\mu$ M), whilst (*S*)-**GSK'896** was two-fold less active (12.8  $\mu$ M). Potency was maintained relative to (*R*)-**GSK'896** on removal of the  $\alpha$ -methyl group in glycine-linked **6.21** ( $pIC_{50} = 6.7$  vs. 6.6) with a concomitant drop in PFI, but an MIC increase was measured (15.8  $\mu$ M vs. 6.5  $\mu$ M). Addition of a second methyl group in  $\alpha$ -methylalanine-linked **6.22** was tolerated, imparting a modest increase in DprE1 activity over (*R*)-**GSK'896** ( $pIC_{50} = 6.9$  vs. 6.6), whilst retaining a low MIC (4.0  $\mu$ M). Lengthening the amino acid side chain was detrimental in the  $\alpha$ -ethylglycine-linked **6.23** ( $pIC_{50} = 5.4$ ), and increasing steric demand further led to an even greater demise in potency for valine-linked **6.24** ( $pIC_{50} = 4.4$ ). Reversing the connectivity of the alanine linker in **6.25** resulted in a dramatic reduction in DprE1 activity relative to the HTS hit ( $pIC_{50} = 4.2$  vs. 7.2), presumably due to a change in positioning of the chiral centre along the length of the molecule.

Methylation of the alanine alpha heteroatom in **6.26** maintained activity relative to **GSK'896** ( $pIC_{50} = 7.2$ ), suggesting this *N*-H was not likely participating as a hydrogen bond donor. A very potent MIC of 2.5  $\mu$ M was observed for *N*-methylated **6.26**. Replacement of the *N*-H for a carbon linkage led to a large drop in activity for **6.27** ( $pIC_{50} = 5.7$ ), whilst potency was maintained relative to (*R*)-**GSK'896** for *O*-linked **6.28** ( $pIC_{50} = 6.7$  vs. 6.6). This suggested that a hydrogen bond acceptor was beneficial at this location, or that an electron rich benzodioxane was preferred (aniline (*R*)-**GSK'896**  $\approx$  ether **6.28** > carbon-linked **6.27**).

Tethering of the amino acid side chain in the lactams  $\gamma$ -**6.29** and  $\delta$ -**6.30** was not tolerated by the enzyme. Analysis of the computed lowest energy conformations of **GSK'896**,  $\gamma$ -**6.29** and  $\delta$ -**6.30** (Fig. 6.9) revealed that the conformationally constrained lactams had significantly different molecular shapes to **GSK'896**.

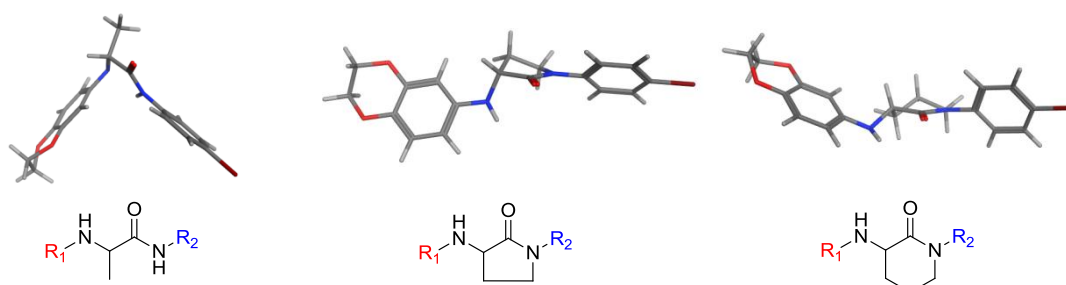


**Figure 6.9.** Side-on views of the lowest energy conformations of **GSK'896** and lactams  $\gamma$ -**6.29** and  $\delta$ -**6.30** computed using MOE<sup>147</sup> (using the (*R*)-enantiomers).  $R_1$  = benzodioxane.  $R_2$  = *p*-bromoaniline.

Figure 6.10 summarises the SAR trends from Table 6.3.

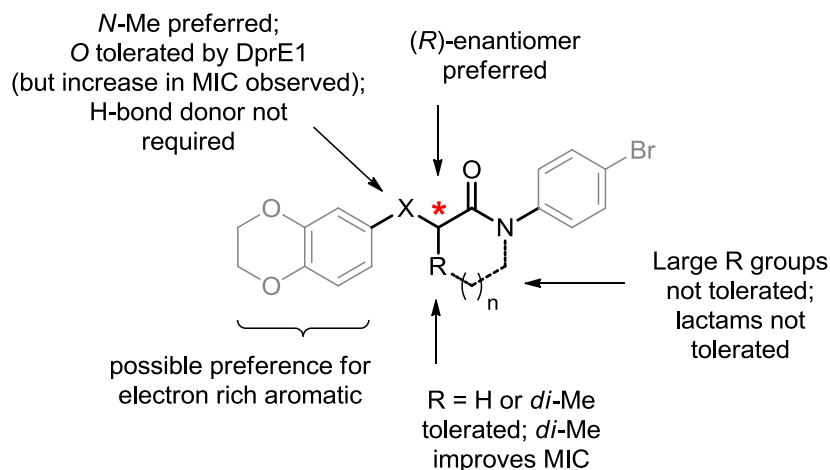


Figure 6.10. SAR around GSK'896 generated from modification of the amino acid linker

#### 6.4.4 Variation of the Aminobenzodioxane Motif of GSK'896

The benzodioxane motif occurred frequently amongst the HTS hits, suggesting a particular recognition of this sub-structure by DprE1. Indeed, benzodioxane-containing fragments **6.19** and **6.20** were highly ligand efficient. The limited SAR from the HTS data and sub-structure searching also indicated that the benzodioxane motif was the most preferable group at this position. Nonetheless, a more complete understanding of the SAR associated with the benzodioxane group was required. Thus, compounds **6.50-6.60** were selected for synthesis (Fig. 6.11). This set encompassed point changes to the saturated ring size and construction (**6.50-6.52**) and heteroatom combination or exclusion (to remove the quinone risk; **6.52-6.56**), aromatic ring electronics (**6.57-6.60**), and lipophilicity (**6.58-6.60**).

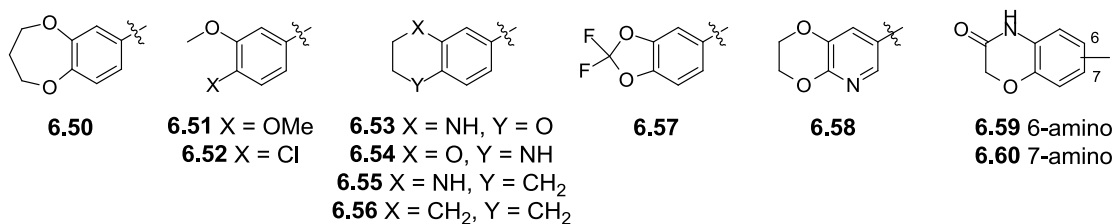
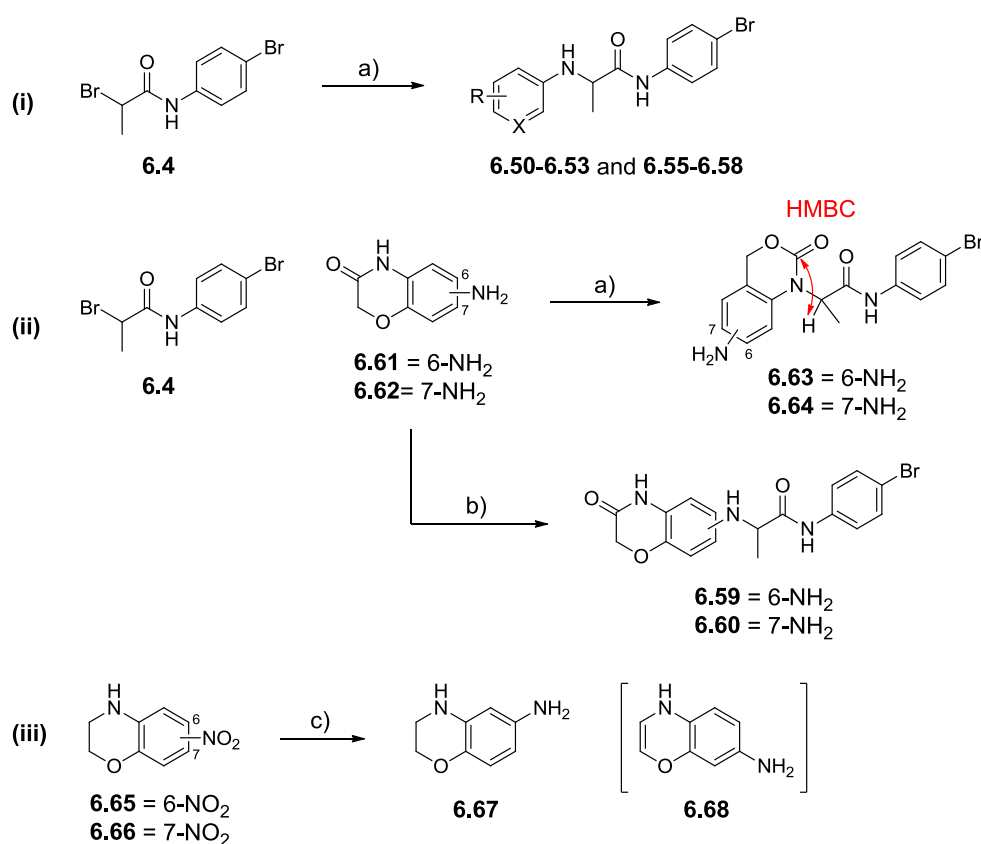


Figure 6.11. Analogues of GSK'896 with variation of the benzodioxane functionality.

##### 6.4.4.1 Synthesis of GSK'896 Analogues with Modifications to the Benzodioxane Motif

In accord with the retrosynthetic disconnection pathway *b* (Scheme 6.2), S<sub>N</sub>2 displacement of  $\alpha$ -bromo amide **6.4** with the appropriate aniline in the presence of base furnished the

benzodioxane variants **6.50-6.53** and **6.55-6.58** (Scheme 6.9i). This strategy could not be applied to the syntheses of benzoxazinones **6.59** and **6.60**, as the lactam nitrogens of **6.61** or **6.62** were alkylated under these conditions, affording **6.63** and **6.64** respectively (Scheme 6.9ii; confirmed by HMBC NMR experiments). Performing the reactions in the absence of base however, did afford **6.59** and **6.60**. The anilines required for the above syntheses were largely commercially available, except the aminodihydrobenzoxazines required for **6.53** and **6.54**. Reduction of 6-nitro-3,4-dihydro-2H-benzo[*b*][1,4]oxazine **6.65** proceeded quantitatively to give 6-amino **6.67** (Scheme 6.9iii) but the corresponding 7-amino regioisomer decomposed to benzoxazine **6.68** during isolation (final compound **6.54** was not pursued further).

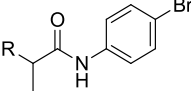


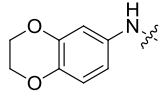
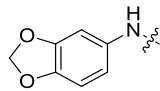
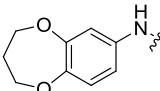
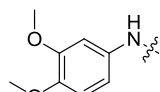
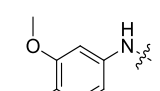
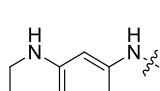
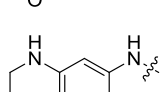
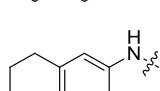
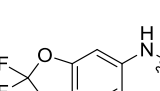
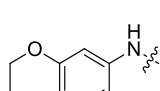
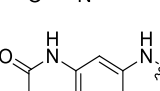
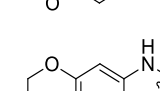
**Scheme 6.9.** a) substituted aniline, K<sub>2</sub>CO<sub>3</sub>, MeCN, 90 °C, 33-81% for **6.51-6.53**, **6.55-6.58** and **6.63-6.64**; for **6.50**, NEt<sub>3</sub>, DMF, 80 °C,  $\mu$ wave, 72%. b) EtOH, reflux, 29-35%. c) 10% Pd/C, H<sub>2</sub>, EtOH, 100% for **6.67**; **6.68** not isolated.

#### 6.4.4.2 Biological and Physicochemical Evaluation of GSK'896 Analogues **6.50-6.53** and **6.55-6.60**

Table 6.4 displays potency, ligand efficiency and physicochemical property data for analogues **6.50-6.53** and **6.55-6.60**.

**Table 6.4.** Potency, ligand efficiency and physicochemical data for compounds **6.50-6.53** and **6.55-6.60**.



No.	R	pIC <sub>50</sub> <sup>a</sup>	LE, LLE <sub>AT</sub>	PFI	MIC (μM)
<b>GSK'896</b>		7.2	0.43, 0.31	7.5	8.0 <sup>b</sup>
<b>HTS-4</b>		6.0	0.37, 0.24	ND	80.0
<b>6.50</b>		6.8	0.39, 0.27	7.7	4.0
<b>6.51</b>		5.7	0.34, 0.23	7.2	40.0
<b>6.52</b>		5.1	0.32, 0.14	8.3	125.0
<b>6.53</b>		5.6	0.33, 0.24	6.8	>125
<b>6.55</b>		5.9	0.35, 0.23	8.0	125.0
<b>6.56</b>		6.2	0.37, 0.16	9.7	16.0
<b>6.57</b>		4.7	0.27, 0.07	8.9	125.0
<b>6.58</b>		5.7	0.34, 0.21	6.0	62.0
<b>6.59</b>		<4	-, -	6.2	ND
<b>6.60</b>		<4 <sup>c</sup>	-, -	5.9	ND

<sup>a</sup> pIC<sub>50</sub> measured in the DprE1 fluorescence assay. <sup>b</sup> Compound tested inactive (MIC > 125 μM) in 1 out of 5 test occasions. <sup>c</sup> Compound failed to fit a curve in 1 out of 4 test occasions. ND = not determined.

Increasing the unsaturated ring size was tolerated by the enzyme, as benzodioxepane **6.50** remained highly potent at DprE1 ( $pIC_{50} = 6.8$ ) and possessed a good MIC ( $4.0 \mu\text{M}$ ). Comparing this result to the loss in potency observed when the unsaturated ring size was decreased (benzodioxole **HTS-4**;  $pIC_{50} = 6.0$ ) suggested that shape complementarity was enhanced for larger, non-planar ring systems (Fig. 6.12). Deconstruction of the saturated ring led to a large reduction in activity in dimethoxy **6.51** and chloro-methoxy **6.52**, revealing a lack of space to accommodate the different steric requirements (Fig. 6.12).

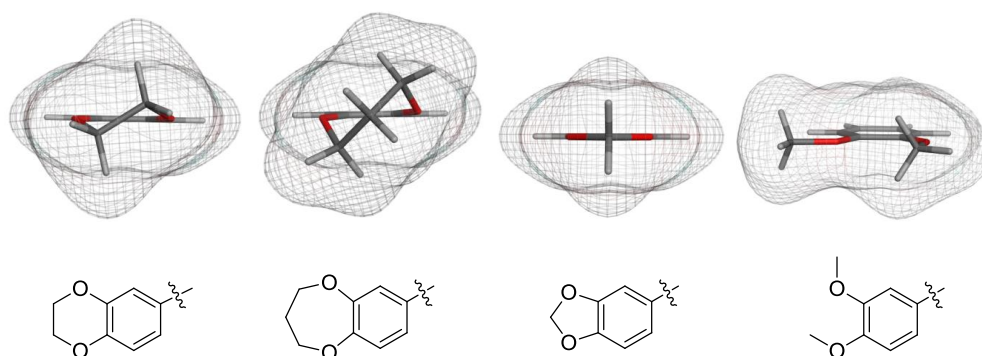


**Figure 6.12.** Computed lowest energy conformations of benzodioxane **GSK'896**, benzodioxepane **6.50**, benzodioxole **HTS-4** and dimethoxy **6.51** with Van der Waal radii shown. The structure energy minimizations were performed using MOE.<sup>147</sup>

Replacement of the dioxane oxygens in nitrogen-analogues **6.53** and **6.55** led to reduced DprE1 activity and a large increase in MIC relative to **GSK'896**. Replacement with two methylene linkages was less detrimental for tetrahydronaphthalene **6.56** ( $pIC_{50} = 6.2$ ), which retained a modest MIC ( $16.0 \mu\text{M}$ ), although the PFI of this lipophilic molecule was particularly high (PFI = 9.7).

Efforts to improve the properties of **GSK'896** through incorporation of polar functionality into the benzodioxane group were unsuccessful. Pyridine **6.58** retained some activity at DprE1 ( $pIC_{50} = 5.7$ ), but benzoxazinones **6.59** and **6.60** were inactive. Whilst polar groups must make productive contact with the target to maintain or improve potency,<sup>148</sup> this result highlighted that the electronics of the aromatic ring may also be important. The poorly active or inactive polar congeners **6.58-6.60** possessed less electron rich aromatic rings than the benzodioxane of **GSK'896**. Notably, electron deficient difluoro-benzodioxole **6.57** was 20-fold less active than the methylene derivative **HTS-4** ( $pIC_{50} = 4.7$  vs. 6.0).

Figure 6.13 summarises the SAR trends from Table 6.4.

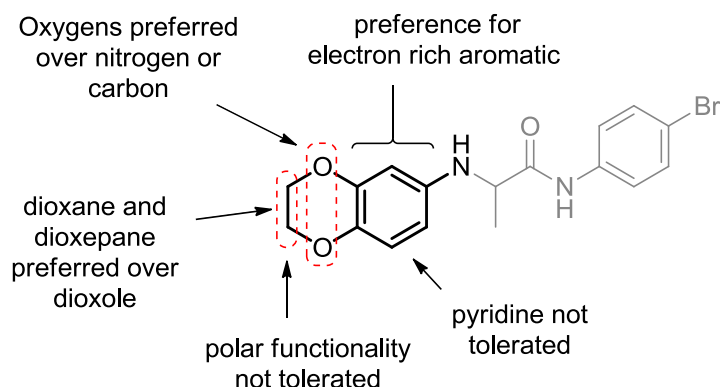


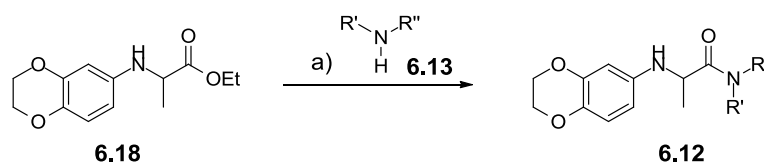
Figure 6.13. SAR around **GSK'896** generated from modification of the aminobenzodioxane motif.

### 6.4.5 Variation of the C-Terminal Aniline of **GSK'896**

Analysis of the data from the HTS and subsequent sub-structure searching exercise indicated that *para*-substitution of the C-terminal aniline was most beneficial (Sect. 6.3). Subsequently, it was envisaged that a Topliss analysis<sup>149</sup> would facilitate further understanding of the SAR associated with the C-terminal aniline. Efforts also focussed on identifying a replacement for the aniline due to the potential mutagenicity risk.

#### 6.4.5.1 Synthesis of **GSK'896** Analogues with Modifications to the C-Terminal Aniline

To achieve the syntheses of **GSK'896** analogues with varied aniline substitution, an array of amide coupling reactions with acid **6.14** was initially anticipated (disconnection pathway *c*, Scheme 6.2). This acid **6.14** however, proved to be unstable to isolation (Sect. 6.4.3.1). Alternatively, trimethylaluminum-mediated aminolysis of the stable ester **6.18** presented a suitable synthetic route. Specifically, the air-stable, moisture-tolerant (and therefore amenable to array synthesis) DABCO adduct of trimethylaluminium<sup>142</sup> was used (as for **6.19** and **6.20**; Scheme 6.3). Scheme 6.10 illustrates general reaction conditions for the compounds presented in the following section. This methodology was suitable for the majority of analogues; different synthetic routes are detailed where an alternative strategy was required.



**Scheme 6.10.** a) amine **6.13**, DABAL-Me<sub>3</sub>, THF, 50 °C, then ester **6.18**, 90 °C.

#### 6.4.5.2 Topliss Analysis

A Topliss analysis is a non-mathematical approach to Hansch's quantitative structure-activity relationship methods<sup>150</sup> (QSAR) that relates certain physicochemical properties to activity in a biological system, specifically concerning the substitution of a benzene ring.<sup>149</sup> In theory, the approach allows the rapid identification of which, if any, physical property descriptors have a significant impact on potency. The property descriptors used in a Topliss analysis are: the *substituent hydrophobicity constant*,  $\pi$  (a measure of the substituents hydrophobicity relative to hydrogen); the *Hammett substituent constant*,  $\sigma$  (a measure of the electron donating or withdrawing capacity of the substituent); and *Taft's steric factor*,  $E$ .<sup>149</sup> The process initiates with the synthesis of 5 synthetically tractable analogues; ranking of their potency then facilitates identification of the probable operative parameters (or combination thereof), and indicates further analogues to synthesise that are likely to have increased potency based on this result. The 5 initial compounds are the unsubstituted parent compound and the 4-methyl, 4-methoxy, 4-chloro and 3,4-dichloro analogues (Fig. 6.14).

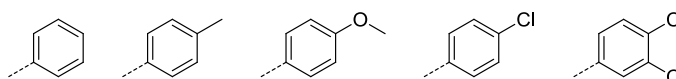


**Figure 6.14.** The initial analogues synthesised as part of a Topliss analysis.

For example, if the order of potency is 3,4-Cl<sub>2</sub> > 4-Cl > 4-Me > 4-OMe ~ 4-H, then this indicates that lipophilicity is important for increased potency (a  $+\pi$  dependency). If the order is 4-OMe > 4-Me > 4-H > 4-Cl > 3,4-Cl<sub>2</sub>, this indicates that electron donating substituents are beneficial, electron withdrawing are not (a  $-\sigma$  dependency). These examples are both linear dependencies; the Topliss method also allows for the identification of non-linear relationships, where combinations of multiple parameters with different weightings are apparent.

The compounds **6.69-6.73** required for the Topliss analysis were synthesised using the DABAL-Me<sub>3</sub> methodology (Scheme 6.10) in 50-82% yield. The data for **6.69-6.73** are presented in Table 6.5.

**Table 6.5.** Potency, ligand efficiency and physicochemical data for compounds **6.69-6.73**.

No.	R	pIC <sub>50</sub> <sup>a</sup>	LE, LLE <sub>AT</sub>	PFI	MIC (μM)
<b>GSK'896</b>		7.2	0.43, 0.31	7.5	8.0 <sup>b</sup>
<b>6.69</b>		4.2 <sup>c</sup>	0.26, 0.19	6.3	>125
<b>6.70</b>		4.8	0.29, 0.20	6.8	125
<b>6.71</b>		5.5	0.31, 0.26	6.1	93.5
<b>6.72</b>		6.0	0.34, 0.20	8.1	28.0
<b>6.73</b>		6.4	0.38, 0.27	7.2	8.0

<sup>a</sup> pIC<sub>50</sub> measured in the DprE1 fluorescence assay. <sup>b</sup> Compound tested inactive (MIC > 125 μM) in 1 out of 5 test occasions. <sup>c</sup> Compound failed to fit a curve in 1 out of 4 test occasions and tested as pIC<sub>50</sub> < 4 in 1 out of 4 test occasions.

The potency data for the Topliss set **6.69-6.73** revealed the following ranking: 4-Cl > 3,4-Cl<sub>2</sub> > 4-OMe > 4-Me > 4-H. Unfortunately this trend did not match any of the potency rankings indicated in the Topliss publication. The most similar ranking was for a 2π-π<sup>2</sup> dependency, but 4-Me **6.70** would be expected to be more active than the 4-OMe **6.71**, and this was not observed. This result suggested that unrecognized influences outside of those considered in the Topliss analysis were operative in this series of compounds, and that the approach could not be used to direct the choice of subsequent compounds to synthesise. No

disadvantage was incurred from synthesising the Topliss set **6.69-6.73** however, as new SAR was generated.

Interestingly, unsubstituted aniline **6.69** was ~1000-fold less active than **GSK'896**, revealing that lipophilic substitution at the 4-position was important for achieving high potency. Comparison of 4-Cl **6.73** ( $pIC_{50} = 6.4$ ) and 3,4-diCl **6.72** ( $pIC_{50} = 6.0$ ) further illustrated that aniline *meta*-substitution was not beneficial.

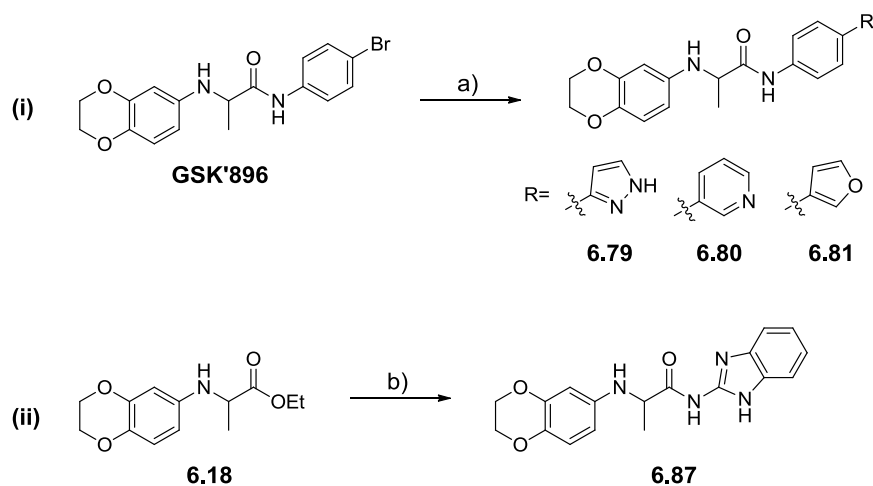
#### **6.4.5.3 Design and Synthesis of Further GSK'896 Analogues with Modification of the C-Terminal Aniline**

Beyond the Topliss analysis, a set of compounds was designed to explore further SAR, investigating whether hydrophilic substituents could be introduced to reduce lipophilicity of the series and whether the aniline could be replaced.

##### Variation of the C-Terminal Aniline: Reducing Lipophilicity

Pyridine analogues **6.74** and **6.75** were prepared to investigate the effect of introducing heteroatoms into this aromatic ring (see Table 6.6 for structures and data summary). As aniline *para*-substitution was deemed necessary for high potency, and *ortho* and *meta* substitution were not beneficial, replacement of the 4-bromine substitution with polar functionality was pursued as a second strategy to reduce lipophilicity of the series. Whilst it appeared that lipophilic steric bulk at the *para*-position engendered potency, it was hoped that replacement with hydrophilic functionality may also be tolerated. Analogues were targeted in which the 4-bromine of **GSK'896** was exchanged for small polar groups (**6.76-6.78**) or a heterocycle (**6.79-6.82**), as well as analogues where the 4-bromoaniline was replaced with a benzo-fused heterocycle (**6.83-6.87**).

Biaryls **6.79-6.81** were prepared *via* a Suzuki reaction between **GSK'896** and the required boronic acids or potassium trifluoroborate salt (Scheme 6.11i). Benzimidazole **6.87** was prepared from the ester **6.18** and 2-aminobenzimidazole using trimethylaluminum (Scheme 6.11ii) as DABAL-Me<sub>3</sub> did not effect this transformation. The remaining analogues were synthesised from the corresponding commercial amine *via* DABAL-Me<sub>3</sub> mediated aminolysis of the ester **6.18** (Scheme 6.10).



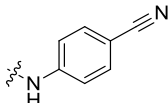
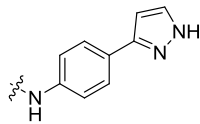
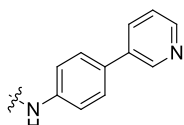
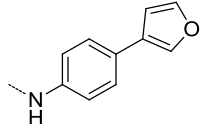
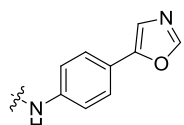
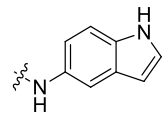
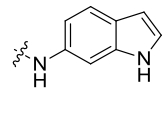
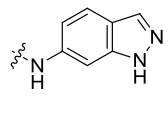
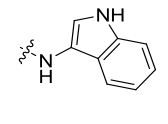
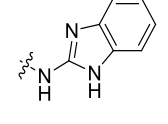
**Scheme 6.11.** a) Pd(OAc)<sub>2</sub> (6 mol%), RuPhos (12 mol%), potassium trifluoro(1H-pyrazol-3-yl)borate, Na<sub>2</sub>CO<sub>3</sub>, EtOH, 85 °C, 39% for **6.79**, OR Pd(PPh<sub>3</sub>)<sub>2</sub>Cl<sub>2</sub> (5 mol%), K<sub>2</sub>CO<sub>3</sub>, pyridin-3-ylboronic acid or furan-3-ylboronic acid, 1,4-dioxane, water, 100 °C, **6.80** = 63%, **6.81** = 66%. b) AlMe<sub>3</sub>, 2-aminobenzimidazole, toluene, 50 °C then **6.18**, 100 °C, 72%.

**Table 6.6.** Potency, ligand efficiency and physicochemical data for compounds **6.74-6.87**.

No.	R	pIC <sub>50</sub> <sup>a</sup>	LE, LLE <sub>AT</sub>	PFI	MIC (μM)
GSK'896		7.2	0.43, 0.31	7.5	8.0 <sup>b</sup>
<b>6.74</b>		5.8	0.35, 0.27	6.2	32.0
<b>6.75</b>		5.2	0.31, 0.24	7.4	80.0
<b>6.76</b>		<4	-, -	4.4	>80
<b>6.77</b>		5.0	0.25, 0.27	5.2	>80

Table 6.6 continued overleaf

Table 6.6 continued from overleaf

No.	R	pIC <sub>50</sub> <sup>a</sup>	LE, LLE <sub>AT</sub>	PFI	MIC (μM)
6.78		5.7	0.33, 0.27	6.2	31.3
6.79		<4	-, -	6.4	78.0
6.80		<4	-, -	7.2	78.0
6.81		4.7 <sup>c</sup>	0.24, 0.15	8.3	>125
6.82		<4	-, -	6.7	>80
6.83		4.5	0.25, 0.21	6.6	>125
6.84		6.1	0.33, 0.29	7.0	32.0
6.85		5.4	0.30, 0.25	6.0	31.3
6.86		<4	-, -	6.8	>125
6.87		5.4	0.30, 0.24	6.7	62.0

<sup>a</sup> pIC<sub>50</sub> measured in the DprE1 fluorescence assay. <sup>b</sup> Compound tested inactive (MIC > 125 μM) in 1 out of 5 test occasions. <sup>c</sup> Compound tested as pIC<sub>50</sub> < 4 in 1 out of 2 test occasions.

Replacing the *p*-bromoaniline with pyridine isomers **6.74** ( $pIC_{50} = 5.8$ ) and **6.75** ( $pIC_{50} = 5.2$ ) resulted in potency losses. In all cases, replacing the aniline 4-bromo substitution with small polar functionality led to a reduction in potency: *N*-methylbenzamide **6.76** was inactive, whilst benzonitrile **6.78** suffered a 30-fold reduction in activity relative to **GSK'896** ( $pIC_{50} = 5.7$  vs.  $7.2$ ). Exchanging the aniline 4-bromo substitution with heterocycles was also unsuccessful, with only lipophilic furan **6.81** showing a measurable  $IC_{50}$  ( $pIC_{50} = 4.7$ ). Interestingly, both pyrazole **6.79** and pyridine **6.80** exhibited modest MICs ( $78 \mu M$ ) despite being inactive against DprE1, suggesting that these compounds were inhibiting *M.tb* growth *via* some other mechanism. Replacement of the 4-bromoaniline with fused nitrogen heterocycles proved more successful as activity was retained for all but one of the analogues **6.83-6.87**, however potency was not maintained relative to **GSK'896**.

The results in Table 6.6 revealed that whilst the compounds did generally exist in improved property space relative to **GSK'896**, it was not possible to maintain potency when substituting the aniline 4-position with polar groups. Considering these data and the potency ranking of the Topliss set (Table 6.5), it is likely that lipophilic contact with the protein at this location was responsible for the enhanced activity of **GSK'896**. Published crystal structures of DprE1 have revealed a hydrophobic pocket deep within the active site of the enzyme.<sup>87,93,113,151</sup> Indeed, the lipophilic thiazole ring of **TCA1**<sup>112</sup> and lipophilic aryl-CF<sub>3</sub> groups of **PBTZ169**<sup>87</sup> (Fig. 6.15), **Ty38c**<sup>111</sup> and **CT319**<sup>113</sup> are seen to bind in this hydrophobic pocket. It was therefore speculated that the *p*-bromo of **GSK'896** interacts with this same hydrophobic cleft, explaining the importance of lipophilic substitution at this position. Computational docking of **GSK'896** into the active site of DprE1 was attempted based on this assumption, in order to gain further insight into the binding mode of this HTS hit and related analogues. However, different binding poses were generated depending on which literature or in-house crystal structure was used to perform the docking study. This was due to the fact that the flexible loops at the entrance to the DprE1 active site (Sect. 3.3) adopt different positions in each of the available crystal structures, which changes the shape of the active site in this region. Ultimately, it was not possible to confidently select one preferred binding mode for **GSK'896**.

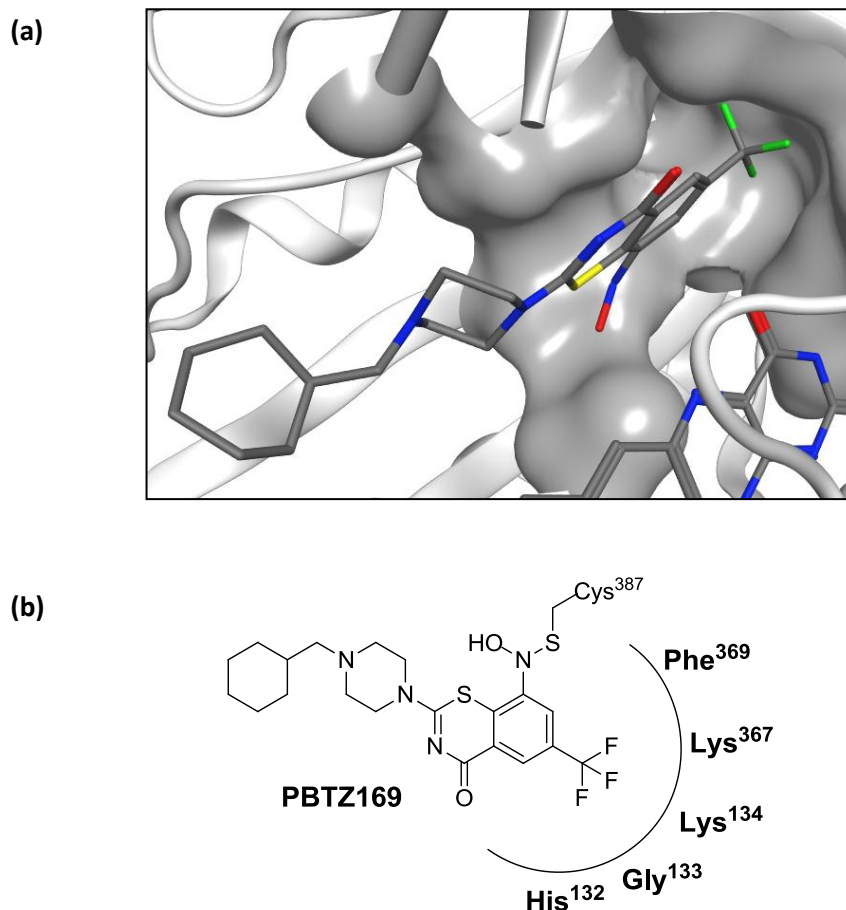


**Figure 6.15.** (a) Crystal structure of **PBTZ169** bound covalently to DprE1 (the *M.Smeg* ortholog).<sup>87</sup> The aryl-CF<sub>3</sub> group occupies a lipophilic cavity. (b) Two-dimensional representation of the lipophilic cavity that interacts with the aryl-CF<sub>3</sub> of **PBTZ169**.

#### Variation of the C-Terminal Aniline: Replacing the Aniline with Saturated Derivatives

To investigate replacement of the C-terminal aniline, various aliphatic amines were targeted, namely cyclohexyl **6.88**, substituted piperidines **6.89** and **6.90**, and benzylic amines **6.91-6.95** (see Table 6.7 for structures and data summary). These compounds were all synthesised from the corresponding commercial amine *via* DABAL-Me<sub>3</sub> mediated aminolysis of the ester **6.18** (Scheme 6.10).

**Table 6.7.** Potency, ligand efficiency and physicochemical data for compounds **6.69** and **6.88-6.95**.

No.	R	pIC <sub>50</sub> <sup>a</sup>	LE, LLE <sub>AT</sub>	PFI	MIC (μM)
<b>GSK'896</b>		7.2	0.43, 0.31	7.5	8.0 <sup>b</sup>
<b>6.69</b>		4.2 <sup>c</sup>	0.26, 0.19	6.3	>125
<b>6.88</b>		4.4	0.27, 0.20	5.4	>125
<b>6.89</b>		<4	-, -	1.7	>125
<b>6.90</b>		<4	-, -	6.8	>125
<b>6.91</b>		<4 <sup>d</sup>	-, -	5.9	>125
<b>6.92</b>		4.2	0.24, 0.22	6.4	>125
<b>6.93</b>		5.6	0.31, 0.26	6.8	>125
<b>6.94</b>		4.4	0.23, 0.14	7.9	78.0
<b>6.95</b>		4.2	0.22, 0.13	7.9	78.0

<sup>a</sup> pIC<sub>50</sub> measured in the DprE1 fluorescence assay. <sup>b</sup> Compound tested inactive (MIC > 125 μM) in 1 out of 5 test occasions. <sup>c</sup> Compound failed to fit a curve in 1 out of 4 test occasions and tested as pIC<sub>50</sub> < 4 in 1 out of 4 test occasions. <sup>d</sup> Compound failed to fit a curve in 2 out of 6 test occasions.

Cyclohexyl **6.88** was equipotent with the unsubstituted aniline **6.69** ( $pIC_{50} = 4.4$  vs. 4.2), potentially representing a replacement for the aniline of **GSK'896**. Further elaborated substituted piperidines **6.89** and **6.90** were inactive however, suggesting the saturated ring did not provide a direct vector towards the lipophilic cavity where the aniline 4-substituent was believed to bind. Whilst benzylamine **6.91** was inactive, isoindoline **6.92** and tetrahydroisoquinoline (THIQ) **6.93** were active, with the latter **6.93** showing enhanced potency at DprE1 compared to unsubstituted aniline **6.69** ( $pIC_{50} = 5.6$  vs. 4.2). Diminished activity was observed for bromo-substituted THIQs **6.94** and **6.95** however, presumably due to a clash with the protein surface as a result of extending the length of the molecule relative to **GSK'896**.

Figure 6.16 summarises the SAR trends associated with the C-terminal alanine.

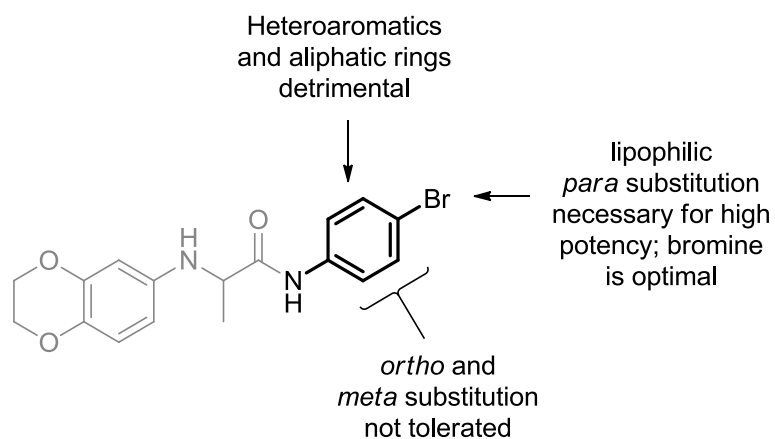


**Figure 6.16.** SAR around **GSK'896** generated from modification of the C-terminal aniline.

## 6.5 Aminobenzodioxane-Phenyl-Propanamides SAR Overview

A thorough investigation into the SAR around **GSK'896** has been performed. The collective body of SAR data generated is summarised in Figure 6.17. Whilst many of the analogues showed good activity at DprE1, the majority of modifications led to a loss in activity relative to the HTS hit, which remained one of the most potent analogues of the series. Some analogues however, displayed an improved MIC relative to **GSK'896**.

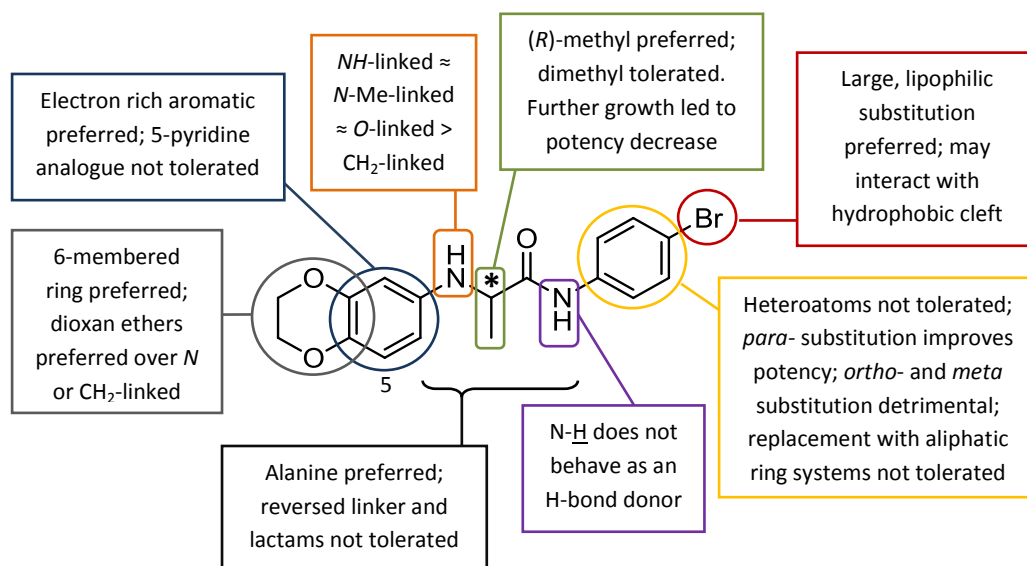


**Figure 6.17.** Structure-activity-relationships for the aminobenzodioxane-phenyl-propanamide series of DprE1 inhibitors.

A key aim was to identify points of change that would improve the physicochemical properties of the HTS hit **GSK'896**, which was too lipophilic in nature. SAR analysis revealed that this was perhaps an intrinsically challenging task. The aromatic rings of **GSK'896** presented logical motifs upon which to introduce polar functionality. However, the C-terminal aniline only tolerated substitution at the 4-position with lipophilic groups, and an electron rich benzodioxane motif was preferred, preventing additional incorporation of polar functionality at this terminus of the molecule. Furthermore, the SAR analysis suggested that the activity in this series was largely driven by lipophilicity. Figure 6.18 plots the activity of **GSK'896** and the new analogues against Chrom Log  $D_{7.4}$ , illustrating this relationship.

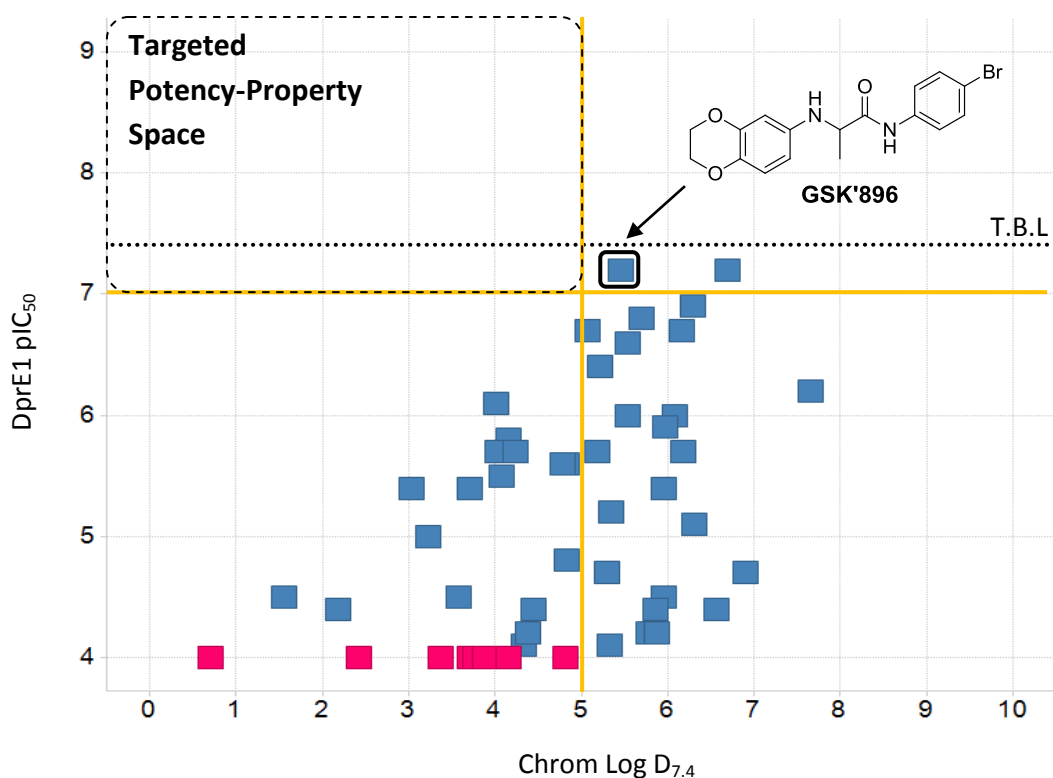


**Figure 6.18.** A plot of Chrom Log  $D_{7.4}$  vs. DprE1  $pIC_{50}$  (measured in the fluorescence assay) of **GSK'896** and all the new analogues presented herein. Colour key: blue =  $pIC_{50} \geq 4$ ; red =  $pIC_{50} < 4$ . T.B.L = tight binding limit. The Chrom Log  $D_{7.4}$  cut-off value of 5 correlates with a PFI of 7 for analogues with two aromatic rings.

The second key aim was to replace or remove the structural motifs that caused developability concerns. Replacement of the benzodioxane aniline with an aromatic ether (**6.28**) was one modification that was successful (although an increase in MIC was observed), but a suitable replacement for the C-terminal aniline was not found. Removing the potential quinone-precursor (the aminobenzodioxane motif) also proved challenging, as all efforts led to reduced activity at DprE1.

## 6.6 Conclusions

In summary, extensive changes around the structure of the HTS hit **GSK'896** were investigated, establishing the aminobenzodioxane-phenyl-propanamides as a novel series of non-covalent DprE1 inhibitors with an unprecedented chemotype. Many of the compounds were highly potent at DprE1 and some analogues exhibited good MICs against the virulent *M.tb* H37Rv. In particular, (*R*)-**GSK'896**,  $\alpha$ -methylalanine **6.22**, *N*-methyl alanine

**6.26** and benzodioxepane **6.50** displayed the most potent MICs (Fig. 6.19). Notably, this series demonstrated target engagement at DprE1 in the DprE1 over-expression MIC assay.

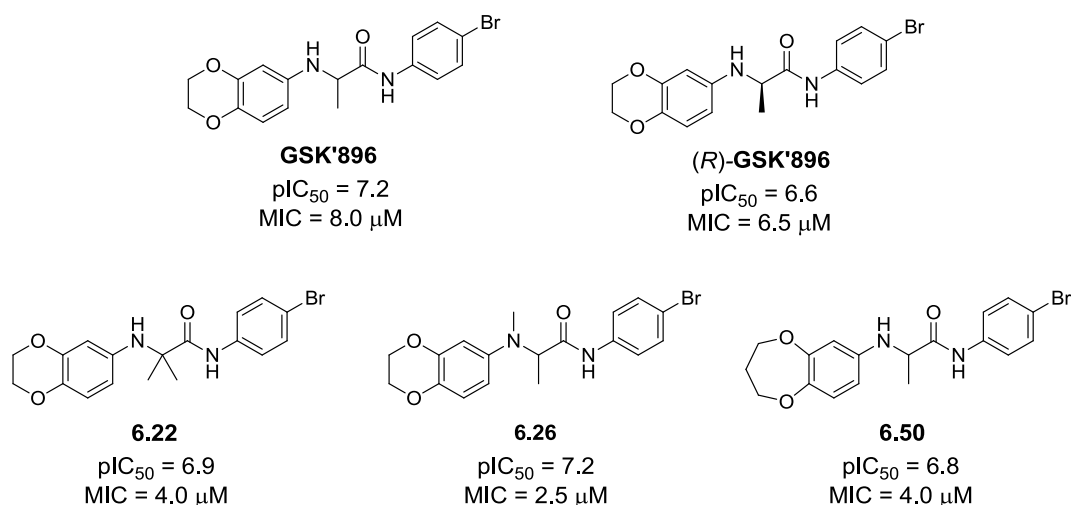


**Figure 6.19.** The most potent analogues of the aminobenzodioxane-phenyl-propanamide series.

In spite of the encouraging potency of several exemplars within this series, it was not possible to demonstrate that DprE1 activity could be maintained whilst improving the physicochemical properties of the molecules. All efforts to improve physicochemical properties resulted in activity losses, and it appeared that potency of this series was largely driven by lipophilicity. The inability to improve upon the property profile of **GSK'896**, in combination with the sub-optimal ADME indicators of the HTS hit (Table 6.1) thus suggested that it was unlikely that this series of molecules could be developed into a medicine. However, whilst not suitable as potential drug candidates, the potent exemplars of the series (Fig. 6.19) represent quality probe molecules<sup>152,153</sup> which could be used to further investigate non-covalent DprE1 inhibition in the context of *M.tb* growth and survival. Frye suggested that quality probes should be highly potent and selective for the intended target *in vitro*, with sufficient mechanistic information to assign activity in a cell-based assay to engagement at the desired target.<sup>152</sup> The aminobenzodioxane-phenyl-propanamides were shown to inhibit mycobacterial growth through target engagement at DprE1 in the over-expression MIC assay, and two exemplars were active against DprE1 at <100 nM (**GSK'896** and **6.26**).

## 6.7 Future Work

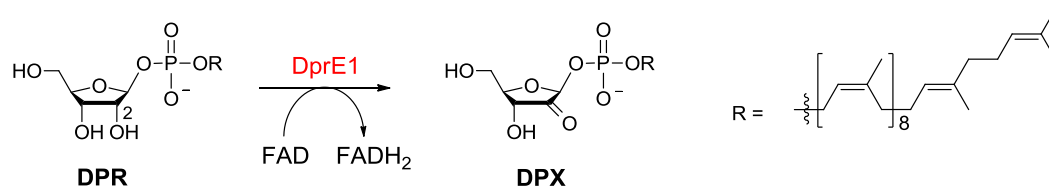
Work is currently on-going in our laboratories to investigate whether there is a critical residue for the binding and activity of non-covalent DprE1 inhibitors. Several mutant strains of *M.tb* resistant to different non-covalent DprE1 inhibitors (published and in-house) have been cultivated, and the DprE1 point mutations have been identified. Screening non-covalent DprE1 inhibitors (including analogues of **GSK'896**) against these *M.tb* mutants for cross-resistance may therefore indicate common residues important for non-covalent inhibition of DprE1, which could have important implications for future inhibitor design.

Efforts to crystallise analogues of **GSK'896** bound to DprE1 are on-going in our laboratories. If any structural information becomes available it would be instructive to re-visit the SAR presented herein to rationalise the difficulties associated with improving the physicochemical properties of the aminobenzodioxane-phenyl-propanamide series. Furthermore, as it was predicted that **GSK'896** interacted with a lipophilic cleft similar to other non-covalent DprE1 inhibitors, it would be interesting to use any structural information to design hybrid series, incorporating structural features from the aminobenzodioxane-phenyl-propanamide series and other non-covalent DprE1 inhibitors. Such hybrid molecules may present a more attractive lead series than the aminobenzodioxane-phenyl-propanamides.

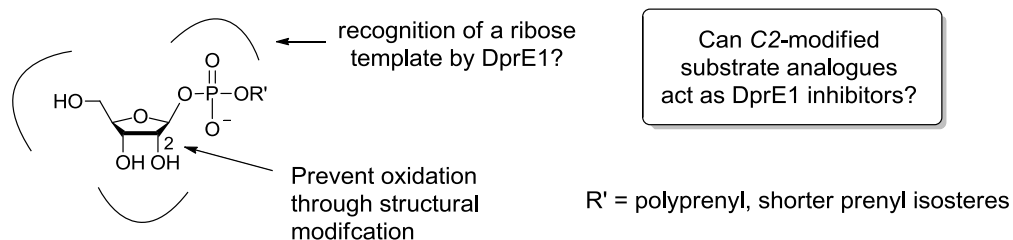
## 7. Substrate Analogues as Inhibitors of DprE1 and Tool Compounds for Chemical Biology

During the course of our efforts to identify inhibitors of DprE1, the possibility of designing substrate analogues as DprE1 inhibitors was investigated. The catalytic role of DprE1 is to oxidise the substrate **DPR** at the ribose C2-position (Chapt. 3; Fig. 7.1a); it was proposed that prevention of this oxidation process *via* structural modification of the substrate at the C2-position could form the basis of inhibitor design (Fig. 7.1b). The value of this approach was considered twofold. Firstly, as DprE1 is predisposed to the recognition of a ribose template, it was predicted that such substrate analogues would act as inhibitors of DprE1. Furthermore, the hydrophilic and highly three-dimensional ribose core represented an attractive motif upon which to design novel DprE1 inhibitors. Secondly, it was intended that the proposed molecules would have value as tool compounds for chemical biology experiments, to probe both the nature of DprE1 and interactions between the protein and small molecule inhibitors (Fig. 7.1c). X-ray crystallography for DprE1 has not routinely delivered liganded crystal structures within our laboratory, so tools with which to investigate mechanism of action were deemed highly valuable.

(a) DprE1-catalysed oxidation



(b) Non-oxidisable substrate analogues as DprE1 inhibitors



(c) Substrate analogues for chemical biology

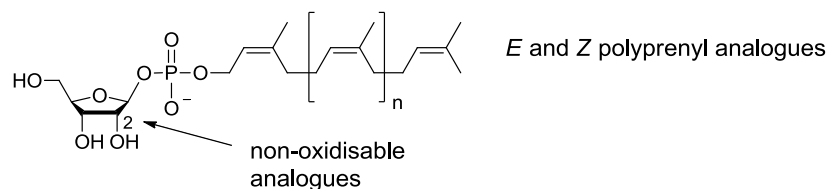


**Figure 7.1.** (a) The DprE1-catalysed oxidation of **DPR**. (b) Non-oxidisable substrate analogues as potential inhibitors of DprE1. (c) Substrate analogues proposed as DprE1 tool molecules for chemical biology experiments.

## 7.1 Project Aims

To investigate the hypotheses outlined above, the aims of this project were:

- Design multiple series of C2-modified DprE1 substrate analogues;
- Develop syntheses of the designed analogue series (amenable to variation of the prenyl functionality);
- Test these analogues as inhibitors of DprE1 and establish SAR trends;
- Investigate the potential of the substrate analogues as chemical biology tools.

## 7.2 Design of Substrate Analogues 7.1-7.3 as Potential DprE1 Inhibitors

### 7.2.1 Design of the C2-Modified Ribose Cores for Series 7.1-7.3

Figure 7.2 illustrates three ribose analogue scaffolds **7.1**, **7.2** and **7.3**, each of which incorporates a structural modification at the C2-position designed to prevent the DprE1-catalysed oxidation: methylated **7.1** contains a tertiary alcohol at the C2-position; the C2-hydroxyl in **7.2** was replaced with a *gem*-difluoromethylene moiety; and acyclic **7.3** lacks the C2-position entirely. An additional design consideration for these analogues concerned the substrate phosphate group. Two active site lysine residues are thought to engage the phosphate group of **DPR**.<sup>151</sup> To maintain these putative interactions, retention of the phosphate group or bioisosteric replacement with a phosphonate group was proposed (phosphonates have successfully been employed as phosphate bioisosteres in medicinal chemistry programmes<sup>154</sup> and in licensed drugs<sup>155</sup>). Whilst C2-methylated **7.1** retained a phosphate group, **7.2** and **7.3** were substituted with phosphonate esters.

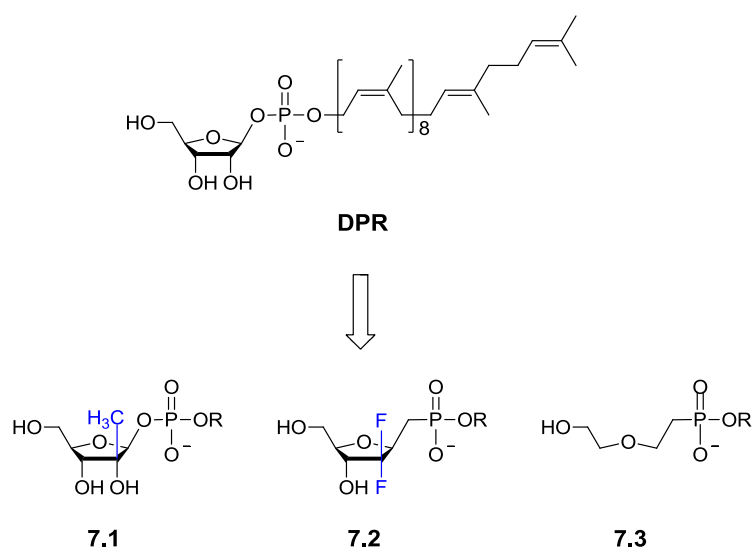


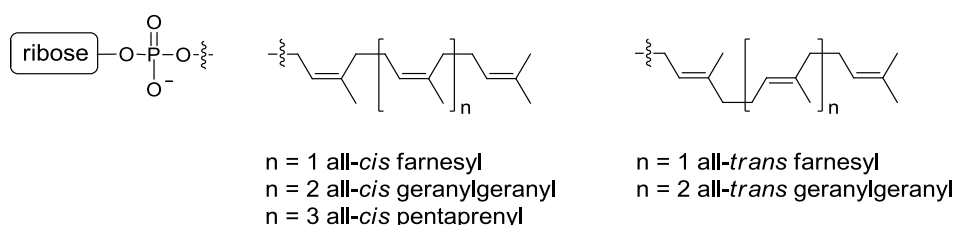
**Figure 7.2.** Design of three series of DprE1 substrate analogues **7.1-7.3** as potential inhibitors of DprE1.

### 7.2.2 Selection of Substituents for Series 7.1-7.3

The highly lipophilic decaprenyl chain of **DPR** is not readily available and represented a synthetically challenging functionality to pursue. However, truncated-lipid analogues are also recognised by DprE1: *E*-**FPR** (all-*trans*-farnesylphosphoryl- $\beta$ -D-ribose) is regularly used

as an oxidisable substrate surrogate in functional DprE1 enzyme assays,<sup>93</sup> and *E*-GGPR (all-*trans*-geranylgeranylphosphoryl- $\beta$ -D-ribose) has been developed for use in the GSK assays (Sect. 4.1). As such, the designed ribose cores **7.1** and **7.2** were substituted with the prenyl lipids farnesol, geranylgeraniol and pentaprenol (Fig. 7.3a). The all-*trans* and all-*cis* farnesyl and geranylgeranyl analogues were targeted, as well as the all-*cis* pentaprenyl analogue, to investigate the effect of prenyl length and geometric isomerism on analogue recognition. In addition, to investigate the replacement of the lipophilic polyprenyl functionality, smaller, less lipophilic and more drug-like substituents were selected for the functionalisation of series **7.1-7.3** (Fig. 7.3b). To probe the effect of substituent choice, groups of varying length, lipophilicity, topology and aromatic ring count were selected, ranging from isopentyl to biphenyl.

(a) farnesyl, geranylgeranyl and pentaprenyl substituents (for series **7.1** and **7.2** only):



(b) small phosphate/ phosphonate substituents (for series **7.1-7.3**):

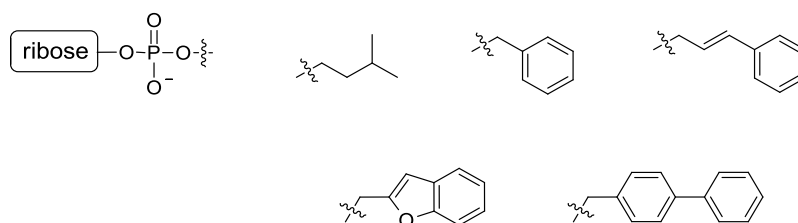


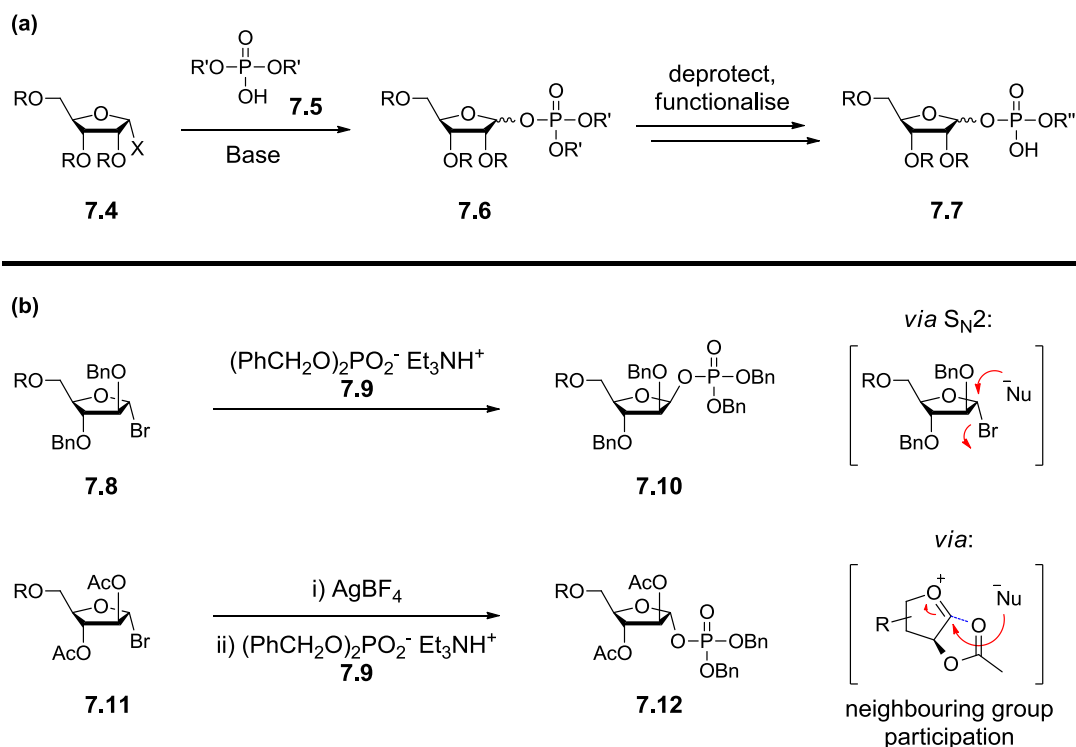
**Figure 7.3.** The proposed phosphate and phosphonate substituents for ribose series **7.1-7.3**.

## 7.3 Synthesis of the 2-Methyl-1-Phosphoryl- $\beta$ -D-Ribofuranoses **7.1**

### 7.3.1 Synthetic Approaches Towards Ribosyl-1-Phosphates

Two main strategies for the synthesis of pentose-1-phosphates are prevalent in the literature. The first and most common procedure is the glycosylation reaction between a nucleophilic phosphate glycosyl acceptor (e.g. phosphate diester **7.5**, Scheme 7.1a) and an

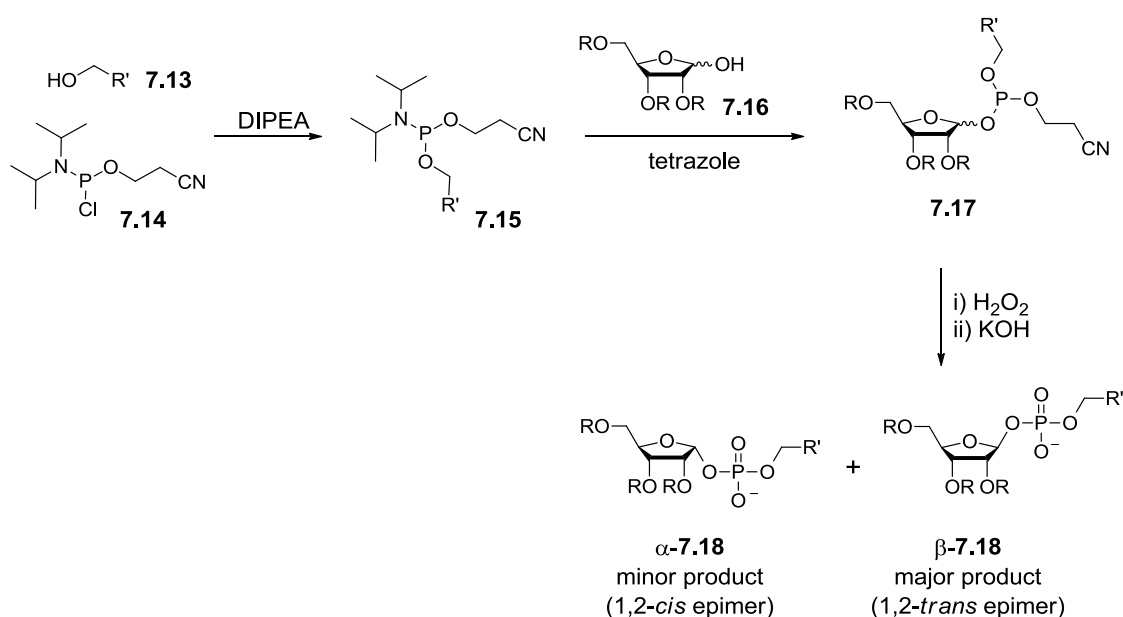
electrophilic glycosyl donor, typically a glycosyl bromide or glycosyl trichloroacetimidate (e.g. ribose **7.4**, X = Br or OCNHCl<sub>3</sub> respectively).<sup>156,157</sup> Deprotection of the resulting phosphate triester **7.6** reveals a site amenable to further functionalisation, providing access to phosphate diester **7.7**. Anomeric selectivity of such glycosylation reactions may be achieved by selecting appropriate protecting groups. Maryanoff *et al.* demonstrated<sup>158</sup> that an  $\alpha$ -bromo arabinose **7.8** protected with non-participating benzyl groups gave  $\beta$ -arabinose **7.10** on treatment with phosphate diester **7.9** (Scheme 7.1b). An analogous reaction with 2,3-di-*O*-acetyl derivative **7.11** gave the  $\alpha$ -arabinose **7.12** by way of anchimeric assistance.



**Scheme 7.1.** (a) Generalised synthesis of a ribosyl-1-phosphate **7.7** by glycosylation of phosphate diester **7.5** with glycosyl donor **7.4** (X = Br or OCNHCl<sub>3</sub>). (b) Anomeric selectivity of glycosylation reactions may be achieved through judicious choice of protecting group for the C2-hydroxyl functionality.

The second strategy for the synthesis of pentose-1-phosphates is the phosphoramidite approach developed by Lee *et al.* (Scheme 7.2).<sup>159</sup> This method involves first the condensation of an alcohol **7.13** with the phosphitilating reagent 2-cyanoethyl *N,N*-diisopropylchlorophosphoramidite **7.14**. Subsequent condensation between the phosphoramidite intermediate **7.15** and a 2,3,5-*O*-silyl protected furanose (e.g. ribose **7.16**) in the presence of tetrazole, gives intermediate phosphite **7.17**. This phosphite **7.17** can then be oxidised to the corresponding phosphate with H<sub>2</sub>O<sub>2</sub>, prior to cleavage of the

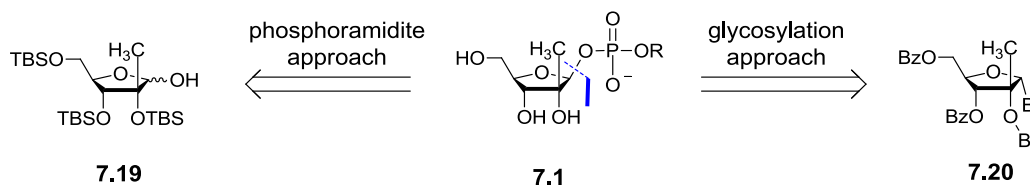
cianoethyl protecting group under basic conditions to give the  $\alpha$ -**7.18** and  $\beta$ -**7.18** phosphates. Notably, this methodology favours the formation of the anomer bearing the 1,2-*trans* configuration: the  $\beta$ -anomer is favoured for ribose sugars and the  $\alpha$ -anomer is favoured for arabinose sugars. The degree of selectivity appears to be dependent on both the reaction temperature, and the sugar and alcohol coupling partners used.<sup>160</sup> Some examples gave complete selectivity for the 1,2-*trans* epimer,<sup>161,162</sup> whilst others provided the 1,2-*trans* epimer as the major product<sup>163</sup> after separation. It was suggested by Lee and co-workers<sup>160</sup> that, given glycosyl-phosphites are highly activated glycosyl donors under mild conditions,<sup>164</sup> the phosphite anomer bearing the 1,2-*cis* configuration may eliminate or rearrange to give the 1,2-*trans* epimer as the major product.



**Scheme 7.2.** A general schematic for the synthesis of ribosyl-1-phosphates *via* the phosphoramidite approach developed by Lee *et al.*<sup>159</sup> R = *tert*-butyldimethylsilyl (TBS).

Considering both synthetic strategies, it was concluded that the phosphoramidite methodology was particularly suited to the synthesis of the 2-methyl-1-phosphoryl- $\beta$ -D-ribofuranoses **7.1**, as the required 1,2-*trans* configured  $\beta$ -riboses could be accessed in relatively few synthetic steps. An uncertainty arose however, as to whether the presence of the C2-methyl group would interfere with the stereoselectivity of the reaction, perhaps through steric encumbrment. However, based on the rationale provided by Lee,<sup>160</sup> whereby the 1,2-*cis* configured phosphite intermediates **7.17** were unstable to elimination or rearrangement, it was reasoned that the 1,2-*trans* configured  $\beta$ -riboses should still be

the major products. In the event that the phosphoramidite methodology was not successful, concurrent efforts to access the ribosyl-1-phosphates **7.1** *via* the glycosylation approach were also pursued in the first instance. Retrosynthetic analyses for each of these methodologies are presented in Scheme 7.3.

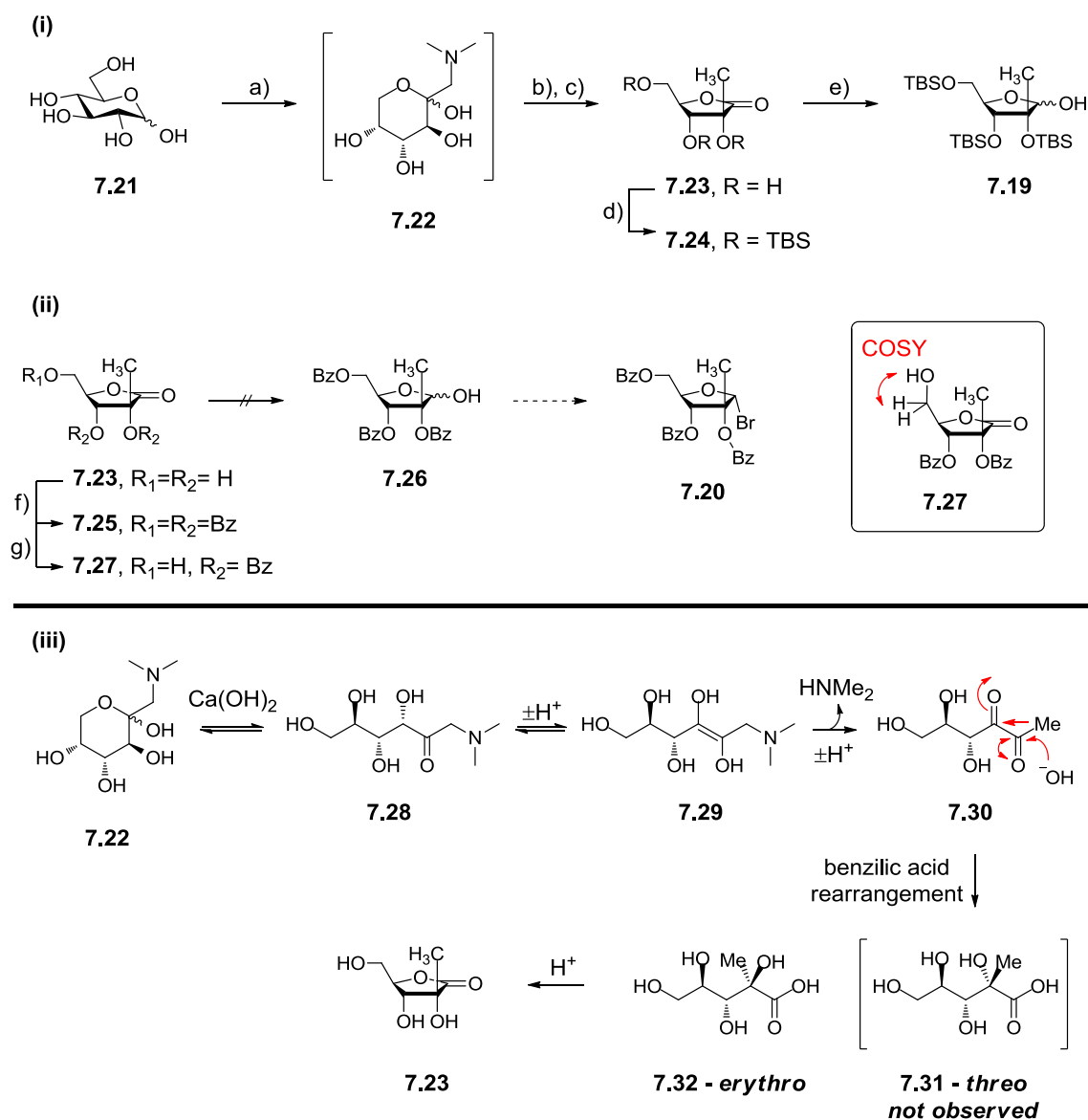


**Scheme 7.3.** Retrosynthetic analysis for 2-methyl-1-phosphoryl- $\beta$ -D-ribofuranoses **7.1**. Disconnection at the anomeric position exploiting the phosphoramidite approach or the glycosylation approach yielded riboses **7.19** or **7.20** respectively.

### 7.3.2 Synthesis of Analogues 7.1a-j

The syntheses of the 2-methyl riboses **7.1** started with the conversion of D-glucose **7.21** into 2-methyl-D-ribo-1,4-lactone **7.23** *via* a reported procedure, as shown in Scheme 7.4i.<sup>165,166</sup> This multi-step reaction proceeded with an Amadori rearrangement of glucose **7.21** to give the Amadori ketose **7.22**. Intermediate **7.22** was then treated with aqueous calcium hydroxide to give, after acidic workup, the lactone **7.23** in 17% yield. A plausible pathway for this reaction is outlined in Scheme 7.4iii.<sup>165,166</sup> Notably, none of the *threo*-sugar **7.31** was formed. The per-silylated **7.24** was next obtained in 85% yield upon treatment of lactone **7.23** with TBSOTf, 2,6-lutidine and catalytic DMAP (Scheme 7.4i). A low temperature reduction of protected lactone **7.24** using DIBAL-H subsequently furnished the anomeric mixture of lactols **7.19** required for the ensuing phosphoramidite coupling reactions.

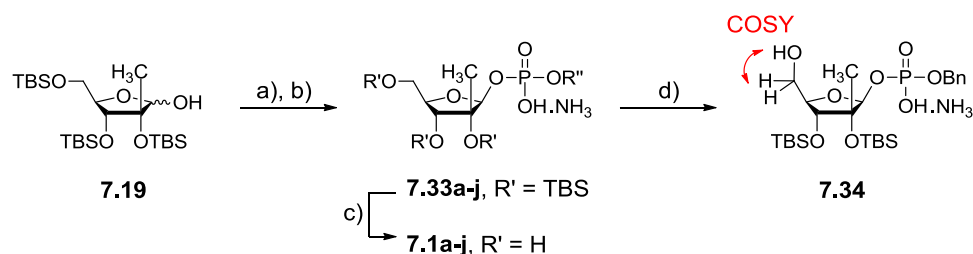
In efforts to access the ribosyl bromide **7.20** required for the alternative glycosylation route, per-benzoylated lactone **7.25** was first synthesised from unprotected lactone **7.23** (Scheme 7.4ii). However, subsequent attempts to selectively reduce the lactone of **7.25** in the presence of the benzoyl protecting groups failed to yield the desired mixture of lactols **7.26**. Reaction of lactone **7.25** with Red-Al and di-*sec*-isoamyl borane gave complex mixtures, DIBAL-H selectively cleaved the C5-protecting group to give dibenzoyl **7.27** (confirmed by COSY NMR; Scheme 7.4ii), and no reaction was observed upon treatment with NaBH<sub>4</sub>. Due to these results, the glycosylation route was not pursued further.



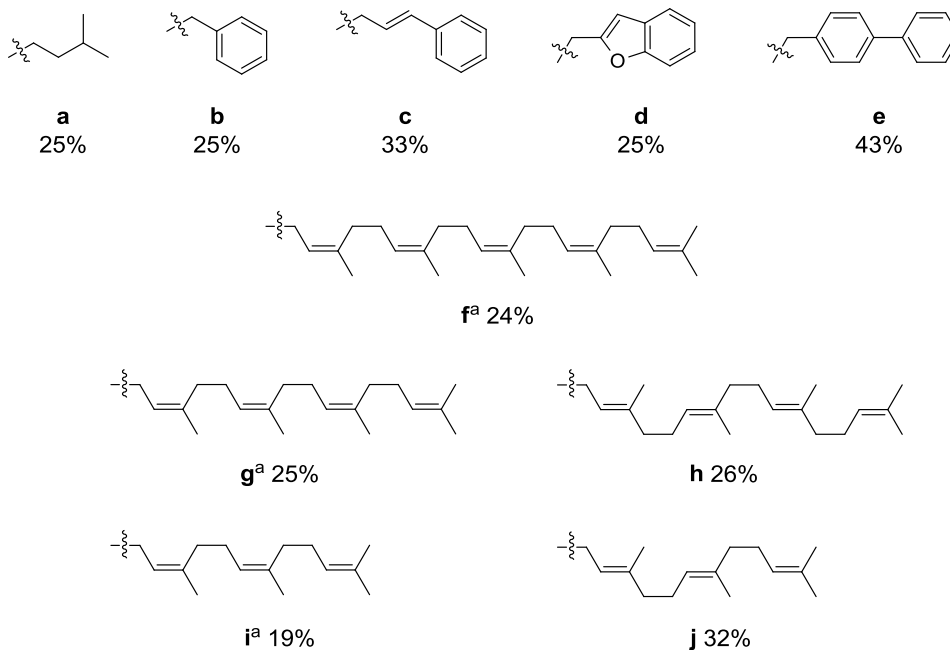
**Scheme 7.4.** (i) a)  $\text{NHEt}_2$ , AcOH, EtOH, 80 °C. b) CaO,  $\text{H}_2\text{O}$ , 70 °C. c) Amberlite IR 120 ion exchange resin  $\text{H}^+$  form,  $\text{H}_2\text{O}$ , 40 °C, 17% yield over 3 steps. d) TBSOTf, 2,6-lutidine, DMAP, DMF, THF, 85%. e) DIBAL-H, -78 °C, toluene 65%. (ii) f) BzCl, pyridine, DCM, reflux, 43%. g) DIBAL-H, -78 °C, THF, 17%. (iii) A plausible reaction pathway (suggested by Fleet *et al.*<sup>165,166</sup>) for the base-catalysed formation of **7.32** from **7.22**.

With tri-TBS protected lactol **7.19** in hand, the phosphoramidite-mediated installation of the anomeric phosphate was next investigated, employing the selected alcohols as coupling partners (Scheme 7.5; the *trans*-polyprenyl alcohol starting materials were commercially available whilst the *cis*-polyprenols were synthesised for the project by GVKBio). After chromatography, the protected intermediates **7.33a-j** were subject to desilylation. However, the use of ammonium fluoride (30 equivalents) in methanolic ammonium hydroxide (5%) as routinely performed by Lee and co-workers was not reproducible when

applied to C2-methylated riboses **7.33**. Under these conditions, benzyl substituted **7.33b** was converted to mono-desilylated **7.34** (confirmed by COSY NMR), after which no further deprotection occurred. Alternatively, treatment of per-TBS intermediates **7.33a-j** with TBAF did effect the global deprotections. The target compounds **7.1a-j** were afforded as the ammonium salts in moderate yields over the two steps, after column chromatography and cation exchange chromatography to remove persistent tetrabutylammonium salts.



**7.1, R'' =**



**Scheme 7.5.** a) R''OH, DIPEA, 2-cyanoethyl *N,N*-diisopropylchlorophosphoramidite **7.14**, DCM, then **7.19**, 1*H*-tetrazole. b) H<sub>2</sub>O<sub>2</sub>, THF, then 5% KOH in MeOH. c) TBAF, THF. The overall yields over steps a) – c) are indicated under the alcohol coupling partners. d) NH<sub>4</sub>F (30 equiv.), 15% NH<sub>4</sub>OH in MeOH, 55 °C, 60%. <sup>a</sup> The *cis*-polyprenyl alcohol starting materials were synthesised by GVKBio.

Whilst the phosphoramidite methodology gave final compounds **7.1a-j** exclusively as single anomers (>95% d.e.), stereochemical assignment was not trivial, as transient 1D NOE experiments did not provide unequivocal evidence for the relative stereochemistry at the

anomeric position. On irradiation of the C2-Me group of cinnamyl **7.1c**, NOEs were observed between the C2-Me and both the 1-H and 3-H protons, with relative integrations of 0.5 and 1.0 respectively (Fig. 7.4a). Irradiating the anomeric 1-H of **7.1c**, NOEs were observed between 1-H and both the 3-H and 4-H protons, with relative integrations of 0.7 and 1.0 respectively (Fig. 7.4b).

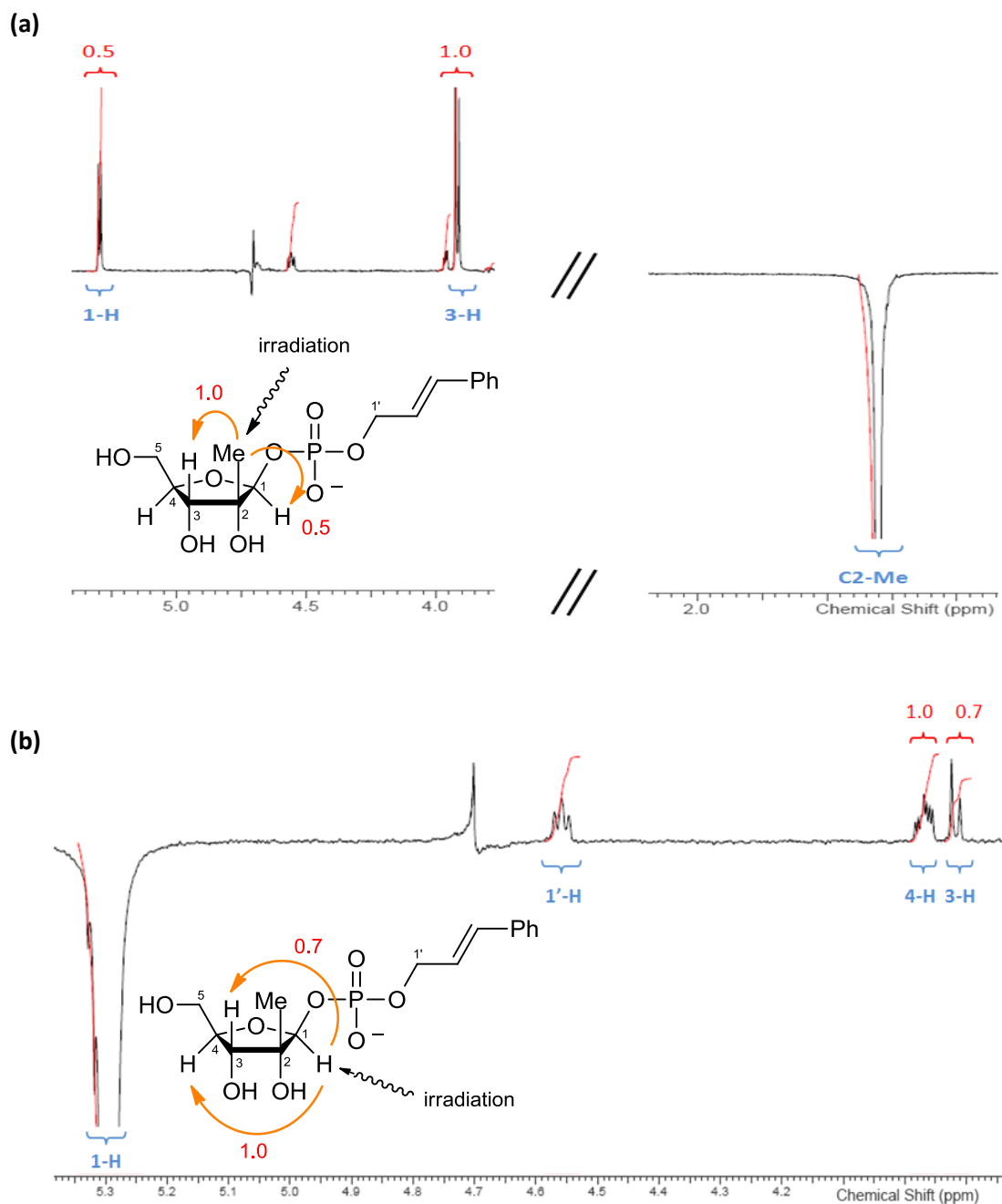


**Figure 7.4.** Transient NOEs observed when a) C2-Me and b) 1-H of **7.1c** were irradiated. Proton numbers are in blue, relative integrations are in red. The NMR solvent was D<sub>2</sub>O; exchangeable protons were not observed.

To aid with the stereochemical assignment at the anomeric position, computational modelling was used to investigate the lowest energy conformations of the possible  $\alpha$ - and  $\beta$ - ribose products. To this end, models of simplified 1-phosphate-C2-methyl riboses  $\alpha$ -7.35 and  $\beta$ -7.35 were generated using MOE<sup>147</sup> (performed by Sean Lynn; Fig. 7.5). The modelled distances between the anomeric 1-H and both the 3-H and 4-H protons were noted (Table 7.1).

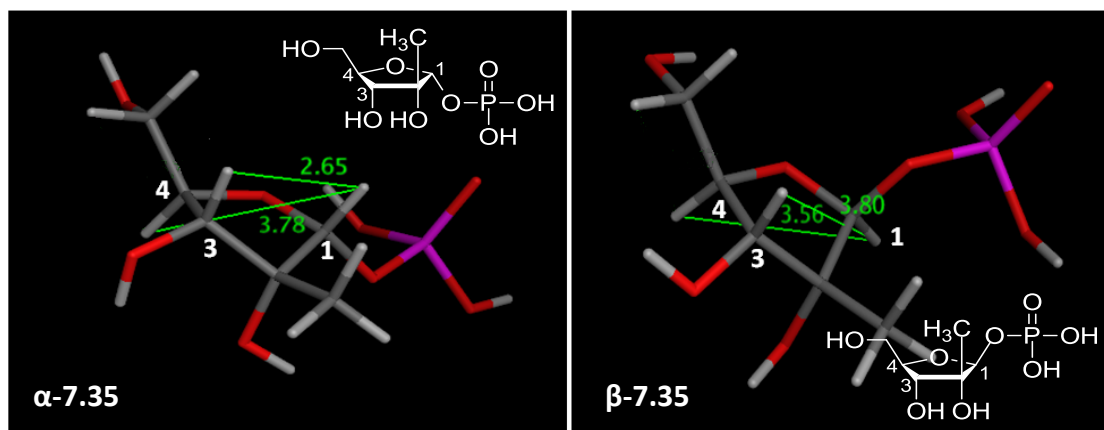


**Figure 7.5.** The lowest energy conformers of simplified 1-phosphate-C2-methylated riboses  $\alpha$ -7.35 and  $\beta$ -7.35 as calculated in MOE (MMFF94x force field). The computed 1H-3H and 1H-4H distances (Å) are shown in green font.

**Table 7.1a).** Energy-minimised geometries for the  $\alpha$ -7.35<sup>a</sup>

$\Delta E$ / Hartree	1H-3H distance / Å	1H-4H distance / Å
0.00	2.65	3.78
0.21	2.63	3.73
0.29	2.63	3.77

**Table 7.1b).** Energy-minimised geometries for the  $\beta$ -7.35<sup>a</sup>

$\Delta E$ / Hartree	H1-H3 distance / Å	H1-H4 distance / Å
0.00	3.80	3.56
0.19	3.80	3.55
0.47	3.80	3.58

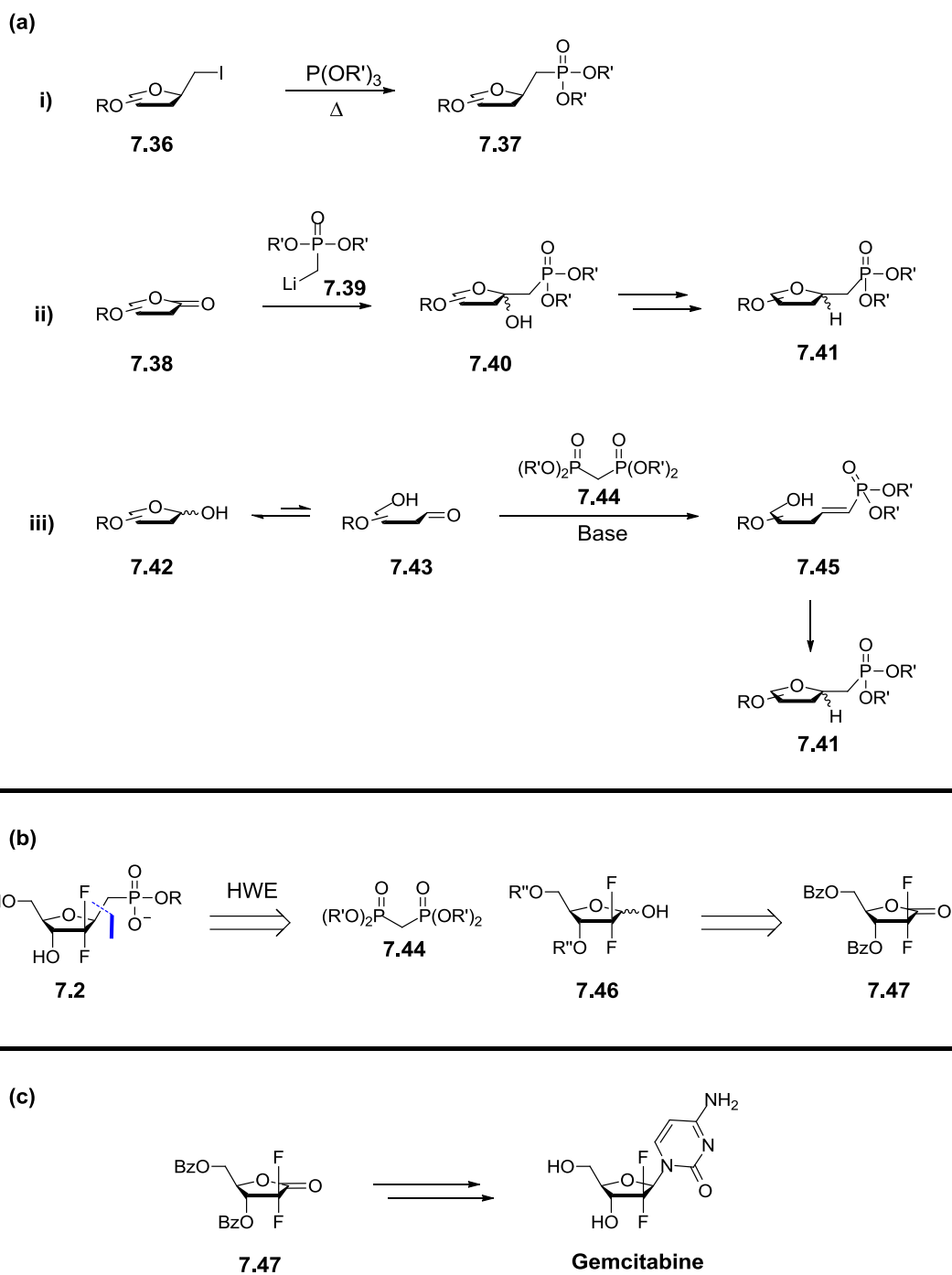
<sup>a</sup> Key: Energy minimisations for  $\alpha$ -7.35 and  $\beta$ -7.35 were calculated in MOE (by Sean Lynn) using an MMFF94x force field model.  $\Delta E$  refers to the energy difference relative to the lowest energy conformer.

The data in Tables 7.1a-b show that  $\alpha$ -**7.35** would expectedly have a short H1-H3 distance ( $\sim 2.65$  Å) and a considerably longer H1-H4 distance ( $\sim 3.78$  Å), whereas the epimer  $\beta$ -**7.35** would display similar H1-H3 and H1-H4 distances ( $\sim 3.80$  and  $3.56$  Å). Therefore, on irradiation of the anomeric proton, a much greater NOE enhancement of 3-H relative to 4-H would be expected for the  $\alpha$ -anomer. However, Figure 7.4b illustrates that the 3-H and 4-H NOE enhancements are roughly equal for cinnamyl **7.1c** (with relative integrals of 0.7 and 1.0), consistent with the modelled conformation of  $\beta$ -**7.35**. Due to the combination of this result and the literature precedent for 1,2-*trans* selectivity, compounds **7.1a-j** were assigned as the desired  $\beta$ -anomers. The modelled dihedral angles about the H-C3-C4-H bonds in both the  $\alpha$ - and  $\beta$ -anomers were between  $-157.3^\circ$  and  $-159.4^\circ$ , which was consistent with the observed coupling  $J_{\text{H3-H4}}$  of 8.3 Hz, adding extra confidence to the models.

## 7.4 Synthesis of the 2,2-Difluororibophosphonates 7.2

### 7.4.1 Synthetic Approaches towards Ribosyl-1-Phosphonates

Three main strategies have been reported for the synthesis of pentose-1-phosphonates: (i) an Arbuzov reaction with an appropriately halogenated pentose of desired anomeric configuration **7.36**<sup>167,168</sup>; (ii) condensation of the lithium anion of a methylphosphonate diester **7.39** with a lactone **7.38**, followed by deoxygenation<sup>169</sup> or dehydration and reduction<sup>170</sup>; and finally (iii) Horner-Wadsworth-Emmons reaction (HWE) between lactol **7.42** and a methylenebisphosphonate **7.44**<sup>171,172</sup> (followed by an intramolecular trapping of the resulting  $\alpha,\beta$ -unsaturated phosphonate diester **7.45**; Scheme 7.6a). The HWE approach was selected on the basis that it facilitated rapid access to the targeted ribosyl-1-phosphonates **7.2**. HWE disconnection of **7.2** gave lactol **7.46**, accessible from **7.47** (Scheme 7.6b), which is a commercially available synthesis intermediate of the cancer drug gemcitabine (Scheme 7.6c).<sup>173</sup>



**Scheme 7.7.** (a) Three approaches to the synthesis of glycosyl-1-phosphonates, *via*: i) an Arbuzov reaction, ii) condensation between lactone **7.38** and lithium anion **7.39**, iii) a HWE reaction. (b) Retrosynthetic analysis for the 2,2-difluororibophosphonates **7.2** *via* the HWE approach gave commercial lactone **7.47**. (c) Retrosynthesis target **7.47** is a commercially available synthesis intermediate of the cancer drug gemcitabine.<sup>173</sup>

## 7.4.2 Synthesis of Analogues 7.2a-f

A selective reduction of the commercially available ((2*R*,3*R*)-3-(benzoyloxy)-4,4-difluoro-5-oxotetrahydrofuran-2-yl)methyl benzoate **7.47** using Red-Al at -78 °C afforded the anomeric mixture of lactols **7.46** in 79% yield (Scheme 7.7).<sup>174</sup> The chemoselectivity for the lactone originated from the di-fluoro substitution alpha to the carbonyl, and the enforced *trans* orientation of the lactone<sup>175</sup> (Fig. 7.6), rendering this functionality much more electrophilic than the benzoyl ester protecting groups present in **7.47**.

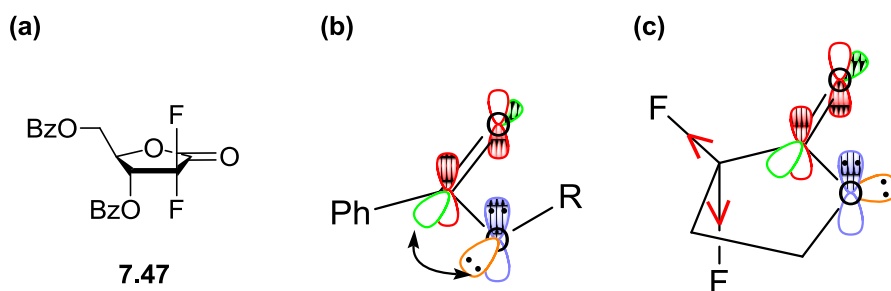
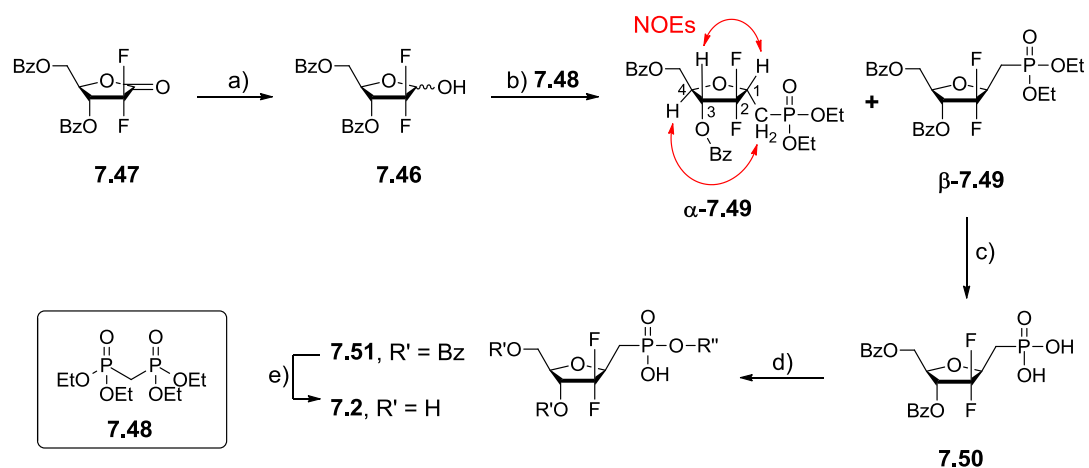
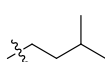


**Figure 7.6.** (a) The structure of **7.47**. (b) The ester is stabilised both by donation of a lone pair on oxygen (blue) into the C-O  $\pi^*$  orbital (red) and by donation of the second lone pair on oxygen (orange) into the C-O  $\sigma^*$  orbital (green). (c) Overlap of the 2<sup>nd</sup> lone pair on oxygen with the C-O  $\sigma^*$  orbital is not possible in the lactone as the ester functionality is constrained in a *trans* orientation. Additionally, the electron withdrawing fluorine substituents on C2 engender further electrophilicity to the lactone carbonyl.

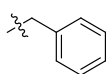
Subsequent Horner-Wadsworth-Emmons reaction between lactols **7.46** and methylenebisphosphonate **7.48** furnished the phosphonates  $\alpha$ -**7.49** and  $\beta$ -**7.49** after chiral chromatography in 23% and 30% yield respectively (Scheme 7.7). Anomeric configurations were assigned using 2-dimensional NOE experiments (Appendix A2). NOE enhancements between H-1 and H-3, and between the phosphonate  $\text{CH}_2$  and H-4, were characteristic of the  $\alpha$ -phosphonate  $\alpha$ -**7.49** (Scheme 7.7). Selective phosphonate ester hydrolysis of  $\beta$ -**7.49** with TMSBr then furnished the  $\beta$ -phosphonate di-acid **7.50** in 80% yield. Facile microwave-assisted one-pot reactions<sup>176</sup> between di-acid **7.50** and the selected alcohols subsequently afforded the mono-esters **7.51a-f** in 42-69% yields (of the poly prenyl analogues, only all-*cis* geranylgeranyl **7.2f** was synthesised for this template). Finally, selective benzoyl ester hydrolysis under mild conditions ( $\text{H}_2\text{O}/\text{MeOH}/\text{Et}_3\text{N}$ , 5:2:1, 3 days) gave the 2,2-difluororibophosphonates **7.2a-f** in moderate to good yields.



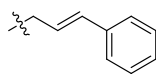
**7.51, 7.2, R'' =**



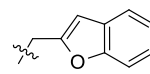
**a**, 67%, 72%



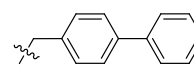
**b**, 69%, 73%



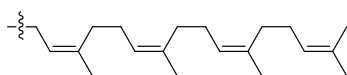
**c**, 69%, 37%



**d**, 47%, 59%



**e**, 42%, 58%

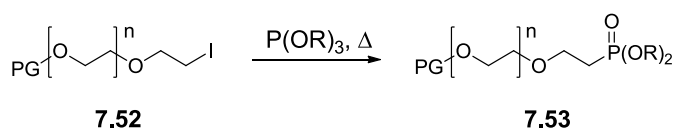


**f**<sup>a</sup>, 29%<sup>b</sup>

**Scheme 7.7.** a) Red-Al, THF, -78 °C, 79%. b) **7.48**, NaH, THF then **7.46**.  $\alpha$ -**7.49** = 23%,  $\beta$ -**7.49** = 30%. c) TMSBr, MeCN, 80%. d) R''OH, Cl<sub>3</sub>CCN, pyr., 90 °C,  $\mu$ -wave irradiation. e) MeOH, H<sub>2</sub>O, NEt<sub>3</sub> 5:2:1, 3 days. Yields for steps d) and e) are shown below the alcohol coupling partners.<sup>a</sup> The *cis*-polyprenyl alcohol starting material was synthesised by GVKBio.<sup>b</sup> Yield over 2 steps from **7.50**.

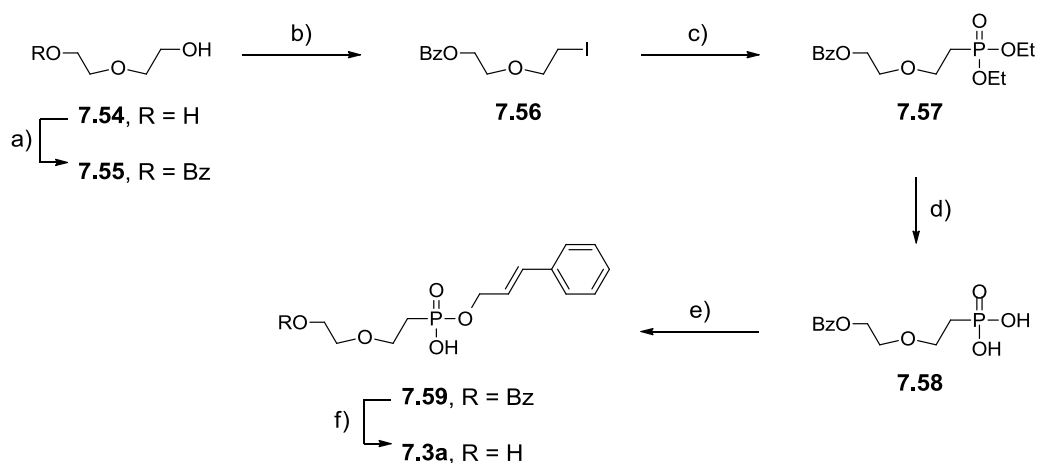
## 7.5 Synthesis of the Acyclic Sugar-Phosphonates 7.3

Many syntheses of phosphonate-substituted polyethylene glycols **7.53** have been reported in the literature, widely adopting an Arbuzov reaction of readily accessible iodinated precursors **7.52** as the key transformation (Scheme 7.8).<sup>177,178</sup>



**Scheme 7.8.** Generalised synthetic strategy for the generation of phosphonate-substituted polyethylene glycols that is widely adopted in the literature. PG = protecting group.

To exploit this methodology, synthesis of the designed acyclic sugar phosphonates **7.3** initiated with the mono-benzoylation of oxydiethanol **7.54**, followed by iodination of the remaining unprotected alcohol<sup>179</sup> to afford iodide **7.56** (Scheme 7.9). An Arbuzov reaction between iodide **7.56** and triethyl phosphite then gave phosphonate diester **7.57** in 95% yield. Subsequent treatment of **7.57** with TMSBr selectively hydrolysed the phosphonate esters to afford the di-acid **7.58** in quantitative yield. Employing the same microwave assisted phosphonate mono-ester synthesis as reported above,<sup>176</sup> cinnamyl alcohol was coupled with di-acid **7.58** to give product **7.59** in 51% yield. Only the cinnamyl analogue **7.3a** was synthesised for this series as emerging SAR indicated this scaffold would not likely yield active analogues (*vide infra*). To complete the synthesis, selective deprotection of the benzoate ester was achieved under mild conditions (H<sub>2</sub>O/MeOH/Et<sub>3</sub>N, 5:2:1, 3 days), affording acyclic sugar phosphonate **7.3a** in 50% yield.



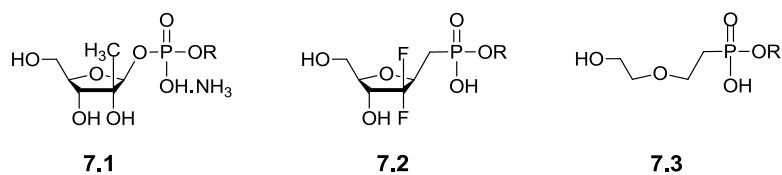
**Scheme 7.9.** a) BzCl, pyr., DCM, 70%. b) PPh<sub>3</sub>, imidazole, I<sub>2</sub>, DCM, 75%. c) P(OEt)<sub>3</sub>, 120 °C, 95%. d) TMSBr, MeCN, 100%. e) cinnamyl alcohol, Cl<sub>3</sub>CCN, pyr., 90 °C,  $\mu$ wave irradiation, 51%. f) MeOH, H<sub>2</sub>O, NEt<sub>3</sub> 5:2:1, 3 days, 50%.

## 7.6 Evaluation of the Substrate Analogues 7.1-7.3 as Inhibitors of

### DprE1

Upon completion of the syntheses of the proposed substrate analogues, these compounds were tested for activity against DprE1 in the fluorescence biochemical assay at high concentration (1 mM, unless otherwise stated in Table 7.2). The potency data for **7.1-7.3** are reported in Table 7.2.

**Table 7.2.** Potency data for the substrate analogues **7.1-7.3**.



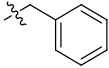
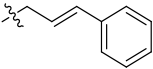
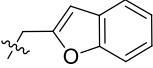
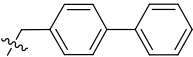
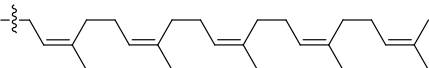
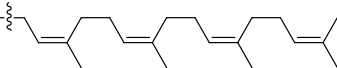
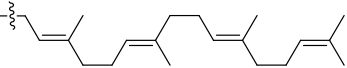
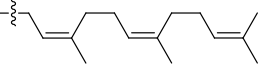
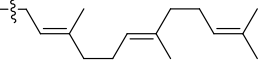
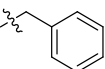
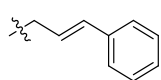
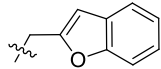
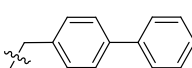
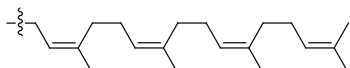
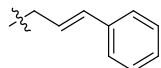
Ribose Template	Analogue	R	pIC <sub>50</sub> [IC <sub>50</sub> ] <sup>a</sup>
7.1	a		<3.0
7.1	b		<3.0
7.1	c		<3.3 <sup>b</sup>
7.1	d		<3.0
7.1	e		<3.0
7.1	f <sup>c</sup>		3.6 [251 μM]
7.1	g		3.6 [251 μM] <sup>d</sup>
7.1	h		<3.3 <sup>e</sup>
7.1	i		<3.0
7.1	j		<3.0

Table continued overleaf.

Table 7.2 continued from overleaf.

Ribose Template	Analogue	R	pIC <sub>50</sub> [IC <sub>50</sub> ] <sup>a</sup>
7.2	a		4.0 [100 μM]
7.2	b		3.2 [631 μM] <sup>d</sup>
7.2	c		4.2 [63 μM]
7.2	d		3.5 [316 μM] <sup>d</sup>
7.2	e		4.2 [63 μM] <sup>d</sup>
7.2	f <sup>c</sup>		3.8 [158 μM]
7.3	a		<3.0

<sup>a</sup> Activities measured in the DprE1 fluorescence assay. <sup>b</sup> On 1 test occasion out of 8 a curve was fitted (pIC<sub>50</sub> = 3.2). <sup>c</sup> Compound screened at 0.5 mM. <sup>d</sup> Compound tested as pIC<sub>50</sub> < 4 in 2 out of 2 test occasions when screened at 0.1 mM. <sup>e</sup> On 1 test occasion out of 6 a curve was fitted (pIC<sub>50</sub> = 3.5).

Of the C2-methylated ribose analogues **7.1**, all the compounds bearing the smaller, non-isoprenyl substituents **7.1a-e** were inactive against DprE1. Furthermore, the farnesyl analogues **7.1i** and **7.1j** and the *trans*-configured geranylgeranyl **7.1h** also showed no quantifiable activity. The longer *cis*-configured polyprenyl analogues geranylgeranyl **7.1g** and pentaprenyl **7.1f** however, were active at DprE1 with high micromolar IC<sub>50</sub> values (251 μM). Conversely, all of the synthesised 2,2-difluororibophosphonates **7.2** exhibited measurable DprE1 inhibitory activity. Cinnamyl **7.2c** and biphenyl **7.2e** were the most potent analogues in this series (IC<sub>50</sub> = 63 μM), and were approximately twofold more active than the geranylgeranyl analogue **7.2f** (IC<sub>50</sub> = 158 μM). Finally, cinnamyl substituted acyclic derivative **7.3a** did not show any activity at DprE1.

The above data revealed that the 2,2-difluororibophosphonate scaffold **7.2** showed greater inhibitory potential than the C2-methylated riboses **7.1** and acyclic derivative **7.3a**, as all analogues in this series **7.2a-f** showed quantifiable activity against DprE1. Whilst it is difficult to rationalise this observation in the absence of a DprE1 crystal structure liganded with substrate or a substrate analogue, it is known that polyfluorinated sugar analogues tend to bind to their target with greater affinity than their hydroxylated analogues.<sup>180</sup> This effect is due to contributions from hydrophobic desolvation of the more lipophilic fluorinated congeners,<sup>181</sup> and the potential to form dipolar interactions mediated by the C-F bonds.<sup>182</sup> Furthermore, the CF<sub>2</sub> group will likely influence the solution-phase conformation of riboses **7.2** via the fluorine *gauche* effect,<sup>183,184</sup> which may improve shape complementarity with the protein thus enhancing activity.

The potency data for the C2-methylated riboses **7.1** indicated that for this series, DprE1 activity was only achieved when the ribose motif was substituted with prenyl functionality of sufficient length: the farnesyl analogues **7.1i** and **7.1j** were inactive whilst the longer *cis*-configured analogues geranylgeranyl **7.1g** and pentaprenyl **7.1f** were active. This suggested that for the C2-methylated riboses **7.1**, activity was not derived from directional polar interactions associated with contact between the ribose motif and DprE1, but rather from lipophilic contact between the ribose substituent and the protein. This order of activity was not observed for the 2,2-difluororibophosphonates **7.2** however: shorter analogues cinnamyl **7.2c** and biphenyl **7.2e** were two-fold more potent than geranylgeranyl **7.2f**, perhaps indicating a different binding mode for this series.

In summary, the data presented herein show that substrate analogues can act as DprE1 inhibitors, albeit with rather weak potency.

## 7.7 DprE1 Substrate Analogues as Tools for Chemical Biology

It was envisioned that the prenyl-substituted substrate-analogues **7.1g-j** could have utility as investigative chemical biology tools. With these tools, we wanted to:

- i) Explore the effect in other assays of prenyl substituent length and geometric isomerism on the binding of the 2-methyl-1-phosphoryl-β-D-ribofuranoses **7.1**;
- ii) Further probe the binding requirements of small molecule DprE1 inhibitors.

## 7.7.1 Thermal Shift Experiments Show that Binding of Substrate Analogues

### 7.1g-j Correlates with Prenyl Substituent Length and Geometric Isomerism

A *ThermoFAD*<sup>185</sup> assay was developed (by Peter Francis at GSK) to investigate the effect of prenyl substituent length and geometric isomerism on the binding of substrate analogues **7.1g-j**. A *ThermoFAD* assay is a biophysical thermal shift experiment that monitors the increase in fluorescence signal of a flavoprotein's cofactor during thermal denaturation, allowing measurement of the thermal melt temperature ( $T_m$ ; Fig. 7.7 illustrates a schematic representation of *ThermoFAD*).<sup>185</sup> Ligands that have affinity for the protein may cause a stabilising or destabilising effect upon binding to the protein, leading to an increase or decrease in melt temperature respectively. Consequently, thermal shift assays have been used to screen libraries of potential ligands for drug targets.<sup>186</sup>

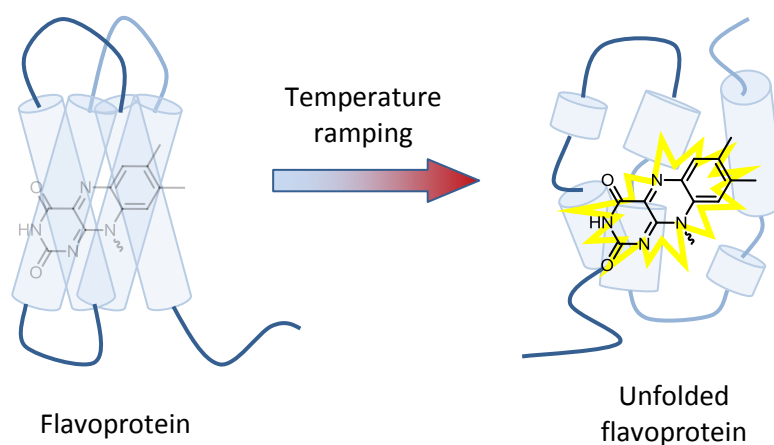


**Figure 7.7.** Schematic for a *ThermoFAD* thermal shift experiment.<sup>185</sup> FAD fluorescence is quenched by the protein environment when the flavoprotein is folded; FAD fluorescence increases as the protein unfolds.<sup>185</sup>

The DprE1  $T_m$  shift assay was performed (by Peter Francis at GSK) using three protocols:

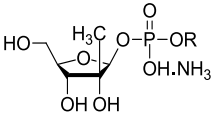
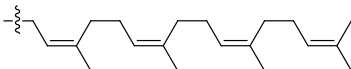
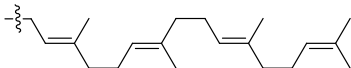
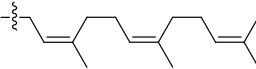
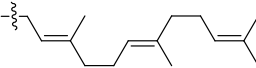
- a) addition of each compound **7.1g-j** only to DprE1;
- b) pre-incubation of DprE1 with oxidisable substrate surrogate *E*-GGPR (all-*trans*-geranylgeranylphosphoryl- $\beta$ -D-ribose), followed by addition of each compound **7.1g-j**;
- c) pre-incubation of DprE1 with each compound **7.1g-j**, followed by addition of substrate surrogate *E*-GGPR.

Table 7.3 displays the results.

**Table 7.3.** DprE1 thermal shift data for compounds **7.1g-j**. The  $T_m$  shift experiments were performed by Peter Francis. Values in red indicate a significant shift from the  $T_m$  of the native DprE1 protein.

		$T_m$ ( $^{\circ}\text{C}$ )	$\Delta T_m$ ( $^{\circ}\text{C}$ )
Native DprE1		43.25	-
DprE1 + <i>E</i> - <b>GGPR</b>		42.99	-0.26

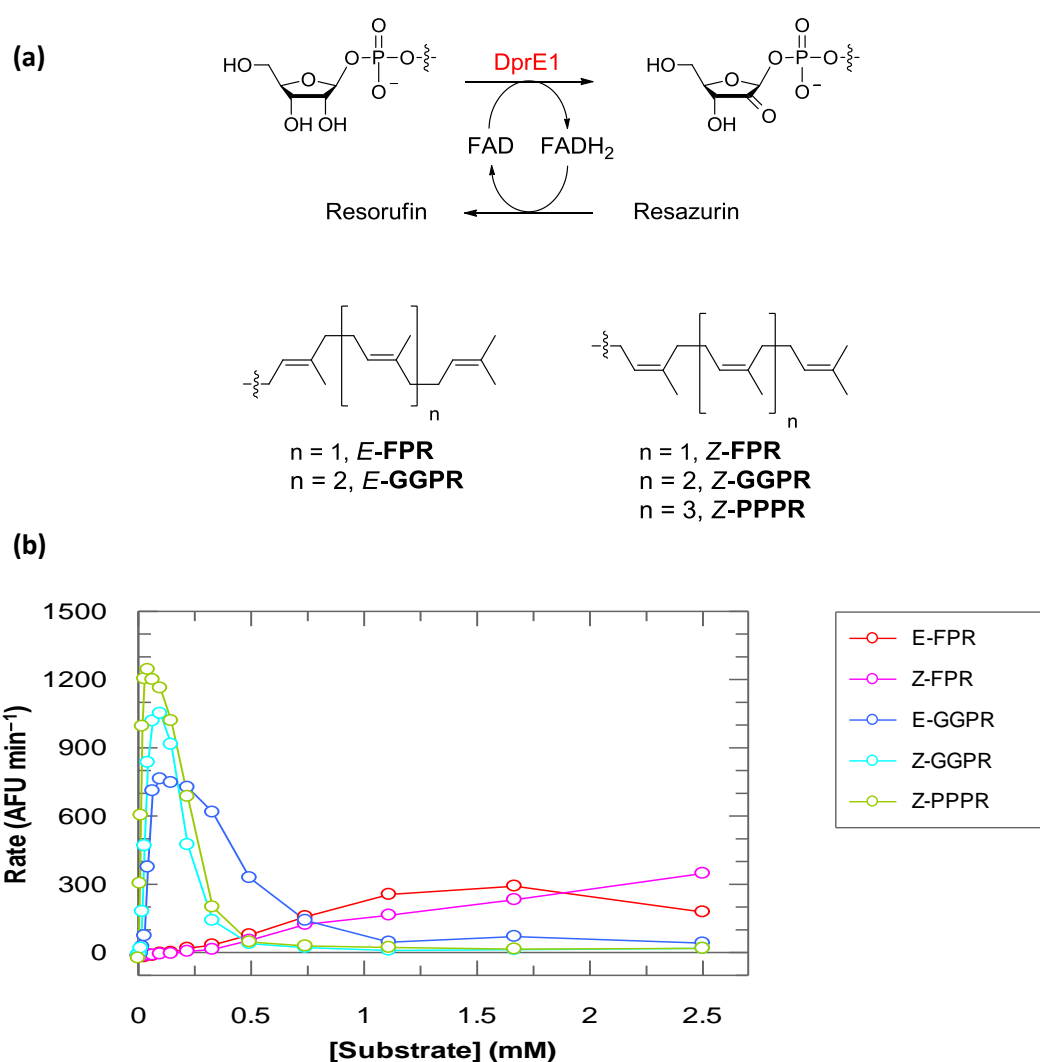
  

	Experiment protocol		
	a)	b)	c)
R=	$\Delta T_m$ ( $^{\circ}\text{C}$ )	$\Delta T_m$ ( $^{\circ}\text{C}$ )	$\Delta T_m$ ( $^{\circ}\text{C}$ )
<b>7.1g</b> 	-3.24	-6.60	-6.71
<b>7.1h</b> 	-0.75	-3.01	-4.40
<b>7.1i</b> 	0.01	-0.73	-0.67
<b>7.1j</b> 	-0.35	-0.38	-0.68

The  $T_m$  shift data in Table 7.2 show that the presence of oxidisable *E*-**GGPR** caused no significant change to the DprE1 thermal melt temperature ( $\Delta T_m = -0.26$   $^{\circ}\text{C}$ ). Non-oxidisable C2-methyl geranylgeranyl **7.1g** and **7.1h** however, did cause a significant decrease in  $T_m$  (indicating a destabilising effect on binding), where all-*cis* **7.1g** caused a greater perturbation. Notably, the magnitude of these shifts was greater in the presence of **GGPR**. Conversely, the shorter farnesyl analogues **7.1i** and **7.1j** had no significant effect on the DprE1 melt temperature. These results indicated that both prenyl substituent length and geometric isomerism were important factors in the binding of the 2-methyl-1-phosphoryl- $\beta$ -D-ribofuranoses **7.1**, suggesting that longer, *cis*-configured prenyl substitution was favourable. This result mirrored the inhibitory activity data for this series **7.1** (Table 7.2): the only analogues that showed measurable activity at DprE1 were the *cis*-configured geranylgeranyl **7.1g** and pentaprenyl **7.1f**, whilst *trans*-geranylgeranyl **7.1h** and the shorter-chain analogues were inactive.

This outcome should be compared to a more recent kinetics analysis investigating the rate of catalytic turnover for oxidisable DprE1 substrates with varied polyprenyl substituents

(this experiment was developed and run by Argyrides Argyrou at GSK; Fig. 7.8a illustrates the assay biochemistry). The data (Fig. 7.8b) show that the initial reaction velocity increased as the prenyl substituent was lengthened, and the *cis*-configured **Z-GGPR** provided a further enhancement in rate over the *trans*-configured **E-GGPR** (in all cases an inhibitory effect was observed at higher concentrations, dependant on isoprenyl substitution length). It was logical to equate the increased velocity with enhanced recognition and binding; these results therefore corroborated the  $T_m$  shift assay data, confirming a preference for longer, *cis*-configured prenyl substituents.



**Figure 7.8.** (a) The enzymatic assay used to investigate the turnover of the oxidisable substrate analogues. The increase in fluorescence signal of resorufin was proportional to substrate turnover rate (*cf.* the DprE1 primary screening assay; Sect. 4.1). This assay was developed and performed by Argyrides Argyrou at GSK. The oxidisable substrates were synthesised by Ben Whitehurst (data not included) and Monica Cacho-Izquierdo at GSK. (b) Plot of rate (AFU min<sup>-1</sup>) versus substrate concentration. AFU = arbitrary fluorescence units.

The observations from the  $T_m$  shift assay and kinetics experiments could be explained by two theories. Physiologically, **DPR** is embedded in the cell membrane.<sup>92</sup> Analogues bearing a longer prenyl substituent may better incorporate into the detergent micelles present under the various assay conditions, presenting the ribose head to the enzyme in a manner more similar to the physiological scenario. Alternatively, it could be that a longer, *cis*-configured prenyl substituent is required to position the ribose motif a sufficient depth into the active site to correctly align the sugar at the ribose binding site. These theories however, and the importance of prenyl substitution length, remain speculative as the 2,2-difluororibophosphonate analogue **7.2f** bearing the *cis*-geranylgeranyl substituent was less potent than the shorter cinnamyl and biphenyl derivatives, **7.2c** and **7.2e** (Table 7.2).

The kinetics data in Fig. 7.8b also suggested a third theory pertaining to the binding of substrate analogues. At high concentrations, the oxidisable analogues were themselves inhibitory, suggesting that these substrates could bind in a non-productive manner (e.g. as illustrated in Fig. 7.9). This may suggest therefore, that the substrate analogues designed as inhibitors of DprE1 show inhibitory activity through non-specific binding interactions, rather than through directional contact with the hydrophilic ribose core.

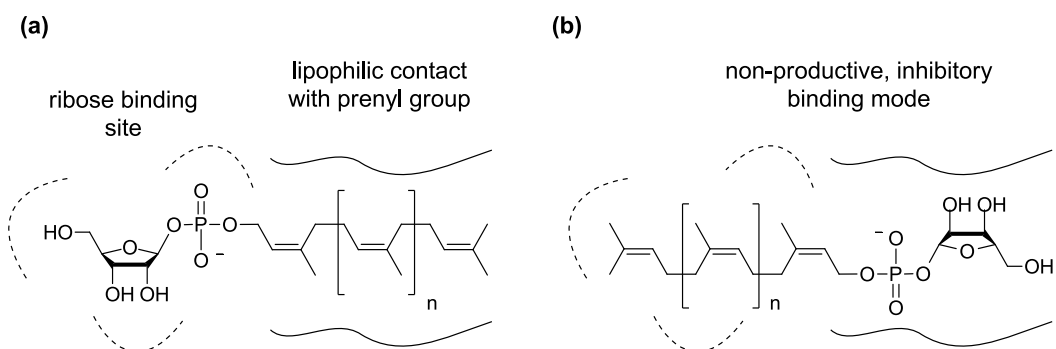


**Figure 7.9.** (a) A productive binding mode of an oxidisable DprE1 substrate in which the ribose occupies the ribose binding site (indicated with dashed lines). (b) A non-productive binding mode, in which the prenyl group occupies the ribose binding site.

### 7.7.2 Substrate Turnover is Not a Binding Pre-requisite for Small Molecule Inhibitors that Bind to DprE1 Only in the Presence of Oxidisable Substrate

During the course of the work to identify small molecule DprE1 inhibitors, it was discovered that some compounds only bound to DprE1 in the presence of oxidisable substrate, and not in its absence.<sup>118</sup> This raised the question of whether oxidative turnover of the substrate

was necessary for the binding of these DprE1 inhibitors. By analogy, it was recently reported that the binding affinity of a novel *M.tb* enoyl-acyl carrier protein reductase (InhA) inhibitor was highly dependent on the oxidation state of the NAD cofactor. Isothermal titration calorimetry showed the inhibitor interacted only weakly with the NAD<sup>+</sup>-bound form of InhA (9.3 μM), but was a tight-binding inhibitor of the NADH-bound form (13.7 nM).<sup>187</sup>

One such DprE1 inhibitor that bound only in the presence of oxidisable substrate was thiadiazole **7.60** (Fig. 7.10). Compound **7.60** caused a dose-dependent quenching of the FAD cofactor fluorescence<sup>118</sup> in the presence of oxidisable *E*-FPR (Fig. 7.10, purple triangles), suggesting inhibitor binding. In the absence of *E*-FPR however, no FAD quenching was observed, suggesting **7.60** did not bind under these conditions (Fig. 7.10, red circles). When *E*-FPR was replaced with non-oxidisable substrates **7.1g**, **7.1h** or **7.1j** however, quenching of the FAD fluorescence was again observed (Fig. 7.10; this effect was not observed in the presence of *cis*-farnesyl **7.1i**).

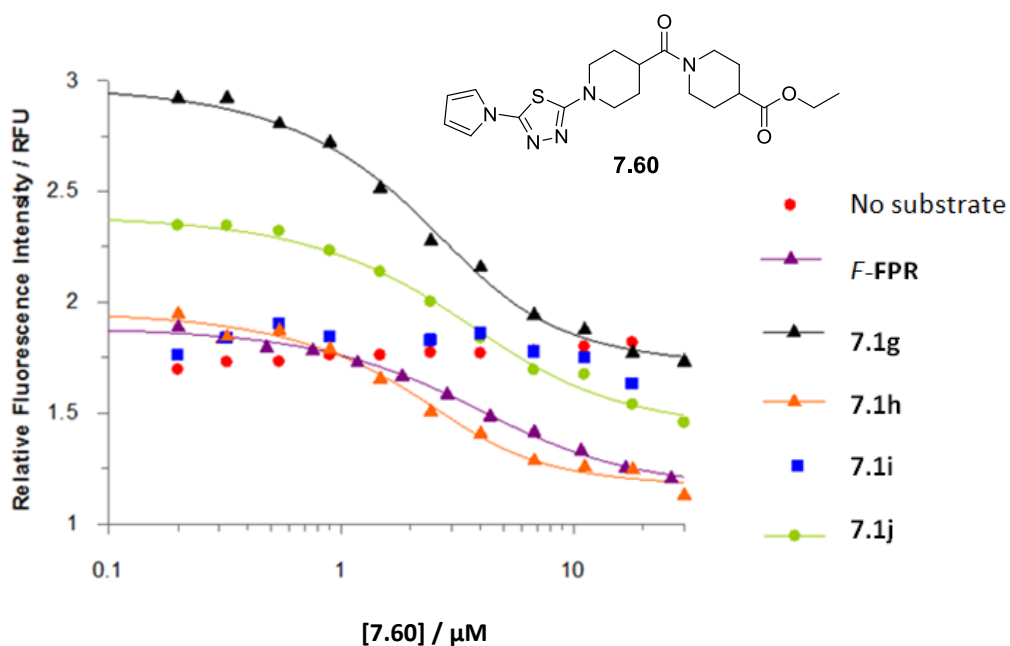


**Figure 7.10.** A dose-dependent fluorescence quench was observed on binding of **7.60** to DprE1 in the presence of *E*-FPR. No such fluorescence quench was observed in the absence of substrate or substrate analogue; fluorescence quenching was observed however in the presence of **7.1g**, **7.1h** and **7.1j**. The assay<sup>118</sup> was developed by Jon Hutchinson and the experiments were performed by Christopher Stubbs at GSK.

These results suggested that catalytic turnover is not a pre-requisite to the binding of DprE1 inhibitors that had only demonstrated binding in the presence of substrate, rather it is merely the presence of the substrate that is necessary. This perhaps indicates an equilibrium process, whereby the substrate must first provide access to the active site *via* disordering of the proximal flexible loops (Sect. 3.3) before the inhibitor **7.60** is able to bind to DprE1. Notably, the HTS hit **GSK'896** described in Chapter 6 only bound to DprE1 in the presence of substrate (*E-FPR*).

## 7.8 Conclusions

This chapter reported the rational design and synthesis of potential DprE1 inhibitors based on the substrate of the enzyme: the 2-methyl-1-phosphoryl- $\beta$ -D-ribofuranoses **7.1**, the 2,2-difluororibophosphonates **7.2**, and the acyclic ribose **7.3a**. Both series **7.1** and **7.2** yielded active DprE1 inhibitors. Notably, the 2,2-difluororibophosphonate scaffold **7.2** afforded modestly potent analogues cinnamyl **7.2c** and biphenyl **7.2e**, which both displayed micromolar activity ( $IC_{50} = 63 \mu\text{M}$ ; Fig. 7.11).

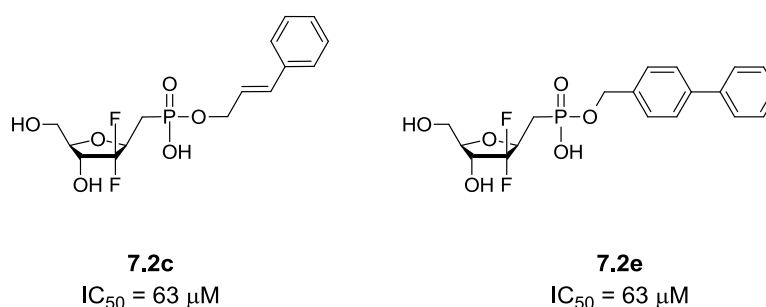


**Figure 7.11.** DprE1 substrate analogues **7.2c** and **7.2e** showed the most potent DprE1 inhibitory activity.

The 2-methyl-1-phosphoryl- $\beta$ -D-ribofuranoses **7.1** were used as tool compounds in chemical biology experiments.  $T_m$  shift experiments revealed that the binding of the C2-methylated analogues **7.1** was enhanced when the ribose motif was functionalised with longer, *cis*-configured prenyl functionality, providing rationale as to why the shorter substrate analogues **7.1a-e** did not exhibit activity against DprE1. The importance of prenyl substitution length and isomerism was also highlighted in experiments investigating the kinetics of oxidisable substrate turnover.

The polyprenyl substituted analogues of C2-methylated **7.1g-j** were also employed to probe the binding interactions of small molecule DprE1 inhibitors. These experiments revealed

that oxidative turnover of the substrate was not a pre-requisite to the binding of DprE1 inhibitors that only bound in the presence of substrate. This result suggested it was merely the presence of substrate that was required for inhibitor binding, probably to facilitate access to a particular protein conformer in which the flexible loops were disordered, providing the inhibitor access to the active site.

## 7.9 Future Work

No resolved crystal structure of DprE1 liganded with substrate is currently available. This structural information would be highly beneficial to the understanding of the enzyme mechanism and biochemistry, and would aid future DprE1 drug discovery efforts. In particular, a crystal structure of DprE1 liganded with substrate could help clarify why certain DprE1 inhibitors require the presence of a substrate analogue to bind to the enzyme. The 2-methyl-1-phosphoryl- $\beta$ -D-ribofuranoses **7.1f-h** and 2,2-difluororibophosphonates **7.2a-f** which showed modest activity at DprE1 represent potential non-oxidisable tools with which to attempt co-crystallisation studies. Whilst efforts to co-crystallise these analogues have been attempted unsuccessfully with *M.tb* DprE1, our laboratory has recently started experimenting with other DprE1 constructs, such as the *M.Smeg* ortholog, which may facilitate successful crystallography. Efforts to generate crystals of DprE1 liganded with substrate analogues **7.1** and **7.2** are thus ongoing.

Work recently reported by Vincent and colleagues suggested another possible substrate analogue to investigate as a DprE1 inhibitor.<sup>180</sup> They reported that a tetra-fluoro UDP-galactofuranose analogue **7.61** showed significantly higher affinity for the bacterial enzyme UDP-galactopyranose mutase (UGM) than the natural hydroxylated substrate UDP-galactofuranose (UDP-Galf; Fig. 7.12).<sup>180</sup> Whilst the origin of this binding phenomenon was unclear, the authors attributed the heightened affinity to the replacement of two adjacent galactofuranose hydroxymethylene groups for two CF<sub>2</sub> groups. As the 2,2-difluororibophosphonate scaffold **7.2** showed the greatest DprE1 inhibitory potential of the three designed DprE1 substrate analogues **7.1-7.3**, it would be interesting to study the inhibitory potential of a tetrafluorinated analogue **7.62**. Moreover, this would facilitate an investigation into whether the benefit of glycosyl hydroxyl replacement with CF<sub>2</sub> groups was additive.

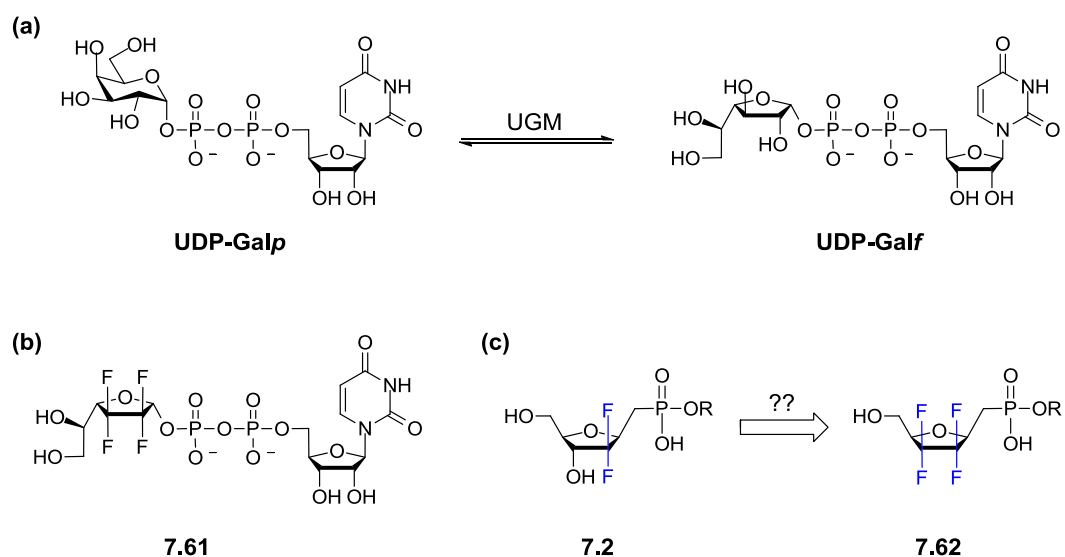


**Figure 7.12.** (a) UDP-galactopyranose mutase (UGM) catalyses the interconversion between UDP-Galp (UDP-galactopyranose) and UDP-Galf (UDP-galactofuranose). (b) Tetrafluorinated UDP-Galf **7.61** had a significantly greater affinity for UGM than the natural substrate UDP-Galf. (c) Tetrafluorinated DprE1 substrate analogue **7.62** may be a better DprE1 inhibitor than difluoro-**7.2**.

## 8. *N*-Acetylglucosamine-1-Phosphate

### Uridyltransferase

*Mycobacterium tuberculosis* *N*-acetylglucosamine-1-phosphate uridyltransferase (*M.tb* GlmU) has recently been identified as a potential drug target for the development of antitubercular medicines with a novel mode of action. GlmU is a bifunctional enzyme involved in the synthesis of an important biosynthetic intermediate required for cell wall peptidoglycan biosynthesis (uridine diphosphate *N*-acetylglucosamine, UDP-GlcNAc),<sup>188</sup> and is essential for optimal mycobacterial growth.<sup>189,190</sup>

#### 8.1 Structure and Biosynthesis of Peptidoglycan

Peptidoglycan (PG) is a heavily cross-linked polymer that is found almost ubiquitously amongst bacteria. The primary function of PG is to rigidify the bacterial cell to withstand osmotic pressure from within, whilst providing a scaffold upon which other structures are supported (Sect. 1.3).<sup>191</sup> PG is essential for mycobacterial cell viability: lack of peptidoglycan results in cell swelling and rupture.<sup>192</sup>

The structure of *M.tb* PG is similar to that of other bacteria, comprising cross-linked chains of alternating  $\beta$ -(1,4) linked *N*-acetylglucosamine residues (GlcNAc) and modified muramic acid residues (Fig. 8.1a).<sup>191</sup> The muramic acid residues are typically *N*-acetylated (*N*-acetylmuramic acid; MurNAc); however, uniquely in mycobacteria they may instead be *N*-acetylated with glycolic acid<sup>193</sup> (*N*-glycolylmuramic acid; MurNGlyc). The muramic acid residues are further modified *via* functionalisation with a short peptide chain. In nascent PG, the peptide is most commonly L-alanyl- $\gamma$ -D-glutamyl-(meso)diaminopimelyl-D-alanyl-D-alanine (Fig. 8b), but one or both of the terminal alanine residues may be lost in mature PG.<sup>192</sup> Peptidic bonds between either two (meso)diaminopimelic acid (DAP) residues, or between a D-alanine residue and a DAP residue form the cross-linkages between different PG strands.<sup>194</sup> Finally, the C6 hydroxyl group of some of the muramic acid residues are linked to arabinogalactan (AG) *via* a phosphodiester bond and a rhamnose-*N*-acetylglucosamine linker<sup>195</sup> (Fig. 3.1; Sect. 3.1).

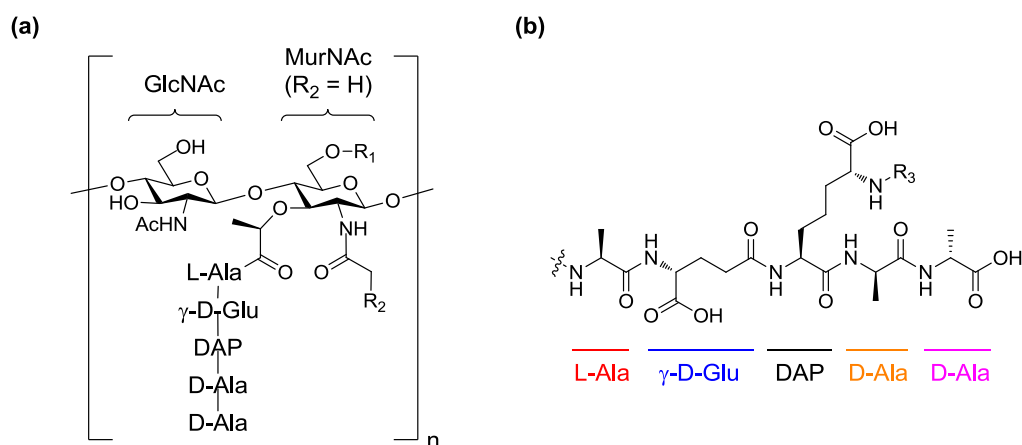


**Figure 8.1.** (a) The structure of a representative monomer of mycobacterial peptidoglycan (prior to peptide trimming).  $R_1 = \text{H}$  or phosphodiester rhamnose-*N*-acetylglucosamine linkage to arabinogalactan;  $R_2 = \text{H}$  (MurNAc) or OH (MurNGlyc). (b) The structure of the pentapeptide chain (prior to peptide trimming).  $R_3 = \text{H}$ , or cross-linked to the penultimate D-Ala or the D-centre of another DAP residue. In mature PG, one or both of the terminal D-Ala residues will be absent. DAP = (meso)diaminopimelic acid.

The genes responsible for the synthesis of PG in *M.tb* are arranged very similarly to those of other bacteria.<sup>196</sup> It is expected therefore, that mycobacterial biosynthesis of PG will be similar to that of bacterial PG, which has been well-characterised.<sup>197</sup> In the first committed steps of PG biosynthesis, uridine diphosphate *N*-acetylglucosamine (UDP-GlcNAc) is converted to uridine diphosphate *N*-acetylmuramic acid (UDP-MurNAc) by the consecutive actions of transferase MurA and reductase MurB (Fig. 8.2, step 1). The UDP-MurNAc pentapeptide is then generated through the sequential addition of amino acid residues onto the lactoyl group of UDP-MurNAc, catalysed by a series of synthetase enzymes (MurC, MurD, MurE and MurF; Fig. 8.2, step 2). Translocase MraY then catalyses the transfer of the phosphoMurNac pentapeptide moiety of UDP-MurNAc pentapeptide to a membrane-bound lipid carrier (decaprenyl phosphate in *M.tb*<sup>198</sup>) to yield Lipid I (Fig. 8.2, step 3). Lipid II is subsequently generated by the addition of a unit of GlcNAc (from UDP-GlcNAc), catalysed by the transferase MurG (Fig. 8.2, step 4). An as yet unidentified “flippase” is then believed to transport Lipid II from the cytoplasmic face of the cell membrane to the periplasmic face (Fig. 8.2, step 5). Transglycosylation then occurs through the transfer of the disaccharide pentapeptide to a growing PG chain with the loss of the polyprenyl lipid carrier (Fig. 8.2, step 6). Finally, transpeptidation reactions catalysed by a variety of penicillin-binding proteins (PBPs) form the cross-linkages between separate glycan strands generating cross-linked PG (Fig. 8.2, step 7).

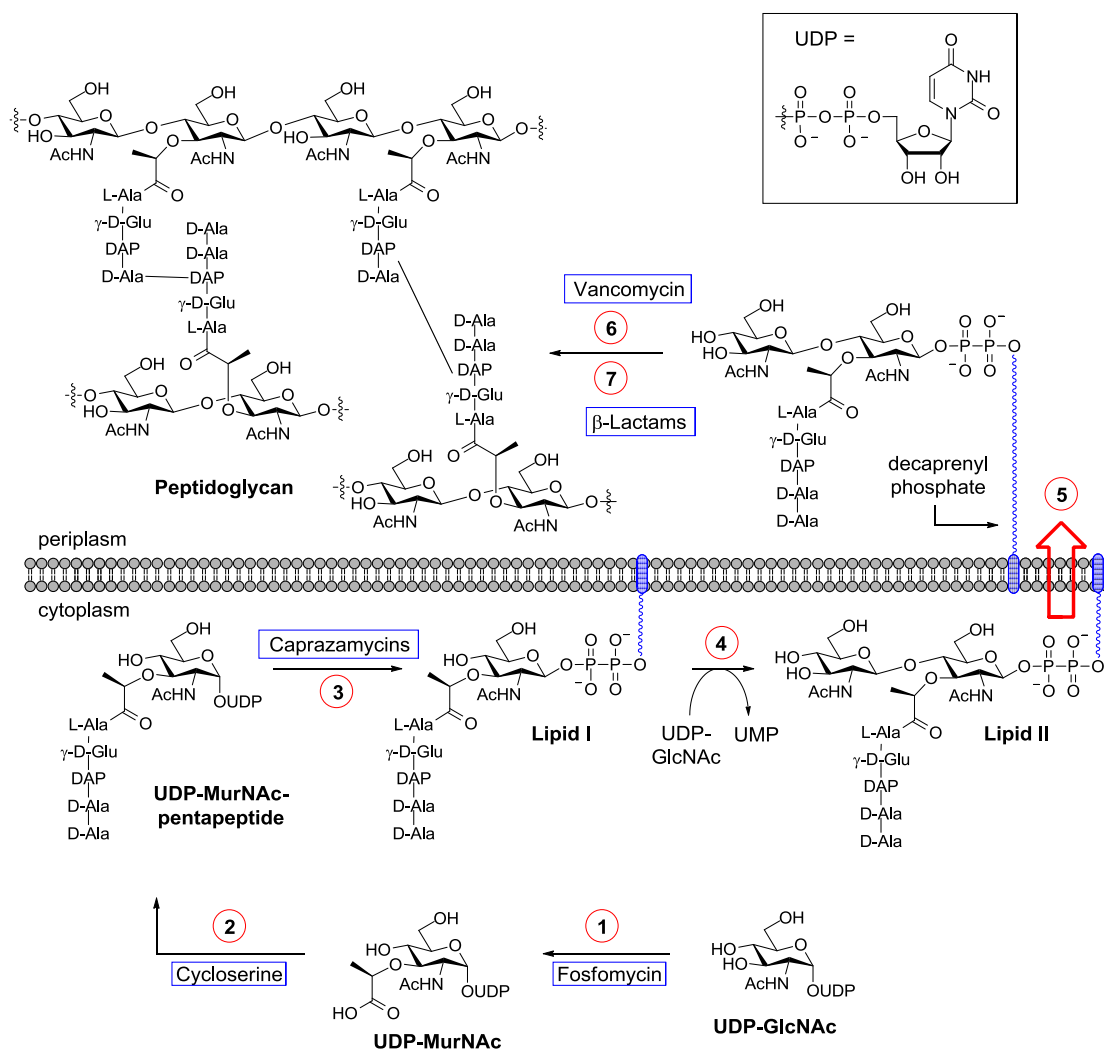


**Figure 8.2.** The biosynthesis of peptidoglycan. 1. MurA, MurB. 2. MurC, MurD, MurE, MurF. 3. MraY. 4. MurG. 5. “Flippase”. 6. Transglycosylation. 7. Transpeptidation. Drugs known to inhibit at specific points of PG synthesis are indicated. UMP = uridine monophosphate.

## 8.2 Drugs Targeting Peptidoglycan Biosynthesis

Figure 8.2 highlights that the bacterial peptidoglycan biosynthesis machinery is a rich source of potential drug targets. Indeed, several antibiotics are known to act as inhibitors of bacterial PG metabolism, including fosfomycin, cycloserine, caprazamycins, vancomycin, and β-lactam antibiotics (indicated in Fig. 8.2). Of these drugs however, only second-line cycloserine is regularly used to treat TB (Sect. 1.3). Fosfomycin (Fig. 8.3) is a broad spectrum epoxide-containing antibiotic that covalently inhibits bacterial MurA *via* alkylation of an active site cysteine.<sup>199</sup> In mycobacteria however, this cysteine is replaced with an aspartic acid residue, so *M.tb* is inherently resistant to fosfomycin.<sup>200</sup> β-lactam antibiotics such as

the penicillins prevent bacterial PG biosynthesis by inhibiting peptidoglycan transpeptidases (penicillin binding proteins),<sup>201</sup> and have been incredibly successful as treatments for many different bacterial infections. Penicillins are also ineffective against *M.tb* however, as mycobacteria express an extremely broad spectrum  $\beta$ -lactamase that hydrolyses the  $\beta$ -lactam ring, rendering these antibiotics inactive.<sup>202,203</sup> However, recent reports indicate that certain carbapenems<sup>204</sup> ( $\beta$ -lactam antibiotics less susceptible to  $\beta$ -lactamase activity) impart an enhanced curative effect against MDR-TB in humans when administered with the  $\beta$ -lactamase inhibitor clavulanate, as part of a combination therapy with other TB medicines<sup>205</sup> (e.g. meropenem; Fig. 8.3). Finally, the recently discovered caprazamycins also show potential promise as novel TB drugs, acting through inhibition of MraY (Fig. 8.3).<sup>206</sup>

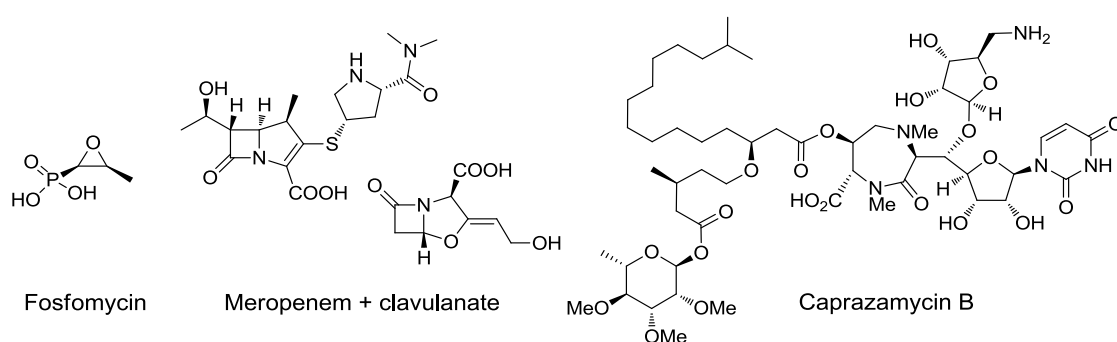


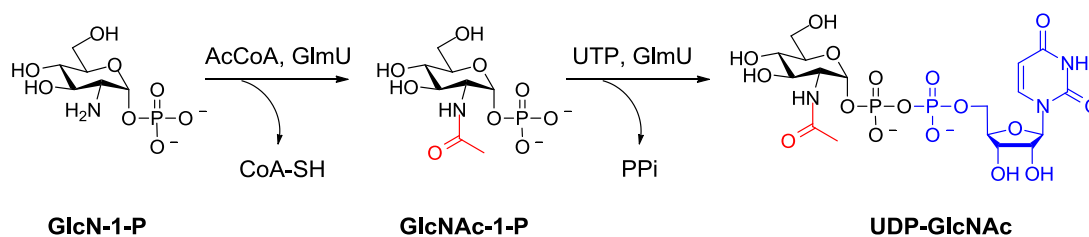
**Figure 8.3.** Drugs and combination therapies that target peptidoglycan biosynthesis. Fosfomycin is ineffective against *M.tb*, but meropenem (in combination with  $\beta$ -lactamase inhibitor clavulanate) and caprazamycin B have potential as treatments for TB.

### 8.3 GlmU Catalyses the Formation of UDP-GlcNAc

GlmU is required for the synthesis of UDP-GlcNAc, the activated nucleotide sugar feedstock for PG biosynthesis (Fig. 8.2). It has been shown that the *glmU* gene is essential for the survival of *M.tb*,<sup>189</sup> and importantly, no human homologue exists. As such, *M.tb* GlmU has recently emerged as a potential new target for the treatment of TB. GlmU is conserved in both Gram-positive and Gram-negative bacteria; whilst some published research has focussed on targeting bacterial GlmU (e.g. *E.coli*, *S.pneumoniae* and *H.influenzae*), relatively little is known about the mycobacterial ortholog.

GlmU is a bifunctional acetyltransferase/uridylyltransferase that catalyses the final two steps in the biosynthesis of UDP-GlcNAc (Scheme 8.1).<sup>188</sup> In the first step, GlmU catalyses the transfer of the acetyl group of acetyl coenzyme A (AcCoA) onto the amine of glucosamine-

1-phosphate (GlcN-1-P) to give *N*-acetylglucosamine-1-phosphate (GlcNAc-1-P). In the second step, GlmU catalyses the uridylation reaction between the newly formed GlcNAc-1-P and uridine triphosphate (UTP) to give UDP-GlcNAc.



**Scheme 8.1.** GlmU is a bifunctional enzyme that catalyses the conversion of GlcN-1-P into UDP-GlcNAc. AcCoA = acetyl coenzyme A. UTP = uridine triphosphate. PP<sub>i</sub> = pyrophosphate.

Structurally, GlmU is folded into two distinct domains that are each responsible for one of the two catalytic activities (Fig. 8.4).<sup>188</sup> The C-terminal domain catalyses the acetylation of GlcN-1-P, whilst the N-terminal domain catalyses the uridylation of GlcNAc-1-P. It is believed that after formation in the C-terminal domain, the acetyltransferase product GlcNAc-1-P freely diffuses to the N-terminal uridytransferase domain.<sup>207</sup> GlmU is trimeric in solution, which represents the biologically functional form of the enzyme;<sup>208</sup> three acetyltransferase active sites are formed upon the association of the GlmU monomers.<sup>207</sup>

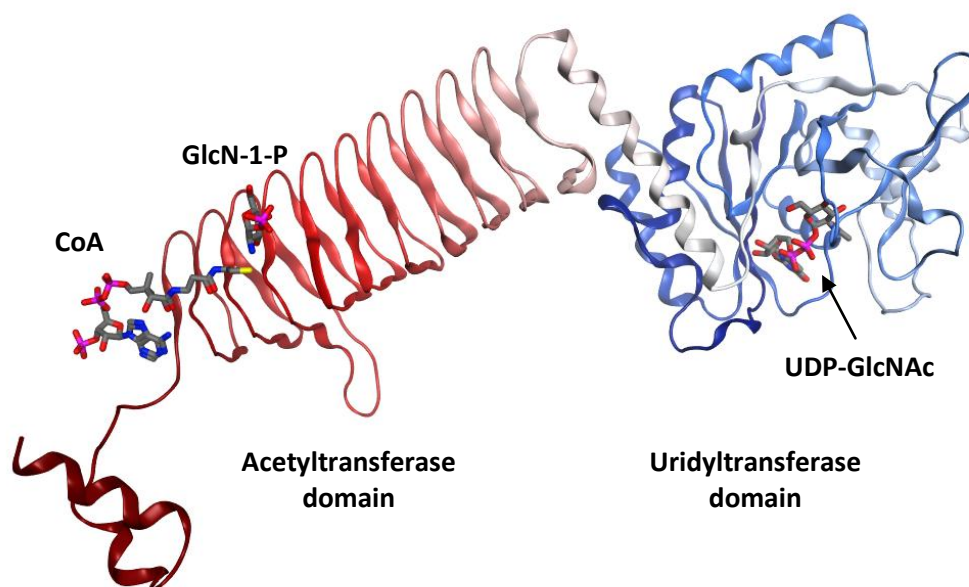


**Figure 8.4.** The structure of monomeric *M.tb* GlmU in complex with coenzyme A (CoA), GlcN-1-P and UDP-GlcNAc. The structure is coloured to indicate the acetyltransferase (red) and uridytransferase (blue) domains.<sup>207</sup>

### 8.3.1 Structural Basis for *M.tb* GlmU Acetyltransferase activity

Site directed mutagenesis experiments by Prakash and co-workers revealed that the catalytic residues involved in the acetyltransferase reaction are the histidine residue His<sup>374</sup>, asparagine Asn<sup>397</sup> and alanine Ala<sup>391</sup>.<sup>207</sup> The authors proposed that whilst His<sup>374</sup> likely deprotonates the amine of GlcN-1-P, Asn<sup>397</sup> enhances the nucleophilicity of the sugar substrate through a hydrogen bonding interaction, and the Ala<sup>391</sup> stabilises the resultant charge on the coenzyme acetyl group (Fig. 8.5).

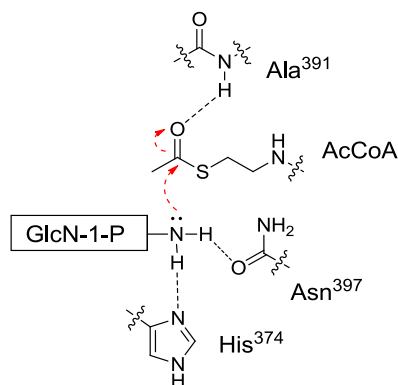


**Figure 8.5.** Schematic for the *M.tb* GlmU-catalysed acetyltransferase reaction, as proposed by Prakash *et al.*<sup>207</sup> The catalytic residues and their likely roles are indicated.

A crystal structure of *M.tb* GlmU bound to AcCoA showed that the coenzyme binds at the interface between two GlmU chains of the trimer, and is further stabilised by contacts with residues from the third monomer.<sup>207</sup> Interestingly, the AcCoA substrate adopts an unusual “U” conformation unique to *M.tb*, as opposed to the “L” conformation commonly observed in other bacterial orthologs of GlmU<sup>207</sup> (Fig. 8.6). The authors identified four residues that likely stabilised the unusual “U” conformation: Ala<sup>451</sup>, Arg<sup>439</sup>, Ile<sup>457</sup> and Arg<sup>455</sup>. A tetra-mutant modified at these residues displayed a marked reduction in acetyltransferase activity, highlighting the importance of this nuanced cofactor binding mode in *M.tb* GlmU. This structural information may be useful for developing GlmU acetyltransferase inhibitors that are specific to *M.tb*.

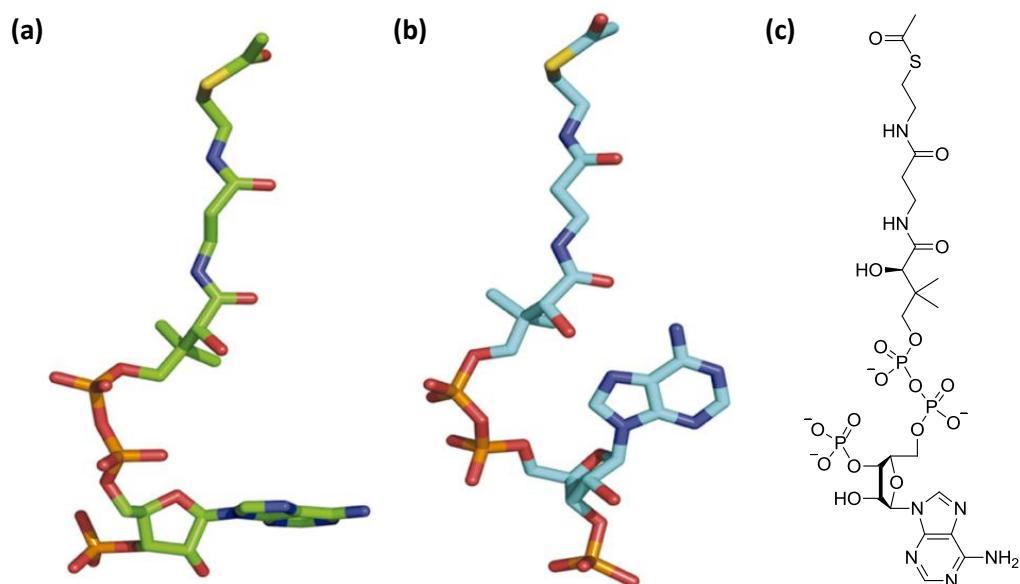


**Figure 8.6.** (a) The structure of AcCoA bound to *E. coli* GlmU displays the common "L" conformation. (b) The structure of AcCoA bound to *M. tb* GlmU revealed an uncommon "U" conformation, unique to *M. tb* (Figures reproduced from J. Biol. Chem. **2012**, 287 (47), 39524- 39537, with permission from the American Society for Biochemistry and Molecular Biology). (c) The chemical structure of AcCoA.

### 8.3.2 Structural Basis for *M. tb* GlmU Uridyltransferase activity

Another crystal structure reported by Prakash *et al.* has shed light on the mechanism of the *M. tb* GlmU-catalysed uridylation of GlcNAc-1-P.<sup>209</sup> The structure shows GlmU bound to the two uridyltransferase products, UDP-GlcNAc and pyrophosphate (PP<sub>i</sub>), and suggested the presence of two metal ions in the active site. Importantly, this identified that the reaction is mediated by two Mg<sup>2+</sup> ions, and not one as was described previously.<sup>188</sup> This crystal structure was used to model the substrates GlcNAc-1-P and UTP into the GlmU uridyltransferase active site (Fig. 8.7), in which the location of the two Mg<sup>2+</sup> ions were suggestive of particular roles. The first magnesium ion (Mg<sup>2+</sup><sub>A</sub>) is believed to enhance the binding of GlcNAc-1-P through a coordination interaction, whilst orientating the nucleophilic phosphate group for attack of UTP. The authors suggested that the second magnesium ion (Mg<sup>2+</sup><sub>B</sub>) activates UTP towards nucleophilic attack by holding the substrate in a strained orientation, and stabilises the transition state by neutralizing the developing negative charge.

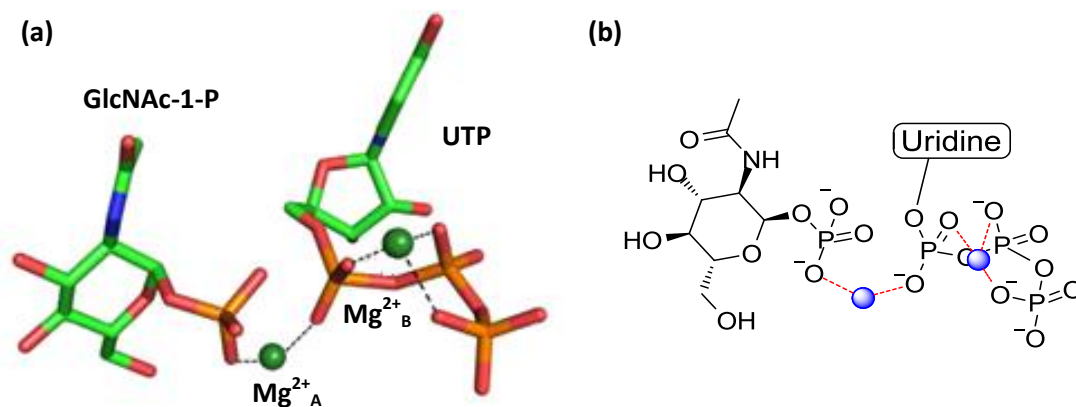


**Figure 8.7.** (a) Uridyltransferase substrates GlcNAc-1-P and UTP modelled in the GlmU active site by Prakash *et al.*<sup>209</sup> Figure reproduced from *J. Mol. Biol.* **2013**, 425 (10), 1745-1759, with permission from Elsevier. (b) Two-dimensional representation of the uridylyltransferase substrates bound in the GlmU active site. The blue spheres represent Mg<sup>2+</sup> ions.

### 8.3.3 Reported Inhibitors of Bacterial and *M.tb* GlmU

Several small molecule inhibitors of bacterial GlmU orthologues have recently been reported, which target either the acetyltransferase<sup>210,211</sup> or uridylyltransferase<sup>212,213</sup> activity of the enzyme. Furthermore, Buurman and co-workers reported that inhibition of the of *H.influenzae* GlmU acetyltransferase functionality prevented incorporation of radiolabeled *N*-acetylglucosamine into bacterial macromolecules.<sup>210</sup> This result was consistent with the inhibition of a key step in UDP-GlcNAc synthesis, thus validating GlmU as an antimicrobial target *in vitro* for the first time.

The first *M.tb* GlmU acetyltransferase inhibitor was reported by Li *et al.* in 2011.<sup>214</sup> Fluoro-sugar **8.1** had a weak IC<sub>50</sub> of 13 mM (Fig. 8.8). Tran *et al.* later reported the first uridylyltransferase inhibitors of *M.tb* GlmU in 2013.<sup>215</sup> The authors noted that the AstraZeneca *H.influenzae* GlmU inhibitor **8.2**<sup>216</sup> was weakly active at *M.tb* GlmU, and subsequently attempted to optimise the inhibitors for the mycobacterial ortholog. Whilst they were unable to quote IC<sub>50</sub> values for the majority of newly synthesised compounds, one exemplar **8.3** was quoted as having a weak IC<sub>50</sub> of 74 μM (pIC<sub>50</sub> = 4.1) against the *M.tb* GlmU uridylyltransferase activity. The majority of their inhibitors however, showed less than 50% uridylyltransferase inhibition at 50 μM. Most recently, Rani and co-workers reported four compounds **8.4-8.7** (Fig. 8.8) as potent *M.tb* GlmU acetyltransferase inhibitors following an HTS campaign.<sup>217</sup> However, based on their molecular structures, all four compounds appeared to be PAINS (pan-assay interference compounds),<sup>218</sup> and it is unlikely

that they were genuine GlmU inhibitors. Indeed, the authors monitored GlmU inhibition using a calorimetric assay that relied on the quantification of CoA produced upon turnover of AcCoA<sup>217</sup>; each of the compounds **8.4-8.7** were Michael acceptors capable of depleting the concentration of CoA, which would lead to the false impression of GlmU inhibition.

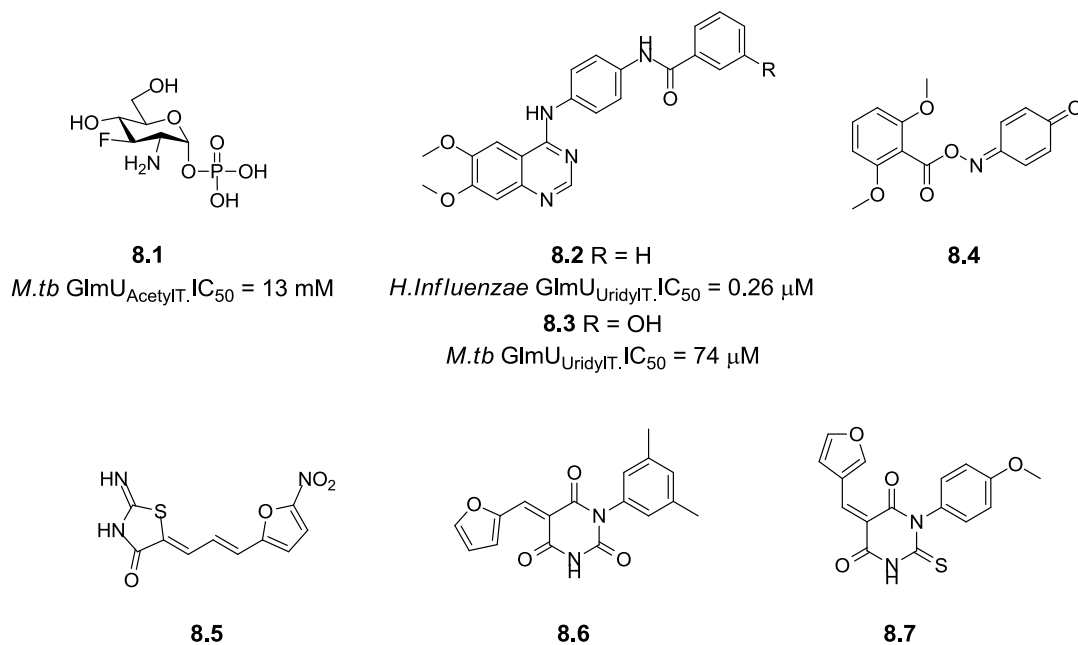


**Figure 8.8.** Compounds **8.1** and **8.3-8.7** are published *M.tb* GlmU inhibitors. **8.2** is a known inhibitor of *H.influenzae* GlmU.<sup>216</sup> Quinones (e.g. **8.4**), rhodanine-related compounds (e.g. **8.5**), and alkyldene barbiturates (e.g. **8.6-8.7**) are known PAINS.<sup>218</sup> It is likely that **8.4-8.7** were not genuine GlmU acetyltransferase inhibitors.

## 8.4 Research Aims

There are currently no quality, potent *M.tb* GlmU inhibitors with which to investigate the biochemistry of this enzyme or the validity of this target for TB chemotherapy. Scientists within GSK are currently working to develop separate *M.tb* GlmU acetyltransferase and uridyltransferase assays which should facilitate the screening of small molecules against both activities of *M.tb* GlmU (this work is being performed by Peter Craggs). To help establish the *M.tb* GlmU acetyltransferase assay, we sought to design a small set of potential GlmU acetyltransferase inhibitors based on the natural substrate, GlcN-1-P (Chapter 9). With these analogues, we hoped to demonstrate inhibition of GlmU acetyltransferase activity, whilst providing chemical matter to help further characterise the mycobacterial GlmU ortholog.

## 9. Glucosamine-1-Phosphate Analogues as Inhibitors of *M.tb* GlmU Acetyltransferase Activity

Inhibitors of the *M.tb* GlmU acetyltransferase activity were required to establish a GSK GlmU functional enzyme assay, and to provide probes with which to investigate the underlying biochemistry of the mycobacterial GlmU ortholog. As no potent *M.tb* GlmU acetyltransferase inhibitors had previously been identified (Sect. 8.3.3), substrate analogues **9.1** were pursued as potential inhibitors (Fig. 9.1). It was hypothesised that these analogues would act as GlmU acetyltransferase inhibitors as this domain of the enzyme is predisposed to the recognition of a glucosamine-1-phosphate template.<sup>207</sup>

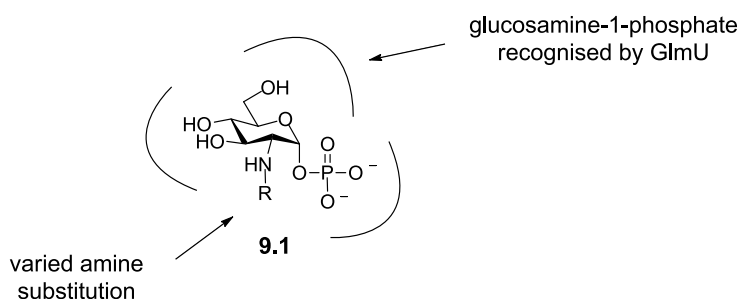


**Figure 9.1.** Analogues of GlcN-1-P as proposed inhibitors of the *M.tb* GlmU acetyltransferase activity.

### 9.1 Project Aims

The aims of this work were as follows:

- i) Design and synthesise a set of GlcN-1-P analogues as potential inhibitors of the *M.tb* GlmU acetyltransferase activity;
- ii) Test these analogues as inhibitors of *M.tb* GlmU acetyltransferase activity and establish SAR trends.

### 9.2 Design of GlcN-1-P Analogues 9.1a-g as Potential Inhibitors of the GlmU Acetyltransferase Activity

The GlmU-catalysed conversion of GlcN-1-P into GlcNAc-1-P is believed to occur *via* the tetrahedral intermediate **9.2**<sup>219,220</sup> (Fig. 9.2a). Transition state analogues that mimic the structure and geometry of a tetrahedral centre through stable isosteric replacement have

precedence as enzyme inhibitors,<sup>221</sup> and many examples are tight-binding inhibitors.<sup>222,223</sup> Tetrahedral functional groups such as sulfonamides,<sup>222,224,225</sup> sulfonates,<sup>226</sup> phosphoramidates<sup>223,227</sup> phosphates,<sup>228,229</sup> phosphonates,<sup>230</sup> chiral alcohols<sup>231</sup> and silanediols<sup>232</sup> have all been utilised in this context (largely to simulate the transition state of peptide or ester bond hydrolysis). This design strategy has been successful in the identification of probes for reaction mechanisms, and has led to marketed drugs (e.g. HIV protease inhibitors<sup>233</sup>). Consequently, it was postulated that structural mimics of tetrahedral intermediate **9.2** may act as GlmU acetyltransferase inhibitors. To this end, simplified tetrahedral intermediate mimics sulfonamide **9.1a** and phosphinic amide **9.1b** were designed (Fig. 9.2b). The carbon backbone of AcCoA interacts with GlmU through lipophilic and polar contacts, contributing to the overall binding interaction of the coenzyme (Fig. 9.2c).<sup>207</sup> It is likely these contacts are maintained by the reaction intermediate **9.2**.<sup>207</sup> In efforts to mimic these interactions, truncated-CoA sulfonamide analogue **9.1c** was designed (Fig. 9.2b).

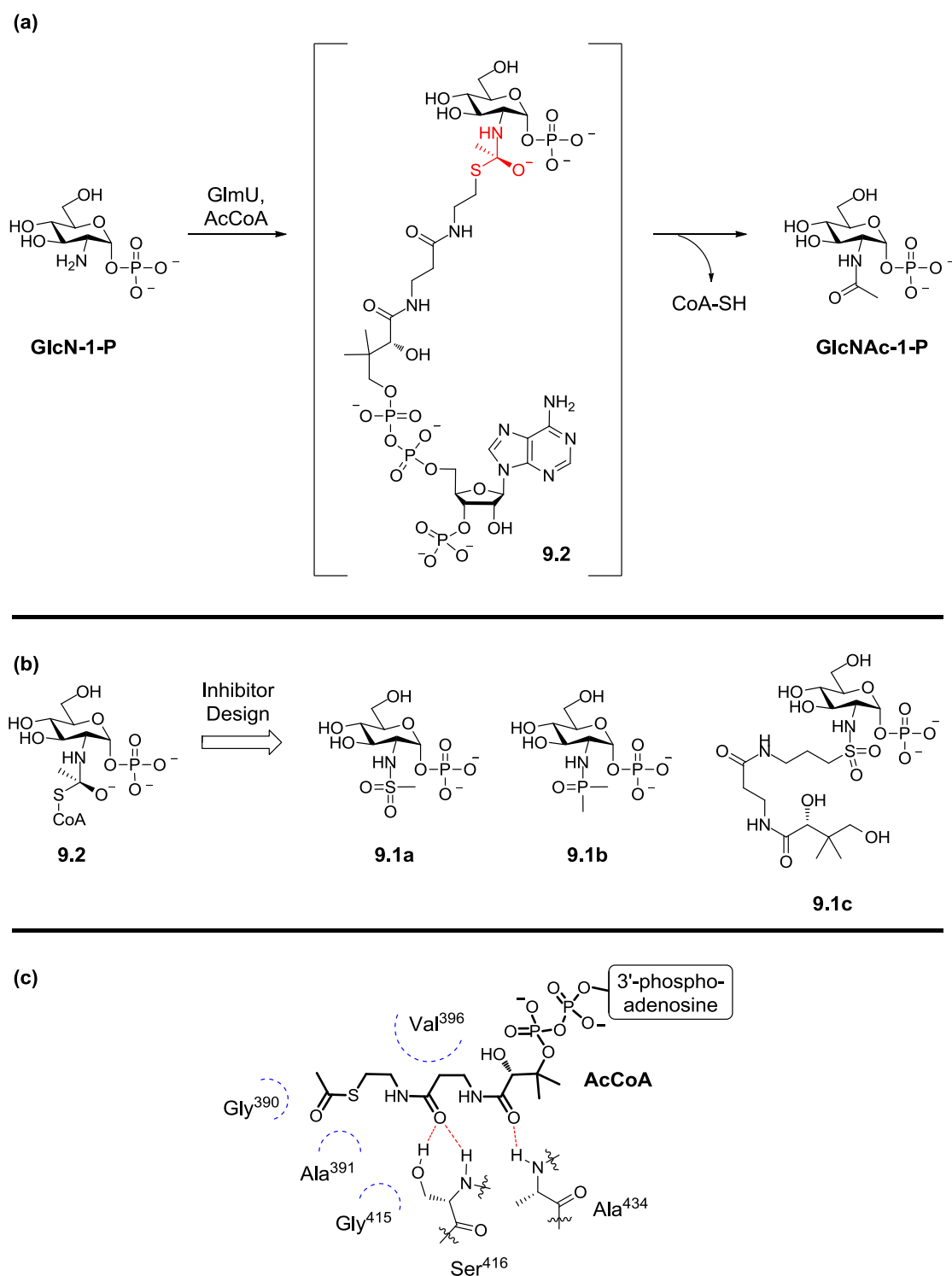


**Figure 9.2** (a) The GlmU-catalysed acetylation of GlcN-1-P is believed to proceed *via* tetrahedral intermediate **9.2** (the depicted stereochemistry of the oxyanion **9.2** is arbitrary).<sup>219,220</sup> The tetrahedral centre targeted for isosteric replacement is highlighted in red. (b) Analogues of the tetrahedral intermediate **9.2** designed as potential inhibitors of the GlmU acetyltransferase functionality. (c) Interactions between the carbon backbone of AcCoA with residues contributed by the three monomers of the GlmU trimer.<sup>207</sup> Hydrophobic contacts are indicated with dashed blue lines; hydrogen bonding interactions are indicated with dashed red lines.

As compounds **9.1a-c** were structurally similar to the GlmU acetyltransferase reaction product, GlcNAc-1-P itself was tested as an inhibitor of this enzymatic function (this analogue was commercially available and did not require synthesis). Amides **9.1d-g** were also targeted to investigate the consequence of varying amide substitution length and steric bulk (Fig. 9.3). **9.1g** was designed to contain a truncate of the carbon backbone present in tetrahedral intermediate **9.2g**.

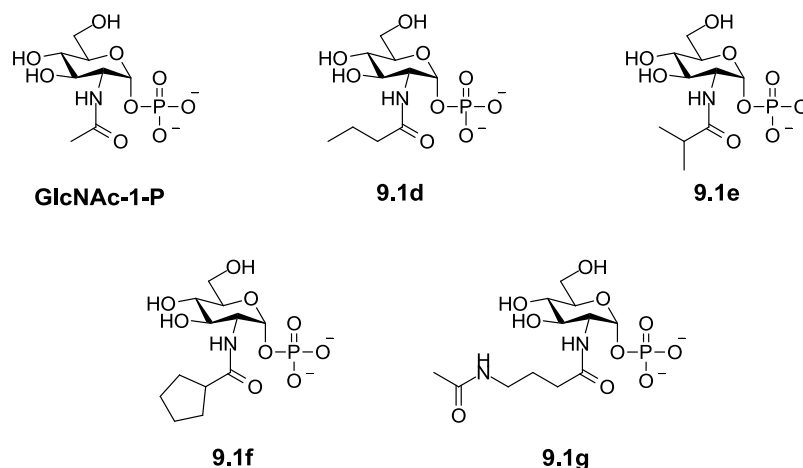
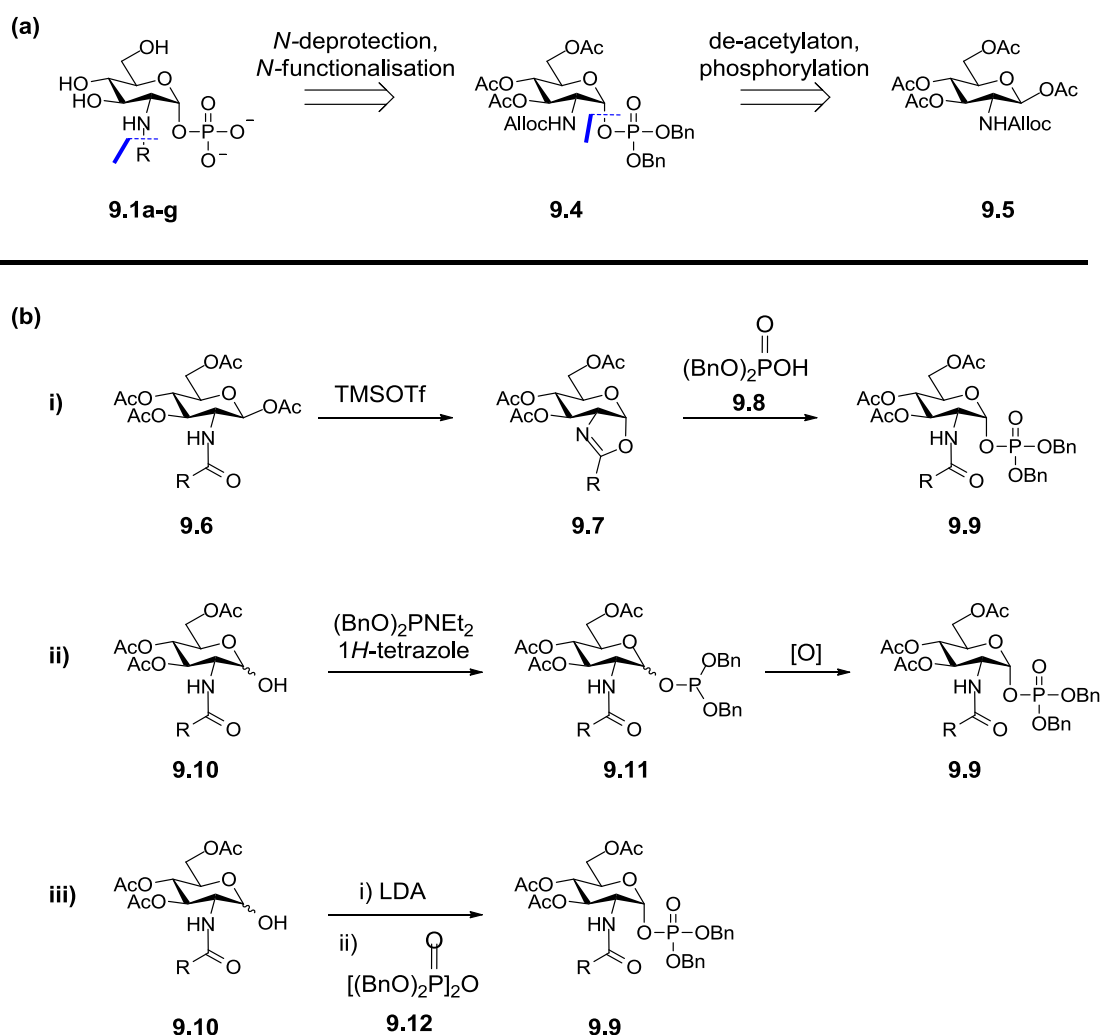


**Figure 9.3.** Amide analogues of GlcN-1-P targeted as potential inhibitors of *M.tb* GlmU acetyltransferase activity.

### 9.3 Synthesis of *N*-functionalised GlcN-1-P Analogues 9.1a-g

Disconnection of analogues **9.1a-g** at the glucosamine nitrogen suggested that protected intermediate  $\alpha$ -glycosyl-1-phosphate **9.4** should provide access to all the targeted compounds **9.1** after *N*-Alloc deprotection and *N*-functionalisation of the resulting secondary amine (Scheme 9.1a). Three strategies are widely employed in the syntheses of glucosamine-1-phosphates such as **9.4** (Scheme 9.1b). The first strategy involves the formation of an electrophilic oxazoline **9.7** from a sugar precursor (e.g. acetate-protected **9.6**), followed by the phosphorolytic opening of the oxazoline sugar **9.7** with an excess of dibenzyl phosphate **9.8** (route i).<sup>234,235</sup> The second and third strategies employ a sugar lactol **9.10**, and proceed either step-wise *via* the phosphite **9.11** (route ii),<sup>236</sup> or directly *via* low temperature metalation of the glycosyl oxygen of **9.10** and reaction with tetrabenzyl pyrophosphate **9.12** (route iii).<sup>237</sup> Generally, the thermodynamic  $\alpha$ -phosphate is obtained as the sole product for each of the three methodologies; it is believed that a *trans* 2-acetamido group will destabilise the  $\beta$ -phosphate by neighbouring group participation.<sup>238</sup>

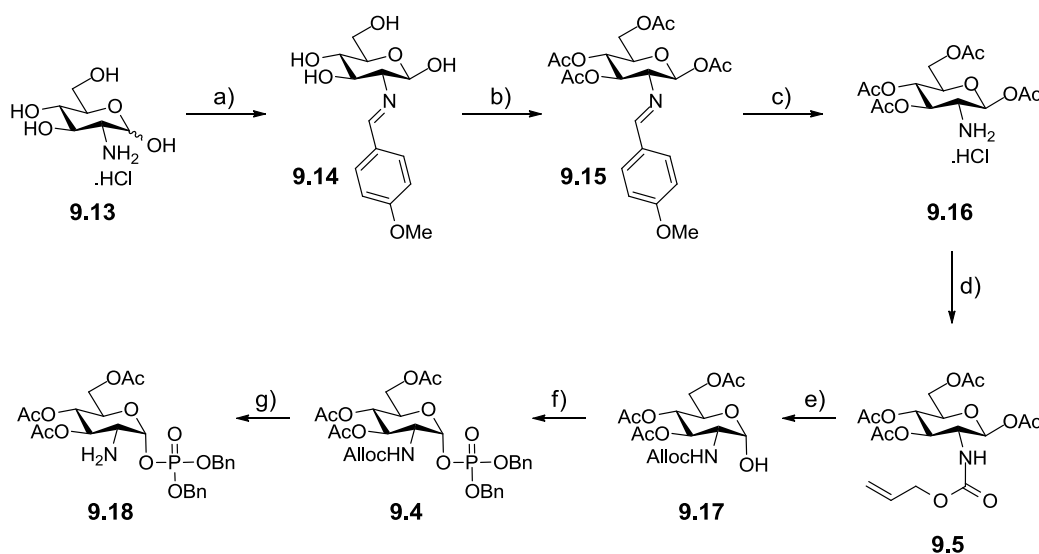
The third strategy (route iii) was chosen as it would facilitate rapid access to glycosyl phosphate **9.4** from a known intermediate **9.5**<sup>239</sup> (Scheme 9.1a).



**Scheme 9.1.** (a) Retrosynthetic analysis of the *N*-functionalised GlcN-1-P analogues **9.1a-g**. (b) Strategies for the synthesis of glycosyl-1-phosphates: i) the oxazoline strategy<sup>234,235</sup>; ii) the phosphite strategy<sup>236</sup>; iii) metalation of sugar lactol **9.10** and reaction with tetrabenzyl pyrophosphate **9.12**.<sup>237</sup>

Synthesis began with a four step procedure to generate the *per-O*-acetylated *N*-Alloc glucosamine **9.5** from glucosamine hydrochloride **9.13**<sup>239,240</sup> (Scheme 9.2). Reaction between **9.13** and *p*-anisaldehyde protected the amine group as the anisaldehyde imine **9.14**; *per*-acetylation of the hydroxyl groups by treatment of **9.14** with acetic anhydride and DMAP in pyridine gave fully-protected **9.15**; acid mediated hydrolysis of the imine protecting group gave **9.16**; and protection of the amine as the allyl carbamate afforded intermediate **9.5** in 50% yield over the four steps. Selective deprotection of the anomeric

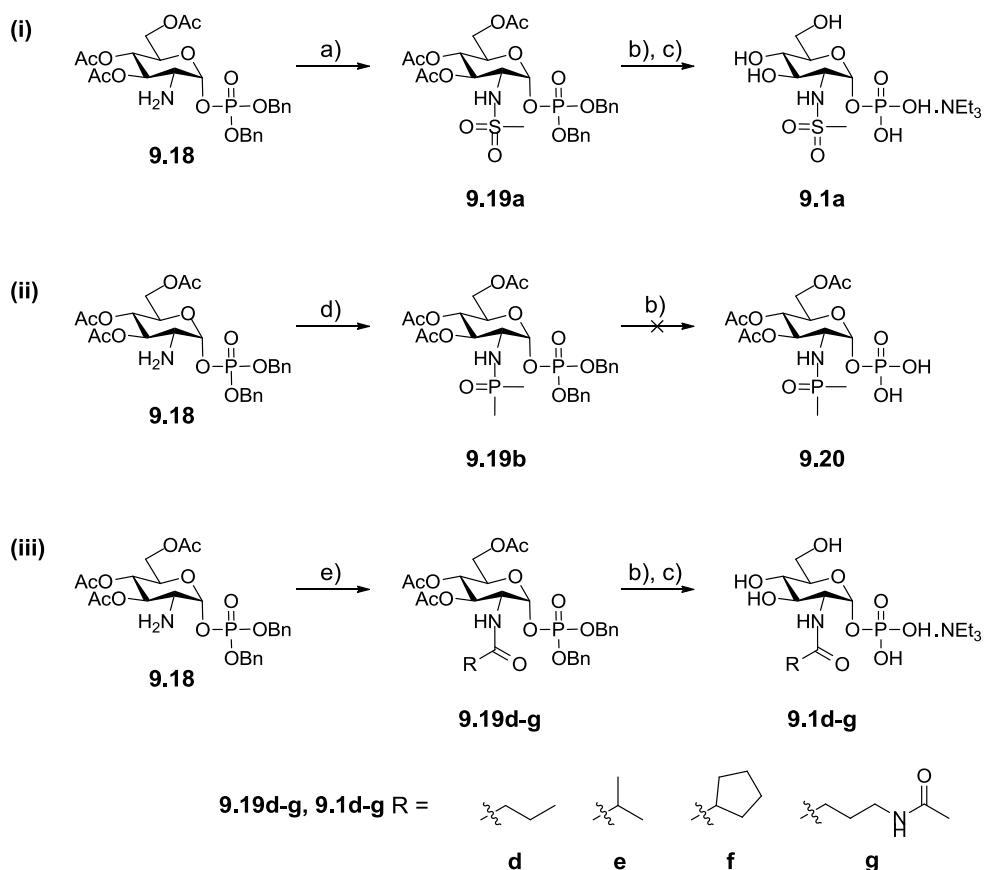
acetate with benzylamine then furnished the sugar lactol **9.17** in 66 % yield. Installation of the phosphate functionality proceeded smoothly on sequential treatment of **9.17** with LDA and tetrabenzyl pyrophosphate. The glycosyl-1-phosphate **9.4** was produced in 69% yield exclusively as the thermodynamic  $\alpha$ -anomer (none of the  $\beta$ -anomer was detected), confirmed by the signal for the anomeric proton in the  $^1\text{H}$  NMR spectrum (doublet of doublets,  $J_{\text{H1-H2}} = 3.5$  Hz,  $J_{\text{H1-P}} = 6.0$  Hz). Finally, treatment of phospho-sugar **9.4** with palladium tetrakis(triphenylphosphine) and diethylamine removed the allyl carbamate protecting group to give the unmasked glucosamine-1-phosphate **9.18** in 91% yield.



**Scheme 9.2** a) 1 M aq. NaOH, *p*-anisaldehyde. b) Ac<sub>2</sub>O, DMAP, pyridine. c) 5 M HCl, acetone, reflux. d) allyl carbonochloridate, NaHCO<sub>3</sub>, DCM, H<sub>2</sub>O, 50% over 4 steps from **9.13**. e) BnNH<sub>2</sub>, THF, 66%. f) LDA, **9.17**, THF, -78°C, then tetrabenzyl pyrophosphate, 69%. g) Pd(Ph<sub>3</sub>P)<sub>4</sub>, Et<sub>2</sub>NH, THF, 91%.

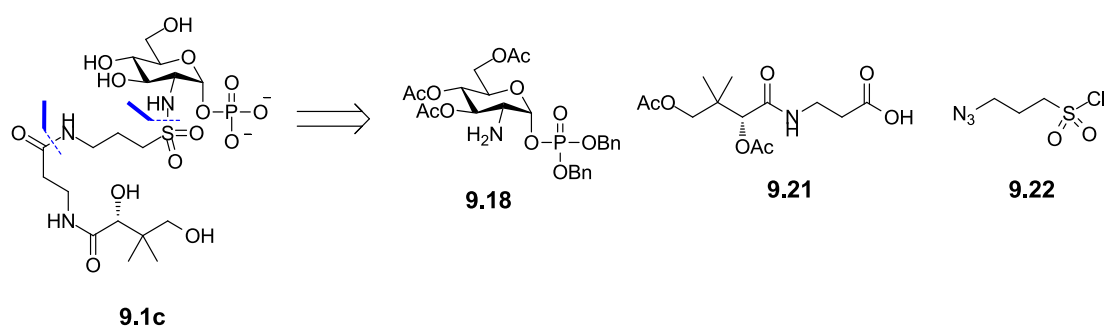
Syntheses of the targeted compounds **9.1a-b** and **9.1d-g** then proceeded as detailed in Scheme 9.3. Reaction of amine **9.18** with mesyl chloride in the presence of triethylamine afforded sulfonamide **9.19a** in 57% yield. Global deprotection of **9.19a** was achieved *via* a two step procedure, initiating with the palladium-mediated hydrogenolysis of the phosphate benzyl esters. Selective cleavage of the hydroxyl acetate groups with a mixture of methanol, water and triethylamine (7:3:1) subsequently gave the targeted analogue **9.1a** in near-quantitative yield over the two steps. Treatment of amine **9.18** with dimethylphosphinic chloride in the presence of *N*-methyl morpholine furnished the phosphinic amide **9.19b** in 63% yield (Scheme 9.3ii). All efforts to isolate the intermediate **9.20** after hydrogenolysis of **9.19b** failed however, as degradation of **9.20** during the

reaction was repeatedly observed (under the same conditions as for **9.19a**). Phosphinic amides are known to be susceptible to hydrolysis under acidic conditions,<sup>241,242</sup> it is possible that degradation occurred upon unmasking of the acidic phosphate di-acid. Due to these stability issues, phosphinic amide **9.1b** was not pursued further. Amide intermediates **9.19d-g** were synthesised from amine **9.18** and the appropriate acid chloride or carboxylic acid in 73-91% yields (Scheme 9.3iii). Global deprotection of the intermediates **9.19d-g** yielded final compounds **9.1d-g** in excellent yields over the two steps.



**Scheme 9.3.** a) MsCl, NEt<sub>3</sub>, DCM, 57%. b) Pd/C, H<sub>2</sub> (1 atm.), MeOH. c) MeOH-H<sub>2</sub>O-Et<sub>3</sub>N (7:3:1), 93-100% yield over 2 steps. d) Me<sub>2</sub>POCl, *N*-methyl morpholine, DCM, 63%. e) For **9.19d-f**, **9.18**, RCOCl, NEt<sub>3</sub>, DCM. **9.19d** = 91% **9.19e** = 74%, **9.19f** = 84% OR for **9.19g**, 4-acetamidobutanoic acid, DIPEA, COMU, DMF, then **9.18**, 73%.

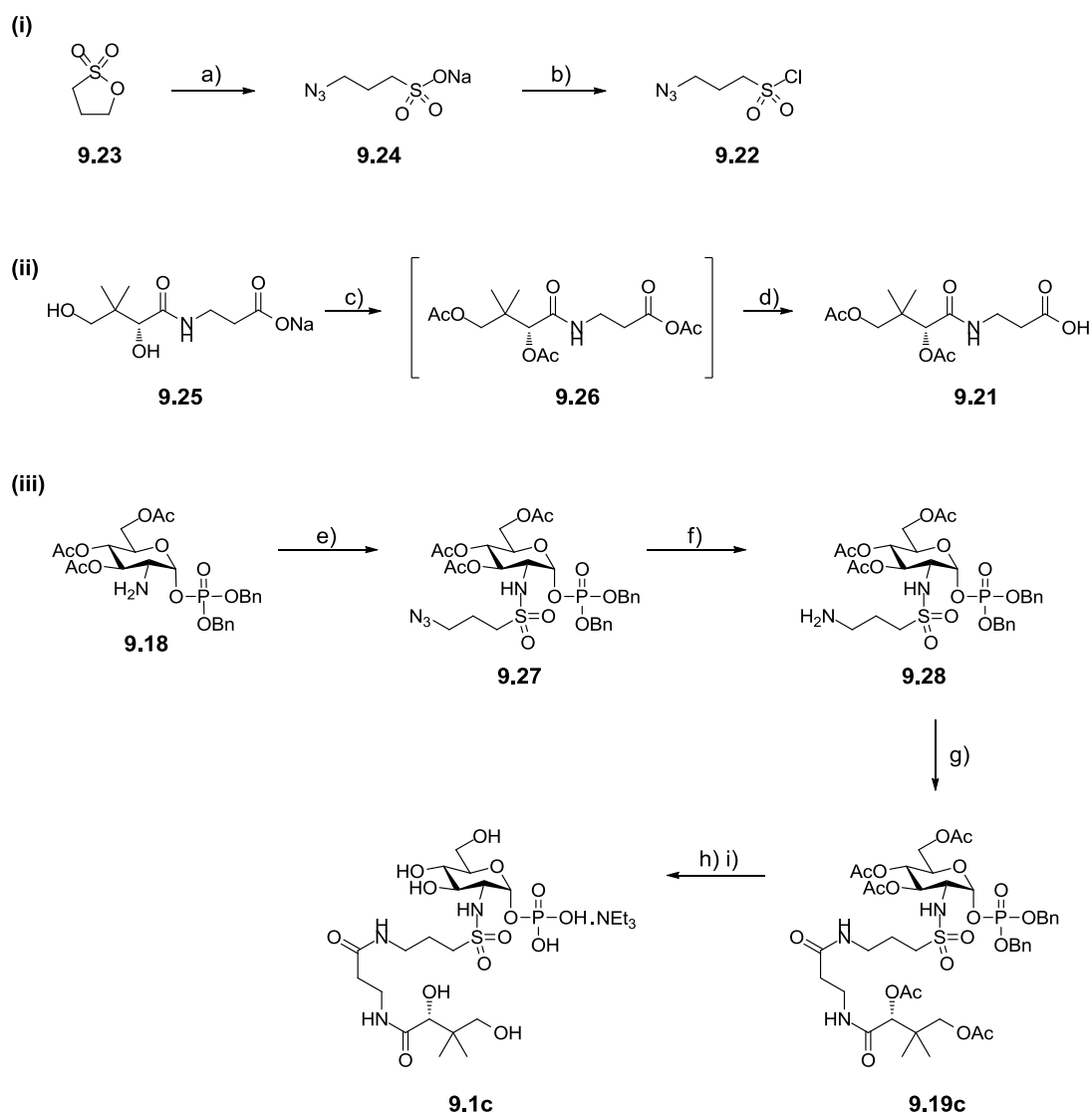
Retrosynthetic disconnection of truncated-CoA sulfonamide analogue **9.1c** yielded the glucosamine-1-phosphate **9.18**, the appropriately protected D-pantothenic acid **9.21**<sup>243</sup> and known 3-azidopropane-1-sulfonyl chloride **9.22**<sup>244</sup> (Scheme 9.4).



**Scheme 9.4.** Retrosynthetic disconnection of sulfonamide **9.1c** afforded glucosamine-1-phosphate **9.18**, protected D-pantothenic acid **9.21**<sup>243</sup> and 3-azidopropane-1-sulfonyl chloride **9.22**.<sup>244</sup>

Ring opening of 1,3-propanesultone **9.23** with sodium azide afforded 3-azidopropane sulfonic acid **9.24** as the sodium salt in 67% yield (Scheme 9.5i). Conversion of **9.24** into sulfonyl chloride **9.22** was then effected in 80% yield by phosphorus pentachloride.<sup>244</sup> The protected D-pantothenic acid **9.21** was synthesised according to a published two-step procedure<sup>243</sup> as follows (Scheme 9.5ii): treatment of D-pantothenic acid sodium salt **9.25** with acetic anhydride and catalytic iodine gave mixed anhydride **9.26**. Stirring this intermediate **9.26** in a mixture of THF and water hydrolysed the anhydride to give the carboxylic acid **9.21** in 59% over two steps.

With the required fragments **9.21** and **9.22** in hand, amino-sugar **9.18** was reacted with the sulfonyl chloride **9.22** to give the sulfonamide **9.27** in 82% yield (Scheme 9.5iii). Reduction of the azide **9.27** was then achieved by treatment with zinc and acetic acid. The resulting amine intermediate **9.28** was used directly in the ensuing amide coupling reaction, pairing **9.28** with the acid **9.21** to afford the advanced intermediate **9.19c** in 50% yield over the two steps. Global deprotection of **9.19c** gave **9.1c** in quantitative yield.

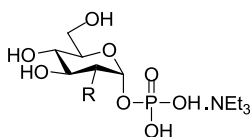


**Scheme 9.5.** a)  $\text{NaN}_3$ ,  $\text{H}_2\text{O}$ , acetone, 67%. b)  $\text{PCl}_5$ , toluene, reflux, 80%. c)  $\text{Ac}_2\text{O}$ ,  $\text{I}_2$  (cat.). d) THF,  $\text{H}_2\text{O}$ , 59% over 2 steps. e) **9.22**,  $\text{NEt}_3$ , DCM, 82%. f), AcOH, Zn, DCM. g) **9.21**, HATU, DIPEA, DMF then **9.28**, 50% over 2 steps. h) Pd/C,  $\text{H}_2$  (1 atm.), MeOH. i) MeOH- $\text{H}_2\text{O}$ - $\text{Et}_3\text{N}$  (7:3:1), 100% over 2 steps.

### 9.3 Biological Evaluation of GlcN-1-P Analogues 9.1a-g

Analogues **9.1a-g** were screened in the GSK GlmU acetyltransferase assay at a concentration of 5 mM (the assay biochemistry is detailed in Appendix A1). Table 9.1 displays the activity data for analogues **9.1a-g**.

**Table 9.1.** Potency data for the substrate analogues **9.1a-g** against the *M.tb* GlmU acetyltransferase activity.



Analogue	R	% Inhibition <sup>a</sup>
<b>9.1a</b>		75
<b>9.1c</b>		25
GlcNAc-1-P <sup>b</sup>		No inhibition
<b>9.1d</b>		45
<b>9.1e</b>		60
<b>9.1f</b>		60
<b>9.1g</b>		50

<sup>a</sup>% inhibition at 5 mM of inhibitor **9.1a-g**. <sup>b</sup> GlcNAc-1-P was commercially available as the disodium salt.

The biological data in Table 9.1 show that the designed analogues **9.1a** and **9.1c-g** were weak inhibitors of the *M.tb* GlmU acetyltransferase activity, exhibiting between 25-75% inhibition at a concentration of 5 mM. The sulfonamide **9.1a** demonstrated the greatest inhibitory effect (75% inhibition), whilst the truncated-CoA sulfonamide analogue **9.1c** was only very weakly active (25% inhibition). Whilst GlcNAc-1-P did not show any inhibition of the GlmU acetyltransferase activity, amides **9.1d-g** were active; branched amides **9.1e** and **9.1f** showed greater inhibition than the linear amide analogues **9.1d** and **9.1g**.

The analogues **9.1a** and **9.1c** designed to mimic the tetrahedral intermediate **9.2** were not significantly biologically active against GlnU, suggesting that the sulfonamide group was not an effective isostere of the tetrahedral oxyanion in this case. This may be because the sulfonamide group adopts a conformation or geometry too dissimilar to that of the tetrahedral intermediate **9.2**, or because it does not possess the same charge and electrostatic potential as **9.2**. Houk and co-workers performed a computational analysis to investigate how faithfully sulfonamide groups reproduce the transition state of protease-catalyzed amide hydrolysis (Fig. 9.4a).<sup>245</sup> They reported that whilst the conformational minima of sulfonamide **9.31** did differ from the tetrahedral intermediate **9.30**, the major inconsistency was the difference in charge and electrostatic potential. The authors concluded that any hydrogen bonding or electrostatic interactions between the tetrahedral intermediate **9.30** and the protease would not be mimicked effectively by the sulfonamide **9.31**. In *M.tb* GlnU, the catalytic alanine Ala<sup>319</sup> is believed to stabilise the charge on intermediate **9.2** via a hydrogen bonding interaction<sup>207</sup> (Sect. 8.3.1; Fig. 9.4b). Based on the analysis by Houk *et al.*, it is plausible to suggest that this interaction was not effectively reproduced by the sulfonamides **9.1a** and **9.1c**.

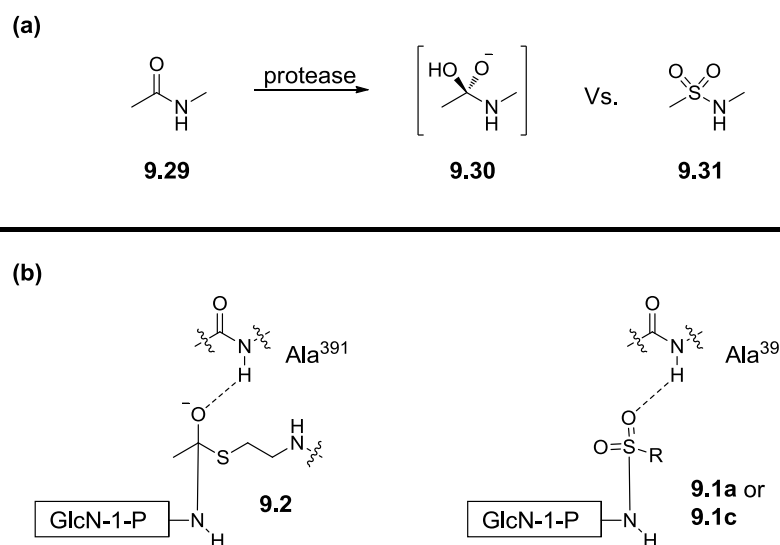


**Figure 9.4.** (a) Houk and co-workers performed calculations to evaluate how faithfully the sulfonamide **9.31** mimics the tetrahedral intermediate **9.30** of the protease-catalysed hydrolysis of amide **9.29**.<sup>245</sup> (b) The GlnU catalytic alanine Ala<sup>391</sup> likely stabilises the charge on tetrahedral intermediate **9.2**<sup>207</sup>; this interaction may not be faithfully reproduced by sulfonamides **9.1a** or **9.1c**.

Conversely, Pisabarro *et al.* demonstrated that sulfonamides can be effective isosteres of a charged tetrahedral intermediate, reporting that transition state analogue **9.33** was a

tight-binding inhibitor of human synovial fluid nonpancreatic secretory phospholipase A<sub>2</sub> (HSF-PLA<sub>2</sub>; Fig. 9.5).<sup>222</sup> The activity of this analogue was attributed to both the sulfonamide tetrahedral geometry and to a hydrogen bond between the sulfonamide N-H and a nitrogen of the catalytic histidine His<sup>48</sup>. The *M.tb* GlmU acetyltransferase domain also has a catalytic histidine residue (His<sup>374</sup>; Sect. 8.3.1; Fig. 8.5), but presumably a comparable hydrogen bonding interaction is not as important for recognition of the sulfonamides **9.1a** and **9.1c**, or that these inhibitors do not interact with this residue.

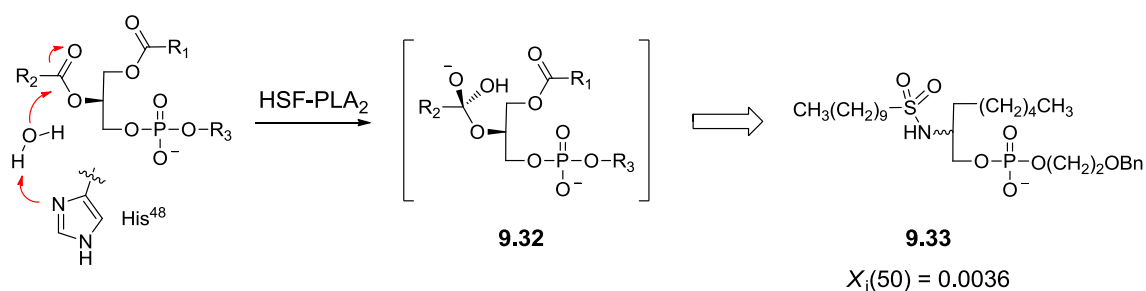


**Figure 9.5.** Sulfonamide **9.33** was an effective analogue of the charged tetrahedral intermediate **9.32**, and was a tight binding inhibitor of HSF-PLA<sub>2</sub>.<sup>222</sup>  $X_i(50) =$  mole fraction of **9.33** giving 50% HSF-PLA<sub>2</sub> activity as expressed by the initial enzymatic rate.<sup>222</sup>

Finally, it is interesting to compare the difference in activity between sulfonamides **9.1a** and **9.1c**. Both analogues were designed to mimic the tetrahedral intermediate **9.2**, but **9.1c** also incorporated sulfonamide substitution to mimic the lipophilic CoA carbon chain (Fig. 9.2c). Analogue **9.1c** was less active than **9.1a**, suggesting that the CoA side chain of **9.1c** did not enhance inhibitor binding. Jagtap and co-workers identified that interactions between the AcCoA backbone phosphates and the GlmU residues Trp<sup>460</sup> and Lys<sup>464</sup> appeared to be important for the binding of AcCoA (Fig. 9.6a).<sup>207</sup> Furthermore, interactions between GlmU and the adenosine component of AcCoA stabilise the unique “U”-shaped binding mode of the cofactor, which facilitates optimal *M.tb* GlmU acetyltransferase activity (Fig. 9.6a; Sect.8.3.1).<sup>207</sup> Analogue **9.1c** lacked both the CoA adenosine and diphosphate motif, perhaps explaining why **9.1c** was a particularly weak GlmU inhibitor.

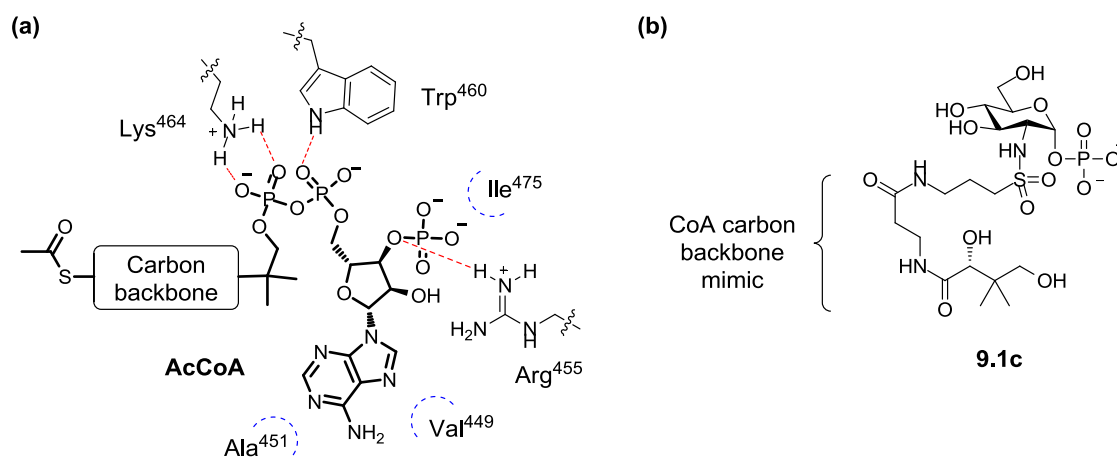


**Figure 9.6.** (a) The adenosine diphosphate motif of AcCoA makes interactions with GlmU that are important for the binding of the cofactor.<sup>207</sup> Hydrophobic contacts are indicated with dashed blue lines; hydrogen bonding interactions are indicated with dashed red lines. (b) The structure of **9.1c**. Whilst inhibitor **9.1c** incorporated a mimic of the lipophilic carbon backbone of AcCoA, it did not contain an adenosine diphosphate motif.

## 9.4 Conclusions

In conclusion, a set of *M.tb* GlmU acetyltransferase inhibitors **9.1a-g** were designed and their syntheses were successfully accomplished in good yields. The compounds **9.1a-g** were shown to exhibit between 25-75% inhibition of GlmU, and provided useful tools to help establish the GlmU acetyltransferase assay. Sulfonamides **9.1a** and **9.1c** were designed to mimic the tetrahedral intermediate **9.2**, but unfortunately they were not significantly active. Analogues of enzyme-catalysed reaction transition states and intermediates have potential to be highly active tight-binding inhibitors, provided they accurately simulate any geometric constraints and contacts with the enzyme.<sup>221</sup> As **9.1a** and **9.1c** did not demonstrate such activity, it appeared that the sulfonamide was not a good mimic of the tetrahedral intermediate **9.2**. This was attributed to the difference in charge and electrostatic potential between oxyanion **9.2** and sulfonamides **9.1a** and **9.1c**.

## 9.5 Future Work

Further work should focus on identifying isosteres that better replicate the oxyanion intermediate **9.2**. Phosphoramidates have proven to be highly successful isosteres of amide bond hydrolysis transition states. Houk *et al.* demonstrated that the charges and electrostatic potential of phosphoramidates are nearly identical to those of the amide

bond hydrolysis tetrahedral intermediate **9.30** (Fig.9.4a).<sup>245</sup> The effectiveness of a phosphoramidate isostere is exemplified by the tight-binding *E.coli* NagA inhibitor **9.36** reported by Xu and colleagues<sup>223</sup> (Fig.9.7a), which was designed to mimic amide bond hydrolysis intermediate **9.35**. Phosphoramidate analogues **9.37** and **9.38** therefore represent attractive targets to pursue as potential GlmU acetyltransferase inhibitors (Fig. 9.7b; the glucosamine-1-phosphonate analogue **9.38** would likely be more stable than the phosphate **9.37**).

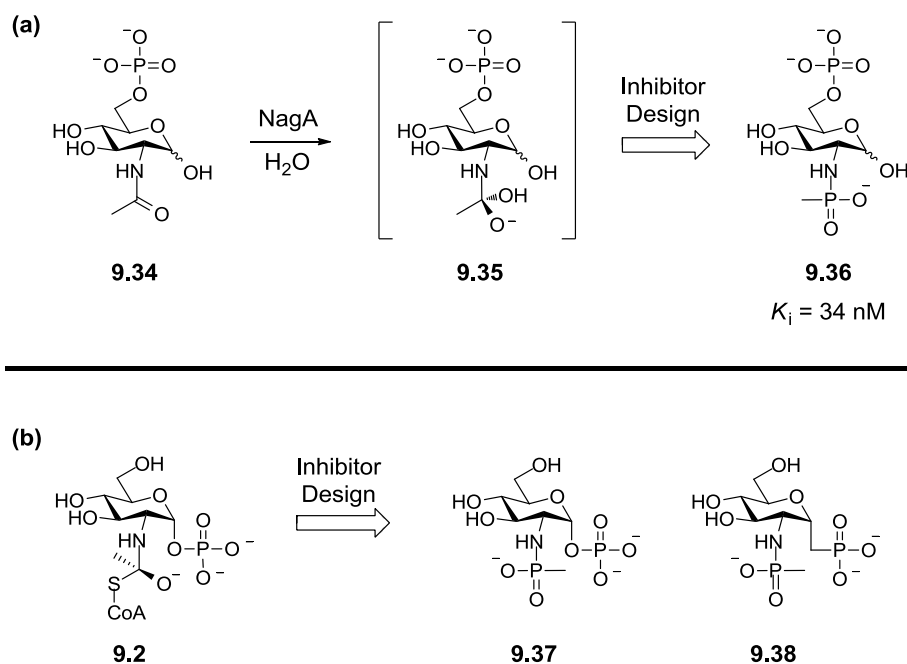


**Figure 9.7. (a)** The phosphoramidate **9.36** was a tight binding inhibitor of the *E.coli* N-acetyl-D-glucosamine-6-phosphate deacetylase (NagA), illustrating that phosphoramidates can be effective mimics of tetrahedral intermediates.<sup>223</sup> **(b)** Proposed phosphoramidate analogues of **9.2** as potential *M.tb* GlmU acetyltransferase inhibitors.

A second consideration for the design of further GlcN-1-P analogues as GlmU acetyltransferase inhibitors stems from the conclusions made about the truncated-CoA sulfonamide analogue **9.1c**. It was postulated that analogue **9.1c** was a particularly weak inhibitor of the GlmU acetyltransferase activity as it lacked the CoA adenosine and diphosphate motif, and therefore it could not form the key interactions important for AcCoA binding (Fig. 9.6a). Consequently, it would be interesting to test the inhibitory potential of an analogue which did contain both motifs, such as **9.1h** (Fig.9.8).

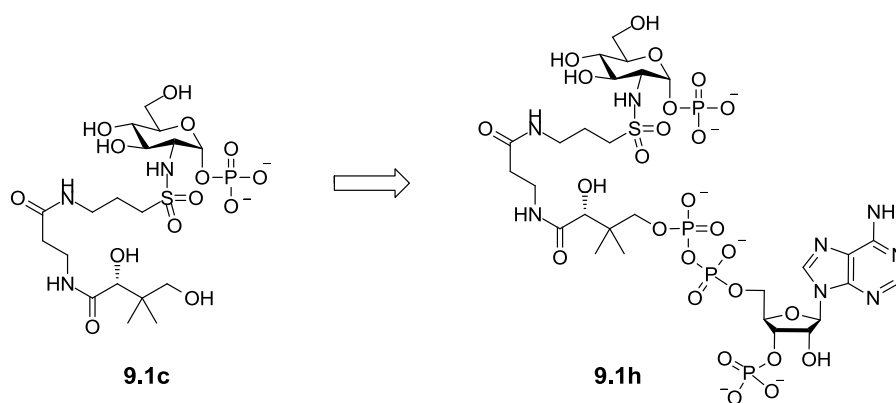


**Fig.9.8.** Newly designed analogue **9.1h** contains the CoA adenosine and diphosphate motif, and may be a more active inhibitor of the GlmU acetyltransferase activity than **9.1c**.

The GlmU acetyltransferase inhibitors **9.1a-g** synthesised in this Chapter are structurally similar to GlcNAc-1-P, the substrate of the GlmU uridylyltransferase domain. This domain catalyses the conversion of GlcNAc-1-P into UDP-GlcNAc (Sect. 8.3). Recently, various academic groups have become interested in exploiting uridylyltransferase enzymes to perform the synthesis of UDP-GlcNAc and unnatural analogues thereof,<sup>246–248</sup> as these activated sugar donors are challenging to synthesise chemically and yields are often poor.<sup>249</sup> Unnatural analogues of UDP-GlcNAc are precursors to unnatural polysaccharides, which are particularly desirable for glycobiology research.<sup>250</sup> In efforts to develop enzymatic syntheses of unnatural UDP-GlcNAc analogues, Masuko and co-workers designed a small set of GlcNAc-1-P analogues **9.39** to test as substrates of the *E.coli* GlmU ortholog, including the propiolamide analogue with a handle for click chemistry (Fig.9.9a).<sup>247</sup> They demonstrated that the GlcNAc-1-P analogues bearing an amide at the C-2 nitrogen did act as substrates, affording the unnatural UDP-GlcNAc analogues **9.40** in moderate to good yields. Similarly, it would be interesting to investigate whether the analogues **9.1a-g** would serve as substrates for the *M.tb* GlmU uridylyltransferase domain (Fig. 9.9b). Masuko *et al.* did not investigate amides with branched or lengthy substitution such as **9.1e-g**, and sulfonamides also remain unexplored as GlmU uridylyltransferase substrates.

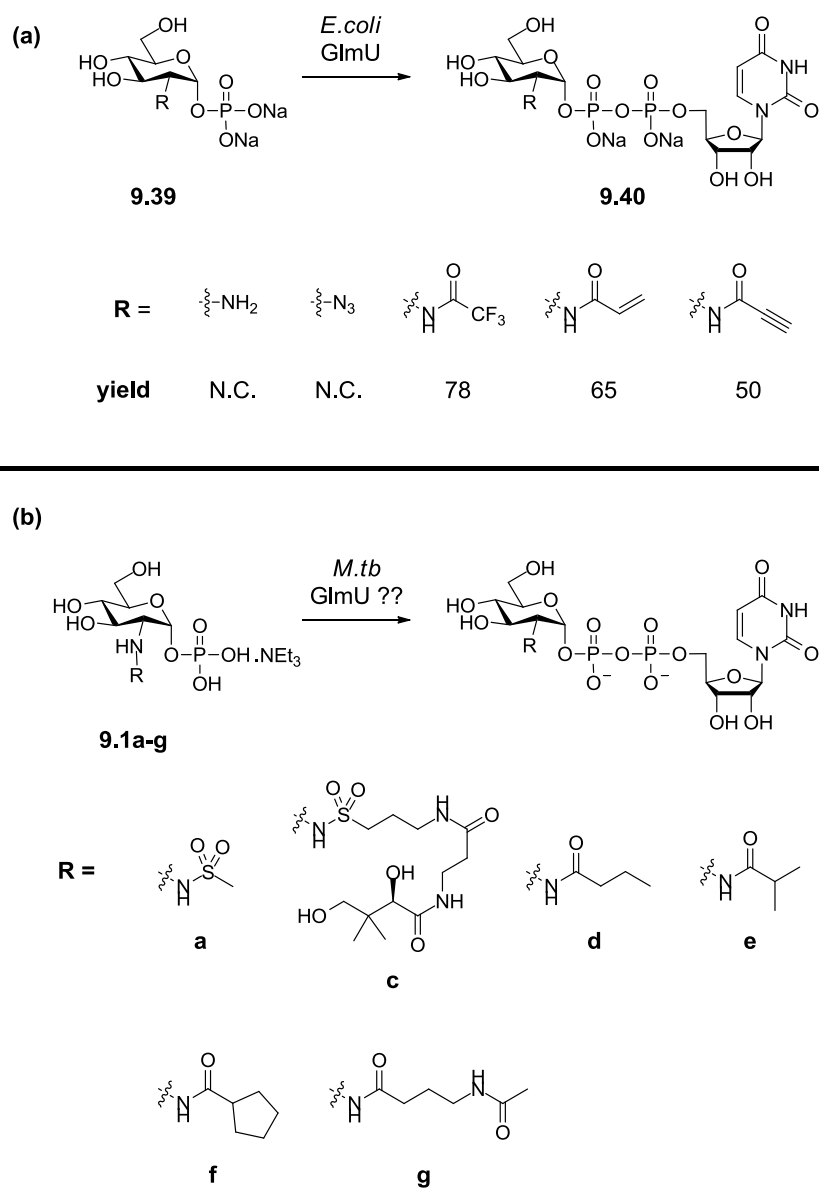


**Figure 9.9.** (a) Masuko and co-workers demonstrated that GlmU from *E.coli* can utilise three unnatural GlcNAc-1-P analogues as substrates for the uridylyltransferase reaction.<sup>247</sup> N.C. = no conversion. (b) Analogues **9.1a-g** could be tested as substrates of the *M.tb* GlmU uridylyltransferase domain to investigate substrate scope of the *M.tb* ortholog.

## 10. Perspectives and Future Directions

### 10.1 A Combined Phenotypic/Target-Based Approach to Tuberculosis Drug Discovery

Historically, phenotypic screening approaches have been the only successful platform for identifying TB drugs: all current TB medicines are derived from phenotypic screens (Sect. 1.2). In contrast, target-based screening approaches have been unsuccessful, despite the benefits of high-throughput biochemical assays and structure-based drug design. Combined approaches however, in which a phenotypic hit is “de-orphaned” and subsequent discovery efforts can adopt a target-based strategy, are anticipated to deliver the next generation of TB therapies.<sup>26</sup> De-orphaning (target identification) has been made possible by recent advances in *M.tb* genomics and proteomics.

The work presented in Chapter 5 demonstrates the prosecution of a combined phenotypic/target-based strategy (Fig. 10.1a illustrates the work-flow). **GSK'710** was identified in a phenotypic screen,<sup>117</sup> and this hit was de-orphaned through the use of an *M.tb* DprE1 over-expressor strain.<sup>118</sup> Subsequent cloning and expression of DprE1 protein facilitated the development of DprE1 enzymatic assays, which in turn enabled rapid SAR and SPR delineation around the **GSK'710** structure. Ultimately, this expedited the discovery of the highly promising lead compounds **GSK'932** and pyrimidin-2(1*H*)-ones **5.32b-c**. Identification of DprE1 as the target also prompted concurrent crystallography efforts to facilitate structure-based drug design. Encouragingly, a crystal structure of a **GSK'932** analogue bound to the *C.bovis* DprE1 ortholog was obtained during the completion of this thesis. Finally, target identification enabled the design of substrate analogues as potential inhibitors of DprE1 (Chapter 7). Whilst these compounds were only weakly active, certain analogues were used as tool molecules to probe the nature of DprE1, providing valuable insight into the binding of GSK small molecule DprE1 inhibitors (including an analogue of **GSK'710**, **7.60**). In conclusion, the combined phenotypic/target-based hit-to-lead strategy has enabled the rapid identification of highly potent cell-active DprE1 lead molecule inhibitors with good physicochemical properties, and facilitated a structural and mechanistic understanding of how the molecules interact with DprE1. This information will collectively support future lead-optimisation efforts (Fig. 10.1a). Figure 10.1b illustrates a

generalised work-flow for a combined phenotypic/target-based strategy, which could be applied to future TB drug discovery programmes.

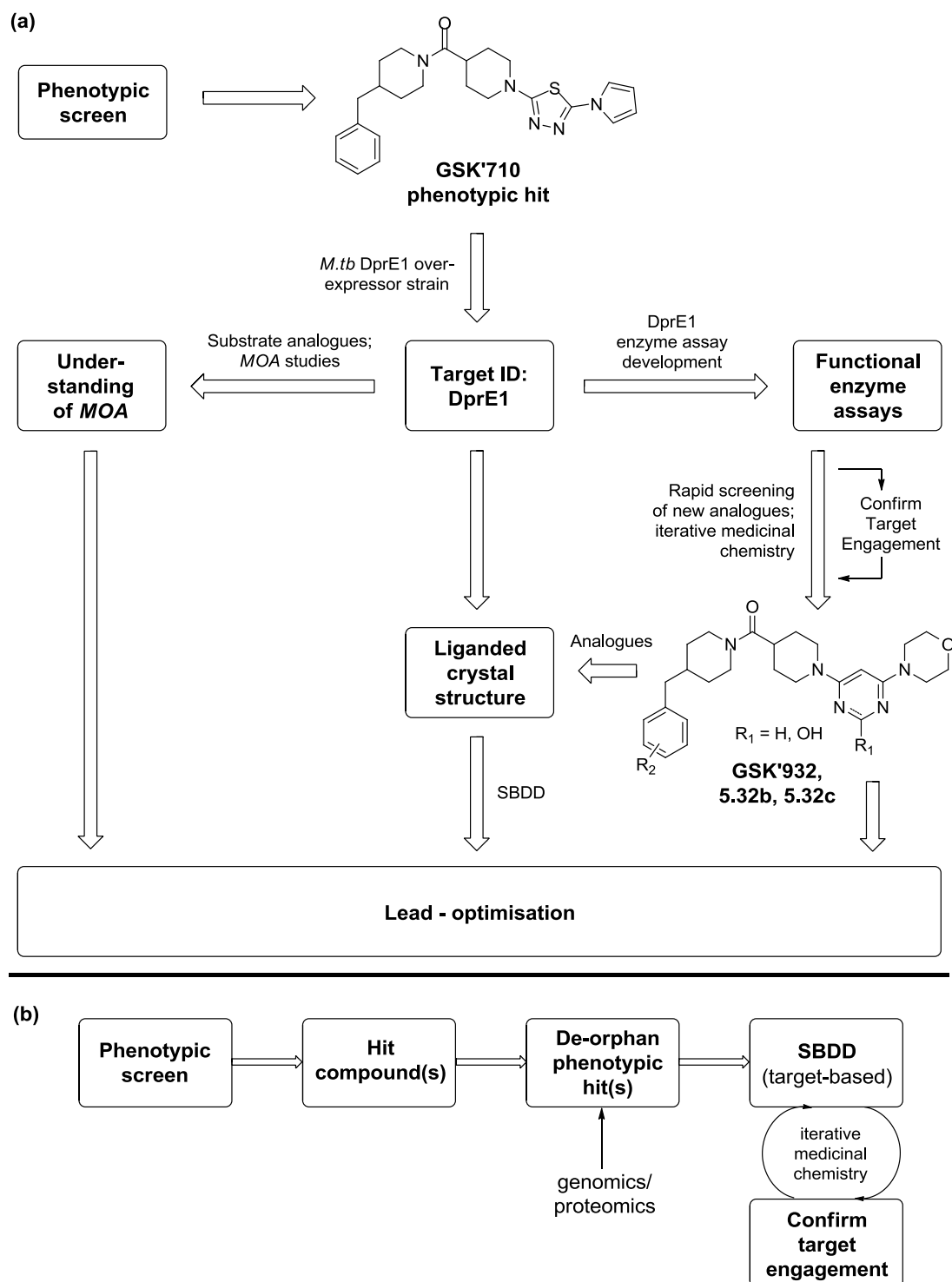


**Figure 10.1.** (a) A schematic of the hit-to-lead activities performed around **GSK'710**. (b) A generalised work-flow for a combined phenotypic/target-based approach to TB drug discovery. *MOA* = mechanism of action; SBDD = structure-based drug design.

## 10.2 Relationship Between Lipophilicity and Antimycobacterial Activity

It is generally believed that improved antimycobacterial activity correlates with lipophilicity across a series, where the more lipophilic analogues have a lower MIC than the more hydrophilic congeners. Smith and Manjunatha at the Novartis Institute for Tropical Diseases illustrated that for four series of molecules (derived from four phenotypic screening hits), an improvement in MIC was accompanied by a significant increase in lipophilicity.<sup>27</sup> The authors linked this result to permeability across the highly lipophilic mycolic acid component of the *M.tb* cell wall. The correlation between MIC and lipophilicity was also demonstrated recently in a comparison between fluoroquinolone analogues (Fig. 10.2), in which the more lipophilic moxifloxacin (cLog P = 0.6) had an 32-fold improved MIC (against *M.smeg*) over the more hydrophilic norfloxacin (cLog P = -0.1).<sup>251</sup>

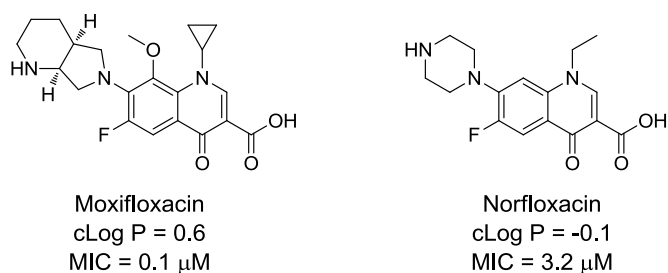


**Figure 10.2.** The more lipophilic fluoroquinolone moxifloxacin was 32-fold more potent against *M.smeg* than the less lipophilic fluoroquinolone norfloxacin.<sup>251</sup>

Analysis of the pyrimidin-2(1*H*)-ones **5.6a** and **5.32a-e** however, revealed that MIC remained roughly constant ( $0.8 \geq \text{MIC} (\mu\text{M}) \geq 3.0$ ) as lipophilicity was increased between the limits  $3.6 \geq \text{Chrom Log } D_{7.4} \geq 5.1$  (Table 10.1). Furthermore, the highly lipophilic phenotypic screening hit **GSK'710** from which **5.6a** and **5.32a-e** were derived (Chrom Log  $D_{7.4} = 6.4$ ) exhibited a similar MIC of 3.8  $\mu$ M. This result indicated that lipophilicity may not always be a key driver of MIC within a series, and highlights that there is no generalised route by which xenobiotics transit across the hydrophobic *M.tb* cell wall. One possibility is that the pyrimidin-2(1*H*)-ones and related analogues may cross the *M.tb* cell wall *via* facilitated diffusion or active transport.<sup>25</sup>



mannosylated glycoconjugates), and was shown to have an MIC of 2.7  $\mu\text{M}$ . Furthermore, **10.1** was active against MDR-TB strains. In conclusion, we have further demonstrated that modified carbohydrates can be highly useful tools for investigating *M.tb* cell wall biosynthesis targets, and emerging data suggests they may also have utility as new medicines.

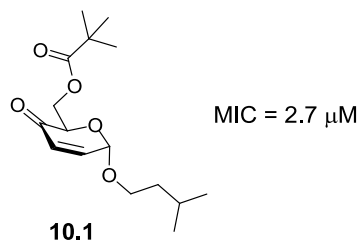


**Figure 10.3.** Deoxysugar **10.1** shows encouraging antimycobacterial activity against *M.tb* and is active against MDR-TB strains. **10.1** is believed to act *via* inhibition of the mycobacterial alpha-mannosidase.<sup>256</sup>

# 11. Experimental

## 11.1 General Experimental

All solvents and reagents, unless otherwise stated, were commercially available and were used without further purification.

### 11.1.1 Nuclear Magnetic Resonance (NMR) Spectroscopy

$^1\text{H}$  NMR spectra were obtained on a Bruker AVI II (600 MHz) spectrometer or Bruker DPX400 (400 MHz) spectrometer.  $^{13}\text{C}$  NMR spectra were obtained on a Bruker AVI500 (125 MHz) spectrometer or Bruker DPX400 (100 MHz) spectrometer.  $^{19}\text{F}$  NMR and  $^{31}\text{P}$  NMR spectra were obtained on a Bruker DPX400 (400 MHz) spectrometer. Chemical shifts were reported in parts per million (ppm) to the nearest 0.01 ppm ( $^1\text{H}$  NMR) or 0.1 ppm ( $^{13}\text{C}$ ), and were referenced to tetramethylsilane. Coupling constants ( $J$ ) were reported in Hz to the nearest 0.1 Hz ( $^1\text{H}$  NMR), or to the nearest 1.0 Hz ( $^{13}\text{C}$ ,  $^{19}\text{F}$ ,  $^{31}\text{P}$  NMR). Spectra were recorded at room temperature unless otherwise stated. Heated spectra were recorded at 120 °C.

### 11.1.2 Liquid Chromatography Mass Spectroscopy (LCMS)

The UPLC analysis was conducted on an Acquity UPLC BEH  $\text{C}_{18}$  column (50 mm x 2.1 mm, i.d. 1.7  $\mu\text{m}$  packing diameter) at 40 °C. The UV detection was a summed signal from wavelength of 210 nm to 350 nm. Mass spectrometry was conducted on a Waters ZQ mass spectrometer, with ionisation by alternate-scan positive and negative electrospray.  $t_{\text{R}}$  = LC retention time. The quoted "area % total" reports the integrated UV peak area as a percentage of the total integrated area of UV peaks present.

Method Using Formic Acid Modifier – "LCMS (formic)": LC and MS conditions as reported above. The solvents used were: A = 0.1% v/v solution of formic acid in water; B = 0.1% v/v solution of formic acid in acetonitrile. The gradient (A:B) was 97:3 to 3:97 over 2 min.

Method Using Ammonium Bicarbonate Modifier – "LCMS (high pH)": LC and MS conditions as reported above. The solvents used were: A = 10 mM ammonium bicarbonate in water adjusted to pH 10 with aq. ammonia solution; B = acetonitrile. The gradient (A:B) was 99:1 to 0:100 over 2 min.

### 11.1.3 Mass Directed Auto-Preparative HPLC (MDAP)

The HPLC separations were conducted on either a Sunfire C<sub>18</sub> column (100 mm x 19 mm, i.d. 5 µm packing diameter) or a Sunfire C<sub>18</sub> column (150 mm x 30 mm, i.d. 5 µm packing diameter) at ambient temperature. The UV detection was a summed signal from wavelength of 210 nm to 350 nm. Mass spectrometry was conducted on a Waters ZQ mass spectrometer, with an ionisation mode of alternate-scan positive and negative electrospray.

Method Using Formic Acid Modifier – “MDAP (formic)”: LC and MS conditions as reported above. The solvents employed were: A = 0.1% v/v solution of formic acid in water; B = 0.1% v/v solution of formic acid in acetonitrile. The purification was run as a gradient (A:B) over either 15 min or 25 min, with a flow rate of 20 ml/min (100 mm x 19 mm, i.d. 5 µm packing diameter) or 40 ml/min (150 mm x 30 mm, i.d. 5 µm packing diameter). See Table 10.1 for method gradients.

Method Using Ammonium Bicarbonate Modifier – “MDAP (high pH)”: LC and MS conditions as reported above. The solvents employed were: A = 10 mM ammonium bicarbonate in water, adjusted to pH 10 with aq. ammonia solution; B = acetonitrile. The purification was run as a gradient (A:B) over either 15 min or 25 min, with a flow rate of 20 ml/min (100 mm x 19 mm, i.d. 5 µm packing diameter) or 40 ml/min (150 mm x 30 mm, i.d. 5 µm packing diameter). See Table 10.1 for method gradients.

**Table 10.1.** Method Gradients for MDAP purification

Method Name	Gradient of MeCN (%) in modified H <sub>2</sub> O
Method A	5 – 30
Method B	15 – 55
Method C	30 – 85
Method D	50 – 99
Method E	80 – 99

#### **11.1.4 High Resolution Mass Spectroscopy (HRMS)**

An Agilent 1100 Liquid Chromatograph equipped with a model G1367A autosampler, a model G1312A binary pump and a HP1100 model G1315B diode array detector was used. All separations were achieved using a Phenomenex Luna C18 (2) reversed phase column (100 x 2.1 mm, 3  $\mu\text{m}$  particle size). ESI (+) high resolution mass spectra (HRMS) were obtained on a Micromass Q-ToF 2 hybrid quadrupole time-of-flight mass spectrometer, equipped with a Z-spray interface, over a mass range of 100 – 1100 Da, with a scan time of 0.9 s and an interscan delay of 0.1 s. Reserpine was used as the external mass calibrant ( $[\text{M}+\text{H}]^+ = 609.2812$  Da). The elemental composition was calculated using MassLynx v4.1 for the  $[\text{M}+\text{H}]^+$ . All measured masses are accurate to within 5 ppm of the calculated mass.

#### **11.1.5 Melting Points**

Melting points were measured on a Stuart automatic melting point apparatus SMP40. For compounds that decomposed over a wide temperature range, it was possible to watch a recorded video of the experiment to manually determine the melting point range.

#### **11.1.6 Optical Rotations**

Optical rotation values were measured on a Jasco P1030 polarimeter and  $[\alpha_D]$  values were reported in  $10^{-1} \text{ deg cm}^2 \text{ g}^{-1}$ .

#### **11.1.7 Infrared (IR) Spectroscopy**

IR spectra were obtained on a Perkin Elmer Spectrum One machine and the data was processed using Perkin Elmer Spectrum software. Absorption frequencies of the higher intensity peaks are reported in wavenumbers ( $\text{cm}^{-1}$ ).

#### **11.1.8 Purification by Column Chromatography**

Column chromatography was conducted on a Teledyne Isco Combiflash<sup>®</sup> Rf automated flash chromatography system, using disposable, normal or reversed phase Redisep cartridges (4 g to 330 g). The system was equipped with a UV variable dual-wavelength detector and a Foxy<sup>®</sup> fraction collector that enabled automated peak cutting, collection, and tracking. Reversed phase chromatography employing modified water (high pH) used a 10 mM aqueous ammonium bicarbonate solution, adjusted to pH 10 with aq. ammonia

solution. Reversed phase chromatography employing modified water (formic) used a 0.1% v/v solution of formic acid in water.

#### **11.1.9 Purification by Solid Phase Extraction**

Strong cation exchange chromatography was performed using Biotage ISOLUTE Flash SCX 2 solid phase extraction cartridges. The cartridge was wetted with 1 column volume of MeOH before the sample was loaded onto the column head in a minimal volume of MeOH. The column was washed with 3 column volumes of MeOH then the compound was eluted in 4 column volumes of 2 M NH<sub>3</sub> in MeOH.

Weak anion exchange chromatography was performed using Biotage ISOLUTE Flash NH<sub>2</sub> (aminopropyl) solid phase extraction cartridge. The cartridge was wetted with 1 column volume of MeOH before the sample was loaded onto the column head in a minimal volume of MeOH. The column was washed with 3 column volumes of MeOH then the compound was eluted in 4 column volumes of MeCN containing 15% v/v conc. NH<sub>4</sub>OH solution.

#### **11.1.10 Microwave Chemistry**

Microwave chemistry was performed using a Biotage Initiator<sup>TM</sup> Microwave Synthesiser. Reaction mixtures were sealed in a Biotage microwave reaction vial (0.5 mL, 2.0 mL or 20 mL) with a Teflon cap.

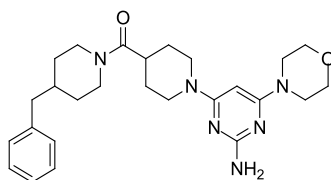
## 11.2 Synthesis of Compounds in Chapter 5

### ***N*4-((3-Isobutylisoxazol-5-yl)methyl)-6-morpholinopyrimidine-2,4-diamine (GSK'295)**



A solution of HCl in 1,4-dioxane (4 M, 2 mL) was added to di-*tert*-butyl (4-chloro-6-morpholinopyrimidin-2-yl)imidodicarbamate **5.19** (13.0 mg, 24.0  $\mu$ mol). This mixture was stirred for 16 hours, after which it was concentrated under reduced pressure. The residue was adsorbed onto diatomaceous earth and purified by reversed phase chromatography, eluting under a gradient of MeCN (10-40%) in modified water (high pH) to afford the title compound **GSK'295** (6.2 mg, 19.0  $\mu$ mol, 76 % yield) as a straw-coloured gum.  $^1\text{H}$  NMR (400 MHz, MeOD- $d_4$ ):  $\delta$  0.95 (d,  $J$  = 6.9 Hz, 6H), 1.89-2.02 (m, 1H), 2.51 (d,  $J$  = 7.3 Hz, 2H), 3.42-3.45 (m, 4H), 3.70-3.73 (m, 4H), 4.58 (s, 2H), 5.19 (s, 1H), 6.15 (s, 1H). *Exchangeable protons not observed.*  $^{13}\text{C}$  NMR (100 MHz, MeOD- $d_4$ ):  $\delta$  22.8 (2C), 29.2, 35.9, 38.1, 46.1 (2C), 67.8 (2C), 75.3, 103.1, 164.3, 164.9, 165.9, 166.0, 172.7. IR  $\nu_{\text{max}}$  (neat): 3335 (br.), 2958, 2856, 1562, 1507, 1436, 1368, 1267, 1228, 1179, 1115, 1002, 873, 792  $\text{cm}^{-1}$ . HR-MS (ESI):  $\text{C}_{16}\text{H}_{25}\text{N}_6\text{O}_2$  [ $\text{M}+\text{H}^+$ ] requires 333.2034, found 333.2035.

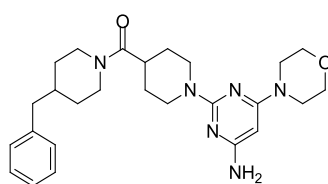
### **(1-(2-Amino-6-morpholinopyrimidin-4-yl)piperidin-4-yl)(4-benzylpiperidin-1-yl)methanone (5.3a)**



To a solution of (4-benzylpiperidin-1-yl)(piperidin-4-yl)methanone hydrochloride (**'932-amine.HCl**, 120 mg, 0.373 mmol) in EtOH (0.9 mL) was added 4-chloro-6-morpholinopyrimidin-2-amine **5.17** (40.0 mg, 0.186 mmol) and DIPEA (98.0  $\mu$ L, 0.559 mmol). The mixture was heated at 150  $^{\circ}\text{C}$  in the microwave for 3 hours, after which time direct purification of the mixture by MDAP (high pH, Method C) afforded the title compound **5.3a** (64.1 mg, 0.138 mmol, 74 % yield) as a straw-coloured foam.  $^1\text{H}$  NMR (600 MHz, DMSO- $d_6$ ):  $\delta$  0.93-1.01 (m, 1H), 1.04-1.12 (m, 1H), 1.40-1.48 (m, 2H), 1.56-1.64 (m,

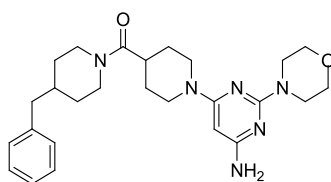
4H), 1.72-1.77 (m, 1H), 2.45 (t,  $J = 12.2$  Hz, 1H), 2.52 (s, 2H), 2.75-2.80 (m, 2H), 2.85 (tt,  $J = 3.7, 11.3$  Hz, 1H), 2.95 (t,  $J = 12.2$  Hz, 1H), 3.40-3.42 (m, 4H), 3.61-3.62 (m, 4H), 3.97 (d,  $J = 12.6$  Hz, 1H), 4.27 (d,  $J = 12.6$  Hz, 2H), 4.35 (d,  $J = 12.6$  Hz, 1H), 5.30 (s, 1H), 5.56 (s, 2H), 7.17-7.20 (m, 3H), 7.27-7.29 (m, 2H).  $^{13}\text{C}$  NMR (125 MHz,  $\text{DMSO-}d_6$ ):  $\delta$  27.8, 28.0, 31.4, 32.6, 37.5 (2C), 41.2, 42.0, 43.3 (2C), 44.3 (2C), 44.8, 66.0 (2C), 73.1, 125.8, 128.1 (2C), 129.0 (2C), 140.0, 162.2, 164.0, 164.6, 172.1. IR  $\nu_{\text{max}}$  (neat): 3342, 2917, 2848, 1628, 1565, 1418, 1370, 1252, 1210, 1188, 1115, 987, 967, 898, 789, 745, 700  $\text{cm}^{-1}$ . HR-MS (ESI):  $\text{C}_{26}\text{H}_{37}\text{N}_6\text{O}_2$  [ $\text{M}+\text{H}^+$ ] requires 465.2973, found 465.2980.

**(1-(4-Amino-6-morpholinopyrimidin-2-yl)piperidin-4-yl)(4-benzylpiperidin-1-yl)methanone (5.3b)**



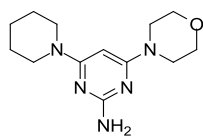
The title compound **5.3b** (22.6 mg, 49.0  $\mu\text{mol}$ , 35 % yield, brown solid) was prepared in the same manner as **5.3a** using the following reagents and solvents: '932-amine.HCl (90.0 mg, 0.280 mmol), 2-chloro-6-morpholinopyrimidin-4-amine **5.21** (30.0 mg, 0.140 mmol), DIPEA (73.0  $\mu\text{L}$ , 0.419 mmol), EtOH (0.9 mL). The compound was purified by MDAP (high pH, Method C). M.pt. 218-224  $^{\circ}\text{C}$  (decomp.).  $^1\text{H}$  NMR (400 MHz,  $\text{DMSO-}d_6$ , heated):  $\delta$  1.06-1.18 (m, 2H), 1.48-1.71 (m, 6H), 1.79-1.89 (m, 1H), 2.58 (d,  $J = 7.0$  Hz, 2H), 2.82-2.92 (m, 5H), 3.39-3.42 (m, 4H), 3.65-3.67 (m, 4H), 4.10-4.17 (m, 2H), 4.47-4.54 (m, 2H), 5.13 (s, 1H), 5.36 (br.s, 2H), 7.17-7.21 (m, 3H), 7.25-7.31 (m, 2H).  $^{13}\text{C}$  NMR (125 MHz,  $\text{DMSO-}d_6$ ):  $\delta$  28.1, 28.2, 31.5, 32.6, 37.5, 37.7, 41.2, 42.0, 42.9 (2C), 44.2 (2C), 44.8, 65.9 (2C), 73.7, 125.8, 128.1 (2C), 129.0 (2C), 140.0, 160.7, 163.7, 164.9, 172.2. IR  $\nu_{\text{max}}$  (neat): 3415, 3322, 2913, 2843, 1619, 1579, 1556, 1431, 1308, 1223, 1117, 998, 786, 698  $\text{cm}^{-1}$ . HR-MS (ESI):  $\text{C}_{26}\text{H}_{37}\text{N}_6\text{O}_2$  [ $\text{M}+\text{H}^+$ ] requires 465.2973, found 465.2989.

**(1-(6-Amino-2-morpholinopyrimidin-4-yl)piperidin-4-yl)(4-benzylpiperidin-1-yl)methanone (5.3c)**



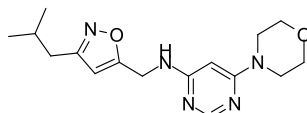
The title compound **5.3c** (40.1 mg, 86.0  $\mu\text{mol}$ , 46 % yield, off-white solid) was prepared in the same manner as **5.3a** using the following reagents and solvents: '932-amine.HCl (120 mg, 0.373 mmol), 6-chloro-2-morpholinopyrimidin-4-amine **5.22** (40.0 mg, 0.186 mmol), DIPEA (98.0  $\mu\text{L}$ , 0.559 mmol), EtOH (0.9 mL). The compound was purified by MDAP (high pH, Method C). M.pt. 186-195  $^{\circ}\text{C}$  (decomp.).  $^1\text{H}$  NMR (400 MHz, DMSO- $d_6$ , heated):  $\delta$  1.07-1.16 (m, 2H), 1.57-1.69 (m, 6H), 1.83-1.86 (m, 1H), 2.58 (d,  $J = 7.3$  Hz, 2H), 2.82-2.94 (m, 5H), 3.61 (br.s, 8H), 4.10-4.16 (m, 4H), 5.18 (s, 1H), 5.29 (br.s, 2H), 7.16-7.22 (m, 3H), 7.27-7.31 (m, 2H).  $^{13}\text{C}$  NMR (125 MHz, DMSO- $d_6$ ):  $\delta$  27.6, 27.9, 31.5, 32.6, 37.5, 37.5, 41.2, 42.1, 43.4 (2C), 44.0 (2C), 44.8, 66.1 (2C), 74.1, 125.8, 128.1 (2C), 129.0 (2C), 140.0, 161.2, 163.0, 164.9, 172.0. IR  $\nu_{\text{max}}$  (neat): 3343, 2915, 2847, 1609, 1562, 1427, 1254, 1208, 1112, 998, 966, 789, 749, 702  $\text{cm}^{-1}$ . HR-MS (ESI):  $\text{C}_{26}\text{H}_{37}\text{N}_6\text{O}_2$  [ $\text{M}+\text{H}^+$ ] requires 465.2973, found 465.2973.

**4-Morpholino-6-(piperidin-1-yl)pyrimidin-2-amine (5.4a)**



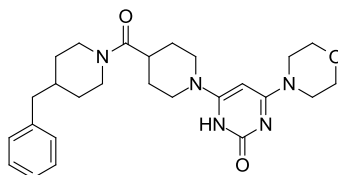
The title compound **5.4a** (55.0 mg, 0.209 mmol, 90 % yield, straw coloured gum) was prepared in the same manner as **5.3a** using the following reagents and solvents: piperidine (69.0  $\mu\text{L}$ , 0.699 mmol), 4-chloro-6-morpholinopyrimidin-2-amine **5.17** (50.0 mg, 0.233 mmol), DIPEA (0.122 mL, 0.699 mmol), EtOH (0.9 mL). The compound was purified by MDAP (high pH, Method B).  $^1\text{H}$  NMR (400 MHz, DMSO- $d_6$ ):  $\delta$  1.43-1.49 (m, 4H), 1.56-1.62 (m, 2H), 3.39-3.41 (m, 4H), 3.45-3.48 (m, 4H), 3.60-3.62 (m, 4H), 5.28 (s, 1H), 5.55 (m, 2H).  $^{13}\text{C}$  NMR (100 MHz, DMSO- $d_6$ ):  $\delta$  24.4, 25.2 (2C), 44.3 (2C), 44.6 (2C), 66.0 (2C), 73.0, 162.1, 163.9, 164.6. IR  $\nu_{\text{max}}$  (neat): 3324, 2932, 2852, 1661, 1612, 1564, 1497, 1442, 1419, 1371, 1256, 1226, 1115, 1020, 990, 900, 854, 790, 727  $\text{cm}^{-1}$ . HR-MS (ESI):  $\text{C}_{13}\text{H}_{22}\text{N}_5\text{O}$  [ $\text{M}+\text{H}^+$ ] requires 264.1819, found 264.1828.

#### ***N*-((3-Isobutylisoxazol-5-yl)methyl)-6-morpholinopyrimidin-4-amine (5.5)**



To a solution of (3-isobutylisoxazol-5-yl)methanamine hydrochloride **5.16** (50.0 mg, 0.262 mmol) in EtOH (0.9 mL) was added 4,6-dichloropyrimidine **5.23** (39.1 mg, 0.262 mmol) and DIPEA (0.114 mL, 0.656 mmol). The mixture was heated to 150 °C in the microwave for 5 minutes. After this time, morpholine (0.115 mL, 1.31 mmol) was added and the reaction mixture was heated in the microwave at 150 °C for 1 hour. Direct purification of the mixture by MDAP (high pH, Method C) afforded the title compound **5.5** (52.4 mg, 0.165 mmol, 63 % yield) as a cream solid. M.pt. 121-123 °C. <sup>1</sup>H NMR (400 MHz, MeOD-*d*<sub>4</sub>): δ 0.95 (d, *J* = 6.6 Hz, 6H), 1.89-2.02 (m, 1H), 2.51 (d, *J* = 7.1 Hz, 2H), 3.49-3.51 (m, 4H), 3.74-3.76 (m, 4H), 4.63 (s, 2H), 5.73 (s, 1H), 6.16 (s, 1H), 8.06 (s, 1H). *Exchangeable protons not observed.* <sup>13</sup>C NMR (100 MHz, MeOD-*d*<sub>4</sub>): δ 22.8 (2C), 29.2, 35.9, 38.0, 45.9 (2C), 67.7 (2C), 83.7, 103.2, 158.5, 164.4, 164.6, 164.9, 172.1. IR  $\nu_{\text{max}}$  (neat): 3237, 3116, 2957, 2869, 1586, 1480, 1433, 1333, 1298, 1258, 1227, 1205, 1115, 982, 961, 882, 846, 800, 761, 700 cm<sup>-1</sup>. HR-MS (ESI): C<sub>16</sub>H<sub>24</sub>N<sub>5</sub>O<sub>2</sub> [M+H<sup>+</sup>] requires 318.1925, found 318.1922.

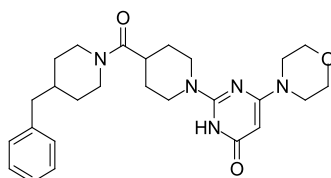
#### **4-(4-(4-Benzylpiperidine-1-carbonyl)piperidin-1-yl)-6-morpholinopyrimidin-2(1H)-one (5.6a)**



To a solution of 4-(6-chloro-2-((4-methoxybenzyl)oxy)pyrimidin-4-yl)morpholine **5.24a** (75.0 mg, 0.223 mmol) and DIPEA (0.117 mL, 0.670 mmol) in EtOH (0.9 mL) was added '932-amine.HCl (144 mg, 0.447 mmol). The mixture was heated to 150 °C in the microwave for 8 hours, after which time direct purification of the reaction mixture by MDAP (high pH, Method B) afforded the title compound **5.6a** (84.2 mg, 0.181 mmol, 81 % yield) as a straw coloured glass that was scratched to give an amorphous white solid. M.pt. 117-123 °C. <sup>1</sup>H NMR (400 MHz, DMSO-*d*<sub>6</sub>): δ 0.95-1.01 (m, 1H), 1.05-1.12 (m, 1H), 1.44-1.65 (m, 6H), 1.70-1.81 (m, 1H), 2.42-2.49 (m, 1H), 2.52-2.54 (m, 2H), 2.86-2.99 (m, 4H), 3.42-3.45 (m, 4H), 3.60-3.63 (m, 4H), 3.98 (d, *J* = 12.6 Hz, 1H), 4.12-4.17 (m, 2H), 4.36 (d, *J* = 12.6 Hz, 1H), 5.21

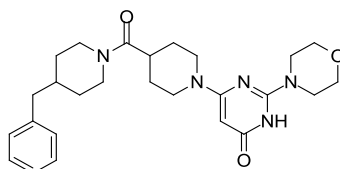
(s, 1H), 7.17-7.21 (m, 3H), 7.27-7.31 (m, 2H), 9.41 (br.s, 1H).  $^{13}\text{C}$  NMR (125 MHz, DMSO- $d_6$ ):  $\delta$  27.8, 28.0, 31.5, 32.6, 37.0, 37.5, 41.2, 42.0, 44.3, 44.8, 44.9 (2C), 48.6, 65.8 (2C), 71.1, 125.8, 128.1 (2C), 129.0 (2C), 140.0, 158.0, 160.6, 162.2, 171.9. IR  $\nu_{\text{max}}$  (neat): 2918, 2851, 1596, 1507, 1441, 1366, 1255, 1205, 1115, 967, 747, 701  $\text{cm}^{-1}$ . HR-MS (ESI):  $\text{C}_{26}\text{H}_{36}\text{N}_5\text{O}_3$   $[\text{M}+\text{H}^+]$  requires 466.2813, found 466.2814.

**2-(4-(4-Benzylpiperidine-1-carbonyl)piperidin-1-yl)-6-morpholinopyrimidin-4(3H)-one (5.6b)**



The title compound **5.6b** (32.5 mg, 70.0  $\mu\text{mol}$ , 47 % yield, straw coloured glass) was prepared in the same manner as **5.6a** using the following reagents and solvents: 4-(2-chloro-6-((4-methoxybenzyl)oxy)pyrimidin-4-yl)morpholine **5.24b** (50.0 mg, 0.149 mmol) DIPEA (78.0  $\mu\text{L}$ , 0.447 mmol), **932**-amine.HCl (96.0 mg, 0.298 mmol), EtOH (0.9 mL). The compound was purified by MDAP (high pH, Method C).  $^1\text{H}$  NMR (400 MHz, DMSO- $d_6$ ):  $\delta$  0.93-1.02 (m, 1H), 1.04-1.13 (m, 1H), 1.40-1.52 (m, 2H), 1.55-1.65 (m, 4H), 1.74-1.78 (m, 1H), 2.41-2.48 (m, 1H), 2.51-2.53 (m, 2H), 2.85-2.98 (m, 4H), 3.38-3.40 (m, 4H), 3.61-3.63 (m, 4H), 3.98 (d,  $J = 12.9$  Hz, 1H), 4.30-4.37 (m, 3H), 4.84 (s, 1H), 7.17-7.21 (m, 3H), 7.27-7.31 (m, 2H), 10.32 (br.s, 1H).  $^{13}\text{C}$  NMR (125 MHz, DMSO- $d_6$ ):  $\delta$  27.8, 28.0, 31.4, 32.6, 37.0, 37.5, 41.2, 42.0, 43.7, 44.2 (3C), 44.8, 65.8 (2C), 76.3, 125.8, 128.1 (2C), 129.0 (2C), 140.0, 154.0, 163.3, 165.4, 171.9. IR  $\nu_{\text{max}}$  (neat): 2916, 2849, 1624, 1559, 1438, 1370, 1296, 1230, 1190, 1114, 999, 967, 785, 747, 700  $\text{cm}^{-1}$ . HR-MS (ESI):  $\text{C}_{26}\text{H}_{36}\text{N}_5\text{O}_3$   $[\text{M}+\text{H}^+]$  requires 466.2813, found 466.2804.

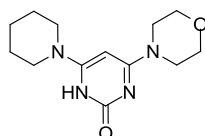
**6-(4-(4-Benzylpiperidine-1-carbonyl)piperidin-1-yl)-2-morpholinopyrimidin-4(3H)-one (5.6c)**



The title compound **5.6c** (42.5 mg, 91.0  $\mu\text{mol}$ , 41 % yield, white solid), was prepared in the same manner as **5.6a** using the following reagents and solvents: 4-(4-chloro-6-((4-methoxybenzyl)oxy)pyrimidin-2-yl)morpholine **5.24c** (75.0 mg, 0.223 mmol), DIPEA (0.117

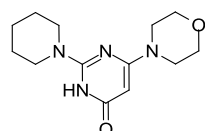
mL, 0.670 mmol), '932-amine.HCl (144 mg, 0.447 mmol), EtOH (0.9 mL). The compound was purified by MDAP (high pH, Method C). M.pt. 119-122 °C. <sup>1</sup>H NMR (400 MHz, DMSO-*d*<sub>6</sub>): δ 0.92-1.13 (m, 2H), 1.42-1.51 (m, 2H), 1.57-1.64 (m, 4H), 1.70-1.82 (m, 1H), 2.43-2.48 (m, 1H), 2.51-2.54 (m, 2H), 2.81-2.99 (m, 4H), 3.52-3.54 (m, 4H), 3.60-3.63 (m, 4H), 3.97 (d, *J* = 12.8 Hz, 1H), 4.14-4.19 (m, 2H), 4.35 (d, *J* = 12.8 Hz, 1H), 4.92 (s, 1H), 7.17-7.21 (m, 3H), 7.27-7.31 (m, 2H), 10.30 (br.s, 1H). <sup>13</sup>C NMR (125 MHz, DMSO-*d*<sub>6</sub>): δ 27.7, 28.0, 31.5, 32.16, 37.3, 37.5, 41.2, 42.1, 43.5 (2C), 44.4 (2C), 44.8, 65.7 (2C), 76.3, 125.8, 128.1 (2C), 129.0 (2C), 140.0, 155.3, 162.7, 165.9, 172.0. IR ν<sub>max</sub> (neat): 2914, 2850, 1621, 1554, 1440, 1378, 1255, 1211, 1115, 968, 783, 746, 700 cm<sup>-1</sup>. HR-MS (ESI): C<sub>26</sub>H<sub>36</sub>N<sub>5</sub>O<sub>3</sub> [M+H<sup>+</sup>] requires 466.2813, found 466.2821.

#### 4-Morpholino-6-(piperidin-1-yl)pyrimidin-2(1H)-one (5.7a)



4-(2-((4-methoxybenzyl)oxy)-6-(piperidin-1-yl)pyrimidin-4-yl)morpholine **5.25a** (60.0 mg, 0.156 mmol) was dissolved in a mixture of DCM/TFA (3 mL, 1:1). This mixture was stirred for 1 hour, after which time it was concentrated to dryness under reduced pressure. The residue was dissolved in DMF (1 mL) and subjected to MDAP purification (high pH, Method A) to give the title compound **5.7a** (36.7 mg, 0.139 mmol, 89 % yield) as a white solid. M.pt. 259-270 °C (decomp.). <sup>1</sup>H NMR (400 MHz, DMSO-*d*<sub>6</sub>): δ 1.47-1.51 (m, 4H), 1.56-1.62 (m, 2H), 3.41-3.45 (m, 8H), 3.60-3.63 (m, 4H), 5.18 (s, 1H), 8.39 (s, 1H). <sup>13</sup>C NMR (125 MHz, DMSO-*d*<sub>6</sub>): δ 24.0, 25.1 (2C), 44.9 (2C), 45.7 (2C), 65.8 (2C), 70.8, 157.9, 160.6, 162.3. IR ν<sub>max</sub> (neat): 2927, 2840, 1596, 1534, 1498, 1427, 1382, 1360, 1265, 1228, 1207, 1115, 1028, 1000, 896, 861, 828, 778, 747 cm<sup>-1</sup>. HR-MS (ESI): C<sub>13</sub>H<sub>21</sub>N<sub>4</sub>O<sub>2</sub> [M+H<sup>+</sup>] requires 265.1659, found 265.1665.

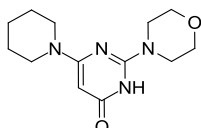
#### 6-Morpholino-2-(piperidin-1-yl)pyrimidin-4(3H)-one (5.7b)



The title compound **5.7b** (38.7 mg, 0.146 mmol, 66 % yield, white solid), was prepared in the same manner as **5.7a** using the following reagents and solvents: 4-(6-((4-methoxybenzyl)oxy)-2-(piperidin-1-yl)pyrimidin-4-yl)morpholine **5.25b** (85.0 mg, 0.221

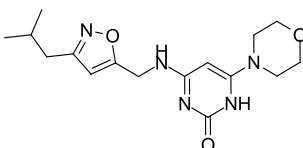
mmol), DCM/TFA (3 mL, 1:1). The compound was purified by MDAP (high pH, Method B). M.pt. 234-243 °C (decomp.). <sup>1</sup>H NMR (400 MHz, DMSO-*d*<sub>6</sub>): δ 1.45-1.51 (m, 4H), 1.56-1.61 (m, 2H), 3.37-3.39 (m, 4H), 3.53-3.56 (m, 4H), 3.60-3.62 (m, 4H), 4.81 (s, 1H), 10.31 (br.s, 1H). <sup>13</sup>C NMR (125 MHz, DMSO-*d*<sub>6</sub>): δ 24.0 25.1 (2C), 44.3 (2C), 45.0 (2C), 65.9 (2C), 76.1, 154.1, 163.3, 165.5. IR ν<sub>max</sub> (neat): 2925, 2849, 1642, 1556, 1444, 1397, 1366, 1278, 1226, 1211, 1120, 1011, 900, 864, 780, 711, 673 cm<sup>-1</sup>. HR-MS (ESI): C<sub>13</sub>H<sub>21</sub>N<sub>4</sub>O<sub>2</sub> [M+H<sup>+</sup>] requires 265.1659, found 265.1649.

#### 2-Morpholino-6-(piperidin-1-yl)pyrimidin-4(3H)-one (5.7c)



The title compound **5.7c** (37.5 mg, 0.142 mmol, 84 % yield, white solid), was prepared in the same manner as **5.7a** using the following reagents and solvents: 4-(4-((4-methoxybenzyl)oxy)-6-(piperidin-1-yl)pyrimidin-2-yl)morpholine **5.25c** (65.0 mg, 0.169 mmol), DCM/TFA (3 mL, 1:1). The compound was purified by MDAP (high pH, Method B). M.pt. 231-253 °C (decomp.). <sup>1</sup>H NMR (400 MHz, DMSO-*d*<sub>6</sub>): δ 1.44-1.50 (m, 4H), 1.56-1.60 (m, 2H), 3.42-3.45 (m, 4H), 3.51-3.53 (m, 4H), 3.60-3.63 (m, 4H), 4.89 (s, 1H), 8.39 (s, 1H). <sup>13</sup>C NMR (100 MHz, DMSO-*d*<sub>6</sub>): δ 24.2, 25.1 (2C), 44.4 (2C), 44.8 (2C), 65.7 (2C), 76.0, 155.5, 162.7, 166.0. IR ν<sub>max</sub> (neat): 2915, 2848, 1621, 1554, 1479, 1441, 1375, 1304, 1267, 1220, 1119, 1023, 1016, 900, 858, 781 cm<sup>-1</sup>. HR-MS (ESI): C<sub>13</sub>H<sub>21</sub>N<sub>4</sub>O<sub>2</sub> [M+H<sup>+</sup>] requires 265.1659, found 265.1664.

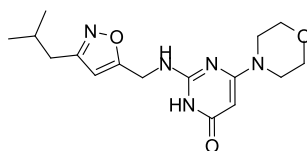
#### 4-(((3-Isobutylisoxazol-5-yl)methyl)amino)-6-morpholinopyrimidin-2(1H)-one (5.8a)



The title compound **5.8a** (13.3 mg, 40.3 μmol, 50 % yield, off-white solid), was prepared in the same manner as **5.7a** using the following reagents and solvents: *N*-(((3-isobutylisoxazol-5-yl)methyl)amino)-2-((4-methoxybenzyl)oxy)-6-morpholinopyrimidin-4-amine **5.26a** (36.0 mg, 79.1 μmol), DCM/TFA (3 mL, 1:1). The compound was purified by MDAP (high pH, Method B). M.pt. 227-230 °C (decomp.). <sup>1</sup>H NMR (400 MHz, DMSO-*d*<sub>6</sub>): δ 0.89 (d, *J* = 6.7 Hz, 6H), 1.86-1.97 (m, 1H), 2.46 (d, *J* = 7.1 Hz, 2H), 3.38-3.40 (m, 4H), 3.59-3.62 (m, 4H), 4.54 (d, *J* =

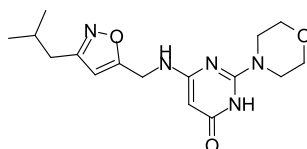
5.0 Hz, 2H), 5.07 (s, 1H), 6.24 (s, 1H), 7.32 (br.s, 1H), 10.06 (br.s, 1H).  $^{13}\text{C}$  NMR (125 MHz, DMSO- $d_6$ ):  $\delta$  22.1 (2C), 27.2, 34.1, 36.5, 44.8 (2C), 65.7 (2C), 69.6, 102.1, 156.5, 162.6, 169.3. Two  $^{13}\text{C}$  signals not observed due to line broadening. IR  $\nu_{\text{max}}$  (neat): 3675, 2961, 2901, 1668, 1598, 1517, 1418, 1367, 1318, 1235, 1115, 1066, 872, 778, 721  $\text{cm}^{-1}$ . HR-MS (ESI):  $\text{C}_{16}\text{H}_{24}\text{N}_5\text{O}_3$  [ $\text{M}+\text{H}^+$ ] requires 334.1874, found 334.1899.

### 2-(((3-Isobutylisoxazol-5-yl)methyl)amino)-6-morpholinopyrimidin-4(3H)-one (5.8b)



The title compound **5.8b** (17.1 mg, 51.0  $\mu\text{mol}$ , 47 % yield, off-white solid), was prepared in the same manner as **5.7a** using the following reagents and solvents: *N*-((3-isobutylisoxazol-5-yl)methyl)-4-((4-methoxybenzyl)oxy)-6-morpholinopyrimidin-2-amine **5.26b** (50.0 mg, 0.110 mmol), DCM/TFA (3 mL, 1:1). The compound was purified by MDAP (high pH, Method B). M.pt. 175-177  $^{\circ}\text{C}$ .  $^1\text{H}$  NMR (400 MHz, DMSO- $d_6$ ):  $\delta$  0.88 (d,  $J$  = 6.8 Hz, 6H), 1.83-1.98 (m, 1H), 2.44 (d,  $J$  = 7.1 Hz, 2H), 3.33-3.36 (m, 4H), 3.56-3.58 (m, 4H), 4.51 (d,  $J$  = 5.4 Hz, 2H), 4.74 (s, 1H), 6.19 (s, 1H), 7.18 (br.s, 1H), 8.41 (s, 1H).  $^{13}\text{C}$  NMR (125 MHz, DMSO- $d_6$ ):  $\delta$  22.1 (2C), 27.3, 34.2, 36.2, 44.3 (2C), 65.8 (2C), 77.2, 101.6, 153.4, 162.6, 163.0, 165.8, 170.2. IR  $\nu_{\text{max}}$  (neat): 3162, 2844, 1617, 1581, 1522, 1443, 1319, 1231, 1115, 1022, 948, 866, 778, 675  $\text{cm}^{-1}$ . HR-MS (ESI):  $\text{C}_{16}\text{H}_{24}\text{N}_5\text{O}_3$  [ $\text{M}+\text{H}^+$ ] requires 334.1874, found 334.1873.

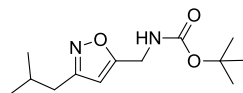
### 6-(((3-Isobutylisoxazol-5-yl)methyl)amino)-2-morpholinopyrimidin-4(3H)-one (5.8c)



The title compound **5.8c** (13.7 mg, 0.041 mmol, 50 % yield, white solid), was prepared in the same manner as **5.7a** using the following reagents and solvents: *N*-((3-isobutylisoxazol-5-yl)methyl)-6-((4-methoxybenzyl)oxy)-2-morpholinopyrimidin-4-amine **5.26c** (37.0 mg, 0.082 mmol), DCM/TFA (3 mL, 1:1). The compound was purified by MDAP (high pH, Method B). M.pt. 197-201  $^{\circ}\text{C}$ .  $^1\text{H}$  NMR (400 MHz, DMSO- $d_6$ ):  $\delta$  0.88 (d,  $J$  = 6.6 Hz, 6H), 1.83-1.97 (m, 1H), 2.44 (d,  $J$  = 7.1 Hz, 2H), 3.50-3.53 (m, 4H), 3.57-3.60 (m, 4H), 4.45-4.47 (m, 2H), 4.76 (s, 1H), 6.16 (s, 1H), 7.17 (br.s, 1H), 10.27 (br.s, 1H).  $^{13}\text{C}$  NMR (125 MHz, DMSO- $d_6$ ):  $\delta$  22.1 (2C),

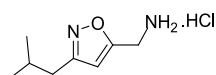
27.3, 34.2, 36.5, 44.3 (2C), 65.7 (2C), 76.5, 101.6, 156.0, 162.5, 163.3, 165.4, 170.6. IR  $\nu_{\max}$  (neat): 2958, 1594, 1553, 1524, 1461, 1411, 1351, 1296, 1270, 1209, 1175, 1022, 923, 866, 744  $\text{cm}^{-1}$ . HR-MS (ESI):  $\text{C}_{16}\text{H}_{24}\text{N}_5\text{O}_3$   $[\text{M}+\text{H}^+]$  requires 334.1874, found 334.1876.

#### ***Tert*-butyl ((3-isobutylisoxazol-5-yl)methyl)carbamate (5.15)**



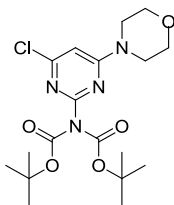
To a solution of hydroxylamine hydrochloride (0.847 g, 12.2 mmol) in water (24 mL) and *tert*-butanol (24 mL) was added 3-methylbutanal **5.14** (1.25 mL, 11.6 mmol) followed by sodium hydroxide (0.488 g, 12.2 mmol). This mixture was stirred for 0.5 hours at room temperature. Chloramine-T trihydrate (3.43 g, 12.2 mmol) was added in small portions, followed by copper(II) sulfate pentahydrate (87.0 mg, 0.348 mmol) and copper turnings (25.0 mg). *Tert*-butyl prop-2-yn-1-ylcarbamate (1.89 g, 12.2 mmol) was added and the pH was adjusted to 6 by addition of 1 M NaOH. Stirring was continued for a further 16 hours. The reaction mixture was poured into ice water (100 mL) and dilute  $\text{NH}_4\text{OH}$  (15 mL) was added, and then the mixture was filtered. The filtrate was adsorbed onto diatomaceous earth and purified by reversed phase chromatography, eluting under a gradient of MeOH (25-60%) in modified water (high pH), affording the title compound **5.15** (1.73 g, 6.80 mmol, 59 % yield) as an orange oil.  $^1\text{H}$  NMR (400 MHz,  $\text{MeOD}-d_4$ ):  $\delta$  0.97 (d,  $J = 6.8$  Hz, 6H), 1.47 (s, 9H), 1.91-2.04 (m, 1H), 2.52 (d,  $J = 7.1$  Hz, 2H), 4.33 (s, 2H), 6.14 (s, 1H). *Exchangeable protons not observed*. LCMS (high pH):  $t_{\text{R}} = 1.09$  min,  $[\text{M}+\text{H}^+]$  255,  $[\text{M}+\text{H}^++\text{MeCN}]$  296; (area % total: 100).

#### **(3-Isobutylisoxazol-5-yl)methanamine hydrochloride salt (5.16)**



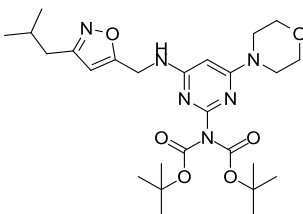
*Tert*-butyl ((3-isobutylisoxazol-5-yl)methyl)carbamate **5.15** (1.48 g, 5.82 mmol) was dissolved in a solution of HCl in 1,4-dioxane (4 M, 25 mL). This mixture was stirred for 2 hours, after which the solvent was removed under reduced pressure. The resulting solid was triturated with  $\text{Et}_2\text{O}$  to afford the title compound **5.16** (1.03 g, 5.40 mmol, 93 % yield) as an off-white solid.  $^1\text{H}$  NMR (400 MHz,  $\text{MeOD}-d_4$ ):  $\delta$  0.99 (d,  $J = 6.6$  Hz, 6H), 1.94-2.08 (m, 1H), 2.59 (d,  $J = 7.1$  Hz, 2H), 4.35 (s, 2H), 6.49 (s, 1H). *Exchangeable protons not observed*. LCMS (high pH):  $t_{\text{R}} = 0.70$  min,  $[\text{M}+\text{H}^+]$  196; (area % total: 100).

### Di-*tert*-butyl (4-chloro-6-morpholinopyrimidin-2-yl)imidodicarbamate (5.18)



To a solution of 4-chloro-6-morpholinopyrimidin-2-amine **5.17** (250 mg, 1.17 mmol) in DMF (7 mL) at 0 °C was added NaH (279 mg, 6.99 mmol, 60% wt/wt). The mixture was stirred for 20 minutes before di-*tert*-butyl dicarbonate (1.02 g, 4.66 mmol) in DMF (3 mL) was added. The solution was stirred for 16 hours, after which time water (30 mL) and EtOAc (30 mL) were added and the organics were separated, dried over MgSO<sub>4</sub> and concentrated under reduced pressure. The crude material was adsorbed onto diatomaceous earth and purified by reversed phase chromatography, eluting under a gradient of MeCN (30-80%) in modified water (high pH) to afford the title compound **5.18** (417 mg, 1.01 mmol, 86 % yield) as a pale orange solid. <sup>1</sup>H NMR (400 MHz, CDCl<sub>3</sub>): δ 1.42 (s, 18H), 3.61-3.67 (m, 8H), 6.92 (s, 1H). LCMS (high pH): t<sub>R</sub> = 1.23 min, [M-Boc+H<sup>+</sup>] 315, 317, [M+H<sup>+</sup>] 415, 417; (area % total: 100).

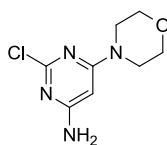
### Di-*tert*-butyl (4-(((3-isobutylisoxazol-5-yl)methyl)amino)-6-morpholinopyrimidin-2-yl)dicarbamate (5.19)



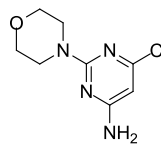
To a solution of di-*tert*-butyl (4-chloro-6-morpholinopyrimidin-2-yl)imidodicarbamate **5.18** (100 mg, 0.241 mmol) in DMF (2 mL) was added caesium carbonate (353 mg, 1.09 mmol), (3-isobutylisoxazol-5-yl)methanamine hydrochloride **5.16** (68.9 mg, 0.362 mmol), XPhos (34.5 mg, 72.0 μmol) and Pd<sub>2</sub>(dba)<sub>3</sub> (24.3 mg, 27.0 μmol). The resulting solution was heated to 80 °C in the microwave for 2 hours. Additional (3-isobutylisoxazol-5-yl)methanamine hydrochloride **5.16** (68.9 mg, 0.362 mmol) and caesium carbonate (118 mg, 0.362 mmol) were added and the mixture was heated to 100 °C for 3 hours in the microwave. After this time aq. sat. NH<sub>4</sub>Cl solution (10 mL) was added and the mixture was extracted with EtOAc (10 mL). The organics were washed with aq. sat. NH<sub>4</sub>Cl solution and brine, then concentrated under reduced pressure. The residue was dissolved in DMSO (1 mL); MDAP

purification of this mixture (high pH, Method C) afforded the title compound **5.19** (16.1 mg, 30.0  $\mu$ mol, 13 % yield) as an orange glass.  $^1\text{H}$  NMR (400 MHz,  $\text{CDCl}_3$ ):  $\delta$  0.95 (d,  $J$  = 6.6 Hz, 6H), 1.49 (s, 18H), 1.90-2.02 (m, 1H), 2.51 (d,  $J$  = 7.0 Hz, 2H), 3.50-3.52 (m, 4H), 3.73-3.75 (m, 4H), 4.59 (d,  $J$  = 6.3 Hz, 2H), 5.28 (br.s, 1H), 5.32 (s, 1H), 6.04 (s, 1H). LCMS (high pH):  $t_R$  = 1.36 min,  $[\text{M-Boc}+\text{H}^+]$  433,  $[\text{M}+\text{H}^+]$  533; (area % total: 91).

### 2-Chloro-6-morpholinopyrimidin-4-amine (**5.21**) & 6-Chloro-2-morpholinopyrimidin-4-amine (**5.22**)



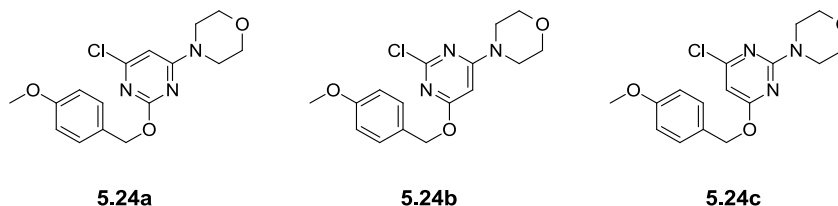
**5.21**



**5.22**

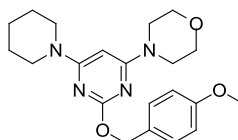
Three separate 20 mL microwave vials each containing a mixture of morpholine (0.531 mL, 6.10 mmol), 2,6-dichloropyrimidin-4-amine **5.20** (1.00 g, 6.10 mmol) and DIPEA (2.66 mL, 15.2 mmol) in ethanol (18 mL) were stirred at 150  $^\circ\text{C}$  in the microwave for 10 minutes. The mixtures were combined, evaporated to dryness, and purified by reversed phase chromatography, eluting under a gradient of MeOH (10-50%) in modified water (high pH), affording 6-chloro-2-morpholinopyrimidin-4-amine **5.22** (2.93 g, 13.7 mmol, 75% yield) as an off-white solid and 2-chloro-6-morpholinopyrimidin-4-amine **5.21** (270 mg, 1.26 mmol, 7 % yield) as a white solid. 2-Chloro-6-morpholinopyrimidin-4-amine **5.21**:  $^1\text{H}$  NMR (400 MHz,  $\text{DMSO}-d_6$ ):  $\delta$  3.37-3.39 (m, 4H), 3.63-3.65 (m, 4H), 5.50 (s, 1H), 6.68 (br.s, 2H). LCMS (formic):  $t_R$  = 0.57 min,  $[\text{M}+\text{H}^+]$  215, 217; (area % total: 100). 6-Chloro-2-morpholinopyrimidin-4-amine **5.22**:  $^1\text{H}$  NMR (400 MHz,  $\text{DMSO}-d_6$ ):  $\delta$  3.58-3.61 (m, 8H), 5.77 (s, 1H), 6.76 (br.s, 2H). LCMS (formic):  $t_R$  = 0.66 min,  $[\text{M}+\text{H}^+]$  215, 217; (area % total: 100).

**4-(6-Chloro-2-((4-methoxybenzyl)oxy)pyrimidin-4-yl)morpholine (5.24a), 4-(2-Chloro-6-((4-methoxybenzyl)oxy)pyrimidin-4-yl)morpholine (5.24b) & 4-(4-Chloro-6-((4-methoxybenzyl)oxy)pyrimidin-2-yl)morpholine (5.24c)**<sup>257</sup>



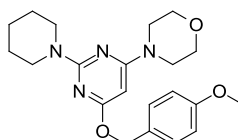
To a solution of 2,4,6-trichloropyrimidine **5.12** (2.51 mL, 21.8 mmol) and caesium carbonate (21.3 g, 65.4 mmol) in acetonitrile (50 mL) was added (4-methoxyphenyl)methanol (2.71 mL, 21.8 mmol). This mixture was stirred at room temperature for 72 hours, after which morpholine (2.28 mL, 26.2 mmol) was added. The resulting mixture was stirred for 16 hours, after which the solvent was removed under reduced pressure. The resulting solid was suspended in EtOAc (200 mL). Water (200 mL) was added and the mixture was separated. The organic layer was washed with water (2 x 200 mL), brine (100 mL), dried over MgSO<sub>4</sub> and concentrated under reduced pressure. The resulting residue was adsorbed onto diatomaceous earth and purified by flash chromatography, eluting under a gradient of TBME (0-25%) in cyclohexane to afford the three regioisomers, which eluted in the following order: 4-(4-chloro-6-((4-methoxybenzyl)oxy)pyrimidin-2-yl)morpholine **5.24c**<sup>257</sup> (2.95 g, 8.79 mmol, 40 % yield, white solid), 4-(2-chloro-6-((4-methoxybenzyl)oxy)pyrimidin-4-yl)morpholine **5.24b**<sup>257</sup> (412 mg, 1.23 mmol, 6 % yield, opaque gum), 4-(6-chloro-2-((4-methoxybenzyl)oxy)pyrimidin-4-yl)morpholine **5.24a**<sup>257</sup> (1.52 g, 4.53 mmol, 21 % yield, transparent gum). Compound **5.24a**: <sup>1</sup>H NMR (400 MHz, DMSO-*d*<sub>6</sub>): δ 3.59-3.65 (m, 8H), 3.76 (s, 3H), 5.22 (s, 2H), 6.61 (s, 1H), 6.92-6.95 (m, 2H), 7.35-7.38 (m, 2H). LCMS (high pH): t<sub>R</sub> = 1.19 min, [M+H<sup>+</sup>] 336; (area % total: 99). Compound **5.24b**: <sup>1</sup>H NMR (400 MHz, DMSO-*d*<sub>6</sub>): δ 3.53-3.55 (m, 4H), 3.63-3.64 (m, 4H), 3.76 (s, 3H), 5.23 (s, 2H), 6.13 (s, 1H), 6.93-6.96 (m, 2H), 7.36-7.38 (m, 2H). LCMS (high pH): t<sub>R</sub> = 1.29 min, [M+H<sup>+</sup>] 336; (area % total: 100). Compound **5.24c**: <sup>1</sup>H NMR (400 MHz, DMSO-*d*<sub>6</sub>): δ 3.64-3.66 (m, 4H), 3.70-3.72 (m, 4H), 3.76 (s, 3H), 5.30 (s, 2H), 6.21 (s, 1H), 6.93-6.95 (m, 2H), 7.36-7.39 (m, 2H). LCMS (high pH): t<sub>R</sub> = 1.40 min, [M+H<sup>+</sup>] 336; (area % total: 99).

#### 4-(2-((4-Methoxybenzyl)oxy)-6-(piperidin-1-yl)pyrimidin-4-yl)morpholine (5.25a)



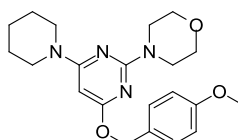
To a solution of 4-(6-chloro-2-((4-methoxybenzyl)oxy)pyrimidin-4-yl)morpholine **5.24a** (75.0 mg, 0.223 mmol) and DIPEA (0.117 mL, 0.670 mmol) in EtOH (0.9 mL) was added piperidine (66.0  $\mu$ L, 0.670 mmol). The mixture was heated to 150  $^{\circ}$ C in the microwave for 5 hours, after which time direct purification of the reaction mixture by MDAP (high pH, Method C) afforded the title compound **5.25a** (61.0 mg, 0.159 mmol, 71 % yield) as a red glass.  $^1$ H NMR (400 MHz, MeOD- $d_4$ ):  $\delta$  1.55-1.61 (m, 4H), 1.65-1.72 (m, 2H), 3.49-3.51 (m, 4H), 3.55-3.58 (m, 4H), 3.71-3.73 (m, 4H), 3.79 (s, 3H), 5.42 (s, 2H), 5.48 (s, 1H), 6.88-6.91 (m, 2H), 7.34-7.38 (m, 2H). LCMS (high pH):  $t_R$  = 1.35 min,  $[M+H]^+$  385; (area % total: 100).

#### 4-(6-((4-Methoxybenzyl)oxy)-2-(piperidin-1-yl)pyrimidin-4-yl)morpholine (5.25b)



The title compound **5.25b** (85.0 mg, 0.221 mmol, 93 % yield, white solid) was prepared in the same manner as **5.25a** using the following reagents and solvents: 4-(2-chloro-6-((4-methoxybenzyl)oxy)pyrimidin-4-yl)morpholine **5.24b** (80.0 mg, 0.238 mmol), DIPEA (0.125 mL, 0.715 mmol), piperidine (71.0  $\mu$ L, 0.715 mmol), EtOH (0.9 mL). The compound was purified by MDAP (high pH, Method D).  $^1$ H NMR (400 MHz, MeOD- $d_4$ ):  $\delta$  1.52-1.58 (m, 4H), 1.64-1.70 (m, 2H), 3.46-3.48 (m, 4H), 3.69-3.75 (m, 8H), 3.80 (s, 3H), 5.22 (s, 2H), 5.33 (s, 1H), 6.89-6.92 (m, 2H), 7.33-7.35 (m, 2H). LCMS (high pH):  $t_R$  = 1.54 min,  $[M+H]^+$  385; (area % total: 100).

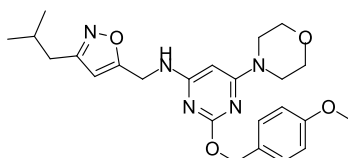
#### 4-(4-((4-Methoxybenzyl)oxy)-6-(piperidin-1-yl)pyrimidin-2-yl)morpholine (5.25c)



The title compound **5.25c** (69.0 mg, 0.179 mmol, 80 % yield, off-white solid) was prepared in the same manner as **5.25a** using the following reagents and solvents: 4-(4-chloro-6-((4-methoxybenzyl)oxy)pyrimidin-2-yl)morpholine **5.24c** (75.0 mg, 0.223 mmol), DIPEA (0.117

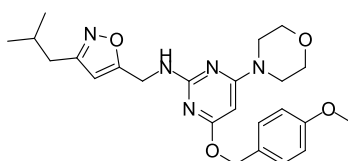
mL, 0.670 mmol), piperidine (66.0  $\mu$ L, 0.670 mmol), EtOH (0.9 mL). The compound was purified by MDAP (high pH, Method D).  $^1\text{H}$  NMR (400 MHz,  $\text{MeOD-}d_4$ ):  $\delta$  1.55-1.60 (m, 4H), 1.66-1.70 (m, 2H), 3.53-3.56 (m, 4H), 3.71 (s, 8H), 3.80 (s, 3H), 5.22 (s, 2H), 5.38 (s, 1H), 6.89-6.93 (m, 2H), 7.32-7.36 (m, 2H). LCMS (high pH):  $t_R = 1.52$  min,  $[\text{M}+\text{H}^+]$  385; (area % total: 100).

***N*-((3-Isobutylisoxazol-5-yl)methyl)-2-((4-methoxybenzyl)oxy)-6-morpholinopyrimidin-4-amine (5.26a)**



To a solution of 4-(6-chloro-2-((4-methoxybenzyl)oxy)pyrimidin-4-yl)morpholine **5.24a** (150 mg, 0.447 mmol) in DMF (3 mL) was added caesium carbonate (655 mg, 2.01 mmol), (3-isobutylisoxazol-5-yl)methanamine hydrochloride **5.16** (128 mg, 0.670 mmol), XPhos (63.9 mg, 0.134 mmol) and  $\text{Pd}_2(\text{dba})_3$  (45.0 mg, 49.0  $\mu$ mol). The resulting solution was heated to 80  $^\circ\text{C}$  in the microwave for 5 hours. Sat. aq.  $\text{NH}_4\text{Cl}$  (10 mL) was added and the mixture was extracted with EtOAc (10 mL). The organics were washed with sat. aq.  $\text{NH}_4\text{Cl}$  solution and brine, dried over sodium sulfate then concentrated *in vacuo*. The residue was dissolved in DMF (2.5 mL); MDAP (high pH, Method C) purification of this mixture afforded the title compound **5.26a** (36.3 mg, 80.0  $\mu$ mol, 18 % yield) as a fluffy white solid.  $^1\text{H}$  NMR (400 MHz,  $\text{DMSO-}d_6$ ):  $\delta$  0.88 (d,  $J = 6.6$  Hz, 6H), 1.84-1.94 (m, 1H), 2.44 (d,  $J = 7.2$  Hz, 2H), 3.38-3.41 (m, 4H), 3.61-3.65 (m, 4H), 3.75 (s, 3H), 4.55 (d,  $J = 6.0$  Hz, 2H), 5.13 (s, 2H), 5.41 (s, 1H), 6.12 (s, 1H), 6.88-6.92 (m, 2H), 7.30-7.35 (m, 3H). LCMS (high pH):  $t_R = 1.27$  min,  $[\text{M}+\text{H}^+]$  454; (area % total: 100).

***N*-((3-Isobutylisoxazol-5-yl)methyl)-4-((4-methoxybenzyl)oxy)-6-morpholinopyrimidin-2-amine (5.26b)**

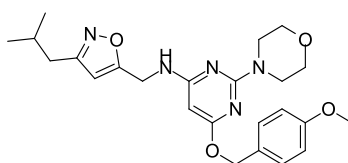


The title compound **5.26b** (54.2 mg, 0.120 mmol, 22 % yield, transparent glass) was prepared in the same manner as **5.26a** using the following reagents and solvents: 4-(2-

chloro-6-((4-methoxybenzyl)oxy)pyrimidin-4-yl)morpholine **5.24b** (180 mg, 0.536 mmol), caesium carbonate (786 mg, 2.41 mmol), (3-isobutylisoxazol-5-yl)methanamine hydrochloride **5.16** (153 mg, 0.804 mmol), XPhos (77.0 mg, 0.161 mmol), Pd<sub>2</sub>(dba)<sub>3</sub> (54.0 mg, 59.0 μmol), DMF (4 mL). The compound was purified by MDAP (high pH, Method C). <sup>1</sup>H NMR (400 MHz, MeOD-*d*<sub>4</sub>): δ 0.93 (d, *J* = 6.6 Hz, 6H), 1.85-1.98 (m, 1H), 2.47 (d, *J* = 7.2 Hz, 2H), 3.45-3.47 (m, 4H), 3.66-3.68 (m, 4H), 3.78 (s, 3H), 4.60 (s, 2H), 5.18 (s, 2H), 5.40 (s, 1H), 6.06 (s, 1H), 6.86-6.90 (m, 2H), 7.29-7.39 (m, 2H). *Exchangeable protons not observed*. LCMS (high pH): t<sub>R</sub> = 1.36 min, did not ionize; (area % total: 90).

Alternatively, a solution of 4-(2-chloro-6-((4-methoxybenzyl)oxy)pyrimidin-4-yl)morpholine **5.24b** (100 mg, 0.298 mmol), (3-isobutylisoxazol-5-yl)methanamine hydrochloride **5.16** (68.1 mg, 0.357 mmol), sodium *tert*-butoxide (86.0 mg, 0.893 mmol), BrettPhos Pd G1 methyl-*t*-butyl ether adduct (11.9 mg, 15.0 μmol) and BrettPhos (8.0 mg, 15.0 μmol) in 1,4-Dioxane (3 mL) was heated to 100 °C in the microwave for 1 hour. After this time, the mixture was diluted with EtOAc (10 mL), washed with water (10 mL) and concentrated under reduced pressure. The crude material was dissolved in MeOH and DMSO (1:1, 2 ml) and purified by MDAP (high pH, Method C) to afford the title compound **5.26b** (67.0 mg, 0.148 mmol, 50 % yield) as a transparent glass. Spectral data were identical to those reported above.

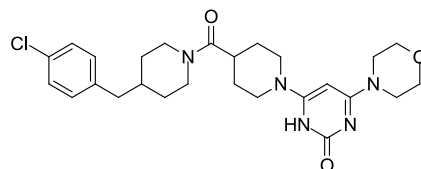
#### ***N*-((3-Isobutylisoxazol-5-yl)methyl)-6-((4-methoxybenzyl)oxy)-2-morpholinopyrimidin-4-amine (5.26c)**



The title compound **5.26c** (37.5 mg, 0.083 mmol, 28 % yield, orange glass) was prepared in the same manner as **5.26a** using the following reagents and solvents: 4-(4-chloro-6-((4-methoxybenzyl)oxy)pyrimidin-2-yl)morpholine **5.24c** (100 mg, 0.298 mmol), caesium carbonate (437 mg, 1.34 mmol), (3-isobutylisoxazol-5-yl)methanamine hydrochloride **5.16** (85.0 mg, 0.447 mmol), XPhos (42.6 mg, 89.0 μmol), Pd<sub>2</sub>(dba)<sub>3</sub> (30.0 mg, 33.1 μmol), DMF (2 mL). The compound was purified by MDAP (high pH, Method D). <sup>1</sup>H NMR (400 MHz, MeOD-*d*<sub>4</sub>): δ 0.93 (d, *J* = 6.6 Hz, 6H), 1.86-1.98 (m, 1H), 2.49 (d, *J* = 7.2 Hz, 2H), 3.62-3.70 (m, 8H), 3.79 (s, 3H), 4.58 (s, 2H), 5.18 (s, 2H), 5.27 (s, 1H), 6.09 (s, 1H), 6.87-6.91 (m, 2H), 7.29-7.33

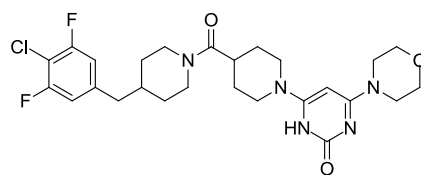
(m, 2H). *Exchangeable protons not observed.* LCMS (high pH):  $t_R = 1.38$  min,  $[M+H]^+$  454; (area % total: 100).

**6-(4-(4-(4-Chlorobenzyl)piperidine-1-carbonyl)piperidin-1-yl)-4-morpholinopyrimidin-2(1H)-one (5.32a)**



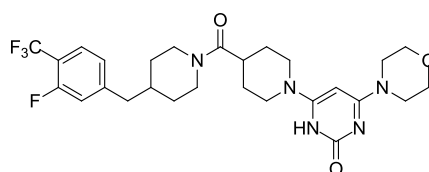
To a solution of 1-(2-((4-methoxybenzyl)oxy)-6-morpholinopyrimidin-4-yl)piperidine-4-carboxylic acid **5.33** (36.0 mg, 84.0  $\mu$ mol) in DMF (0.5 mL) was added DIPEA (44.0  $\mu$ L, 0.252 mmol) and HATU (38.3 mg, 0.101 mmol). The mixture was stirred for 30 minutes at room temperature, after which 4-(4-chlorobenzyl)piperidine hydrochloride **5.34a** (22.8 mg, 92.0  $\mu$ mol) was added. The mixture was stirred at room temperature for 2 hours after which EtOAc (10 mL) was added and the organics were washed sequentially with water (10 mL), sat. aq.  $\text{NaHCO}_3$  (10 mL) and brine (10 mL), then dried over  $\text{MgSO}_4$  and concentrated under reduced pressure. The crude material was dissolved in a mixture of DCM:TFA (1:1, 1 mL) and stirred at room temperature for 20 hours. After this time, the mixture was concentrated, dissolved in MeOH and subject to purification by MDAP (high pH, Method C) to afford the title compound **5.32a** (40.1 mg, 83.0  $\mu$ mol, 98 % yield) as a straw coloured glass.  $^1\text{H}$  NMR (400 MHz,  $\text{MeOD-}d_4$ ):  $\delta$  1.15 (qd,  $J = 3.9, 12.7$  Hz, 2H), 1.68-1.90 (m, 7H), 2.56-2.63 (m, 3H), 3.00-3.14 (m, 4H), 3.52-3.55 (m, 4H), 3.74-3.77 (m, 4H), 4.07-4.19 (m, 3H), 4.51 (d,  $J = 12.7$  Hz, 1H), 5.29 (s, 1H), 7.16-7.18 (m, 2H), 7.27-7.29 (m, 2H). *Exchangeable protons not observed.*  $^{13}\text{C}$  NMR (125 MHz,  $\text{MeOD-}d_4$ ):  $\delta$  29.1, 29.3, 32.9, 34.0, 38.7, 39.2, 42.9, 43.4, 46.8, 46.8, 46.9, 47.3 (2C), 67.2 (2C), 72.0 (m), 129.3 (2C), 131.7 (2C), 132.8, 140.1, 155.4, 159.8 (m), 163.1 (m), 174.5.  $\nu_{\text{max}}$  (neat): 2922, 1666, 1603, 1428, 1368, 1197, 1172, 1116, 1015, 968, 832, 798, 719  $\text{cm}^{-1}$ . HR-MS (ESI):  $\text{C}_{26}\text{H}_{35}\text{ClN}_5\text{O}_3$   $[M+H]^+$  requires 500.2423, found 500.2420.

**6-(4-(4-(4-Chloro-3,5-difluorobenzyl)piperidine-1-carbonyl)piperidin-1-yl)-4-morpholinopyrimidin-2(1H)-one (5.32b)**



The title compound **5.32b** (25.8 mg, 48.0  $\mu\text{mol}$ , 69 % yield, transparent gum) was prepared in the same manner as **5.32a** using the following reagents and solvents: 1-(2-((4-methoxybenzyl)oxy)-6-morpholinopyrimidin-4-yl)piperidine-4-carboxylic acid **5.33** (30.0 mg, 70.0  $\mu\text{mol}$ ), DIPEA (36.7  $\mu\text{L}$ , 0.210 mmol), HATU (31.9 mg, 84.0  $\mu\text{mol}$ ), DMF (0.5 mL), 4-(4-chloro-3,5-difluorobenzyl)piperidine hydrochloride **5.34b** (21.7 mg, 77.0  $\mu\text{mol}$ ), *then* DCM:TFA (1:1, 1 mL). The compound was purified by MDAP (high pH, Method C).  $^1\text{H}$  NMR (400 MHz, MeOD- $d_4$ ):  $\delta$  1.08-1.27 (m, 2H), 1.65-1.82 (m, 6H), 1.84-1.94 (m, 1H), 2.56-2.66 (m, 3H), 2.97-3.15 (m, 4H), 3.52 (br.s, 4H), 3.73-3.76 (m, 4H), 4.08-4.26 (m, 3H), 4.52 (d,  $J$  = 12.6 Hz, 1H), 5.27 (s, 1H), 6.99-7.03 (m, 2H). *Exchangeable protons not observed.*  $^{13}\text{C}$  NMR (125 MHz, MeOD- $d_4$ ):  $\delta$  27.8, 28.0, 31.4, 32.4, 37.5, 37.8, 41.5, 41.9, 44.7 (br. m, 3C), 45.4 (2C), 66.1 (2C), 71.5, 106.8 (t,  $J$  = 21 Hz), 112.4 (dd,  $J$  = 3, 19 Hz, 2C), 142 (m), 158.5 (dd,  $J$  = 4, 247 Hz, 2C), 159.2, 173.4. *Two  $^{13}\text{C}$  signals not observed due to line broadening.*  $^{19}\text{F}$  NMR (376 MHz, MeOD- $d_4$ ):  $\delta$  -116.4.  $\nu_{\text{max}}$  (neat): 2922, 1595, 1507, 1432, 1365, 1255, 1203, 1114, 1022, 960, 857, 782, 650  $\text{cm}^{-1}$ . HR-MS (ESI):  $\text{C}_{26}\text{H}_{33}\text{ClF}_2\text{N}_5\text{O}_3$  [ $\text{M}+\text{H}^+$ ] requires 536.2235, found 536.2226.

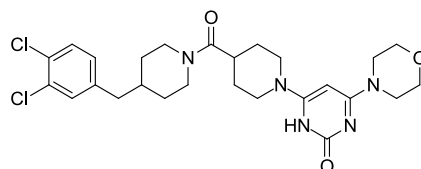
**6-(4-(4-(3-Fluoro-4-(trifluoromethyl)benzyl)piperidine-1-carbonyl)piperidin-1-yl)-4-morpholinopyrimidin-2(1H)-one (5.32c)**



The title compound **5.32c** (23.8 mg, 43.0  $\mu\text{mol}$ , 53 % yield, light brown gum) was prepared in the same manner as **5.32a** using the following reagents and solvents: 1-(2-((4-methoxybenzyl)oxy)-6-morpholinopyrimidin-4-yl)piperidine-4-carboxylic acid **5.33** (35.0 mg, 82.0  $\mu\text{mol}$ ), DIPEA (42.8  $\mu\text{L}$ , 0.245 mmol), HATU (37.3 mg, 98.0  $\mu\text{mol}$ ), DMF (0.5 mL), 4-(3-fluoro-4-(trifluoromethyl)benzyl)piperidine hydrochloride **5.34c** (26.8 mg, 90.0  $\mu\text{mol}$ ), *then*

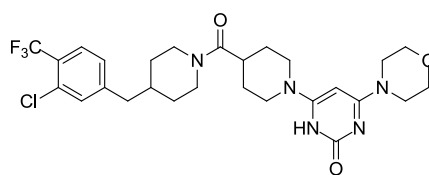
DCM:TFA (1:1, 1 mL). The compound was purified by MDAP (high pH, Method C).  $^1\text{H}$  NMR (400 MHz, MeOD- $d_4$ ):  $\delta$  1.11-1.25 (m, 2H), 1.66-1.75 (m, 6H), 1.85-1.94 (m, 1H), 2.56-2.67 (m, 3H), 2.96-3.11 (m, 4H), 3.47-3.52 (m, 4H), 3.71-3.74 (m, 4H), 4.06-4.20 (m, 3H), 4.50 (d,  $J = 12.4$  Hz, 1H), 5.25 (s, 1H), 7.11-7.20 (m, 2H), 7.58 (t,  $J = 7.8$  Hz, 1H). *Exchangeable protons not observed.*  $^{13}\text{C}$  NMR (125 MHz, MeOD- $d_4$ ):  $\delta$  29.2, 29.4, 32.8, 33.9, 38.9, 39.2, 43.1, 43.3, 46.1 (2C), 46.8, 46.8 (2C), 67.4 (2C), 72.7 (m), 116.8 (m), 118.4 (d,  $J = 20$  Hz), 124.4 (q,  $J = 273$  Hz), 126.4 (d,  $J = 4$  Hz), 128.0 (m, 2C), 149.7 (d,  $J = 8$  Hz), 160.0, 160.5, 162.0, 174.8.  $^{19}\text{F}$  NMR (376 MHz, MeOD- $d_4$ ):  $\delta$  -117 (m, 1F), -61.9 (d,  $J = 12$  Hz, 3F).  $\nu_{\text{max}}$  (neat): 2922, 1597, 1508, 1431, 1385, 1323, 1252, 1206, 1175, 1119, 1045, 994, 783, 751, 660  $\text{cm}^{-1}$ . HR-MS (ESI):  $\text{C}_{27}\text{H}_{34}\text{F}_4\text{N}_5\text{O}_3$  [ $\text{M}+\text{H}^+$ ] requires 552.2592, found 552.2576.

**6-(4-(4-(3,4-Dichlorobenzyl)piperidine-1-carbonyl)piperidin-1-yl)-4-morpholinopyrimidin-2(1H)-one (5.32d)**



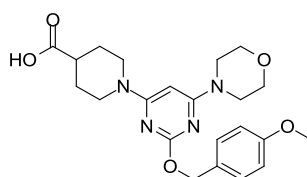
The title compound **5.32d** (15.6 mg, 29.1  $\mu\text{mol}$ , 63 % yield, opaque gum) was prepared in the same manner as **5.32a** using the following reagents and solvents: 1-(2-((4-methoxybenzyl)oxy)-6-morpholinopyrimidin-4-yl)piperidine-4-carboxylic acid **5.33** (20.0 mg, 47.0  $\mu\text{mol}$ ), DIPEA (24.5  $\mu\text{l}$ , 0.140 mmol), HATU (21.3 mg, 56.0  $\mu\text{mol}$ ), DMF (0.5 mL), 4-(3,4-dichlorobenzyl)piperidine hydrochloride **5.34d** (14.4 mg, 54.0  $\mu\text{mol}$ ), *then* DCM:TFA (1:1, 1 mL). The compound was purified by MDAP (high pH, Method C).  $^1\text{H}$  NMR (400 MHz, MeOD- $d_4$ ):  $\delta$  1.07-1.26 (m, 2H), 1.68-1.91 (m, 7H), 2.57-2.63 (m, 3H), 2.97-3.12 (m, 4H), 3.51-3.53 (m, 4H), 3.73-3.76 (m, 4H), 4.08-4.24 (m, 3H), 4.49-4.55 (m, 1H), 5.27 (s, 1H), 7.14 (dd,  $J = 2.0, 8.3$  Hz, 1H), 7.38 (d,  $J = 2.0$  Hz, 1H), 7.44 (d,  $J = 8.3$  Hz, 1H). *Exchangeable protons not observed.*  $^{13}\text{C}$  NMR (100 MHz, MeOD- $d_4$ ):  $\delta$  29.2, 29.4, 32.8, 33.9, 39.1, 39.2, 42.6, 43.3, 46.2, 46.8 (2C), 67.4 (2C), 130.1, 130.8, 131.3, 132.1, 133.0, 142.4, 160.5, 174.8. *Five  $^{13}\text{C}$  signals not observed due to line broadening.*  $\nu_{\text{max}}$  (neat): 2921, 2852, 1594, 1506, 1437, 1365, 1255, 1205, 1114, 1021, 969, 782, 689  $\text{cm}^{-1}$ . HR-MS (ESI):  $\text{C}_{26}\text{H}_{34}\text{Cl}_2\text{N}_5\text{O}_3$  [ $\text{M}+\text{H}^+$ ] requires 534.2033, found 534.2024.

**6-(4-(4-(3-Chloro-4-(trifluoromethyl)benzyl)piperidine-1-carbonyl)piperidin-1-yl)-4-morpholinopyrimidin-2(1H)-one (5.32e)**



The title compound **5.32e** (15.1 mg, 27.0  $\mu\text{mol}$ , 57 % yield, brown gum) was prepared in the same manner as **5.32a** using the following reagents and solvents: 1-(2-((4-methoxybenzyl)oxy)-6-morpholinopyrimidin-4-yl)piperidine-4-carboxylic acid **5.33** (20.0 mg, 47.0  $\mu\text{mol}$ ), DIPEA (24.0  $\mu\text{L}$ , 0.140 mmol), HATU (21.3 mg, 56.0  $\mu\text{mol}$ ), DMF (0.28 mL), 4-(3-chloro-4-(trifluoromethyl)benzyl)piperidine **5.34e** (14.3 mg, 51.0  $\mu\text{mol}$ ), then DCM:TFA (1:1, 1 mL). The compound was purified by MDAP (high pH, Method C).  $^1\text{H}$  NMR (400 MHz,  $\text{MeOD-}d_4$ ):  $\delta$  1.11-1.25 (m, 2H), 1.67-1.77 (m, 6H), 1.89-1.92 (m, 1H), 2.56-2.66 (m, 3H), 2.99-3.11 (m, 4H), 3.49 (br.s, 4H), 3.71-3.73 (m, 4H), 4.06-4.18 (m, 3H), 4.50 (d,  $J = 12.1$  Hz, 1H), 5.25 (s, 1H), 7.30 (d,  $J = 8.1$  Hz, 1H), 7.46 (s, 1H), 7.67 (d,  $J = 8.1$  Hz, 1H). *Exchangeable protons not observed.*  $^{13}\text{C}$  NMR (100 MHz,  $\text{MeOD-}d_4$ ):  $\delta$  27.8 (2C), 31.4, 32.5, 37.6, 37.8, 41.5, 41.9, 45.4 (2C), 66.1 (2C), 123.3 (q,  $J = 271$  Hz), 125.6 (m), 127.2 (m), 127.7, 131.5 (m), 131.7, 146.9, 159.1, 173.5. *Six  $^{13}\text{C}$  signals not observed due to line broadening.*  $^{19}\text{F}$  NMR (376 MHz,  $\text{MeOD-}d_4$ ):  $\delta$  -63.0.  $\nu_{\text{max}}$  (neat): 2923, 1595, 1500, 1437, 1382, 1315, 1256, 1174, 1120, 1103, 1026, 969, 839, 782, 696  $\text{cm}^{-1}$ . HR-MS (ESI):  $\text{C}_{27}\text{H}_{34}\text{ClF}_3\text{N}_5\text{O}_3$  [ $\text{M}+\text{H}^+$ ] requires 568.2297, found 568.2295.

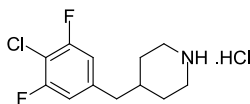
**1-(2-((4-Methoxybenzyl)oxy)-6-morpholinopyrimidin-4-yl)piperidine-4-carboxylic acid (5.33)**



To a solution of ethyl 1-(2-((4-methoxybenzyl)oxy)-6-morpholinopyrimidin-4-yl)piperidine-4-carboxylate **5.39** (300 mg, 0.657 mmol) in water (1.2 mL) and 1,4-dioxane (1.2 mL) was added  $\text{LiOH}\cdot\text{H}_2\text{O}$  (138 mg, 3.29 mmol). This mixture was stirred at room temperature for 3 hours, after which time it was concentrated under reduced pressure and adsorbed onto diatomaceous earth. The crude material was purified by reversed phase chromatography, eluting under a gradient of MeCN (10-30%) in modified water (high pH) to afford the title

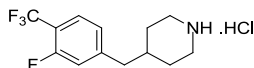
compound **5.33** (247 mg, 0.576 mmol, 88 % yield) as a collapsed white foam.  $^1\text{H}$  NMR (400 MHz,  $\text{MeOD-}d_4$ ):  $\delta$  1.59-1.69 (m, 2H), 1.91-1.95 (m, 2H), 2.47-2.55 (m, 1H), 2.95-3.02 (m, 2H), 3.51-3.53 (m, 4H), 3.72-3.74 (m, 4H), 3.80 (s, 3H), 4.25-4.31 (m, 2H), 5.25 (s, 2H), 5.53 (s, 1H), 6.89-6.92 (m, 2H), 7.35-7.39 (m, 2H). *Exchangeable protons not observed*. LCMS (high pH):  $t_{\text{R}}$  = 0.71 min,  $[\text{M}+\text{H}^+]$  429; (area % total: 99).

#### 4-(4-Chloro-3,5-difluorobenzyl)piperidine hydrochloride (**5.34b**)



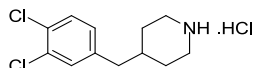
To a solution of *tert*-butyl 4-methylenepiperidine-1-carboxylate **5.36** (100 mg, 0.507 mmol) in THF (0.5 mL) was added 9-BBN dimer (123 mg, 0.507 mmol). This mixture was heated to reflux for 1 hour. After cooling to room temperature, the solution was added to a mixture of 5-bromo-2-chloro-1,3-difluorobenzene (115 mg, 0.507 mmol),  $\text{PdCl}_2\text{dppf}$  (20.8 mg, 25.0  $\mu\text{mol}$ ) and  $\text{K}_2\text{CO}_3$  (98.0 mg, 0.710 mmol) in DMF (1 mL) and water (0.1 mL). This mixture was heated to 60  $^\circ\text{C}$  for 18 hours. The mixture was poured into water, the pH was adjusted to 11 by the addition of 2M NaOH, followed by extraction with EtOAc. The organics were washed with brine, dried over  $\text{MgSO}_4$  and concentrated. The crude material was purified by reversed phase chromatography, eluting under a gradient of MeCN (30-50%) in modified water (high pH) to afford the intermediate **5.38a** (106 mg). This material was dissolved in a 4M solution of HCl in 1,4-dioxane (1 mL). Stirring was continued at room temperature for 1 hour, after which the solvent was removed under reduced pressure. The crude material was dissolved in methanol (1 mL) and loaded on to a 5 g Biotage ISOLUTE Flash SCX 2 cartridge, washing with 3 column volumes of MeOH and eluting with 4 column volumes of 2M ammonia in MeOH. The appropriate fractions were concentrated and the resulting material was dissolved in a 4M solution of HCl in 1,4-dioxane (1 mL), stirred for 2 minutes then concentrated under reduced pressure to afford the title compound **5.34b** (77.3 mg, 0.274 mmol, 54 % yield) as a white solid.  $^1\text{H}$  NMR (400 MHz,  $\text{MeOD-}d_4$ ):  $\delta$  1.42-1.35 (m, 2H), 1.85-2.01 (m, 3H), 2.65 (d,  $J$  = 6.9 Hz, 2H), 2.97 (t,  $J$  = 12.7 Hz, 2H), 3.36-3.42 (m, 2H), 7.02-7.06 (m, 2H). *Exchangeable protons not observed*. LCMS (high pH):  $t_{\text{R}}$  = 0.99 min,  $[\text{M}+\text{H}^+]$  246,  $[\text{M}+\text{H}^++\text{MeCN}]$  287; (area % total: 97).

#### 4-(3-Fluoro-4-(trifluoromethyl)benzyl)piperidine hydrochloride (5.34c)



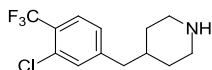
The title compound **5.34c** (85.4 mg, 0.287 mmol, 57 % yield, white solid) was prepared in the same manner as **5.34b** using the following reagents and solvents: *tert*-butyl 4-methylenepiperidine-1-carboxylate **5.36** (100 mg, 0.507 mmol), 9-BBN dimer (123 mg, 0.507 mmol), THF (0.5 mL), *then* 4-bromo-2-fluoro-1-(trifluoromethyl)benzene (123 mg, 0.507 mmol), PdCl<sub>2</sub>dppf (20.8 mg, 25.0 μmol), K<sub>2</sub>CO<sub>3</sub> (98.0 mg, 0.710 mmol), DMF (1 mL), water (0.1 mL), *then* HCl in 1,4-dioxane (1 mL). <sup>1</sup>H NMR (400 MHz, MeOD-*d*<sub>4</sub>): δ 1.44-1.55 (m, 2H), 1.84-1.91 (m, 2H), 1.94-2.05 (m, 1H), 2.74 (d, *J* = 7.3 Hz, 2H), 2.98 (t, *J* = 11.9 Hz, 2H), 3.37-3.41 (m, 2H), 7.22-7.25 (m, 2H), 7.62 (t, *J* = 7.8 Hz, 1H). *Exchangeable protons not observed*. LCMS (high pH): *t*<sub>R</sub> = 1.30 min, [M+H<sup>+</sup>] 262, [M+H<sup>+</sup>+MeCN] 303; (area % total: 90).

#### 4-(3,4-Dichlorobenzyl)piperidine hydrochloride (5.34d)<sup>258</sup>



The title compound **5.34d** (21.0 mg, 75.0 μmol, 15 % yield, transparent gum) was prepared in the same manner as **5.34b**, except a commercial solution of 9-BBN in THF (0.5 M) was used in place of 9-BBN dimer and THF. The following reagents and solvents were used: 9-BBN (0.5 M in THF, 1.01 mL, 0.507 mmol), *tert*-butyl 4-methylenepiperidine-1-carboxylate **5.36** (100 mg, 0.507 mmol), *then* 4-bromo-1,2-dichlorobenzene (115 mg, 0.507 mmol), PdCl<sub>2</sub>dppf (20.8 mg, 25.0 μmol), K<sub>2</sub>CO<sub>3</sub> (98.0 mg, 0.710 mmol), DMF (1 mL), water (0.1 mL) *then* HCl in 1,4-dioxane (1 mL). <sup>1</sup>H NMR (400 MHz, MeOD-*d*<sub>4</sub>): δ 1.41-1.51 (m, 2H), 1.83-1.96 (m, 3H), 2.62 (d, *J* = 7.1 Hz, 2H), 2.95 (t, *J* = 12.1 Hz, 2H), 3.36-3.40 (m, 2H), 7.16 (dd, *J* = 2.0, 8.2 Hz, 1H), 7.40 (d, *J* = 2.0 Hz, 1H), 7.45 (d, *J* = 8.2 Hz, 1H). *Exchangeable protons not observed*. LCMS (high pH): *t*<sub>R</sub> = 1.28 min, [M+H<sup>+</sup>] 244; (area % total: 100).

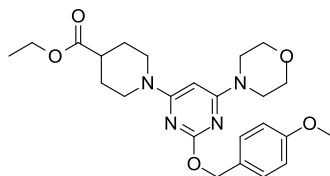
#### 4-(3-chloro-4-(trifluoromethyl)benzyl)piperidine (5.34e)



9-BBN (0.5 M in THF, 1.01 mL, 0.507 mmol) was added to *tert*-butyl 4-methylenepiperidine-1-carboxylate **5.36** (100 mg, 0.507 mmol). This mixture was heated to reflux for 1 hour. After cooling to room temperature, the solution was added to a mixture of 4-bromo-2-chloro-1-(trifluoromethyl)benzene (132 mg, 0.507 mmol), PdCl<sub>2</sub>dppf (20.8 mg, 25.0 μmol) and K<sub>2</sub>CO<sub>3</sub> (98.0 mg, 0.710 mmol) in DMF (1 mL) and water (0.1 mL). This mixture was

heated to 60 °C for 18 hours. The mixture was poured into water, the pH was adjusted to 11 by the addition of 2M NaOH, followed by extraction with EtOAc. The organics were washed with brine, dried over MgSO<sub>4</sub> and concentrated. The crude material was purified by reversed phase chromatography, eluting under a gradient of MeCN (20-70%) in modified water (high pH). The fractions containing the title compound were combined and concentrated. This material was dissolved in MeOH (1 mL) and loaded on to a Biotage 5g ISOLUTE Flash SCX 2 cartridge, washing with 3 column volumes of MeOH and eluting with 4 column volumes of 2M ammonia in MeOH to afford the title compound **5.34e** (24.7 mg, 89.0 μmol, 18 % yield) as a straw coloured gum. <sup>1</sup>H NMR (400 MHz, MeOD-*d*<sub>4</sub>): δ 1.23 (qd, *J* = 3.8, 12.4 Hz, 2H), 1.60-1.67 (m, 2H), 1.71-1.79 (m, 1H), 2.57 (dt, *J* = 2.1, 12.4 Hz, 2H), 2.63 (d, *J* = 7.2 Hz, 2H), 3.01-3.08 (m, 2H), 7.30 (d, *J* = 8.1 Hz, 1H), 7.45 (s, 1H), 7.68 (d, *J* = 8.1 Hz, 1H). *Exchangeable protons not observed*. LCMS (high pH): *t*<sub>R</sub> = 1.30 min, [M+H<sup>+</sup>] 278, [M+H<sup>+</sup>+MeCN] 319; (area % total: 100).

**Ethyl 1-(2-((4-methoxybenzyl)oxy)-6-morpholinopyrimidin-4-yl)piperidine-4-carboxylate (5.39)**



A suspension of 4-(6-chloro-2-((4-methoxybenzyl)oxy)pyrimidin-4-yl)morpholine **5.24a** (300 mg, 0.893 mmol), DIPEA (0.312 mL, 1.79 mmol) and ethyl piperidine-4-carboxylate **5.35** (0.165 mL, 1.07 mmol) in EtOH (4.5 mL) was heated to 120 °C under microwave irradiation for 3 hours. Additional ethyl piperidine-4-carboxylate **5.35** (0.165 mL, 1.07 mmol) and DIPEA (0.312 mL, 1.79 mmol) were added and the mixture was heated to 120 °C under microwave irradiation for a further 2 hours. The mixture was concentrated *in vacuo* and the crude material was purified by reversed phase chromatography, eluting under a gradient of MeCN (20-60%) in modified water (high pH) to afford the title compound **5.39** (353 mg, 0.773 mmol, 87 % yield) as a transparent gum. <sup>1</sup>H NMR (400 MHz, MeOD-*d*<sub>4</sub>): δ 1.26 (t, *J* = 7.3 Hz, 3H), 1.58-1.67 (m, 2H), 1.91-1.95 (m, 2H), 2.58-2.65 (m, 1H), 2.96-3.05 (m, 2H), 3.51-3.54 (m, 4H), 3.71-3.73 (m, 4H), 3.79 (s, 3H), 4.15 (q, *J* = 7.3 Hz, 2H), 4.25 (dt, *J* = 3.5, 13.8 Hz, 2H), 5.26 (s, 2H), 5.54 (s, 1H), 6.68-6.91 (m, 2H), 7.34-7.38 (m, 2H). LCMS (high pH): *t*<sub>R</sub> = 1.28 min, [M+H<sup>+</sup>] 457; (area % total: 99).

## 11.3 Synthesis of Compounds in Chapter 6

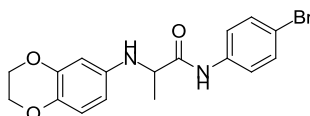
### General Procedure A for the Synthesis of GSK'896 Analogues *via* DABAL-Me<sub>3</sub> Mediated Aminolysis of Ester **6.18** or **6.42**<sup>142</sup>

To a solution of DABAL-Me<sub>3</sub> (122 mg, 0.478 mmol) in THF (2.5 mL) in a microwave vial was added the appropriate amine (0.478 mmol). The vial was sealed with a Teflon septum and heated to 50 °C for 1 hour. After this time, a solution of the ester **6.18** or **6.42** (0.239 mmol) in THF (0.5 mL) was added *via* syringe and the mixture was heated to reflux for 18 hours. The reaction was quenched by the careful addition of HCl (2M, 5 mL) at room temperature. DCM (5 mL) was added to the vial and the biphasic mixture was stirred vigorously for 10 minutes, after which the layers were separated by passage through a hydrophobic frit. The organics were removed under reduced pressure to give a residue that was dissolved in MeOH (< 3mL) and subjected to MDAP purification to afford the amide product.

### General procedure B for the S<sub>N</sub>2 Displacement of an α-Bromo or α-Tosyl Amide with an Aniline or Phenol

To a solution of the aniline or phenol (0.235 mmol) and potassium carbonate (54.0 mg, 0.391 mmol) in MeCN (2 mL) was added the α-bromo or α-tosyl amide (0.195 mmol). The mixture was heated to 90 °C for 18 hours, after which it was filtered and the solid was washed with MeCN. The filtrate was evaporated under reduced pressure, and the residue was dissolved in DMF (2 mL). This mixture was subjected to MDAP purification to afford the product.

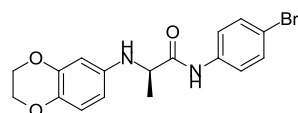
### *N*-(4-Bromophenyl)-2-((2,3-dihydrobenzo[*b*][1,4]dioxin-6-yl)amino)propanamide (GSK'896)



A mixture of 2-bromo-*N*-(4-bromophenyl)propanamide **6.4** (40.0 mg, 0.130 mmol), 2,3-dihydrobenzo[*b*][1,4]dioxin-6-amine **6.5** (18.0 μL, 0.143 mmol) and triethylamine (36.0 μL, 0.261 mmol) in DMF (0.7 mL) was heated to 80 °C under microwave irradiation for 4.5 hours. Direct purification of the reaction mixture by MDAP (high pH, Method C) afforded the title compound **GSK'896** (30.7 mg, 0.081 mmol, 63 % yield) as a light brown gum. <sup>1</sup>H NMR (400 MHz, MeOD-*d*<sub>4</sub>): δ 1.49 (d, *J* = 7.1 Hz, 3H), 3.84 (q, *J* = 7.1 Hz, 1H), 4.11-4.14 (m, 2H), 4.16-4.18 (m, 2H), 6.19-6.22 (m, 2H), 6.63-6.66 (m, 1H), 7.42-7.45 (m, 2H), 7.48-7.53

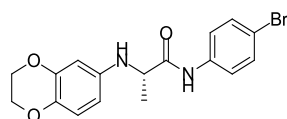
(m, 2H). Exchangeable protons not observed.  $^{13}\text{C}$  NMR (100 MHz, MeOD- $d_4$ ):  $\delta$  19.3, 56.9, 65.4, 65.9, 103.6, 108.4, 117.8, 118.5, 123.1 (2C), 132.8 (2C), 137.8, 138.6, 143.3, 145.4, 176.4.  $\nu_{\text{max}}$  (neat): 3318, 2872, 1668, 1626, 1589, 1504, 1394, 1320, 1280, 1240, 1208, 1175, 1067, 1008, 920, 884, 823, 743  $\text{cm}^{-1}$ . HR-MS (ESI):  $\text{C}_{17}\text{H}_{18}\text{BrN}_2\text{O}_3$  [ $\text{M}+\text{H}^+$ ] requires 377.0495, found 377.0513.

**(R)-N-(4-Bromophenyl)-2-((2,3-dihydrobenzo[*b*][1,4]dioxin-6-yl)amino)propanamide**  
**((R)-GSK'896)**



To a solution of 4-bromoaniline (65.3 mg, 0.379 mmol) in DCM (0.5 mL) under nitrogen was added  $\text{AlMe}_3$  (2M in toluene, 0.190 mL, 0.379 mmol) at 0 °C. This mixture was warmed to ambient temperature and stirred for 1 hour, after which time (*R*)-methyl 2-((2,3-dihydrobenzo[*b*][1,4]dioxin-6-yl)amino)propanoate (*R*)-**6.33** (60.0 mg, 0.253 mmol) in DCM (0.5 mL) was added dropwise at 0°C. This mixture was stirred at room temperature for 18 hours. The solution was cooled to 0 °C and quenched by the dropwise addition of aqueous 1M HCl (2 mL). The organics were dried by passage through a hydrophobic frit and the solution was concentrated under reduced pressure. The residue was dissolved in MeOH (1 mL) and this mixture was subjected to MDAP purification (high pH, Method C) to afford the title compound (*R*)-**GSK'896** (71.8 mg, 0.190 mmol, 75 % yield) as a cream gum.  $[\alpha_D]_{589}^{20.6^\circ\text{C}}$  [c 0.1, MeOD- $d_4$ ]: +64. Other spectral data were identical to those reported for **GSK'896**. HR-MS (ESI):  $\text{C}_{17}\text{H}_{18}\text{BrN}_2\text{O}_3$  [ $\text{M}+\text{H}^+$ ] requires 377.0495, found 377.0511.

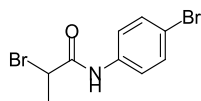
**(S)-N-(4-bromophenyl)-2-((2,3-dihydrobenzo[*b*][1,4]dioxin-6-yl)amino)propanamide**  
**((S)-GSK'896)**



The title compound (*S*)-**GSK'896** (46.1 mg, 0.122 mmol, 73 % yield, cream gum), was prepared in the same manner as (*R*)-**GSK'896** using the following reagents and solvents: 4-bromoaniline (43.5 mg, 0.253 mmol) in DCM (0.5 mL),  $\text{AlMe}_3$  (2 M in toluene, 0.126 mL, 0.253 mmol), (*S*)-methyl 2-((2,3-dihydrobenzo[*b*][1,4]dioxin-6-yl)amino)propanoate (*S*)-**6.33** (40.0 mg, 0.169 mmol) in DCM (0.5 mL). The compound was purified by MDAP (high pH, Method C).  $[\alpha_D]_{589}^{20.6^\circ\text{C}}$  [c 0.1, MeOD- $d_4$ ]: -60. Other spectral data were identical to those

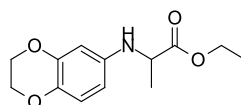
reported for **GSK'896**. HR-MS (ESI):  $C_{17}H_{18}BrN_2O_3$   $[M+H]^+$  requires 377.0495, found 377.0509.

#### 2-Bromo-*N*-(4-bromophenyl)propanamide (**6.4**)



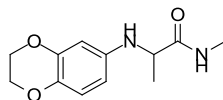
To a solution of 4-bromoaniline (800 mg, 4.65 mmol) in DCM (40 mL) at 0 °C was added 2-bromopropanoyl chloride **6.3** (0.61 mL, 6.05 mmol) in DCM (5 mL) dropwise. After warming to room temperature, sodium bicarbonate (586 mg, 6.98 mmol) was added. The resulting mixture was stirred at room temperature overnight. The mixture was washed with saturated sodium bicarbonate solution, separated and dried by passage through a hydrophobic frit. The organics were concentrated under reduced pressure to give the title compound **6.4** (1.39 g, 4.53 mmol, 97 % yield) as a white solid that was used without further purification.  $^1H$  NMR (400 MHz,  $CDCl_3$ ):  $\delta$  1.99 (d,  $J = 7.1$  Hz, 3H), 4.56 (q,  $J = 7.1$  Hz, 1H), 7.45-7.51 (m, 4H), 8.04 (br.s, 1H). LCMS (high pH):  $t_R = 1.13$  min,  $[M+H]^+$  307; (area % total: 96).

#### Ethyl 2-((2,3-dihydrobenzo[*b*][1,4]dioxin-6-yl)amino)propanoate (**6.18**)



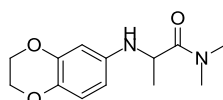
To a solution of 2,3-dihydrobenzo[*b*][1,4]dioxin-6-amine **6.5** (3.51 g, 23.2 mmol) and potassium carbonate (5.34 g, 38.7 mmol) in MeCN (220 mL) was added ethyl 2-bromopropanoate **6.17** (2.51 mL, 19.3 mmol). This mixture was heated to reflux for 18 hours, after which the solid material was filtered off and washed with MeCN. The filtrate was concentrated, adsorbed onto diatomaceous earth and purified by flash chromatography, eluting under a gradient of TBME (0-25%) in cyclohexane to afford the title compound **6.18** (3.56 g, 14.2 mmol, 73% yield) as a yellow oil.  $^1H$  NMR (400 MHz,  $CDCl_3$ ):  $\delta$  1.27 (t,  $J = 7.2$  Hz, 3H), 1.45 (d,  $J = 6.9$  Hz, 3H), 3.90 (br.s, 1H), 4.02 (q,  $J = 6.9$  Hz, 1H), 4.17-4.21 (m, 4H), 4.23-4.25 (m, 2H), 6.16-6.19 (m, 2H), 6.69-6.72 (m, 1H). LCMS (high pH):  $t_R = 1.01$  min,  $[M+H]^+$  252; (area % total: 97).

### 2-((2,3-Dihydrobenzo[*b*][1,4]dioxin-6-yl)amino)-*N*-methylpropanamide (6.19)



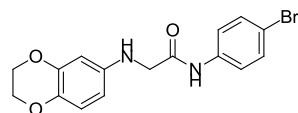
The title compound **6.19** (35.0 mg, 0.148 mmol, 62 % yield, orange gum), was prepared according to general procedure **A** using the following reagents and solvents: methylamine (2M in THF, 0.239 mL, 0.478 mmol), DABAL-Me<sub>3</sub> (122 mg, 0.478 mmol), THF (2.5 mL), *then* ethyl 2-((2,3-dihydrobenzo[*b*][1,4]dioxin-6-yl)amino)propanoate **6.18** (60.0 mg, 0.239 mmol) in THF (0.5 mL). The compound was purified by MDAP (high pH, Method A). <sup>1</sup>H NMR (400 MHz, MeOH): δ 1.40 (d, *J* = 7.1 Hz, 3H), 2.72 (s, 3H), 3.65 (q, *J* = 7.1 Hz, 1H), 4.12-4.14 (m, 2H), 4.17-4.19 (m, 2H), 6.09 (d, *J* = 2.6 Hz, 1H), 6.12 (dd, *J* = 2.6, 8.4 Hz, 1H), 6.62 (d, *J* = 8.4 Hz, 1H). *Exchangeable protons not observed.* <sup>13</sup>C NMR (100 MHz, MeOD-*d*<sub>4</sub>): δ 19.4, 26.2, 56.3, 65.4, 65.9, 103.2, 108.1, 118.4, 137.6, 143.5, 145.4, 178.5. *v*<sub>max</sub> (neat): 3326, 2932, 1651, 1509, 1325, 1279, 1241, 1212, 1068, 885, 797 cm<sup>-1</sup>. HR-MS (ESI): C<sub>12</sub>H<sub>17</sub>N<sub>2</sub>O<sub>3</sub> [M+H<sup>+</sup>] requires 237.1234, found 237.1227.

### 2-((2,3-Dihydrobenzo[*b*][1,4]dioxin-6-yl)amino)-*N,N*-dimethylpropanamide (6.20)



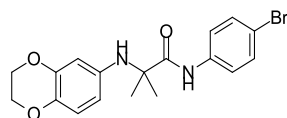
The title compound **6.20** (27.6 mg, 0.110 mmol, 46 % yield, orange gum), was prepared according to general procedure **A** using the following reagents and solvents: dimethylamine (2M in THF, 0.239 mL, 0.478 mmol), DABAL-Me<sub>3</sub> (122 mg, 0.478 mmol), THF (2.5 mL), *then* ethyl 2-((2,3-dihydrobenzo[*b*][1,4]dioxin-6-yl)amino)propanoate **6.18** (60.0 mg, 0.239 mmol) in THF (0.5 mL). The compound was purified by MDAP (high pH, Method A). <sup>1</sup>H NMR (400 MHz, MeOH): δ 1.32 (d, *J* = 6.8 Hz, 3H), 2.94 (s, 3H), 3.18 (s, 3H), 4.12-4.15 (m, 2H), 4.17-4.19 (m, 2H), 4.42 (q, *J* = 6.8 Hz, 1H), 6.19-6.21 (m, 2H), 6.61-6.64 (m, 1H). *Exchangeable protons not observed.* <sup>13</sup>C NMR (100 MHz, MeOD-*d*<sub>4</sub>): δ 18.2, 36.2, 37.3, 51.3, 65.4, 65.9, 104.3, 109.2, 118.4, 137.8, 143.3, 145.4, 176.5. *v*<sub>max</sub> (neat): 3339, 2976, 2930, 2873, 1641, 1592, 1507, 1397, 1328, 1279, 1241, 1211, 1126, 1068, 926, 885, 799, 742 cm<sup>-1</sup>. HR-MS (ESI): C<sub>13</sub>H<sub>19</sub>N<sub>2</sub>O<sub>3</sub> [M+H<sup>+</sup>] requires 251.1390, found 251.1383.

***N*-(4-Bromophenyl)-2-((2,3-dihydrobenzo[*b*][1,4]dioxin-6-yl)amino)acetamide (6.21)**



The title compound **6.21** (38.7 mg, 0.107 mmol, 62 % yield, brown gum), was prepared according to general procedure **B** using the following reagents and solvents: 2-bromo-*N*-(4-bromophenyl)acetamide **6.35** (50.0 mg, 0.171 mmol), 2,3-dihydrobenzo[*b*][1,4]dioxin-6-amine **6.5** (31.0 mg, 0.205 mmol), potassium carbonate (47.2 mg, 0.341 mmol), MeCN (2 mL). The compound was purified by MDAP (high pH, Method C).  $^1\text{H}$  NMR (400 MHz, DMSO- $d_6$ ):  $\delta$  3.77 (d,  $J$  = 5.9 Hz, 2H), 4.09-4.11 (m, 2H), 4.14-4.16 (m, 2H), 5.64 (t,  $J$  = 5.9 Hz, 1H), 6.09-6.10 (m, 1H), 6.13 (dd,  $J$  = 2.7, 8.6 Hz, 1H), 6.61 (d,  $J$  = 8.6 Hz, 1H), 7.47-7.50 (m, 2H), 7.58-7.62 (m, 2H), 10.05 (s, 1H).  $^{13}\text{C}$  NMR (100 MHz, DMSO- $d_6$ ):  $\delta$  48.1, 63.7, 64.3, 100.7, 106.0, 114.8, 117.2, 121.1 (2C), 131.5 (2C), 134.9, 138.2, 143.1, 143.6, 169.7.  $\nu_{\text{max}}$  (neat): 3321, 2977, 2874, 2473, 1651, 1587, 1509, 1488, 1442, 1385, 1303, 1210, 1067, 1008, 909, 881, 826, 801, 759, 700  $\text{cm}^{-1}$ . HR-MS (ESI):  $\text{C}_{16}\text{H}_{16}\text{BrN}_2\text{O}_3$  [ $\text{M}+\text{H}^+$ ] requires 363.0339, found 363.0344.

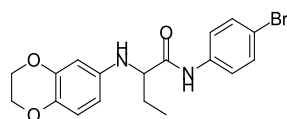
***N*-(4-Bromophenyl)-2-((2,3-dihydrobenzo[*b*][1,4]dioxin-6-yl)amino)-2-methylpropanamide (6.22)**



To a solution of 2,3-dihydrobenzo[*b*][1,4]dioxin-6-amine **6.5** (49.5 mg, 0.328 mmol) in THF (2 mL) was added NaH (14.2 mg, 0.355 mmol, 60% wt/wt). This mixture was stirred for 10 minutes, after which time 2-bromo-*N*-(4-bromophenyl)-2-methylpropanamide **6.36** (88.0 mg, 0.273 mmol) in THF (2 mL) was added. The mixture was stirred overnight at room temperature. Water (10 mL) was added and the mixture was extracted with EtOAc (3 x 10 mL). The combined organics were washed with brine, dried over  $\text{MgSO}_4$ , and concentrated. The residue was dissolved in MeOH (1 mL) and purified by MDAP (high pH, Method D) to afford the title compound **6.22** (60.4 mg, 0.154 mmol, 57 % yield) as a light brown solid. M.pt. 145-146  $^{\circ}\text{C}$ .  $^1\text{H}$  NMR (400 MHz, DMSO- $d_6$ ):  $\delta$  1.40 (s, 6H), 4.07-4.09 (m, 2H), 4.12-4.14 (m, 2H), 5.45 (s, 1H), 6.05-6.09 (m, 2H), 6.59 (d,  $J$  = 8.5 Hz, 1H), 7.44-7.47 (m, 2H), 7.62-7.66 (m, 2H), 9.85 (s, 1H).  $^{13}\text{C}$  NMR (100 MHz, DMSO- $d_6$ ):  $\delta$  25.2 (2C), 57.8, 63.6, 64.2, 103.5, 108.5, 114.8, 116.9, 121.7 (2C), 131.3 (2C), 135.4, 138.4, 140.6, 143.3, 175.2.  $\nu_{\text{max}}$  (neat): 3296, 2978, 2927, 2875, 1671, 1591, 1503, 1392, 1312, 1282, 1240, 1207, 1171, 1068, 1005,

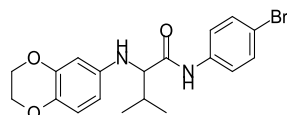
913, 882, 804, 710  $\text{cm}^{-1}$ . HR-MS (ESI):  $\text{C}_{18}\text{H}_{20}\text{BrN}_2\text{O}_3$   $[\text{M}+\text{H}^+]$  requires 391.0652, found 391.0653.

***N*-(4-bromophenyl)-2-((2,3-dihydrobenzo[*b*][1,4]dioxin-6-yl)amino)butanamide (6.23)**



The title compound **6.23** (37.0 mg, 0.095 mmol, 58 % yield, orange gum), was prepared according to general procedure **B** using the following reagents and solvents: 2-bromo-*N*-(4-bromophenyl)butanamide **6.37** (52.2 mg, 0.163 mmol), 2,3-dihydrobenzo[*b*][1,4]dioxin-6-amine **6.5** (29.5 mg, 0.195 mmol), potassium carbonate (44.9 mg, 0.325 mmol), MeCN (2 mL). The compound was purified by MDAP (high pH, Method C).  $^1\text{H}$  NMR (400 MHz, MeOD- $d_4$ ):  $\delta$  1.08 (t,  $J = 7.6$  Hz, 3H), 1.79-1.95 (m, 2H), 3.71 (dd,  $J = 6.0, 7.5$  Hz, 1H), 4.11-4.13 (m, 2H), 4.16-4.18 (m, 2H), 6.20-6.23 (m, 2H), 6.62-6.65 (m, 1H), 7.42-7.45 (m, 2H), 7.47-7.51 (m, 2H). *Exchangeable protons not observed.*  $^{13}\text{C}$  NMR (100 MHz, MeOD- $d_4$ ):  $\delta$  11.0, 27.6, 62.9, 65.4, 65.9, 103.5, 108.3, 117.8, 118.5, 123.1 (2C), 132.8 (2C), 137.7, 138.5, 143.6, 145.4, 175.7.  $\nu_{\text{max}}$  (neat): 3322, 2970, 2931, 2875, 1667, 1590, 1505, 1395, 1323, 1281, 1209, 1176, 1069, 1009, 921, 886, 825, 737  $\text{cm}^{-1}$ . HR-MS (ESI):  $\text{C}_{18}\text{H}_{20}\text{BrN}_2\text{O}_4$   $[\text{M}+\text{H}^+]$  requires 391.0652, found 391.0665.

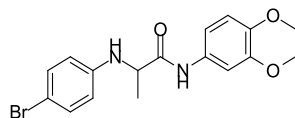
***N*-(4-Bromophenyl)-2-((2,3-dihydrobenzo[*b*][1,4]dioxin-6-yl)amino)-3-methylbutanamide (6.24)**



The title compound **6.24** (52.1 mg, 0.129 mmol, 62 % yield, straw coloured glass), was prepared according to general procedure **B** using the following reagents and solvents: 2-bromo-*N*-(4-bromophenyl)-3-methylbutanamide **6.38** (70.0 mg, 0.209 mmol), 2,3-dihydrobenzo[*b*][1,4]dioxin-6-amine **6.5** (37.9 mg, 0.251 mmol), potassium carbonate (57.8 mg, 0.418 mmol), MeCN (2 mL). The compound was purified by MDAP (high pH, Method C).  $^1\text{H}$  NMR (400 MHz, DMSO- $d_6$ ):  $\delta$  0.96 (d,  $J = 6.9$  Hz, 3H), 1.02 (d,  $J = 6.9$  Hz, 3H), 1.94-2.06 (m, 1H), 3.57 (dd,  $J = 7.7, 8.6$  Hz, 1H), 4.07-4.09 (m, 2H), 4.12-4.15 (m, 2H), 5.34 (d,  $J = 8.6$  Hz, 1H), 6.19-6.22 (m, 2H), 6.58 (d,  $J = 8.7$  Hz, 1H), 7.46-7.49 (m, 2H), 7.58-7.59 (m, 2H), 10.07 (s, 1H).  $^{13}\text{C}$  NMR (100 MHz, DMSO- $d_6$ ):  $\delta$  19.2, 19.3, 31.1, 63.6, 64.3, 64.3, 101.1, 106.5, 114.9, 117.0, 121.2 (2C), 131.5 (2C), 134.8, 138.0, 143.0, 143.5, 172.5.  $\nu_{\text{max}}$  (neat):

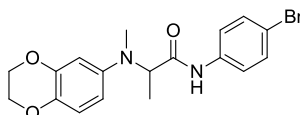
3313 (br.), 2964, 2929, 2872, 1660, 1591, 1502, 1393, 1303, 1279, 1240, 1209, 1172, 1068, 1008, 921, 885, 822 cm<sup>-1</sup>. HR-MS (ESI): C<sub>19</sub>H<sub>22</sub>BrN<sub>2</sub>O<sub>3</sub> [M+H<sup>+</sup>] requires 405.0808, found 405.0798.

### 2-((4-Bromophenyl)amino)-*N*-(2,3-dihydrobenzo[*b*][1,4]dioxin-6-yl)propanamide (6.25)



The title compound **6.25** (59.0 mg, 0.156 mmol, 32 % yield, straw coloured glass), was prepared according to general procedure **B** using the following reagents and solvents: 2-bromo-*N*-(2,3-dihydrobenzo[*b*][1,4]dioxin-6-yl)propanamide **6.39** (141 mg, 0.496 mmol), 4-bromoaniline (102 mg, 0.595 mmol), potassium carbonate (137 mg, 0.992 mmol), MeCN (2 mL). The compound was purified by MDAP (high pH, Method C). <sup>1</sup>H NMR (400 MHz, DMSO-*d*<sub>6</sub>): δ 1.36 (d, *J* = 6.7 Hz, 3H), 3.95 (q, *J* = 6.7 Hz, 1H), 4.16-4.22 (m, 5H), 6.53-6.57 (m, 2H), 6.76 (d, *J* = 8.8 Hz, 1H), 6.97 (dd, *J* = 2.5, 8.8 Hz, 1H), 7.20-7.24 (m, 3H), 9.83 (s, 1H). <sup>13</sup>C NMR (100 MHz, DMSO-*d*<sub>6</sub>): δ 18.7, 48.6, 52.9, 63.9, 64.1, 107.1, 108.4, 111.5, 112.5, 114.5, 116.7, 131.4, 132.5, 139.4, 142.9, 147.1, 172.2. *v*<sub>max</sub> (neat): 3325, 2977, 2932, 2874, 1659, 1594, 1504, 1457, 1429, 1300, 1285, 1241, 1203, 1165, 1065, 919, 886, 811, 742 cm<sup>-1</sup>. HR-MS (ESI): C<sub>17</sub>H<sub>18</sub>BrN<sub>2</sub>O<sub>3</sub> [M+H<sup>+</sup>] requires 377.0495, found 377.0511.

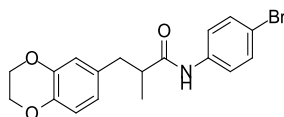
### *N*-(4-Bromophenyl)-2-((2,3-dihydrobenzo[*b*][1,4]dioxin-6-yl)(methyl)amino)propanamide (6.26)



The title compound **6.26** (37.6 mg, 96.0 μmol, 49 % yield, brown gum), was prepared according to general procedure **B** using the following reagents and solvents: 2-bromo-*N*-(4-bromophenyl)propanamide **6.4** (60.0 mg, 0.195 mmol), *N*-methyl-2,3-dihydrobenzo[*b*][1,4]dioxin-6-amine **6.40** (38.7 mg, 0.235 mmol), potassium carbonate (54.0 mg, 0.391 mmol), MeCN (2 mL). The compound was purified by MDAP (high pH, Method C). <sup>1</sup>H NMR (400 MHz, DMSO-*d*<sub>6</sub>): δ 1.26 (d, *J* = 6.8 Hz, 3H), 2.75 (s, 3H), 4.13-4.15 (m, 2H), 4.18-4.20 (m, 2H), 4.42 (q, *J* = 6.8 Hz, 1H), 6.37-6.40 (m, 2H), 6.70-6.72 (m, 1H), 7.46-7.50 (m, 2H), 7.60-7.64 (m, 2H), 10.01 (s, 1H). <sup>13</sup>C NMR (100 MHz, DMSO-*d*<sub>6</sub>): δ 12.9, 33.8, 58.6, 63.8, 64.3, 103.2, 107.6, 114.8, 116.9, 121.5 (2C), 131.4 (2C), 135.6, 138.3, 143.5, 144.4, 171.8. *v*<sub>max</sub> (neat): 3261, 2977, 2927, 2869, 1670, 1585, 1505, 1395, 1296, 1244,

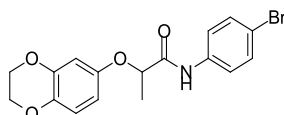
1227, 1182, 1108, 1066, 1007, 915, 858, 819, 790, 716  $\text{cm}^{-1}$ . HR-MS (ESI):  $\text{C}_{18}\text{H}_{20}\text{BrN}_2\text{O}_3$   $[\text{M}+\text{H}^+]$  requires 391.0652, found 391.0653.

***N*-(4-Bromophenyl)-3-(2,3-dihydrobenzo[*b*][1,4]dioxin-6-yl)-2-methylpropanamide (6.27)**



The title compound **6.27** (99.5 mg, 0.264 mmol, 83 % yield, straw coloured solid), was prepared according to general procedure **A** using the following reagents and solvents: *p*-bromoaniline (110 mg, 0.639 mmol), DABAL- $\text{Me}_3$  (164 mg, 0.639 mmol), THF (3 mL), *then* ethyl 3-(2,3-dihydrobenzo[*b*][1,4]dioxin-6-yl)-2-methylpropanoate **6.42** (80.0 mg, 0.320 mmol) in THF (0.5 mL). The compound was purified by MDAP (high pH, Method C). M.pt. 130-133  $^{\circ}\text{C}$ .  $^1\text{H}$  NMR (400 MHz,  $\text{MeOD-}d_4$ ):  $\delta$  1.19 (d,  $J = 6.7$  Hz, 3H), 2.59 (dd,  $J = 6.8, 13.6$  Hz, 1H), 2.68-2.76 (m, 1H), 2.87 (dd,  $J = 8.1, 13.6$  Hz, 1H), 4.18 (s, 4H), 6.65 (dd,  $J = 2.8, 8.1$  Hz, 1H), 6.70-6.72 (m, 2H), 7.39-7.44 (m, 4H). *Exchangeable protons not observed*.  $^{13}\text{C}$  NMR (100 MHz,  $\text{MeOD-}d_4$ ):  $\delta$  18.0, 40.6, 45.1, 65.5, 65.6, 117.4, 117.9, 118.6, 122.8, 123.1 (2C), 132.7 (2C), 134.0, 139.1, 143.5, 144.7, 177.3.  $\nu_{\text{max}}$  (neat): 2967, 2923, 2398, 1632, 1589, 1492, 1505, 1462, 1433, 1397, 1336, 1307, 1288, 1206, 1128, 1066, 1008, 918, 863, 770, 738  $\text{cm}^{-1}$ . HR-MS (ESI):  $\text{C}_{18}\text{H}_{19}\text{BrNO}_3$   $[\text{M}+\text{H}^+]$  requires 376.0543, found 376.0546.

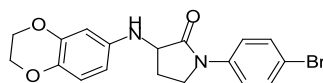
***N*-(4-Bromophenyl)-2-((2,3-dihydrobenzo[*b*][1,4]dioxin-6-yl)oxy)propanamide (6.28)**



The title compound **6.28** (48.4 mg, 0.128 mmol, 66 % yield, orange gum), was prepared according to general procedure **B** using the following reagents and solvents: 2-bromo-*N*-(4-bromophenyl)propanamide **6.4** (60.0 mg, 0.195 mmol), 2,3-dihydrobenzo[*b*][1,4]dioxin-6-ol **6.43** (35.7 mg, 0.235 mmol), potassium carbonate (54.0 mg, 0.391 mmol), MeCN (2 mL). The compound was purified by MDAP (high pH, Method C).  $^1\text{H}$  NMR (400 MHz,  $\text{MeOD-}d_4$ ):  $\delta$  1.58 (d,  $J = 6.8$  Hz, 3H), 4.16-4.18 (m, 2H), 4.20-4.22 (m, 2H), 4.68 (q,  $J = 6.8$  Hz, 1H), 6.49 (dd,  $J = 2.8, 8.6$  Hz, 1H), 6.53 (d,  $J = 2.8$  Hz, 1H), 6.75 (d,  $J = 8.6$  Hz, 1H), 7.43-7.47 (m, 2H), 7.51-7.55 (m, 2H). *Exchangeable protons not observed*.  $^{13}\text{C}$  NMR (100 MHz,  $\text{MeOD-}d_4$ ):  $\delta$  19.1, 65.3, 65.8, 76.9, 106.0, 109.9, 118.1, 118.5, 123.5 (2C), 132.8 (2C), 138.3, 140.2, 145.4, 153.0, 173.5.  $\nu_{\text{max}}$  (neat): 3313, 2982, 2934, 1680, 1590, 1521, 1496, 1489, 1395, 1301,

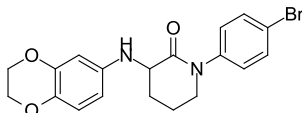
1239, 1198, 1158, 1065, 1008, 970, 920, 824, 734  $\text{cm}^{-1}$ . HR-MS (ESI):  $\text{C}_{17}\text{H}_{17}\text{BrNO}_4$  [ $\text{M}+\text{H}^+$ ] requires 378.0336, found 378.0346.

**1-(4-Bromophenyl)-3-((2,3-dihydrobenzo[*b*][1,4]dioxin-6-yl)amino)pyrrolidin-2-one (6.29)**



The title compound **6.29** (40.9 mg, 0.105 mmol, 67 % yield, light brown solid), was prepared according to general procedure **B** using the following reagents and solvents: 3-bromo-1-(4-bromophenyl)pyrrolidin-2-one **6.46** (50.0 mg, 0.157 mmol), 2,3-dihydrobenzo[*b*][1,4]dioxin-6-amine **6.5** (28.4 mg, 0.188 mmol), potassium carbonate (43.3 mg, 0.313 mmol), MeCN (2 mL). The compound was purified by MDAP (high pH, Method C). M.pt. 130-145 °C (decomp.).  $^1\text{H}$  NMR (400 MHz,  $\text{DMSO}-d_6$ ):  $\delta$  1.86 (ddt,  $J = 9.5, 9.5, 12.2$  Hz, 1H), 2.53-2.60 (m, 1H), 3.74-3.83 (m, 2H), 4.10-4.12 (m, 2H), 4.16-4.18 (m, 2H), 4.21-4.27 (m, 1H), 5.51 (d,  $J = 7.0$  Hz, 1H), 6.21-6.24 (m, 2H), 6.61 (d,  $J = 8.6$  Hz, 1H), 7.57-7.61 (m, 2H), 7.68-7.72 (m, 2H).  $^{13}\text{C}$  NMR (100 MHz,  $\text{DMSO}-d_6$ ):  $\delta$  26.4, 44.3, 55.6, 63.7, 64.3, 101.3, 106.4, 115.9, 117.0, 121.0 (2C), 131.5 (2C), 134.7, 138.9, 142.7, 143.6, 173.1.  $\nu_{\text{max}}$  (neat): 3324, 2969, 2919, 2869, 1686, 1623, 1587, 1507, 1487, 1415, 1390, 1306, 1202, 1179, 1069, 1007, 922, 883, 830, 708  $\text{cm}^{-1}$ . HR-MS (ESI):  $\text{C}_{18}\text{H}_{18}\text{BrN}_2\text{O}_3$  [ $\text{M}+\text{H}^+$ ] requires 389.0495, found 389.0511.

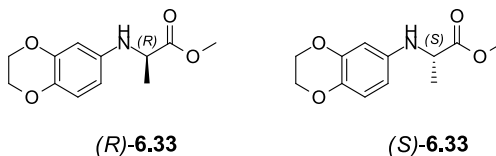
**1-(4-Bromophenyl)-3-((2,3-dihydrobenzo[*b*][1,4]dioxin-6-yl)amino)piperidin-2-one (6.30)**



The title compound **6.30** (40.2 mg, 99.2  $\mu\text{mol}$ , 62% yield, white solid), was prepared according to general procedure **B** using the following reagents and solvents: 1-(4-bromophenyl)-2-oxopiperidin-3-yl 4-methylbenzenesulfonate **6.49** (68.0 mg, 0.160 mmol), 2,3-dihydrobenzo[*b*][1,4]dioxin-6-amine **6.5** (29.1 mg, 0.192 mmol), potassium carbonate (44.3 mg, 0.321 mmol), MeCN (2 mL). The compound was purified by MDAP (high pH, Method C). M.pt. 165-167 °C.  $^1\text{H}$  NMR (400 MHz,  $\text{DMSO}-d_6$ ):  $\delta$  1.68-1.78 (m, 1H), 1.96-2.02 (m, 2H), 2.19-2.27 (m, 1H), 3.64-3.75 (m, 2H), 4.00-4.05 (m, 1H), 4.09-4.11 (m, 2H), 4.15-4.17 (m, 2H), 5.34 (d,  $J = 7.0$  Hz, 1H), 6.18-6.22 (m, 2H), 6.59 (d,  $J = 8.0$  Hz, 1H), 7.26-7.30 (m, 2H), 7.55-7.59 (m, 2H).  $^{13}\text{C}$  NMR (100 MHz,  $\text{DMSO}-d_6$ ):  $\delta$  20.5, 27.1, 49.5, 53.8, 63.7, 64.3, 101.2, 106.5, 116.9, 118.3, 127.9 (2C), 131.5 (2C), 134.5, 142.4, 142.9, 143.5, 170.5.  $\nu_{\text{max}}$  (neat): 3340, 2973, 2870, 2481, 1650, 1586, 1508, 1486, 1321, 1304, 1277, 1229, 1146,

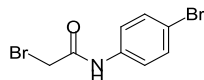
1069, 1010, 917, 884, 835, 811, 736  $\text{cm}^{-1}$ . HR-MS (ESI):  $\text{C}_{19}\text{H}_{20}\text{BrN}_2\text{O}_3$   $[\text{M}+\text{H}^+]$  requires 403.0652, found 403.0669.

**(R)-Methyl 2-((2,3-dihydrobenzo[*b*][1,4]dioxin-6-yl)amino)propanoate (R)-6.33 and (S)-methyl 2-((2,3-dihydrobenzo[*b*][1,4]dioxin-6-yl)amino)propanoate (S)-6.33**



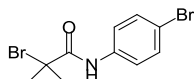
Into a dry round bottom flask was added (*R*)-methyl 2-aminopropanoate hydrochloride (*R*)-**6.32** or (*S*)-methyl 2-aminopropanoate hydrochloride (*S*)-**6.32** (500 mg, 3.58 mmol), (2,3-dihydrobenzo[*b*][1,4]dioxin-6-yl)boronic acid **6.31** (1.03 g, 5.73 mmol), copper(II) acetate (716 mg, 3.94 mmol) and powdered 4Å molecular sieves (1.34 g). The flask was sealed with a septum, evacuated and backfilled with oxygen. DCM (30 mL) and triethylamine (0.899 mL, 6.45 mmol) were added, and the mixture was stirred at room temperature for 36 hours. The reaction mixture was quenched with 2 M ammonia in MeOH (13 mL), and then filtered through a pad of Celite. The volatiles were removed under reduced pressure and the resulting crude oil was adsorbed onto diatomaceous earth and purified by reversed phase chromatography, eluting under a gradient of MeCN (0-40%) in modified water (formic) to afford a viscous brown gum. Further purification by flash chromatography, eluting under a gradient of EtOAc (0-15%) in cyclohexane, afforded either (*R*)-methyl 2-((2,3-dihydrobenzo[*b*][1,4]dioxin-6-yl)amino)propanoate (*R*)-**6.33** (127 mg, 0.535 mmol, 15 % yield) as a transparent gum, or (*S*)-methyl 2-((2,3-dihydrobenzo[*b*][1,4]dioxin-6-yl)amino)propanoate (*S*)-**6.33** (123 mg, 0.518 mmol, 14 % yield) as a transparent gum. (*R*)-**6.33**:  $[\alpha_D]_{589}^{22.7^\circ\text{C}}$  [c 0.2,  $\text{CH}_2\text{Cl}_2$ ]: +82.  $^1\text{H}$  NMR (400 MHz,  $\text{CDCl}_3$ ):  $\delta$  1.45 (d,  $J = 6.9$  Hz, 3H), 3.75 (s, 3H), 3.89 (br.s, 1H), 4.03-4.08 (m, 1H), 4.19-4.21 (m, 2H), 4.23-4.25 (m, 2H), 6.16-6.19 (m, 2H), 6.70-6.73 (m, 1H). LCMS (formic):  $t_R = 0.80$  min,  $[\text{M}+\text{H}^+]$  238; (area % total: 100). (*S*)-**6.33**:  $[\alpha_D]_{589}^{22.7^\circ\text{C}}$  [c 0.2,  $\text{CH}_2\text{Cl}_2$ ]: -76. Spectral data were identical to those reported for (*R*)-**6.33**. LCMS (formic):  $t_R = 0.80$  min,  $[\text{M}+\text{H}^+]$  238; (area % total: 100).

### 2-Bromo-*N*-(4-bromophenyl)acetamide (6.35)



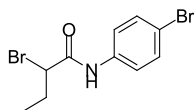
To a mixture of *p*-bromoaniline (200 mg, 1.16 mmol) in DCM (9 mL) at 0 °C was added a solution of 2-bromoacetyl bromide (0.116 mL, 1.34 mmol) in DCM (4.5 mL). The mixture was stirred at room temperature for 20 hours. After this time, sodium bicarbonate (147 mg, 1.74 mmol) was added and the mixture was stirred for 2 hours. Saturated sodium bicarbonate solution (20 mL) was added and the mixture was stirred vigorously. The organic layer was separated, washed with brine and dried over a hydrophobic frit. The organics were removed under reduced pressure to afford the title compound **6.35** (319 mg, 1.09 mmol, 94 % yield) as a white solid that was used without further purification. <sup>1</sup>H NMR (400 MHz, CDCl<sub>3</sub>): δ 4.04 (s, 2H), 7.45-7.52 (m, 4H), 8.12 (br.s, 1H). LCMS (high pH): t<sub>R</sub> = 0.94 min, did not ionize; (area % total: 98).

### 2-Bromo-*N*-(4-bromophenyl)-2-methylpropanamide (6.36)



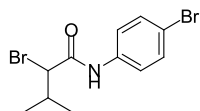
The title compound **6.36** (401 mg, 1.25 mmol, 72 % yield, white solid), was prepared in the same manner as **6.35** using the following reagents and solvents: *p*-bromoaniline (300 mg, 1.74 mmol), DCM (9 mL), 2-bromo-2-methylpropanoyl bromide (0.248 mL, 2.01 mmol) in DCM (4.5 mL), sodium bicarbonate (220 mg, 2.62 mmol). <sup>1</sup>H NMR (400 MHz, CDCl<sub>3</sub>): δ 2.07 (s, 6H), 7.45-7.51 (m, 4H), 8.46 (br.s, 1H). LCMS (high pH): t<sub>R</sub> = 1.24 min, [M+H<sup>+</sup>] 319, 321, 323; (area % total: 100).

### 2-Bromo-*N*-(4-bromophenyl)butanamide (6.37)



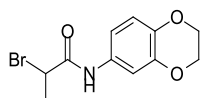
The title compound **6.37** (149 mg, 0.463 mmol, 100 % yield, white solid), was prepared in the same manner as **6.35** using the following reagents and solvents: *p*-bromoaniline (80.0 mg, 0.465 mmol), DCM (3.6 mL), 2-bromobutanoyl chloride (0.058 mL, 0.535 mmol) in DCM (1 mL), sodium bicarbonate (58.6 mg, 0.698 mmol). <sup>1</sup>H NMR (400 MHz, CDCl<sub>3</sub>): δ 1.13 (t, *J* = 7.1 Hz, 3H), 2.11-2.22 (m, 1H), 2.23-2.33 (m, 1H), 4.44 (dd, *J* = 5.1, 7.8 Hz, 1H), 7.45-7.51 (m, 4H), 8.08 (br.s, 1H). LCMS (high pH): t<sub>R</sub> = 1.21 min, [M+H<sup>+</sup>] 319, 322, 324; (area % total: 80).

### 2-bromo-N-(4-bromophenyl)-3-methylbutanamide (6.38)



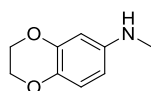
To a mixture of 2-bromo-3-methylbutanoic acid (150 mg, 0.829 mmol), 4-bromoaniline (150 mg, 0.870 mmol), and DMAP (10.1 mg, 0.083 mmol) in DCM (3 mL) was added *N,N'*-diisopropylcarbodiimide (0.141 mL, 0.911 mmol) at 0 °C. The mixture was allowed to warm to room temperature and was stirred for 20 hours. After this time, the mixture was diluted with DCM (5 mL) and quenched with water (10 mL). The resulting solution was extracted with DCM (2 x 10 mL), and the combined organics were dried over a hydrophobic frit and concentrated *in vacuo*. The residue was adsorbed onto diatomaceous earth and purified by flash chromatography, eluting under a gradient of TBME (0-20%) in cyclohexane to afford the title compound **6.38** (212 mg, 0.633 mmol, 76 % yield) as a white solid. <sup>1</sup>H NMR (400 MHz, CDCl<sub>3</sub>): δ 1.06 (d, *J* = 6.7 Hz, 3H), 1.14 (d, *J* = 6.7 Hz, 3H), 2.46-2.54 (m, 1H), 4.45 (d, *J* = 4.5 Hz, 1H), 7.45-7.51 (m, 4H), 8.20 (br.s, 1H). LCMS (high pH): *t*<sub>R</sub> = 1.27 min, [M+H<sup>+</sup>] 333, 335, 337; (area % total: 98).

### 2-Bromo-N-(2,3-dihydrobenzo[*b*][1,4]dioxin-6-yl)propanamide (6.39)



The title compound **6.39** (141 mg, 0.496 mmol, 100 % yield, light brown solid), was prepared in the same manner as **6.35** using the following reagents and solvents: 2,3-dihydrobenzo[*b*][1,4]dioxin-6-amine **6.5** (75.0 mg, 0.496 mmol), DCM (3.6 mL), 2-bromopropanoyl chloride (0.058 mL, 0.571 mmol) in DCM (1 mL), sodium bicarbonate (62.5 mg, 0.744 mmol). <sup>1</sup>H NMR (400 MHz, DMSO-*d*<sub>6</sub>): δ 1.73 (d, *J* = 6.9 Hz, 3H), 4.19-4.24 (m, 4H), 4.65 (q, *J* = 6.9 Hz, 1H), 6.81 (d, *J* = 8.9 Hz, 1H), 6.98 (dd, *J* = 2.4, 8.9 Hz, 1H), 7.23 (d, *J* = 2.4 Hz, 1H), 10.14 (br.s, 1H). LCMS (high pH): *t*<sub>R</sub> = 0.92 min, [M+H<sup>+</sup>] 285, 287; (area % total: 95).

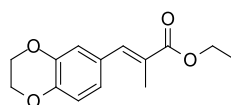
### *N*-Methyl-2,3-dihydrobenzo[*b*][1,4]dioxin-6-amine (6.40)<sup>259</sup>



To a solution of sodium methoxide (268 mg, 4.96 mmol) in MeOH (3 mL), paraformaldehyde (298 mg, 9.92 mmol) and 2,3-dihydrobenzo[*b*][1,4]dioxin-6-amine **6.5** (150 mg, 0.992 mmol) were added. This mixture was stirred at room temperature for 20

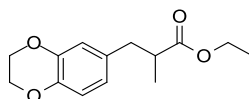
hours. Sodium borohydride (113 mg, 2.98 mmol) was then added in portions, and the mixture was stirred for a further 3 hours at 40 °C. After this time the mixture was filtered and the organics were removed under reduced pressure. The residue was dissolved in DCM, washed with water and brine then dried over a hydrophobic frit. The organics were removed, under reduced pressure to afford the title compound **6.40** (153 mg, 0.926 mmol, 93 % yield) as a light brown oil that was used without further purification. <sup>1</sup>H NMR (400 MHz, DMSO-*d*<sub>6</sub>): δ 2.58 (d, *J* = 5.4 Hz, 3H), 4.09-4.11 (m, 2H), 4.15-4.17 (m, 2H), 5.16 (q, *J* = 5.4 Hz, 1H), 6.02 (d, *J* = 2.7 Hz, 1H), 6.05 (dd, *J* = 2.7, 8.6 Hz, 1H), 6.59 (d, *J* = 8.6 Hz, 1H). LCMS (high pH): *t*<sub>R</sub> = 0.77 min, [M+H<sup>+</sup>] 166; (area % total: 97).

**(E)-Ethyl 3-(2,3-dihydrobenzo[*b*][1,4]dioxin-6-yl)-2-methylacrylate (S.I. 1)**



To a solution of ethyl 2-(diethoxyphosphoryl)propanoate **6.44** (2.09 mL, 9.75 mmol) in THF (15 mL) at 0 °C under an atmosphere of nitrogen was added NaH (390 mg, 9.75 mmol, 60% wt/wt) portion-wise. This mixture was stirred for 20 minutes at the same temperature, after which time 2,3-dihydrobenzo[*b*][1,4]dioxine-6-carbaldehyde **6.41** (800 mg, 4.87 mmol) in THF (5 mL) was added dropwise. This mixture was warmed to room temperature and stirred for 18 hours, after which water (60 mL) was added and the organics were extracted with EtOAc (3 x 60 mL). The combined organics were dried over MgSO<sub>4</sub> and concentrated. The residue was adsorbed onto diatomaceous earth and purified by flash chromatography, eluting under a gradient of TBME (0-15%) in cyclohexane to afford the title compound **S.I. 1** (1.21 g, 4.87 mmol, 100 % yield) as a transparent oil. <sup>1</sup>H NMR (400 MHz, CDCl<sub>3</sub>): δ 1.36 (t, *J* = 7.2 Hz, 3H), 2.14 (d, *J* = 2.0 Hz, 3H), 4.27-4.32 (m, 6H), 6.89 (d, *J* = 8.3 Hz, 1H), 6.94 (dd, *J* = 2.0 Hz, 8.3 Hz, 1H), 6.99 (d, *J* = 2.0 Hz, 1H), 7.59 (br.s, 1H). LCMS (high pH): *t*<sub>R</sub> = 1.25 min, [M+H<sup>+</sup>] 249; (area % total: 100).

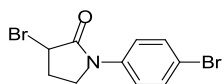
**Ethyl 3-(2,3-dihydrobenzo[*b*][1,4]dioxin-6-yl)-2-methylpropanoate (6.42)**



A mixture of (*E*)-ethyl 3-(2,3-dihydrobenzo[*b*][1,4]dioxin-6-yl)-2-methylacrylate **S.I. 1** (500 mg, 2.01 mmol), and 10% Pd/C (50.0 mg, 0.047 mmol) in EtOH (10 mL) was stirred under an

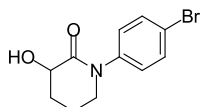
atmosphere of hydrogen at room temperature for 24 hours, after which the mixture was filtered through Celite and the organics were removed under reduced pressure to afford the title compound **6.42** (488 mg, 1.95 mmol, 97 % yield) as a transparent oil that was used without further purification.  $^1\text{H NMR}$  (400 MHz,  $\text{CDCl}_3$ ):  $\delta$  1.15 (d,  $J = 6.7$  Hz, 3H), 1.23 (t,  $J = 7.1$  Hz, 3H), 2.57 (dd,  $J = 7.9, 13.4$  Hz, 1H), 2.63-2.72 (m, 1H), 2.93 (dd,  $J = 6.8, 13.4$  Hz, 1H), 4.12 (q,  $J = 7.1$  Hz, 2H), 4.25 (s, 4H), 6.64 (dd,  $J = 2.2, 8.1$  Hz, 1H), 6.69 (d,  $J = 2.2$  Hz, 1H), 6.78 (d,  $J = 8.1$  Hz, 1H). LCMS (high pH):  $t_R = 1.20$  min,  $[\text{M}+\text{H}^+]$  251; (area % total: 100).

### 3-Bromo-1-(4-bromophenyl)pyrrolidin-2-one (**6.46**)<sup>260</sup>



To a slurry of *p*-bromoaniline (300 mg, 1.74 mmol) and sodium phosphate (164 mg, 0.959 mmol) in MeCN (3 mL) at 0 °C was added 2,4-dibromobutyryl chloride **6.45** (0.273 mL, 2.01 mmol) dropwise. The mixture was stirred for 2 hours at room temperature, after which potassium carbonate (482 mg, 3.49 mmol) was added and the mixture was stirred for 18 hours at the same temperature. The mixture was filtered and the solid was washed with MeCN. The organics were evaporated under reduced pressure, adsorbed onto diatomaceous earth and purified by flash chromatography, eluting under a gradient of TBME (0-25%) in cyclohexane to give the title compound **6.46**<sup>260</sup> (379 mg, 1.19 mmol, 68 % yield) as a white solid.  $^1\text{H NMR}$  (400 MHz,  $\text{DMSO}-d_6$ ):  $\delta$  2.34 (ddt,  $J = 3.6, 7.3, 14.3$  Hz, 1H), 2.72-2.81 (ddt,  $J = 7.3, 7.3, 14.3$  Hz, 1H), 3.84-3.98 (m, 2H), 4.90 (dd,  $J = 3.6, 7.3$  Hz, 1H), 7.59-7.63 (m, 2H), 7.66-7.71 (m, 2H). LCMS (high pH):  $t_R = 1.12$  min,  $[\text{M}+\text{H}^+]$  317, 319, 321; (area % total: 98).

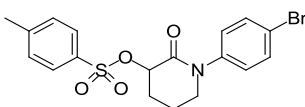
### 1-(4-Bromophenyl)-3-hydroxypiperidin-2-one (**6.48**)



A mixture of 1-bromo-4-iodobenzene (983 mg, 3.47 mmol), 3-hydroxypiperidin-2-one **6.47** (400 mg, 3.47 mmol), caesium carbonate (1.70 g, 5.21 mmol), XantPhos (302 mg, 0.521 mmol) and  $\text{Pd}(\text{OAc})_2$  (46.8 mg, 0.208 mmol) were sealed in a microwave vial with a Teflon septum. The vial was evacuated and back filled with nitrogen, and 1,4-Dioxane (12 mL) was added. The mixture was heated at 100 °C for 7 hours under microwave irradiation, after which time the solvents were removed under reduced pressure. The residue was dissolved

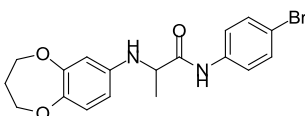
in a mixture of saturated ammonium chloride (10 mL) and EtOAc (10 mL). The organics were separated and the aqueous layer was extracted with EtOAc (2 x 10 mL). The combined organics were dried over sodium sulfate and concentrated under reduced pressure. The crude material was adsorbed onto diatomaceous earth and purified by reversed phase chromatography eluting under a gradient of MeCN (10-35%) in modified water (high pH) to afford the title compound **6.48** (376 mg, 1.39 mmol, 40 % yield) as a white solid.  $^1\text{H}$  NMR (400 MHz, DMSO- $d_6$ ):  $\delta$  1.71-1.80 (m, 1H), 1.82-2.01 (m, 2H), 2.08-2.14 (m, 1H), 3.51-3.57 (m, 1H), 3.64-3.70 (m, 1H), 4.05-4.10 (m, 1H), 5.27 (d,  $J$  = 5.3 Hz, 1H), 7.24-7.29 (m, 2H), 7.56-7.59 (m, 2H). LCMS (high pH):  $t_R$  = 0.84 min,  $[\text{M}+\text{H}^+]$  269, 271; (area % total: 100).

#### 1-(4-Bromophenyl)-2-oxopiperidin-3-yl 4-methylbenzenesulfonate (6.49)



To a solution of 1-(4-bromophenyl)-3-hydroxypiperidin-2-one **6.48** (60.0 mg, 0.222 mmol) and DABCO (125 mg, 1.11 mmol) in DCM (3 mL) at 0 °C was added 4-toluenesulfonyl chloride (169 mg, 0.888 mmol) portion-wise. The mixture was warmed to room temperature and stirred for 1 hour, after which time DCM (7 mL) was added and the mixture was extracted with aq. HCl (1 M, 10 mL). The organics were washed with brine (10 mL), concentrated *in vacuo*, adsorbed onto diatomaceous earth and purified by flash chromatography, eluting under a gradient of EtOAc (0-50%) in cyclohexane to afford the title compound **6.49** (69.2 mg, 0.163 mmol, 73 % yield) as a white solid.  $^1\text{H}$  NMR (400 MHz,  $\text{CDCl}_3$ ):  $\delta$  1.97-2.07 (m, 1H), 2.18-2.25 (m, 1H), 2.37-2.41 (m, 2H), 2.43 (s, 3H), 3.60 (ddd,  $J$  = 5.1, 6.3, 11.8 Hz, 1H), 3.70 (ddd,  $J$  = 5.1, 7.8, 12.5 Hz, 1H), 5.03 (dd,  $J$  = 5.9, 7.3 Hz, 1H), 7.07-7.11 (m, 2H), 7.33 (d,  $J$  = 8.0 Hz, 2H), 7.49-7.52 (m, 2H), 7.90-7.93 (m, 2H). LCMS (high pH):  $t_R$  = 1.26 min;  $[\text{M}+\text{H}^+]$  423, 425; (area % total: 100).

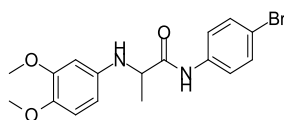
#### *N*-(4-Bromophenyl)-2-((3,4-dihydro-2*H*-benzo[*b*][1,4]dioxepin-7-yl)amino)propanamide (6.50)



A mixture of 2-bromo-*N*-(4-bromophenyl)propanamide **6.4** (40.0 mg, 0.130 mmol), 3,4-dihydro-2*H*-benzo[*b*][1,4]dioxepin-7-amine (23.7, 0.143 mmol) and triethylamine (36.0  $\mu\text{L}$ , 0.261 mmol) in DMF (0.7 mL) was heated to 80 °C under microwave irradiation for 3 hours.

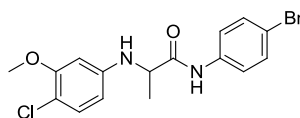
Direct purification of the reaction mixture by MDAP (high pH, Method C) afforded the title compound **6.50** (36.6 mg, 94.0  $\mu\text{mol}$ , 72 % yield) as a brown gum that was scratched to give a solid. M.pt. 130-132  $^{\circ}\text{C}$ .  $^1\text{H}$  NMR (400 MHz,  $\text{MeOD-}d_4$ ):  $\delta$  1.50 (d,  $J = 7.1$  Hz, 3H), 2.04-2.11 (m, 2H), 3.87 (q,  $J = 7.1$  Hz, 1H), 4.01 (dd,  $J = 5.1, 5.9$  Hz, 2H), 4.08 (dd,  $J = 5.1, 5.9$  Hz, 2H), 6.27 (dd,  $J = 2.6, 8.5$  Hz, 1H), 6.32 (d,  $J = 2.6$  Hz, 1H), 6.79 (d,  $J = 8.5$  Hz, 1H), 7.42-7.46 (m, 2H), 7.48-7.52 (m, 2H). *Exchangeable protons not observed*.  $^{13}\text{C}$  NMR (100 MHz,  $\text{MeOD-}d_4$ ):  $\delta$  19.3, 33.9, 56.6, 72.2, 72.3, 107.6, 109.7, 117.8, 123.1 (2C), 123.2, 132.8 (2C), 138.6, 145.3, 145.3, 153.7, 176.2.  $\nu_{\text{max}}$  (neat): 3321, 1667, 1587, 1488, 1393, 1298, 1260, 1207, 1172, 1045, 1007, 811  $\text{cm}^{-1}$ . HR-MS (ESI):  $\text{C}_{18}\text{H}_{20}\text{BrN}_2\text{O}_3$   $[\text{M}+\text{H}^+]$  requires 391.0652, found 391.0672.

#### ***N*-(4-Bromophenyl)-2-((3,4-dimethoxyphenyl)amino)propanamide (6.51)**



The title compound **6.51** (24.6 mg, 0.065 mmol, 33 % yield, straw coloured gum), was prepared according to general procedure **B** using the following reagents and solvents: 2-bromo-*N*-(4-bromophenyl)propanamide **6.4** (60.0 mg, 0.195 mmol), 3,4-dimethoxyaniline (35.9 mg, 0.235 mmol), potassium carbonate (54.0 mg, 0.391 mmol), MeCN (2 mL). The compound was purified by MDAP (high pH, Method C).  $^1\text{H}$  NMR (400 MHz,  $\text{MeOD-}d_4$ ):  $\delta$  1.52 (d,  $J = 7.1$  Hz, 3H), 3.73 (s, 3H), 3.78 (s, 3H), 3.90 (q,  $J = 7.1$  Hz, 1H), 6.16 (dd,  $J = 2.7, 8.5$  Hz, 1H), 6.42 (d,  $J = 2.7$  Hz, 1H), 6.78 (d,  $J = 8.5$  Hz, 1H), 7.42-7.45 (m, 2H), 7.48-7.51 (m, 2H). *Exchangeable protons not observed*.  $^{13}\text{C}$  NMR (100 MHz,  $\text{MeOD-}d_4$ ):  $\delta$  19.3, 56.3, 56.9, 57.6, 101.3, 105.6, 115.5, 117.8, 123.1 (2C), 132.8 (2C), 138.6, 143.4, 143.8, 151.6, 176.4.  $\nu_{\text{max}}$  (neat): 3318, 2934, 1662, 1590, 1514, 1488, 1441, 1394, 1301, 1230, 1132, 1023, 1008, 977, 823, 763, 721  $\text{cm}^{-1}$ . HR-MS (ESI):  $\text{C}_{17}\text{H}_{20}\text{BrNO}_3$   $[\text{M}+\text{H}^+]$  requires 379.0652, found 379.0654.

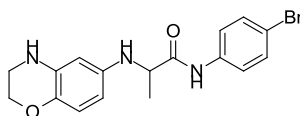
#### ***N*-(4-Bromophenyl)-2-((4-chloro-3-methoxyphenyl)amino)propanamide (6.52)**



The title compound **6.52** (29.9 mg, 0.078 mmol, 40% yield, brown glass), was prepared according to general procedure **B** using the following reagents and solvents: 2-bromo-*N*-(4-bromophenyl)propanamide **6.4** (60.0 mg, 0.195 mmol), 4-chloro-3-methoxyaniline (37.0 mg, 0.235 mmol), potassium carbonate (54.0 mg, 0.391 mmol), MeCN (2 mL). The

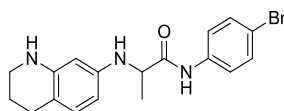
compound was purified by MDAP (high pH, Method C).  $^1\text{H}$  NMR (400 MHz,  $\text{DMSO-}d_6$ ):  $\delta$  1.40 (d,  $J = 6.7$  Hz, 3H), 3.74 (s, 3H), 4.02-4.09 (m, 1H), 6.13-6.17 (m, 2H), 6.41 (d,  $J = 2.3$  Hz, 1H), 7.06 (d,  $J = 8.5$  Hz, 1H), 7.46-7.50 (m, 2H), 7.56-7.60 (m, 2H), 10.20 (s, 1H).  $^{13}\text{C}$  NMR (100 MHz,  $\text{DMSO-}d_6$ ):  $\delta$  18.6, 53.0, 55.5, 97.9, 105.0, 108.1, 115.0, 121.2 (2C), 129.7, 131.5 (2C), 138.1, 148.1, 154.8, 173.0.  $\nu_{\text{max}}$  (neat): 3329, 2975, 1665, 1588, 1488, 1394, 1321, 1212, 1180, 1066, 1009, 816, 674  $\text{cm}^{-1}$ . HR-MS (ESI):  $\text{C}_{16}\text{H}_{17}\text{BrClN}_2\text{O}_2$  [ $\text{M}+\text{H}^+$ ] requires 383.0156, found 383.0170.

***N*-(4-Bromophenyl)-2-((3,4-dihydro-2*H*-benzo[*b*][1,4]oxazin-6-yl)amino)propanamide (6.53)**



The title compound **6.53** (46.1 mg, 0.122 mmol, 63% yield, brown glass), was prepared according to general procedure **B** using the following reagents and solvents: 2-bromo-*N*-(4-bromophenyl)propanamide **6.4** (60.0 mg, 0.195 mmol), 3,4-dihydro-2*H*-benzo[*b*][1,4]oxazin-6-amine **6.67** (35.3 mg, 0.235 mmol), potassium carbonate (54.0 mg, 0.391 mmol), MeCN (2 mL). The compound was purified by MDAP (high pH, Method C).  $^1\text{H}$  NMR (400 MHz,  $\text{DMSO-}d_6$ ):  $\delta$  1.35 (d,  $J = 7.0$  Hz, 3H), 3.17-3.20 (m, 2H), 3.78-3.85 (m, 1H), 3.96 (t,  $J = 4.3$  Hz, 2H), 5.20 (d,  $J = 7.6$  Hz, 1H), 5.54-5.55 (m, 1H), 5.79 (dd,  $J = 2.7, 8.5$  Hz, 1H), 5.86 (d,  $J = 2.7$  Hz, 1H), 6.38 (d,  $J = 8.5$  Hz, 1H), 7.45-7.49 (m, 2H), 7.58-7.62 (m, 2H), 9.95 (s, 1H).  $^{13}\text{C}$  NMR (100 MHz,  $\text{DMSO-}d_6$ ):  $\delta$  18.5, 40.3, 54.3, 64.3, 99.9, 101.9, 114.8, 116.0, 121.2 (2C), 131.4 (2C), 134.5, 134.9, 135.5, 138.3, 173.9.  $\nu_{\text{max}}$  (neat): 3311, 2870, 1669, 1620, 1588, 1505, 1394, 1324, 1281, 1209, 1089, 1071, 1007, 885, 820, 676  $\text{cm}^{-1}$ . HR-MS (ESI):  $\text{C}_{17}\text{H}_{19}\text{BrN}_3\text{O}_2$  [ $\text{M}+\text{H}^+$ ] requires 376.0655, found 376.0656.

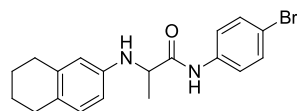
***N*-(4-Bromophenyl)-2-((1,2,3,4-tetrahydroquinolin-7-yl)amino)propanamide (6.55)**



The title compound **6.55** (59.0 mg, 0.158 mmol, 81% yield, brown glass), was prepared according to general procedure **B** using the following reagents and solvents: 2-bromo-*N*-(4-bromophenyl)propanamide **6.4** (60.0 mg, 0.195 mmol), 1,2,3,4-tetrahydroquinolin-7-amine (34.8 mg, 0.235 mmol), potassium carbonate (54.0 mg, 0.391 mmol), MeCN (2 mL). The

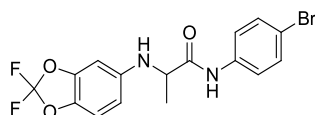
compound was purified by MDAP (high pH, Method C).  $^1\text{H}$  NMR (400 MHz,  $\text{DMSO-}d_6$ ):  $\delta$  1.35 (d,  $J = 7.0$  Hz, 3H), 1.68-1.74 (m, 2H), 2.48-2.51 (m, 2H), 3.06-3.09 (m, 2H), 3.82-3.89 (m, 1H), 5.30 (d,  $J = 7.8$  Hz, 1H), 5.34 (m, 1H), 5.70 (d,  $J = 2.3$  Hz, 1H), 5.79 (dd,  $J = 2.3, 7.9$  Hz, 1H), 6.53 (d,  $J = 7.9$  Hz, 1H), 7.45-7.49 (m, 2H), 7.58-7.61 (m, 2H), 9.94 (s, 1H).  $^{13}\text{C}$  NMR (100 MHz,  $\text{DMSO-}d_6$ ):  $\delta$  18.9, 22.2, 26.0, 40.9, 53.8, 97.9, 101.7, 109.6, 114.7, 121.2 (2C), 129.2, 131.4 (2C), 138.3, 145.6, 146.4, 173.8.  $\nu_{\text{max}}$  (neat): 3323, 2926, 2838, 1667, 1618, 1587, 1504, 1488, 1393, 1320, 1209, 1183, 1071, 1007, 819  $\text{cm}^{-1}$ . HR-MS (ESI):  $\text{C}_{18}\text{H}_{21}\text{BrN}_3\text{O}$  [ $\text{M}+\text{H}^+$ ] requires 374.0863, found 374.0887.

#### ***N*-(4-Bromophenyl)-2-((5,6,7,8-tetrahydronaphthalen-2-yl)amino)propanamide (6.56)**



The title compound **6.56** (27.5 mg, 0.074 mmol, 38 % yield, brown gum), was prepared according to general procedure **B** using the following reagents and solvents: 2-bromo-*N*-(4-bromophenyl)propanamide **6.4** (60.0 mg, 0.195 mmol), 5,6,7,8-tetrahydronaphthalen-2-amine (34.5 mg, 0.235 mmol), potassium carbonate (54.0 mg, 0.391 mmol), MeCN (2 mL). The compound was purified by MDAP (high pH, Method D).  $^1\text{H}$  NMR (400 MHz,  $\text{DMSO-}d_6$ ):  $\delta$  1.36 (d,  $J = 6.8$  Hz, 3H), 1.62-1.69 (m, 4H), 2.54-2.58 (m, 4H), 3.93-4.00 (m, 1H), 5.5d (d,  $J = 7.9$  Hz, 1H), 6.30-6.31 (m, 1H), 6.37-6.40 (m, 1H), 6.75 (d,  $J = 8.1$  Hz, 1H), 7.43-7.49 (m, 2H), 7.55-7.60 (m, 2H), 10.06 (s, 1H).  $^{13}\text{C}$  NMR (100 MHz  $\text{DMSO-}d_6$ ):  $\delta$  18.8, 22.9, 23.2, 27.9, 29.1, 53.4, 111.1, 112.7, 114.8, 121.2 (2C), 124.8, 129.2, 131.4 (2C), 136.6, 138.2, 145.3, 173.6.  $\nu_{\text{max}}$  (neat): 3304, 2928, 1675, 1601, 1539, 1505, 1485, 1449, 1392, 1296, 1246, 1171, 1071, 1007, 861, 823, 798, 700  $\text{cm}^{-1}$ . HR-MS (ESI):  $\text{C}_{19}\text{H}_{22}\text{BrN}_2\text{O}$  [ $\text{M}+\text{H}^+$ ] requires 373.0910, found 373.0913.

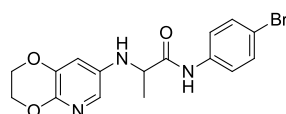
#### ***N*-(4-Bromophenyl)-2-((2,2-difluorobenzo[d][1,3]dioxol-5-yl)amino)propanamide (6.57)**



The title compound **6.57** (29.9 mg, 0.075 mmol, 38% yield, straw coloured glass), was prepared according to general procedure **B** using the following reagents and solvents: 2-bromo-*N*-(4-bromophenyl)propanamide **6.4** (60.0 mg, 0.195 mmol), 2,2-

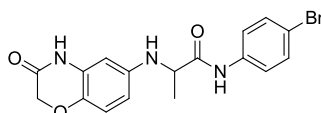
difluorobenzo[*d*][1,3]dioxol-5-amine (40.6 mg, 0.235 mmol), potassium carbonate (54.0 mg, 0.391 mmol), MeCN (2 mL). The compound was purified by MDAP (high pH, Method C). <sup>1</sup>H NMR (400 MHz, MeOD-*d*<sub>4</sub>): δ 1.53 (d, *J* = 7.0 Hz, 3H), 3.94 (q, *J* = 7.0 Hz, 1H), 6.34 (dd, *J* = 2.2, 8.5 Hz, 1H), 6.55 (d, *J* = 2.2 Hz, 1H), 6.94 (d, *J* = 8.5 Hz, 1H), 7.43-7.45 (m, 2H), 7.49-7.52 (m, 2H). *Exchangeable protons not observed.* <sup>13</sup>C NMR (100 MHz, MeOD-*d*<sub>4</sub>): δ 19.2, 56.4, 97.0, 108.1, 110.8, 117.9, 123.2 (2C), 132.8 (2C), 133.1 (t, *J* = 252 Hz), 137.3, 138.6, 145.8, 146.3, 175.7. *v*<sub>max</sub> (neat): 3259, 1669, 1589, 1489, 1395, 1228, 1184, 1143, 1071, 1033, 899, 821 790, 702 cm<sup>-1</sup>. HR-MS (ESI): C<sub>16</sub>H<sub>14</sub>BrF<sub>2</sub>N<sub>2</sub>O<sub>3</sub> [M+H<sup>+</sup>] requires 399.0150, found 399.0169.

***N*-(4-Bromophenyl)-2-((2,3-dihydro-[1,4]dioxino[2,3-*b*]pyridin-7-yl)amino)propanamide (6.58)**



The title compound **6.58** (29.0 mg, 0.077 mmol, 39 % yield, brown gum), was prepared according to general procedure **B** using the following reagents and solvents: 2-bromo-*N*-(4-bromophenyl)propanamide **6.4** (60.0 mg, 0.195 mmol), 2,3-dihydro-[1,4]dioxino[2,3-*b*]pyridin-7-amine (35.7 mg, 0.235 mmol), potassium carbonate (54.0 mg, 0.391 mmol), MeCN (2 mL). The compound was purified by MDAP (high pH, Method B). <sup>1</sup>H NMR (400 MHz, MeOD-*d*<sub>4</sub>): δ 1.51 (d, *J* = 7.1 Hz, 3H), 3.92 (q, *J* = 7.1 Hz, 1H), 4.20-4.22 (m, 2H), 4.31-4.33 (m, 2H), 6.69 (d, *J* = 2.5 Hz, 1H), 7.18 (d, *J* = 2.5 Hz, 1H), 7.43-7.46 (m, 2H), 7.49-7.53 (m, 2H). *Exchangeable protons not observed.* <sup>13</sup>C NMR (100 MHz, MeOD-*d*<sub>4</sub>): δ 19.2, 56.2, 65.6, 65.9, 112.4, 117.9, 123.1 (2C), 124.7, 132.8 (2C), 138.6, 141.3, 142.1, 145.2, 175.6. *v*<sub>max</sub> (neat): 3319, 2973, 1659, 1587, 1528, 1477, 1395, 1278, 1222, 1178, 1072, 1052, 1009, 931. 888, 817, 729 cm<sup>-1</sup>. HR-MS (ESI): C<sub>16</sub>H<sub>17</sub>BrN<sub>3</sub>O<sub>3</sub> [M+H<sup>+</sup>] requires 378.0448, found 378.0460.

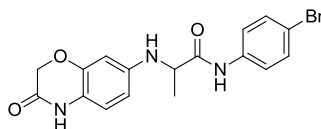
***N*-(4-Bromophenyl)-2-((3-oxo-3,4-dihydro-2*H*-benzo[*b*][1,4]oxazin-6-yl)amino)propanamide (6.59)**



A mixture of 6-amino-2*H*-benzo[*b*][1,4]oxazin-3(4*H*)-one **6.61** (40.0 mg, 0.244 mmol) and 2-bromo-*N*-phenylpropanamide **6.4** (61.1 mg, 0.268 mmol) in EtOH (2 mL) was heated to reflux for 48 hours, after which the mixture was concentrated under reduced pressure and

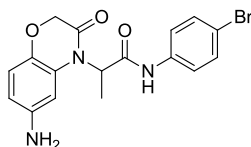
the crude material was subjected to MDAP purification (high pH) to afford the title compound **6.59** (33.0 mg, 0.085 mmol, 35% yield) as a light brown solid. The compound was purified by MDAP (high pH, Method C). M.pt. 223-234 °C.  $^1\text{H}$  NMR (400 MHz, DMSO- $d_6$ ):  $\delta$  1.38 (d,  $J$  = 6.8 Hz, 3H), 3.86-3.93 (m, 1H), 4.83 (s, 2H), 5.76 (d,  $J$  = 7.5 Hz, 1H), 6.16 (dd,  $J$  = 2.7, 8.8 Hz, 1H), 6.22 (s,  $J$  = 2.7 Hz, 1H), 6.70 (d,  $J$  = 8.8 Hz, 1H), 7.46-7.49 (m, 2H), 7.57-7.61 (m, 2H), 10.06 (br.s, 1H), 10.55 (br.s, 1H).  $^{13}\text{C}$  NMR (100 MHz, DMSO- $d_6$ ):  $\delta$  18.8, 53.8, 66.9, 100.7, 106.6, 114.8, 116.3, 121.3 (2C), 127.8, 131.4 (2C), 134.9, 138.2, 143.4, 165.5, 173.4.  $\nu_{\text{max}}$  (neat): 3270, 1693, 1680, 1632, 1589, 1524, 1491, 1392, 1334, 1273, 1214, 1162, 1049, 1011, 839, 822, 788  $\text{cm}^{-1}$ . HR-MS (ESI):  $\text{C}_{17}\text{H}_{17}\text{BrN}_3\text{O}_3$  [ $\text{M}+\text{H}^+$ ] requires 390.0448, found 390.0449.

***N*-(4-Bromophenyl)-2-((3-oxo-3,4-dihydro-2*H*-benzo[*b*][1,4]oxazin-7-yl)amino)propanamide (6.60)**



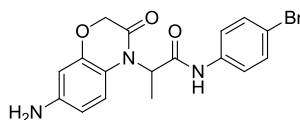
The title compound **6.60** (27.6 mg, 0.071 mmol, 29% yield, light brown solid), was prepared in the same manner as **6.59** using the following reagents and solvents: 7-amino-2*H*-benzo[*b*][1,4]oxazin-3(4*H*)-one **6.62** (40.0 mg, 0.244 mmol), 2-bromo-*N*-phenylpropanamide **6.4** (61.1 mg, 0.268 mmol), EtOH (2 mL). The compound was purified by MDAP (high pH, Method B). M.pt. 228-230 °C.  $^1\text{H}$  NMR (400 MHz, DMSO- $d_6$ ):  $\delta$  1.37 (d,  $J$  = 6.8 Hz, 3H), 3.91-3.98 (m, 1H), 4.43 (s, 2H), 5.80 (d,  $J$  = 7.9 Hz, 1H), 6.21-6.24 (m, 2H), 6.62-6.64 (m, 1H), 7.46-7.50 (m, 2H), 7.56-7.61 (m, 2H), 10.08-10.32 (br. m, 2H).  $^{13}\text{C}$  NMR (100 MHz, DMSO- $d_6$ ):  $\delta$  18.7, 53.4, 66.8, 100.8, 106.7, 114.9, 116.3, 117.4, 121.2 (2C), 131.5 (2C), 138.2, 144.1, 144.3, 163.9, 173.4.  $\nu_{\text{max}}$  (neat): 3322, 3247, 3044, 1667, 1593, 1506, 1361, 1322, 1278, 1233, 1211, 1190, 1066, 944, 881, 814, 793, 682  $\text{cm}^{-1}$ . HR-MS (ESI):  $\text{C}_{17}\text{H}_{17}\text{BrN}_3\text{O}_3$  [ $\text{M}+\text{H}^+$ ] requires 390.0448, found 390.0439.

**2-(6-amino-3-oxo-2H-benzo[*b*][1,4]oxazin-4(3H)-yl)-N-(4-bromophenyl)propanamide  
(6.63)**



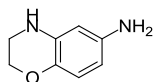
The title compound **6.63** (40.1 mg, 0.103 mmol, 53 % yield, brown glass), was prepared according to general procedure **B** using the following reagents and solvents: 2-bromo-*N*-(4-bromophenyl)propanamide **6.4** (60.0 mg, 0.195 mmol), 6-amino-2*H*-benzo[*b*][1,4]oxazin-3(4*H*)-one (38.5 mg, 0.235 mmol), potassium carbonate (54.0 mg, 0.391 mmol), MeCN (2 mL). The compound was purified by MDAP (high pH, Method B). <sup>1</sup>H NMR (400 MHz, DMSO-*d*<sub>6</sub>): δ 1.50 (d, *J* = 7.1 Hz, 3H), 4.50 (s, 2H), 4.87 (br. s, 2H), 5.25 (q, *J* = 7.1 Hz, 1H), 6.20 (dd, *J* = 2.4, 8.5 Hz, 1H), 6.35 (d, *J* = 2.4 Hz, 1H), 6.71 (d, *J* = 8.5 Hz, 1H), 7.46-7.49 (m, 2H), 7.52-7.55 (m, 2H), 9.80 (s, 1H). LCMS (high pH): *t*<sub>R</sub> = 0.96 [M+H<sup>+</sup>] 390, 392; (area % total: 100).

**2-(7-Amino-3-oxo-2H-benzo[*b*][1,4]oxazin-4(3H)-yl)-N-(4-bromophenyl)propanamide  
(6.64)**



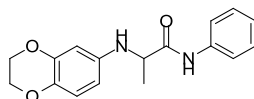
The title compound **6.64** (29.5 mg, 0.076 mmol, 39 % yield, brown glass), was prepared according to general procedure **B** using the following reagents and solvents: 2-bromo-*N*-(4-bromophenyl)propanamide **6.4** (60.0 mg, 0.195 mmol), 7-amino-2*H*-benzo[*b*][1,4]oxazin-3(4*H*)-one (38.5 mg, 0.235 mmol), potassium carbonate (54.0 mg, 0.391 mmol), MeCN (2 mL). The compound was purified by MDAP (high pH, Method C). <sup>1</sup>H NMR (400 MHz, DMSO-*d*<sub>6</sub>): δ 1.43 (d, *J* = 7.0 Hz, 3H), 4.54 (s, 2H), 5.01 (br.s, 2H), 5.34 (q, *J* = 7.0 Hz, 1H), 6.20 (dd, *J* = 2.5, 8.7 Hz, 1H), 6.25 (d, *J* = 2.5 Hz, 1H), 6.73 (d, *J* = 8.7 Hz, 1H), 7.45-7.48 (m, 2H), 5.51-7.53 (m, 2H), 9.80 (s, 1H). LCMS (high pH): *t*<sub>R</sub> = 1.00 min, [M+H<sup>+</sup>] 390, 392; (area % total: 88).

### 3,4-Dihydro-2H-benzo[*b*][1,4]oxazin-6-amine (6.67)<sup>261</sup>



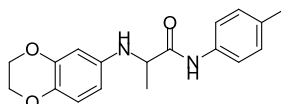
A mixture of 6-nitro-3,4-dihydro-2H-benzo[*b*][1,4]oxazine **6.65** (350 mg, 1.94 mmol) and 10% Pd/C (60.0 mg) in EtOH (10 mL) was stirred under an atmosphere of hydrogen for 18 hours. After this time, the mixture was filtered over a frit and the organics were removed under reduced pressure to afford the title compound **6.67** (291 mg, 1.94 mmol, 100% yield) as an orange gum that was used without further purification. <sup>1</sup>H NMR (400 MHz, CDCl<sub>3</sub>): δ 3.35 (br.s, 3H), 3.39-3.41 (m, 2H), 4.18-4.20 (m, 2H), 5.99 (d, *J* = 2.7 Hz, 1H), 6.04 (dd, *J* = 2.7, 8.4 Hz, 1H), 6.61 (d, *J* = 8.4 Hz, 1H). LCMS (high pH): *t*<sub>R</sub> = 0.50 min, [M+H<sup>+</sup>] 150; (area % total: 89).

### 2-((2,3-Dihydrobenzo[*b*][1,4]dioxin-6-yl)amino)-*N*-phenylpropanamide (6.69)



The title compound **6.69** (48.2 mg, 0.162 mmol, 68 % yield, straw coloured glass), was prepared according to general procedure **A** using the following reagents and solvents: aniline (44.0 μL, 0.478 mmol), DABAL-Me<sub>3</sub> (122 mg, 0.478 mmol), THF (2.5 mL), *then* ethyl 2-((2,3-dihydrobenzo[*b*][1,4]dioxin-6-yl)amino)propanoate **6.18** (60.0 mg, 0.239 mmol) in THF (0.5 mL). The compound was purified by MDAP (high pH, Method C). <sup>1</sup>H NMR (400 MHz, DMSO-*d*<sub>6</sub>): δ 1.36 (d, *J* = 6.8 Hz, 3H), 3.87-3.94 (m, 1H), 4.07-4.10 (m, 2H), 4.13-4.15 (m, 2H), 5.52 (d, *J* = 8.0 Hz, 1H), 6.12-6.17 (m, 2H), 6.59 (d, *J* = 8.4 Hz, 1H), 7.02-7.06 (m, 1H), 7.27-7.31 (m, 2H), 7.59-7.62 (m, 2H), 9.91 (s, 1H). <sup>13</sup>C NMR (100 MHz, DMSO-*d*<sub>6</sub>): δ 18.9, 53.8, 63.6, 64.2, 101.1, 106.5, 117.1, 119.1 (2C), 123.3, 128.7 (2C), 134.9, 138.9, 142.5, 143.6, 173.4. *v*<sub>max</sub> (neat): 3322 (br.), 2976, 2929, 2873, 1664, 1596, 1502, 1440, 1317, 1280, 1240, 1208, 1066, 919, 884, 830, 795, 753 cm<sup>-1</sup>. HR-MS (ESI): C<sub>17</sub>H<sub>19</sub>N<sub>2</sub>O<sub>3</sub> [M+H<sup>+</sup>] requires 299.1390, found 299.1396.

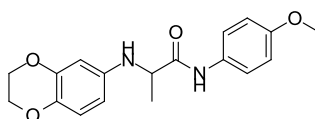
### 2-((2,3-Dihydrobenzo[*b*][1,4]dioxin-6-yl)amino)-*N*-(*p*-tolyl)propanamide (6.70)



The title compound **6.70** (58.0 mg, 0.186 mmol, 78 % yield, straw coloured solid), was prepared according to general procedure **A** using the following reagents and solvents: *p*-

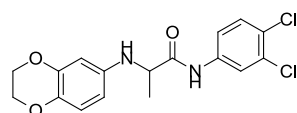
toluidine (51.2 mg, 0.478 mmol), DABAL-Me<sub>3</sub> (122 mg, 0.478 mmol), THF (2.5 mL), *then* ethyl 2-((2,3-dihydrobenzo[*b*][1,4]dioxin-6-yl)amino)propanoate **6.18** (60.0 mg, 0.239 mmol) in THF (0.5 mL). The compound was purified by MDAP (high pH, Method C). M.pt. 125-127 °C. <sup>1</sup>H NMR (400 MHz, DMSO-*d*<sub>6</sub>): δ 1.35 (d, *J* = 6.9 Hz, 3H), 2.24 (s, 3H), 3.83-3.92 (m, 1H), 4.07-4.09 (m, 2H), 4.13-4.15 (m, 2H), 5.50 (br.d, *J* = 7.6 Hz, 1H), 6.11 (d, *J* = 2.8 Hz, 1H), 6.15 (dd, *J* = 2.8, 8.5 Hz, 1H), 6.59 (d, *J* = 8.5 Hz, 1H), 7.09 (d, *J* = 8.2 Hz, 2H), 7.46-7.50 (m, 2H), 9.81 (s, 1H). <sup>13</sup>C NMR (100 MHz, DMSO-*d*<sub>6</sub>): δ 18.9, 20.4, 53.7, 60.6, 64.3, 101.1, 106.5, 117.1, 119.2 (2C), 129.0 (2C), 132.1, 134.9, 136.4, 142.5, 143.5, 173.1. *v*<sub>max</sub> (neat): 3325, 2976, 2927, 2873, 1661, 1596, 1505, 1453, 1405, 1317, 1280, 1240, 1208, 1176, 1067, 920, 885, 814, 735 cm<sup>-1</sup>. HR-MS (ESI): C<sub>18</sub>H<sub>21</sub>N<sub>2</sub>O<sub>3</sub> [M+H<sup>+</sup>] requires 313.1547, found 313.1549.

### 2-((2,3-Dihydrobenzo[*b*][1,4]dioxin-6-yl)amino)-*N*-(4-methoxyphenyl)propanamide (**6.71**)



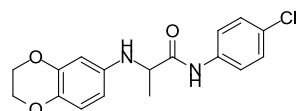
The title compound **6.71** (51.8 mg, 0.158 mmol, 66 % yield, straw coloured gum), was prepared according to general procedure **A** using the following reagents and solvents: 4-methoxyaniline (58.8 mg, 0.478 mmol), DABAL-Me<sub>3</sub> (122 mg, 0.478 mmol), THF (2.5 mL), *then* ethyl 2-((2,3-dihydrobenzo[*b*][1,4]dioxin-6-yl)amino)propanoate **6.18** (60.0 mg, 0.239 mmol) in THF (0.5 mL). The compound was purified by MDAP (high pH, Method C). <sup>1</sup>H NMR (400 MHz, DMSO-*d*<sub>6</sub>): δ 1.35 (d, *J* = 6.8 Hz, 3H), 3.71 (s, 3H), 3.82-3.89 (m, 1H), 4.07-4.10 (m, 2H), 4.13-4.15 (m, 2H), 5.48 (d, *J* = 7.7 Hz, 1H), 6.12 (d, *J* = 2.7 Hz, 1H), 6.15 (dd, *J* = 2.7, 8.6 Hz, 1H), 6.59 (d, *J* = 8.6 Hz, 1H), 6.85-6.89 (m, 2H), 7.49-7.53 (m, 2H), 9.76 (s, 1H). <sup>13</sup>C NMR (100 MHz, DMSO-*d*<sub>6</sub>): δ 18.9, 53.7, 55.1, 63.6, 64.3, 101.1, 106.5, 113.8 (2C), 117.1, 120.7 (2C), 132.0, 134.9, 142.5, 143.5, 155.2, 172.8. *v*<sub>max</sub> (neat): 3320, 2932, 1658, 1596, 1507, 1456, 1412, 1322, 1280, 1240, 1209, 1175, 1067, 1033, 919, 884, 827, 743 cm<sup>-1</sup>. HR-MS (ESI): C<sub>18</sub>H<sub>21</sub>N<sub>2</sub>O<sub>4</sub> [M+H<sup>+</sup>] requires 329.1496, found 329.1502.

***N*-(3,4-Dichlorophenyl)-2-((2,3-dihydrobenzo[*b*][1,4]dioxin-6-yl)amino)propanamide (6.72)**



The title compound **6.72** (43.6 mg, 0.119 mmol, 50 % yield, pale brown glass that was scratched to give a solid), was prepared according to general procedure **A** using the following reagents and solvents: 3,4-dichloroaniline (77.0 mg, 0.478 mmol), DABAL-Me<sub>3</sub> (122 mg, 0.478 mmol), THF (2.5 mL), *then* ethyl 2-((2,3-dihydrobenzo[*b*][1,4]dioxin-6-yl)amino)propanoate **6.18** (60.0 mg, 0.239 mmol) in THF (0.5 mL). The compound was purified by MDAP (high pH, Method C). M.pt. 128-130 °C. <sup>1</sup>H NMR (400 MHz, DMSO-*d*<sub>6</sub>): δ 1.37 (d, *J* = 6.9 Hz, 3H), 3.85-3.92 (m, 1H), 4.08-4.09 (m, 2H), 4.13-4.15 (m, 2H), 5.54 (d, *J* = 7.3 Hz, 1H), 6.10 (d, *J* = 2.3 Hz, 1H), 6.13 (dd, *J* = 2.3, 8.3 Hz, 1H), 6.60 (d, *J* = 8.3 Hz, 1H), 7.53-7.58 (m, 2H), 8.01-8.02 (m, 1H), 10.23 (s, 1H). <sup>13</sup>C NMR (100 MHz, DMSO-*d*<sub>6</sub>): δ 18.6, 54.0, 63.6, 64.3, 101.1, 106.3, 117.1, 119.3, 120.4, 124.7, 130.6, 130.9, 135.0, 138.9, 142.4, 143.5, 174.0.  $\nu_{\max}$  (neat): 3300, 2975, 2873, 1672, 1592, 1504, 1474, 1377, 1321, 1280, 1240, 1208, 1176, 1125, 1067, 1027, 922, 884, 814, 676 cm<sup>-1</sup>. HR-MS (ESI): C<sub>17</sub>H<sub>17</sub>Cl<sub>2</sub>N<sub>2</sub>O<sub>3</sub> [M+H<sup>+</sup>] requires 367.0611, found 367.0620.

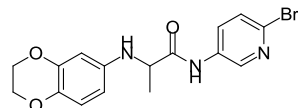
***N*-(4-chlorophenyl)-2-((2,3-dihydrobenzo[*b*][1,4]dioxin-6-yl)amino)propanamide (6.73)**



The title compound **6.73** (65.1 mg, 0.196 mmol, 82 % yield, straw coloured gum that was scratched to give a solid), was prepared according to general procedure **A** using the following reagents and solvents: 4-chloroaniline (60.9 mg, 0.478 mmol), DABAL-Me<sub>3</sub> (122 mg, 0.478 mmol), THF (2.5 mL), *then* ethyl 2-((2,3-dihydrobenzo[*b*][1,4]dioxin-6-yl)amino)propanoate **6.18** (60.0 mg, 0.239 mmol) in THF (0.5 mL). The compound was purified by MDAP (high pH, Method C). M.pt. 145-147 °C. <sup>1</sup>H NMR (400 MHz, DMSO-*d*<sub>6</sub>): δ 1.37 (d, *J* = 7.0 Hz, 3H), 3.86-3.93 (m, 1H), 4.07-4.09 (m, 2H), 4.13-4.15 (m, 2H), 5.52 (br.s, 1H), 6.11 (d, *J* = 2.7 Hz, 1H), 6.14 (dd, *J* = 2.7, 8.4 Hz, 1H), 6.60 (d, *J* = 8.4 Hz, 1H), 7.33-7.37 (m, 2H), 7.63-7.66 (m, 2H), 10.05 (s, 1H). <sup>13</sup>C NMR (100 MHz, DMSO-*d*<sub>6</sub>): δ 18.8, 53.8, 63.6, 64.3, 101.1, 106.4, 117.1, 120.8 (2C), 126.8, 128.5 (2C), 134.9, 137.8, 142.4, 143.5, 173.6.  $\nu_{\max}$  (neat): 3320, 2985, 1678, 1590, 1511, 1490, 1398, 1282, 1209, 1178, 1089, 1068, 1010,

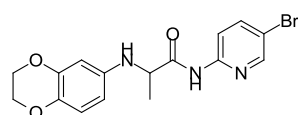
921, 883, 838, 675  $\text{cm}^{-1}$ . HR-MS (ESI):  $\text{C}_{17}\text{H}_{18}\text{ClN}_2\text{O}_3$   $[\text{M}+\text{H}^+]$  requires 333.1001, found 333.1008.

***N*-(6-Bromopyridin-3-yl)-2-((2,3-dihydrobenzo[*b*][1,4]dioxin-6-yl)amino)propanamide  
(6.74)**



The title compound **6.74** (43.2 mg, 0.114 mmol, 48 % yield, pale brown solid), was prepared according to general procedure **A** using the following reagents and solvents: 6-bromopyridin-3-amine (83.0 mg, 0.478 mmol), DABAL- $\text{Me}_3$  (122 mg, 0.478 mmol), THF (2.5 mL), *then* ethyl 2-((2,3-dihydrobenzo[*b*][1,4]dioxin-6-yl)amino)propanoate **6.18** (60.0 mg, 0.239 mmol) in THF (0.5 mL). The compound was purified by MDAP (high pH, Method C). M.pt. 175-177  $^{\circ}\text{C}$ .  $^1\text{H}$  NMR (400 MHz,  $\text{DMSO-}d_6$ ):  $\delta$  1.38 (d,  $J = 6.9$  Hz, 3H), 3.88-3.95 (m, 1H), 4.07-4.10 (m, 2H), 4.13-4.15 (m, 2H), 5.58 (d,  $J = 7.5$  Hz, 1H), 6.11 (d,  $J = 2.8$  Hz, 1H), 6.13 (dd,  $J = 2.8, 8.3$  Hz, 1H), 6.60 (d,  $J = 8.3$  Hz, 1H), 7.58 (d,  $J = 8.7$  Hz, 1H), 8.03 (dd,  $J = 2.9, 8.7$  Hz, 1H), 8.62 (d,  $J = 2.9$  Hz, 1H), 10.32 (s, 1H).  $^{13}\text{C}$  NMR (100 MHz,  $\text{DMSO-}d_6$ ):  $\delta$  18.6, 53.9, 63.6, 64.3, 101.1, 106.3, 117.2, 127.8, 129.7, 134.0, 135.0, 135.5, 141.1, 142.4, 143.6, 174.3.  $\nu_{\text{max}}$  (neat): 3361, 3322, 1677, 1600, 1572, 1508, 1491, 1465, 1368, 1319, 1211, 1068, 919, 881, 828, 801, 724  $\text{cm}^{-1}$ . HR-MS (ESI):  $\text{C}_{16}\text{H}_{17}\text{BrN}_3\text{O}_3$   $[\text{M}+\text{H}^+]$  requires 378.0448, found 378.0436.

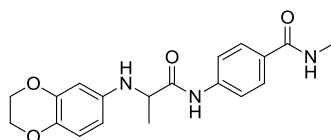
***N*-(5-Bromopyridin-2-yl)-2-((2,3-dihydrobenzo[*b*][1,4]dioxin-6-yl)amino)propanamide  
(6.75)**



The title compound **6.75** (35.5 mg, 94.0  $\mu\text{mol}$ , 39 % yield, brown gum), was prepared according to general procedure **A** using the following reagents and solvents: 5-bromopyridin-2-amine (83.0 mg, 0.478 mmol), DABAL- $\text{Me}_3$  (122 mg, 0.478 mmol), THF (2.5 mL), *then* ethyl 2-((2,3-dihydrobenzo[*b*][1,4]dioxin-6-yl)amino)propanoate **6.18** (60.0 mg, 0.239 mmol) in THF (0.5 mL). The compound was purified by MDAP (high pH, Method C).  $^1\text{H}$  NMR (400 MHz,  $\text{MeOD-}d_4$ ):  $\delta$  1.50 (d,  $J = 7.1$  Hz, 3H), 3.88 (q,  $J = 7.1$  Hz, 1H), 4.11-4.13 (m, 2H), 4.15-4.18 (m, 2H), 6.18-6.22 (m, 2H), 6.64 (d,  $J = 8.4$  Hz, 1H), 7.91 (dd,  $J = 2.5, 8.8$  Hz, 1H), 8.13 (d,  $J = 8.8$  Hz, 1H), 8.32 (d,  $J = 2.5$  Hz, 1H). *Exchangeable protons not observed.*

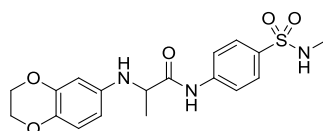
$^{13}\text{C}$  NMR (100 MHz, MeOD- $d_4$ ):  $\delta$  19.1, 57.0, 65.3, 65.9, 103.5, 108.3, 115.7, 116.4, 118.5, 138.0, 142.0, 143.2, 145.4, 149.9, 151.4, 176.5.  $\nu_{\text{max}}$  (neat): 3344, 2970, 1684, 1598, 1566, 1505, 1486, 1377, 1319, 1299, 1239, 1212, 1124, 1070, 1005, 921, 886, 803, 827, 743, 690  $\text{cm}^{-1}$ . HR-MS (ESI):  $\text{C}_{16}\text{H}_{17}\text{BrN}_3\text{O}_3$  [ $\text{M}+\text{H}^+$ ] requires 378.0448, found 378.0450.

**4-((2,3-Dihydrobenzo[*b*][1,4]dioxin-6-yl)amino)propanamido)-*N*-methylbenzamide (6.76)**



The title compound **6.76** (54.1 mg, 0.152 mmol, 64 % yield, pale yellow glass), was prepared according to general procedure **A** using the following reagents and solvents: 4-amino-*N*-methylbenzamide (71.8 mg, 0.478 mmol), DABAL- $\text{Me}_3$  (122 mg, 0.478 mmol), THF (2.5 mL), *then* ethyl 2-((2,3-dihydrobenzo[*b*][1,4]dioxin-6-yl)amino)propanoate **6.18** (60.0 mg, 0.239 mmol) in THF (0.5 mL). The compound was purified by MDAP (high pH, Method B).  $^1\text{H}$  NMR (400 MHz, DMSO- $d_6$ ):  $\delta$  1.37 (d,  $J = 6.9$  Hz, 3H), 2.76 (d,  $J = 4.4$  Hz, 3H), 3.89-3.96 (m, 1H), 4.07-4.09 (m, 2H), 4.13-4.15 (m, 2H), 5.55 (d,  $J = 8.0$  Hz, 1H), 6.11 (d,  $J = 2.5$  Hz, 1H), 6.14 (dd,  $J = 2.5, 8.4$  Hz, 1H), 6.60 (d,  $J = 8.4$  Hz, 1H), 7.66-7.68 (m, 2H), 7.77-7.80 (m, 2H), 8.29 (q,  $J = 4.4$  Hz, 1H), 10.13 (s, 1H).  $^{13}\text{C}$  NMR (100 MHz, DMSO- $d_6$ ):  $\delta$  18.8, 26.2, 53.8, 63.6, 64.3, 101.1, 106.4, 117.1, 118.4 (2C), 127.8 (2C), 129.1, 134.9, 141.2, 142.5, 143.6, 166.0, 173.8.  $\nu_{\text{max}}$  (neat): 3316, 2976, 2933, 1627, 1598, 1501, 1405, 1290, 1241, 1209, 1177, 1067, 920, 885, 848, 765  $\text{cm}^{-1}$ . HR-MS (ESI):  $\text{C}_{19}\text{H}_{22}\text{N}_3\text{O}_4$  [ $\text{M}+\text{H}^+$ ] requires 356.1605, found 356.1571.

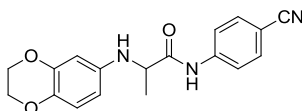
**2-((2,3-Dihydrobenzo[*b*][1,4]dioxin-6-yl)amino)-*N*-(4-(*N*-methylsulfamoyl)phenyl)propanamide (6.77)**



The title compound **6.77** (40.8 mg, 0.123 mmol, 51 % yield, brown glass), was prepared according to general procedure **A** using the following reagents and solvents: 4-amino-*N*-methylbenzenesulfonamide (89.0 mg, 0.478 mmol), DABAL- $\text{Me}_3$  (122 mg, 0.478 mmol), THF (2.5 mL), *then* ethyl 2-((2,3-dihydrobenzo[*b*][1,4]dioxin-6-yl)amino)propanoate **6.18** (60.0

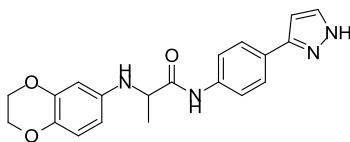
mg, 0.239 mmol) in THF (0.5 mL). The compound was purified by MDAP (high pH, Method B).  $^1\text{H}$  NMR (400 MHz,  $\text{DMSO-}d_6$ ):  $\delta$  1.38 (d,  $J = 6.9$  Hz, 3H), 2.38 (s, 3H), 3.92-3.98 (m, 1H), 4.07-4.09 (m, 2H), 4.13-4.15 (m, 2H), 5.58 (d,  $J = 8.3$  Hz, 1H), 6.11 (d,  $J = 2.3$  Hz, 1H), 6.14 (dd,  $J = 2.3, 8.4$  Hz, 1H), 6.60 (d,  $J = 8.4$  Hz, 1H), 7.35 (br.s, 1H), 7.69-7.72 (m, 2H), 7.80-7.83 (m, 2H), 10.20 (br.s, 1H).  $^{13}\text{C}$  NMR (100 MHz,  $\text{DMSO-}d_6$ ):  $\delta$  18.7, 28.6, 53.9, 63.6, 64.3, 101.2, 106.4, 117.2, 119.0 (2C), 127.8 (2C), 133.3, 134.9, 142.3, 142.4, 143.6, 174.2.  $\nu_{\text{max}}$  (neat): 3308, 1677, 1590, 1504, 1400, 1319, 1210, 1154, 1066, 920, 884, 827, 690  $\text{cm}^{-1}$ . HR-MS (ESI):  $\text{C}_{18}\text{H}_{22}\text{N}_3\text{O}_5\text{S}$  [ $\text{M}+\text{H}^+$ ] requires 392.1275, found 392.1276.

***N*-(4-Cyanophenyl)-2-((2,3-dihydrobenzo[*b*][1,4]dioxin-6-yl)amino)propanamide (6.78)**



The title compound **6.78** (55.6 mg, 0.172 mmol, 72 % yield, brown solid), was prepared according to general procedure **A** using the following reagents and solvents: 4-aminobenzonitrile (56.4 mg, 0.478 mmol), DABAL- $\text{Me}_3$  (122 mg, 0.478 mmol), THF (2.5 mL), *then* ethyl 2-((2,3-dihydrobenzo[*b*][1,4]dioxin-6-yl)amino)propanoate **6.18** (60.0 mg, 0.239 mmol) in THF (0.5 mL). The compound was purified by MDAP (high pH, Method B). M.pt. 140-141  $^\circ\text{C}$ .  $^1\text{H}$  NMR (400 MHz,  $\text{DMSO-}d_6$ ):  $\delta$  1.38 (d,  $J = 6.8$  Hz, 3H), 3.90-3.98 (m, 1H), 4.07-4.09 (m, 2H), 4.13-4.14 (m, 2H), 5.60 (d,  $J = 7.5$  Hz, 1H), 6.10 (d,  $J = 2.5$  Hz, 1H), 6.13 (dd,  $J = 2.5, 8.7$  Hz, 1H), 6.60 (d,  $J = 8.7$  Hz, 1H), 7.75-7.77 (m, 2H), 7.81-7.83 (m, 2H), 10.42 (s, 1H).  $^{13}\text{C}$  NMR (100 MHz,  $\text{DMSO-}d_6$ ):  $\delta$  18.7, 53.9, 63.6, 64.3, 101.0, 105.0, 106.4, 117.2, 119.0, 119.3 (2C), 133.2 (2C), 135.0, 142.4, 143.0, 143.6, 174.4.  $\nu_{\text{max}}$  (neat): 3308, 2977, 2873, 2224, 1686, 1597, 1507, 1407, 1314, 1281, 1241, 1208, 1174, 1067, 920, 884, 835, 701  $\text{cm}^{-1}$ . HR-MS (ESI):  $\text{C}_{18}\text{H}_{18}\text{N}_3\text{O}_3$  [ $\text{M}+\text{H}^+$ ] requires 324.1343, found 324.1346.

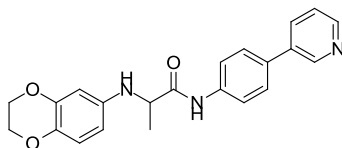
***N*-(4-(1*H*-pyrazol-3-yl)phenyl)-2-((2,3-dihydrobenzo[*b*][1,4]dioxin-6-yl)amino)propanamide (6.79)**



A vial charged with potassium trifluoro(1*H*-pyrazol-3-yl)borate (29.1 mg, 0.167 mmol), *N*-(4-bromophenyl)-2-((2,3-dihydrobenzo[*b*][1,4]dioxin-6-yl)amino)propanamide **GSK'896** (60.0 mg, 0.159 mmol), palladium(II) acetate (2.14 mg, 9.54  $\mu\text{mol}$ ), RuPhos (8.91 mg, 19.0  $\mu\text{mol}$ )

and Na<sub>2</sub>CO<sub>3</sub> (33.7 mg, 0.318 mmol) was sealed with a Teflon cap, evacuated and purged with nitrogen. EtOH (0.9 mL) was added *via* syringe and the mixture was heated to 85 °C for 12 hours. DMF (1 mL) was added and the mixture was heated to 100 °C for 5 hours. The reaction mixture was filtered and the organics were concentrated. The residue was dissolved in DMF (2 mL) and subjected to purification by MDAP (high pH, Method B) to afford the title compound **6.79** (22.5 mg, 62.3 μmol, 39 % yield) as a straw coloured glass. <sup>1</sup>H NMR (400 MHz, MeOD-*d*<sub>4</sub>): δ 1.51 (d, *J* = 7.2 Hz, 3H), 3.87 (q, *J* = 7.2 Hz, 1H), 4.12-4.14 (m, 2H), 4.16-4.19 (m, 2H), 6.22-6.24 (m, 2H), 6.63-6.66 (m, 2H), 7.60-7.73 (m, 5H). *Exchangeable protons not observed.* <sup>13</sup>C NMR (100 MHz, MeOD-*d*<sub>4</sub>): δ 19.3, 56.9, 65.4, 65.9, 103.1, 103.6, 108.4, 118.5 (2C), 121.5, 127.2 (2C), 137.9, 143.4, 145.4, 176.3. *Four <sup>13</sup>C signals not observed due to line broadening* *v*<sub>max</sub> (neat): 3297 (br.), 2974, 1664, 1597, 1505, 1453, 1410, 1316, 1279, 1241, 1209, 1176. 1066, 921, 884, 836, 768 cm<sup>-1</sup>. HR-MS (ESI): C<sub>20</sub>H<sub>21</sub>N<sub>4</sub>O<sub>3</sub> [M+H<sup>+</sup>] requires 365.1608, found 365.1610.

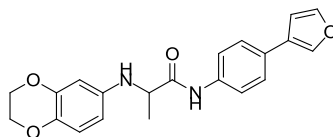
**2-((2,3-Dihydrobenzo[*b*][1,4]dioxin-6-yl)amino)-*N*-(4-(pyridin-3-yl)phenyl)propanamide (6.80)**



A mixture of the pyridin-3-ylboronic acid (29.3 mg, 0.239 mmol), *N*-(4-bromophenyl)-2-((2,3-dihydrobenzo[*b*][1,4]dioxin-6-yl)amino)propanamide **GSK'896** (60.0 mg, 0.159 mmol), Pd(PPh<sub>3</sub>)<sub>2</sub>Cl<sub>2</sub> (5.58 mg, 7.95 μmol) and potassium carbonate (65.9 mg, 0.477 mmol) was sealed in a microwave vial and placed under atmosphere of nitrogen. 1,4-Dioxane (1 mL) and water (1 mL) were added and the mixture was heated to 100 °C for 18 hours. Water (5 mL) was added and the mixture was extracted with EtOAc (10 mL x 3). The combined organics were washed with brine (20 mL) and dried over a hydrophobic frit. The organics were concentrated and the residue was dissolved in DMF (2 mL) and subjected to purification by MDAP (high pH, Method B) to afford the title compound **6.80** (37.4 mg, 0.100 mmol, 63 % yield) as a white solid. M.pt. 180-182 °C. <sup>1</sup>H NMR (400 MHz, DMSO-*d*<sub>6</sub>): δ 1.39 (d, *J* = 7.3 Hz, 3H), 3.90-3.97 (m, 1H), 4.07-4.09 (m, 2H), 4.13-4.15 (m, 2H), 5.55 (d, *J* = 8.4 Hz, 1H), 6.14 (d, *J* = 2.7 Hz, 1H), 6.16 (dd, *J* = 2.7, 8.6 Hz, 1H), 6.60 (d, *J* = 8.6 Hz, 1H), 7.46 (ddd, *J* = 0.7, 4.7, 7.9 Hz, 1H), 7.67-7.71 (m, 2H), 7.74-7.77 (m, 2H), 8.02-8.05 (m, 1H), 8.53 (dd, *J* = 1.7, 4.7 Hz, 1H), 8.87 (dd, *J* = 0.7, 2.5 Hz, 1H), 10.08 (s, 1H). <sup>13</sup>C NMR (100 MHz, DMSO-*d*<sub>6</sub>): δ 18.8, 53.8, 63.6, 64.3, 101.1, 106.5, 117.1, 119.7 (2C), 123.8, 127.1 (2C), 131.7,

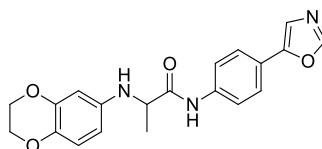
133.5, 133.9, 134.9, 139.0, 142.5, 143.6, 147.2, 148.0, 173.6.  $\nu_{\max}$  (neat): 3663, 3337, 3271, 2988, 1674, 1587, 1523, 1497, 1427, 1318, 1275, 1216, 1172, 1071, 1020, 1001, 885, 840, 800, 706  $\text{cm}^{-1}$ . HR-MS (ESI):  $\text{C}_{22}\text{H}_{22}\text{N}_3\text{O}_3$  [ $\text{M}+\text{H}^+$ ] requires 376.1656, found 376.1654.

**2-((2,3-Dihydrobenzo[*b*][1,4]dioxin-6-yl)amino)-*N*-(4-(furan-3-yl)phenyl)propanamide (6.81)**



The title compound **6.81** (38.1 mg, 0.105 mmol, 66 % yield, straw coloured gum that was scratched to give a solid), was prepared in the same manner as **6.80** using the following reagents and solvents: furan-3-ylboronic acid (21.0 mg, 0.188 mmol), *N*-(4-bromophenyl)-2-((2,3-dihydrobenzo[*b*][1,4]dioxin-6-yl)amino)propanamide **GSK'896** (60.0 mg, 0.159 mmol),  $\text{Pd}(\text{PPh}_3)_2\text{Cl}_2$  (5.58 mg, 7.95  $\mu\text{mol}$ ) and potassium carbonate (65.9 mg, 0.477 mmol), 1,4-dioxane (1 mL), water (1 mL). The reaction time was 18 hours. The compound was purified by MDAP (high pH, Method C). M.pt. 168-170  $^\circ\text{C}$ .  $^1\text{H}$  NMR (400 MHz,  $\text{DMSO}-d_6$ ):  $\delta$  1.37 (d,  $J$  = 6.4 Hz, 3H), 3.87-3.94 (m, 1H), 4.07-4.09 (m, 2H), 4.13-4.15 (m, 2H), 5.52 (d,  $J$  = 8.2 Hz, 1H), 6.13-6.18 (m, 2H), 6.60 (d,  $J$  = 8.9 Hz, 1H), 6.91 (dd,  $J$  = 0.7, 1.7 Hz, 1H), 7.53-7.56 (m, 2H), 7.62-7.64 (m, 2H), 7.71 (t,  $J$  = 1.7 Hz, 1H), 8.10-8.11 (m, 1H), 9.96 (s, 1H).  $^{13}\text{C}$  NMR (100 MHz,  $\text{DMSO}-d_6$ ):  $\delta$  18.8, 53.8, 63.6, 64.3, 101.1, 106.4, 108.6, 117.1, 119.4 (2C), 125.4, 125.8 (2C), 127.0, 134.9, 137.7, 138.7, 142.5, 143.6, 144.1, 173.3.  $\nu_{\max}$  (neat): 2864, 2478, 1668, 1631, 1591, 1512, 1450, 1409, 1323, 1282, 1226, 1160, 1067, 1050, 1013, 918, 874, 842, 787  $\text{cm}^{-1}$ . HR-MS (ESI):  $\text{C}_{21}\text{H}_{21}\text{N}_2\text{O}_4$  [ $\text{M}+\text{H}^+$ ] requires 365.1496, found 365.1493.

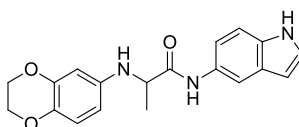
**2-((2,3-Dihydrobenzo[*b*][1,4]dioxin-6-yl)amino)-*N*-(4-(oxazol-5-yl)phenyl)propanamide (6.82)**



The title compound **6.82** (63.0 mg, 0.173 mmol, 72 % yield, brown gum), was prepared according to general procedure **A** using the following reagents and solvents: 4-(oxazol-5-yl)aniline (76.5 mg, 0.478 mmol), DABAL- $\text{Me}_3$  (122 mg, 0.478 mmol), THF (2.5 mL), then ethyl 2-((2,3-dihydrobenzo[*b*][1,4]dioxin-6-yl)amino)propanoate **6.18** (60.0 mg, 0.239 mmol) in THF (0.5 mL). The compound was purified by MDAP (high pH, Method B).  $^1\text{H}$  NMR

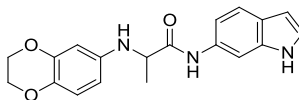
(400 MHz, DMSO- $d_6$ )  $\delta$  1.38 (d,  $J$  = 6.9 Hz, 3H), 3.88-3.95 (m, 1H), 4.07-4.09 (m, 2H), 4.13-4.15 (m, 2H), 5.54 (d,  $J$  = 7.8 Hz, 1H), 6.12 (d,  $J$  = 2.6 Hz, 1H), 6.15 (dd,  $J$  = 2.6, 8.6 Hz, 1H), 6.60 (d,  $J$  = 8.6 Hz, 1H), 7.58 (s, 1H), 7.65-7.68 (m, 2H), 7.72-7.74 (m, 2H), 8.39 (s, 1H), 10.10 (br.s, 1H).  $^{13}\text{C}$  NMR (100 MHz, DMSO- $d_6$ ):  $\delta$  18.8, 53.8, 63.6, 64.3, 101.1, 106.4, 117.1, 119.5 (2C), 121.0, 122.4, 124.7 (2C), 134.9, 139.2, 142.5, 143.6, 150.4, 151.4, 173.7.  $\nu_{\text{max}}$  (neat): 3312 (br.), 1669, 1596, 1506, 1409, 1315, 1280, 1241, 1209, 1177, 1067, 941, 919, 884, 824, 744  $\text{cm}^{-1}$ . HR-MS (ESI):  $\text{C}_{20}\text{H}_{20}\text{N}_3\text{O}_4$  [ $\text{M}+\text{H}^+$ ] requires 366.1448, found 366.1446.

### 2-((2,3-Dihydrobenzo[*b*][1,4]dioxin-6-yl)amino)-*N*-(1*H*-indol-5-yl)propanamide (6.83)



The title compound **6.83** (23.1 mg, 68.0  $\mu\text{mol}$ , 29 % yield, red solid), was prepared according to general procedure **A** using the following reagents and solvents: 1*H*-indol-5-amine (63.1 mg, 0.478 mmol), DABAL- $\text{Me}_3$  (122 mg, 0.478 mmol), THF (2.5 mL), *then* ethyl 2-((2,3-dihydrobenzo[*b*][1,4]dioxin-6-yl)amino)propanoate **6.18** (60.0 mg, 0.239 mmol) in THF (0.5 mL). The compound was purified by MDAP (high pH, Method B). M.pt. 190-192  $^\circ\text{C}$ .  $^1\text{H}$  NMR (400 MHz, DMSO- $d_6$ ):  $\delta$  1.38 (d,  $J$  = 6.9 Hz, 3H), 3.86-3.93 (m, 1H), 4.07-4.09 (m, 2H), 4.13-4.15 (m, 2H), 5.49 (d,  $J$  = 8.3 Hz, 1H), 6.15-6.19 (m, 2H), 6.36-6.37 (m, 1H), 8.60 (d,  $J$  = 8.5 Hz, 1H), 7.20 (dd,  $J$  = 1.8, 8.9 Hz, 1H), 7.29-7.31 (m, 2H), 7.85 (d,  $J$  = 1.8 Hz, 1H), 9.67 (s, 1H), 10.98 (br.s, 1H).  $^{13}\text{C}$  NMR (100 MHz DMSO- $d_6$ ):  $\delta$  19.0, 53.8, 63.7, 64.3, 101.0, 101.2, 106.5, 110.7, 111.1, 114.8, 117.1, 125.9, 127.4, 130.8, 132.7, 134.8, 142.6, 143.6, 172.6.  $\nu_{\text{max}}$  (neat): 3328, 2977, 2927, 2872, 1639, 1599, 1508, 1449, 1323, 1279, 1213, 1179, 1127, 1068, 920, 886, 800, 749  $\text{cm}^{-1}$ . HR-MS (ESI):  $\text{C}_{19}\text{H}_{20}\text{N}_3\text{O}_3$  [ $\text{M}+\text{H}^+$ ] requires 338.1499, found 338.1500.

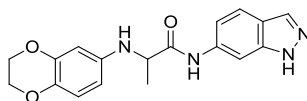
### 2-((2,3-Dihydrobenzo[*b*][1,4]dioxin-6-yl)amino)-*N*-(1*H*-indol-6-yl)propanamide (6.84)



The title compound **6.84** (31.0 mg, 92.0  $\mu\text{mol}$ , 39 % yield, dark green solid), was prepared according to general procedure **A** using the following reagents and solvents: 1*H*-indol-6-amine (63.1 mg, 0.478 mmol), DABAL- $\text{Me}_3$  (122 mg, 0.478 mmol), THF (2.5 mL), *then* ethyl 2-((2,3-dihydrobenzo[*b*][1,4]dioxin-6-yl)amino)propanoate **6.18** (60.0 mg, 0.239 mmol) in

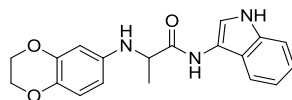
THF (0.5 mL). The compound was purified by MDAP (high pH, Method B). M.pt. 149-151 °C.  $^1\text{H}$  NMR (400 MHz,  $\text{DMSO-}d_6$ ):  $\delta$  1.38 (d,  $J$  = 6.8 Hz, 3H), 3.88-3.95 (m, 1H), 4.07-4.09 (m, 2H), 4.12-4.15 (m, 2H), 5.51 (d,  $J$  = 8.0 Hz, 1H), 6.15 (d,  $J$  = 2.5 Hz, 1H), 6.17 (dd,  $J$  = 2.5, 8.9 Hz, 1H), 6.34-6.35 (m, 1H), 6.60 (d,  $J$  = 8.9 Hz, 1H), 7.03 (dd,  $J$  = 1.8, 8.4 Hz, 1H), 7.24-7.26 (m, 1H), 7.42 (d,  $J$  = 8.4 Hz, 1H), 7.94-7.95 (m, 1H), 9.77 (s, 1H), 10.98 (br.s, 1H).  $^{13}\text{C}$  NMR (100 MHz  $\text{DMSO-}d_6$ ):  $\delta$  19.0, 53.8, 63.6, 64.5, 100.9, 101.1, 102.2, 106.5, 112.3, 117.1, 119.7, 123.9, 124.9, 132.9, 134.8, 135.8, 142.6, 143.5, 172.8.  $\nu_{\text{max}}$  (neat): 3372, 3309, 3241, 2974, 1650, 1584, 1507, 1486, 1453, 1417, 1351, 1319, 1279, 1242, 1210, 1176, 1069, 963, 887, 792, 733  $\text{cm}^{-1}$ . HR-MS (ESI):  $\text{C}_{19}\text{H}_{20}\text{N}_3\text{O}_3$  [ $\text{M}+\text{H}^+$ ] requires 338.1499, found 338.1500.

### 2-((2,3-Dihydrobenzo[*b*][1,4]dioxin-6-yl)amino)-*N*-(1*H*-indazol-6-yl)propanamide (6.85)



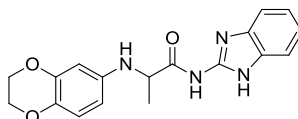
The title compound **6.85** (47.0 mg, 0.139 mmol, 58 % yield, cream solid), was prepared according to general procedure **A** using the following reagents and solvents: 1*H*-indazol-6-amine (63.6 mg, 0.478 mmol), DABAL- $\text{Me}_3$  (122 mg, 0.478 mmol), THF (2.5 mL), then ethyl 2-((2,3-dihydrobenzo[*b*][1,4]dioxin-6-yl)amino)propanoate **6.18** (60.0 mg, 0.239 mmol) in THF (0.5 mL). The compound was purified by MDAP (high pH, Method B). M.pt. 208-210 °C.  $^1\text{H}$  NMR (400 MHz,  $\text{DMSO-}d_6$ ):  $\delta$  1.37 (d,  $J$  = 6.8 Hz, 3H), 3.92-3.99 (m, 1H), 4.07-4.08 (m, 2H), 4.12-4.14 (m, 2H), 5.58 (d,  $J$  = 8.0 Hz, 1H), 6.14 (d,  $J$  = 2.5 Hz, 1H), 6.17 (dd,  $J$  = 2.5, 8.6 Hz, 1H), 6.60 (d,  $J$  = 8.6 Hz, 1H), 7.13 (d,  $J$  = 8.5 Hz, 1H), 7.65 (d,  $J$  = 8.5 Hz, 1H), 7.96 (s, 1H), 8.14 (s, 1H), 10.10 (br.s, 1H), 12.89 (br.s, 1H).  $^{13}\text{C}$  NMR (100 MHz  $\text{DMSO-}d_6$ ):  $\delta$  18.9, 53.8, 63.6, 64.3, 99.0, 101.1, 106.5, 114.1, 117.1, 119.1, 120.6, 133.2, 134.9, 137.0, 140.3, 142.5, 143.6, 173.7.  $\nu_{\text{max}}$  (neat): 3246, 3045, 1664, 1632, 1593, 1538, 1508, 1322, 1278, 1238, 1211, 1187, 1066, 944, 921, 881, 856, 834, 793  $\text{cm}^{-1}$ . HR-MS (ESI):  $\text{C}_{18}\text{H}_{19}\text{N}_4\text{O}_3$  [ $\text{M}+\text{H}^+$ ] requires 339.1452, found 339.1460.

## 2-((2,3-Dihydrobenzo[*b*][1,4]dioxin-6-yl)amino)-*N*-(1*H*-indol-3-yl)propanamide (6.86)



The title compound **6.86** (6.8 mg, 19.9  $\mu\text{mol}$ , 8 % yield, red glass), was prepared according to general procedure **A** using the following reagents and solvents: 1*H*-indol-3-amine (63.1 mg, 0.478 mmol), DABAL-Me<sub>3</sub> (122 mg, 0.478 mmol), THF (2.5 mL), *then* ethyl 2-((2,3-dihydrobenzo[*b*][1,4]dioxin-6-yl)amino)propanoate **6.18** (60.0 mg, 0.239 mmol) in THF (0.5 mL). The compound was purified by MDAP (high pH, Method B). <sup>1</sup>H NMR (400 MHz, MeOD-*d*<sub>4</sub>):  $\delta$  1.55 (d, *J* = 6.8 Hz, 3H), 3.99 (q, *J* = 6.8 Hz, 1H), 4.12-4.14 (m, 2H), 4.17-4.19 (m, 2H), 6.27-6.30 (m, 2H), 6.66-6.68 (m, 1H), 6.99-7.03 (m, 1H), 7.10-7.14 (m, 1H), 7.34 (d, *J* = 8.4 Hz, 1H), 7.42 (d, *J* = 8.4 Hz, 1H), 7.54 (s, 1H). *Exchangeable protons not observed.* <sup>13</sup>C NMR (100 MHz MeOD-*d*<sub>4</sub>):  $\delta$  19.6, 56.3, 65.4, 65.9, 103.8, 108.6, 112.4, 114.7, 118.2, 118.5, 119.9, 122.9, 122.9, 127.4, 135.8, 137.9, 143.4, 145.5, 175.8.  $\nu_{\text{max}}$  (neat): 3319, 1651, 1595, 1566, 1506, 1456, 1321, 1280, 1239, 1207, 1177, 1066, 921, 884, 795, 740 cm<sup>-1</sup>. HR-MS (ESI): C<sub>19</sub>H<sub>20</sub>N<sub>3</sub>O<sub>3</sub> [M+H<sup>+</sup>] requires 338.1499, found 338.1498.

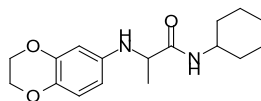
## *N*-(1*H*-benzo[*d*]imidazol-2-yl)-2-((2,3-dihydrobenzo[*b*][1,4]dioxin-6-yl)amino)propanamide (6.87)



To a suspension of 1*H*-benzo[*d*]imidazol-2-amine (159 mg, 1.19 mmol) in toluene (2 mL) was added AlMe<sub>3</sub> (2M in toluene, 0.597 mL, 1.19 mmol) dropwise. This mixture was stirred for 30 minutes at 50 °C after which time ethyl 2-((2,3-dihydrobenzo[*b*][1,4]dioxin-6-yl)amino)propanoate **6.18** (60.0 mg, 0.239 mmol) in toluene (0.5 mL) was added and the mixture was heated to 100 °C for 3 hours. After this time, water (5 mL) was added to quench the reaction, and EtOAc (5 mL) was added. The mixture was filtered, the organics were separated and the aqueous layer was washed with EtOAc (2 x 5 mL). The combined organics were dried over MgSO<sub>4</sub>, filtered and concentrated. The residue was dissolved in MeOH (2 mL) and purified by MDAP (high pH, Method B) to afford the title compound **6.87** (57.8 mg, 0.171 mmol, 72 % yield) as a brown gum. <sup>1</sup>H NMR (400 MHz, DMSO-*d*<sub>6</sub>):  $\delta$  1.41 (d, *J* = 7.0 Hz, 3H), 4.06-4.07 (m, 2H), 4.11-4.14 (m, 3H), 5.58 (d, *J* = 9.0 Hz, 1H), 6.15 (d, *J* = 2.6 Hz, 1H), 6.17 (dd, *J* = 2.6, 8.5 Hz, 1H), 6.59 (d, *J* = 8.5 Hz, 1H), 7.06-7.09 (m, 2H), 7.42-7.43

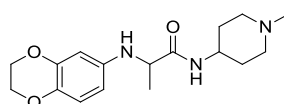
(m, 2H), 11.53 (br.s, 1H), 12.00 (br.s, 1H).  $^{13}\text{C}$  NMR (100 MHz DMSO- $d_6$ ):  $\delta$  18.5, 53.0, 63.6, 64.3, 101.1, 106.5, 111.5, 116.8, 117.2, 121.0 (2C), 132.6, 135.0, 140.4, 142.3, 143.6, 146.3, 174.8.  $\nu_{\text{max}}$  (neat): 3380, 2872, 1682, 1629, 1562, 1506, 1454, 1309, 1272, 1207, 1175, 1067, 1021, 924, 885, 795, 742  $\text{cm}^{-1}$ . HR-MS (ESI):  $\text{C}_{18}\text{H}_{19}\text{N}_4\text{O}_3$  [ $\text{M}+\text{H}^+$ ] requires 339.1452, found 339.1454.

#### ***N*-cyclohexyl-2-((2,3-dihydrobenzo[*b*][1,4]dioxin-6-yl)amino)propanamide (6.88)**



The title compound **6.88** (57.9 mg, 0.190 mmol, 80 % yield, straw coloured gum), was prepared according to general procedure **A** using the following reagents and solvents: cyclohexylamine (55.0  $\mu\text{L}$ , 0.478 mmol), DABAL- $\text{Me}_3$  (122 mg, 0.478 mmol), THF (2.5 mL), *then* ethyl 2-((2,3-dihydrobenzo[*b*][1,4]dioxin-6-yl)amino)propanoate **6.18** (60.0 mg, 0.239 mmol) in THF (0.5 mL). The compound was purified by MDAP (high pH, Method C).  $^1\text{H}$  NMR (400 MHz, MeOH):  $\delta$  1.11-1.26 (m, 3H), 1.28-1.41 (m, 5H), 1.57-1.83 (m, 5H), 3.60-3.69 (m, 2H), 4.12-4.14 (m, 2H), 4.17-4.19 (m, 2H), 6.13-6.15 (m, 2H), 6.62 (dd,  $J = 2.6, 9.4$  Hz, 1H). *Exchangeable protons not observed.*  $^{13}\text{C}$  NMR (100 MHz, MeOD- $d_4$ ):  $\delta$  19.4, 25.9, 25.9, 26.5, 33.5, 33.5, 49.4, 56.3, 65.4, 65.9, 103.6, 108.3, 118.4, 137.7, 143.4, 145.4, 176.7.  $\nu_{\text{max}}$  (neat): 3312, 2930, 2854, 1644, 1507, 1451, 1321, 1279, 1240, 1208, 1178, 1068, 921, 885, 832, 735  $\text{cm}^{-1}$ . HR-MS (ESI):  $\text{C}_{17}\text{H}_{25}\text{N}_2\text{O}_3$  [ $\text{M}+\text{H}^+$ ] requires 305.1860, found 305.1844.

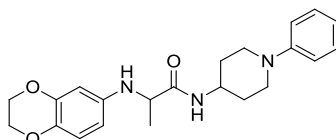
#### **2-((2,3-Dihydrobenzo[*b*][1,4]dioxin-6-yl)amino)-*N*-(1-methylpiperidin-4-yl)propanamide (6.89)**



The title compound **6.89** (61.0 mg, 0.191 mmol, 80 % yield, straw coloured gum), was prepared according to general procedure **A** using the following reagents and solvents: 4-(*tert*-butyl)cyclohexanamine (74.2 mg, 0.478 mmol), DABAL- $\text{Me}_3$  (122 mg, 0.478 mmol), THF (2.5 mL), *then* ethyl 2-((2,3-dihydrobenzo[*b*][1,4]dioxin-6-yl)amino)propanoate **6.18** (60.0 mg, 0.239 mmol) in THF (0.5 mL). The compound was purified by MDAP (high pH, Method B).  $^1\text{H}$  NMR (400 MHz, MeOD- $d_4$ ):  $\delta$  1.40 (d,  $J = 6.8$  Hz, 3H), 1.56-1.71 (m, 2H), 1.84-1.95 (m, 2H), 2.52 (s, 3H), 2.55-2.63 (m, 2H), 3.05 (t,  $J = 13.1$  Hz, 2H), 3.71 (q,  $J = 6.8$  Hz, 1H), 3.75-3.82 (m, 1H), 4.13-4.14 (m, 2H), 4.17-4.19 (m, 2H), 6.13-6.16 (m, 2H), 6.61-6.64 (m,

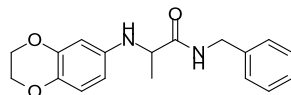
1H). *Exchangeable protons not observed.*  $^{13}\text{C}$  NMR (100 MHz, MeOD- $d_4$ ):  $\delta$  19.3, 30.9, 30.9, 44.9, 45.9, 54.6 (2C), 56.2, 65.4, 65.9, 103.5, 108.4, 118.4, 137.7, 143.4, 145.4, 177.4.  $\nu_{\text{max}}$  (neat): 3289, 2933, 2788, 1650, 1626, 1595, 1505, 1452, 1377, 1323, 1278, 1240, 1209, 1178, 1066, 919, 884, 796, 745  $\text{cm}^{-1}$ . HR-MS (ESI):  $\text{C}_{17}\text{H}_{26}\text{N}_3\text{O}_3$  [ $\text{M}+\text{H}^+$ ] requires 320.1969, found 320.1986.

**2-((2,3-Dihydrobenzo[*b*][1,4]dioxin-6-yl)amino)-*N*-(1-phenylpiperidin-4-yl)propanamide (6.90)**



The title compound **6.90** (54.3 mg, 0.142 mmol, 60 % yield, light brown solid), was prepared according to general procedure **A** using the following reagents and solvents: 1-phenylpiperidin-4-amine (84.0 mg, 0.478 mmol), DABAL- $\text{Me}_3$  (122 mg, 0.478 mmol), THF (2.5 mL), *then* ethyl 2-((2,3-dihydrobenzo[*b*][1,4]dioxin-6-yl)amino)propanoate **6.18** (60.0 mg, 0.239 mmol) in THF (0.5 mL). The compound was purified by MDAP (high pH, Method C). M.pt. 115-117  $^{\circ}\text{C}$ .  $^1\text{H}$  NMR (400 MHz, DMSO- $d_6$ , heated):  $\delta$  1.27 (d,  $J$  = 6.5 Hz, 3H), 1.32-1.42 (m, 2H), 1.94-1.99 (m, 2H), 3.11-3.17 (m, 2H), 3.49-3.56 (m, 1H), 4.06-4.13 (m, 4H), 4.17-4.19 (m, 2H), 4.32-4.39 (m, 1H), 4.75 (d,  $J$  = 8.4 Hz, 1H), 4.93 (d,  $J$  = 8.2 Hz, 1H), 6.16-6.19 (m, 2H), 6.54-6.60 (m, 2H), 6.64-6.66 (m, 2H), 7.06-7.10 (m, 2H).  $^{13}\text{C}$  NMR (100 MHz, DMSO- $d_6$ ):  $\delta$  18.0, 18.3, 31.5 (m), 32.4 (m), 43.2 (m), 48.3 (m), 48.5 (m), 63.6, 64.3, 101.3, 106.5 (m), 112.5 (2C), 115.5 (m), 117.0, 128.9 (2C), 134.6, 142.4, 143.6, 147.6, 171.6 (m).  $\nu_{\text{max}}$  (neat): 3352, 2988, 2868, 1634, 1599, 1507, 1449, 1311, 1207, 1127, 1067, 885, 824, 799, 750, 694  $\text{cm}^{-1}$ . HR-MS (ESI):  $\text{C}_{22}\text{H}_{28}\text{N}_3\text{O}_3$  [ $\text{M}+\text{H}^+$ ] requires 382.2125, found 382.2130.

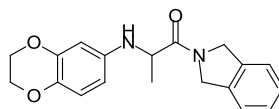
***N*-benzyl-2-((2,3-dihydrobenzo[*b*][1,4]dioxin-6-yl)amino)propanamide (6.91)**



The title compound **6.91** (49.2 mg, 0.158 mmol, 66 % yield, cream gum), was prepared according to general procedure **A** using the following reagents and solvents: benzylamine (52.0  $\mu\text{L}$ , 0.478 mmol), DABAL- $\text{Me}_3$  (122 mg, 0.478 mmol), THF (2.5 mL), *then* ethyl 2-((2,3-dihydrobenzo[*b*][1,4]dioxin-6-yl)amino)propanoate **6.18** (60.0 mg, 0.239 mmol) in THF (0.5 mL). The compound was purified by MDAP (high pH, Method B).  $^1\text{H}$  NMR (400 MHz, MeOH):  $\delta$  1.43 (d,  $J$  = 6.9 Hz, 3H), 3.77 (q,  $J$  = 6.9 Hz, 1H), 4.13-4.15 (m, 2H), 4.17-4.19 (m, 2H), 4.32

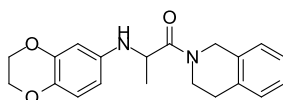
(d,  $J = 15.0$  Hz, 1H), 4.40 (d,  $J = 15.0$  Hz, 1H), 6.14-6.17 (m, 2H), 6.61-6.64 (m, 1H), 7.13-7.27 (m, 5H). *Exchangeable protons not observed.*  $^{13}\text{C}$  NMR (100 MHz, MeOD- $d_4$ ):  $\delta$  19.4, 43.7, 56.3, 65.4, 65.9, 103.6, 108.5, 118.4, 128.0, 128.3 (2C), 129.4 (2C), 137.7, 139.8, 143.4, 145.4, 177.9.  $\nu_{\text{max}}$  (neat): 3327, 3031, 2976, 2930, 2873, 1650, 1597, 1508, 1454, 1323, 1279, 1240, 1209, 1179, 1068, 915, 885, 797, 733  $\text{cm}^{-1}$ . HR-MS (ESI):  $\text{C}_{18}\text{H}_{21}\text{N}_2\text{O}_3$  [ $\text{M}+\text{H}^+$ ] requires 313.1547, found 313.1549.

### 2-((2,3-Dihydrobenzo[*b*][1,4]dioxin-6-yl)amino)-1-(isoindolin-2-yl)propan-1-one (6.92)



The title compound **6.92** (27.4 mg, 84.0  $\mu\text{mol}$ , 35 % yield, black gum), was prepared according to general procedure **A** using the following reagents and solvents: isoindoline (54.0  $\mu\text{L}$ , 0.478 mmol), DABAL- $\text{Me}_3$  (122 mg, 0.478 mmol), THF (2.5 mL), *then* ethyl 2-((2,3-dihydrobenzo[*b*][1,4]dioxin-6-yl)amino)propanoate **6.18** (60.0 mg, 0.239 mmol) in THF (0.5 mL). The compound was purified by MDAP (high pH, Method C).  $^1\text{H}$  NMR (400 MHz, DMSO- $d_6$ ):  $\delta$  1.29 (d,  $J = 6.5$  Hz, 3H), 4.07-4.11 (m, 2H), 4.13-4.15 (m, 2H), 4.20-4.27 (m, 1H), 4.66 (AB system,  $J = 17.3$  Hz, 2H), 4.91 (d,  $J = 14.7$  Hz, 1H), 5.08 (d,  $J = 14.7$  Hz, 1H), 5.37 (d,  $J = 9.2$  Hz, 1H), 6.13-6.17 (m, 2H), 6.58 (d,  $J = 8.4$  Hz, 1H), 7.30-7.38 (m, 4H).  $^{13}\text{C}$  NMR (100 MHz, DMSO- $d_6$ ):  $\delta$  17.2, 50.2, 51.4, 52.0, 63.6, 64.3, 101.2, 106.4, 117.1, 122.8, 123.0, 127.4, 127.4, 134.7, 135.9, 136.8, 142.5, 143.6, 172.2.  $\nu_{\text{max}}$  (neat): 3303, 2864, 1641, 1596, 1528, 1502, 1452, 1425, 1339, 1275, 1222, 1170, 1067, 886, 820, 765  $\text{cm}^{-1}$ . HR-MS (ESI):  $\text{C}_{19}\text{H}_{21}\text{N}_2\text{O}_3$  [ $\text{M}+\text{H}^+$ ] requires 325.1547, found 325.1558.

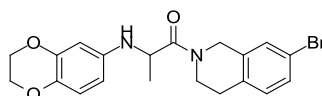
### 2-((2,3-Dihydrobenzo[*b*][1,4]dioxin-6-yl)amino)-1-(3,4-dihydroisoquinolin-2(1*H*)-yl)propan-1-one (6.93)



The title compound **6.93** (53.9 mg, 0.159 mmol, 67 % yield, brown gum), was prepared according to general procedure **A** using the following reagents and solvents: 1,2,3,4-tetrahydroisoquinoline (60.0  $\mu\text{L}$ , 0.478 mmol), DABAL- $\text{Me}_3$  (122 mg, 0.478 mmol), THF (2.5 mL), *then* ethyl 2-((2,3-dihydrobenzo[*b*][1,4]dioxin-6-yl)amino)propanoate **6.18** (60.0 mg, 0.239 mmol) in THF (0.5 mL). The compound was purified by MDAP (high pH, Method C).  $^1\text{H}$  NMR (400 MHz, DMSO- $d_6$ , heated):  $\delta$  1.28 (d,  $J = 6.7$  Hz, 3H), 2.85 (t,  $J = 6.3$  Hz, 2H), 3.72-

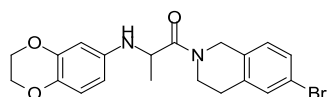
3.83 (m, 2H), 4.10-4.12 (m, 2H), 4.15-4.17 (m, 2H), 4.42 (q,  $J = 6.7$  Hz, 1H), 4.69 (s, 2H), 6.16-6.20 (m, 2H), 6.56 (d,  $J = 8.3$  Hz, 1H), 7.17-7.19 (m, 4H). *N-H* not observed.  $^{13}\text{C}$  NMR (100 MHz,  $\text{DMSO-}d_6$ ):  $\delta$  17.9 (m), 27.8-29.0 (m), 42.1-43.9 (m), 46.1, 48.7 (m), 63.6, 64.3, 101.3 (m), 106.5, 117.0 (m), 126.1-126.5 (m, 3C), 128.4 (m), 133.4 (m), 134.3 (m), 134.7, 142.4, 143.6, 172.2.  $\nu_{\text{max}}$  (neat): 3341 (br.), 2974, 2928, 1637, 1507, 1447, 1369, 1327, 1279, 1242, 1208, 1176, 1067, 973, 925, 885, 796, 747  $\text{cm}^{-1}$ . HR-MS (ESI):  $\text{C}_{20}\text{H}_{23}\text{N}_2\text{O}_3$  [ $\text{M}+\text{H}^+$ ] requires 339.1703, found 339.1720.

**1-(7-Bromo-3,4-dihydroisoquinolin-2(1H)-yl)-2-((2,3-dihydrobenzo[*b*][1,4]dioxin-6-yl)amino)propan-1-one (6.94)**



The title compound **6.94** (63.9 mg, 0.153 mmol, 64 % yield, straw coloured glass that was scratched to give a solid), was prepared according to general procedure **A** using the following reagents and solvents: 7-bromo-1,2,3,4-tetrahydroisoquinoline (101 mg, 0.478 mmol), DABAL- $\text{Me}_3$  (122 mg, 0.478 mmol), THF (2.5 mL), *then* ethyl 2-((2,3-dihydrobenzo[*b*][1,4]dioxin-6-yl)amino)propanoate **6.18** (60.0 mg, 0.239 mmol) in THF (0.5 mL). The compound was purified by MDAP (high pH, Method C). M.pt. 142-144  $^{\circ}\text{C}$ .  $^1\text{H}$  NMR (400 MHz,  $\text{DMSO-}d_6$ , heated):  $\delta$  1.27-1.28 (m, 3H), 3.20-3.23 (m, 1H), 3.74-3.77 (m, 2H), 4.09-4.11 (m, 2H), 4.14-4.16 (m, 2H), 4.37-4.44 (m, 1H), 4.65-4.78 (m, 3H), 6.15-6.19 (m, 2H), 6.55-6.57 (m, 1H), 7.11-7.13 (m, 1H), 7.32-7.39 (m, 2H). *N-H* not observed.  $^{13}\text{C}$  NMR (100 MHz,  $\text{DMSO-}d_6$ , heated):  $\delta$  18.6, 28.5, 41.6, 45.3, 50.2, 64.4, 64.9, 102.6, 107.5, 117.4, 119.4, 129.4, 129.7, 130.9, 134.6, 135.9, 136.7, 142.7, 144.4, 172.9.  $\nu_{\text{max}}$  (neat): 3375, 2976, 2928, 2871, 1637, 1592, 1508, 1447, 1326, 1278, 1241, 1206, 1177, 1122, 1067, 1048, 927, 883, 803, 742  $\text{cm}^{-1}$ . HR-MS (ESI):  $\text{C}_{20}\text{H}_{22}\text{BrN}_2\text{O}_3$  [ $\text{M}+\text{H}^+$ ] requires 417.0808, found 417.0814.

**1-(6-Bromo-3,4-dihydroisoquinolin-2(1H)-yl)-2-((2,3-dihydrobenzo[*b*][1,4]dioxin-6-yl)amino)propan-1-one (6.95)**



The title compound **6.95** (63.5 mg, 0.153 mmol, 64 % yield, straw coloured glass that was scratched to give a solid), was prepared according to general procedure **A** using the following reagents and solvents: 6-bromo-1,2,3,4-tetrahydroisoquinoline (101 mg, 0.478 mmol), DABAL-Me<sub>3</sub> (122 mg, 0.478 mmol), THF (2.5 mL), *then* ethyl 2-((2,3-dihydrobenzo[*b*][1,4]dioxin-6-yl)amino)propanoate **6.18** (60.0 mg, 0.239 mmol) in THF (0.5 mL). The compound was purified by MDAP (high pH, Method C). M.pt. 140-143 °C. <sup>1</sup>H NMR (400 MHz, DMSO-*d*<sub>6</sub>, heated): δ 1.27-1.29 (m, 3H), 2.85-2.87 (m, 1H), 3.75-3.78 (m, 2H), 4.10-4.12 (m, 2H), 4.15-4.17 (m, 2H), 4.40-4.45 (m, 1H), 4.66-4.79 (m, 3H), 6.16-6.20 (m, 2H), 6.55-6.57 (m, 1H), 7.12-7.14 (m, 1H), 7.33-7.40 (m, 2H). *N-H* not observed. <sup>13</sup>C NMR (100 MHz, DMSO-*d*<sub>6</sub>, heated): δ 18.6, 28.5, 41.6, 45.3, 50.2, 64.4, 64.9, 102.6, 107.5, 117.4, 119.4, 129.4, 129.7, 130.9, 134.6, 135.9, 136.7, 142.7, 144.4, 172.9.  $\nu_{\max}$  (neat): 3376, 2975, 1636, 1591, 1508, 1447, 1326, 1278, 1241, 1206, 1178, 1122, 1067, 1048, 927, 883, 803, 742 cm<sup>-1</sup>. HR-MS (ESI): C<sub>20</sub>H<sub>22</sub>BrN<sub>2</sub>O<sub>3</sub> [M+H<sup>+</sup>] requires 417.0808, found 417.0806.

## 11.4 Synthesis of Compounds in Chapter 7

### General Procedure C for the Synthesis of Glycosyl-1-Phosphates 7.1a-e via the Phosphoramidite Methodology<sup>159</sup> and Subsequent Deprotection

To a stirred solution of the alcohol coupling partner (0.976 mmol) and DIPEA (0.207 mL, 1.18 mmol) in DCM (14 mL) at 0 °C was added 3-((chloro-(diisopropylamino)phosphino)oxy)propanenitrile (0.238 mL, 1.07 mmol) dropwise. The mixture was warmed to room temperature and stirred for 1 hour, before being cooled to 0 °C. A solution of (3*R*,4*R*,5*R*)-3,4-bis((*tert*-butyldimethylsilyl)oxy)-5-(((*tert*-butyldimethylsilyl)oxy)methyl)-3-methyltetrahydrofuran-2-ol **7.19** (300 mg, 0.592 mmol) in DCM (10 mL) was added followed by 1*H*-tetrazole (99 mg, 1.42 mmol), and the mixture was allowed to warm to room temperature and left to stir for 4 hours. The mixture was then washed with 5% aq. NaHCO<sub>3</sub> solution (3 x 15 mL) and the aq. layer was back-extracted with DCM (30 mL). The combined organics were dried by passage through a hydrophobic frit and concentrated under reduced pressure to give a colourless oil that was dissolved in THF (30 mL). To this mixture was added H<sub>2</sub>O<sub>2</sub> (35% w/w in water, 0.233 mL, 2.66 mmol). After 30 seconds of stirring, a 5% solution of potassium hydroxide in methanol (20 mL) was added and this mixture was stirred for 30 minutes before being concentrated under reduced pressure to approximately 1/4 the volume. The resulting mixture was partitioned between DCM (250 mL) and water (250 mL). The organic phase was washed with brine and concentrated *in vacuo* to afford the crude material that was adsorbed onto diatomaceous earth and purified by reversed phase chromatography, eluting under a gradient of MeCN (0-50%) in modified water (high pH) to give the intermediate *per*-silylated ribose **7.33**. The purified material obtained directly from the column was concentrated and dissolved in THF (5 mL), to which TBAF (1.0 M in THF, 8.88 mL, 8.80 mmol) was added dropwise. This solution was stirred for 24 hours after which time it was concentrated under reduced pressure. The crude material was adsorbed onto diatomaceous earth and purified by flash chromatography, eluting under a gradient of MeOH containing 1% v/v conc. NH<sub>4</sub>OH solution (0-30%) in DCM. The appropriate fractions were combined and concentrated; the resulting material was purified again by flash chromatography under the same conditions. This material was dissolved in MeOH (1 mL) and loaded onto the head of a 25 g Biotage ISOLUTE Flash NH<sub>2</sub> (aminopropyl) solid phase extraction cartridge. The cartridge was washed with 4 column volumes of

MeOH then the pure glycosyl-1-phosphate **7.1a-e** was eluted in 4 column volumes of MeCN containing 15% v/v conc. NH<sub>4</sub>OH solution.

**General Procedure D for the Deprotection of *per*-Silylated Intermediates **7.33f-j** to Afford Polyprenyl Substituted Glycosyl-1-Phosphates **7.1f-j****

TBAF (1 M in THF, 1.82 mL, 1.82 mmol) was added dropwise to a solution of the *per*-silyl protected intermediate **7.33f-j** (0.182 mmol) in THF (6 mL). This solution was stirred for 24 hours after which time it was concentrated under reduced pressure. The crude material was adsorbed onto diatomaceous earth and purified by flash chromatography, eluting under a gradient of MeOH containing 1% v/v conc. NH<sub>4</sub>OH solution (0-20%) in DCM. The appropriate fractions were combined and concentrated; the resulting material was purified again by flash chromatography under the same conditions. This material was dissolved in MeOH (1 mL) and loaded onto the head of a 25 g Biotage ISOLUTE Flash NH<sub>2</sub> (aminopropyl) solid phase extraction cartridge. The cartridge was washed with 4 column volumes of MeOH then the pure glycosyl-1-phosphate **7.1f-j** was eluted in 4 column volumes of MeCN containing 15% v/v conc. NH<sub>4</sub>OH solution.

**General Procedure E for the Benzoyl Ester Deprotection of **7.51a-e** and **7.59****

The dibenzoyl protected compound **7.51a-e** or **7.59** (0.093 mmol) was dissolved in a mixture of MeOH-H<sub>2</sub>O-NEt<sub>3</sub> (5:2:1, 5 mL) and stirred for 72 hours at room temperature. After this time, the reaction mixture was evaporated to dryness, adsorbed onto diatomaceous earth and purified by reversed phase chromatography, eluting under a gradient of MeCN in modified water (formic acid) to give the product.

**General Procedure F for the Synthesis of *per*-Silylated Polyprenyl Intermediates **7.33f-j** via the Phosphoramidite Methodology<sup>159</sup>**

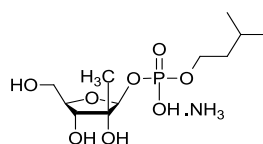
To a stirred solution of the prenyl alcohol (0.976 mmol) in DCM (14 mL) at 0 °C was added 3-((chloro(diisopropylamino)phosphino)oxy)propanenitrile (0.238 mL, 1.07 mmol) dropwise. The mixture was warmed to room temperature and stirred for 1 hour, before being cooled to 0 °C. A solution of (3*R*,4*R*,5*R*)-3,4-bis((*tert*-butyldimethylsilyl)oxy)-5-(((*tert*-butyldimethylsilyl)oxy)methyl)-3-methyltetrahydrofuran-2-ol **7.19** (300 mg, 0.592 mmol) in DCM (10 mL) was added followed by 1*H*-tetrazole (99 mg, 1.42 mmol), and the mixture was allowed to warm to room temperature and left to stir for 4 hours. The mixture was then washed with 5% aq. NaHCO<sub>3</sub> solution (3 x 15 mL) and the aq. layer was back-extracted with DCM (30 mL). The combined organics were dried by passage through a hydrophobic frit and

concentrated under reduced pressure to give a colourless oil that was dissolved in THF (30 mL). To this mixture was added H<sub>2</sub>O<sub>2</sub> (35% w/w in water, 0.233 mL, 2.66 mmol). After 30 seconds of stirring, a 5% solution of potassium hydroxide in methanol (20 mL) was added and this mixture was stirred for 30 minutes before being concentrated under reduced pressure to approximately 1/4 the volume. The resulting mixture was partitioned between DCM (250 mL) and water (250 mL). The organic phase was washed with brine and concentrated *in vacuo* to afford the crude material that was adsorbed onto diatomaceous earth and purified by flash chromatography, eluting under a gradient of MeOH containing 1% v/v conc. NH<sub>4</sub>OH solution (0-10%) in DCM affording the *per*-silylated intermediates **7.33f-j**.

### General Procedure G for the One-Pot Microwave Assisted Synthesis<sup>176</sup> of Phosphonate Monoesters **7.51a-e** and **7.59**

A mixture of the phosphonate di-acid **7.50** or **7.58** (0.219 mmol), anhydrous pyridine (0.6 mL), 2,2,2-trichloroacetonitrile (0.6 mL) and the appropriate alcohol (0.329 mmol) was sealed in a microwave vial with a Teflon septum and subjected to microwave irradiation at 90 °C for 25 minutes (or until consumption of the phosphonate di-acid was observed by LCMS), after which time the mixture was evaporated to dryness. The crude material was adsorbed onto diatomaceous earth and purified by reversed phase chromatography, eluting under a gradient of MeCN in modified water (formic acid) to give the product.

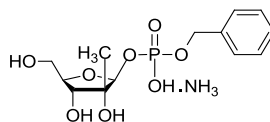
### (2*S*,3*R*,4*R*,5*R*)-3,4-dihydroxy-5-(hydroxymethyl)-3-methyltetrahydrofuran-2-yl isopentyl hydrogen phosphate, ammonia salt (**7.1a**)



The title compound **7.1a** (36.0 mg, 0.115 mmol, 19% yield, transparent glass), was prepared according to general procedure **C** using the following reagents and solvents: 3-methylbutan-1-ol (0.106 mL, 0.976 mmol), DIPEA (0.207 mL, 1.18 mmol), DCM (14 mL), 3-((chloro(diisopropylamino)phosphino)oxy)propanenitrile (0.238 mL, 1.07 mmol), *then* lactol **7.19** (300 mg, 0.592 mmol) in DCM (10 mL), 1*H*-tetrazole (99.0 mg, 1.42 mmol), *then* THF (30 mL), H<sub>2</sub>O<sub>2</sub> (0.233 mL, 2.66 mmol), 5% methanolic potassium hydroxide solution (20 mL), *then* THF (3 mL), TBAF (1.0 M in THF, 4.57 mL, 4.57 mmol). The intermediate **7.33a** was

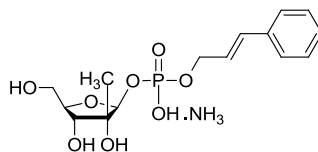
purified by normal phase chromatography, eluting under a gradient of MeOH containing 1% v/v conc. NH<sub>4</sub>OH solution (5-15%) in DCM.  $[\alpha_D]_{589}^{21.9^\circ C}$  [c 1, MeOH]: +52. <sup>1</sup>H NMR (400 MHz, MeOD-*d*<sub>4</sub>): δ 0.94 (d, *J* = 6.9 Hz, 6H), 1.33 (s, 3H), 1.53 (q, *J* = 6.8 Hz, 2H), 1.71-1.84 (m, 1H), 3.59-3.63 (m, 1H), 3.82-3.85 (m, 1H), 3.90-3.97 (m, 4H), 5.29 (d, *J* = 4.9 Hz, 1H). *Exchangeable protons not observed.* <sup>13</sup>C NMR (100 MHz, MeOD-*d*<sub>4</sub>): δ 19.7, 22.9 (2C), 25.8, 40.6 (d, *J* = 8 Hz), 63.4, 65.2 (d, *J* = 6 Hz), 74.8, 80.1 (d, *J* = 10 Hz), 85.2, 105.3 (d, *J* = 7 Hz). <sup>31</sup>P NMR (162 MHz, MeOD-*d*<sub>4</sub>): δ -1.2.  $\nu_{\max}$  (neat): 3213 (br.), 2925, 1658, 1457, 1260, 1192, 1061, 1030, 970, 872, 750 cm<sup>-1</sup>. HR-MS (ESI): C<sub>11</sub>H<sub>24</sub>O<sub>8</sub>P [M+H<sup>+</sup>] requires 315.1209, found 315.1205.

**Benzyl ((3*R*,4*R*,5*R*)-3,4-dihydroxy-5-(hydroxymethyl)-3-methyltetrahydrofuran-2-yl) hydrogen phosphate, ammonia salt (7.1b)**



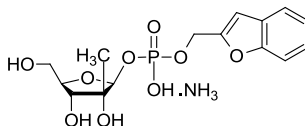
The title compound **7.1b** (51.0 mg, 0.145 mmol, 24% yield, opaque white gum), was prepared according to general procedure **C** using the following reagents and solvents: phenylmethanol (0.101 mL, 0.976 mmol), DIPEA (0.207 mL, 1.184 mmol), DCM (14 mL), 3-((chloro(diisopropylamino)phosphino)oxy)propanenitrile (0.238 mL, 1.07 mmol), *then* lactol **7.19** (300 mg, 0.592 mmol) in DCM (10 mL), 1*H*-tetrazole (99.0 mg, 1.42 mmol), *then* THF (30 mL), H<sub>2</sub>O<sub>2</sub> (0.233 mL, 2.66 mmol), 5% methanolic potassium hydroxide solution (20 mL), *then* THF (6 mL), TBAF (1.0 M in THF, 8.88 mL, 8.88 mmol).  $[\alpha_D]_{589}^{21.3^\circ C}$  [c 1, MeOH]: +9. <sup>1</sup>H NMR (400 MHz, MeOD-*d*<sub>4</sub>): δ 1.27 (s, 3H), 3.58-3.60 (m, 1H), 3.80-3.85 (m, 1H), 3.91-3.94 (m, 2H), 4.90-4.96 (m, 2H), 5.34 (d, *J* = 4.9 Hz, 1H), 7.25-7.29 (m, 1H), 7.32-7.36 (m, 2H), 7.41-7.43 (m, 2H). *Exchangeable protons not observed.* <sup>13</sup>C NMR (100 MHz, MeOD-*d*<sub>4</sub>): δ 19.7, 63.7, 68.5 (d, *J* = 5 Hz), 72.0, 80.2 (d, *J* = 10 Hz), 85.5, 105.6 (d, *J* = 6 Hz), 128.5 (2C), 128.7, 129.4 (2C), 139.8 (d, *J* = 8 Hz). <sup>31</sup>P NMR (162 MHz, MeOD-*d*<sub>4</sub>): δ -1.4.  $\nu_{\max}$  (neat): 3207 (br.), 1454, 1198, 1064, 1024, 972, 867, 732, 695 cm<sup>-1</sup>. HR-MS (ESI): C<sub>13</sub>H<sub>20</sub>O<sub>8</sub>P [M+H<sup>+</sup>] requires 335.0896, found 335.0890.

**Cinnamyl ((2S,3R,4R,5R)-3,4-dihydroxy-5-(hydroxymethyl)-3-methyltetrahydrofuran-2-yl) hydrogen phosphate, ammonia salt (7.1c)**



The title compound **7.1c** (73.1 mg, 0.193 mmol, 33 % yield, straw coloured glass), was prepared according to general procedure **C** using the following reagents and solvents: (*E*)-3-phenylprop-2-en-1-ol (0.125 mL, 0.976 mmol), DIPEA (0.207 mL, 1.184 mmol), DCM (14 mL), 3-((chloro(diisopropylamino)phosphino)oxy)propanenitrile (0.238 mL, 1.07 mmol), then lactol **7.19** (300 mg, 0.592 mmol) in DCM (10 mL), 1*H*-tetrazole (99.0 mg, 1.42 mmol), then THF (30 mL), H<sub>2</sub>O<sub>2</sub> (0.233 mL, 2.66 mmol), 5% methanolic potassium hydroxide solution (20 mL), then THF (6 mL), TBAF (1.0 M in THF, 3.1 mL, 3.1 mmol).  $[\alpha_D]_{589}^{21.9^\circ C}$  [c 1, MeOH]: -23. <sup>1</sup>H NMR (400 MHz, MeOD-*d*<sub>4</sub>): δ 1.34 (s, 3H), 3.60-3.67 (m, 1H), 3.83-3.88 (m, 1H), 3.94-3.98 (m, 2H), 4.56-4.59 (m, 2H), 5.35 (d, *J* = 4.9 Hz, 1H), 6.38 (dt, *J* = 5.7, 15.9 Hz, 1H), 6.69 (d, *J* = 15.9 Hz, 1H), 7.21-7.25 (m, 1H), 7.29-7.33 (m, 2H), 7.41-7.44 (m, 2H). *Exchangeable protons not observed.* <sup>1</sup>H NMR (600 MHz, D<sub>2</sub>O): 1.30 (s, 3H), 3.64 (dd, *J* = 5.6, 12.5 Hz, 1H), 3.80 (dd, *J* = 3.0, 12.5 Hz, 1H), 3.91 (d, *J* = 8.3 Hz, 1H), 3.97 (ddd, *J* = 3.0, 5.6, 8.3 Hz, 1H), 4.55-4.57 (m, 2H), 5.29 (d, *J* = 6.1 Hz, 1H), 6.41 (dt, *J* = 6.0, 15.9 Hz, 1H), 6.73 (d, *J* = 15.9 Hz, 1H), 7.31-7.33 (m, 1H), 7.38-7.41 (m, 2H), 7.50-7.52 (m, 2H). *Exchangeable protons not observed.* <sup>13</sup>C NMR (100 MHz, MeOD-*d*<sub>4</sub>): δ 19.7, 63.6, 67.3 (d, *J* = 6 Hz), 74.9, 80.1 (d, *J* = 10 Hz), 85.3, 105.4 (d, *J* = 7 Hz), 127.1 (d, *J* = 8 Hz), 127.5 (2C), 128.6, 129.5 (2C), 132.8, 138.2. <sup>31</sup>P NMR (162 MHz, MeOD-*d*<sub>4</sub>): δ -1.1. *v*<sub>max</sub> (neat): 3205 (br.), 1662, 1448, 1375, 1196, 1085, 1064, 1021, 961, 872, 731, 688 cm<sup>-1</sup>. HR-MS (ESI): C<sub>15</sub>H<sub>22</sub>O<sub>8</sub>P [M+H<sup>+</sup>] requires 361.1047, found 361.1041.

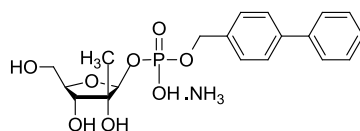
**Benzofuran-2-ylmethyl ((2S,3R,4R,5R)-3,4-dihydroxy-5-(hydroxymethyl)-3-methyltetrahydrofuran-2-yl) hydrogen phosphate, ammonia salt (7.1d)**



The title compound **7.1d** (58.6 mg, 0.148 mmol, 25 % yield, transparent glass), was prepared according to general procedure **C** using the following reagents and solvents: benzofuran-2-ylmethanol (145 mg, 0.976 mmol), DIPEA (0.207 mL, 1.184 mmol), DCM (14

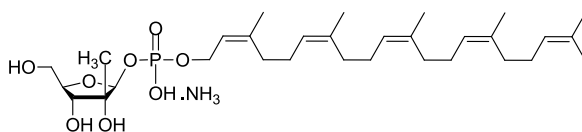
mL), 3-((chloro(diisopropylamino)phosphino)oxy)propanenitrile (0.238 mL, 1.07 mmol), then lactol **7.19** (300 mg, 0.592 mmol) in DCM (10 mL), 1*H*-tetrazole (99.0 mg, 1.42 mmol), then THF (30 mL), H<sub>2</sub>O<sub>2</sub> (0.233 mL, 2.66 mmol), 5% methanolic potassium hydroxide solution (20 mL), then THF (6 mL), TBAF (1.0 M in THF, 5.90 mL, 5.90 mmol).  $[\alpha_D]_{589}^{21.9^\circ C}$  [c 1, MeOH]: -52. <sup>1</sup>H NMR (400 MHz, MeOD-*d*<sub>4</sub>): δ 1.30 (s, 3H), 3.63 (dd, *J* = 4.3, 13.0 Hz, 1H), 3.82-3.86 (m, 1H), 3.93-3.98 (m, 2H), 5.03 (d, *J* = 7.0 Hz, 2H), 5.36 (d, *J* = 5.1 Hz, 1H), 6.83 (s, 1H), 7.21 (td, *J* = 1.0, 7.3 Hz, 1H), 7.26-7.30 (m, 1H), 7.44-7.48 (m, 1H), 7.56-7.59 (m, 1H). *Exchangeable protons not observed.* <sup>13</sup>C NMR (100 MHz, MeOD-*d*<sub>4</sub>): δ 19.6, 61.2 (d, *J* = 6 Hz), 63.6, 74.9, 80.0 (d, *J* = 10 Hz), 85.3, 105.5 (d, *J* = 6 Hz), 106.3, 112.0, 122.2, 123.8, 125.4, 129.6, 155.7 (d, *J* = 9 Hz), 156.6. <sup>31</sup>P NMR (162 MHz, MeOD-*d*<sub>4</sub>): δ -1.6.  $\nu_{\max}$  (neat): 3204 (br.), 1660, 1453, 1204, 1090, 1066, 1025, 927, 866, 737 cm<sup>-1</sup>. HR-MS (ESI): C<sub>15</sub>H<sub>20</sub>O<sub>9</sub>P [M+H<sup>+</sup>] requires 375.0840, found 375.0843.

**[1,1'-Biphenyl]-4-ylmethyl((2*S*,3*R*,4*R*,5*R*)-3,4-dihydroxy-5-(hydroxymethyl)-3-methyltetrahydrofuran-2-yl) hydrogen phosphate, ammonia salt (**7.1e**)**



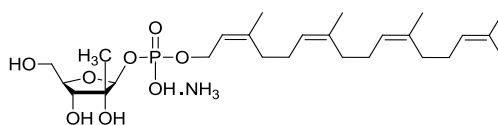
The title compound **7.1e** (109 mg, 0.256 mmol, 43 % yield, white foam), was prepared according to general procedure **C** using the following reagents and solvents: [1,1'-biphenyl]-4-ylmethanol (180 mg, 0.976 mmol), DIPEA (0.207 mL, 1.184 mmol), DCM (14 mL), 3-((chloro(diisopropylamino)phosphino)oxy)propanenitrile (0.238 mL, 1.07 mmol), then lactol **7.19** (300 mg, 0.592 mmol) in DCM (10 mL), 1*H*-tetrazole (99.0 mg, 1.42 mmol), then THF (30 mL), H<sub>2</sub>O<sub>2</sub> (0.233 mL, 2.66 mmol), 5% methanolic potassium hydroxide solution (20 mL), then THF (6 mL), TBAF (1.0 M in THF, 5.92 mL, 5.92 mmol).  $[\alpha_D]_{589}^{21.9^\circ C}$  [c 1, MeOH]: -11. <sup>1</sup>H NMR (400 MHz, MeOD-*d*<sub>4</sub>): δ 1.30 (s, 3H), 3.60-3.64 (m, 1H), 3.82-3.85 (m, 1H), 3.93-3.98 (m, 2H), 5.00 (d, *J* = 6.5 Hz, 2H), 5.36 (d, *J* = 4.9 Hz, 1H), 7.31-7.36 (m, 1H), 7.42-7.46 (m, 2H), 7.50-7.52 (m, 2H), 7.60-7.64 (m, 4H). *Exchangeable protons not observed.* <sup>13</sup>C NMR (100 MHz, MeOD-*d*<sub>4</sub>): δ 19.6, 63.6, 68.1 (d, *J* = 6 Hz), 74.9, 80.1 (d, *J* = 10 Hz), 85.3, 105.4 (d, *J* = 7 Hz), 127.9 (2C), 127.9 (2C), 128.3, 128.9 (2C), 129.8 (2C), 138.9 (d, *J* = 8 Hz), 141.8, 142.3. <sup>31</sup>P NMR (162 MHz, MeOD-*d*<sub>4</sub>): δ -1.3.  $\nu_{\max}$  (neat): 3201 (br.), 1648, 1451, 1198, 1090, 1064, 1031, 972, 874, 819, 757, 694 cm<sup>-1</sup>. HR-MS (ESI): C<sub>19</sub>H<sub>24</sub>O<sub>8</sub>P [M+H<sup>+</sup>] requires 411.1203, found 411.1208.

**(2S,3R,4R,5R)-3,4-Dihydroxy-5-(hydroxymethyl)-3-methyltetrahydrofuran-2-yl  
((2Z,6Z,10Z,14Z)-3,7,11,15,19-pentamethylcosa-2,6,10,14,18-pentaen-1-yl) hydrogen  
phosphate, ammonia salt (7.1f)**



The title compound **7.1f** (56.3 mg, 0.094 mmol, 57% yield, white gum), was prepared according to general procedure **D** using the following reagents and solvents: *per*-silylated intermediate **7.33f** (155 mg, 0.164 mmol), THF (7 mL), TBAF (1 M in THF, 1.64 mL, 1.64 mmol).  $[\alpha_D]_{589}^{20.1^\circ C}$  [c 0.1, MeOH]: -8.  $^1\text{H}$  NMR (400 MHz, MeOD- $d_4$ ):  $\delta$  1.33 (s, 3H), 1.63 (s, 3H), 1.70 (s, 12H), 1.75 (d,  $J = 1\text{H}$ , 3H), 2.03-2.15 (m, 16H), 3.61 (dd,  $J = 4.5, 12.5$  Hz, 1H), 3.83 (dd,  $J = 2.5, 12.5$  Hz, 1H), 3.94 (ddd,  $J = 2.5, 4.5, 7.8$  Hz, 1H), 3.97 (d,  $J = 7.8$  Hz, 1H), 4.42 (t,  $J = 7.0$  Hz, 2H), 5.12-5.19 (m, 4H), 5.30 (d,  $J = 4.8$  Hz, 1H), 5.42 (dt,  $J = 1.0, 7.0$  Hz, 1H). *Exchangeable protons not observed.*  $^{13}\text{C}$  NMR (100 MHz, MeOD- $d_4$ ):  $\delta$  17.8, 19.7, 23.7-23.8 (m, 4C), 26.0, 27.5-27.6 (m, 3C), 27.7, 32.9, 33.2, 33.3, 33.3, 63.3 (d,  $J = 6$  Hz), 63.4, 74.8, 80.1 (d,  $J = 10$  Hz), 85.3, 105.3 (d,  $J = 7$  Hz), 123.4 (d,  $J = 8$  Hz), 125.4, 125.8, 126.1, 126.1, 132.3, 136.3, 136.3, 136.6, 140.6.  $^{31}\text{P}$  NMR (162 MHz, MeOD- $d_4$ ):  $\delta$  -1.0.  $\nu_{\text{max}}$  (neat): 3214, 2927, 1447, 1376, 1204, 1092, 1025, 966, 862  $\text{cm}^{-1}$ . (ESI):  $\text{C}_{31}\text{H}_{54}\text{O}_8\text{P}$  [ $\text{M}+\text{H}^+$ ] requires 585.3551, found 585.3536.

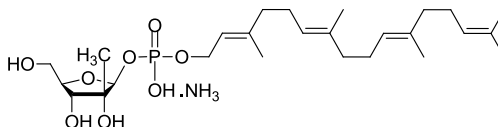
**(2S,3R,4R,5R)-3,4-Dihydroxy-5-(hydroxymethyl)-3-methyltetrahydrofuran-2-yl  
((2Z,6Z,10Z)-3,7,11,15-tetramethylhexadeca-2,6,10,14-tetraen-1-yl) hydrogen phosphate,  
ammonia salt (7.1g)**



The title compound **7.1g** (58.5 mg, 0.110 mmol, 60% yield, white gum), was prepared according to general procedure **D** using the following reagents and solvents: *per*-silylated intermediate **7.33g** (156 mg, 0.182 mmol), THF (6 mL), TBAF (1 M in THF, 1.82 mL, 1.82 mmol).  $[\alpha_D]_{589}^{21.2^\circ C}$  [c 1, MeOH]: -93.  $^1\text{H}$  NMR (400 MHz, MeOD- $d_4$ ):  $\delta$  1.34 (s, 3H), 1.63 (s, 3H), 1.70 (s, 9H), 1.76 (d,  $J = 1.0$  Hz, 3H), 2.03-2.15 (m, 12H), 3.61 (dd,  $J = 4.1, 12.4$  Hz, 1H), 3.84 (dd,  $J = 2.2, 12.4$  Hz, 1H), 3.92-3.98 (m, 2H), 4.42 (t,  $J = 6.8$  Hz, 2H), 5.12-5.18 (m, 3H), 5.30 (d,  $J = 4.8$  Hz, 1H), 5.42 (dt,  $J = 1.0, 6.8$  Hz, 1H). *Exchangeable protons not observed.*  $^{13}\text{C}$

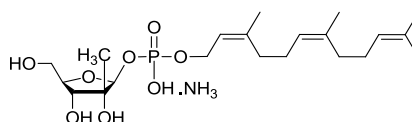
NMR (100 MHz, MeOD-*d*<sub>4</sub>):  $\delta$  17.8, 19.7, 23.7, 23.7, 23.8, 26.0, 27.5, 27.6, 27.7, 32.9, 33.2, 33.3, 63.3 (d, *J* = 6 Hz), 63.4, 74.8, 80.1 (d, *J* = 10 Hz), 85.2, 105.3 (d, *J* = 6 Hz), 123.3 (d, *J* = 8 Hz), 125.4, 125.7, 126.1, 132.4, 136.3, 136.6, 140.6. <sup>31</sup>P NMR (162 MHz, MeOD-*d*<sub>4</sub>):  $\delta$  -1.1.  $\nu_{\max}$  (neat): 3209, 2926, 2854, 1448, 1377, 1198, 1091, 1026, 973, 877, 736 cm<sup>-1</sup>. HR-MS (ESI): C<sub>26</sub>H<sub>46</sub>O<sub>8</sub>P [M+H<sup>+</sup>] requires 517.2925, found 517.2923.

**(2*S*,3*R*,4*R*,5*R*)-3,4-Dihydroxy-5-(hydroxymethyl)-3-methyltetrahydrofuran-2-yl ((2*E*,6*E*,10*E*)-3,7,11,15-tetramethylhexadeca-2,6,10,14-tetraen-1-yl) hydrogen phosphate, ammonia salt (7.1h)**



The title compound **7.1h** (69.6 mg, 0.130 mmol, 47 % yield, opaque gum), was prepared according to general procedure **D** using the following reagents and solvents: *per*-silylated intermediate **7.33h** (241 mg, 0.275 mmol), THF (5 mL), TBAF (1 M in THF, 2.75 mL, 2.75 mmol).  $[\alpha_D]_{589}^{19.3^\circ C}$  [c 1, MeOH]: -167. <sup>1</sup>H NMR (400 MHz, MeOD-*d*<sub>4</sub>):  $\delta$  1.34 (s, 3H), 1.62-1.64 (m, 9H), 1.69 (d, *J* = 1.0 Hz, 3H), 1.71 (s, 3H), 1.97-2.19 (m, 12H), 3.61 (dd, *J* = 4.2, 12.5 Hz, 1H), 3.83 (dd, *J* = 1.7, 12.5 Hz, 1H), 3.92-3.98 (m, 2H), 4.44 (t, *J* = 6.8 Hz, 2H), 5.09-5.17 (m, 3H), 5.30 (d, *J* = 4.7 Hz, 1H), 5.42 (dt, *J* = 1.0, 6.8 Hz, 1H). *Exchangeable protons not observed*. <sup>13</sup>C NMR (100 MHz, MeOD-*d*<sub>4</sub>):  $\delta$  16.1 (2C), 16.1, 16.6, 17.8, 19.7, 25.9, 27.5, 27.6, 27.8, 40.7, 40.8, 40.9, 63.4, 63.5 (d, *J* = 6 Hz), 74.8, 80.1 (d, *J* = 10 Hz), 85.3, 105.3 (d, *J* = 6 Hz), 122.3 (d, *J* = 8 Hz), 125.2, 125.5, 132.0, 135.9, 136.2, 140.8. <sup>31</sup>P NMR (162 MHz, MeOH):  $\delta$  -1.1.  $\nu_{\max}$  (neat): 3193 (br.), 2926, 1447, 1377, 1203, 1092, 1024, 972, 864, 736 cm<sup>-1</sup>. HR-MS (ESI): C<sub>26</sub>H<sub>46</sub>O<sub>8</sub>P [M+H<sup>+</sup>] requires 517.2925, found 517.2935.

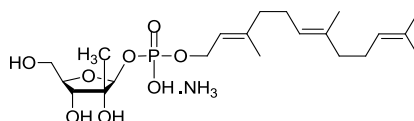
**(2*S*,3*R*,4*R*,5*R*)-3,4-Dihydroxy-5-(hydroxymethyl)-3-methyltetrahydrofuran-2-yl ((2*Z*,6*Z*)-3,7,11-trimethyldodeca-2,6,10-trien-1-yl) hydrogen phosphate, ammonia salt (7.1i)**



The title compound **7.1i** (42.6 mg, 0.092 mmol, 60 % yield, white gum), was prepared according to general procedure **D** using the following reagents and solvents: *per*-silylated intermediate **7.33i** (124 mg, 0.153 mmol), THF (6 mL), TBAF (1 M in THF, 1.53 mL, 1.53 mmol).  $[\alpha_D]_{589}^{19.3^\circ C}$  [c 1, MeOH]: -86. <sup>1</sup>H NMR (400 MHz, MeOD-*d*<sub>4</sub>):  $\delta$  1.34 (s, 3H), 1.63 (s,

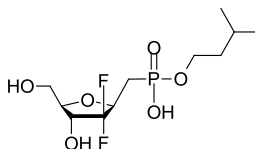
3H), 1.70 (s, 6H), 1.76 (d,  $J = 1.0$  Hz, 3H), 2.04-2.15 (m, 8H), 3.61 (dd,  $J = 3.9, 12.9$  Hz, 1H), 3.82-3.85 (m, 1H), 3.94-3.97 (m, 2H), 4.42 (t,  $J = 6.8$  Hz, 2H), 5.13-5.16 (m, 2H), 5.30 (d,  $J = 4.5$  Hz, 1H), 4.52 (td,  $J = 1.0, 6.8$  Hz, 1H). *Exchangeable protons not observed.*  $^{13}\text{C}$  NMR (100 MHz, MeOD- $d_4$ ):  $\delta$  17.8, 19.7, 23.7, 23.7, 25.9, 27.5, 27.7, 32.9, 33.3, 63.3 (d,  $J = 6$  Hz), 63.5, 74.8, 80.1 (d,  $J = 9$  Hz), 85.3, 105.3 (d,  $J = 7$  Hz), 123.4 (d,  $J = 8$  Hz), 125.3, 125.7, 132.4, 136.6, 140.6.  $^{31}\text{P}$  NMR (162 MHz, MeOD- $d_4$ ):  $\delta$  -1.1.  $\nu_{\text{max}}$  (neat): 3353 (br.), 2930, 1715, 1378, 1067, 977  $\text{cm}^{-1}$ . HR-MS (ESI):  $\text{C}_{21}\text{H}_{38}\text{O}_8\text{P}$  [ $\text{M}+\text{H}^+$ ] requires 449.2299, found 449.2303.

**(2S,3R,4R,5R)-3,4-Dihydroxy-5-(hydroxymethyl)-3-methyltetrahydrofuran-2-yl ((2E,6E)-3,7,11-trimethyldodeca-2,6,10-trien-1-yl) hydrogen phosphate, ammonia salt (7.1j)**



The title compound **7.1j** (64.5 mg, 0.144 mmol, 59 % yield, transparent glass), was prepared according to general procedure **D** using the following reagents and solvents: *per*-silylated intermediate **7.33j** (193 mg, 0.244 mmol), THF (1 mL), TBAF (1 M in THF, 2.44 mL, 2.44 mmol).  $[\alpha_D]_{589}^{21.9^\circ\text{C}}$  [c 1, MeOH]: -120.  $^1\text{H}$  NMR (400 MHz, MeOD- $d_4$ ):  $\delta$  1.34 (s, 3H), 1.62 (s, 6H), 1.69 (d,  $J = 1.0$  Hz, 3H), 1.71 (s, 3H), 1.98-2.17 (m, 8H), 3.61 (dd,  $J = 4.3, 12.2$  Hz, 1H), 3.83 (dd,  $J = 2.4, 12.2$  Hz, 1H), 3.94 (ddd,  $J = 2.4, 4.3, 8.1$  Hz, 1H), 3.97 (d,  $J = 8.1$  Hz, 1H), 4.45 (t,  $J = 6.8$  Hz, 2H), 5.09-5.17 (m, 2H), 5.31 (d,  $J = 4.9$  Hz, 1H), 5.42 (td,  $J = 1.0, 6.8$  Hz, 1H). *Exchangeable protons not observed.*  $^{13}\text{C}$  NMR (125 MHz, MeOD- $d_4$ ):  $\delta$  14.7, 15.1, 16.3, 18.3, 24.5, 26.0, 26.4, 39.2, 39.4, 62.0, 62.1 (d,  $J = 6$  Hz), 73.4, 78.7 (d,  $J = 10$  Hz), 83.7, 103.9 (d,  $J = 7$  Hz), 121.0 (d,  $J = 9$  Hz), 123.8, 124.0, 130.7, 134.8, 139.3.  $^{31}\text{P}$  NMR (162 MHz, MeOD- $d_4$ ):  $\delta$  -1.0.  $\nu_{\text{max}}$  (neat): 3222 (br.), 2925, 1452, 1379, 1200, 1092, 1025, 974, 882, 736  $\text{cm}^{-1}$ . HR-MS (ESI):  $\text{C}_{21}\text{H}_{38}\text{O}_8\text{P}$  [ $\text{M}+\text{H}^+$ ] requires 449.2299, found 449.2289.

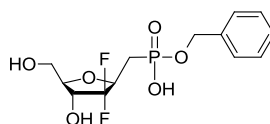
**Isopentyl hydrogen (((2R,4R,5R)-3,3-difluoro-4-hydroxy-5-(hydroxymethyl)tetrahydrofuran-2-yl)methyl)phosphonate (7.2a)**



The title compound **7.2a** (32.4 mg, 0.102 mmol, 72 % yield, transparent colourless glass), was prepared according to general procedure **E** using the following reagents: ((2R,3R,5R)-3-

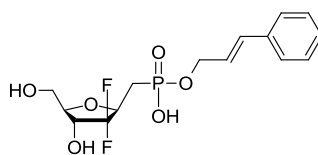
(benzoyloxy)-4,4-difluoro-5-((hydroxy(isopentyloxy)phosphoryl)methyl)tetrahydrofuran-2-yl)methyl benzoate **7.51a** (74.0 mg, 0.141 mmol). The compound was purified by reversed phase chromatography: 0-20% MeCN in modified water (formic).  $[\alpha_D]_{589}^{20.3^\circ C}$  [c 1, MeOH]: +105.  $^1\text{H}$  NMR (600 MHz, MeOD- $d_4$ ):  $\delta$  0.96 (d,  $J$  = 6.6 Hz, 6H), 1.56 (dt,  $J$  = 6.0, 6.2 Hz, 2H), 1.75-1.82 (m, 1H), 2.01-2.14 (m, 2H), 3.63-3.67 (m, 1H), 3.75-3.80 (m, 2H), 3.97-4.02 (m, 1H), 4.05-4.09 (m, 2H), 4.16-4.24 (m, 1H). *Exchangeable protons not observed.*  $^{13}\text{C}$  NMR (125 MHz, MeOD- $d_4$ ):  $\delta$  22.9 (2C), 25.9, 26.7 (d,  $J$  = 142 Hz), 40.6, 62.4, 65.2, 73.3 (dd,  $J$  = 18, 32 Hz), 77.0 (t,  $J$  = 25 Hz), 85.1 (d,  $J$  = 4 Hz), 125.8 (td,  $J$  = 11, 257 Hz).  $^{19}\text{F}$  NMR (376 MHz, MeOD- $d_4$ ):  $\delta$  -121.9 (d,  $J$  = 238 Hz, 1F), -118.3 (d,  $J$  = 238 Hz, 1F).  $^{31}\text{P}$  NMR (162 MHz, MeOD- $d_4$ ):  $\delta$  24.4.  $\nu_{\text{max}}$  (neat): 3315 (br.), 2958, 1461, 1202, 1051, 1005  $\text{cm}^{-1}$ . HR-MS (ESI):  $\text{C}_{11}\text{H}_{22}\text{F}_2\text{O}_6\text{P}$  [ $\text{M}+\text{H}^+$ ] requires 319.1117, found 319.1114.

**Benzyl hydrogen (((2R,4R,5R)-3,3-difluoro-4-hydroxy-5-(hydroxymethyl)tetrahydrofuran-2-yl)methyl)phosphonate (7.2b)**



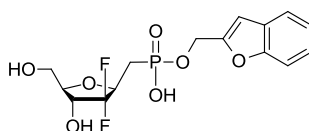
The title compound **7.2b** (23.0 mg, 68.0  $\mu\text{mol}$ , 73 % yield, transparent colourless glass), was prepared according to general procedure **E** using the following reagents: ((2R,3R,5R)-3-(benzoyloxy)-5-(((benzyloxy)(hydroxy)phosphoryl)methyl)-4,4-difluorotetrahydrofuran-2-yl)methyl benzoate **7.51b** (51.0 mg, 93.0  $\mu\text{mol}$ ). The compound was purified by reversed phase chromatography: 0-20% MeCN in modified water (formic).  $[\alpha_D]_{589}^{21.6^\circ C}$  [c 1, MeOD- $d_4$ ): -30.  $^1\text{H}$  NMR (600 MHz, MeOD- $d_4$ ):  $\delta$  2.03-2.18 (m, 2H), 3.64 (dd,  $J$  = 6.0, 12.8 Hz, 1H), 3.73-3.79 (m, 2H), 4.00 (dt,  $J$  = 4.4, 15.9 Hz, 1H), 4.15-4.27 (m, 1H), 5.08 (d,  $J$  = 7.3 Hz, 2H), 7.31-7.49 (m, 5H). *Exchangeable protons not observed.*  $^{13}\text{C}$  NMR (125 MHz, MeOD- $d_4$ ):  $\delta$  27.0 (d,  $J$  = 141 Hz), 62.2, 68.0, 73.1 (dd,  $J$  = 19, 40 Hz), 77.0 (t,  $J$  = 28 Hz), 84.9 (d,  $J$  = 4 Hz), 125.7 (td,  $J$  = 12, 256 Hz), 128.7 (2C), 129.0, 129.5 (2C), 138.7 (d,  $J$  = 6 Hz).  $^{19}\text{F}$  NMR (376 MHz, MeOD- $d_4$ ):  $\delta$  -121.8 (d,  $J$  = 236 Hz, 1F), -118.3 (d,  $J$  = 236 Hz, 1F).  $^{31}\text{P}$  NMR (162 MHz, MeOD- $d_4$ ):  $\delta$  24.7.  $\nu_{\text{max}}$  (neat): 3306 (br.), 2925, 1455, 1204, 1011, 862, 736, 696  $\text{cm}^{-1}$ . HR-MS (ESI):  $\text{C}_{13}\text{H}_{18}\text{F}_2\text{O}_6\text{P}$  [ $\text{M}+\text{H}^+$ ] requires 339.0804, found 339.0800.

**Cinnamyl hydrogen (((2*R*,4*R*,5*R*)-3,3-difluoro-4-hydroxy-5-(hydroxymethyl)tetrahydrofuran-2-yl)methyl)phosphonate (7.2c)**



The title compound **7.2c** (19.5 mg, 54.0  $\mu\text{mol}$ , 37 % yield, transparent colourless glass), was prepared according to general procedure **E** using the following reagents: (2*R*,3*R*,5*R*)-3-(benzoyloxy)-5-(((cinnamyloxy)(hydroxy)phosphoryl)methyl)-4,4-difluorotetrahydrofuran-2-yl)methyl benzoate **7.51c** (83.0 mg, 0.145 mmol). The compound was purified by reversed phase chromatography: 0-20% MeCN in modified water (formic).  $[\alpha_D]_{589}^{20.3^\circ\text{C}}$  [c 1, MeOH]: +35.  $^1\text{H}$  NMR (600 MHz, MeOD- $d_4$ ):  $\delta$  2.03-2.17 (m, 2H), 3.63-3.67 (m, 1H), 3.77-3.81 (m, 2H), 3.97-4.03 (m, 1H), 4.21-4.28 (m, 1H), 4.67-4.71 (m, 2H), 6.39 (dt,  $J = 5.3, 15.7$  Hz, 1H), 6.72 (d,  $J = 15.7$  Hz, 1H), 7.52 (t,  $J = 7.3$  Hz, 1H), 7.32 (t,  $J = 7.3$  Hz, 2H), 7.44 (d,  $J = 7.3$  Hz, 2H). *Exchangeable protons not observed.*  $^{13}\text{C}$  NMR (125 MHz, MeOD- $d_4$ ):  $\delta$  27.1 (d,  $J = 141$  Hz), 62.3, 66.9, 73.1 (dd,  $J = 18, 32$  Hz), 77.0 (t,  $J = 29$  Hz), 84.9 (d,  $J = 4$  Hz), 124.0-127.7 (m), 126.1, 127.6 (2C), 128.9, 129.6 (2C), 133.9, 137.9.  $^{19}\text{F}$  NMR (376 MHz, MeOD- $d_4$ ):  $\delta$  -121.7 (d,  $J = 237$  Hz, 1F), -118.3 (d,  $J = 237$  Hz, 1F).  $^{31}\text{P}$  NMR (162 MHz, MeOD- $d_4$ ):  $\delta$  24.2.  $\nu_{\text{max}}$  (neat): 3307 (br.), 2926, 1695, 1451, 1202, 1012, 740, 692  $\text{cm}^{-1}$ . HR-MS (ESI):  $\text{C}_{15}\text{H}_{20}\text{F}_2\text{O}_6\text{P}$  [M+H $^+$ ] requires 365.0960, found 365.0964.

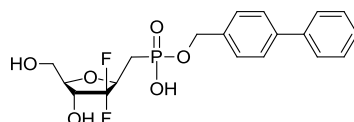
**Benzofuran-2-ylmethyl hydrogen (((2*R*,4*R*,5*R*)-3,3-difluoro-4-hydroxy-5-(hydroxymethyl)tetrahydrofuran-2-yl)methyl)phosphonate (7.2d)**



The title compound **7.2d** (21.3 mg, 56.0  $\mu\text{mol}$ , 59 % yield, transparent colourless glass), was prepared according to general procedure **E** using the following reagents: (2*R*,3*R*,5*R*)-5-(((benzofuran-2-ylmethoxy)(hydroxy)phosphoryl)methyl)-2-((benzoyloxy)methyl)-4,4-difluorotetrahydrofuran-3-yl benzoate **7.51d** (56 mg, 95.0  $\mu\text{mol}$ ). The compound was purified by reversed phase chromatography: 0-20% MeCN in modified water (formic).  $[\alpha_D]_{589}^{20.3^\circ\text{C}}$  [c 1, MeOH]: -50.  $^1\text{H}$  NMR (600 MHz, MeOD- $d_4$ ):  $\delta$  2.07-2.18 (m, 2H), 3.61-3.66 (m, 1H), 3.75-3.81 (m, 2H), 3.95-4.01 (m, 1H), 4.22-4.29 (m, 1H), 5.16 (br.s, 2H), 6.87 (s, 1H), 7.23 (t,  $J = 7.3$  Hz, 1H), 7.30 (t,  $J = 7.3$  Hz, 1H), 7.47 (d,  $J = 7.30$  Hz, 1H), 7.58 (d,  $J = 7.30$  Hz, 1H). *Exchangeable protons not observed.*  $^{13}\text{C}$  NMR (125 MHz, MeOD- $d_4$ ):  $\delta$  27.1 (d,  $J = 144$

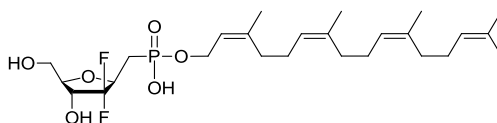
Hz), 60.7, 62.3, 73.1 (dd,  $J = 18, 30$  Hz), 76.8-77.3 (m), 84.9, 107.2, 112.1, 122.4, 124.0, 124.2-127.4 (m), 125.8, 129.4, 154.8, 156.7.  $^{19}\text{F}$  NMR (376 MHz, MeOD- $d_4$ ):  $\delta$  -121.8 (d,  $J = 236$  Hz, 1F), -118.3 (d,  $J = 236$  Hz, 1F).  $^{31}\text{P}$  NMR (162 MHz, MeOD- $d_4$ ):  $\delta$  23.9.  $\nu_{\text{max}}$  (neat): 3300 (br.), 2932, 1453, 1262, 1200, 1068, 1009, 943, 878, 814, 733, 702  $\text{cm}^{-1}$ . HR-MS (ESI):  $\text{C}_{15}\text{H}_{18}\text{F}_2\text{O}_7\text{P}$  [ $\text{M}+\text{H}^+$ ] requires 379.0753, found 379.0757.

**[1,1'-Biphenyl]-4-ylmethyl hydrogen (((2*R*,4*R*,5*R*)-3,3-difluoro-4-hydroxy-5-(hydroxymethyl)tetrahydrofuran-2-yl)methyl)phosphonate (7.2e)**



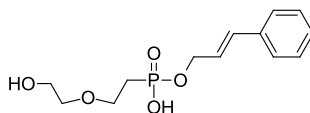
The title compound **7.2e** (15.0 mg, 36.0  $\mu\text{mol}$ , 58 % yield, transparent colourless glass), was prepared according to general procedure **E** using the following reagents: (2*R*,3*R*,5*R*)-5-(((1,1'-biphenyl)-4-ylmethoxy)(hydroxy)phosphoryl)methyl)-2-((benzoyloxy)methyl)-4,4-difluorotetrahydrofuran-3-yl benzoate **7.51e** (39.0 mg, 63.0  $\mu\text{mol}$ ). The compound was purified by reversed phase chromatography: 0-20% MeCN in modified water (formic).  $[\alpha_D]_{589}^{20.3^\circ\text{C}}$  [ $c$  0.5, MeOH]: +107.  $^1\text{H}$  NMR (600 MHz, MeOD- $d_4$ ):  $\delta$  2.05-2.16 (m, 2H), 3.63-3.66 (m, 1H), 3.75-3.79 (m, 2H), 3.97-4.04 (m, 1H), 4.22-4.26 (m, 1H), 5.10 (d,  $J = 7.3$  Hz, 2H), 7.34 (t,  $J = 7.3$  Hz, 1H), 7.44 (t,  $J = 7.3$  Hz, 2H), 7.51 (d,  $J = 7.3$  Hz, 2H), 7.62-7.64 (m, 4H). *Exchangeable protons not observed.*  $^{13}\text{C}$  NMR (125 MHz, MeOD- $d_4$ ):  $\delta$  27.1 (d,  $J = 140$  Hz), 62.2, 67.7 (d,  $J = 6$  Hz), 73.1 (dd,  $J = 19, 32$  Hz), 77.0 (t,  $J = 27$  Hz), 84.9 (d,  $J = 4$  Hz), 125.7-129.8(m), 128.0 (2C), 128.0 (2C), 128.4, 129.2 (2C), 129.8 (2C), 137.8 (d,  $J = 7$  Hz), 142.1, 142.3.  $^{19}\text{F}$  NMR (376 MHz, MeOD- $d_4$ ):  $\delta$  -121.7 (d,  $J = 238$  Hz, 1F), -118.3 (d,  $J = 238$  Hz, 1F).  $^{31}\text{P}$  NMR (162 MHz, MeOD- $d_4$ ):  $\delta$  24.0.  $\nu_{\text{max}}$  (neat): 3299 (br.), 2925, 1653, 1487, 1409, 1201, 1003, 865, 757, 735, 696  $\text{cm}^{-1}$ . HR-MS (ESI):  $\text{C}_{19}\text{H}_{22}\text{F}_2\text{O}_6\text{P}$  [ $\text{M}+\text{H}^+$ ] requires 415.1117, found 415.1116.

**(2Z,6Z,10Z)-3,7,11,15-Tetramethylhexadeca-2,6,10,14-tetraen-1-yl hydrogen (((2R,4R,5R)-3,3-difluoro-4-hydroxy-5-(hydroxymethyl)tetrahydrofuran-2-yl)methyl)phosphonate (7.2f)**



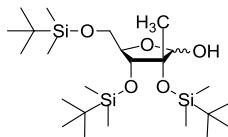
A mixture of (((2R,4R,5R)-4-(benzoyloxy)-5-((benzoyloxy)methyl)-3,3-difluorotetrahydrofuran-2-yl)methyl)phosphonic acid **7.50** (60.0 mg, 0.131 mmol), anhydrous pyridine (0.3 mL), 2,2,2-trichloroacetonitrile (0.3 mL) and (2Z,6Z,10Z)-3,7,11,15-tetramethylhexadeca-2,6,10,14-tetraen-1-ol (49.7 mg, 0.171 mmol) was sealed in a microwave vial with a Teflon septum and subjected to microwave irradiation at 90 °C for 40 minutes, after which time the mixture was evaporated to dryness, adsorbed onto diatomaceous earth and purified by flash chromatography, eluting under a gradient of MeOH containing 1% v/v conc. NH<sub>4</sub>OH solution (0-40%) in DCM to afford the intermediate **7.51f** (38 mg). Intermediate **7.51f** (38 mg, 52.0 μmol) was dissolved in a mixture of MeOH-H<sub>2</sub>O-NEt<sub>3</sub> (5:2:1, 5 mL) and stirred for 3 days at room temperature. After this time the mixture was evaporated to dryness, adsorbed onto diatomaceous earth and purified by flash chromatography, eluting under a gradient of MeOH containing 1% v/v NH<sub>4</sub>OH solution (0-45%) in DCM to afford the title compound **7.2f** (19.7 mg, 38.0 μmol, 29 % yield over two steps) as an opaque gum.  $[\alpha_D]_{589}^{18.6^\circ C}$  [c 0.2, MeOH]: -19. <sup>1</sup>H NMR (600 MHz, MeOD-*d*<sub>4</sub>): δ 1.63 (s, 3H), 1.70 (s, 9H), 1.76 (s, 3H), 1.82-1.94 (m, 2H), 2.04-2.16 (m, 12H), 3.61 (dd, *J* = 5.6, 12.2 Hz, 1H), 3.72-3.74 (m, 1H), 3.79 (dd, *J* = 2.9, 12.2 Hz, 1H), 3.93-3.98 (m, 1H), 4.17-4.25 (m, 1H), 4.43 (t, *J* = 6.9 Hz, 2H), 5.13-5.16 (m, 3H), 5.42 (t, *J* = 6.9 Hz, 1H). *Exchangeable protons not observed.* <sup>13</sup>C NMR (125 MHz, MeOD-*d*<sub>4</sub>): δ 17.9, 23.8, 23.9, 23.9, 26.1, 27.7, 27.7, 27.9, 27.9 (dd, *J* = 4, 137 Hz), 33.0, 33.4, 33.5, 62.1 (d, *J* = 6 Hz), 62.5, 73.3 (dd, *J* = 18, 31 Hz), 78.1 (ddd, *J* = 5, 26, 31 Hz), 84.5 (d, *J* = 5 Hz), 123.9 (d, *J* = 7 Hz), 125.5, 125.9, 126.2 (td, *J* = 13, 256 Hz), 126.3, 132.5, 136.5, 136.7, 140.7. <sup>19</sup>F NMR (376 MHz, MeOD-*d*<sub>4</sub>): δ -121.1 (d, *J* = 235 Hz, 1F), -118.4 (d, *J* = 235 Hz, 1F). <sup>31</sup>P NMR (162 MHz, MeOD-*d*<sub>4</sub>): δ 20.1.  $\nu_{\max}$  (neat): 3196 (br.), 2917, 1448, 1376, 1195, 1163, 1066, 1004, 805 cm<sup>-1</sup>. HR-MS (ESI): C<sub>26</sub>H<sub>34</sub>F<sub>2</sub>O<sub>6</sub>P [M+H<sup>+</sup>] requires 521.2838, found 521.2835.

### Cinnamyl hydrogen (2-(2-hydroxyethoxy)ethyl)phosphonate (7.3a)



The title compound **7.3a** (40.0 mg, 0.140 mmol, 50 % yield, transparent colourless glass), was prepared according to general procedure **E** using the following reagents: (*E*)-2-(2-((cinnamyloxy)(hydroxy)phosphoryl)ethoxy)ethyl benzoate **7.59** (109 mg, 0.279 mmol). The compound was purified by reversed phase chromatography: 0-30% MeCN in modified water (formic). <sup>1</sup>H NMR (400 MHz, MeOD-*d*<sub>4</sub>): δ 2.08-2.23 (m, 2H), 3.53-3.59 (m, 2H), 3.65-3.84 (m, 4H), 4.66-4.72 (m, 2H), 6.38 (dt, *J* = 5.2, 15.9 Hz, 1H), 6.73 (d, *J* = 15.9 Hz, 1H), 7.23-7.28 (m, 1H), 7.31-7.35 (m, 2H), 7.43-7.46 (m, 2H). *Exchangeable protons not observed.* <sup>13</sup>C NMR (100 MHz, MeOD-*d*<sub>4</sub>): δ 29.0 (m), 62.1, 66.4, 66.8, 73.2, 125.7 (d, *J* = 4.0 Hz), 127.6 (2C), 129.0, 129.6 (2C), 134.2, 137.8. <sup>31</sup>P NMR (162 MHz, MeOD-*d*<sub>4</sub>): δ 27.7. *v*<sub>max</sub> (neat): 3333 (br.), 2874, 1717, 1450, 1360, 1178, 1112, 1068, 993, 961, 874, 811, 734, 691 cm<sup>-1</sup>. HR-MS (ESI): C<sub>13</sub>H<sub>20</sub>O<sub>5</sub>P [M+H<sup>+</sup>] requires 287.1043, found 287.1044.

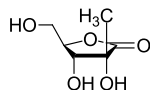
### (3*R*,4*R*,5*R*)-3,4-Bis((*tert*-butyldimethylsilyl)oxy)-5-(((*tert*-butyldimethylsilyl)oxy)methyl)-3-methyltetrahydrofuran-2-ol (7.19)



To a solution of (3*R*,4*R*,5*R*)-3,4-bis((*tert*-butyldimethylsilyl)oxy)-5-(((*tert*-butyldimethylsilyl)oxy)methyl)-3-methyldihydrofuran-2(3*H*)-one **7.24** (3.50 g, 6.93 mmol) in anhydrous toluene (100 mL) at -78 °C was added diisobutylaluminum hydride (25% in toluene, 14.0 mL, 20.8 mmol) dropwise. This mixture was stirred at the same temperature for 12 hours after which time MeOH (20 mL) was added dropwise. This mixture was allowed to warm to room temperature and then EtOAc/cyclohexane 50:50 (100 mL) was added and this mixture was stirred for 2 hours, after which the solution was filtered through Celite. The solvent was evaporated under reduced pressure to give the crude material which was adsorbed onto diatomaceous earth and purified by flash chromatography, eluting under a gradient of TBME (0-5%) in cyclohexane, affording the title compound **7.19** (2.27 g, 4.48 mmol, 65 % yield) as a transparent viscous oil. <sup>1</sup>H NMR (400 MHz, CDCl<sub>3</sub>): δ 0.09-0.16 (18H), 0.90-0.94 (27H), 1.32 - 1.34 (m, 3H), 2.91 (d, *J* = 7.3 Hz,

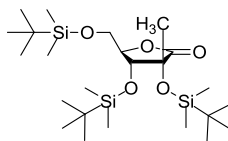
0.7H), 3.63-3.69 (m, 1H), 3.72 (d,  $J = 12.8$  Hz, 0.3H), 3.81-3.86 (m, 1H), 3.91 (dt,  $J = 2.2, 7.8$  Hz, 0.3H), 3.96-4.00 (m, 1H), 4.11 (d,  $J = 7.3$  Hz, 0.7H), 4.83-4.87 (m, 1H). LCMS (high pH): desired mass not detected. HR-MS (ESI):  $C_{24}H_{55}O_5Si_3$   $[M+H^+]$  requires 507.3357, desired mass not detected.

**(3R,4R,5R)-3,4-Dihydroxy-5-(hydroxymethyl)-3-methyldihydrofuran-2(3H)-one (7.23)**<sup>165,166</sup>



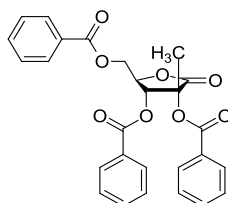
D-glucose (20.0 g, 111 mmol) was suspended in EtOH (30 mL) and glacial acetic acid (6.36 mL, 111 mmol), to which dimethylamine (5.6 M in EtOH, 21.8 mL, 122 mmol) was added dropwise at room temperature. The mixture was stirred at 80 °C for 1.5 hours, after which time additional dimethylamine (5.6 M in EtOH, 5 mL, 28.0 mmol) was added and the mixture was stirred for a further 2 hours. The solution was concentrated under reduced pressure to give a viscous dark oil which was dissolved in water (50 mL). Calcium oxide (12.5 g, 222 mmol) was added and the aqueous solution was stirred at 70 °C for 24 hours. Oxalic acid dihydrate (42.0 g, 333 mmol) was added to the suspension and the reaction mixture was filtered through Celite. The filtrate was then passed through a column packed with Amberlite IR 120 ion exchange resin ( $H^+$  form) and the mixture was reduced to 1/3 the volume under reduced pressure. This solution was heated at 40 °C for 18 hours. After this time, the solvent was removed *in vacuo* to give an oil, which was dissolved in a mixture of acetone (100 mL) and water (10 mL), to which Fuller's Earth (12.0 g) was added. This mixture was heated to reflux for 0.5 hours, and the organic phase was decanted and filtered. The solid remaining in the flask was then extracted a further three times with 10% aqueous acetone (3 x 35 mL), heating to reflux for 5 minutes and decanting the acetone each time. The combined filtrates were concentrated under reduced pressure to give a dark brown viscous oily solid that was recrystallized from boiling acetone to give the title compound **7.23**<sup>165,166</sup> (3.14 g, 19.4 mmol, 17% yield) as a light brown solid. M.pt. 162-169 °C (lit.<sup>166</sup> 158-159 °C).  $^1H$  NMR (400 MHz, MeOD- $d_4$ ):  $\delta$  1.41 (s, 3H), 3.72 (dd,  $J = 4.5, 12.8$  Hz, 1H), 3.91 (d,  $J = 7.8$  Hz, 1H), 3.95 (dd,  $J = 2.3, 12.8$  Hz, 1H), 4.29 (ddd,  $J = 2.3, 4.5, 7.8$  Hz, 1H). *Exchangeable protons not observed.*  $^{13}C$  NMR (100 MHz, MeOD- $d_4$ ):  $\delta$  21.1, 61.1, 73.6, 73.7, 84.5, 178.0.

**(3R,4R,5R)-3,4-Bis((*tert*-butyldimethylsilyloxy)-5-(((*tert*-butyldimethylsilyloxy)methyl)-3-methyldihydrofuran-2(3H)-one (7.24)**



(3R,4R,5R)-3,4-Dihydroxy-5-(hydroxymethyl)-3-methyldihydrofuran-2(3H)-one **7.23** (3.00 g, 18.5 mmol) was dissolved in DMF(20 mL) and THF (20 mL), to which 2,6-lutidine (8.62 mL, 74.0 mmol) and *tert*-butyldimethyl((trifluoromethyl)sulfonyl)silane (12.0 mL, 55.5 mmol) and DMAP (0.678 g, 5.55 mmol) were added sequentially at 0 °C. This mixture was stirred at room temperature for 24 hours, after which time it was concentrated *in vacuo* and the residue was dissolved in EtOAc. The organics were washed with aq. CuSO<sub>4</sub> solution (2 x 100 mL) then dried by passage through a hydrophobic frit. The crude material was adsorbed onto diatomaceous earth and purified by flash chromatography eluting in 100% cyclohexane to give the title compound **7.24** (7.90 g, 15.7 mmol, 85 % yield) as a white solid. M.pt. 72-73 °C.  $[\alpha_D]_{589}^{21.7^\circ C}$  [c 1, CDCl<sub>3</sub>]: +104°. <sup>1</sup>H NMR (400 MHz, CDCl<sub>3</sub>): δ 0.08 (s, 3H), 0.10 (s, 3H), 0.12 (s, 3H), 0.14-0.15 (m, 6H), 0.18 (s, 3H), 0.88-0.91 (m, 18H), 0.94 (s, 9H), 1.43 (s, 3H), 3.80 (dd, *J* = 2.3, 12.4 Hz, 1H), 4.00-4.06 (m, 2H), 4.23 (dt, *J* = 2.3, 8.1 Hz, 1H). <sup>13</sup>C NMR (100 MHz, CDCl<sub>3</sub>): δ -5.5, -5.3, -4.9, -4.2, -4.1, -2.7, 18.0, 18.3, 18.3, 21.5, 25.5 (3C), 25.7 (3C), 25.8 (3C), 59.3, 73.8, 75.2, 82.0, 174.6.  $\nu_{max}$  (neat): 2931, 2858, 1790, 1462, 1390, 1254, 1199, 1137, 1113, 1057, 1006, 938, 879, 830, 775, 673 cm<sup>-1</sup>. HR-MS (ESI): C<sub>24</sub>H<sub>53</sub>O<sub>5</sub>Si<sub>3</sub> [M+H<sup>+</sup>] requires 505.3195, found 505.3181.

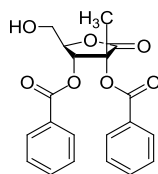
**(3R,4R,5R)-5-((Benzoyloxy)methyl)-3-methyl-2-oxotetrahydrofuran-3,4-diyl dibenzoate (7.25)**



To a mixture of benzoyl chloride (0.573 mL, 4.93 mmol) and pyridine (0.698 mL, 8.63 mmol) in DCM (1 mL) at 0 °C was added (3R,4R,5R)-3,4-dihydroxy-5-(hydroxymethyl)-3-methyldihydrofuran-2(3H)-one **7.23** (100 mg, 0.617 mmol) portion-wise. This mixture was stirred for 18 hours at reflux. Additional benzoyl chloride (0.300 mL, 2.58 mmol) and pyridine (0.300 mL, 3.73 mmol) were added and the mixture was stirred for a further 4

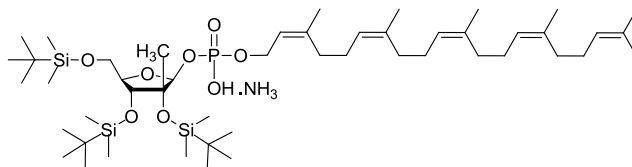
hours at reflux. After this time the mixture was diluted with DCM, washed with sat. sodium bicarbonate solution and water, then the organics were dried by passage through a hydrophobic frit. The organics were concentrated under reduced pressure to give the crude material which was adsorbed onto diatomaceous earth and purified by reversed phase chromatography, eluting under a gradient of MeCN (30-70%) in modified water (formic acid) to give the title compound **7.25** (127 mg, 0.268 mmol, 43 % yield) as a white solid. M.pt. 136-139 °C.  $[\alpha_D]_{589}^{22.0^\circ C}$  [c 1, CDCl<sub>3</sub>]: +31. <sup>1</sup>H NMR (400 MHz, DMSO-*d*<sub>6</sub>): δ 1.91 (s, 3H), 4.76-4.85 (m, 2H), 5.19 (td, *J* = 3.7, 5.4 Hz, 1H), 5.55 (d, *J* = 5.4 Hz, 1H), 7.27-7.31 (m, 2H), 7.43-7.47 (m, 2H), 7.50-7.57 (m, 3H), 7.60-7.65 (m, 1H), 7.68-7.72 (m, 3H), 7.87-7.90 (m, 2H), 7.98-8.01 (m, 2H). <sup>13</sup>C NMR (100 MHz, CDCl<sub>3</sub>): δ 23.7, 63.1, 72.5, 75.3, 79.5, 127.8, 127.8, 128.3 (2C), 128.4 (2C), 128.6 (2C), 129.2, 129.6 (2C), 129.7 (2C), 129.9 (2C), 133.5, 133.7, 133.8, 165.4, 165.9, 166.0, 172.6.  $\nu_{\max}$  (neat): 1793, 1726, 1452, 1269, 1110, 1069, 708 cm<sup>-1</sup>. HR-MS (ESI): C<sub>27</sub>H<sub>23</sub>O<sub>8</sub> [M+H<sup>+</sup>] requires 475.1388, found 475.1371.

**(3*R*,4*R*,5*R*)-5-(Hydroxymethyl)-3-methyl-2-oxotetrahydrofuran-3,4-diyl dibenzoate (7.27)**



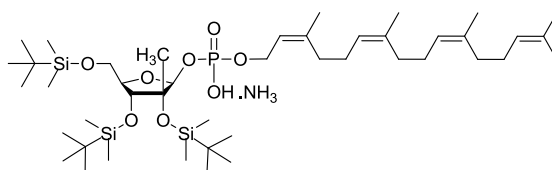
To a solution of (3*R*,4*R*,5*R*)-5-((benzoyloxy)methyl)-3-methyl-2-oxotetrahydrofuran-3,4-diyl dibenzoate **7.25** (100 mg, 0.211 mmol) in THF (1 mL) at -78 °C was added DIBAL-H (1 M in THF, 0.263 mL, 0.263 mmol). The solution was stirred for 20 hours, after which time MeOH (0.1 mL) was added. The organics were removed under reduced pressure and the residue was dissolved in DMF and DMSO (1:1, 1 mL); MDAP (formic, Method C) purification of this mixture afforded the title compound **7.27** (13.0 mg, 35.0 μmol, 17% yield) as a transparent glass. <sup>1</sup>H NMR (400 MHz, DMSO-*d*<sub>6</sub>): δ 1.84 (s, 3H), 3.77 (ddd, *J* = 2.9, 5.9, 12.4 Hz, 1H), 3.87 (ddd, *J* = 2.6, 4.6, 12.4 Hz, 1H), 4.81-4.84 (m, 1H), 5.48-5.50 (m, 2H), 7.25-7.29 (m, 2H), 7.40-7.44 (m, 2H), 7.48-7.52 (m, 1H), 7.57-7.62 (m, 1H), 7.67-6.69 (m, 2H), 7.84-7.87 (m, 2H). LCMS (formic): *t*<sub>R</sub> = 1.07 min, [M+H<sup>+</sup>] 371, [M+NH<sub>4</sub><sup>+</sup>] 388; (area % total: 99).

**(2*S*,3*R*,4*R*,5*R*)-3,4-Bis((*tert*-butyldimethylsilyl)oxy)-5-(((*tert*-butyldimethylsilyl)oxy)methyl)-3-methyltetrahydrofuran-2-yl ((2*Z*,6*Z*,10*Z*,14*Z*)-3,7,11,15,19-pentamethylcosa-2,6,10,14,18-pentaen-1-yl) hydrogen phosphate, ammonia salt (7.33f)**



The title compound **7.33f** (155.5 mg, 0.165 mmol, 42 % yield, transparent gum), was prepared according to general procedure **F** using the following reagents: (2*Z*,6*Z*,10*Z*,14*Z*)-3,7,11,15,19-pentamethylcosa-2,6,10,14,18-pentaen-1-ol (233 mg, 0.651 mmol), DIPEA (0.138 mL, 0.789 mmol), DCM (9.3 mL), 3-((chloro(diisopropylamino)phosphino)oxy)propanenitrile (0.158 mL, 0.710 mmol), *then* lactol **7.19** (200 mg, 0.395 mmol) in DCM (6.7 mL), 1*H*-tetrazole (66.3 mg, 0.947 mmol), *then* THF (20 mL), H<sub>2</sub>O<sub>2</sub> (0.155 mL, 1.78 mmol), 5% methanolic potassium hydroxide solution (14 mL). <sup>1</sup>H NMR (400 MHz, CDCl<sub>3</sub>): δ 0.05 (s, 3H), 0.09 (s, 3H), 0.12 (s, 9H), 0.15 (s, 3H), 0.90-0.92 (m, 27H), 1.32 (s, 3H), 1.62 (s, 3H), 1.68-1.72 (m, 15H), 2.01-2.10 (m, 16H), 3.68-3.75 (m, 2H), 3.87 (d, *J* = 10.2 Hz, 1H), 3.94-3.99 (m, 1H), 4.34-4.43 (m, 2H), 5.07-5.17 (m, 4H), 5.21 (d, *J* = 6.9 Hz, 1H), 5.39 (t, *J* = 6.2 Hz, 1H), 7.54 (br.s, 1H).

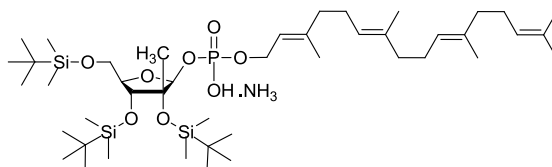
**(2*S*,3*R*,4*R*,5*R*)-3,4-Bis((*tert*-butyldimethylsilyl)oxy)-5-(((*tert*-butyldimethylsilyl)oxy)methyl)-3-methyltetrahydrofuran-2-yl ((2*Z*,6*Z*,10*Z*)-3,7,11,15-tetramethylhexadeca-2,6,10,14-tetraen-1-yl) hydrogen phosphate, ammonia salt (7.33g)**



The title compound **7.33g** (209 mg, 0.243 mmol, 41 % yield, white gum), was prepared according to general procedure **F** using the following reagents: (2*Z*,6*Z*,10*Z*)-3,7,11,15-tetramethylhexadeca-2,6,10,14-tetraen-1-ol (284 mg, 0.976 mmol), DIPEA (0.207 mL, 1.18 mmol), DCM (14 mL), 3-((chloro(diisopropylamino)phosphino)oxy)propanenitrile (0.238 mL, 1.07 mmol), *then* lactol **7.19** (300 mg, 0.592 mmol) in DCM (10 mL), 1*H*-tetrazole (99.0 mg, 1.42 mmol), *then* THF (30 mL), H<sub>2</sub>O<sub>2</sub> (0.233 mL, 2.66 mmol), 5% methanolic potassium hydroxide solution (20 mL). <sup>1</sup>H NMR (400 MHz, MeOD-*d*<sub>4</sub>): δ 0.11 (s, 3H), 0.12 (s, 3H), 0.13

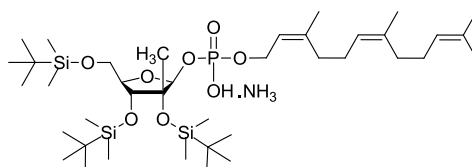
(s, 3H), 0.15 (s, 3H), 0.17 (s, 3H), 0.21 (s, 3H), 0.93-0.96 (m, 27H), 1.40 (s, 3H), 1.63 (s, 3H), 1.70 (s, 9H), 1.75 (d,  $J = 0.8$  Hz, 3H), 2.07-2.15 (m, 12H), 3.76 (dd,  $J = 7.2, 11.3$  Hz, 1H), 3.85 (d,  $J = 8.3$  Hz, 1H), 3.91-4.00 (m, 2H), 4.43-4.47 (m, 2H), 5.12-5.19 (m, 3H), 5.37 (d,  $J = 6.8$  Hz, 1H), 5.44 (td,  $J = 0.8, 6.9$  Hz, 1H). *Exchangeable protons not observed.*

**(2*S*,3*R*,4*R*,5*R*)-3,4-Bis(*tert*-butyldimethylsilyloxy)-5-(((*tert*-butyldimethylsilyloxy)methyl)-3-methyltetrahydrofuran-2-yl ((2*E*,6*E*,10*E*)-3,7,11,15-tetramethylhexadeca-2,6,10,14-tetraen-1-yl) hydrogen phosphate, ammonia salt (7.33h)**



The title compound **7.33h** (247 mg, 0.287 mmol, 55 % yield, transparent gum), was prepared according to general procedure **F** using the following reagents: (2*E*,6*E*,10*E*)-3,7,11,15-tetramethylhexadeca-2,6,10,14-tetraen-1-ol (0.284 mL, 0.859 mmol), DIPEA (0.182 mL, 1.04 mmol), DCM (12 mL), 3-((chloro(diisopropylamino)phosphino)oxy)propanenitrile (0.209 mL, 0.937 mmol), *then* lactol **7.19** (264 mg, 0.521 mmol) in DCM (8.5 mL), 1*H*-tetrazole (88.0 mg, 1.25 mmol), *then* THF (25 mL), H<sub>2</sub>O<sub>2</sub> (0.205 mL, 2.34 mmol), 5% methanolic potassium hydroxide solution (15 mL). <sup>1</sup>H NMR (400 MHz, CDCl<sub>3</sub>):  $\delta$  0.05 (s, 3H), 0.09 (s, 3H), 0.12-0.14 (m, 12H), 0.88 (s, 9H), 0.90-0.92 (m, 18H), 1.33 (s, 3H), 1.60 (s, 9H), 1.65 (s, 3H), 1.68 (d,  $J = 0.8$  Hz, 3H), 1.95-2.13 (m, 12H), 3.69-3.76 (m, 2H), 3.86-3.91 (m, 1H), 3.95-4.01 (m, 1H), 4.34-4.46 (m, 2H), 5.07-5.14 (m, 3H), 5.22 (d,  $J = 6.3$  Hz, 1H), 5.37 (t,  $J = 6.2$  Hz, 1H), 7.34 (br.s, 1H).

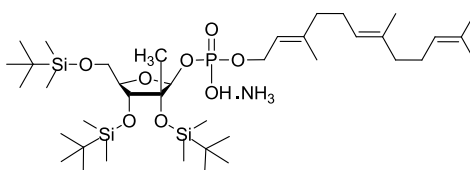
**(2*S*,3*R*,4*R*,5*R*)-3,4-Bis(*tert*-butyldimethylsilyloxy)-5-(((*tert*-butyldimethylsilyloxy)methyl)-3-methyltetrahydrofuran-2-yl ((2*Z*,6*Z*)-3,7,11-trimethyldodeca-2,6,10-trien-1-yl) hydrogen phosphate, ammonia salt (7.33i)**



The title compound **7.33i** (146 mg, 0.185 mmol, 31 % yield, transparent gum), was prepared according to general procedure **F** using the following reagents: (2*Z*,6*Z*)-3,7,11-trimethyldodeca-2,6,10-trien-1-ol (217 mg, 0.976 mmol), DIPEA (0.207 mL, 1.18 mmol),

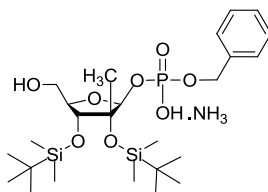
DCM (14 mL), 3-((chloro(diisopropylamino)phosphino)oxy)propanenitrile (0.238 mL, 1.07 mmol), then lactol **7.19** (300 mg, 0.592 mmol) in DCM (10 mL), 1*H*-tetrazole (99.0 mg, 1.42 mmol), then THF (30 mL), H<sub>2</sub>O<sub>2</sub> (0.233 mL, 2.66 mmol), 5% methanolic potassium hydroxide solution (20 mL). <sup>1</sup>H NMR (400 MHz, MeOD-*d*<sub>4</sub>): δ 0.11-0.17 (m, 15H), 0.21 (s, 3H), 0.93-0.96 (m, 27H), 1.40 (s, 3H), 1.63 (s, 3H), 1.70 (s, 6H), 1.76 (s, 3H), 2.05-2.16 (m, 8H), 3.75 (dd, *J* = 7.1, 11.2 Hz, 1H), 3.85 (d, *J* = 8.2 Hz, 1H), 3.91-4.00 (m, 2H), 4.39-4.49 (m, 2H), 5.12-5.18 (m, 2H), 5.37 (d, *J* = 6.9 Hz, 1H), 5.54 (t, *J* = 6.1 Hz, 1H). *Exchangeable protons not observed.*

**(2*S*,3*R*,4*R*,5*R*)-3,4-Bis((*tert*-butyldimethylsilyl)oxy)-5-(((*tert*-butyldimethylsilyl)oxy)methyl)-3-methyltetrahydrofuran-2-yl ((2*E*,6*E*)-3,7,11-trimethyldodeca-2,6,10-trien-1-yl) hydrogen phosphate, ammonia salt (**7.33j**)**



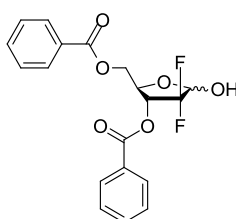
The title compound **7.33j** (257 mg, 0.325 mmol, 55 % yield, white gum), was prepared according to general procedure **F** using the following reagents: (2*E*,6*E*)-3,7,11-trimethyldodeca-2,6,10-trien-1-ol (0.247 mL, 0.976 mmol), DIPEA (0.207 mL, 1.18 mmol), DCM (14 mL), 3-((chloro(diisopropylamino)phosphino)oxy)propanenitrile (0.238 mL, 1.07 mmol), then lactol **7.19** (300 mg, 0.592 mmol) in DCM (10 mL), 1*H*-tetrazole (99.0 mg, 1.42 mmol), then THF (30 mL), H<sub>2</sub>O<sub>2</sub> (0.233 mL, 2.66 mmol), 5% methanolic potassium hydroxide solution (20 mL). <sup>1</sup>H NMR (400 MHz, MeOD-*d*<sub>4</sub>): δ 0.10-0.21 (m, 18 H), 0.93-0.96 (m, 27 H), 1.41 (s, 3H), 1.61 (s, 6H), 1.69 (d, *J* = 0.8 Hz, 3H), 1.71 (s, 3H), 1.98-2.17 (m, 8H), 3.75 (dd, *J* = 7.2, 11.6 Hz, 1H), 3.85 (d, *J* = 8.3 Hz, 1H), 3.92 (dd, *J* = 2.0, 11.6 Hz, 1H), 3.95-4.00 (m, 1H), 4.44-4.51 (m, 2H), 5.09-5.16 (m, 2H), 5.37 (d, *J* = 7.0 Hz, 1H), 5.44 (td, *J* = 0.8, 6.6 Hz, 1H). *Exchangeable protons not observed.*

**Benzyl ((2*S*,3*R*,4*R*,5*R*)-3,4-bis((tert-butyldimethylsilyl)oxy)-5-(hydroxymethyl)-3-methyltetrahydrofuran-2-yl) hydrogen phosphate, ammonia salt (7.34)**



To a solution of benzyl ((3*R*,4*R*,5*R*)-3,4-bis((tert-butyldimethylsilyl)oxy)-5-(((tert-butyldimethylsilyl)oxy)methyl)-3-methyltetrahydrofuran-2-yl) hydrogen phosphate, ammonia salt **7.33a** (401 mg, 0.592 mmol) in a 15% solution of conc.  $\text{NH}_4\text{OH}$  in MeOH (4 mL) was added ammonium fluoride (658 mg, 17.8 mmol). This mixture was stirred at 55 °C for 20 hours, after which time it was cooled to room temperature and diluted with DCM (4 mL). The insoluble material was filtered off and washed with a mixture of DCM and MeOH (4:1, 2 x 5 mL). The organics were concentrated under reduced pressure and the resulting material was dissolved in MeOH (1 mL) and purified by MDAP (high pH, Method C) to afford the title compound **7.34** (200 mg, 0.355 mmol, 60%) as a transparent gum.  $^1\text{H}$  NMR (400 MHz,  $\text{DMSO-}d_6$ ):  $\delta$  0.08 (s, 12 H), 0.85 (s, 9H), 0.89 (s, 9H), 1.14 (s, 3H), 3.20 (m, 1H), 3.65-3.70 (m, 2H), 4.16 (d,  $J = 7.9$  Hz, 1H), 4.66-4.73 (m, 2H), 5.00 (d,  $J = 1.9$  Hz, 1H), 6.01 (br.s, 1H), 7.23-7.26 (m, 1H), 7.30-7.34 (m, 4H). *P-OH* not observed. LCMS (high pH):  $t_R = 1.29$  min,  $[\text{M}+\text{H}^+]$  563; (area % total: 95).

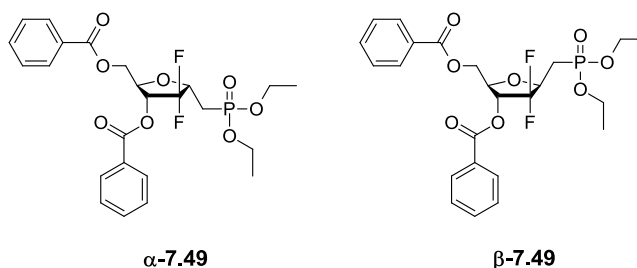
**((2*R*,3*R*)-3-(Benzoyloxy)-4,4-difluoro-5-hydroxytetrahydrofuran-2-yl)methyl benzoate (7.46)<sup>262</sup>**



Red-Al (25% in toluene, 0.614 mL, 2.05 mmol) was added slowly to a solution of ((2*R*,3*R*)-3-(benzyloxy)-4,4-difluoro-5-oxotetrahydrofuran-2-yl)methyl benzoate **7.47** (700 mg, 1.86 mmol) in THF (30 mL) at -78 °C under an atmosphere of nitrogen. The reaction mixture was stirred for 2 hours at the same temperature after which the reaction was quenched by the careful addition of 1N HCl (until pH 2 was reached). The mixture was extracted with EtOAc (3 x 100 mL) and the combined organics were washed with 5% sodium bicarbonate (100

mL) and water (100 mL), dried by passage through a hydrophobic frit then concentrated under reduced pressure. The crude material was adsorbed onto diatomaceous earth and purified by flash chromatography, eluting under a gradient of EtOAc in cyclohexane (10-30%) to give the title compound **7.46** (555 mg, 1.47 mmol, 79 % yield) as a clear glass.  $^1\text{H}$  NMR (400 MHz,  $\text{CDCl}_3$ ):  $\delta$  3.25 (d,  $J = 4.3$  Hz, 0.66H), 3.54 (d,  $J = 5.4$  Hz, 0.34H), 4.47-4.51 (m, 0.34H) 4.63 (dd,  $J = 4.5, 12.2$  Hz, 0.66H), 4.69-4.74 (m, 1 H), 4.76-4.81 (m, 1H), 5.36-5.40 (m, 0.34H), 5.50-5.55 (m, 1.32H), 5.75 (td,  $J = 6.0, 10.0$  Hz, 0.34H), 7.39-7.52 (m, 4H), 7.56-7.60 (m, 1H), 7.62-7.67 (m, 1H), 8.05-8.12 (m, 4H).  $^{19}\text{F}$  NMR (376 MHz,  $\text{CDCl}_3$ ):  $\delta$  -125.2 (d,  $J = 244$  Hz, 0.5F), -125.1 (d,  $J = 252$  Hz, 1F), -123.5 (d,  $J = 244$  Hz, 0.5F), -109.2 (d,  $J = 252$  Hz, 1F). LCMS (formic):  $t_{\text{R}} = 1.13$  min,  $[\text{M}+\text{H}^+]$  379,  $[\text{M}+\text{NH}_4]$  396;  $t_{\text{R}} = 1.14$  min,  $[\text{M}+\text{H}^+]$  378,  $[\text{M}+\text{NH}_4]$  396 (mixture of 2 anomers; area % total: 95).

**((2R,3R,5S)-3-(Benzoyloxy)-5-((diethoxyphosphoryl)methyl)-4,4-difluorotetrahydrofuran-2-yl)methyl benzoate ( $\alpha$ -7.49)** and **((2R,3R,5R)-3-(Benzoyloxy)-5-((diethoxyphosphoryl)methyl)-4,4-difluorotetrahydrofuran-2-yl)methyl benzoate ( $\beta$ -7.49)**



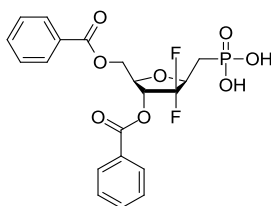
To a solution of tetraethyl methylenebis(phosphonate) (0.991 mL, 3.99 mmol) in THF (35 mL) under nitrogen at room temperature was added sodium hydride (60% wt. in mineral oil, 0.160 g, 3.99 mmol). This mixture was allowed to stir for 30 minutes after which time ((2R,3R)-3-(benzoyloxy)-4,4-difluoro-5-hydroxytetrahydrofuran-2-yl)methyl benzoate **7.46** (1.44 g, 3.80 mmol) in THF (35 mL) was added. This mixture was stirred at room temperature for 18 hours, after which water (50 mL) and DCM (50 mL) were added and the organics were separated. The aqueous layer was washed with DCM (3x 50 mL) and the combined organics were dried by passage through a hydrophobic frit. The organics were concentrated under reduced pressure to give the crude material which was adsorbed onto diatomaceous earth and purified by flash chromatography eluting under a gradient of TBME in cyclohexane (0-50%) to give the purified mixture of anomers (1.30 g). The mixture of anomers was then separated using a 4.6mmid x 25cm Chiralpak AD-H column, eluting under a mixture of EtOH in heptane (30:70) yielding the title compounds  **$\beta$ -7.49** (574 mg,

1.12 mmol, 30 % yield) and  **$\alpha$ -7.49** (438 mg, 0.855 mmol, 23 % yield) as the fast and slow running fractions respectively, as viscous transparent gums.

((2*R*,3*R*,5*S*)-3-(Benzyloxy)-5-((diethoxyphosphoryl)methyl)-4,4-difluorotetrahydrofuran-2-yl)methyl benzoate  **$\alpha$ -7.49**:  $[\alpha_D]_{589}^{21.5^\circ C}$  [c 1, CDCl<sub>3</sub>]: +36. <sup>1</sup>H NMR (400 MHz, CDCl<sub>3</sub>):  $\delta$  1.30-1.35 (m, 6H), 2.24-2.29 (m, 2H), 4.13-4.18 (m, 4H), 4.57 (q, *J* = 4.6 Hz, 1H), 4.61 (dd, *J* = 4.6, 11.9 Hz, 1H), 4.64 (dd, *J* = 4.2, 11.9 Hz, 1H), 4.68-4.74 (m, 1H), 5.67 (dt, *J* = 6.0, 11.6 Hz, 1H), 7.41-7.44 (m, 2H), 7.47-7.50 (m, 2H), 7.55-7.58 (m, 1H), 7.62-7.65 (m, 1H), 8.05-8.07 (m, 2H), 8.08-8.09 (m, 2H). <sup>13</sup>C NMR (100 MHz, CDCl<sub>3</sub>):  $\delta$  16.3 (d, *J* = 4 Hz), 16.4 (d, *J* = 4 Hz), 25.6 (d, *J* = 143 Hz), 62.0 (d, *J* = 7 Hz), 62.2 (d, *J* = 7 Hz), 63.8, 73.4 (dd, *J* = 18, 32 Hz), 75.7-76.3 (m), 78.7 (dd, *J* = 2, 6 Hz), 123.8 (HMBC) 128.3, 128.5 (2C), 128.7 (2C), 129.4, 129.7 (2C), 130.0 (2C), 133.3, 134.0, 165.0, 166.0. <sup>19</sup>F NMR (376 MHz, CDCl<sub>3</sub>):  $\delta$  -124.5 (d, *J* = 234 Hz, 1F), -109.7 (d, *J* = 234 Hz, 1F). <sup>31</sup>P NMR (162 MHz, CDCl<sub>3</sub>):  $\delta$  25.6 (d, *J* = 4 Hz).  $\nu_{\max}$  (neat): 2982, 1728, 1602, 1452, 1268, 1097, 1026, 965, 711 cm<sup>-1</sup>. HR-MS (ESI): C<sub>24</sub>H<sub>28</sub>F<sub>2</sub>O<sub>8</sub>P [M+H<sup>+</sup>] requires 513.1484, found 513.1465.

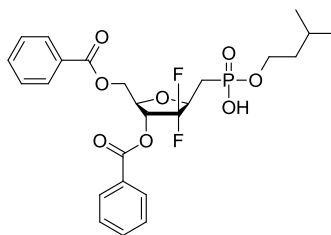
((2*R*,3*R*,5*R*)-3-(Benzyloxy)-5-((diethoxyphosphoryl)methyl)-4,4-difluorotetrahydrofuran-2-yl)methyl benzoate  **$\beta$ -7.49**:  $[\alpha_D]_{589}^{21.5^\circ C}$  [c 1, CDCl<sub>3</sub>]: -64. <sup>1</sup>H NMR (400 MHz, CDCl<sub>3</sub>):  $\delta$  1.30 (t, *J* = 7.0 Hz, 3H), 1.35 (t, *J* = 7.0 Hz, 3H), 2.17-2.29 (m, 2H), 4.09-4.18 (m, 4H), 4.39-4.50 (m, 2H), 4.60 (dd, *J* = 5.1, 11.7 Hz, 1H), 4.68 (dd, *J* = 3.7, 11.7 Hz, 1H), 5.50 (dd, *J* = 4.4, 14.6 Hz, 1H), 7.42-7.45 (m, 2H), 7.47-7.51 (m, 2H), 7.56-7.60 (m, 1H), 7.62-7.66 (m, 1H), 8.03-8.09 (m, 4H). <sup>13</sup>C NMR (100 MHz, CDCl<sub>3</sub>):  $\delta$  16.3, 16.3, 24.5 (dd, *J* = 5, 145 Hz), 61.9 (d, *J* = 6 Hz), 62.5 (d, *J* = 7 Hz), 63.3, 73.3 (dd, *J* = 17, 37 Hz), 75.6 (ddd, *J* = 5, 26, 30 Hz), 79.8 (t, *J* = 4 Hz), 122.8 (HMBC) 128.3, 128.4 (2C), 128.6 (2C), 129.4, 129.7 (2C), 130.0 (2C), 133.3, 133.9, 164.9, 167.0. <sup>19</sup>F NMR (376 MHz, CDCl<sub>3</sub>):  $\delta$  -121.5 (d, *J* = 244 Hz, 1F), -116.2 (d, *J* = 244 Hz, 1F). <sup>31</sup>P NMR (162 MHz, CDCl<sub>3</sub>):  $\delta$  25.9.  $\nu_{\max}$  (neat): 2983, 1725, 1601, 1452, 1266, 1106, 1025, 965, 805, 711 cm<sup>-1</sup>. HR-MS (ESI): C<sub>24</sub>H<sub>28</sub>F<sub>2</sub>O<sub>8</sub>P [M+H<sup>+</sup>] requires 513.1484, found 513.1465.

**((2*R*,4*R*,5*R*)-4-(Benzoyloxy)-5-((benzoyloxy)methyl)-3,3-difluorotetrahydrofuran-2-yl)methyl)phosphonic acid (7.50)**



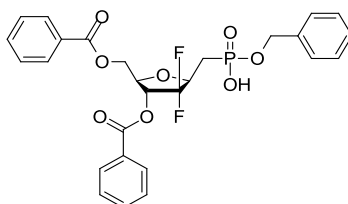
To a solution of ((2*R*,3*R*,5*R*)-3-(benzoyloxy)-5-((diethoxyphosphoryl)methyl)-4,4-difluorotetrahydrofuran-2-yl)methyl benzoate **β-7.49** (521 mg, 1.02 mmol) in MeCN (15 mL) under an atmosphere of nitrogen at room temperature was added TMSBr (1.06 mL, 8.13 mmol). This mixture was stirred at the same temperature for 3 hours, after which time the organics were removed under reduced pressure and the remaining TMSBr was co-evaporated with MeCN (3 x 10 mL). The crude material was adsorbed onto diatomaceous earth and purified by reversed phase chromatography, eluting under a gradient of MeCN (30-50%) in modified water (formic acid). The resulting hygroscopic material was dried azeotropically with toluene (5 x 5 mL) to afford the title compound **7.50** (372 mg, 0.815 mmol, 80 % yield) as a collapsed white foam.  $[\alpha_D]_{589}^{21.5^\circ\text{C}}$  [c 1, CDCl<sub>3</sub>]: -7. <sup>1</sup>H NMR (400 MHz, DMSO-*d*<sub>6</sub>): δ 1.86-1.94 (m, 1H), 1.96-2.03 (m, 1H), 2.90-4.0 (br.s, 2H), 4.27-4.34 (m, 1H), 4.54-4.56 (m, 1 H), 4.58-4.61 (m, 2H), 5.49 (dd, *J* = 5.5, 15.7 Hz, 1H), 7.50-7.52 (m, 2H), 7.56-7.59 (m, 2H), 7.65-7.68 (m, 1H), 7.72-7.74 (m, 1H), 7.95-7.97 (m, 2H), 8.04-8.07 (m, 2H). <sup>13</sup>C NMR (100 MHz, DMSO-*d*<sub>6</sub>): δ 26.5 (dd, *J* = 3, 138 Hz), 63.2, 73.1 (dd, *J* = 17, 37 Hz), 75.8-76.3 (m), 78.1, 123.0 (m), 128.2, 128.7 (2C), 128.9 (2C), 129.1 (2C), 129.2, 129.5 (2C), 133.5, 134.1, 164.4, 165.3. <sup>19</sup>F NMR (376 MHz, CDCl<sub>3</sub>): δ -121.0 (d, *J* = 242 Hz, 1F), -116.0 (d, *J* = 242 Hz, 1F). <sup>31</sup>P NMR (162 MHz, DMSO-*d*<sub>6</sub>): δ 18.8.  $\nu_{\text{max}}$  (neat): 2904 (br.), 1727, 1453, 1269, 1107, 1026, 709 cm<sup>-1</sup>. HR-MS (ESI): C<sub>20</sub>H<sub>20</sub>F<sub>2</sub>O<sub>8</sub>P [M+H<sup>+</sup>] requires 457.0858, found 457.0840.

**((2R,3R,5R)-3-(Benzoyloxy)-4,4-difluoro-5-((hydroxy(isopentyloxy)phosphoryl)methyl)tetrahydrofuran-2-yl)methyl benzoate (7.51a)**



The title compound **7.51a** (77.6 mg, 0.147 mmol, 67 % yield, colourless glass), was prepared according to general procedure **G** using the following reagents and solvents: (((2R,4R,5R)-4-(benzoyloxy)-5-((benzoyloxy)methyl)-3,3-difluorotetrahydrofuran-2-yl)methyl)phosphonic acid **7.50** (100 mg, 0.219 mmol), 3-methylbutan-1-ol (36.0  $\mu$ L, 0.329 mmol), pyridine (0.6 mL), 2,2,2-trichloroacetonitrile (0.6 mL).  $[\alpha_D]_{589}^{20.3^\circ C}$  [c 1, CDCl<sub>3</sub>]: +108. <sup>1</sup>H NMR (600 MHz, CDCl<sub>3</sub>):  $\delta$  0.88 (d,  $J$  = 6.6 Hz, 6H), 1.54 (q,  $J$  = 6.4 Hz, 2H), 1.67-1.77 (m, 1H), 2.20-2.33 (m, 2H), 4.05-4.11 (m, 2H), 4.37-4.48 (m, 2H), 4.58 (dd,  $J$  = 3.5, 11.7 Hz, 1H), 4.67 (dd,  $J$  = 2.8, 11.7 Hz, 1H), 5.51 (dd,  $J$  = 4.5, 15.0 Hz, 1H), 7.42 (t,  $J$  = 8.0 Hz, 2H), 7.50 (t,  $J$  = 8.0 Hz, 2H), 7.54-7.58 (m, 1H), 7.60-7.64 (m, 1H), 8.03-8.07 (m, 4H), 10.50 (br.s, 1H). <sup>13</sup>C NMR (100 MHz, CDCl<sub>3</sub>):  $\delta$  22.3, 22.3, 24.5, 24.8 (d,  $J$  = 148 Hz), 39.0, 63.1, 64.3-64.4 (m), 73.3 (dd,  $J$  = 18, 38 Hz), 75.3-75.7 (m), 79.8, 121.8 (HMBC), 128.4, 128.4 (2C), 128.6 (2C), 129.5, 129.7 (2C), 130.0 (2C), 133.2, 133.9, 164.9, 166.1. <sup>19</sup>F NMR (376 MHz, CDCl<sub>3</sub>):  $\delta$  -121.2 (d,  $J$  = 239 Hz, 1F), -116.4 (d,  $J$  = 239 Hz, 1F). <sup>31</sup>P NMR (162 MHz, CDCl<sub>3</sub>):  $\delta$  27.6.  $\nu_{max}$  (neat): 2959, 1726, 1602, 1453, 1267, 1207, 1106, 1067, 1022, 710 cm<sup>-1</sup>. HR-MS (ESI): C<sub>25</sub>H<sub>30</sub>F<sub>2</sub>O<sub>8</sub>P [M+H<sup>+</sup>] requires 527.1641, found 527.1636.

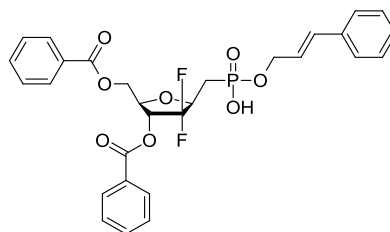
**((2R,3R,5R)-3-(Benzoyloxy)-5-(((benzoyloxy)(hydroxy)phosphoryl)methyl)-4,4-difluorotetrahydrofuran-2-yl)methyl benzoate (7.51b)**



The title compound **7.51b** (83.0 mg, 0.152 mmol, 69 % yield, colourless glass), was prepared according to general procedure **G** using the following reagents and solvents: (((2R,4R,5R)-4-(benzoyloxy)-5-((benzoyloxy)methyl)-3,3-difluorotetrahydrofuran-2-yl)methyl)phosphonic acid **7.50** (100 mg, 0.219 mmol), phenylmethanol (34.0  $\mu$ L, 0.329 mmol), pyridine (0.6 mL),

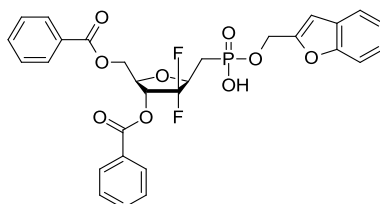
2,2,2-trichloroacetonitrile (0.6 mL).  $[\alpha_D]_{589}^{23.6^\circ C}$  [c 1, CDCl<sub>3</sub>]: +12. <sup>1</sup>H NMR (400 MHz, CDCl<sub>3</sub>): δ 2.27 (dd, *J* = 6.3, 19.0 Hz, 2H), 4.35-4.48 (m, 2H), 4.53 (dd, *J* = 4.2, 12.0 Hz, 1H), 4.65 (dd, *J* = 3.9, 12.0 Hz, 1H), 5.08 (d, *J* = 7.9 Hz, 2H), 5.49 (dd, *J* = 4.9, 14.9 Hz, 1H), 7.24-7.48 (m, 9H), 7.52-7.56 (m, 1H), 7.60-7.64 (m, 1H), 8.00-8.06 (m, 4H), 9.73 (br.s, 1H). <sup>13</sup>C NMR (100 MHz, CDCl<sub>3</sub>): δ 25.1 (d, *J* = 147 Hz), 63.1, 67.2 (d, *J* = 6 Hz), 73.3, (dd, *J* = 17, 37 Hz), 75.2-75.8 (m), 79.8, 120.1-125.3 (m), 127.6 (2C), 128.3, 128.4, 128.4 (2C), 128.5 (2C), 128.6 (2C), 129.4, 129.7 (2C), 130.0 (2C), 133.2, 133.9, 136.1 (d, *J* = 7 Hz), 164.9, 166.1. <sup>19</sup>F NMR (376 MHz, CDCl<sub>3</sub>): δ -121.1 (d, *J* = 244 Hz, 1F), -116.1 (d, *J* = 244 Hz, 1F). <sup>31</sup>P NMR (162 MHz, CDCl<sub>3</sub>): δ 28.2.  $\nu_{\max}$  (neat): 2948, 1726, 1453, 1268, 1107, 1022, 710 cm<sup>-1</sup>. HR-MS (ESI): C<sub>27</sub>H<sub>26</sub>F<sub>2</sub>O<sub>8</sub>P [M+H<sup>+</sup>] requires 547.1328, found 547.1311.

**((2*R*,3*R*,5*R*)-3-(Benzoyloxy)-5-(((cinnamyloxy)(hydroxy)phosphoryl)methyl)-4,4-difluorotetrahydrofuran-2-yl)methyl benzoate (7.51c)**



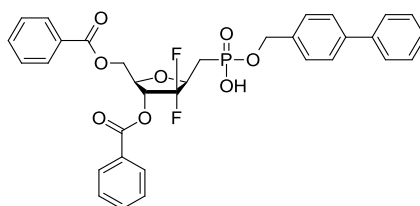
The title compound **7.51c** (86.2 mg, 0.151 mmol, 69 % yield, yellow glass), was prepared according to general procedure **G** using the following reagents and solvents: (((2*R*,4*R*,5*R*)-4-(benzoyloxy)-5-((benzoyloxy)methyl)-3,3-difluorotetrahydrofuran-2-yl)methyl)phosphonic acid **7.50** (100 mg, 0.219 mmol), (*E*)-3-phenylprop-2-en-1-ol (42.0 μL, 0.329 mmol), pyridine (0.6 mL), 2,2,2-trichloroacetonitrile (0.6 mL).  $[\alpha_D]_{589}^{20.3^\circ C}$  [c 1, CDCl<sub>3</sub>]: +108. <sup>1</sup>H NMR (600 MHz, CDCl<sub>3</sub>): δ 2.28-2.32 (m, 2H), 4.36-4.51 (m, 2H), 4.56-4.76 (m, 4H), 5.50 (dd, *J* = 3.7, 14.9 Hz, 1H), 6.23-6.27 (m, 1H), 6.62 (d, *J* = 15.9 Hz, 1H), 7.21-7.47 (m, 10H), 7.53 (t, *J* = 7.3 Hz, 1H), 7.60 (t, *J* = 7.3 Hz, 1H), 8.03 (t, *J* = 7.3 Hz, 4H). <sup>13</sup>C NMR (600 MHz, CDCl<sub>3</sub>): δ 25.0 (d, *J* = 146 Hz), 63.1, 66.4, 73.3 (dd, *J* = 17, 38 Hz), 75.4-75.9 (m), 79.8, 120.9-124.5 (m), 123.8, 126.7 (2C), 128.0, 128.4, 128.4 (2C), 128.6 (2C), 128.6 (2C), 129.4, 129.7 (2C), 130.0 (2C), 133.2, 133.7, 133.9, 136.1, 164.9, 166.1. <sup>19</sup>F NMR (376 MHz, CDCl<sub>3</sub>): δ -121.1 (d, *J* = 243 Hz, 1H), -116.0 (d, *J* = 243 Hz, 1H). <sup>31</sup>P NMR (162 MHz, CDCl<sub>3</sub>): δ 27.5.  $\nu_{\max}$  (neat): 2957, 1725, 1601, 1452, 1267, 1207, 1106, 1070, 1014, 968, 710 cm<sup>-1</sup>. HR-MS (ESI): C<sub>29</sub>H<sub>28</sub>F<sub>2</sub>O<sub>8</sub>P [M+H<sup>+</sup>] requires 573.1484, found 573.1462.

**(2R,3R,5R)-5-(((Benzofuran-2-ylmethoxy)(hydroxy)phosphoryl)methyl)-2-((benzoyloxy)methyl)-4,4-difluorotetrahydrofuran-3-yl benzoate (7.51d)**



The title compound **7.51d** (59.7 mg, 0.102 mmol, 47 % yield, colourless glass), was prepared according to general procedure **G** using the following reagents and solvents: (((2R,4R,5R)-4-(benzoyloxy)-5-((benzoyloxy)methyl)-3,3-difluorotetrahydrofuran-2-yl)methyl)phosphonic acid **7.50** (100 mg, 0.219 mmol), benzofuran-2-ylmethanol (48.7 mg, 0.329 mmol), pyridine (0.6 mL), 2,2,2-trichloroacetonitrile (0.6 mL).  $[\alpha_D]_{589}^{20.3^\circ C}$  [c 1, CDCl<sub>3</sub>]: +92. <sup>1</sup>H NMR (600 MHz, CDCl<sub>3</sub>): δ 2.25-2.36 (m, 2H), 4.33 (br.s, 1H), 4.39-4.51 (m, 2H), 4.59-4.65 (m, 1H), 5.17 (d, *J* = 7.7 Hz, 2H), 5.45 (dd, *J* = 5.0, 15.0 Hz, 1H), 6.68 (s, 1H), 7.13 (t, *J* = 7.4 Hz, 1H), 7.19 (t, *J* = 7.4 Hz, 1H), 7.28-7.45 (m, 6H), 7.48 (t, *J* = 7.4 Hz, 1H), 7.57 (t, *J* = 7.4 Hz, 1H), 7.93-8.05 (m, 4H), 9.71 (br.s, 1H). <sup>13</sup>C NMR (600 MHz, CDCl<sub>3</sub>): δ 25.1 (d, *J* = 148 Hz), 59.9 (d, *J* = 6 Hz), 63.1, 73.2 (dd, *J* = 15, 37 Hz), 75.4-75.8 (m), 79.8, 106.7, 111.3, 120.9-124.5 (m), 121.3, 122.8, 124.8, 127.7, 128.4 (3C), 128.5 (2C), 129.3, 129.7 (2C), 130.0 (2C), 133.2, 133.8, 152.8 (d, *J* = 7 Hz), 155.2, 164.9, 166.2. <sup>19</sup>F NMR (376 MHz, CDCl<sub>3</sub>): δ -120.9 (d, *J* = 238 Hz, 1F), -115.9 (d, *J* = 238 Hz, 1F). <sup>31</sup>P NMR (162 MHz, CDCl<sub>3</sub>): δ 26.7. *v*<sub>max</sub> (neat): 2958, 1727, 1602, 1453, 1317, 1269, 1108, 1070, 1025, 710 cm<sup>-1</sup>. HR-MS (ESI): C<sub>29</sub>H<sub>26</sub>F<sub>2</sub>O<sub>3</sub>P [M+H<sup>+</sup>] requires 587.1277, found 587.1274.

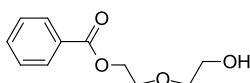
**(2R,3R,5R)-5-(((1,1'-Biphenyl)-4-ylmethoxy)(hydroxy)phosphoryl)methyl)-2-((benzoyloxy)methyl)-4,4-difluorotetrahydrofuran-3-yl benzoate (7.51e)**



The title compound **7.51e** (65.2 mg, 0.105 mmol, 42 % yield, yellow glass), was prepared according to general procedure **G** using the following reagents and solvents: (((2R,4R,5R)-4-(benzoyloxy)-5-((benzoyloxy)methyl)-3,3-difluorotetrahydrofuran-2-yl)methyl)phosphonic acid **7.50** (115 mg, 0.252 mmol), [1,1'-biphenyl]-4-ylmethanol (69.6 mg, 0.378 mmol), pyridine (0.6 mL), 2,2,2-trichloroacetonitrile (0.6 mL).  $[\alpha_D]_{589}^{20.3^\circ C}$  [c 1, CDCl<sub>3</sub>]: +111. <sup>1</sup>H NMR

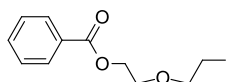
(400 MHz, CDCl<sub>3</sub>):  $\delta$  2.27-2.33 (m, 2H), 4.39-4.55 (m, 3H), 4.69 (dd,  $J$  = 3.2, 12.1 Hz, 1H), 5.11 (d,  $J$  = 6.2 Hz, 2H), 5.50 (dd,  $J$  = 4.9, 15.3 Hz, 1H), 6.41 (br.s, 1H), 7.28-7.53 (m, 14H), 7.58 (t,  $J$  = 7.6 Hz, 1H), 8.02 (t,  $J$  = 7.0 Hz, 4H). <sup>13</sup>C NMR (100 MHz, CDCl<sub>3</sub>):  $\delta$  25.1 (d,  $J$  = 141 Hz), 63.1, 67.0, 73.2 (dd,  $J$  = 17, 37 Hz), 75.6-75.9 (m), 79.9, 121.7 (HMBC), 127.1 (2C), 127.2 (2C), 127.4, 128.1 (2C), 128.3, 128.4 (2C), 128.6 (2C), 128.7 (2C), 129.4, 129.7 (2C), 130.0 (2C), 133.2, 134.8, 135.2 (d,  $J$  = 7 Hz), 140.5, 141.1, 164.9, 166.2. <sup>19</sup>F NMR (376 MHz, CDCl<sub>3</sub>):  $\delta$  -121.1 (d,  $J$  = 245 Hz, 1F), -116.0 (d,  $J$  = 245 Hz, 1F). <sup>31</sup>P NMR (162 MHz, CDCl<sub>3</sub>):  $\delta$  26.8.  $\nu_{\text{max}}$  (neat): 3032, 2891, 1726, 1602, 1489, 1452, 1317, 1268, 1212, 1178, 1107, 1070, 1025, 1005, 759, 710 cm<sup>-1</sup>. HR-MS (ESI): C<sub>33</sub>H<sub>30</sub>F<sub>2</sub>O<sub>8</sub>P [M+H<sup>+</sup>] requires 623.1641, found 623.1638.

### 2-(2-Hydroxyethoxy)ethyl benzoate (**7.55**)<sup>263</sup>



To a solution of 2,2'-oxydiethanol (8.10 mL, 85.0 mmol) and pyridine (2.53 mL, 31.3 mmol) in DCM (30 mL) at 0 °C was added benzoyl chloride (3.30 mL, 28.5 mmol) dropwise. The mixture was stirred for 20 hours at room temperature, after which time EtOAc (200 mL) was added. The organics were washed with water (3 x 100 mL) and brine (100 mL), dried over Na<sub>2</sub>SO<sub>4</sub> and concentrated under reduced pressure. The crude material was adsorbed onto diatomaceous earth and purified by flash chromatography, eluting under a gradient of EtOAc (30-40%) in cyclohexane, affording the title compound **7.55**<sup>263</sup> (4.19 g, 19.9 mmol, 70 % yield) as a transparent oil. <sup>1</sup>H NMR (400 MHz, CDCl<sub>3</sub>):  $\delta$  2.25 (t,  $J$  = 5.8 Hz, 1H), 3.65-3.68 (m, 2H), 3.75-3.78 (m, 2H), 3.84-3.87 (m, 2H), 4.50-4.52 (m, 2H), 7.44-7.47 (m, 2H), 7.55-7.59 (m, 1H), 8.06-8.08 (m, 2H). <sup>13</sup>C NMR (100 MHz, CDCl<sub>3</sub>):  $\delta$  61.8, 64.0, 69.2, 72.4, 128.4 (2C), 129.7 (2C), 130.0, 133.0, 166.6.

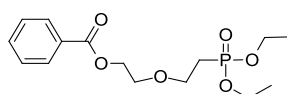
### 2-(2-Iodoethoxy)ethyl benzoate (**7.56**)



To a solution of 2-(2-hydroxyethoxy)ethyl benzoate **7.55** (1.50 g, 7.14 mmol) in DCM (35 mL) was added triphenylphosphine (2.81 g, 10.7 mmol), imidazole (1.46 g, 21.4 mmol) and iodine (2.54 g, 9.99 mmol) at room temperature. The mixture was stirred for 2 hours at the same temperature, after which the reaction mixture was filtered through a pad of Celite. The pad was washed with DCM (2 x 30 mL) and the combined filtrate was concentrated under reduced pressure. Cyclohexane (30 mL) and Et<sub>2</sub>O (30 mL) were added to the resulting

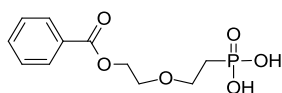
residue and the solids were filtered off over a pad of Celite, which was washed with Et<sub>2</sub>O (3 x 30 mL). The organics were concentrated, adsorbed onto diatomaceous earth and purified by flash chromatography, eluting in a mixture of TBME (5-15%) in cyclohexane to afford the title compound **7.56** (1.72 g, 5.37 mmol, 75 % yield) as a transparent oil. <sup>1</sup>H NMR (400 MHz, CDCl<sub>3</sub>): δ 3.29 (t, *J* = 6.8 Hz, 2H), 3.82 (t, *J* = 6.8 Hz, 2H), 3.84-3.87 (m, 2H), 4.49-4.52 (m, 2H), 7.44-7.48 (m, 2H), 7.58 (tt, *J* = 1.5, 6.8 Hz, 1H), 8.08-8.10 (m, 2H). <sup>13</sup>C NMR (100 MHz, CDCl<sub>3</sub>): δ 2.6, 64.0, 68.9, 71.9, 128.4 (2C), 129.7 (2C), 130.0, 133.0, 166.5. *v*<sub>max</sub> (neat): 2953, 2870, 1716, 1601, 1451, 1358, 1270, 1175, 1098, 1070, 1028, 710 cm<sup>-1</sup>. HR-MS (ESI): C<sub>11</sub>H<sub>14</sub>O<sub>3</sub> [M+H<sup>+</sup>] requires 320.9982, found 320.9982.

### 2-(2-(Diethoxyphosphoryl)ethoxy)ethyl benzoate (7.57)



A mixture of 2-(2-iodoethoxy)ethyl benzoate **7.56** (1.70 g, 5.31 mmol) and triethyl phosphite (5.57 ml, 31.9 mmol) was heated to 120 °C under an atmosphere of nitrogen for 20 hours. After this time the remaining triethyl phosphite was removed under high vacuum and the resulting oil was adsorbed onto diatomaceous earth and purified by reversed phase chromatography, eluting under a gradient of MeCN (20-40%) in modified water (formic acid) to afford the title compound **7.57** (1.66 g, 5.03 mmol, 95 % yield) as a transparent oil. <sup>1</sup>H NMR (400 MHz, CDCl<sub>3</sub>): δ 1.29 (t, *J* = 7.3 Hz, 6H), 2.12 (dt, *J* = 7.5, 18.9 Hz, 2H), 3.75-3.82 (m, 4H), 4.04-4.13 (m, 4H), 4.45-4.47 (m, 2H), 7.41-7.45 (m, 2H), 7.55 (tt, *J* = 1.2, 7.3 Hz, 1H), 8.04-8.06 (m, 2H). <sup>13</sup>C NMR (100 MHz, CDCl<sub>3</sub>): δ 16.4, 16.4, 26.6 (d, *J* = 140 Hz), 61.6, 61.7, 64.0, 65.2, 68.8, 128.3 (2C), 129.6 (2C), 130.0, 133.0, 166.5. <sup>31</sup>P NMR (162 MHz, CDCl<sub>3</sub>): δ 28.4. *v*<sub>max</sub> (neat): 3459 (br.), 2981, 2905, 1717, 1452, 1389, 1271, 1099, 1023, 957, 795, 712 cm<sup>-1</sup>. HR-MS (ESI): C<sub>15</sub>H<sub>24</sub>O<sub>6</sub>P [M+H<sup>+</sup>] requires 331.1305, found 331.1307.

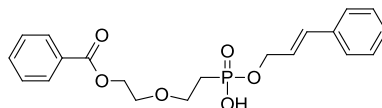
### (2-(2-(Benzoyloxy)ethoxy)ethyl)phosphonic acid (7.58)



The title compound **7.58** (1.00 g, 3.65 mmol, 100 % yield, straw coloured oil) was prepared in the same manner as **7.50** using the following reagents and solvents: 2-(2-(diethoxyphosphoryl)ethoxy)ethyl benzoate **7.57** (1.20 g, 3.63 mmol), MeCN (50 mL), TMSBr (4.71 mL, 36.3 mmol). The compound was purified by reversed phase

chromatography: 0-35% MeCN in modified water (formic).  $^1\text{H}$  NMR (400 MHz,  $\text{DMSO-}d_6$ ):  $\delta$  1.89 (dt,  $J = 7.8, 16.2$  Hz, 2H), 3.66 (dt,  $J = 7.7, 8.0$  Hz, 2H), 3.71-3.74 (m, 2H), 4.38-4.40 (m, 2H), 7.54 (t,  $J = 7.9$  Hz, 2H), 7.65-7.69 (m, 1H), 7.97-7.99 (m, 2H), 9.43 (br.s, 2H).  $^{13}\text{C}$  NMR (100 MHz,  $\text{DMSO-}d_6$ ):  $\delta$  28.9 (d,  $J = 134$  Hz), 64.0, 65.5, 67.8, 128.8 (2C), 129.2 (2C), 129.7, 133.3, 165.7.  $^{31}\text{P}$  NMR (162 MHz,  $\text{DMSO-}d_6$ ):  $\delta$  22.1.  $\nu_{\text{max}}$  (neat): 2879 (br.), 2280 (br.), 1715, 1601, 1452, 1386, 1272, 1175, 1096, 1001, 931, 709  $\text{cm}^{-1}$ . HR-MS (ESI):  $\text{C}_{11}\text{H}_{16}\text{O}_6\text{P}$  [ $\text{M}+\text{H}^+$ ] requires 275.0679, found 275.0677.

**(E)-2-(2-((Cinnamyloxy)(hydroxy)phosphoryl)ethoxy)ethyl benzoate (7.59)**



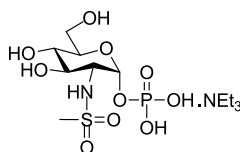
The title compound **7.59** (145 mg, 0.371 mmol, 51 % yield, brown glass), was prepared according to general procedure **G** using the following reagents and solvents: (2-(2-(benzyloxy)ethoxy)ethyl)phosphonic acid **7.58** (200 mg, 0.729 mmol), (*E*)-3-phenylprop-2-en-1-ol (0.141 mL, 1.094 mmol), pyridine (2 mL), 2,2,2-trichloroacetonitrile (2 mL). The compound was purified by reversed phase chromatography: 30-60% MeCN in modified water (formic).  $^1\text{H}$  NMR (400 MHz,  $\text{CDCl}_3$ ):  $\delta$  2.21 (dt,  $J = 6.9, 18.9$  Hz, 2H), 3.76-3.88 (m, 4H), 4.45-4.47 (m, 2H), 4.69 (t,  $J = 6.9$  Hz, 2H), 6.26 (dt,  $J = 5.9, 15.6$  Hz, 1H), 6.63 (d,  $J = 15.6$  Hz, 1H), 7.24-7.38 (m, 5H), 7.44 (t,  $J = 7.8$  Hz, 2H), 7.53-7.58 (m, 1H), 8.06-8.08 (m, 2H), 10.62 (br.s, 1H).  $^{13}\text{C}$  NMR (100 MHz,  $\text{CDCl}_3$ ):  $\delta$  27.4 (d,  $J = 142$  Hz), 64.0, 65.1, 65.8 (d,  $J = 5$  Hz), 68.8, 123.8 (d,  $J = 6$  Hz), 126.7 (2C), 128.1, 128.4 (2C), 128.6 (2C), 129.7 (2C), 130.0, 133.0, 133.6, 136.0, 166.5.  $^{31}\text{P}$  NMR (162 MHz,  $\text{CDCl}_3$ ):  $\delta$  31.3.  $\nu_{\text{max}}$  (neat): 2878, 1716, 1601, 1451, 1383, 1271, 1176, 1099, 995, 965, 711  $\text{cm}^{-1}$ . HR-MS (ESI):  $\text{C}_{20}\text{H}_{24}\text{O}_6\text{P}$  [ $\text{M}+\text{H}^+$ ] requires 391.1305, found 391.1310.

## 11.5 Synthesis of Compounds in Chapter 9

### General Procedure H for the Global Deprotection of Intermediates 9.19a-g

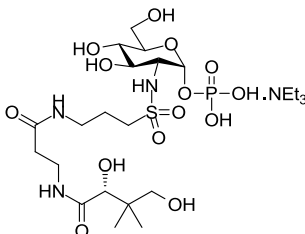
A mixture of the protected intermediate **9.19a-g** (0.079 mmol) and Pd/C (5 mg) in MeOH (9 mL) was stirred under 1 atmosphere of hydrogen at room temperature for 18 hours. The mixture was filtered through a pad of Celite, which was washed through with EtOAc (20 mL). The organics were concentrated under reduced pressure and the residue was dissolved in MeOH (5 mL). Triethylamine (22.0  $\mu$ L, 0.157 mmol) was added to quench the phosphate acid and the mixture was concentrated *in vacuo*. This material was dissolved in a mixture of MeOH-H<sub>2</sub>O-NEt<sub>3</sub> (7:3:1, 3 mL) then stirred at room temperature for 18 hours. After this time the reaction mixture was concentrated and dried azeotropically with toluene (5 x 3 mL). The material was lyophilised twice from water (5 mL) to afford the final compounds **9.1a-g** as off-white lyophilisates.

### (2R,3R,4R,5S,6R)-4,5-Dihydroxy-6-(hydroxymethyl)-3-(methylsulfonamido)tetrahydro-2H-pyran-2-yl dihydrogen phosphate, 1.3 triethylammonium salt (**9.1a**)



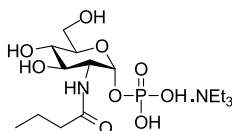
The title compound **9.1a** (40.5 mg, 0.092 mmol, 93 % yield, off-white lyophilisate), was prepared according to general procedure **H** using the following reagents and solvents: protected intermediate **9.19a** (63.8 mg, 0.099 mmol), Pd/C (6 mg), MeOH (10 mL), *then* triethylamine (28.0  $\mu$ L, 0.198 mmol), *then* MeOH-H<sub>2</sub>O-NEt<sub>3</sub> (7:3:1, 3 mL).  $[\alpha_D]_{589}^{21.3^\circ C}$  [*c* 0.2, D<sub>2</sub>O]: +61. <sup>1</sup>H NMR (400 MHz, MeOD-*d*<sub>4</sub>):  $\delta$  1.26 (t, *J* = 7.5 Hz, N(CH<sub>2</sub>CH<sub>3</sub>)<sub>3</sub>, 12H), 3.06-3.12 (m, N(CH<sub>2</sub>CH<sub>3</sub>)<sub>3</sub> & sulfonamide CH<sub>3</sub>, 11H), 3.32-3.39 (m, 2H), 3.36-3.71 (m, 2H), 3.83-3.92 (m, 2H), 5.55 (dd, *J* = 3.6, 6.7 Hz, 1H). *Exchangeable protons not observed.* <sup>13</sup>C NMR (100 MHz, MeOD-*d*<sub>4</sub>):  $\delta$  9.4 (N(CH<sub>2</sub>CH<sub>3</sub>)<sub>3</sub>), 42.5, 47.5 (N(CH<sub>2</sub>CH<sub>3</sub>)<sub>3</sub>), 59.9 (d, *J* = 8 Hz), 62.8, 72.3, 73.6, 74.3, 96.2 (d, *J* = 6 Hz). <sup>31</sup>P NMR (162 MHz, MeOD-*d*<sub>4</sub>):  $\delta$  -0.3.  $\nu_{\max}$  (neat): 3203 (br.), 2932, 1456, 1308, 1146, 1090, 1037, 931, 835, 762, 719 cm<sup>-1</sup>. HR-MS (ESI): C<sub>7</sub>H<sub>17</sub>NO<sub>10</sub>PS [M+H<sup>+</sup>] requires 338.0311, found 338.0319.

**(2R,3R,4R,5S,6R)-3-(3-(3-((R)-2,4-dihydroxy-3,3-dimethylbutanamido)propanamido)propylsulfonamido)-4,5-dihydroxy-6-(hydroxymethyl)tetrahydro-2H-pyran-2-yl dihydrogen phosphate, ditriethylammonium salt (9.1c)**



The title compound **9.1c** (25.0 mg, 0.037 mmol, 100 % yield, off-white lyophilisate), was prepared according to general procedure **H** using the following reagents and solvents: Protected intermediate **9.19c** (36.0 mg, 0.037 mmol), Pd/C (2.5 mg), MeOH (4 mL), *then* triethylamine (10.3  $\mu$ L, 0.074 mmol), *then* MeOH-H<sub>2</sub>O-NEt<sub>3</sub> (7:3:1, 3 mL).  $[\alpha_D]_{589}^{22.9^\circ C}$  [*c* 0.2, MeOH]: +44. <sup>1</sup>H NMR (400 MHz, MeOD-*d*<sub>4</sub>):  $\delta$  0.93 (s, 3H), 0.95 (s, 3H), 1.31 (t, *J* = 6.9 Hz, N(CH<sub>2</sub>CH<sub>3</sub>)<sub>3</sub>, 18H), 2.00-2.10 (m, 2H), 2.46 (t, *J* = 6.6 Hz, 2H), 3.16 (q, *J* = 6.9 Hz, N(CH<sub>2</sub>CH<sub>3</sub>)<sub>3</sub>, 12H), 3.17-3.40 (m, 7H), 3.49-3.52 (m, 3H), 3.66-3.72 (m, 2H), 3.83-3.91 (m, 2H), 3.94 (s, 1H), 5.54 (dd, *J* = 3.2, 6.6 Hz, 1H). *Exchangeable protons not observed.* <sup>13</sup>C NMR (100 MHz, MeOD-*d*<sub>4</sub>):  $\delta$  9.2 (N(CH<sub>2</sub>CH<sub>3</sub>)<sub>3</sub>), 20.9, 21.4, 25.0, 36.4, 36.6, 38.9, 40.4, 47.5 (N(CH<sub>2</sub>CH<sub>3</sub>)<sub>3</sub>), 52.5, 59.7 (d, *J* = 8 Hz), 62.7, 70.4, 72.4, 73.4, 74.3, 77.2, 96.5 (d, *J* = 7 Hz), 174.0, 176.0. <sup>31</sup>P NMR (162 MHz, MeOD-*d*<sub>4</sub>):  $\delta$  -0.4.  $\nu_{max}$  (neat): 3378 (br.), 2983, 2686, 1645, 1555, 1451, 1397, 1302, 1037, 943, 837, 729 cm<sup>-1</sup>. HR-MS (ESI): C<sub>18</sub>H<sub>37</sub>N<sub>3</sub>O<sub>14</sub>PS [M+H<sup>+</sup>] requires 582.1728, found 582.1708.

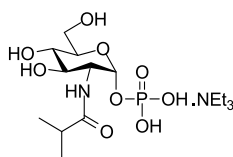
**(2R,3R,4R,5S,6R)-3-Butyramido-4,5-dihydroxy-6-(hydroxymethyl)tetrahydro-2H-pyran-2-yl dihydrogen phosphate, 1.4 triethylammonium salt (9.1d)<sup>264</sup>**



The title compound **9.1d** (33.0 mg, 0.077 mmol, 97 % yield, off-white lyophilisate), was prepared according to general procedure **H** using the following reagents and solvents: protected intermediate **9.19d** (50.0 mg, 0.079 mmol), Pd/C (5 mg), MeOH (9 mL), *then* triethylamine (22.0  $\mu$ L, 0.157 mmol), *then* MeOH-H<sub>2</sub>O-NEt<sub>3</sub> (7:3:1, 3 mL).  $[\alpha_D]_{589}^{21.1^\circ C}$  [*c* 0.25,

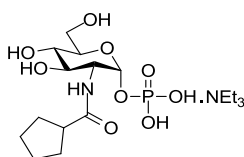
MeOH]: -206.  $^1\text{H}$  NMR (400 MHz, MeOD- $d_4$ ):  $\delta$  0.98 (t,  $J$  = 7.7 Hz, 3H), 1.29 (t,  $J$  = 7.3 Hz,  $\text{N}(\text{CH}_2\text{CH}_3)_3$ , 13H), 1.63-1.72 (m, 2H), 2.27 (t,  $J$  = 7.8 Hz, 2H), 3.10 (q,  $J$  = 7.3 Hz,  $\text{N}(\text{CH}_2\text{CH}_3)_3$ , 8H), 3.38 (dd,  $J$  = 9.3, 9.3 Hz, 1H), 3.67-3.73 (m, 2H), 3.83-3.93 (m, 2H), 3.98 (dt,  $J$  = 3.2, 10.6 Hz, 1H), 5.46 (dd,  $J$  = 3.2, 7.0 Hz, 1H). *Exchangeable protons not observed.*  $^{13}\text{C}$  NMR (100 MHz, MeOD- $d_4$ ):  $\delta$  9.5 ( $\text{N}(\text{CH}_2\text{CH}_3)_3$ ), 14.1, 20.3, 39.1, 47.5 ( $\text{N}(\text{CH}_2\text{CH}_3)_3$ ), 55.4 (d,  $J$  = 8 Hz), 62.9, 72.3, 73.4, 74.6, 95.4 (d,  $J$  = 6 Hz), 176.8.  $^{31}\text{P}$  NMR (162 MHz, MeOD- $d_4$ ):  $\delta$  -0.4.  $\nu_{\text{max}}$  (neat): 3265, 2928, 1645, 1547, 1455, 1393, 1029, 918, 837, 721  $\text{cm}^{-1}$ . HR-MS (ESI):  $\text{C}_{10}\text{H}_{21}\text{NO}_9\text{P}$  [ $\text{M}+\text{H}^+$ ] requires 330.0948, found 330.0947.

**(2R,3R,4R,5S,6R)-4,5-Dihydroxy-6-(hydroxymethyl)-3-isobutyramidotetrahydro-2H-pyran-2-yl dihydrogen phosphate, 1.4 triethylammonium salt (9.1e)**<sup>264</sup>



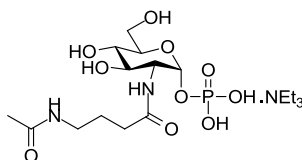
The title compound **9.1e** (41.1 mg, 0.095 mmol, 99 % yield, off-white lyophilisate), was prepared according to general procedure **H** using the following reagents and solvents: protected intermediate **9.19e** (61.0 mg, 0.096 mmol), Pd/C (6 mg), MeOH (10 mL), *then* triethylamine (27.0  $\mu\text{L}$ , 0.192 mmol), *then* MeOH- $\text{H}_2\text{O}$ - $\text{NEt}_3$  (7:3:1, 3 mL).  $[\alpha_D]_{589}^{21.1^\circ\text{C}}$  [c 0.25, MeOH]: +61.  $^1\text{H}$  NMR (400 MHz, MeOD- $d_4$ ):  $\delta$  1.14 (d,  $J$  = 6.9 Hz, 3H), 1.16 (d,  $J$  = 6.9 Hz, 3H), 1.29 (t,  $J$  = 7.3 Hz,  $\text{N}(\text{CH}_2\text{CH}_3)_3$ , 13H), 2.55 (sept,  $J$  = 6.9 Hz, 1H), 3.11 (q,  $J$  = 7.3 Hz,  $\text{N}(\text{CH}_2\text{CH}_3)_3$ , 8H), 3.39 (dd,  $J$  = 9.0, 9.8 Hz, 1H), 3.68-3.74 (m, 2H), 3.85 (dd,  $J$  = 2.3, 11.9 Hz, 1H), 3.88 (ddd,  $J$  = 2.3, 5.5, 9.8 Hz, 1H), 3.96 (dt,  $J$  = 3.4, 10.3 Hz, 1H), 5.46 (dd,  $J$  = 3.4, 7.1 Hz, 1H). *Exchangeable protons not observed.*  $^{13}\text{C}$  NMR (125 MHz, MeOD- $d_4$ ):  $\delta$  9.7 ( $\text{N}(\text{CH}_2\text{CH}_3)_3$ ), 20.0, 20.2, 36.4, 47.8 ( $\text{N}(\text{CH}_2\text{CH}_3)_3$ ), 55.4 (d,  $J$  = 8 Hz), 63.0, 72.5, 73.5, 74.8, 95.6 (d,  $J$  = 6 Hz), 181.0.  $^{31}\text{P}$  NMR (162 MHz, MeOD- $d_4$ ):  $\delta$  -0.7.  $\nu_{\text{max}}$  (neat): 3264 (br.), 2972, 1646, 1544, 1456, 1392, 1086, 1028, 917, 837, 720  $\text{cm}^{-1}$ . HR-MS (ESI):  $\text{C}_{10}\text{H}_{21}\text{NO}_9\text{P}$  [ $\text{M}+\text{H}^+$ ] requires 330.0948, found 330.0948.

**(2R,3R,4R,5S,6R)-3-(Cyclopentanecarboxamido)-4,5-dihydroxy-6-(hydroxymethyl)tetrahydro-2H-pyran-2-yl dihydrogen phosphate, 1.5 triethylamine salt (9.1f)**



The title compound **9.1f** (31.0 mg, 0.068 mmol, 100 % yield, off-white lyophilisate), was prepared according to general procedure **H** using the following reagents and solvents: protected intermediate **9.19f** (45.0 mg, 0.068 mmol), Pd/C (5 mg), MeOH (8 mL), *then* triethylamine (19.0  $\mu$ L, 0.136 mmol), *then* MeOH-H<sub>2</sub>O-NEt<sub>3</sub> (7:3:1, 3 mL).  $[\alpha_D]_{589}^{21.1^\circ C}$  [c 0.25, MeOH]: +6. <sup>1</sup>H NMR (400 MHz, MeOD-*d*<sub>4</sub>):  $\delta$  1.29 (t, *J* = 7.3 Hz, N(CH<sub>2</sub>CH<sub>3</sub>)<sub>3</sub>, 14H), 1.56-1.64 (m, 2H), 1.72-1.82 (m, 4H), 1.86-1.96 (m, 2H), 2.76 (quin, *J* = 7.7 Hz, 1H), 3.08-3.14 (m, N(CH<sub>2</sub>CH<sub>3</sub>)<sub>3</sub>, 9H) 3.38 (t, *J* = 9.5 Hz, 1H), 3.67-3.74 (m, 2H), 3.84-3.99 (m, 3H), 5.46 (dd, *J* = 2.6, 5.7 Hz, 1H). *Exchangeable protons not observed.* <sup>13</sup>C NMR (100 MHz, MeOD-*d*<sub>4</sub>):  $\delta$  9.4 (N(CH<sub>2</sub>CH<sub>3</sub>)<sub>3</sub>), 27.1 (2C), 31.3, 31.8, 46.5, 47.4 (N(CH<sub>2</sub>CH<sub>3</sub>)<sub>3</sub>), 55.6 (m), 62.9, 72.4, 73.6, 74.5, 95.3, 180.0. <sup>31</sup>P NMR (162 MHz, CDCl<sub>3</sub>):  $\delta$  -0.4.  $\nu_{\max}$  (neat): 3272 (br.), 2950, 1644, 1543, 1451, 1394, 1089, 1027, 938, 863, 837, 720 cm<sup>-1</sup>. HR-MS (ESI): C<sub>12</sub>H<sub>23</sub>NO<sub>9</sub>P [M+H<sup>+</sup>] requires 356.1105, found 356.1107.

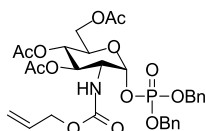
**(2R,3R,4R,5S,6R)-3-(4-Acetamidobutanamido)-4,5-dihydroxy-6-(hydroxymethyl)tetrahydro-2H-pyran-2-yl dihydrogen phosphate, 1.7 triethylammonium salt (9.1g)**



The title compound **9.1g** (38.6 mg, 0.079 mmol, 100 % yield, off-white lyophilisate), was prepared according to general procedure **H** using the following reagents and solvents: protected intermediate **9.19g** (55.0 mg, 0.079 mmol), Pd/C (5 mg), MeOH (9 mL), *then* triethylamine (22.0  $\mu$ L, 0.159 mmol), *then* MeOH-H<sub>2</sub>O-NEt<sub>3</sub> (7:3:1, 3 mL).  $[\alpha_D]_{589}^{21.1^\circ C}$  [c 0.25, MeOH]: +43. <sup>1</sup>H NMR (400 MHz, MeOD-*d*<sub>4</sub>):  $\delta$  1.30 (t, *J* = 6.9 Hz, N(CH<sub>2</sub>CH<sub>3</sub>)<sub>3</sub>, 15H), 1.80-1.88 (m, 2H), 1.96 (s, 3H), 2.32 (td, *J* = 2.5, 7.3 Hz, 2H), 3.13 (q, *J* = 6.9 Hz, N(CH<sub>2</sub>CH<sub>3</sub>)<sub>3</sub>, 10H), 3.23-3.27 (m, 2H), 3.39 (t, *J* = 9.3 Hz, 1H), 3.68-3.75 (m, 2H), 3.84-3.93 (m, 2H), 3.98 (dt, *J* = 3.5, 10.5 Hz, 1H), 5.47 (dd, *J* = 3.5, 7.3 Hz, 1H). *Exchangeable protons not observed.* <sup>13</sup>C NMR

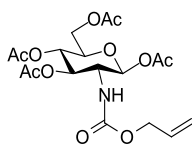
(100 MHz, CDCl<sub>3</sub>): δ 9.4 (N(CH<sub>2</sub>CH<sub>3</sub>)<sub>3</sub>), 22.6, 26.3, 34.3, 39.8, 47.6 (N(CH<sub>2</sub>CH<sub>3</sub>)<sub>3</sub>), 55.5 (d, *J* = 8 Hz), 62.9, 72.2, 73.3, 74.6, 95.4 (d, *J* = 5 Hz), 173.4, 176.0. <sup>31</sup>P NMR (162 MHz, CDCl<sub>3</sub>): δ -0.4. *v*<sub>max</sub> (neat): 3267 (br.), 2927, 1643, 1550, 1447, 1370, 1088, 1036, 918, 837, 721 cm<sup>-1</sup>. HR-MS (ESI): C<sub>12</sub>H<sub>24</sub>N<sub>2</sub>O<sub>10</sub>P [M+H<sup>+</sup>] requires 387.1163, found 387.1163.

**(2*R*,3*S*,4*R*,5*R*,6*R*)-2-(Acetoxymethyl)-5-(((allyloxy)carbonyl)amino)-6-((bis(benzyloxy)phosphoryl)oxy)tetrahydro-2*H*-pyran-3,4-diyl diacetate (9.4)**



To a solution of (2*R*,3*S*,4*R*,5*R*,6*S*)-2-(acetoxymethyl)-5-(((allyloxy)carbonyl)amino)-6-hydroxytetrahydro-2*H*-pyran-3,4-diyl diacetate **9.17** (2.78 g, 7.14 mmol) in THF (172 mL) at -78 °C was added LDA (2 M in THF/heptane/ethylbenzene, 3.93 mL, 7.85 mmol) dropwise. After stirring at the same temperature for 15 minutes, a solution of tetrabenzyl pyrophosphate (5.00 g, 9.28 mmol) in THF (65 mL) was added. The reaction was warmed to 0 °C and stirred for 2 hours. After this time, the mixture was diluted with DCM (300 mL), washed with aq. sat. NaHCO<sub>3</sub> (500 mL) and brine (500 mL), dried by passage through hydrophobic frit and concentrated under reduced pressure. The crude material was adsorbed onto diatomaceous earth and purified by flash chromatography, eluting under a gradient of EtOAc (30-45%) in cyclohexane to afford the title compound **9.4** (3.22 g, 4.95 mmol, 69 % yield) as a transparent gum. [*α*<sub>D</sub>]<sub>21.3°C</sub><sup>21.3°C</sup> [c 1, CDCl<sub>3</sub>]: +71. <sup>1</sup>H NMR (400 MHz, MeOD-*d*<sub>4</sub>): δ 1.97 (s, 3H), 2.01 (s, 3H), 2.03 (s, 3H), 3.95-4.02 (m, 2H), 4.07 (dt, *J* = 3.5, 11.0 Hz, 1H), 4.17 (dd, *J* = 4.0, 12.0 Hz, 1H), 4.43-4.50 (m, 1H), 4.52-4.58 (m, 1H), 5.07 (t, *J* = 9.5 Hz, 1H), 5.11-5.30 (m, 7H), 5.75 (dd, *J* = 3.5, 6.0, 1H), 5.84-5.95 (m, 1H), 7.38-7.42 (m, 10H). *Exchangeable protons not observed.* <sup>13</sup>C NMR (100 MHz, MeOD-*d*<sub>4</sub>): δ 20.6, 20.6, 20.6, 54.9 (d, *J* = 8 Hz), 62.7, 66.8, 69.7, 70.8, 71.2, 71.2, 71.3, 97.8 (d, *J* = 7 Hz), 117.9, 128.9, 129.1 (2C), 129.2 (2C), 129.5, 129.8 (2C), 129.9 (2C), 134.1, 136.9, 137.0, 158.1, 171.1, 171.9, 172.1. <sup>31</sup>P NMR (162 MHz, MeOD-*d*<sub>4</sub>): δ -2.8. *v*<sub>max</sub> (neat): 3253, 3065, 2955, 1745, 1722, 1538, 1366, 1221, 997, 948, 734, 696 cm<sup>-1</sup>. HR-MS (ESI): C<sub>30</sub>H<sub>37</sub>NO<sub>13</sub>P [M+H<sup>+</sup>] requires 650.1997, found 650.2004.

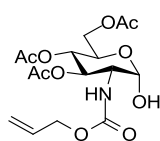
**(2*S*,3*R*,4*R*,5*S*,6*R*)-6-(Acetoxymethyl)-3-(((allyloxy)carbonyl)amino)tetrahydro-2*H*-pyran-2,4,5-triyl triacetate (9.5)**<sup>239,240</sup>



To a vigorously stirred solution of D-glucosamine hydrochloride (13.6 g, 63.2 mmol) in a 1M aqueous solution of NaOH (65 mL) was added 4-methoxybenzaldehyde (7.75 mL, 63.8 mmol). This mixture was stirred vigorously for 5 minutes, after which time it was cooled to 0 °C and stirring was continued for 1 hour. The solid was filtered and washed sequentially with water (2 x 200 mL), a 1:1 MeOH/Et<sub>2</sub>O mixture (200 mL) and then with Et<sub>2</sub>O (200 mL). The solid was dried azeotropically with toluene (5 x 100 mL) to afford crude (2*R*,3*R*,4*R*,5*S*,6*R*)-6-(hydroxymethyl)-3-((*E*)-(4-methoxybenzylidene)amino)tetrahydro-2*H*-pyran-2,4,5-triol **9.14**<sup>240</sup> (14.9 g), which was used in the next step without purification. To a solution of **9.14** (14.8 g, 49.8 mmol) in pyridine (80 mL) at 0 °C was added acetic anhydride (44 mL) and DMAP (608 mg, 4.98 mmol). This mixture was warmed to room temperature and stirred for 16 hours. The solution was poured into 500 mL of ice water and stirred for 5 minutes. The precipitate was filtered, washed with water (2 x 100 mL) and Et<sub>2</sub>O (2 x 100 mL) to afford crude (2*S*,3*R*,4*R*,5*S*,6*R*)-6-(acetoxymethyl)-3-((*E*)-(4-methoxybenzylidene)amino)tetrahydro-2*H*-pyran-2,4,5-triyl triacetate **9.15**<sup>240</sup> (19.8 g) as a white solid, after azeotropic drying with toluene (5 x 100 mL). A solution of **9.15** (19.6 g, 42.1 mmol) in acetone (100 mL) was heated to reflux, to which a 5M aqueous solution of HCl (11 mL) was added. After 5 minutes a thick white precipitate had formed, and the mixture was cooled to room temperature. The solid was filtered and washed with acetone (2 x 200 mL) and ether (2 x 200 mL) then dried azeotropically with toluene (5 x 500 mL) to afford the crude product (2*S*,3*R*,4*R*,5*S*,6*R*)-6-(acetoxymethyl)-3-aminotetrahydro-2*H*-pyran-2,4,5-triyl triacetate hydrochloride **9.16**<sup>240</sup> (14.4 g) that was used in the next step without purification. To a vigorously stirred biphasic mixture of **9.16** (14.3 g, 37.3 mmol) in DCM (100 mL) and water (100 mL) was added sodium bicarbonate (11.9 g, 142 mmol). This mixture was stirred until the solid had fully dissolved, after which allyl carbonochloridate (5.94 mL, 55.9 mmol) was added dropwise. This mixture was stirred vigorously for a further 2 hours. After this time, the layers were separated and the aqueous layer was extracted with DCM (2x 200 mL). The combined organics were washed with water (300 mL) and brine (300 mL) and then dried by passage through a hydrophobic frit. The crude material was

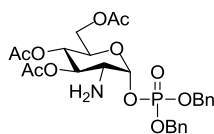
purified by flash chromatography, eluting under a gradient of EtOAc (20-70%) in cyclohexane to afford the title compound **9.5**<sup>239,240</sup> (13.8 g, 31.9 mmol, 50 % yield over 4 steps) as a white solid. <sup>1</sup>H NMR (400 MHz, CDCl<sub>3</sub>): δ 2.05 (s, 3H), 2.06 (s, 3H), 2.10 (s, 3H), 2.13 (s, 3H), 3.83 (ddd, *J* = 2.2, 4.5, 9.8 Hz, 1H), 3.95 (q, *J* = 9.6 Hz, 1H), 4.13 (dd, *J* = 2.2, 12.5 Hz, 1H), 4.30 (dd, *J* = 4.5, 12.5 Hz, 1H), 4.57 (d, *J* = 3.4 Hz, 2H), 4.96 (br.d, *J* = 9.6 Hz, 1H), 5.12 (t, *J* = 9.2 Hz, 1H), 5.18-5.31 (m, 3H), 5.72 (d, *J* = 8.7 Hz, 1H), 5.84-5.96 (m, 1H). <sup>13</sup>C NMR (100 MHz, CDCl<sub>3</sub>): δ 20.6, 20.6, 20.7, 20.9, 54.9, 61.7, 65.8, 68.0, 72.4, 72.8, 92.6, 117.7, 132.5, 155.5, 169.3, 169.3, 170.6, 170.8.

**(2R,3S,4R,5R,6S)-2-(acetoxymethyl)-5-(((allyloxy)carbonyl)amino)-6-hydroxytetrahydro-2H-pyran-3,4-diyl diacetate (9.17)**



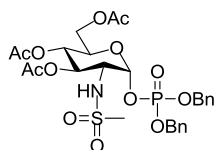
To a solution of (2*S*,3*R*,4*R*,5*S*,6*R*)-6-(acetoxymethyl)-3-(((allyloxy)carbonyl)amino) tetrahydro-2*H*-pyran-2,4,5-triyl triacetate **9.5**<sup>239,240</sup> (6.00 g, 13.9 mmol) in THF (30 mL) was added benzylamine (1.82 mL, 16.7 mmol) dropwise. This mixture was stirred at room temperature for 8 hours, after which time the solution was diluted with DCM (30 mL), washed sequentially with water (60 mL), aq. 1N HCl (60 mL), sat. aq. NaHCO<sub>3</sub> (60 mL) and brine (60 mL), then dried by passage through hydrophobic frit. The residue was subject to flash chromatography, eluting under a gradient of EtOAc (20-55%) in cyclohexane to afford the title compound **9.17** (3.59 g, 9.22 mmol, 66 % yield) as a transparent gum.  $[\alpha_D]_{589}^{212.2^\circ C}$  [c 1, CDCl<sub>3</sub>]: +168. <sup>1</sup>H NMR (400 MHz, MeOD-*d*<sub>4</sub>): δ 1.97 (s, 3H), 2.01 (s, 3H), 2.04 (s, 3H), 3.87 (dd, *J* = 3.4, 10.7 Hz, 1H), 4.06-4.09 (m, 1H), 4.21-4.26 (m, 2H), 4.49 (dd, *J* = 5.0, 13.6 Hz, 1H), 4.56 (ddt, *J* = 1.4, 5.4, 13.6 Hz, 1H), 5.00 (t, *J* = 9.8 Hz, 1H), 5.13 (d, *J* = 3.4 Hz, 1H), 5.17 (d, *J* = 10.3 Hz, 1H), 5.26-5.29 (m, 2H), 5.88-5.95 (m, 1H). *Exchangeable protons not observed.* <sup>13</sup>C NMR (100 MHz, MeOD-*d*<sub>4</sub>): δ 20.8 (2C), 20.9, 55.7, 63.8, 66.7, 68.4, 70.7, 72.8, 93.0, 117.7, 134.5, 158.4, 171.6, 172.3, 172.6.  $\nu_{\max}$  (neat): 3409, 2959, 1743, 1440, 1367, 1224, 1021, 776, 735 cm<sup>-1</sup>. HR-MS (ESI): C<sub>16</sub>H<sub>24</sub>NO<sub>10</sub> [M+H<sup>+</sup>] requires 390.1395, found 390.1396.

**(2R,3S,4R,5R,6R)-2-(acetoxymethyl)-5-amino-6-  
((bis(benzyloxy)phosphoryl)oxy)tetrahydro-2H-pyran-3,4-diyl diacetate (9.18)**



To a solution of (2R,3S,4R,5R,6R)-2-(acetoxymethyl)-5-(((allyloxy)carbonyl)amino)-6-((bis(benzyloxy)phosphoryl)oxy)tetrahydro-2H-pyran-3,4-diyl diacetate **9.4** (3.16 g, 4.86 mmol) in THF (100 mL) was added diethylamine (1.02 mL, 9.73 mmol) and Pd(Ph<sub>3</sub>P)<sub>4</sub> (0.281 g, 0.243 mmol). The solution was stirred at room temperature for 45 minutes, after which it was concentrated under reduced pressure. The residue was adsorbed onto diatomaceous earth and purified by flash chromatography, eluting under a gradient of MeOH (0-4%) in DCM to afford the title compound **9.18** (2.51 g, 4.44 mmol, 91 % yield) as a transparent oil.  $[\alpha_D]_{589}^{21.3^\circ C}$  [c 1, CDCl<sub>3</sub>]: +20. <sup>1</sup>H NMR (400 MHz, CDCl<sub>3</sub>): δ 1.07 (br.s, 2H), 1.99 (s, 3H), 2.01 (s, 3H), 2.06 (s, 3H), 2.97 (dt, *J* = 3.5, 9.8 Hz, 1H), 3.86 (dd, *J* = 2.2, 12.5 Hz, 1H), 4.04 (ddd, *J* = 2.2, 4.1, 10.0 Hz, 1H), 4.17 (dd, *J* = 4.1, 12.5 Hz, 1H), 4.96-5.17 (m, 6H), 5.69 (dd, *J* = 3.5, 5.9 Hz, 1H), 7.34-7.38 (m, 10H). <sup>13</sup>C NMR (100 MHz, CDCl<sub>3</sub>): δ 20.6 (2C), 20.8, 54.4 (d, *J* = 8 Hz), 61.5, 68.0, 69.6, 69.6, 69.8 (d, *J* = 5 Hz), 73.4, 98.7 (d, *J* = 7 Hz), 127.9 (2C), 128.0 (2C), 128.7 (2C), 128.7 (2C), 128.7, 128.8, 135.5 (d, *J* = 2 Hz), 135.5 (d, *J* = 2 Hz), 169.6, 170.5, 170.6. <sup>31</sup>P NMR (162 MHz, CDCl<sub>3</sub>): δ -1.8.  $\nu_{\max}$  (neat): 3035, 2956, 1742, 1456, 1366, 1222, 1122, 1010, 940, 741, 697 cm<sup>-1</sup>. HR-MS (ESI): C<sub>26</sub>H<sub>33</sub>NO<sub>11</sub>P [M+H<sup>+</sup>] requires 566.1791, found 566.1797.

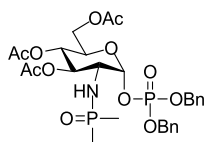
**(3S,4R,5R,6R)-2-(Acetoxymethyl)-6-((bis(benzyloxy)phosphoryl)oxy)-5-  
(methylsulfonamido)tetrahydro-2H-pyran-3,4-diyl diacetate (9.19a)**



To a solution of (2R,3S,4R,5R,6R)-2-(acetoxymethyl)-5-amino-6-((bis(benzyloxy)phosphoryl)oxy)tetrahydro-2H-pyran-3,4-diyl diacetate **9.18** (324 mg, 0.573 mmol) and Et<sub>3</sub>N (0.319 mL, 2.29 mmol) in DCM (4 mL) at 0 °C was added methanesulfonyl chloride (0.134 mL, 1.72 mmol). This solution was stirred at room temperature for 16 hours, after which time it was adsorbed directly onto diatomaceous earth and purified by flash chromatography, eluting under a gradient of EtOAc (50-60%) in cyclohexane, affording the

title compound **9.19a** (212 mg, 0.329 mmol, 57 % yield) as a transparent gum.  $[\alpha_D]_{589}^{21.3^\circ C}$  [c 1, CDCl<sub>3</sub>]: +89. <sup>1</sup>H NMR (400 MHz, CDCl<sub>3</sub>): δ 2.02 (s, 3H), 2.03 (s, 3H), 2.06 (s, 3H), 2.87 (s, 3H), 3.76-3.83 (m, 1H), 3.94 (dd, *J* = 2.2, 12.7 Hz, 1H), 4.09-4.13 (m, 1H), 4.18 (dd, *J* = 4.0, 12.7 Hz, 1H), 5.07-5.22 (m, 6H), 5.49 (dd, *J* = 3.0, 9.4 Hz, 1H), 5.74 (dd, *J* = 3.2, 6.2 Hz, 1H), 7.33-7.39 (m, 10 H). <sup>13</sup>C NMR (100 MHz, CDCl<sub>3</sub>): δ 20.5, 20.6, 20.7, 42.0, 55.6 (d, *J* = 8 Hz), 61.1, 67.8, 69.5, 69.9, 70.0, 70.1, 97.0 (d, *J* = 7 Hz), 128.0 (2C), 128.2 (2C), 128.7 (2C), 128.8 (2C), 128.8, 128.9, 135.2 (d, *J* = 7 Hz), 135.3, (d, *J* = 7 Hz), 169.3, 170.5 (2C). <sup>31</sup>P NMR (162 MHz, CDCl<sub>3</sub>): δ -2.7.  $\nu_{\max}$  (neat): 3146, 2958, 1745, 1456, 1366, 1325, 1218, 1154, 1122, 1009, 950, 734, 697 cm<sup>-1</sup>. HR-MS (ESI): C<sub>27</sub>H<sub>35</sub>NO<sub>13</sub>PS [M+H<sup>+</sup>] requires 644.1561, found 644.1562.

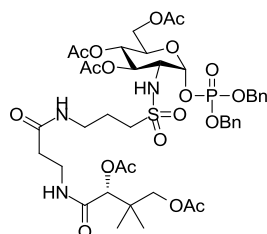
**(2R,3S,4R,5R,6R)-2-(Acetoxymethyl)-6-((bis(benzyloxy)phosphoryl)oxy)-5-((dimethylphosphoryl)amino)tetrahydro-2H-pyran-3,4-diyl diacetate (9.19b)**



To a solution of (2R,3S,4R,5R,6R)-2-(acetoxymethyl)-5-amino-6-((bis(benzyloxy)phosphoryl)oxy)tetrahydro-2H-pyran-3,4-diyl diacetate **9.18** (140 mg, 0.248 mmol) and N-methylmorpholine (82.0 μL, 0.743 mmol) in DCM (2 mL) at 0 °C was added dimethylphosphinic chloride (55.7 mg, 0.495 mmol) in DCM (1 mL) dropwise. This mixture was stirred at the same temperature for 10 minutes then at room temperature for 6 hrs. The mixture was concentrated under reduced pressure, adsorbed onto diatomaceous earth and purified by flash chromatography, eluting under a gradient of MeOH (0-2%) in DCM to afford the title compound **9.19b** (99.4 mg, 0.155 mmol, 63 % yield) as a transparent gum.  $[\alpha_D]_{589}^{21.8^\circ C}$  [c 1, CH<sub>2</sub>Cl<sub>2</sub>]: +130. <sup>1</sup>H NMR (400 MHz, CDCl<sub>3</sub>): δ 1.31 (d, *J* = 8.7 Hz, 3H), 1.34 (d, *J* = 8.7 Hz, 3H), 2.02 (s, 3H), 2.03 (s, 3H), 2.08 (s, 3H), 2.72 (t, *J* = 11.6 Hz, 1H), 3.52-3.62 (m, 1H), 3.93 (dd, *J* = 2.2, 12.4 Hz, 1H), 3.97-4.00 (m, 1H), 4.14 (dd, *J* = 4.0, 12.4 Hz, 1H), 5.05-5.16 (m, 6H), 5.71 (dd, *J* = 3.6, 6.2 Hz, 1H), 7.34-7.41 (m, 10H). <sup>13</sup>C NMR (100 MHz, CDCl<sub>3</sub>): δ 16.8 (d, *J* = 60 Hz), 17.6 (d, *J* = 60 Hz), 20.5, 20.6, 20.9, 52.9 (d, *J* = 8 Hz), 61.3, 67.7, 69.6, 69.9 (d, *J* = 2 Hz), 70.0 (d, *J* = 2 Hz), 71.1 (d, *J* = 4.5 Hz), 98.4 (dd, *J* = 2, 7 Hz), 128.1 (2C), 128.2 (2C), 128.8 (2C), 128.8 (2C), 128.9 (2C), 135.5 (d, *J* = 7 Hz), 135.4 (d, *J* = 7 Hz), 169.2, 170.5, 170.8. <sup>31</sup>P NMR (162 MHz, CDCl<sub>3</sub>): δ -2.2, 38.5.  $\nu_{\max}$  (neat): 3239, 1742, 1456, 1366,

1220, 1130, 1035, 1011, 941, 741, 698  $\text{cm}^{-1}$ . HR-MS (ESI):  $\text{C}_{28}\text{H}_{38}\text{NO}_{12}\text{P}_2$   $[\text{M}+\text{H}^+]$  requires 642.1864, found 642.1890.

**(2R,3S,4R,5R,6R)-2-(Acetoxymethyl)-6-((bis(benzyloxy)phosphoryl)oxy)-5-(3-(3-((R)-2,4-diacetoxy-3,3-dimethylbutanamido)propanamido)propylsulfonamido)tetrahydro-2H-pyran-3,4-diyl diacetate (9.19c)**

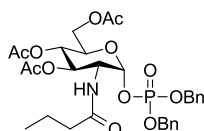


A suspension of (2R,3S,4R,5R,6R)-2-(acetoxymethyl)-5-(3-azidopropylsulfonamido)-6-((bis(benzyloxy)phosphoryl)oxy)tetrahydro-2H-pyran-3,4-diyl diacetate **9.27** (162 mg, 0.227 mmol), acetic acid (78.0  $\mu\text{l}$ , 1.36 mmol) and zinc (149 mg, 2.27 mmol) in DCM (12 mL) was stirred at room temperature for 1 hour. The mixture was filtered, washed with sat.  $\text{NaHCO}_3$  and brine, then concentrated under reduced pressure to afford the crude amine intermediate **9.28** (160 mg).

To a solution of (R)-3-(2,4-diacetoxy-3,3-dimethylbutanamido)propanoic acid **9.21** (78.0 mg, 0.256 mmol) and DIPEA (122  $\mu\text{l}$ , 0.699 mmol) in DMF (1.4 mL) was added HATU (106 mg, 0.280 mmol). This mixture was stirred at room temperature for 15 minutes, after which a solution of the crude amine **9.28** (160 mg) in DMF (0.5 mL) was added. This mixture was stirred for a further 45 minutes. EtOAc was added (5 mL) and the organics were washed with sat  $\text{NaHCO}_2$  and brine, dried over  $\text{MgSO}_4$  and concentrated. The crude material was adsorbed onto diatomaceous earth and purified by flash chromatography, eluting under a gradient of MeOH (0-4%) in DCM to afford the title compound **9.19c** (110 mg, 0.113 mmol, 50 % yield) as a transparent gum.  $[\alpha_D]_{589}^{22.9^\circ\text{C}}$  [c 0.4, MeOH]: +51.  $^1\text{H}$  NMR (400 MHz,  $\text{CDCl}_3$ ):  $\delta$  1.04 (s, 3H), 1.07 (s, 3H), 1.87-1.93 (m, 2H), 2.01 (s, 3H), 2.05 (s, 3H), 2.07 (s, 3H), 2.11 (s, 3H), 2.16 (s, 3H), 2.39 (t,  $J = 5.6$  Hz, 2H), 3.00 (t,  $J = 7.7$  Hz, 2H), 3.19-3.26 (m, 1H), 3.35-3.43 (m, 1H), 3.47-3.58 (m, 2H), 3.81-3.91 (m, 3H), 3.96-4.00 (m, 1H), 4.03 (d,  $J = 11.0$  Hz, 1H), 4.15 (dd,  $J = 4.0, 12.6$  Hz, 1H), 4.81 (d,  $J = 9.3$  Hz, 1H), 4.90 (s, 1H), 5.08-5.18 (m, 6H), 5.74 (dd,  $J = 3.4, 6.4$  Hz, 1H), 6.76 (t,  $J = 5.6$  Hz, 1H), 6.98 (t,  $J = 5.8$  Hz, 1H), 7.38-7.46 (m, 10H).  $^{13}\text{C}$  NMR (100 MHz,  $\text{CDCl}_3$ ):  $\delta$  20.5, 20.6, 20.7, 20.8, 20.8, 21.4, 23.8, 34.9, 35.3, 37.1,

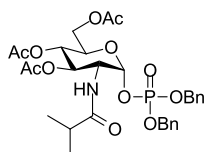
37.2, 52.0, 55.4 (d,  $J = 8$  Hz), 61.1, 67.5, 69.3, 69.7 (2C), 70.1 (d,  $J = 5$  Hz), 70.5 (d,  $J = 6$  Hz), 77.2, 96.7 (d,  $J = 6$  Hz), 128.0 (2C), 128.0 (2C), 128.8 (2C), 129.0 (2C), 129.0, 129.3, 135.1, 135.1, 168.1, 169.1, 170.2, 170.4, 171.0, 171.0, 172.1.  $^{31}\text{P}$  NMR (162 MHz,  $\text{CDCl}_3$ ):  $\delta$  -2.3.  $\nu_{\text{max}}$  (neat): 3302 (br.), 2962, 1743, 1660, 1535, 1456, 1375, 1234, 1122, 1037, 955, 743, 698  $\text{cm}^{-1}$ . HR-MS (ESI):  $\text{C}_{42}\text{H}_{59}\text{N}_3\text{O}_{19}\text{P}$  [ $\text{M}+\text{H}^+$ ] requires 972.3196, found 972.3187.

**(2R,3S,4R,5R,6R)-2-(Acetoxymethyl)-6-((bis(benzyloxy)phosphoryl)oxy)-5-butynamidotetrahydro-2H-pyran-3,4-diyl diacetate (9.19d)**



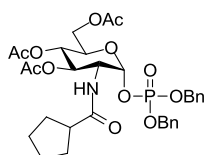
To a solution of (2R,3S,4R,5R,6R)-2-(acetoxymethyl)-5-amino-6-((bis(benzyloxy)phosphoryl)oxy)tetrahydro-2H-pyran-3,4-diyl diacetate **9.18** (100 mg, 0.177 mmol) and triethylamine (49.0  $\mu\text{L}$ , 0.354 mmol) in DCM (3 mL) at 0  $^{\circ}\text{C}$  was added butyryl chloride (28.0  $\mu\text{L}$ , 0.265 mmol). The mixture was warmed to room temperature and stirred for 3 hours after which time DCM (10 mL) was added. The organics were washed with sat.  $\text{NaHCO}_3$  and brine, dried by passage through a hydrophobic frit and concentrated under reduced pressure. The crude material was adsorbed onto diatomaceous earth and purified by flash chromatography, eluting under a gradient of EtOAc (30-70%) in cyclohexane to afford the title compound **9.19d** (102 mg, 0.160 mmol, 91 % yield) as a viscous transparent oil.  $[\alpha_D]_{589}^{21.8^{\circ}\text{C}}$  [c 1,  $\text{CH}_2\text{Cl}_2$ ]: +253.  $^1\text{H}$  NMR (400 MHz,  $\text{CDCl}_3$ ):  $\delta$  0.84 (t,  $J = 7.32$  Hz, 3H), 1.44-1.55 (m, 2H), 1.85-1.95 (m, 2H), 2.01 (s, 3H), 2.03 (s, 3H), 2.04 (s, 3H), 3.94 (dd,  $J = 2.3, 12.5$  Hz, 1H), 4.02 (ddd,  $J = 2.3, 3.8, 9.6$  Hz, 1H), 4.15 (dd,  $J = 3.8, 12.5$  Hz, 1H), 4.39-4.45 (m, 1H), 5.03-5.21 (m, 6H), 5.65-5.70 (m, 2H), 7.35-7.42 (m, 10H).  $^{13}\text{C}$  NMR (100 MHz,  $\text{CDCl}_3$ ):  $\delta$  13.6, 18.8, 20.5, 20.6, 20.6, 38.2, 51.6 (d,  $J = 8$  Hz), 61.3, 67.4, 69.7, 69.8-69.9 (m, 2C), 70.1, 96.4 (d,  $J = 7$  Hz), 128.0 (2C), 128.1 (2C), 128.8 (2C), 128.8 (2C), 128.9 (2C), 135.2 (d,  $J = 7$  Hz), 135.3 (d,  $J = 7$  Hz), 169.1, 170.5, 171.1, 173.0.  $^{31}\text{P}$  NMR (162 MHz,  $\text{CDCl}_3$ ):  $\delta$  -2.4.  $\nu_{\text{max}}$  (neat): 3281, 2963, 1744, 1677, 1543, 1366, 1222, 1008, 950, 737, 696  $\text{cm}^{-1}$ . HR-MS (ESI):  $\text{C}_{30}\text{H}_{39}\text{NO}_{12}\text{P}$  [ $\text{M}+\text{H}^+$ ] requires 636.2204, found 636.2226.

**(2R,3S,4R,5R,6R)-2-(Acetoxymethyl)-5-amino-6-((bis(benzyloxy)phosphoryl)oxy)tetrahydro-2H-pyran-3,4-diyl diacetate (9.19e)**



The title compound **9.19e** (83.1 mg, 0.131 mmol, 74 % yield, viscous transparent oil) was prepared in the same manner as **9.19d** using the following reagents and solvents: (2R,3S,4R,5R,6R)-2-(acetoxymethyl)-5-amino-6-((bis(benzyloxy)phosphoryl)oxy)tetrahydro-2H-pyran-3,4-diyl diacetate **9.18** (100 mg, 0.177 mmol), triethylamine (49.0  $\mu$ L, 0.354 mmol), isobutyryl chloride (28.0  $\mu$ L, 0.265 mmol), DCM (3 mL). The compound was purified by flash chromatography eluting under a gradient of 30-70% EtOAc in cyclohexane.  $[\alpha_D]_{589}^{21.8^\circ C}$  [c 1, CH<sub>2</sub>Cl<sub>2</sub>]: -63. <sup>1</sup>H NMR (400 MHz, CDCl<sub>3</sub>):  $\delta$  1.00 (d,  $J$  = 7.1 Hz, 6H), 2.01 (s, 3H), 2.03 (s, 3H), 2.05 (s, 3H), 2.06-2.13 (m, 1H), 3.94 (dd,  $J$  = 2.4, 12.5 Hz, 1H), 4.02 (ddd,  $J$  = 2.4, 3.9, 9.6 Hz, 1H), 4.16 (dd,  $J$  = 3.9, 12.5 Hz, 1H), 4.38-4.44 (m, 1H), 5.04-5.23 (m, 6H), 5.63 (d,  $J$  = 9.3 Hz, 1H), 5.69 (dd,  $J$  = 3.0, 5.7 Hz, 1H), 7.34-7.43 (m, 10H). <sup>13</sup>C NMR (100 MHz, CDCl<sub>3</sub>):  $\delta$  19.0, 19.4, 20.5, 20.6, 20.6, 35.3, 51.1 (d,  $J$  = 8 Hz), 61.3, 67.3, 69.7, 69.8 (d,  $J$  = 6 Hz), 69.9 (d,  $J$  = 6 Hz), 70.2, 96.4 (d,  $J$  = 7 Hz), 128.0 (2C), 128.1 (2C), 128.8 (2C), 128.8 (2C), 128.9 (2C), 135.2 (d, 7 Hz), 135.3 (d,  $J$  = 7 Hz), 169.1, 170.5, 171.1, 176.9. <sup>31</sup>P NMR (162 MHz, CDCl<sub>3</sub>):  $\delta$  -2.4.  $\nu_{max}$  (neat): 3282, 2967, 1747, 1682, 1536, 1366, 1275, 1226, 1035, 956, 744, 697 cm<sup>-1</sup>. HR-MS (ESI): C<sub>30</sub>H<sub>39</sub>NO<sub>12</sub>P [M+H<sup>+</sup>] requires 636.2204, found 636.2229.

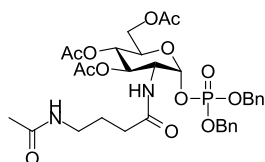
**(2R,3S,4R,5R,6R)-2-(Acetoxymethyl)-6-((bis(benzyloxy)phosphoryl)oxy)-5-(cyclopentanecarboxamido)tetrahydro-2H-pyran-3,4-diyl diacetate (9.19f)**



The title compound **9.19f** (80.9mg, 0.122 mmol, 84 % yield, viscous transparent oil) was prepared in the same manner as **9.19d** using the following reagents and solvents: (2R,3S,4R,5R,6R)-2-(acetoxymethyl)-5-amino-6-((bis(benzyloxy)phosphoryl)oxy)tetrahydro-2H-pyran-3,4-diyl diacetate **9.18** (82.5 mg, 0.146 mmol), triethylamine (41.0  $\mu$ L, 0.292 mmol), cyclopentanecarbonyl chloride (27.0  $\mu$ L, 0.219 mmol), DCM (2.5 mL). The

compound was purified by flash chromatography eluting under a gradient of 30-50% EtOAc in cyclohexane.  $[\alpha_D]_{589}^{21.1^\circ C}$  [c 0.5, CH<sub>2</sub>Cl<sub>2</sub>]: +67. <sup>1</sup>H NMR (400 MHz, CDCl<sub>3</sub>): δ 1.47-1.57 (m, 3H), 1.60-1.73 (m, 5H), 2.00 (s, 3H), 2.01 (s, 3H), 2.03 (s, 3H), 2.17-2.24 (m, 1H), 3.94 (dd, *J* = 2.0, 12.5 Hz, 1H), 4.01 (ddd, *J* = 2.0, 4.1, 10.1 Hz, 1H), 4.15 (dd, *J* = 4.1, 12.5 Hz, 1H), 4.39-4.43 (m, 1H), 5.03-5.22 (m, 6H), 5.64-5.70 (m, 2H), 7.34-7.41 (m, 10H). <sup>13</sup>C NMR (100 MHz, CDCl<sub>3</sub>): δ 20.5, 20.6 (2C), 25.6, 25.8, 29.6, 30.6, 45.5, 51.6 (d, *J* = 8 Hz), 61.3, 67.3, 69.7, 69.8-69.9 (m, 2C), 70.2, 96.5 (d, *J* = 7 Hz), 128.0 (2C), 128.0 (2C), 128.7 (2C), 128.8 (2C), 128.9, 128.9, 135.5 (d, *J* = 7 Hz), 135.4 (d, *J* = 7 Hz), 169.1, 170.5, 171.1, 176.1. <sup>31</sup>P NMR (162 MHz, CDCl<sub>3</sub>): δ -2.4.  $\nu_{\max}$  (neat): 3279, 2959, 1745, 1673, 1524, 1366, 1225, 1151, 1035, 998, 953, 740, 697 cm<sup>-1</sup>. HR-MS (ESI): C<sub>32</sub>H<sub>41</sub>NO<sub>12</sub>P [M+H<sup>+</sup>] requires 662.2361, found 662.2345.

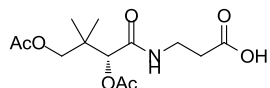
**(2*R*,3*S*,4*R*,5*R*,6*R*)-5-(4-Acetamidobutanamido)-2-(acetoxymethyl)-6-((bis(benzyloxy)phosphoryl)oxy)tetrahydro-2*H*-pyran-3,4-diyl diacetate (9.19g)**



To a solution of 4-acetamidobutanoic acid (39.5 mg, 0.272 mmol) in DMF (2.2 mL) was added DIPEA (86.0 μL, 0.495 mmol) and COMU (127 mg, 0.297 mmol). The mixture was stirred at room temperature for 10 minutes, after which time (2*R*,3*S*,4*R*,5*R*,6*R*)-2-(acetoxymethyl)-5-amino-6-((bis(benzyloxy)phosphoryl)oxy)tetrahydro-2*H*-pyran-3,4-diyl diacetate **9.18** (140 mg, 0.248 mmol) in DMF (2.2 mL) was added. this mixture was stirred at room temperature for 1 hour after which time it was diluted with EtOAc (20 mL), washed with water (20 mL) and brine (20 mL), dried over Na<sub>2</sub>SO<sub>4</sub> and concentrated. The crude material was adsorbed onto diatomaceous earth and purified by flash chromatography, eluting under a gradient of MeOH (0-2%) in DCM to afford the title compound **9.19g** (126 mg, 0.182 mmol, 73 % yield) as a collapsed white foam.  $[\alpha_D]_{589}^{21.8^\circ C}$  [c 1, CH<sub>2</sub>Cl<sub>2</sub>]: +34. <sup>1</sup>H NMR (400 MHz, CDCl<sub>3</sub>): δ 1.67-1.74 (m, 2H), 1.95 (s, 3H), 1.99-2.04 (m, 8H), 2.05 (s, 3H), 3.06-3.14 (m, 1H), 3.20-3.28 (m, 1H), 3.94-4.03 (m, 2H), 4.15 (dd, *J* = 3.9, 12.2 Hz, 1H), 4.36-4.43 (m, 1H), 5.06-5.20 (m, 6H), 5.70 (dd, *J* = 3.3, 6.4 Hz, 1H), 5.97 (d, *J* = 9.0 Hz, 1H), 6.21-6.25 (m, 1H), 7.34-7.42 (m, 10H). <sup>13</sup>C NMR (100 MHz, CDCl<sub>3</sub>): δ 20.5, 20.6, 20.7, 23.2, 24.7, 33.1, 38.6, 51.8 (d, *J* = 8 Hz), 61.3, 67.4, 69.7, 70.0-70.1 (m, 3C), 96.0 (d, *J* = 6 Hz), 128.0 (2C), 128.1 (2C), 128.8 (2C), 128.9 (2C), 129.0, 129.0, 135.1 (d, *J* = 7 Hz), 135.3 (d, *J* = 6 Hz), 169.1,

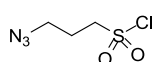
170.3, 170.5, 171.1, 172.8.  $^{31}\text{P}$  NMR (162 MHz,  $\text{CDCl}_3$ ):  $\delta$  -2.5.  $\nu_{\text{max}}$  (neat): 3281, 2954, 1748, 1653, 1546, 1367, 1228, 1036, 955, 742, 698  $\text{cm}^{-1}$ . HR-MS (ESI):  $\text{C}_{32}\text{H}_{42}\text{N}_2\text{O}_{13}\text{P}$  [ $\text{M}+\text{H}^+$ ] requires 693.2419, found 693.2472.

**(R)-3-(2,4-Diacetoxy-3,3-dimethylbutanamido)propanoic acid (9.21)**<sup>243</sup>



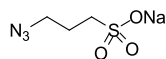
To a suspension of D-pantothenic acid sodium salt (530 mg, 2.20 mmol) in acetic anhydride (10 mL) at 0 °C was added catalytic iodine (38.0 mg, 0.150 mmol). This mixture was stirred at 0 °C for 2 hours then at room temperature for 72 hours. The solvent was removed under reduced pressure (azeotroping with toluene) to afford an oil that was dissolved in DCM and washed with 1 M  $\text{Na}_2\text{S}_2\text{O}_3$  solution. The organics were dried by passage through a hydrophobic frit, then concentrated *in vacuo* to afford the intermediate anhydride (**9.26**). The crude material was dissolved in a mixture of THF and water (2:1, 8 mL) and stirred at room temperature for 16 hours. After removal of the solvents under reduced pressure and azeotropic drying with toluene (3 x 10 mL), the title compound **9.21**<sup>243</sup> (395 mg, 1.30 mmol, 59 % yield) was obtained as a viscous yellow oil.  $^1\text{H}$  NMR (400 MHz,  $\text{CDCl}_3$ ):  $\delta$  1.05 (s, 3H), 1.08 (s, 3H), 2.08 (s, 3H), 2.15 (s, 3H), 2.61 (t,  $J$  = 5.8 Hz, 2H), 3.48-3.54 (m, 1H), 3.56-3.63 (m, 1H), 3.85 (d,  $J$  = 11.0 Hz, 1H), 4.05 (d,  $J$  = 11.0 Hz, 1H), 4.98 (s, 1H), 6.11 (br.s, 1H), 6.70 (t,  $J$  = 6.1 Hz, 1H).  $^{13}\text{C}$  NMR (100 MHz,  $\text{CDCl}_3$ ):  $\delta$  20.7, 20.8 (2C), 21.3, 33.4, 34.5, 37.2, 69.3, 76.9, 168.2, 169.9, 171.1, 176.1.

**3-Azidopropane-1-sulfonyl chloride (9.22)**<sup>244</sup>



To a suspension of 3-azidopropane-1-sulfonic acid sodium salt **9.24** (700 mg, 3.72 mmol) in toluene (10.5 mL) was added  $\text{PCl}_5$  (1.55 g, 7.44 mmol). This mixture was heated to reflux for 2 hours. After this time, the mixture cooled to room temperature and the volatiles were removed under reduced pressure. The residue was dissolved in DCM, washed with water and brine and dried over a hydrophobic frit. The crude material was adsorbed onto diatomaceous earth and purified by flash chromatography, eluting under a gradient of EtOAc (0-10%) in cyclohexane to afford the title compound **9.22**<sup>244</sup> (547 mg, 2.98 mmol, 80 % yield) as a transparent oil.  $^1\text{H}$  NMR (400 MHz,  $\text{CDCl}_3$ ):  $\delta$  2.28-2.35 (m, 2H), 3.61 (t,  $J$  = 6.1 Hz, 2H), 3.78-3.82 (m, 2H).  $^{13}\text{C}$  NMR (100 MHz,  $\text{CDCl}_3$ ):  $\delta$  24.3, 48.6, 62.4.

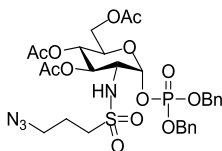
### 3-Azidopropane-1-sulfonic acid sodium salt (**9.24**)<sup>244</sup>



To a stirred solution of sodium azide (1.00 g, 15.4 mmol) in water (7.2 mL) was added a solution of 1,2-oxathiolane 2,2-dioxide (1.35 mL, 15.4 mmol) in acetone (7.2 mL). This mixture was stirred at room temperature for 18 hours after which the solution was concentrated to dryness *in vacuo*. The resulting solid was filtered, washed with ether (20 mL), acetone (20 mL), then dried azeotropically with toluene (4 x 20 mL) to afford the title compound **9.24**<sup>244</sup> (1.93 g, 10.2 mmol, 67 % yield) as a white solid. <sup>1</sup>H NMR (400 MHz, DMSO-*d*<sub>6</sub>): δ 1.84 (quin, *J* = 7.1 Hz, 2H), 2.48-2.52 (m, 2H), 3.42 (t, *J* = 7.1 Hz, 2H). <sup>13</sup>C NMR (100 MHz, DMSO-*d*<sub>6</sub>): δ 25.9, 48.2, 49.9.

### (2*R*,3*S*,4*R*,5*R*,6*R*)-2-(Acetoxymethyl)-5-(3-azidopropylsulfonamido)-6

### ((bis(benzyloxy)phosphoryl)oxy)tetrahydro-2*H*-pyran-3,4-diyl diacetate (**9.27**)



To a solution of (2*R*,3*S*,4*R*,5*R*,6*R*)-2-(acetoxymethyl)-5-amino-6-((bis(benzyloxy)phosphoryl)oxy)tetrahydro-2*H*-pyran-3,4-diyl diacetate **9.18** (285 mg, 0.504 mmol) and NEt<sub>3</sub> (0.281 mL, 2.02 mmol) in DCM (3.2 mL) was added 3-azidopropane-1-sulfonyl chloride **9.22** (139 mg, 0.756 mmol) in DCM (1.6 mL) at 0 °C. This solution was stirred at room temperature for 1 hour, after which it was adsorbed onto diatomaceous earth and purified by flash chromatography, eluting under a gradient of EtOAc (20-50%) in cyclohexane to afford the title compound **9.27** (296 mg, 0.416 mmol, 82 % yield) as a viscous transparent oil. [ $\alpha_D$ ]<sub>589</sub><sup>22.9°C</sup> [c 0.2, MeOH]: +78. <sup>1</sup>H NMR (400 MHz, CDCl<sub>3</sub>): δ 1.96-2.01 (m, 2H), 2.03 (s, 3H), 2.05 (s, 3H), 2.10 (s, 3H), 2.98-3.03 (m, 2H), 3.43 (t, *J* = 6.6 Hz, 2H), 3.77 (tt, *J* = 3.2, 9.8 Hz, 1H), 3.91 (dd, *J* = 2.2, 12.3 Hz, 1H), 4.02-4.06 (m, 1H), 4.17 (dd, *J* = 4.1, 12.3 Hz, 1H), 4.94 (d, *J* = 9.8 Hz, 1H), 5.08-5.19 (m, 6H), 5.75 (dd, *J* = 3.2, 5.7 Hz, 1H), 7.36-7.43 (m, 10H). <sup>13</sup>C NMR (100 MHz, CDCl<sub>3</sub>): δ 20.5, 20.6, 20.7, 23.5, 49.5, 51.7, 55.7 (d, *J* = 8 Hz), 61.1, 67.6, 69.5, 69.7, 70.1-70.2, (m, 2C), 97.0 (d, *J* = 7 Hz), 128.1 (2C), 128.1 (2C), 128.8 (2C), 128.9 (2C), 128.9, 129.0, 135.2-135.3 (m, 2C), 169.2, 170.5, 170.7. <sup>31</sup>P NMR (162 MHz, CDCl<sub>3</sub>): δ -2.4.  $\nu_{\max}$  (neat): 2967, 2099, 1745, 1456, 1366, 1218, 1121, 1037, 997, 952, 739, 697 cm<sup>-1</sup>. HR-MS (ESI): C<sub>29</sub>H<sub>38</sub>N<sub>4</sub>O<sub>13</sub>PS [M+H<sup>+</sup>] requires 713.1888, found 713.1919.

## 12. References

- (1) World Health Organisation Tuberculosis Fact Sheet No. 4.
- (2) World Health Organisation Global Tuberculosis Report 2014.
- (3) Paulson, T. *Nature* **2015**, 502 (7470), S2.
- (4) Migliori, G. B.; Dheda, K.; Centis, R.; Mwaba, P.; Bates, M.; O'Grady, J.; Hoelscher, M.; Zumla, A. *Trop. Med. Int. Heal.* **2010**, 15 (9), 1052.
- (5) Pawlowski, A.; Jansson, M.; Sköld, M.; Rottenberg, M. E.; Källenius, G. *PLoS Pathog.* **2012**, 8 (2), 1.
- (6) World Health Organisation Global Tuberculosis Report 2012.
- (7) Elder, N. C. *Arch. Fam. Med.* **1992**, 1 (1), 91.
- (8) Russell, D. G. *Nat. Rev. Mol. Cell Bio.* **2001**, 2 (8), 1.
- (9) Russell, D. G.; Barry, C. E.; Flynn, J. L. *Science*. **2010**, 328 (5980), 852.
- (10) Koul, A.; Arnoult, E.; Lounis, N.; Guillemont, J.; Andries, K. *Nature* **2011**, 469 (7331), 483.
- (11) Davis, C. E. *Chest* **1985**, 88 (5), 726.
- (12) Mitchison, D. A. *Int. J. Tuberc. Lung Dis.* **2000**, 4 (9), 796.
- (13) Mikusova, K.; Slayden, R. a.; Besra, G. S.; Brennan, P. J. *Antimicrob. Agents Chemother.* **1995**, 39 (11), 2484.
- (14) Zhang, Y. *Annu. Rev. Pharmacol. Toxicol.* **2005**, 45 (1), 529.
- (15) Zumla, A.; Nahid, P.; Cole, S. T. *Nat. Rev. Drug Discov.* **2013**, 12 (5), 388.
- (16) Dorman, S. E.; Chaisson, R. E. *Nat. Med.* **2007**, 13 (3), 295.
- (17) Koenig, R. *Science*. **2008**, 319 (5865), 894.
- (18) World Health Organization Tuberculosis Fact Sheet No. 104.
- (19) Andries, K.; Verhasselt, P.; Guillemont, J.; Neefs, J.; Winkler, H.; Gestel, J. Van; Timmerman, P.; Zhu, M.; Lee, E.; Williams, P.; Chaffoy, D. De; Huitric, E.; Hoffner, S.; Cambau, E.; Truffot-pernot, C.; Lounis, N.; Jarlier, V. *Science*. **2005**, 307 (5707), 223.
- (20) Cohen, J. *Science*. **2013**, 339 (12), 130.
- (21) Matsumoto, M.; Hashizume, H.; Tomishige, T.; Kawasaki, M.; Tsubouchi, H.; Sasaki, H.; Shimokawa, Y.; Komatsu, M. *PLoS Med.* **2006**, 3 (11), 2131.
- (22) Xavier, A.; Lakshmanan, M. *J Pharmacol. Pharmacother.* **2014**, 5 (3), 222.
- (23) Sharma, U. *Expert Opin. Drug Discov.* **2011**, 6 (11), 1171.

- (24) Dartois, V.; Barry, C. E. *Bioorg. Med. Chem. Lett.* **2013**, *23* (17), 4741.
- (25) Sarathy, J. P.; Dartois, V.; Lee, E. J. D. *Pharmaceuticals* **2012**, *5* (11), 1210.
- (26) Cooper, C. B. *J. Med. Chem.* **2013**, *56* (20), 7755.
- (27) Manjunatha, U. H.; Smith, P. W. *Bioorg. Med. Chem.* **2014**, *23* (16), 5087.
- (28) Swinney, D. C.; Anthony, J. *Nat. Rev. Drug Discov.* **2011**, *10* (7), 507.
- (29) Cole, S. T.; Brosch, R.; Parkhill, J.; Garnier, T.; Churcher, C.; Harris, D.; Gordon, S. V.; Eiglmeier, K.; Gas, S.; Barry, C. E.; Tekaia, F.; Badcock, K.; Basham, D.; Brown, D.; Chillingworth, T.; Connor, R.; Davies, R.; Devlin, K.; Feltwell, T.; Gentles, S.; Hamlin, N.; Holroyd, S.; Hornsby, T.; Jagels, K.; Krogh, A.; McLean, J.; Moule, S.; Murphy, L.; Oliver, K.; Osborne, J.; Quail, M. A.; Rajandream, M. A.; Rogers, J.; Rutter, S.; Seeger, K.; Skelton, J.; Squares, R.; Squares, S.; Sulston, J. E.; Taylor, K.; Whitehead, S.; Barrell, B. G. *Nature* **1998**, *393* (6685), 537.
- (30) Payne, D. J.; Gwynn, M. N.; Holmes, D. J.; Pompliano, D. L. *Nat. Rev. Drug Discov.* **2007**, *6* (1), 29.
- (31) Rozwarski, D. A.; Grant, G. A.; Barton, D. H. R.; Jr, W. R. J.; Sacchettini, J. C. *Science*. **1993**, *279* (5347), 19.
- (32) Baulard, A. R.; Betts, J. C.; Engohang-ndong, J.; Quan, S.; Patrick, J.; Loch, C.; Besra, G. S.; Wood, G.; State, C.; Collins, F. *J. Biol. Chem.* **2000**, *275* (36), 28326.
- (33) Belanger, A. E.; Besra, G. S.; Ford, M. E.; Mikusova, K.; Belisle, J. T.; Brennan, P. J.; Inamint, J. M. *Proc. Natl. Acad. Sci. USA* **1996**, *93* (21), 11919.
- (34) Feng, Z. *Antimicrob. Agents Chemother.* **2003**, *47* (1), 283.
- (35) Mdluli, K.; Spigelman, M. *Curr. Opin. Pharm.* **2006**, *6* (5), 459.
- (36) Stocks, M.; Alcaraz, L.; Griffen, E. *On Medicinal Chemistry*; Sci-ink Ltd, 2007.
- (37) Lipinski, C. A.; Lombardo, F.; Dominy, B. W.; Feeney, P. J. *Adv. Drug Deliv. Rev.* **1997**, *23* (1), 3.
- (38) Gleeson, M. P. *J. Med. Chem.* **2008**, *51* (4), 817.
- (39) Hughes, J. D.; Blagg, J.; Price, D. A.; Bailey, S.; Decrescenzo, G. A.; Devraj, R. V.; Ellsworth, E.; Fobian, Y. M.; Gibbs, M. E.; Gilles, R. W.; Greene, N.; Huang, E.; Krieger-Burke, T.; Loesel, J.; Wager, T.; Whiteley, L.; Zhang, Y. *Bioorg. Med. Chem. Lett.* **2008**, *18* (17), 4872.
- (40) Leeson, P. D.; Springthorpe, B. *Nat. Rev. Drug Discov.* **2007**, *6* (11), 881.
- (41) Gleeson, M. P.; Hersey, A.; Montanari, D.; Overington, J. *Nat. Rev. Drug Discov.* **2011**, *10* (3), 197.
- (42) Hann, M. M. *Med. Chem. Commun.* **2011**, *2* (5), 349.
- (43) Hann, M. M.; Keserü, G. M. *Nat. Rev. Drug Discov.* **2012**, *11* (5), 355.

- (44) van de Waterbeemd, H.; Smith, D. A.; Beaumont, K.; Walker, D. K. *J. Med. Chem.* **2001**, *44* (9), 1313.
- (45) Zhao, H. *Drug Discov. Today* **2011**, *16* (3-4), 158.
- (46) Kola, I.; Landis, J. *Nat. Rev. Drug Discov.* **2004**, *3* (8), 711.
- (47) Waring, M. J. *Expert Opin. Drug Discov.* **2010**, *5* (3), 235.
- (48) Young, R. J. *Top. Med. Chem.* **2015**, *9*, 1.
- (49) Kerns, E.; Di, L. *Drug-Like Properties: Concepts, Structure Design and Methods, from ADME to Toxicity Optimization*; Academic Press, 2008.
- (50) Valkó, K.; Bevan, C.; Reynolds, D. *Anal. Chem.* **1997**, *69* (11), 2022.
- (51) Hill, A. P.; Young, R. J. *Drug Discov. Today* **2010**, *15* (15-16), 648.
- (52) Wenlock, M. C.; Austin, R. P.; Barton, P.; Davis, A. M.; Leeson, P. D. *J. Med. Chem.* **2003**, *46* (7), 1250.
- (53) Hansch, C.; Björkroth, J. P.; Leo, A. *J. Pharm. Sci.* **1987**, *76* (9), 663.
- (54) Ritchie, T. J.; Macdonald, S. J. F. *Drug Discov. Today* **2009**, *14* (21-22), 1011.
- (55) Ritchie, T. J.; Macdonald, S. J. F.; Young, R. J.; Pickett, S. D. *Drug Discov. Today* **2011**, *16* (3-4), 164.
- (56) Lovering, F.; Bikker, J.; Humblet, C. *J. Med. Chem.* **2009**, *52* (21), 6752.
- (57) Lovering, F. *Med. Chem. Commun.* **2013**, *4* (3), 515.
- (58) Manallack, D. T. *Perspect. Med. Chem.* **2008**, *1*, 25.
- (59) Kerns, E. H.; Di, L.; Petusky, S.; Farris, M.; Ley, R.; Jupp, P. *J. Pharm. Sci.* **2004**, *93* (6), 1440.
- (60) Ghuman, J.; Zunszain, P. A.; Petitpas, I.; Bhattacharya, A. A.; Otagiri, M.; Curry, S. *J. Mol. Biol.* **2005**, *353* (1), 38.
- (61) Jamieson, C.; Moir, E. M.; Rankovic, Z.; Wishart, G. *J. Med. Chem.* **2006**, *49* (17), 5029.
- (62) Kell, D. B.; Dobson, P. D.; Oliver, S. G. *Drug Discov. Today* **2011**, *16* (15-16), 704.
- (63) Sugano, K.; Kansy, M.; Artursson, P.; Avdeef, A.; Bendels, S.; Di, L.; Ecker, G. F.; Faller, B.; Fischer, H.; Gerebtzoff, G.; Lennernaes, H.; Senner, F. *Nat. Rev. Drug Discov.* **2010**, *9* (8), 597.
- (64) Kubinyi, H. *Prog. Drug Res.* **1979**, *23*, 97.
- (65) Young, R. J.; Green, D. V. S.; Luscombe, C. N.; Hill, A. P. *Drug Discov. Today* **2011**, *16* (17-18), 822.
- (66) Waring, M. J. *Bioorg. Med. Chem. Lett.* **2009**, *19* (10), 2844.

- (67) Riley, R. J.; McGinnity, D. F.; Austin, R. P. *Drug Metab. Dispos.* **2005**, *33* (9), 1304.
- (68) Tandon, M.; O'Donnell, M.-M.; Porte, A.; Vensel, D.; Yang, D.; Palma, R.; Beresford, A.; Ashwell, M. A. *Bioorg. Med. Chem. Lett.* **2004**, *14* (7), 1709.
- (69) Lewis, D. F. V.; Lake, B. G.; Dickins, M. J. *Enzym. Inhib. Med. Chem.* **2007**, *22* (1), 1.
- (70) Fermini, B.; Fossa, A. *Nat. Rev. Drug Discov.* **2003**, *2* (6), 439.
- (71) Waring, M. J.; Johnstone, C. *Bioorg. Med. Chem. Lett.* **2007**, *17* (6), 1759.
- (72) Fletcher, S. R.; Burkamp, F.; Blurton, P.; Cheng, S. K. F.; Clarkson, R.; O'Connor, D.; Spinks, D.; Tudge, M.; van Niel, M. B.; Patel, S.; Chapman, K.; Marwood, R.; Shephard, S.; Bentley, G.; Cook, G. P.; Bristow, L. J.; Castro, J. L.; Hutson, P. H.; MacLeod, A. M. *J. Med. Chem.* **2002**, *45* (2), 492.
- (73) Bowes, J.; Brown, A. J.; Hamon, J.; Jarolimek, W.; Sridhar, A.; Waldron, G.; Whitebread, S. *Nat. Rev. Drug Discov.* **2012**, *11* (12), 909.
- (74) Hopkins, A. L.; Keserü, G. M.; Leeson, P. D.; Rees, D. C.; Reynolds, C. H. *Nat. Rev. Drug Discov.* **2014**, *13* (2), 105.
- (75) Hopkins, A. L.; Groom, C. R.; Alex, A. *Drug Discov. Today* **2004**, *9* (10), 430.
- (76) Mortenson, P. N.; Murray, C. W. *J. Comput. Aided Mol. Des.* **2011**, *25* (7), 663.
- (77) Shultz, M. D. *Bioorg. Med. Chem. Lett.* **2013**, *23* (21), 5980.
- (78) Bembenek, S. D.; Tounge, B. A.; Reynolds, C. H. *Drug Discov. Today* **2009**, *14* (5-6), 278.
- (79) Carr, R. A. E.; Congreve, M.; Murray, C. W.; Rees, D. C. *Drug Discov. Today* **2005**, *10* (14), 10.
- (80) Manuscript in Preparation, Whitehurst, B. C.; Burley, G. A.; Young, R. J. *et al.*
- (81) Teague, S.; Davis, A.; Leeson, P.; Oprea, T. *Angew. Chem. Int. Ed.* **1999**, *38* (24), 3743.
- (82) Adapted from the "GSK Lead Quality Panel".
- (83) O'Shea, R.; Moser, H. E. *J. Med. Chem.* **2008**, *51* (10), 2871.
- (84) Faller, M.; Niederweis, M.; Schulz, G. E. *Science.* **2004**, *303* (5661), 1189.
- (85) Makarov, V.; Manina, G.; Mikusova, K.; Möllmann, U.; Ryabova, O.; Saint-Joanis, B.; Dhar, N.; Pasca, M. R.; Buroni, S.; Lucarelli, A. P.; Milano, A.; De Rossi, E.; Belanova, M.; Bobovska, A.; Dianiskova, P.; Kordulakova, J.; Sala, C.; Fullam, E.; Schneider, P.; McKinney, J. D.; Brodin, P.; Christophe, T.; Waddell, S.; Butcher, P.; Albrethsen, J.; Rosenkrands, I.; Brosch, R.; Nandi, V.; Bharath, S.; Gaonkar, S.; Shandil, R. K.; Balasubramanian, V.; Balganes, T.; Tyagi, S.; Grosset, J.; Riccardi, G.; Cole, S. T. *Science.* **2009**, *324* (5928), 801.
- (86) Manina, G.; Pasca, M. R.; Buroni, S.; Rossi, E. De; Riccardi, G. *Curr. Med. Chem.* **2010**, *17* (27), 3099.

- (87) Makarov, V.; Lechartier, B.; Zhang, M.; Sar, A. M. Van Der; Raadsen, S. A.; Hartkoorn, R. C.; Ryabova, O. B.; Vocat, A.; Decosterd, L. A.; Widmer, N.; Buclin, T.; Bitter, W.; Andries, K.; Pojer, F.; Dyson, P. J.; Cole, S. T. *EMBO Mol. Med.* **2014**, *6* (3), 372.
- (88) Alderwick, L. J.; Lloyd, G. S.; Lloyd, A. J.; Lovering, A. L.; Eggeling, L.; Besra, G. S. *Glycobiology* **2011**, *21* (4), 410.
- (89) Lee, R. E. B.; Li, W.; Chatterjee, D.; Lee, R. E. *Glycobiology* **2005**, *15* (2), 139.
- (90) Kolly, G. S.; Boldrin, F.; Sala, C.; Dhar, N.; Hartkoorn, R. C.; Ventura, M.; Serafini, A.; McKinney, J. D.; Manganelli, R.; Cole, S. T. *Mol. Microbiol.* **2014**, *92* (1), 194.
- (91) Mikusová, K.; Huang, H.; Yagi, T.; Vereecke, D.; Haeze, W. D.; Michael, S.; Brennan, P. J.; Mcneil, M. R.; Crick, C.; Holsters, M.; Scherman, M. S.; Crick, D. C. *J. Bacteriol.* **2005**, *187* (23), 8020.
- (92) Brečik, M.; Centárová, I.; Mukherjee, R.; Kolly, G. S.; Huszár, S.; Bobovská, A.; Kilacsková, E.; Mokošová, V.; Svetlíková, Z.; Šarkan, M.; Neres, J.; Korduláková, J.; Cole, S. T.; Mikušová, K. *ACS Chem. Biol.* **2015**, *10* (7), 1631.
- (93) Neres, J.; Pojer, F.; Molteni, E.; Chiarelli, L. R.; Dhar, N.; Boy-Röttger, S.; Buroni, S.; Fullam, E.; Degiacomi, G.; Lucarelli, A. P.; Read, R. J.; Zanoni, G.; Edmondson, D. E.; De Rossi, E.; Pasca, M. R.; McKinney, J. D.; Dyson, P. J.; Riccardi, G.; Mattevi, A.; Cole, S. T.; Binda, C. *Sci. Transl. Med.* **2012**, *4* (150), 1.
- (94) Crellin, P. K.; Brammananth, R.; Coppel, R. L. *PLoS Pathog.* **2011**, *6* (2), 1.
- (95) Grover, S.; Alderwick, L. J.; Mishra, A. K.; Krumbach, K.; Marienhagen, J.; Eggeling, L.; Bhatt, A.; Besra, G. S. *J. Biol. Chem.* **2014**, *289* (9), 6178.
- (96) Meniche, X.; de Sousa-d'Auria, C.; Van-der-Rest, B.; Bhamidi, S.; Huc, E.; Huang, H.; De Paepe, D.; Tropis, M.; McNeil, M.; Daffé, M.; Houssin, C. *Microbiology* **2008**, *154* (8), 2315.
- (97) Makarov, V.; Cole, S. T.; Mollmann, U. WO07134625, 2007.
- (98) Trefzer, C.; Rengifo-Gonzalez, M.; Hinner, M. J.; Schneider, P.; Makarov, V.; Cole, S. T.; Johnsson, K. *J. Am. Chem. Soc.* **2010**, *132* (39), 13663.
- (99) Trefzer, C.; Henrieta, S.; Buroni, S.; Bobovska, A.; Nenci, S.; Molteni, E.; Pojer, F.; Pasca, M. R.; Makarov, V.; Cole, S. T.; Riccardi, G. *J. Am. Chem. Soc.* **2012**, *134* (2), 912.
- (100) Landge, S.; Mullick, A.; Nagalapur, K.; Neres, J.; Subbulakshmi, V.; Murugan, K.; Ghosh, A.; Sadler, C.; Fellows, M.; Humnabadkar, V.; Mahadevaswamy, J.; Vachaspati, P.; Sharma, S.; Kaur, P.; Mallya, M.; Rudrapatna, S.; Awasthy, D.; Sambandamurthy, V.; Pojer, F.; Cole, S.; Balganes, T.; Ugarkar, B.; Balasubramanian; Bandodkar, B.; Panda, M.; Ramachandran, V. *Bioorg. Med. Chem.* **2015**, *23* (24), 7694.
- (101) Magnet, S.; Hartkoorn, R. C.; Székely, R.; Pató, J.; Triccas, J. a; Schneider, P.; Szántai-Kis, C.; Orfi, L.; Chambon, M.; Banfi, D.; Bueno, M.; Turcatti, G.; Kéri, G.; Cole, S. T. *Tuberculosis* **2010**, *90* (6), 354.

- (102) Christophe, T.; Jackson, M.; Jeon, H. K.; Fenistein, D.; Contreras-Dominguez, M.; Kim, J.; Genovesio, A.; Carralot, J.-P.; Ewann, F.; Kim, E. H.; Lee, S. Y.; Kang, S.; Seo, M. J.; Park, E. J.; Skovierová, H.; Pham, H.; Riccardi, G.; Nam, J. Y.; Marsollier, L.; Kempf, M.; Joly-Guillou, M.-L.; Oh, T.; Shin, W. K.; No, Z.; Nehrbass, U.; Brosch, R.; Cole, S. T.; Brodin, P. *PLoS Pathog.* **2009**, *5* (10), 1.
- (103) Strauss, M. J. *Ind. Eng. Chem. Prod. Res. Dev.* **1979**, *18* (3), 158.
- (104) Manina, G.; Bellinzoni, M.; Pasca, M. R.; Neres, J.; Milano, A.; Ribeiro, A. L. D. J. L.; Buroni, S.; Skovierová, H.; Dianišková, P.; Mikušová, K.; Marák, J.; Makarov, V.; Giganti, D.; Haouz, A.; Lucarelli, A. P.; Degiacomi, G.; Piazza, A.; Chiarelli, L. R.; De Rossi, E.; Salina, E.; Cole, S. T.; Alzari, P. M.; Riccardi, G. *Mol. Microbiol.* **2010**, *77* (5), 1172.
- (105) Makarov, V.; Neres, J.; Hartkoorn, R. C.; Ryabova, O. B.; Kazakova, E.; Šarkan, M.; Huszár, S.; Piton, J.; Kolly, G. S.; Vocat, A.; Conroy, T. M.; Mikušová, K.; Cole, S. T. *Antimicrob. Agents Chemother.* **2015**, *59* (8), 4446.
- (106) Hameed, S.; Shinde, V.; Bathula, C.; Humnabadkar, V.; Kumar, N.; Reddy, J.; Panduga, V.; Sharma, S.; Ambady, A.; Hegde, N.; Whiteaker, J.; McLaughlin, R. E.; Gardner, H.; Madhavapeddi, P.; Ramachandran, V.; Kaur, P.; Narayan, A.; Guptha, S.; Awasthy, D.; Narayan, C.; Mahadevaswamy, J.; Vishwas, K. G.; Ahuja, V.; Srivastava, A.; Prabhakar, K. R.; Bharath, S.; Kale, R.; Ramaiah, M.; Choudhury, N. R.; Sambandamurthy, V. K.; Solapure, S.; Iyer, P. S.; Narayanan, S.; Chatterji, M. *J. Med. Chem.* **2013**, *56* (23), 9701.
- (107) Naik, M.; Humnabadkar, V.; Tantry, S. J.; Panda, M.; Narayan, A.; Guptha, S.; Panduga, V.; Manjrekar, P.; Jena, L. K.; Koushik, K.; Shanbhag, G.; Jatheendranath, S.; Manjunatha, M. R.; Gorai, G.; Bathula, C.; Rudrapatna, S.; Achar, V.; Sharma, S.; Ambady, A.; Hegde, N.; Mahadevaswamy, J.; Kaur, P.; Sambandamurthy, V. K.; Awasthy, D.; Narayan, C.; Ravishankar, S.; Madhavapeddi, P.; Reddy, J.; Prabhakar, K.; Saralaya, R.; Chatterji, M.; Whiteaker, J.; McLaughlin, B.; Chiarelli, L. R.; Riccardi, G.; Pasca, M. R.; Binda, C.; Neres, J.; Dhar, N.; Signorino-Gelo, F.; McKinney, J. D.; Ramachandran, V.; Shandil, R.; Tommasi, R.; Iyer, P. S.; Narayanan, S.; Hosagrahara, V.; Kavanagh, S.; Dinesh, N.; Ghorpade, S. R. *J. Med. Chem.* **2014**, *57* (12), 5419.
- (108) Panda, M.; Ramachandran, S.; Ramachandran, V.; Shirude, P. S.; Humnabadkar, V.; Nagalapur, K.; Sharma, S.; Kaur, P.; Guptha, S.; Narayan, A.; Mahadevaswamy, J.; Ambady, A.; Hegde, N.; Rudrapatna, S. S.; Hosagrahara, V. P.; Sambandamurthy, V. K.; Raichurkar, A. *J. Med. Chem.* **2014**, *57* (11), 4761.
- (109) Shirude, P. S.; Shandil, R. K.; Manjunatha, M. R.; Sadler, C.; Panda, M.; Panduga, V.; Reddy, J.; Saralaya, R.; Nanduri, R.; Ambady, A.; Ravishankar, S.; Sambandamurthy, V. K.; Humnabadkar, V.; Jena, L. K.; Suresh, R. S.; Srivastava, A.; Prabhakar, K. R.; Whiteaker, J.; McLaughlin, R. E.; Sharma, S.; Cooper, C. B.; Mdluli, K.; Butler, S.; Iyer, P. S.; Narayanan, S.; Chatterji, M. *J. Med. Chem.* **2014**, *57* (13), 5728.
- (110) Chatterji, M.; Shandil, R.; Manjunatha, M. R.; Solapure, S.; Ramachandran, V.; Kumar, N.; Saralaya, R.; Panduga, V.; Reddy, J.; K R, P.; Sharma, S.; Sadler, C.; Cooper, C. B.; Mdluli, K.; Iyer, P. S.; Narayanan, S.; Shirude, P. S. *Antimicrob. Agents Chemother.* **2014**, *58* (9), 5325.

- (111) Hartkoorn, R. C.; Chiarelli, L. R.; Gadupudi, R.; Pasca, M. R.; Mori, G.; Venturelli, A.; Savina, S.; Makarov, V.; Kolly, G. S.; Molteni, E.; Binda, C.; Dhar, N.; Ferrari, S.; Brodin, P.; Delorme, V.; Luisa, A.; Lopes, D. J.; Farina, D.; Saxena, P.; Pojer, F.; Carta, A.; Luciani, R.; Porta, A.; Zanoni, G.; Rossi, E. De; Costi, M. P.; Riccardi, G. *ACS Chem. Biol.* **2015**, *10* (3), 705.
- (112) Wang, F.; Sambandan, D.; Halder, R.; Wang, J.; Batt, S. M.; Weinrick, B.; Ahmad, I.; Yang, P.; Zhang, Y.; Kim, J.; Hassani, M.; Huszar, S.; Trefzer, C.; Ma, Z.; Kaneko, T.; Mdluli, K. E.; Franzblau, S.; Chatterjee, a. K.; Johnson, K.; Mikusova, K.; Besra, G. S.; Futterer, K.; Jacobs, W. R.; Schultz, P. G. *Proc. Natl. Acad. Sci. USA* **2013**, *110* (27), 15848.
- (113) Batt, S. M.; Jabeen, T.; Bhowruth, V.; Quill, L.; Lund, P. a; Eggeling, L.; Alderwick, L. J.; Fütterer, K.; Besra, G. S. *Proc. Natl. Acad. Sci. USA* **2012**, *109* (28), 11354.
- (114) Jankute, M.; Byng, C. V; Alderwick, L. J.; Besra, G. S. *Glycoconj. J.* **2014**, *31* (6-7), 475.
- (115) Johnson, K. a.; Goody, R. S. *Biochemistry* **2011**, *50* (39), 8264.
- (116) Anderson, A. C. *Chem. Biol.* **2003**, *10* (9), 787.
- (117) Ballell, L.; Bates, R. H.; Young, R. J.; Alvarez-Gomez, D.; Alvarez-Ruiz, E.; Barroso, V.; Blanco, D.; Crespo, B.; Escribano, J.; González, R.; Lozano, S.; Huss, S.; Santos-Villarejo, A.; Martín-Plaza, J. J.; Mendoza, A.; Rebollo-Lopez, M. J.; Remuñan-Blanco, M.; Lavandera, J. L.; Pérez-Herran, E.; Gamo-Benito, F. J.; García-Bustos, J. F.; Barros, D.; Castro, J. P.; Cammack, N. *ChemMedChem* **2013**, *8* (2), 313.
- (118) Batt, S. M.; Cacho Izquierdo, M.; Castro Pichel, J.; Stubbs, C. J.; Vela-Glez Del Peral, L.; Pérez-Herrán, E.; Dhar, N.; Mouzon, B.; Rees, M.; Hutchinson, J. P.; Young, R. J.; McKinney, J. D.; Barros Aguirre, D.; Ballell, L.; Besra, G. S.; Argyrou, A. *ACS Infect. Dis.* **2015**, Just Accepted Manuscript; DOI: 10.1021/acsinfecdis.
- (119) GSK Unpublished data.
- (120) *GSK Chrom Log D7.4 calculator; available in-house.*
- (121) Giordanetto, F.; Wållberg, A.; Cassel, J.; Ghosal, S.; Kossenjans, M.; Yuan, Z.-Q.; Wang, X.; Liang, L. *Bioorg. Med. Chem. Lett.* **2012**, *22* (21), 6665.
- (122) Hansen, T. V; Wu, P.; Fokin, V. V. *J. Org. Chem.* **2005**, *70* (19), 7761.
- (123) Li, C.; Rosenau, A. *Tetrahedron Lett.* **2009**, *50* (43), 5888.
- (124) Surry, D. S.; Buchwald, S. L. *Angew. Chem. Int. Ed.* **2008**, *47* (34), 6338.
- (125) Fors, B. P.; Watson, D. a; Biscoe, M. R.; Buchwald, S. L. *J. Am. Chem. Soc.* **2008**, *130* (41), 13552.
- (126) Sharif, S.; Rucker, R. P.; Chandrasoma, N.; Mitchell, D.; Rodriguez, M. J.; Froese, R. D. J.; Organ, M. G. *Angew. Chem. Int. Ed.* **2015**, *54* (33), 9507.
- (127) Baell, J.; Walters, M. A. *Nature* **2014**, *513* (7519), 481.
- (128) Young, R. J. *Bioorg. Med. Chem. Lett* **2011**, *21* (21), 6228.

- (129) Rullas, J.; García, J. I.; Beltrán, M.; Cardona, P.-J.; Cáceres, N.; García-Bustos, J. F.; Angulo-Barturen, I. *Antimicrob. Agents Chemother.* **2010**, *54* (5), 2262.
- (130) Cruciani, G.; Carosati, E.; De Boeck, B.; Ethirajulu, K.; Mackie, C.; Howe, T.; Vianello, R. *J. Med. Chem.* **2005**, *48* (22), 6970.
- (131) MetaSite, Molecular Discovery, Via Pieve di Campo, 36, 06135, Ponte San Giovanni, Perugia, Italy, <http://www.moldiscovery.com/software/metasite/>.
- (132) Vice, S.; Bara, T.; Bauer, A.; Evans, C. A.; Ford, J.; Josien, H.; McCombie, S.; Miller, M.; Nazareno, D.; Palani, A.; Tagat, J. *J. Org. Chem.* **2001**, *66* (7), 2487.
- (133) Desai, P. V.; Raub, T. J.; Blanco, M. J. *Bioorg. Med. Chem. Lett.* **2012**, *22* (21), 6540.
- (134) The Daylight TPSA calculator is available from Daylight Chemical Information Systems, Santa Fe, NM. <http://www.daylight.com>.
- (135) Cox, C. D.; Breslin, M. J.; Whitman, D. B.; Coleman, P. J.; Garbaccio, R. M.; Fraley, M. E.; Zrada, M. M.; Buser, C. a.; Walsh, E. S.; Hamilton, K.; Lobell, R. B.; Tao, W.; Abrams, M. T.; South, V. J.; Huber, H. E.; Kohl, N. E.; Hartman, G. D. *Bioorg. Med. Chem. Lett.* **2007**, *17* (10), 2697.
- (136) Travis, A. S. *The Chemistry of Anilines*; Wiley-VCH Verlag GmbH, 2007.
- (137) Holt, M.; Ju, C. *Handb. Exp. Pharmacol.* **2009**, *196*, 3.
- (138) Schweigert, N.; Zehnder, a. J. B.; Eggen, R. I. L. *Environ. Microbiol.* **2001**, *3* (2), 81.
- (139) Kumagai, Y.; Fukuto, J. M.; Cho, A. K. *Curr. Med. Chem.* **1994**, *4*, 254.
- (140) Powis, G.; Hodnett, E. M.; Santone, K. S.; Lee See, K.; Melder, D. C. *Cancer Res.* **1986**, *47*, 2363.
- (141) Hinson, J. A.; Roberts, D. W.; James, L. P. *Handb. Exp. Pharmacol.* **2010**, *196*, 369.
- (142) Novak, A.; Humphreys, L. D.; Walker, M. D.; Woodward, S. *Tetrahedron Lett.* **2006**, *47* (32), 5767.
- (143) Ma, D.; Zhang, Y.; Yao, J.; Wu, S.; Tao, F. *J. Am. Chem. Soc.* **1998**, *8* (15), 12459.
- (144) Narendar, N.; Velmathi, S. *Tetrahedron Lett.* **2009**, *50* (36), 5159.
- (145) Ma, D.; Xia, C. *Org. Lett.* **2001**, *3* (16), 2583.
- (146) Lam, P. Y. .; Bonne, D.; Vincent, G.; Clark, C. G.; Combs, A. P. *Tetrahedron Lett.* **2003**, *44* (8), 1691.
- (147) Molecular Operating Environment (MOE) v.2014.09, available from the Chemical Computing Group, [https://www.chemcomp.com/MOE-Molecular\\_Operating\\_Environment.htm](https://www.chemcomp.com/MOE-Molecular_Operating_Environment.htm).
- (148) Freire, E. *Drug Discov. Today* **2008**, *13* (19-20), 869.
- (149) Topliss, J. G. *J. Med. Chem.* **1977**, *20* (4), 463.

- (150) Hansch, C.; Fujita, T. *J. Am. Chem. Soc.* **1964**, *86* (8), 1616.
- (151) Li, H.; Jögl, G. *Proteins* **2012**, *81* (3), 538.
- (152) Frye, S. V. *Nat. Chem. Biol.* **2010**, *6* (3), 159.
- (153) Bunnage, M. E.; Chekler, E. L. P.; Jones, L. H. *Nat. Chem. Biol.* **2013**, *9* (4), 195.
- (154) Elliott, T. S.; Slowey, A.; Ye, Y.; Conway, S. J. *Med. Chem. Commun.* **2012**, *3* (7), 735.
- (155) Pertusati, F.; Serpi, M.; McGuigan, C. *Antivir. Chem. Chemother.* **2011**, *22* (5), 181.
- (156) Liav, A.; Brennan, P. J. *Tetrahedron Lett.* **2005**, *46* (16), 2937.
- (157) Luo, Y.; Zechel, D. L. *Can. J. Chem.* **2006**, *84* (4), 743.
- (158) Maryanoff, B. E.; Reitz, A. B.; Tutwiler, G. F.; Benkovic, S. J.; Benkovic, P. A.; Pilkid, S. *J. Am. Chem. Soc.* **1984**, *106* (25), 7851.
- (159) Westerduin, P.; Veeneman, G. H.; Marugg, J. E.; Boom, J. H. Van. *Tetrahedron Lett.* **1986**, *27* (10), 1211.
- (160) Lee, R.; Brennan, P.; Besra, G. *Bioorg. Med. Chem. Lett.* **1998**, *8* (8), 951.
- (161) Liav, A.; Swiezewska, E.; Ciepichal, E.; Brennan, P. J. *Tetrahedron Lett.* **2006**, *47* (49), 8781.
- (162) Liav, A.; Ciepichal, E.; Swiezewska, E.; Bobovská, A.; Dianišková, P.; Blaško, J.; Mikušová, K.; Brennan, P. J. *Tetrahedron Lett.* **2009**, *50* (19), 2242.
- (163) Lee, R. E.; Mikusova, K.; Brennan, P. J.; Besra, G. S. *J. Am. Chem. Soc.* **1995**, *117* (48), 11829.
- (164) Aoki, S.; Kondo, H.; Wong, C. *Method. Enzym.* **1994**, *247* (13), 193.
- (165) Booth, K. V.; Cruz, F. P. da; Hotchkiss, D. J.; Jenkinson, S. F.; Jones, N. A.; Weymouth-Wilson, A. C.; Clarkson, R.; Heinz, T.; Fleet, G. W. J. *Tetrahedron: Asymmetry* **2008**, *19* (20), 2417.
- (166) Hotchkiss, D. J.; Jenkinson, S. F.; Storer, R.; Heinz, T.; Fleet, G. W. J. *Tetrahedron Lett.* **2006**, *47* (3), 315.
- (167) Swahn, B.-M.; Edvinsson, K.; Kallin, E.; Larsson, U.; Berge, O. *Bioorg. Med. Chem.* **1997**, *5* (7), 1293.
- (168) Choi, S.; Mansoorabadi, S.; Liu, Y.; Chien, T.; Liu, H.-W. *J. Am. Chem. Soc.* **2012**, *134* (34), 13946.
- (169) Centrone, C.; Lowary, T. *J. Org. Chem.* **2002**, *67* (25), 8862.
- (170) Caravano, A.; Mengin-Lecreulx, D.; Brondello, J.-M.; Vincent, S. P.; Sinaÿ, P. *J. Chem. Eur.* **2003**, *9* (23), 5888.
- (171) Meyer, R.; Stone, T.; Jesthi, P. *J. Med. Chem.* **1984**, *27* (8), 1095.

- (172) Grison, C.; Chobli, H. J. *Carbohydr. Chem.* **2009**, *28* (1), 12.
- (173) Brown, K.; Dixey, M.; Weymouth-Wilson, A.; Linclau, B. *Carbohydr. Res.* **2014**, *387* (1), 59.
- (174) Dabur Pharma Limited. WO2006/92808 A1, 2006.
- (175) Wothers, P.; Greeves, N.; Warren, S.; Clayden, J. *Organic Chemistry*, 8th ed.; Oxford University Press, 2008.
- (176) Shih, H.-W.; Chen, K.-T.; Cheng, W.-C. *Tetrahedron Lett.* **2012**, *53* (2), 243.
- (177) Lartigue, L.; Oumzil, K.; Guari, Y.; Larionova, J.; Guérin, C.; Montero, J.-L.; Barragan-Montero, V.; Sangregorio, C.; Caneschi, A.; Innocenti, C.; Kalaivani, T.; Arosio, P.; Lascialfari, A. *Org. Lett.* **2009**, *11* (14), 2992.
- (178) Nickel, S.; Kaschani, F.; Colby, T.; van der Hoorn, R. A. L.; Kaiser, M. *Bioorg. Med. Chem. Lett.* **2012**, *20* (2), 601.
- (179) Garegg, P. J.; Samuelsson, B. *Synthesis.* **1979**, *6*, 469.
- (180) N'Go, I.; Golten, S.; Ardá, A.; Cañada, J.; Jiménez-Barbero, J.; Linclau, B.; Vincent, S. P. *Chem. Eur. J.* **2014**, *20* (1), 106.
- (181) Mecinović, J.; Snyder, P. W.; Mirica, K. a.; Bai, S.; MacK, E. T.; Kwant, R. L.; Moustakas, D. T.; Héroux, A.; Whitesides, G. M. *J. Am. Chem. Soc.* **2011**, *133* (35), 14017.
- (182) Müller, K.; Faeh, C.; Diederich, F. *Science.* **2007**, *317* (5846), 1881.
- (183) Zheng, F.; Fu, L.; Wang, R.; Qing, F.-L. *Org. Biomol. Chem.* **2010**, *8* (1), 163.
- (184) Tavasli, M.; O'Hagan, D.; Pearson, C.; Petty, M. C. *Chem. Commun.* **2002**, *1* (11), 1226.
- (185) Forneris, F.; Orru, R.; Bonivento, D.; Chiarelli, L. R.; Mattevi, A. *FEBS J.* **2009**, *276* (10), 2833.
- (186) Parks, D. J.; Lafrance, L. V.; Calvo, R. R.; Milkiewicz, K. L.; Gupta, V.; Lattanze, J.; Ramachandren, K.; Carver, T. E.; Petrella, E. C.; Cummings, M. D.; Maguire, D.; Grasberger, B. L.; Lu, T. *Bioorg. Med. Chem. Lett.* **2005**, *15* (3), 765.
- (187) Shirude, P. S.; Madhavapeddi, P.; Naik, M.; Murugan, K.; Shinde, V.; Nandishaiah, R.; Bhat, J.; Kumar, A.; Hameed, S.; Davies, G.; McMiken, H.; Hegde, N.; Ambady, A.; Venkatraman, J.; Panda, M.; Bandodkar, B.; Sambandamurthy, V. K.; Read, J. A. *J. Med. Chem.* **2013**, *56* (21), 8533.
- (188) Zhang, Z.; Bulloch, E. M. M.; Bunker, R. D.; Baker, E. N.; Squire, C. J. *Acta Crystallogr. Sect. D* **2009**, *65* (3), 275.
- (189) Sassetti, C. M.; Boyd, D. H.; Rubin, E. J. *Mol. Microbiol.* **2003**, *48* (1), 77.
- (190) Zhang, W.; Jones, V. C.; Scherman, M. S.; Mahapatra, S.; Crick, D.; Bhamidi, S.; Xin, Y.; McNeil, M. R.; Ma, Y. *Int. J. Biochem. Cell Biol.* **2008**, *40* (11), 2560.

- (191) Kaur, D.; Guerin, M. E.; Skovierová, H.; Brennan, P. J.; Jackson, M. *Adv. Appl. Microbiol.* **2009**, *69* (09), 23.
- (192) van Heijenoort, J. *Glycobiology* **2001**, *11* (3), 25.
- (193) Raymond, J. B.; Mahapatra, S.; Crick, D. C.; Pavelka, M. S. *J. Biol. Chem.* **2005**, *280* (1), 326.
- (194) Wietzerbin, J.; Das, B. C.; Petit, J. F.; Lederer, E.; Leyh-Bouille, M.; Ghuysen, J. M. *Biochemistry* **1974**, *13* (17), 3471.
- (195) McNeil, M.; Daffe, M.; Brennan, P. J. *J. Biol. Chem.* **1990**, *265* (30), 18200.
- (196) Mahapatra, S.; Crick, D. C.; Brennan, P. J. *J. Bacteriol.* **2000**, *182* (23), 6827.
- (197) van Heijenoort, J. *Cell. Mol. Life Sci.* **1998**, *54* (4), 300.
- (198) Crick, D. C.; Mahapatra, S.; Brennan, P. J. *Glycobiology* **2001**, *11* (9), 107.
- (199) Kahan, F. M.; Kahan, J. S.; Cassidy, P. J.; Kropp, H. *Ann. N. Y. Acad. Sci.* **1974**, *235*, 364.
- (200) Kim, D. H.; Lees, W. J.; Kempell, K. E.; Lane, W. S.; Duncan, K.; Walsh, C. T. *Biochemistry* **1996**, *35* (15), 4923.
- (201) Waxman, D. J.; Strominger, J. L. *Annu. Rev. Biochem.* **1983**, *52*, 825.
- (202) Wivagg, C. N.; Bhattacharyya, R. P.; Hung, D. T. *J. Antibiot.* **2014**, *67* (9), 645.
- (203) Tremblay, L. W.; Fan, F.; Blanchard, J. S. *Biochemistry* **2010**, *49* (17), 3766.
- (204) Netto, E. M.; Owendale, P. J.; Reed, S. G.; Coler, R. N.; Badaro, R. *Science*. **2009**, *323* (5918), 1215.
- (205) De Lorenzo, S.; Alffenaar, J. W.; Sotgiu, G.; Centis, R.; D'Ambrosio, L.; Tiberi, S.; Bolhuis, M. S.; van Altena, R.; Viggiani, P.; Piana, A.; Spanevello, A.; Migliori, G. B. *Eur. Respir. J.* **2013**, *41* (6), 1386.
- (206) Ishizaki, Y.; Hayashi, C.; Inoue, K.; Igarashi, M.; Takahashi, Y.; Pujari, V.; Crick, D. C.; Brennan, P. J.; Nomoto, A. *J. Biol. Chem.* **2013**, *288* (42), 30309.
- (207) Jagtap, P. K. A.; Soni, V.; Vithani, N.; Jhingan, G. D.; Bais, V. S.; Nandicoori, V. K.; Prakash, B. *J. Biol. Chem.* **2012**, *287* (47), 39524.
- (208) Pompeo, F.; Bourne, Y.; van Heijenoort, J.; Fassy, F.; Mengin-Lecreulx, D. *J. Biol. Chem.* **2001**, *276* (6), 3833.
- (209) Jagtap, P. K. A.; Verma, S. K.; Vithani, N.; Bais, V. S.; Prakash, B. *J. Mol. Biol.* **2013**, *425* (10), 1745.
- (210) Buurman, E. T.; Andrews, B.; Gao, N.; Hu, J.; Keating, T. a.; Lahiri, S.; Otterbein, L. R.; Patten, A. D.; Stokes, S. S.; Shapiro, A. B. *J. Biol. Chem.* **2011**, *286* (47), 40734.
- (211) Green, O. M.; McKenzie, A. R.; Shapiro, A. B.; Otterbein, L.; Ni, H.; Patten, A.; Stokes, S.; Albert, R.; Kawatkar, S.; Breed, J. *Bioorg. Med. Chem. Lett.* **2012**, *22* (4), 1510.

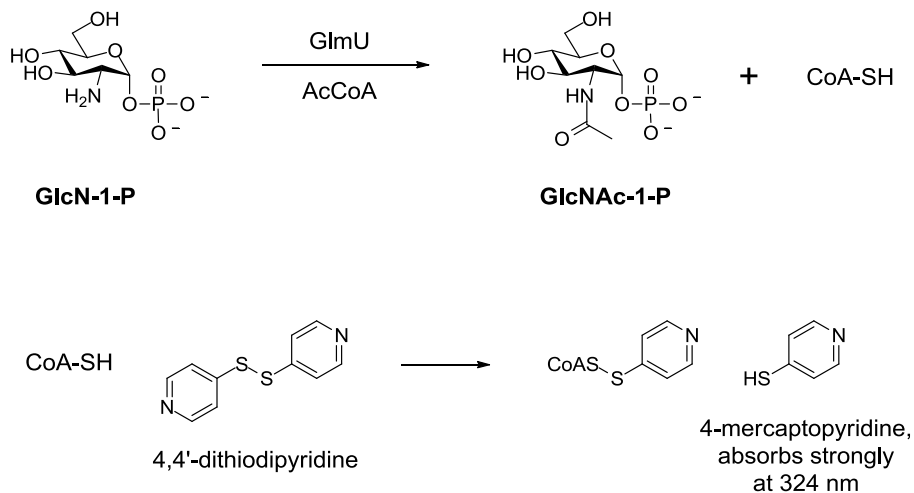
- (212) Doig, P.; Boriack-Sjodin, P. A.; Dumas, J.; Hu, J.; Itoh, K.; Johnson, K.; Kazmirski, S.; Kinoshita, T.; Kuroda, S.; Sato, T.; Sugimoto, K.; Tohyama, K.; Aoi, H.; Wakamatsu, K.; Wang, H. *Bioorg. Med. Chem. Lett.* **2014**, *22* (21), 6256.
- (213) Mochalkin, I.; Lightle, S.; Narasimhan, L.; Bornemeier, D.; Melnick, M.; Vanderroest, S.; McDowell, L. *Protein Sci.* **2008**, *17* (3), 577.
- (214) Li, Y.; Zhou, Y.; Ma, Y.; Li, X. *Carbohydr. Res.* **2011**, *346* (13), 1714.
- (215) Tran, A. T.; Wen, D.; West, N. P.; Baker, E. N.; Britton, W. J.; Payne, R. J. *Org. Biomol. Chem.* **2013**, *11* (46), 8113.
- (216) Larsen, N. A.; Nash, T. J.; Morningstar, M.; Shapiro, A. B.; Joubran, C.; Blackett, C. J.; Patten, A. D.; Boriack-Sjodin, P. A.; Doig, P. *Biochem. J.* **2012**, *446* (3), 405.
- (217) Rani, C.; Mehra, R.; Sharma, R.; Chib, R.; Wazir, P.; Nargotra, A.; Khan, I. A. *Tuberculosis* **2015**, *15*, 30015.
- (218) Baell, J. B.; Holloway, G. A. *J. Med. Chem.* **2010**, *53* (7), 2719.
- (219) Schwartz, B.; Drueckhammer, D. G. *J. Am. Chem. Soc.* **1996**, *118* (41), 9826.
- (220) Olsen, L. R.; Vetting, M. W.; Roderick, S. L. *Protein Sci.* **2007**, *16* (718), 1230.
- (221) Gluza, K.; Kafarski, P. In *Transition State Analogues of Enzymatic Reaction as Potential Drugs, Drug Discovery*; InTech, 2013; pp 325–372.
- (222) Pisabarro, M. T.; Pf, J. A. R.; Palomer, A.; Cabr, F.; Garck, I. I. L.; Wade, R. C.; Gago, F.; Maulen, D.; Carganicoll, G. *J. Med. Chem.* **1994**, *37* (3), 337.
- (223) Xu, C.; Hall, R.; Cummings, J.; Raushel, F. M. *J. Am. Chem. Soc.* **2006**, *128* (13), 4244.
- (224) Cama, E.; Shin, H.; Christianson, D. W. *J. Am. Chem. Soc.* **2003**, *125* (43), 13052.
- (225) Moree, W. J.; Marel, G. A. Van Der; Liskamp, R. J. *J. Org. Chem.* **1996**, *60* (16), 5157.
- (226) Kovac, A.; Wilson, R. A.; Besra, G. S.; Filipic, M.; Kikelj, D.; Gobec, S. *J. Enzyme Inhib. Med. Chem.* **2006**, *21* (4), 391.
- (227) Bartlett, P. a; Marlowe, C. K. *Biochemistry* **1983**, *22* (20), 4618.
- (228) Harrison, A. N.; Reichau, S.; Parker, E. J. *Bioorg. Med. Chem. Lett.* **2012**, *22* (2), 907.
- (229) Yuan, W.; Gelb, M. *J. Am. Chem. Soc.* **1988**, *110* (8), 2665.
- (230) Bartlett, P. A.; Marlowe, C. K. *Biochemistry* **1987**, *26* (26), 8553.
- (231) Pagano, P. J.; Chong, K. T. *J. Infect. Dis.* **1995**, *171* (1), 61.
- (232) Chen, C.-A.; Sieburth, S. M.; Glekas, A.; Hewitt, G. W.; Trainor, G. L.; Erickson-Viitanen, S.; Garber, S. S.; Cordova, B.; Jeffry, S.; Klabe, R. M. *Chem. Biol.* **2001**, *8* (12), 1161.
- (233) Brik, A.; Wong, C.-H. *Org. Biomol. Chem.* **2003**, *1* (1), 5.

- (234) Bano, S.; Hamdard, J. *Tetrahedron Lett.* **1970**, *55*, 4803.
- (235) Warren, C.; Herscovics, A.; Jeanloz, R. *Carbohydr. Res.* **1978**, *45* (5), 181.
- (236) Sim, M. M.; Kondo, H.; Wong, C. H. *J. Am. Chem. Soc.* **1993**, *115* (6), 2260.
- (237) Inage, M.; Chaki, H.; Kusumoto, S.; Shiba, T. *Chem. Lett.* **1982**, *8*, 1281.
- (238) Sabesan, S.; Neira, S. *Carbohydr. Res.* **1992**, *223*, 169.
- (239) Boullanger, P.; Bonoub, J.; Descotes, G. *Can. J. Chem.* **1987**, *65* (6), 1343.
- (240) Kong, H.; Chen, W.; Lu, H.; Yang, Q.; Dong, Y.; Wang, D.; Zhang, J. *Carbohydr. Res.* **2015**, *413*, 135.
- (241) Ramage, R.; Atrash, B.; Hopton, D.; Parrott, M. J. *J. Chem. Soc., Perkin Trans. 1* **1985**, *8*, 1217.
- (242) Modro, T.; Lawry, M.; Murphy, E. *J. Org. Chem.* **1978**, *43* (26), 5000.
- (243) Tosin, M.; Spiteller, D.; Spencer, J. B. *Chembiochem* **2009**, *10* (10), 1714.
- (244) Kong, X.; Atfani, M.; Bachand, B.; Bouzide, A.; Ciblat, S.; Levesque, S.; Migneault, D.; Valade, I.; Wu, X.; Delorme, D. US 2008/0146642 A1, 2008.
- (245) Radkiewicz, J. L.; McAllister, M.; Goldstein, E.; Houk, K. N. *J. Org. Chem.* **1998**, *63* (5), 1419.
- (246) Guan, W.; Cai, L.; Fang, J.; Wu, B.; George Wang, P. *Chem. Commun.* **2009**, *45*, 6976.
- (247) Masuko, S.; Bera, S.; Green, D. E.; Weïwer, M.; Liu, J.; Deangelis, P. L.; Linhardt, R. J. *J. Org. Chem.* **2012**, *77* (3), 1449.
- (248) Chen, Y.; Thon, V.; Li, Y.; Yu, H.; Ding, L.; Lau, K.; Qu, J.; Hie, L.; Chen, X. *Chem. Commun.* **2011**, *47* (38), 10815.
- (249) Chang, R.; Moquist, P.; Finney, N. S. *Carbohydr. Res.* **2004**, *339* (8), 1531.
- (250) Yi, W.; Liu, X.; Li, Y.; Li, J.; Xia, C.; Zhou, G.; Zhang, W.; Zhao, W.; Chen, X.; Wang, P. G. *Proc. Natl. Acad. Sci. USA* **2009**, *106* (11), 4207.
- (251) Danilchanka, O.; Pavlenok, M.; Niederweis, M. *Antimicrob. Agents Chemother.* **2008**, *52* (9), 3127.
- (252) Grewal, R. K.; Yan, W.; Besra, G. S.; Brennanc, P. J.; Fleeta, G. W. *J. Tetrahedron Lett.* **1997**, *38* (38), 6733.
- (253) Saquib, M.; Husain, I.; Sharma, S.; Yadav, G.; Singh, V. K.; Sharma, S. K.; Shah, P.; Siddiqi, M. I.; Kumar, B.; Lal, J.; Jain, G. K.; Srivastava, B. S.; Srivastava, R.; Shaw, A. K. *Eur. J. Med. Chem.* **2011**, *46* (6), 2217.
- (254) Taveira, A. F.; Hyaric, M. Le; Reis, E. F. C.; Araújo, D. P.; Ferreira, A. P.; de Souza, M. A.; Alves, L. L.; Lourenço, M. C. S.; Vicente, F. R. C.; de Almeida, M. V. *Bioorg. Med. Chem.* **2007**, *15* (24), 7789.

- (255) Musicki, B.; Periers, a M.; Laurin, P.; Ferroud, D.; Benedetti, Y.; Lachaud, S.; Chatreaux, F.; Haesslein, J. L.; Iltis, A.; Pierre, C.; Khider, J.; Tessot, N.; Airault, M.; Demasse, J.; Dupuis-Hamelin, C.; Lassaigue, P.; Bonnefoy, A.; Vicat, P.; Klich, M. *Bioorg. Med. Chem. Lett.* **2000**, *10* (15), 1695.
- (256) Kashyap, V.; Sharma, S.; Singh, V.; Sharma, S. K.; Saquib, M.; Srivastava, R.; Shaw, A. K. *Antimicrob. Agents Chemother.* **2014**, *58* (6), 3530.
- (257) Giordanetto, F.; Wällberg, A.; Cassel, J.; Ghosal, S.; Kossenjans, M.; Yuan, Z.-Q.; Wang, X.; Liang, L. *Bioorg. Med. Chem. Lett.* **2012**, *22* (21), 6665.
- (258) Ting, P. C.; Umland, S. P.; Aslanian, R.; Cao, J.; Garlisi, C. G.; Huang, Y.; Jakway, J.; Liu, Z.; Shah, H.; Tian, F.; Wan, Y.; Shih, N. Y. *Bioorg Med Chem Lett* **2005**, *15* (12), 3020.
- (259) Mateu, M.; Capilla, A. .; Harrak, Y.; Pujol, M. *Tetrahedron* **2002**, *58* (26), 5241.
- (260) Colson, P.-J.; Przybyla, C. A.; Wise, B. E.; Babiak, K. A.; Seaney, L. M.; Korte, D. E. *Tetrahedron: Asymmetry* **1998**, *9* (15), 2587.
- (261) Doherty, E. M.; Fotsch, C.; Bo, Y.; Chakrabarti, P. P.; Chen, N.; Gavva, N.; Han, N.; Kelly, M. G.; Kincaid, J.; Klionsky, L.; Liu, Q.; Ognyanov, V. I.; Tamir, R.; Wang, X.; Zhu, J.; Norman, M. H.; Treanor, J. J. S. *J. Med. Chem.* **2005**, *48* (1), 71.
- (262) Polturi, R. B.; Venkata, S. H.; Betini, R. WO2005/95430 A1, 2005.
- (263) Wiseman, R. L.; Johnson, S. M.; Kelker, M. S.; Foss, T.; Wilson, I. A.; Kelly, J. W. *J. Am. Chem. Soc.* **2005**, *127* (15), 5540.
- (264) Lazarević, D.; Thiem, J. *Carbohydr. Res.* **2006**, *341* (5), 569.

## 13. Appendix

### A1. The GlmU Acetyltransferase Assay

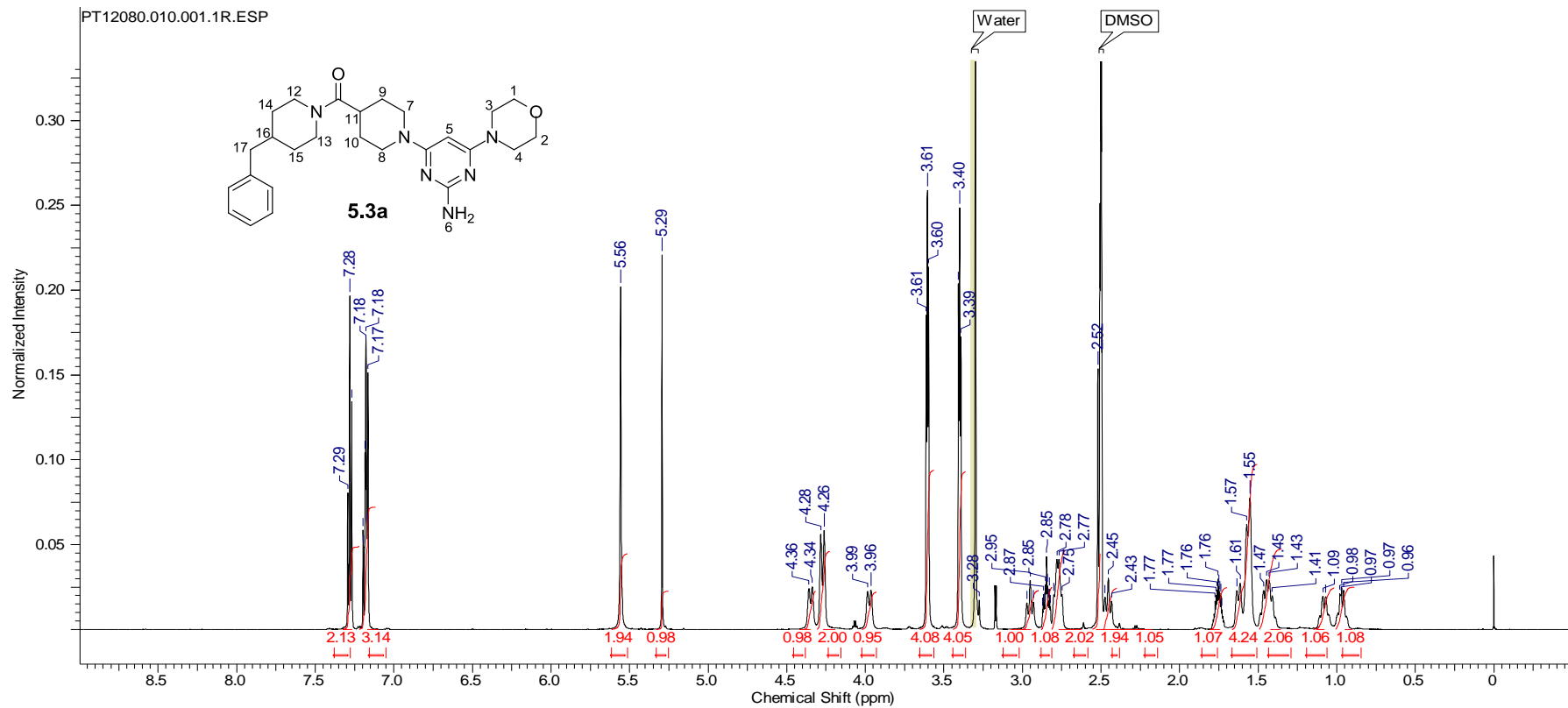


**Scheme A.1.** The GSK GlmU acetyltransferase enzyme assay developed by Peter Craggs. GlmU converts GlcN-1-P and AcCoA into GlcNAc-1-P and CoA-SH. CoA-SH then reacts with 4,4'-dithiodipyridine to give 4-mercaptopyridine, which absorbs strongly at 324 nm. Inhibition of GlmU acetyltransferase activity reduces the formation of 4-mercaptopyridine and thus reduces the absorption signal at 324 nm.

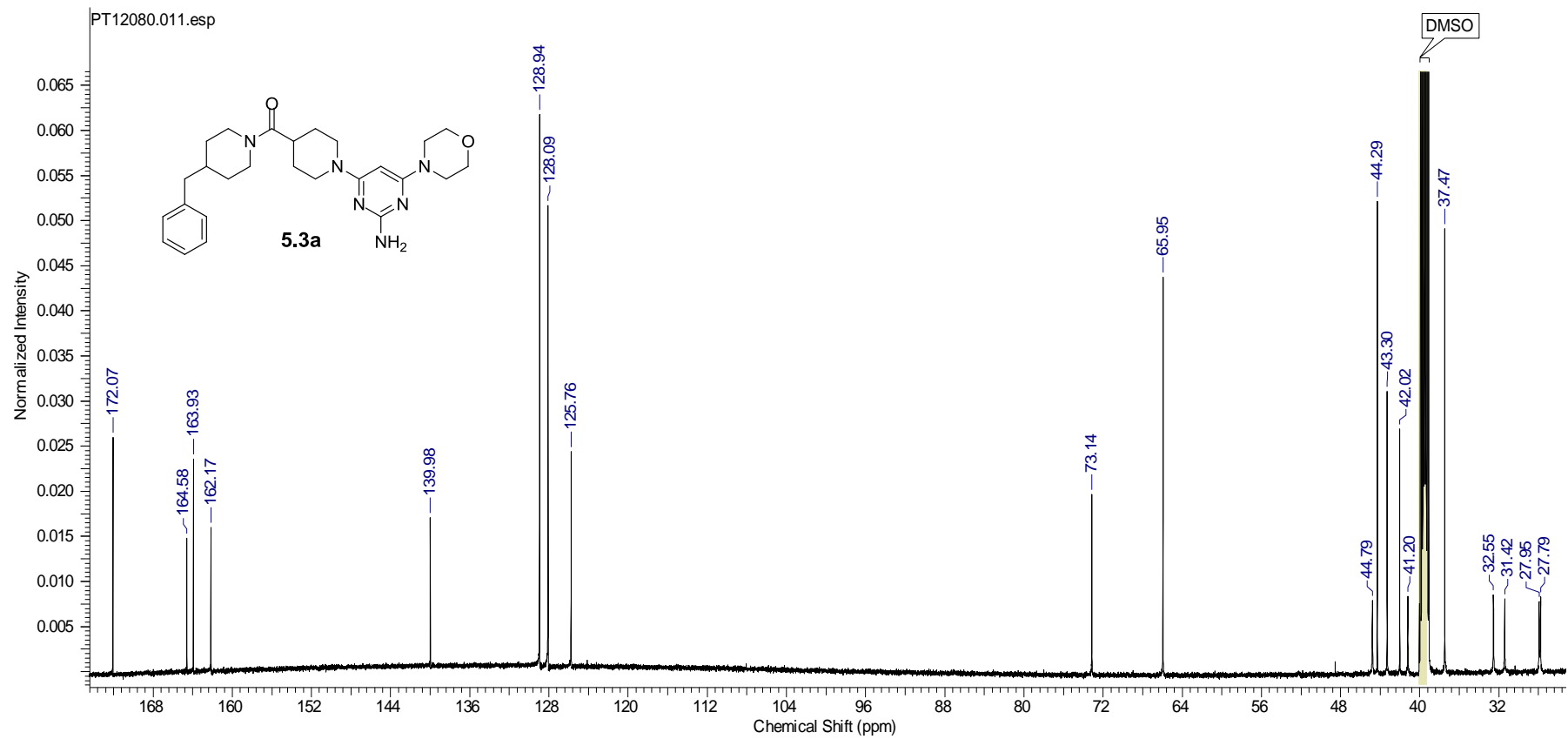
### A2. Representative NMR Spectra

Appendix A2 contains the NMR spectra for the following compounds:

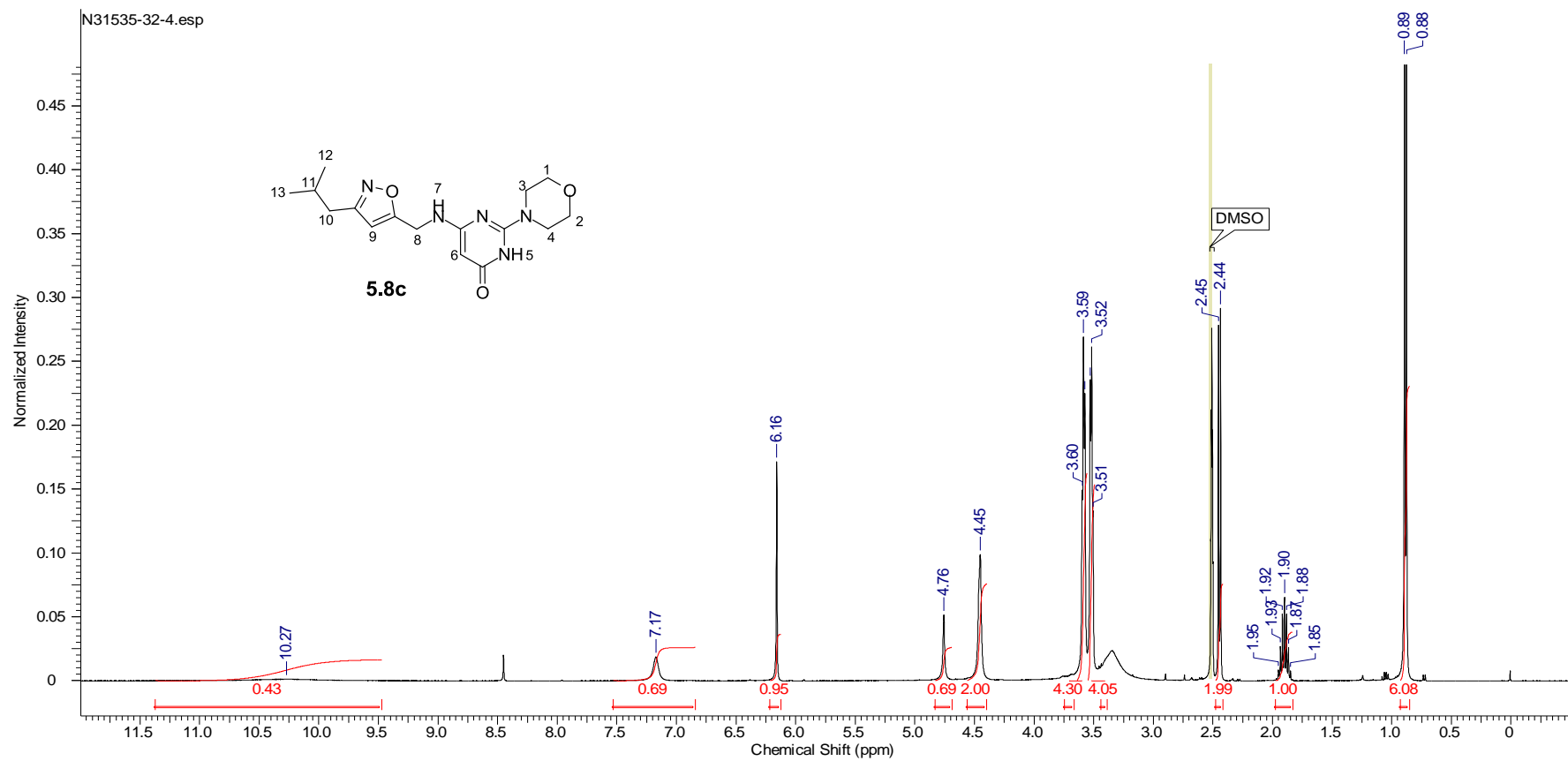
**5.3a, 5.8c, 5.21, 6.26, 7.1c, 7.2f,  $\alpha$ -7.49, 9.1d, 9.19c.**



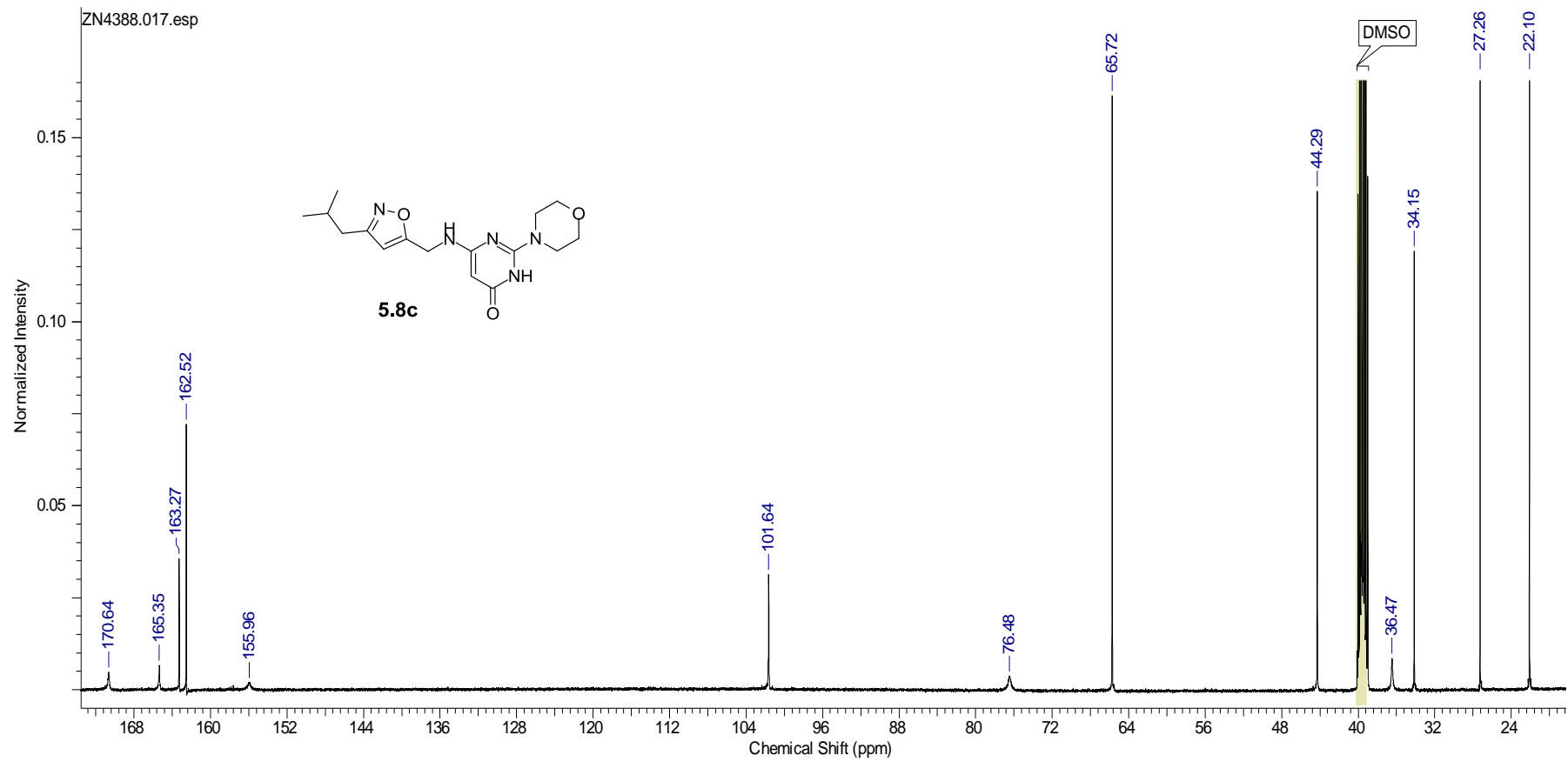
$^1\text{H}$  NMR (600 MHz,  $\text{DMSO}-d_6$ ):  $\delta$  0.93-1.01 (m, 1H, H-14 *ax.*), 1.04-1.12 (m, 1H, H-15 *ax.*), 1.40-1.48 (m, 2H, H-9 *ax.*, H-10 *ax.*), 1.56-1.64 (m, 4H, H-9 *eq.*, H-10 *eq.*, H-14 *eq.*, H-15 *eq.*), 1.72-1.77 (m, 1H, H-16), 2.45 (t,  $J = 12.2$  Hz, 1H, H-12 *ax.*), 2.52 (s, 2H, H-17), 2.75-2.80 (m, 2H, H-7 *ax.*, H-8 *ax.*), 2.85 (tt,  $J = 3.7, 11.3$  Hz, 1H, H-11), 2.95 (t,  $J = 12.2$  Hz, 1H, H-13 *ax.*), 3.40-3.42 (m, 4H, H-3, H-4), 3.61-3.62 (m, 4H, H-1, H-2), 3.97 (d,  $J = 12.6$  Hz, 1H, H-12 *eq.*), 4.27 (d,  $J = 12.6$  Hz, 2H, H-7 *eq.*, H-8 *eq.*), 4.35 (d,  $J = 12.6$  Hz, 1H, H-13 *eq.*), 5.30 (s, 1H, H-5), 5.56 (s, 2H, H-6), 7.17-7.20 (m, 3H, Ar-H), 7.27-7.29 (m, 2H, Ar-H).



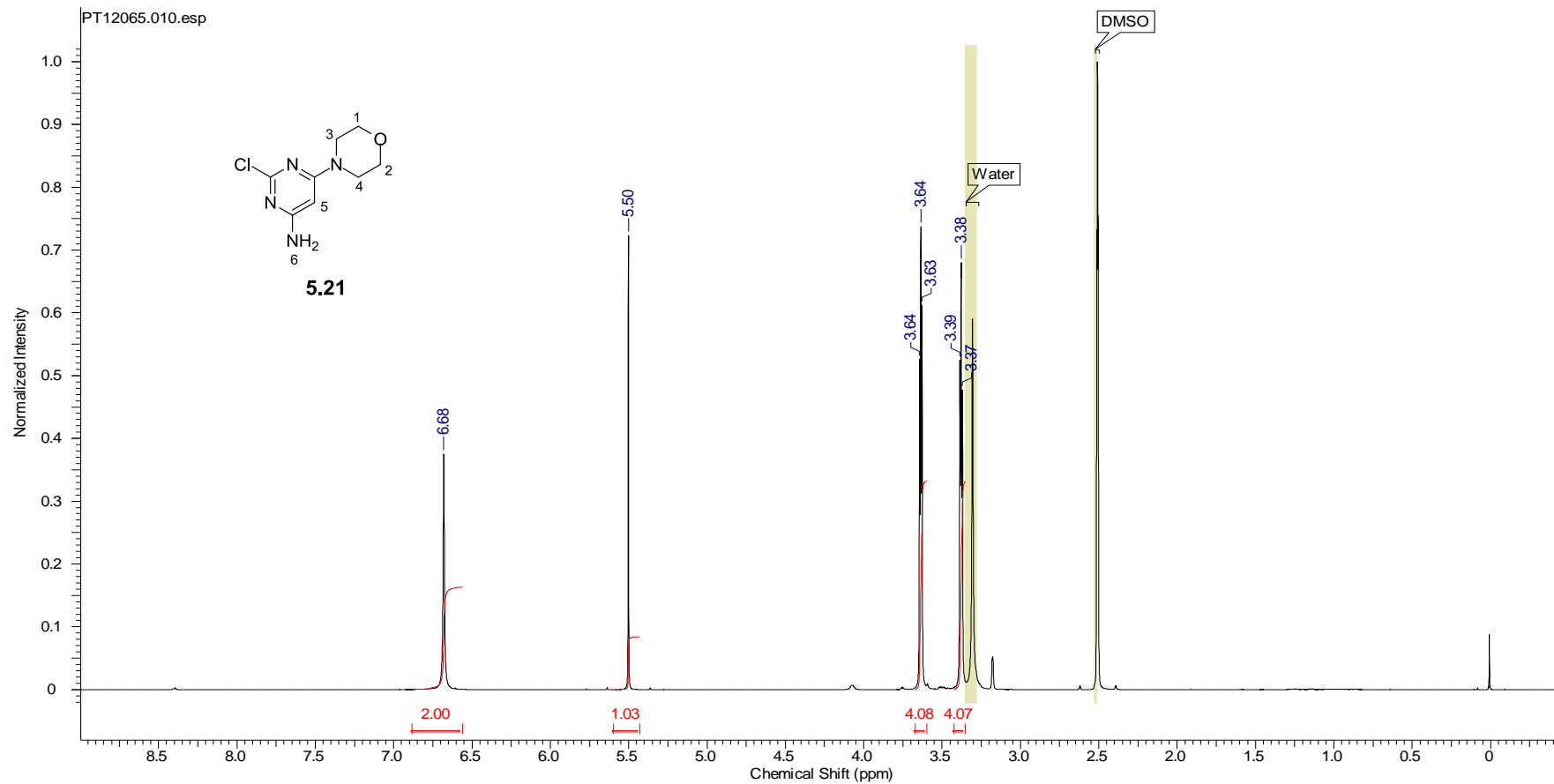
$^{13}\text{C}$  NMR (125 MHz,  $\text{DMSO-}d_6$ ):  $\delta$  27.8, 28.0, 31.4, 32.6, 37.5 (2C), 41.2, 42.0, 43.3 (2C), 44.3 (2C), 44.8, 66.0 (2C), 73.1, 125.8, 128.1 (2C), 129.0 (2C), 140.0, 162.2, 164.0, 164.6, 172.1.



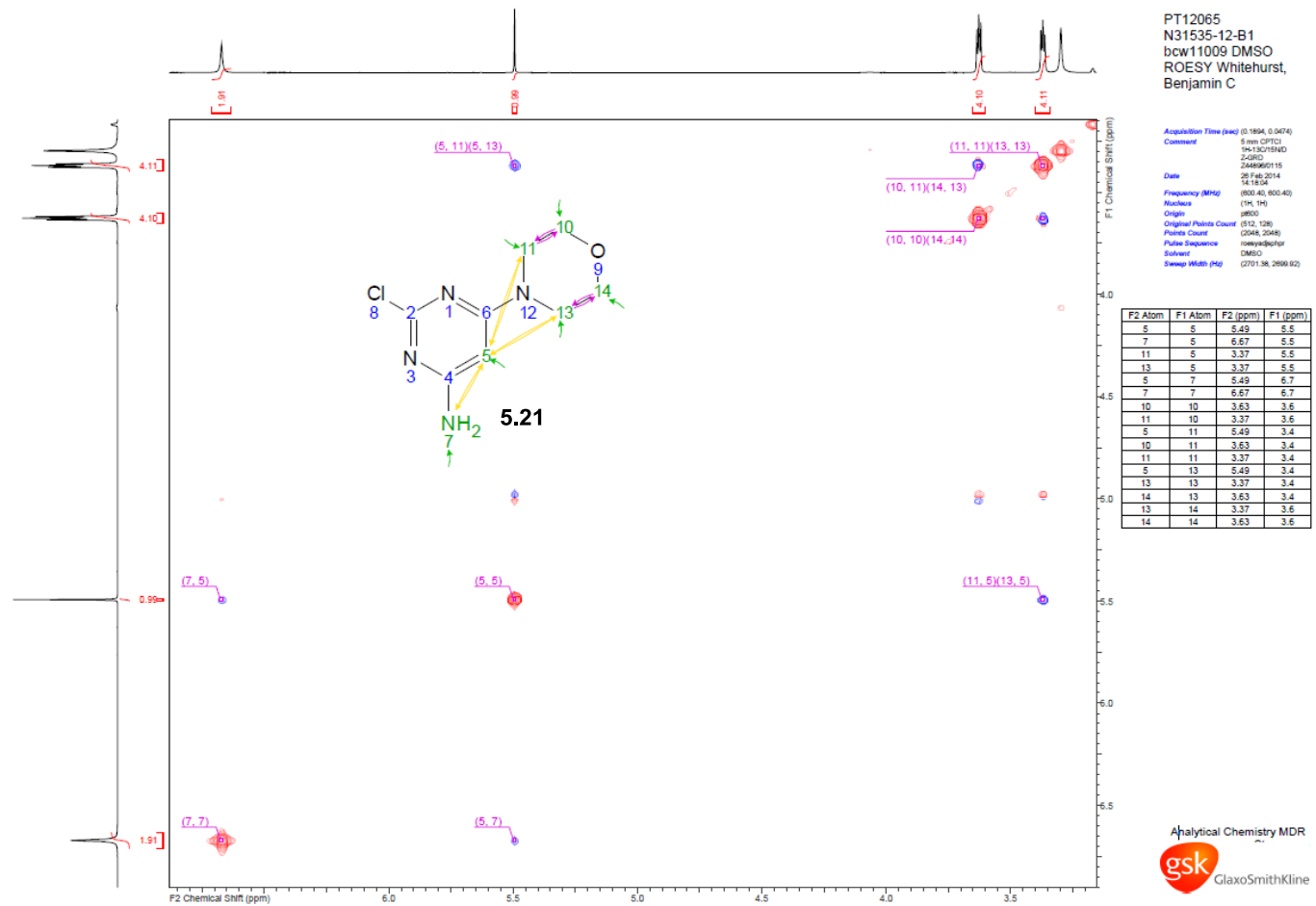
$^1\text{H}$  NMR (400 MHz,  $\text{DMSO}-d_6$ ):  $\delta$  0.88 (d,  $J = 6.6$  Hz, 6H, H-13, H-12), 1.83-1.97 (m, 1H, H-11), 2.44 (d,  $J = 7.1$  Hz, 2H, H-10), 3.50-3.53 (m, 4H, H-3, H-4), 3.57-3.60 (m, 4H, H-1, H-2), 4.45-4.47 (m, 2H, H-8), 4.76 (s, 1H, H-6), 6.16 (s, 1H, H-9), 7.17 (br.s, 1H, H-7), 10.27 (br.s, 1H, H-5).



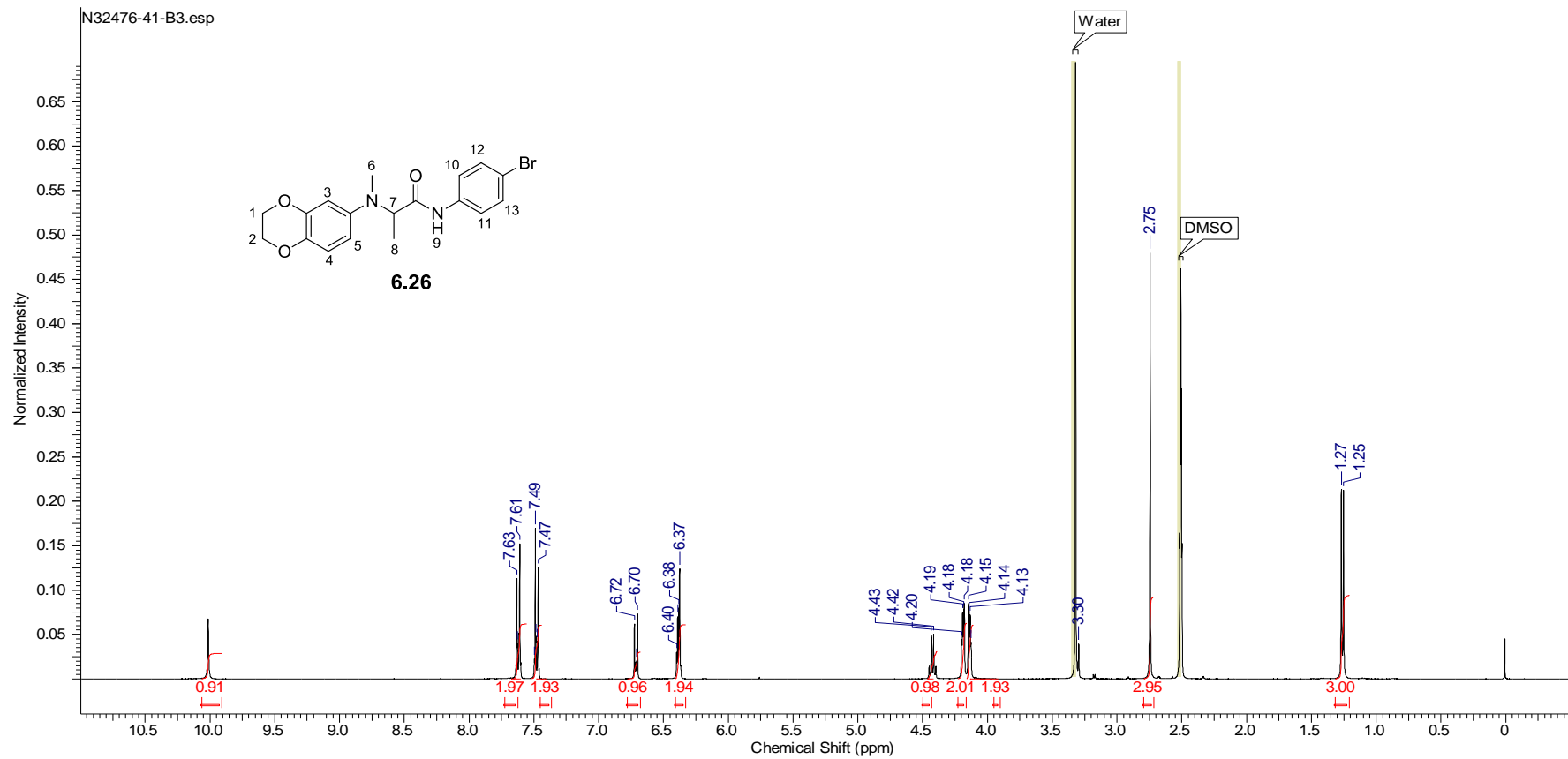
$^{13}\text{C}$  NMR (125 MHz,  $\text{DMSO-}d_6$ ):  $\delta$  22.1 (2C), 27.3, 34.2, 36.5, 44.3 (2C), 65.7 (2C), 76.5, 101.6, 156.0, 162.5, 163.3, 165.4, 170.6.



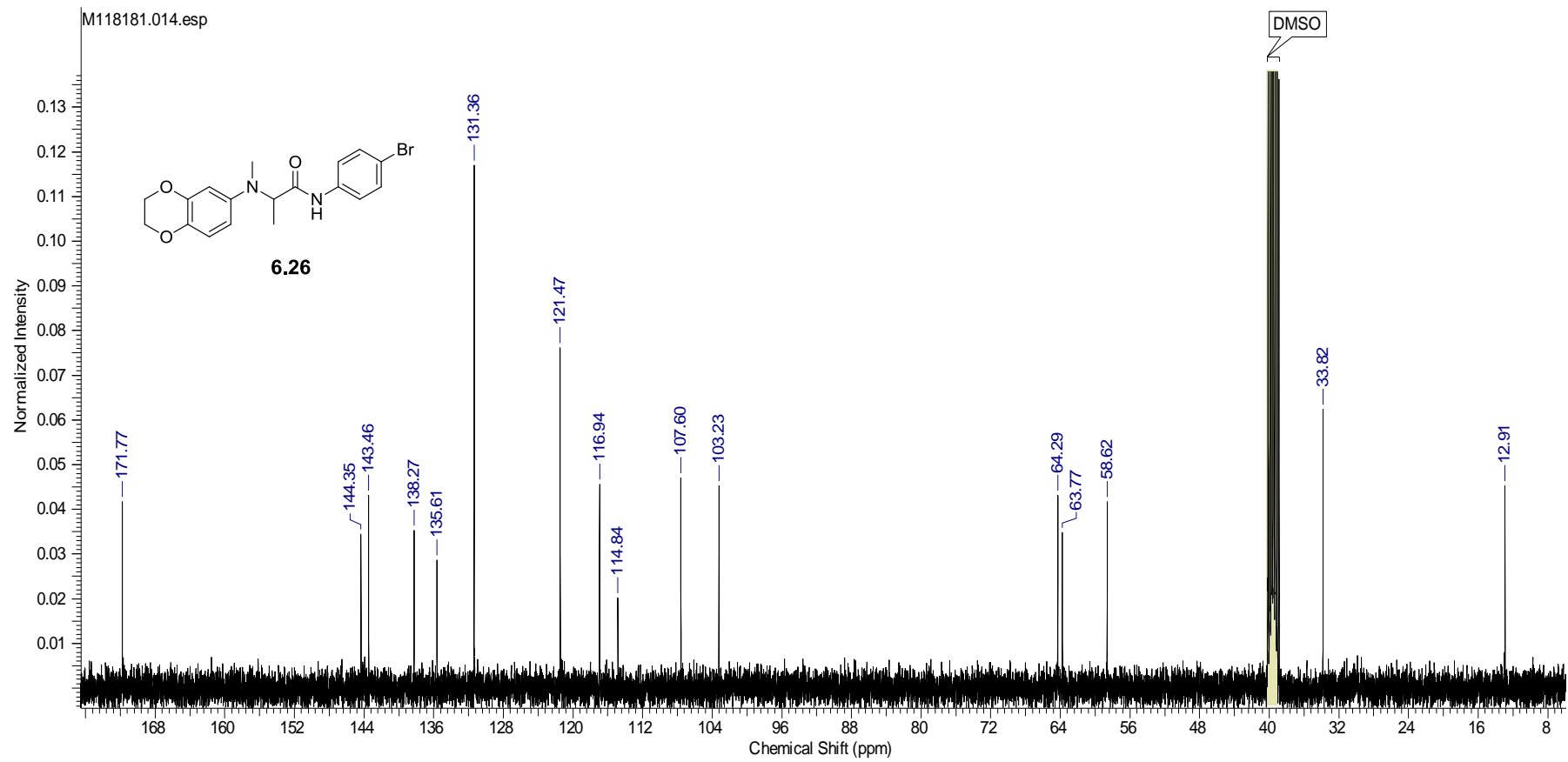
$^1\text{H}$  NMR (400 MHz,  $\text{DMSO-}d_6$ ):  $\delta$  3.37-3.39 (m, 4H, H-3, H-4), 3.63-3.65 (m, 4H, H-1, H-2), 5.50 (s, 1H, H-5), 6.68 (br.s, 2H, H-6).



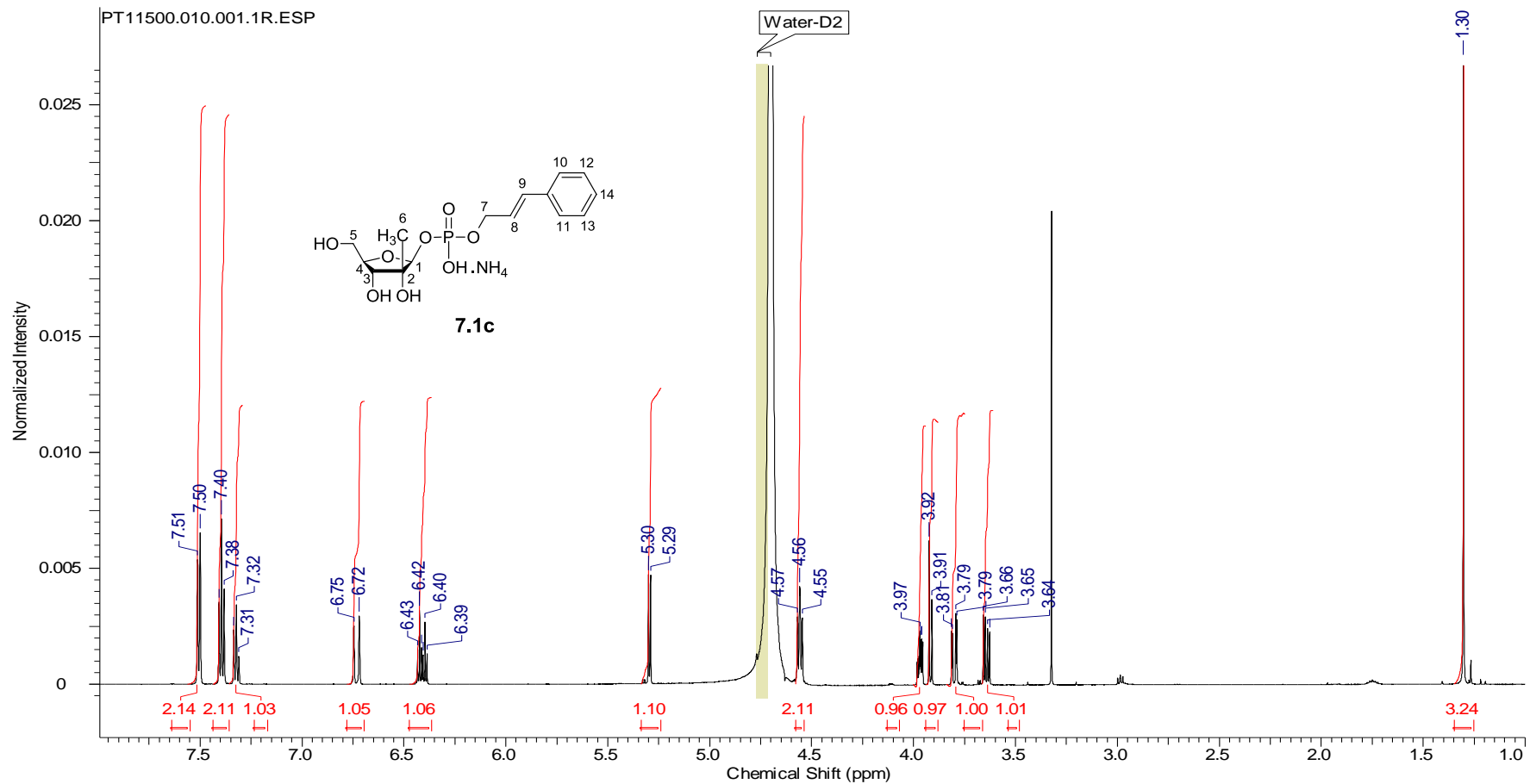
ROESY NMR spectrum for 5.21.



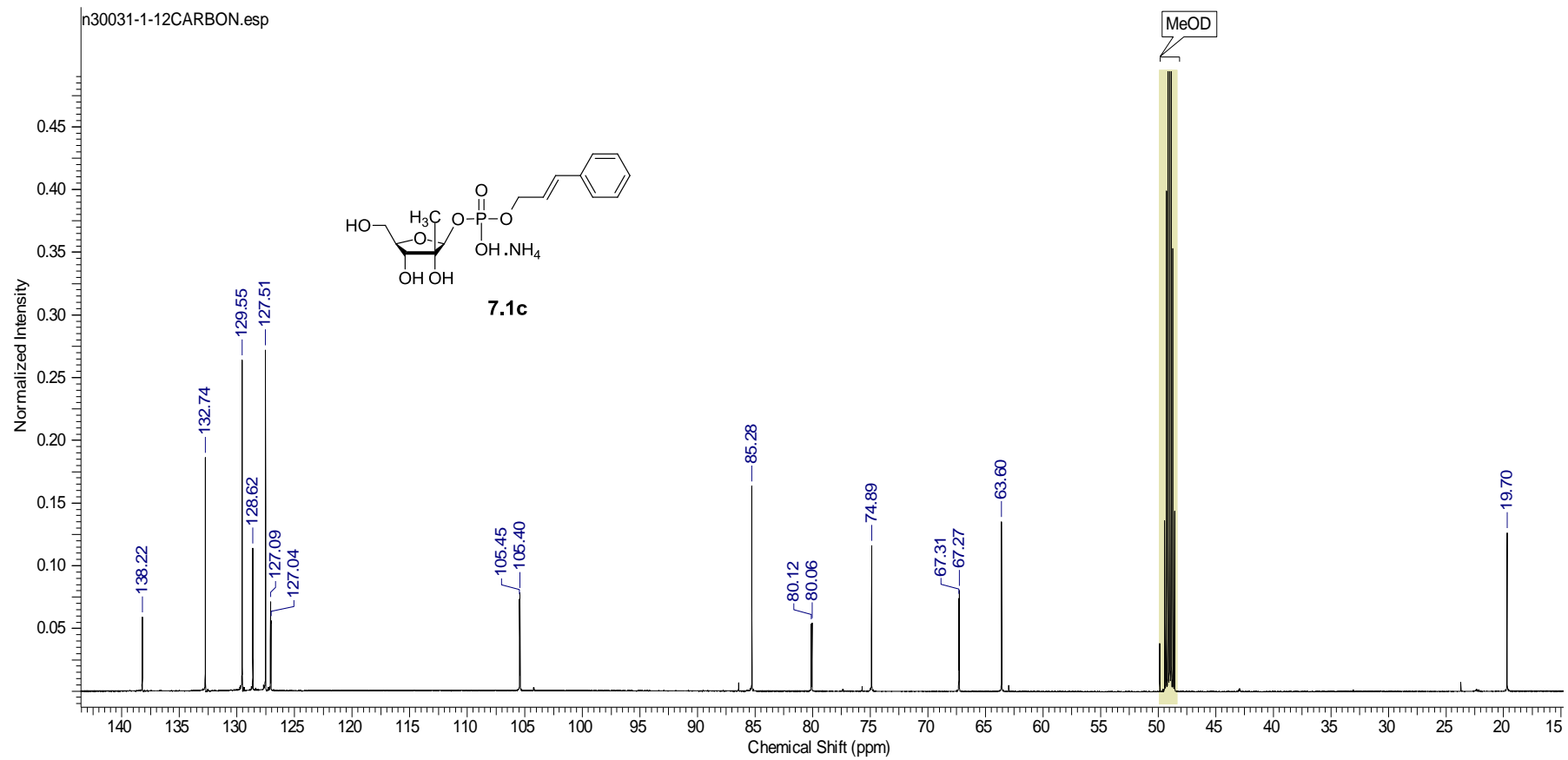
$^1\text{H}$  NMR (400 MHz,  $\text{DMSO}-d_6$ ):  $\delta$  1.26 (d,  $J = 6.8$  Hz, 3H, H-8), 2.75 (s, 3H, H-6), 4.13-4.15 (m, 2H, H-1, H-2), 4.18-4.20 (m, 2H, H-1, H-2), 4.42 (q,  $J = 6.8$  Hz, 1H, H-7), 6.37-6.40 (m, 2H, H-3, H-5), 6.70-6.72 (m, 1H, H-4), 7.46-7.50 (m, 2H, H-12, H-13), 7.60-7.64 (m, 2H, H-10, H-11), 10.01 (s, 1H, H-9).



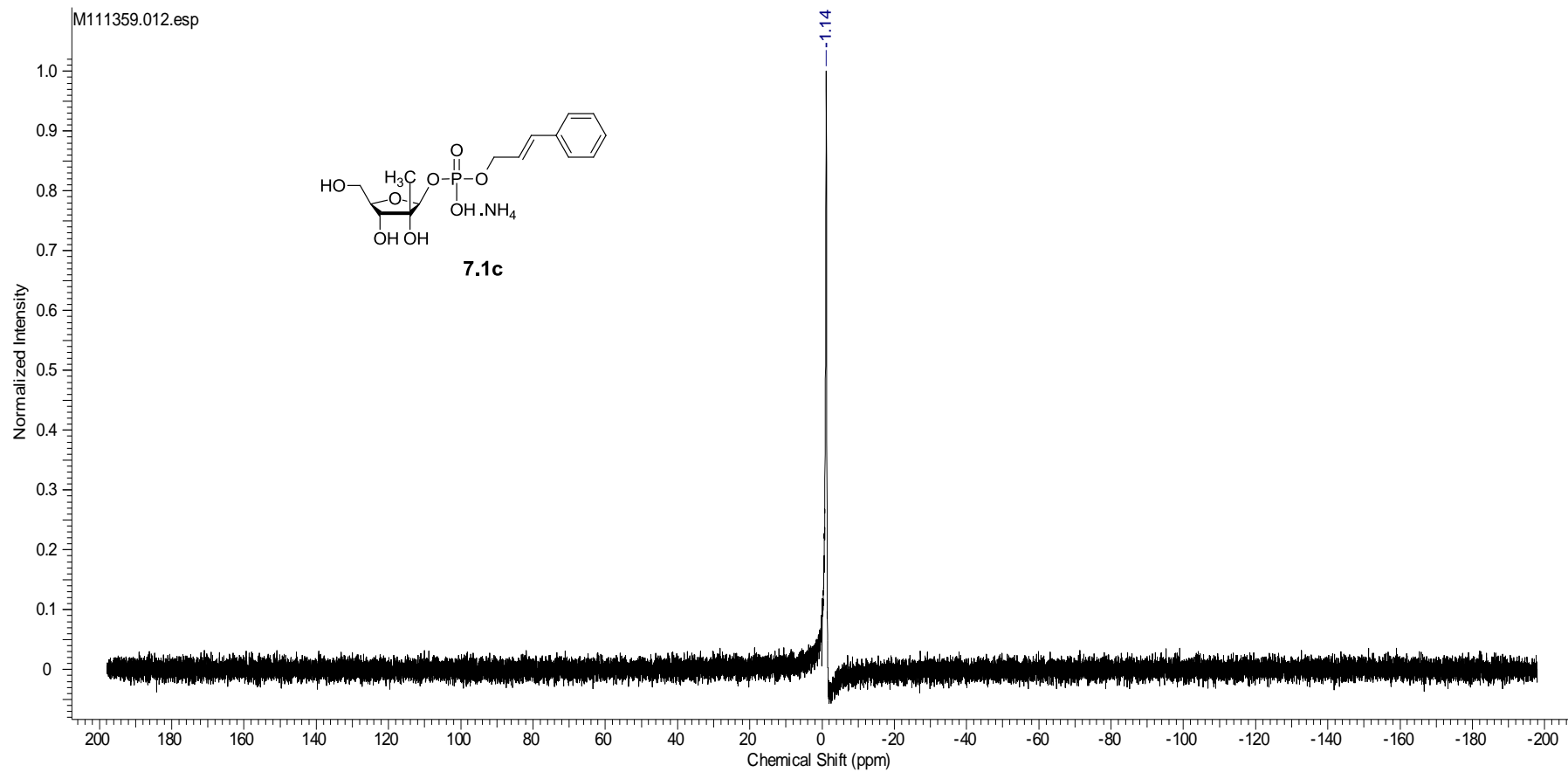
$^{13}\text{C}$  NMR (100 MHz,  $\text{DMSO}-d_6$ ):  $\delta$  12.9, 33.8, 58.6, 63.8, 64.3, 103.2, 107.6, 114.8, 116.9, 121.5 (2C), 131.4 (2C), 135.6, 138.3, 143.5, 144.4, 171.8.



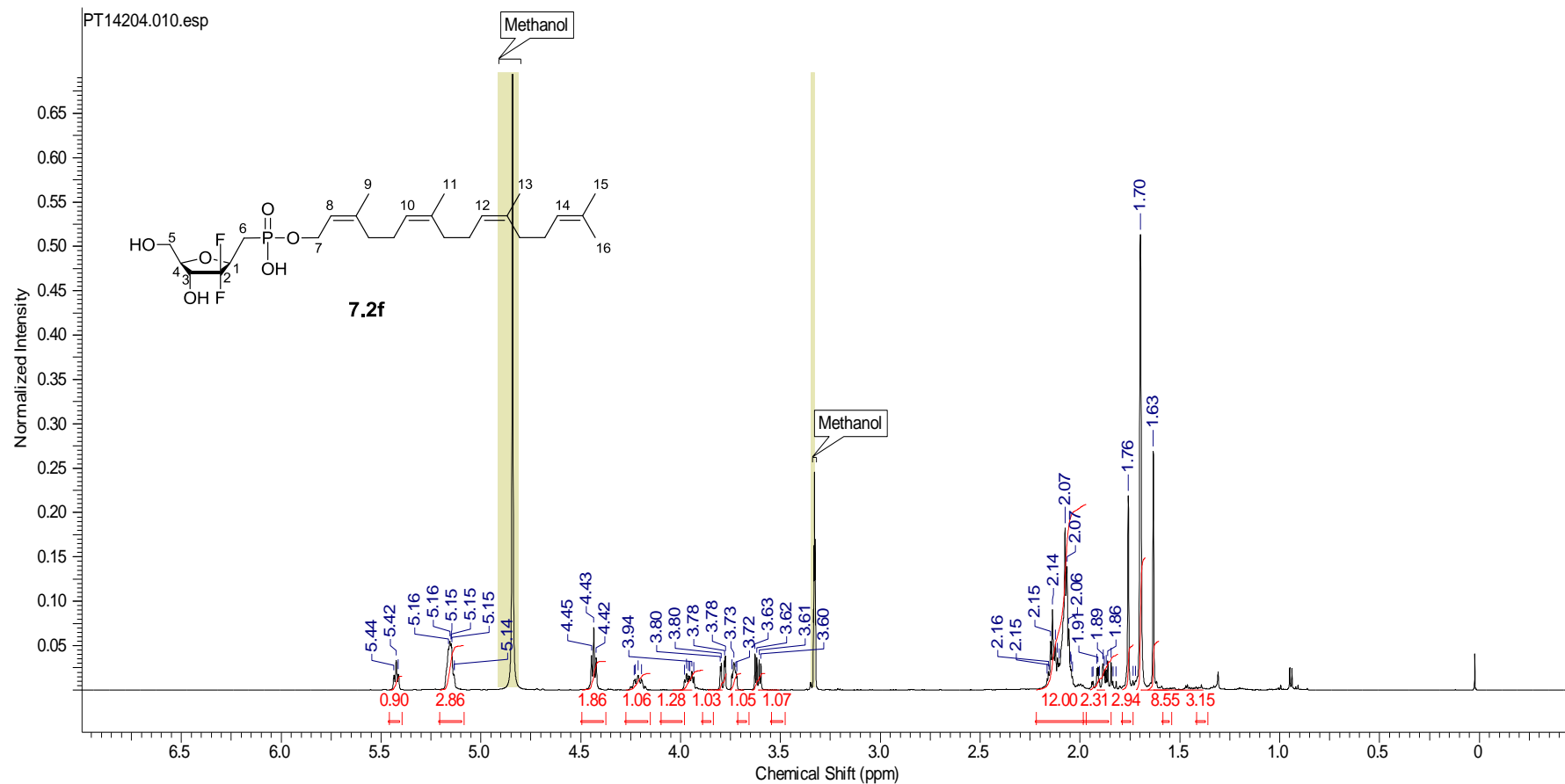
$^1\text{H}$  NMR (600 MHz,  $\text{D}_2\text{O}$ ): 1.30 (s, 3H, H-6), 3.64 (dd,  $J = 5.6, 12.5$  Hz, 1H, H-5'), 3.80 (dd,  $J = 3.0, 12.5$  Hz, 1H, H-5''), 3.91 (d,  $J = 8.3$  Hz, 1H, H-3), 3.97 (ddd,  $J = 3.0, 5.6, 8.3$  Hz, 1H, H-4), 4.55-4.57 (m, 2H, H-7), 5.29 (d,  $J = 6.1$  Hz, 1H, H-1), 6.41 (dt,  $J = 6.0, 15.9$  Hz, 1H, H-8), 6.73 (d,  $J = 15.9$  Hz, 1H, H-9), 7.31-7.33 (m, 1H, H-14), 7.38-7.41 (m, 2H, H-12, H-13), 7.50-7.52 (m, 2H, H-10, H-11). *Exchangeable protons not observed.*



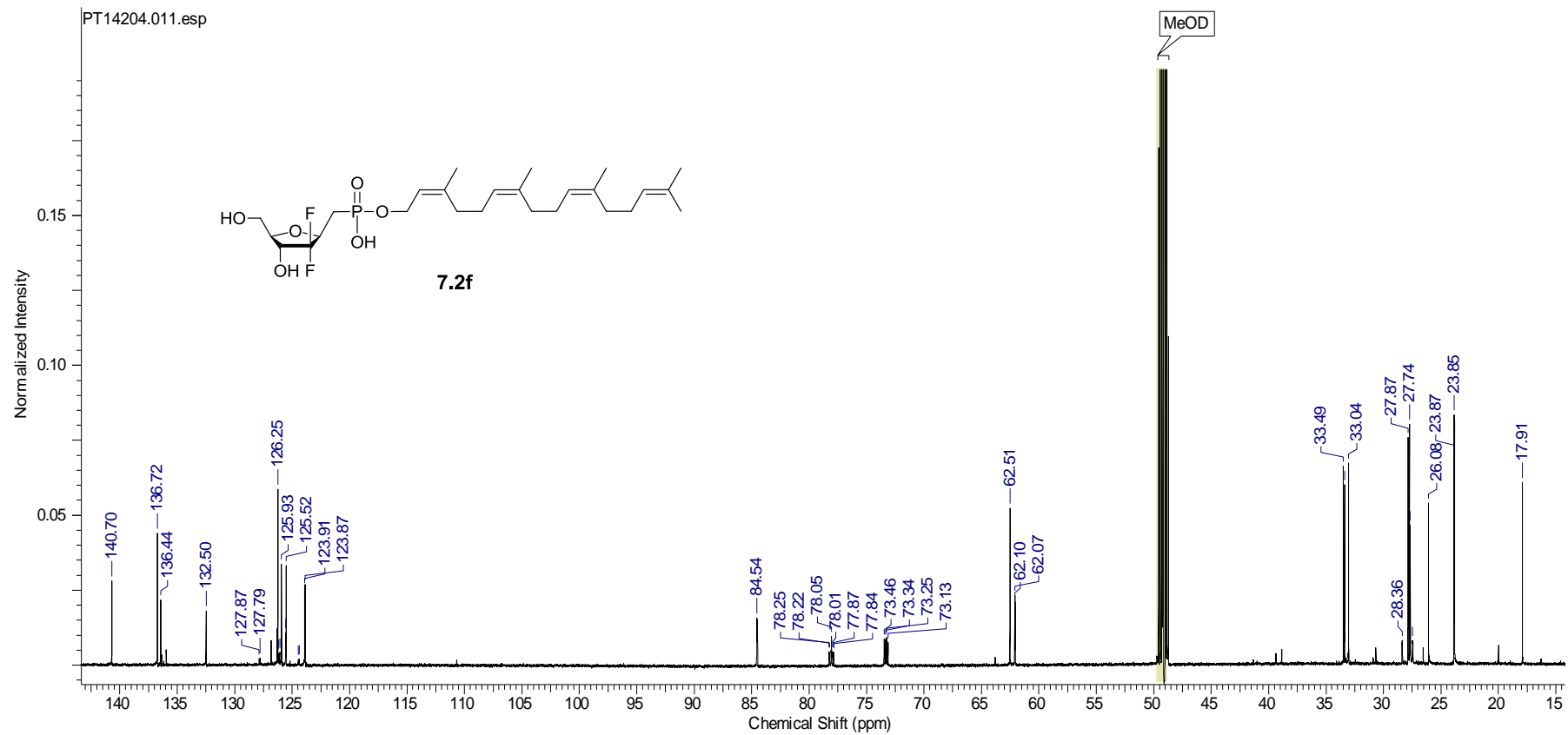
$^{13}\text{C}$  NMR (100 MHz, MeOD- $d_4$ ):  $\delta$  19.7, 63.6, 67.3 (d,  $J = 6$  Hz), 74.9, 80.1 (d,  $J = 10$  Hz) 85.3, 105.4 (d,  $J = 7$  Hz), 127.1 (d,  $J = 8$  Hz), 127.5 (2C), 128.6, 129.6 (2C), 132.7, 138.2.



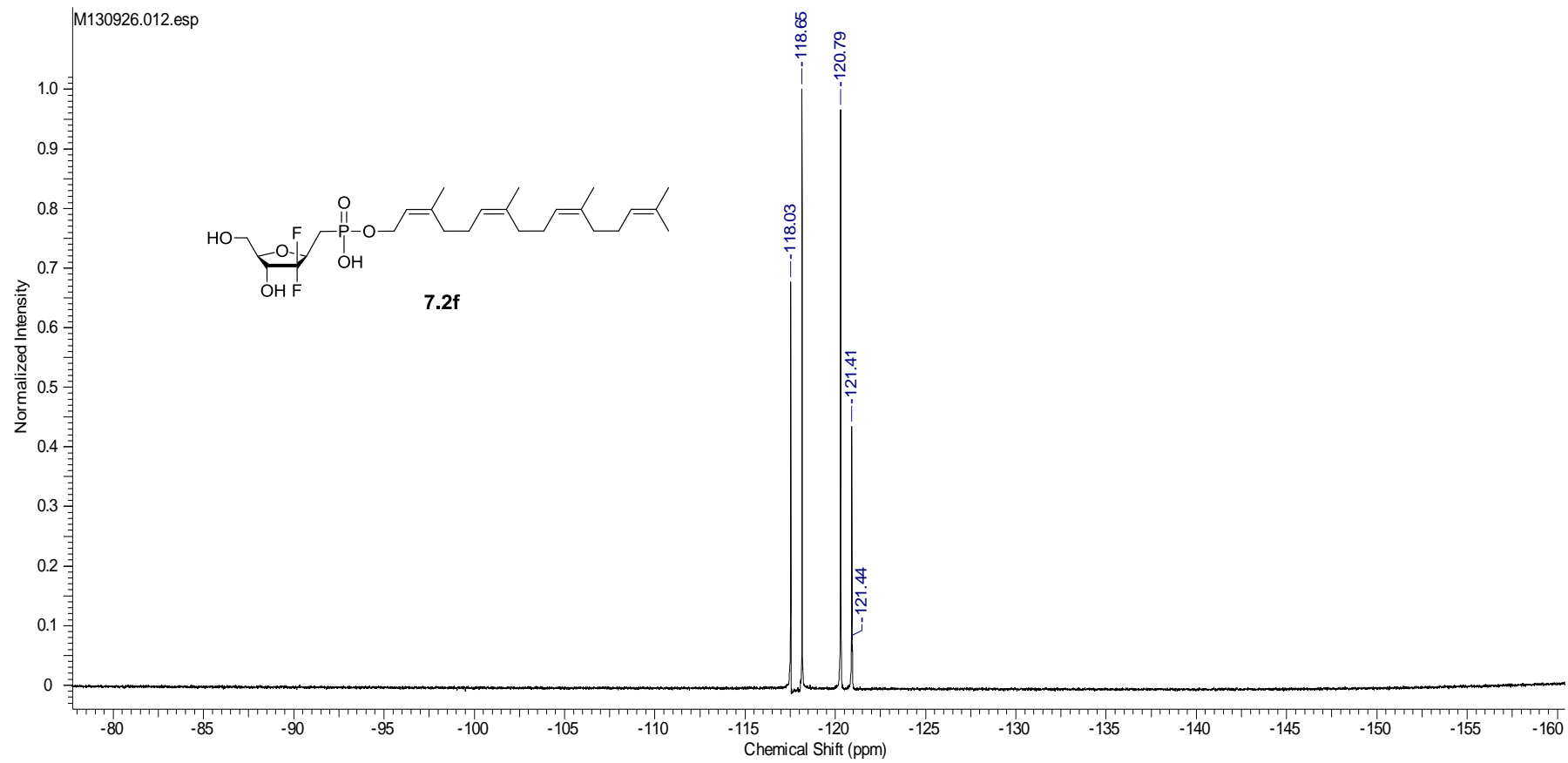
$^{31}\text{P}$  NMR (162 MHz, MeOD- $d_4$ ):  $\delta$  -1.1.



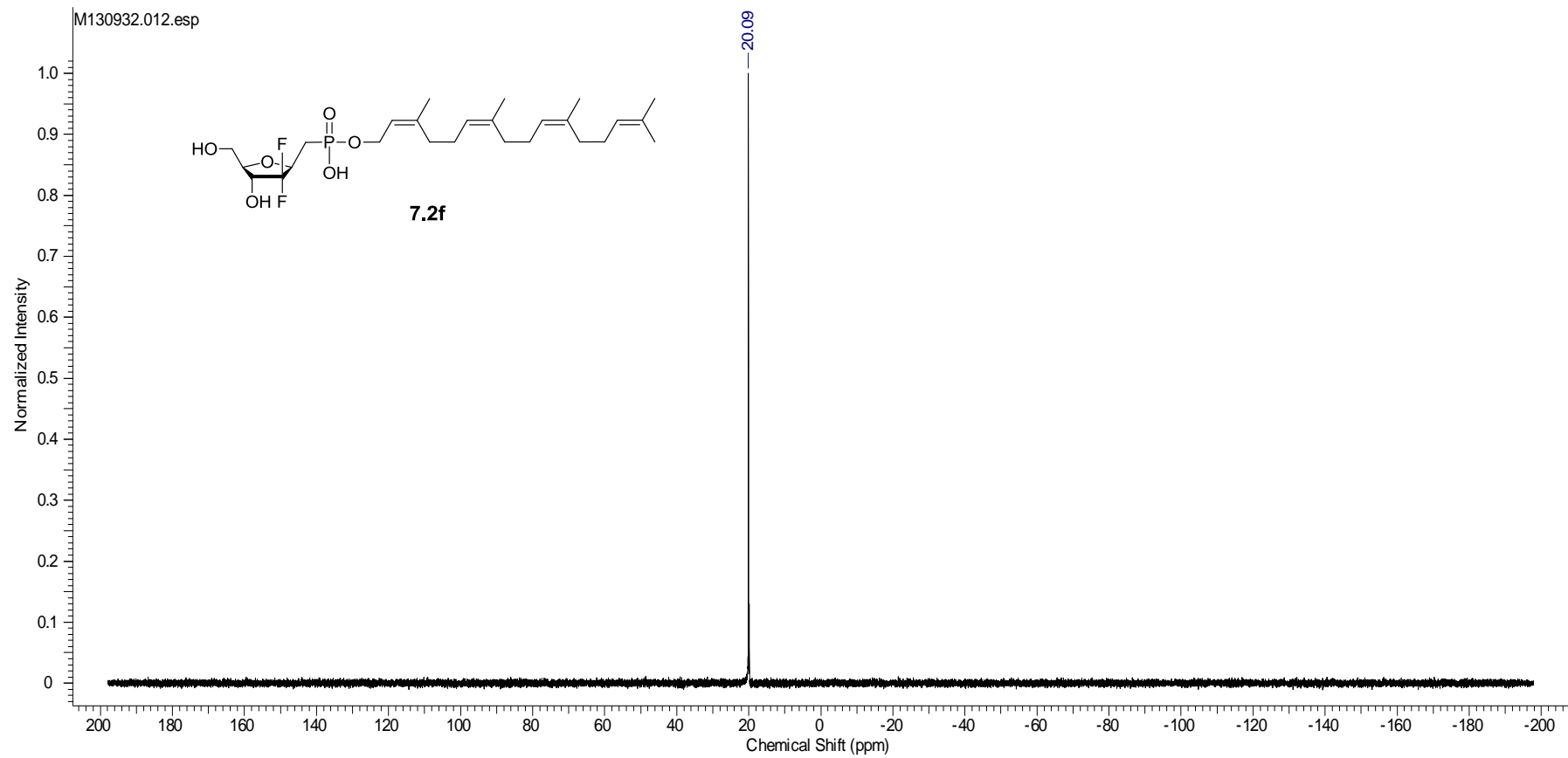
$^1\text{H}$  NMR (600 MHz,  $\text{MeOD-}d_4$ ):  $\delta$  1.63 (s, 3H, H-16), 1.70 (s, 9H, H-11, H-13, H-15), 1.76 (s, 3H, H-9), 1.82-1.94 (m, 2H, H-6), 2.04-2.16 (m, 12H,  $6\times\text{CH}_2$ ), 3.61 (dd,  $J = 5.6, 12.2$  Hz, 1H, H-5'), 3.72-3.74 (m, 1H, H-4), 3.79 (dd,  $J = 2.9, 12.2$  Hz, 1H, H-5''), 3.93-3.98 (m, 1H, H-3), 4.17-4.25 (m, 1H, H-1), 4.43 (t,  $J = 6.9$  Hz, 2H, H-7), 5.13-5.16 (m, 3H, H-10, H-12, H-14), 5.42 (t,  $J = 6.9$  Hz, 1H, H-8). *Exchangeable protons not observed.*



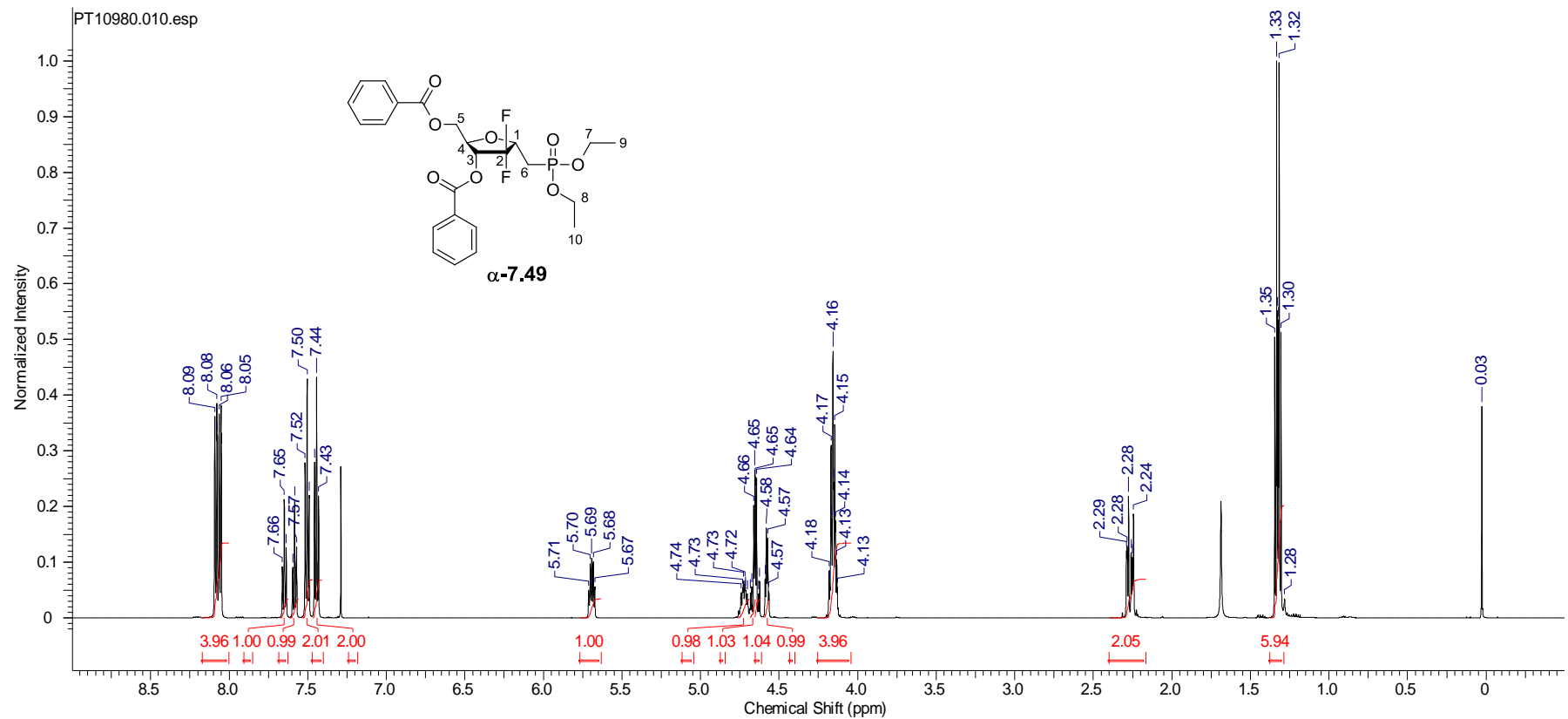
$^{13}\text{C}$  NMR (125 MHz,  $\text{MeOD-}d_4$ ):  $\delta$  17.9, 23.8, 23.9, 23.9, 26.1, 27.7, 27.7, 27.9, 27.9 (dd,  $J = 4, 137$  Hz), 33.0, 33.4, 33.5, 62.1 (d,  $J = 6$  Hz), 62.5, 73.3 (dd,  $J = 18, 31$  Hz), 78.1 (ddd,  $J = 5, 26, 31$  Hz), 84.5 (d,  $J = 5$  Hz), 123.9 (d,  $J = 7$  Hz), 125.5, 125.9, 126.2 (td,  $J = 13, 256$  Hz), 126.3, 132.5, 136.5, 136.7, 140.7.



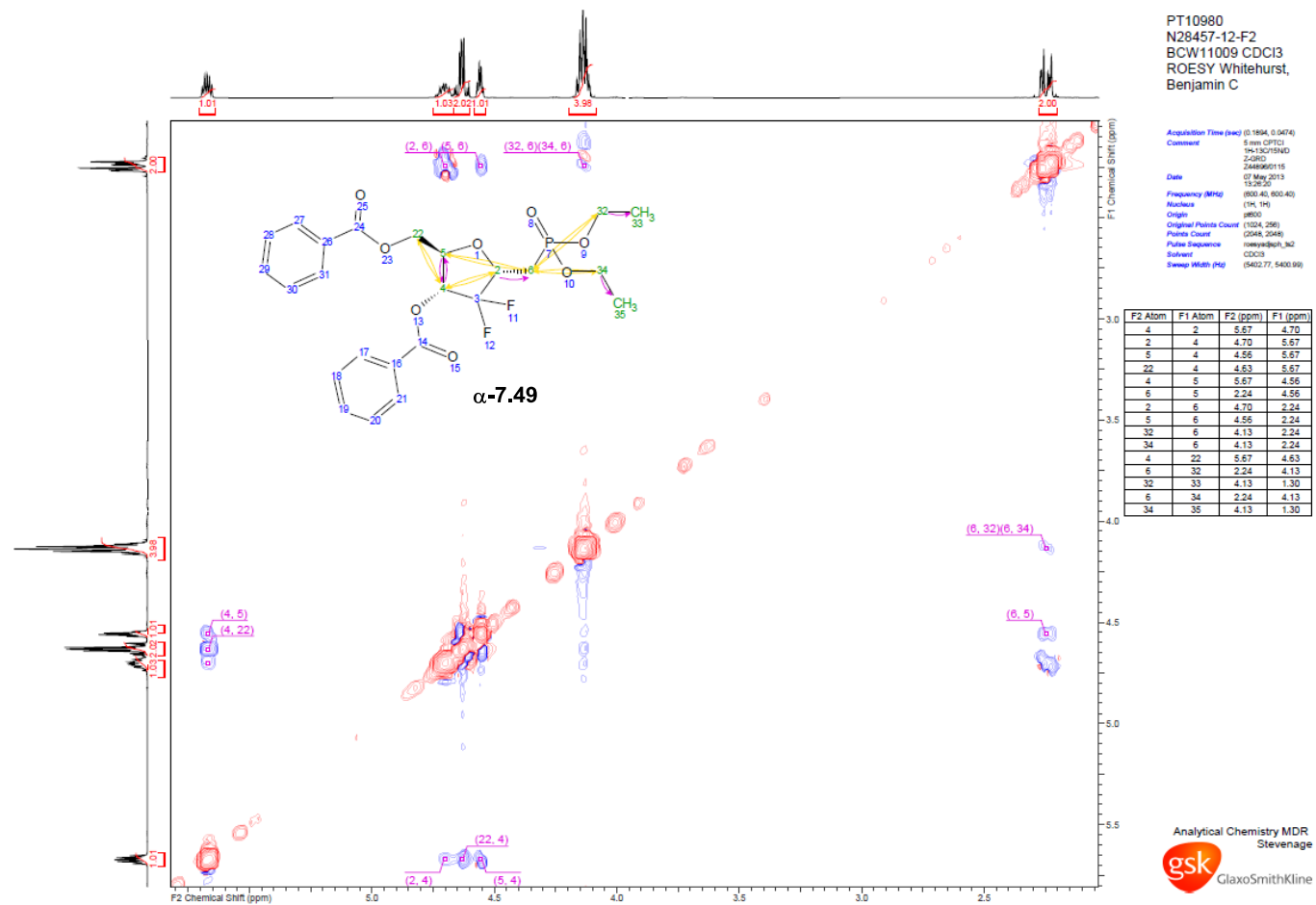
$^{19}\text{F}$  NMR (376 MHz,  $\text{MeOD-}d_4$ ):  $\delta$  -121.1 (d,  $J = 235$  Hz, 1F), -118.4 (d,  $J = 235$  Hz, 1F).



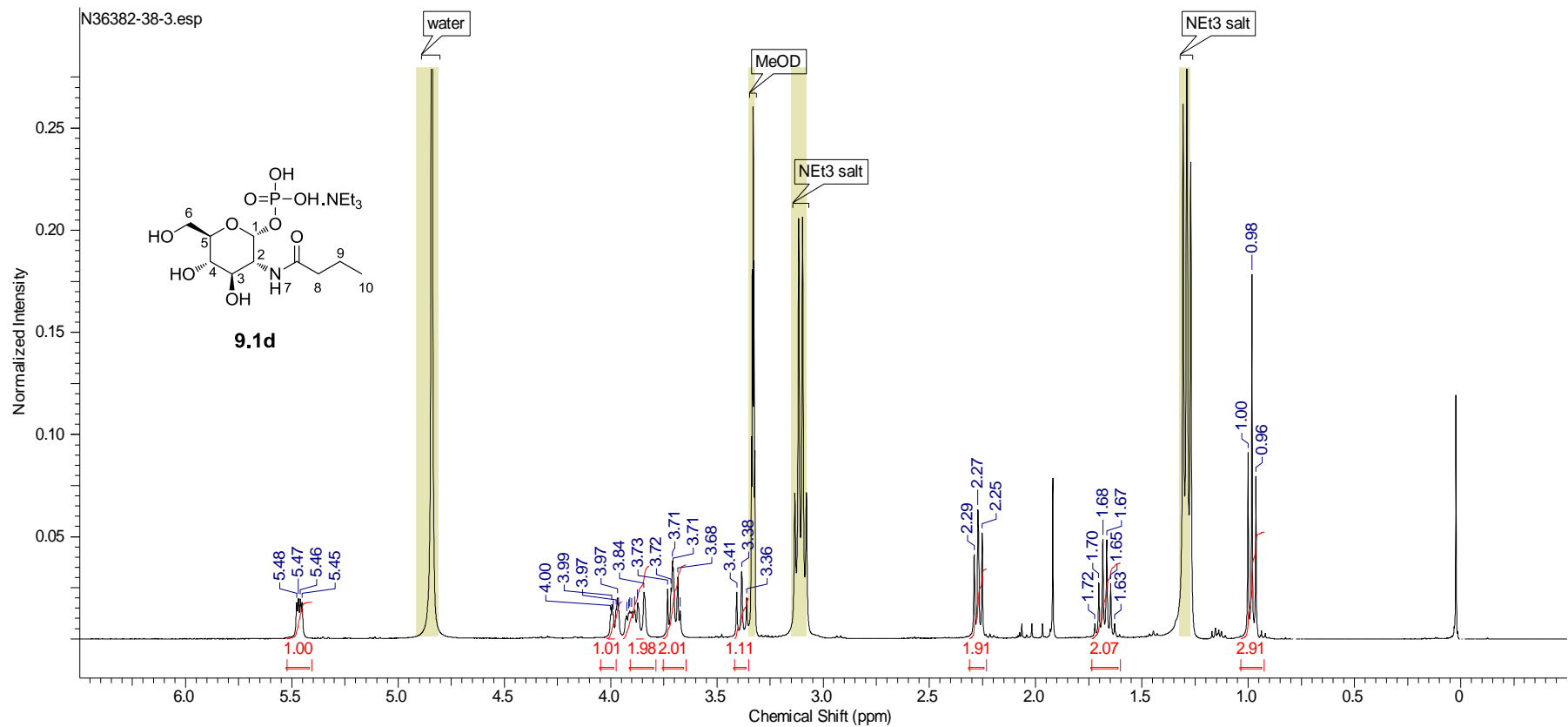
$^{31}\text{P}$  NMR (162 MHz,  $\text{MeOD-}d_4$ ):  $\delta$  20.1.



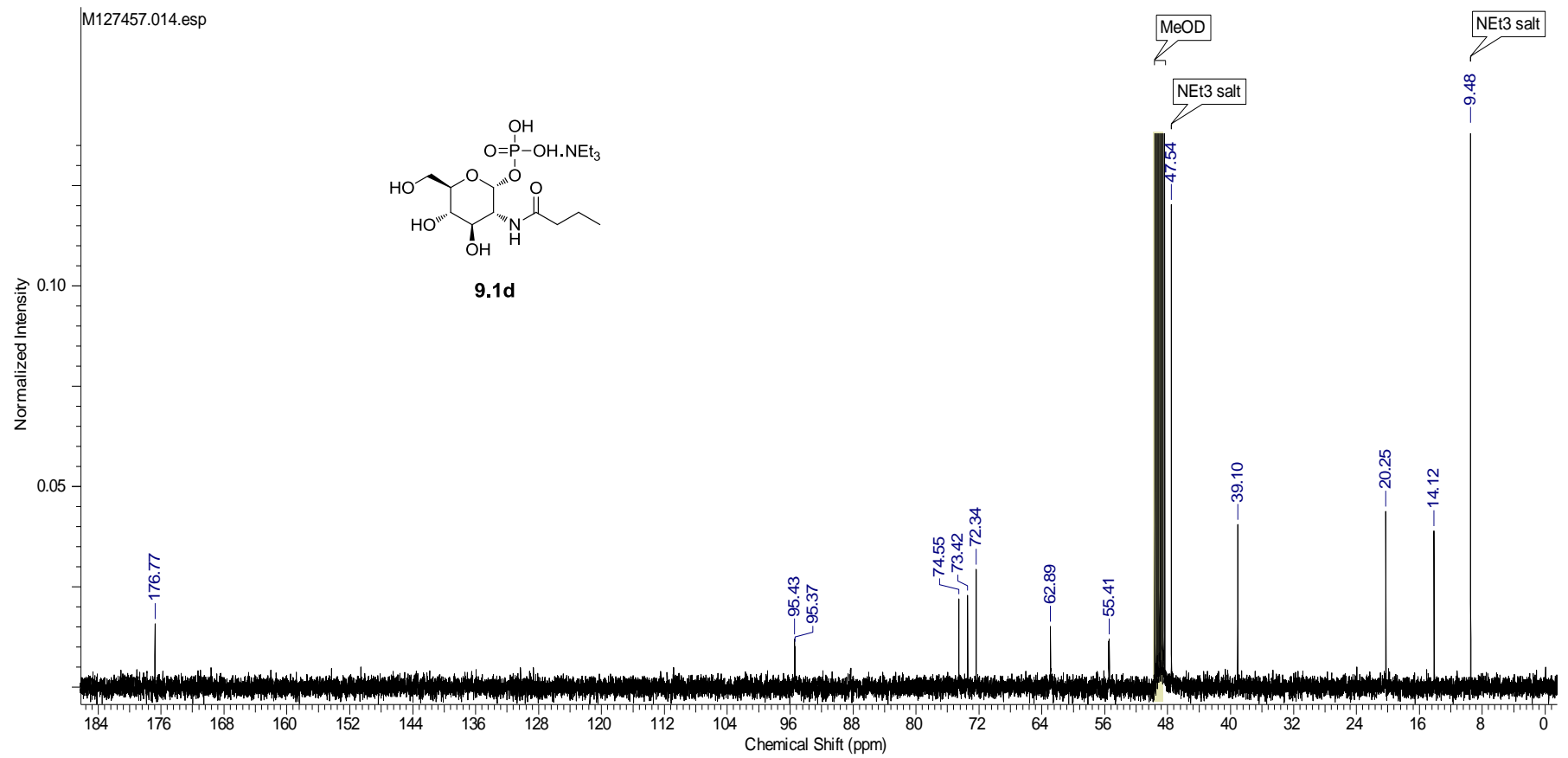
$^1\text{H}$  NMR (400 MHz,  $\text{CDCl}_3$ ):  $\delta$  1.30-1.35 (m, 6H, H-9, H-10), 2.24-2.29 (m, 2H, H-6), 4.13-4.18 (m, 4H, H-7, H-8), 4.57 (q,  $J = 4.6$  Hz, 1H, H-4), 4.61 (dd,  $J = 4.6, 11.9$  Hz, 1H, H-5'), 4.64 (dd,  $J = 4.2, 11.9$  Hz, 1H, H-5''), 4.68-4.74 (m, 1H, H-1), 5.67 (dt,  $J = 6.0, 11.6$  Hz, 1H, H-3), 7.41-7.44 (m, 2H, Ar-H), 7.47-7.50 (m, 2H, Ar-H), 7.55-7.58 (m, 1H, Ar-H), 7.62-7.65 (m, 1H, Ar-H), 8.05-8.07 (m, 2H, Ar-H), 8.08-8.09 (m, 2H, Ar-H).



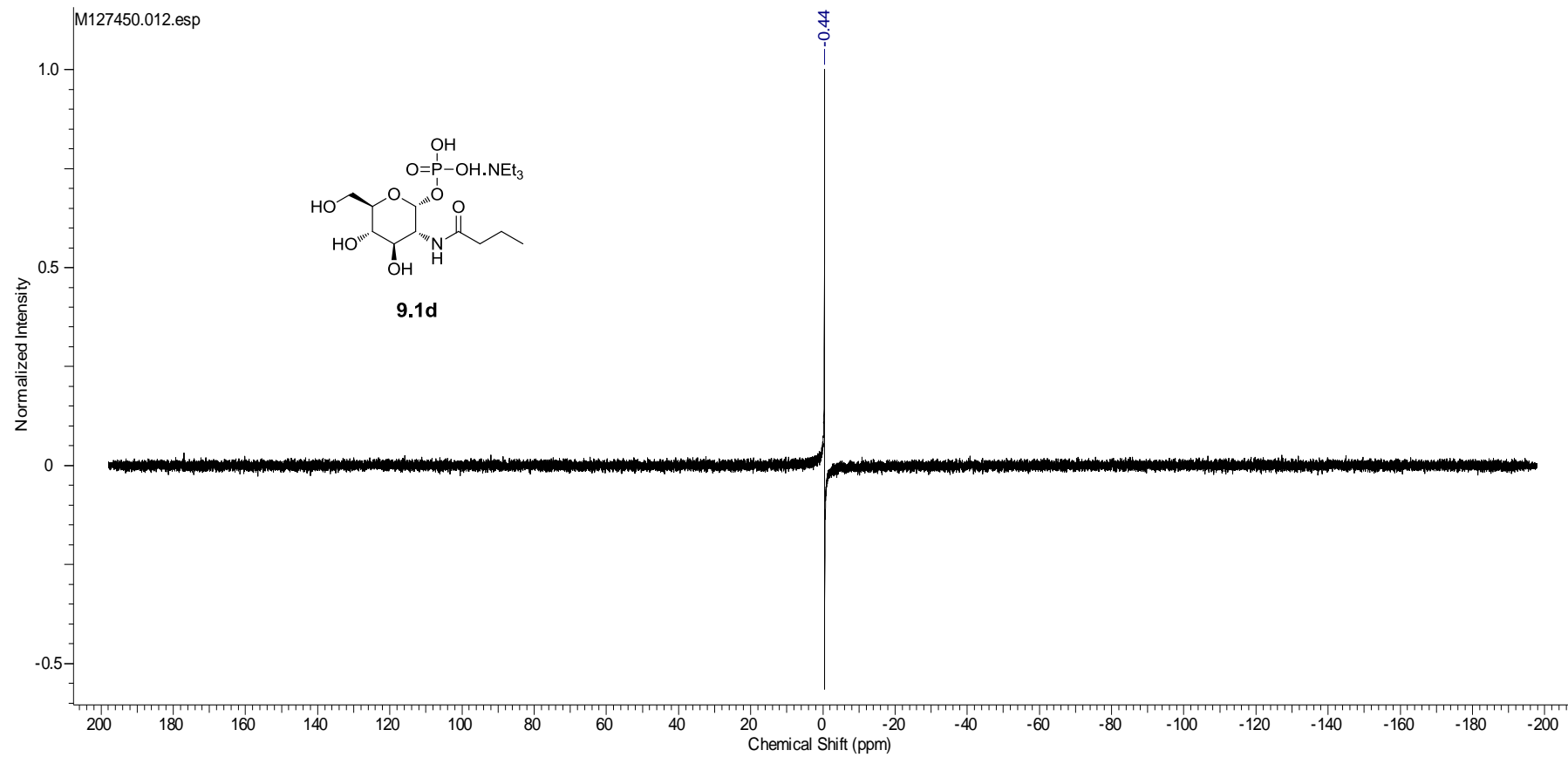
ROESY NMR spectrum for  $\alpha$ -7.49.



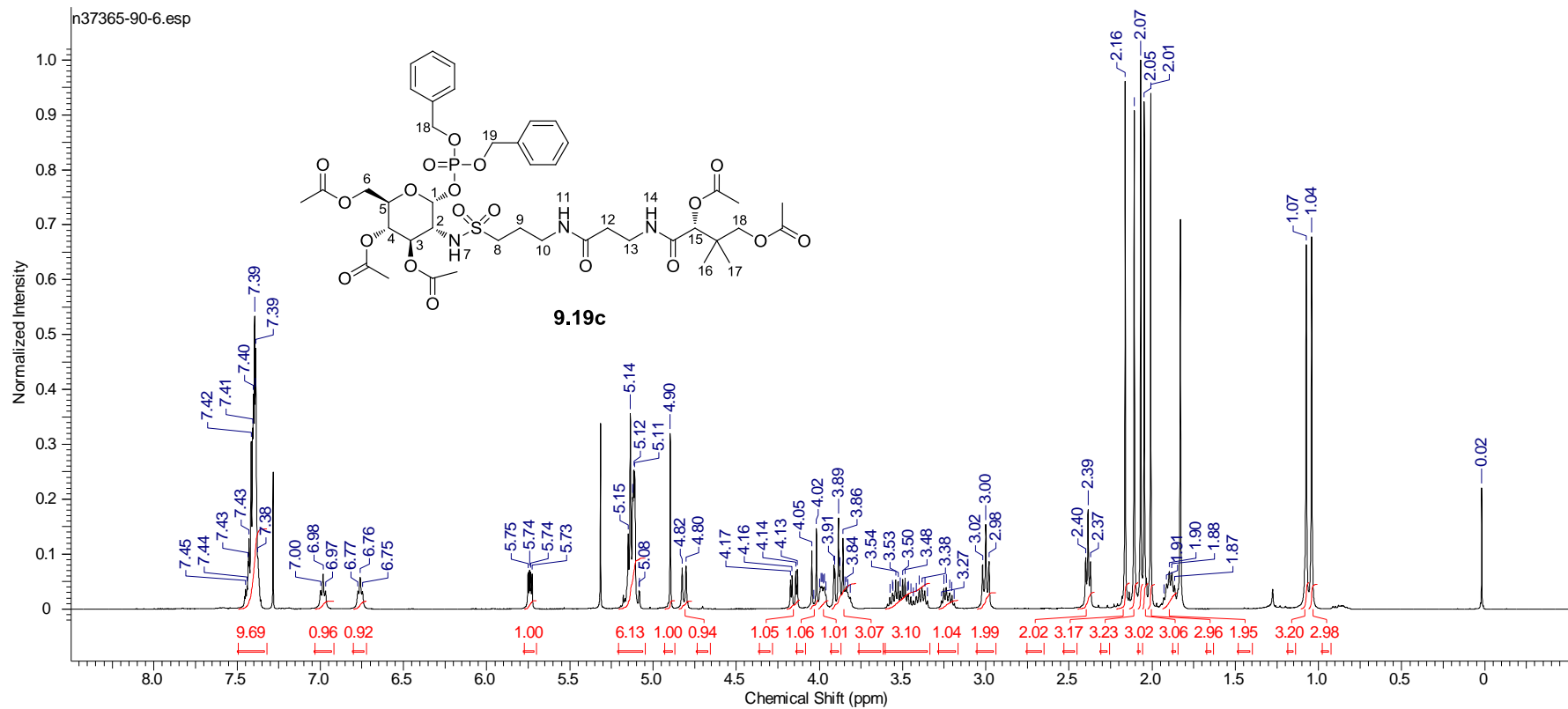
<sup>1</sup>H NMR (400 MHz, MeOD-*d*<sub>4</sub>): δ 0.98 (t, *J* = 7.7 Hz, 3H, H-10), 1.29 (t, *J* = 7.3 Hz, N(CH<sub>2</sub>CH<sub>3</sub>)<sub>3</sub>, 13H), 1.63-1.72 (m, 2H, H-9), 2.27 (t, *J* = 7.8 Hz, 2H, H-8), 3.10 (q, *J* = 7.3 Hz, N(CH<sub>2</sub>CH<sub>3</sub>)<sub>3</sub>, 8H), 3.38 (dd, *J* = 9.3, 9.3 Hz, 1H, H-4), 3.67-3.73 (m, 2H, H-3, H-6'), 3.83-3.93 (m, 2H, H-5, H-6''), 3.98 (dt, *J* = 3.2, 10.6 Hz, 1H, H-2), 5.46 (dd, *J* = 3.2, 7.0 Hz, 1H, H-1). Exchangeable protons not observed.



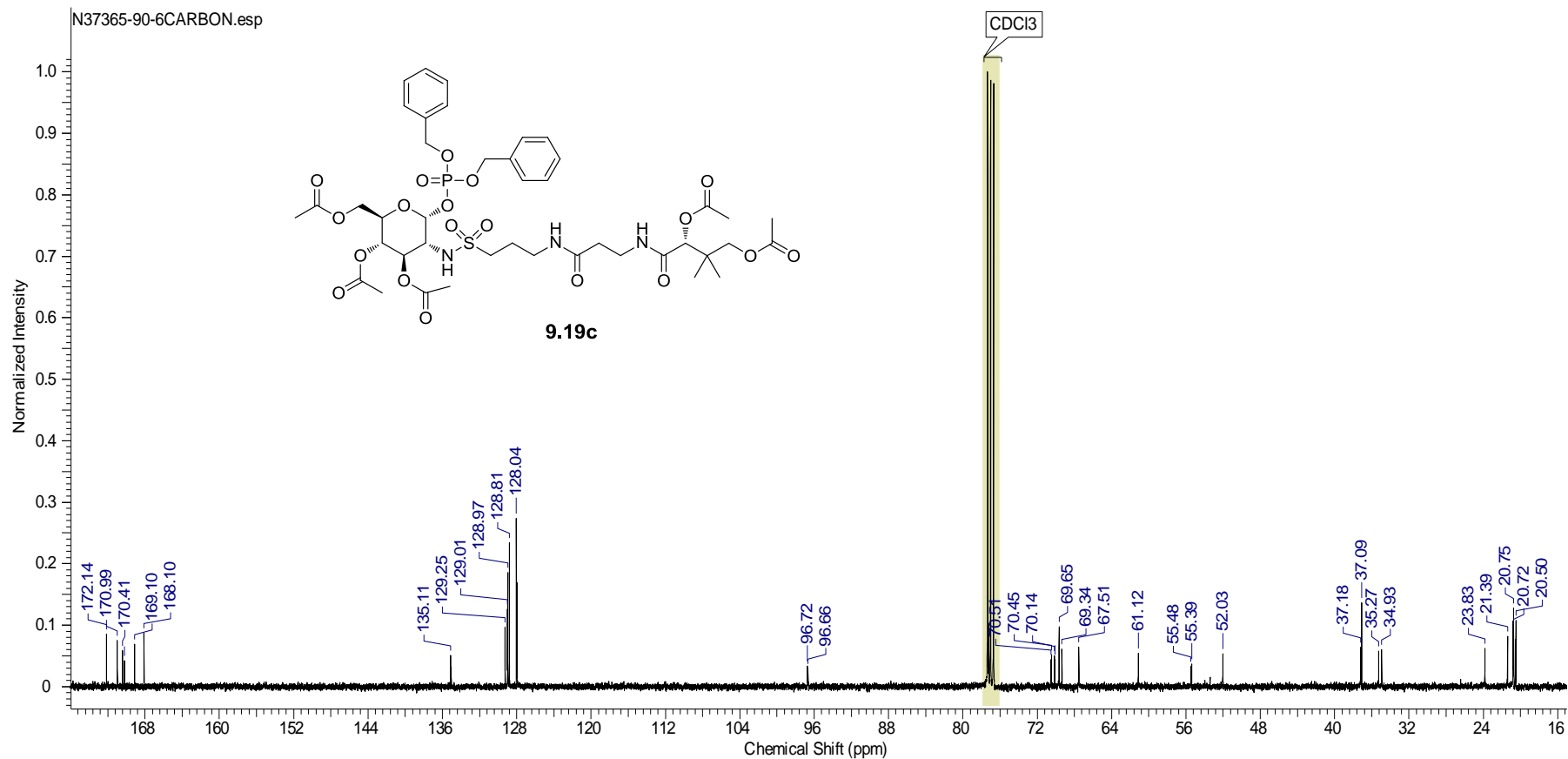
$^{13}\text{C}$  NMR (100 MHz, MeOD- $d_4$ ):  $\delta$  9.5 ( $\text{N}(\text{CH}_2\text{CH}_3)_3$ ), 14.1, 20.3, 39.1, 47.5 ( $\text{N}(\text{CH}_2\text{CH}_3)_3$ ), 55.4 (d,  $J = 8$  Hz), 62.9, 72.3, 73.4, 74.6, 95.4 (d,  $J = 6$  Hz), 176.8.



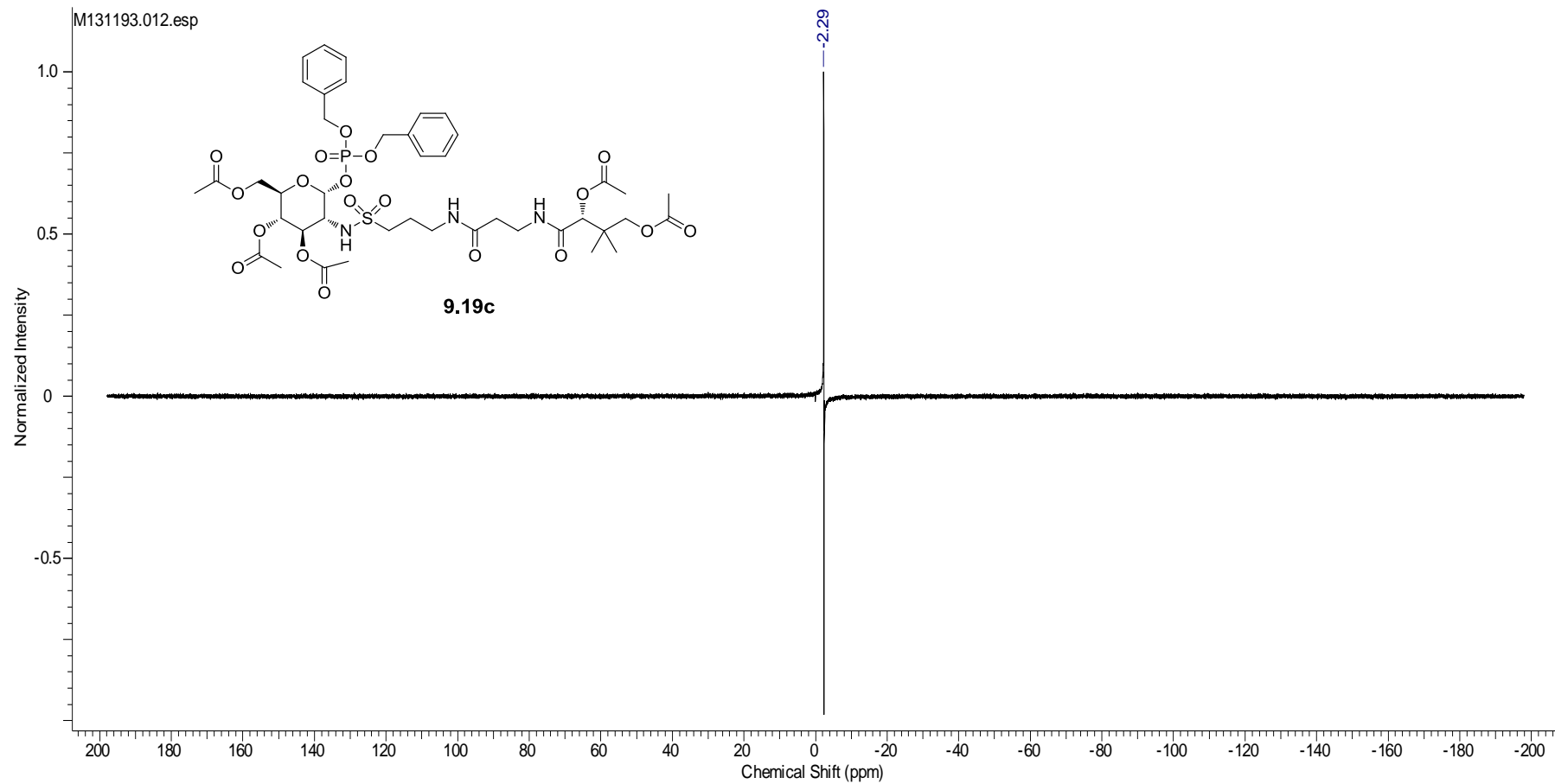
$^{31}\text{P}$  NMR (162 MHz, MeOD- $d_4$ ):  $\delta$  -0.4.



<sup>1</sup>H NMR (400 MHz, CDCl<sub>3</sub>): δ 1.04 (s, 3H, H-16), 1.07 (s, 3H, H-17), 1.87-1.93 (m, 2H, H-9), 2.01 (s, 3H, Ac CH<sub>3</sub>), 2.05 (s, 3H, Ac CH<sub>3</sub>), 2.07 (s, 3H, Ac CH<sub>3</sub>), 2.11 (s, 3H, Ac CH<sub>3</sub>), 2.16 (s, 3H, Ac CH<sub>3</sub>), 2.39 (t, *J* = 5.6 Hz, 2H, H-12), 3.00 (t, *J* = 7.7 Hz, 2H, H-8), 3.19-3.26 (m, 1H, H-10'), 3.35-3.43 (m, 1H, H-10''), 3.47-3.58 (m, 2H, H-13), 3.81-3.91 (m, 3H, H-2, H-6', H-18'), 3.96-4.00 (m, 1H, H-5), 4.03 (d, *J* = 11.0 Hz, 1H, H-18''), 4.15 (dd, *J* = 4.0, 12.6 Hz, 1H, H-6''), 4.81 (d, *J* = 9.3 Hz, 1H, H-7), 4.90 (s, 1H, H-15), 5.08-5.18 (m, 6H, H-3, H-4, H-18, H-19), 5.74 (dd, *J* = 3.4, 6.4 Hz, 1H, H-1), 6.76 (t, *J* = 5.6 Hz, 1H, H-11), 6.98 (t, *J* = 5.8 Hz, 1H, H-14), 7.38-7.46 (m, 10H, Ar-H).



<sup>13</sup>C NMR (100 MHz, CDCl<sub>3</sub>): δ 20.5, 20.6, 20.7, 20.8, 20.8, 20.8, 21.4, 23.8, 34.9, 35.3, 37.1, 37.2, 52.0, 55.4 (d, *J* = 8 Hz), 61.1, 67.5, 69.3, 69.7 (2C), 70.1 (d, *J* = 5 Hz), 70.5 (d, *J* = 6 Hz), 77.2, 96.7 (d, *J* = 6 Hz), 128.0 (2C), 128.0 (2C), 128.8 (2C), 129.0 (2C), 129.0, 129.3, 135.1, 135.1, 168.1, 169.1, 170.2, 170.4, 171.0, 171.0, 172.1.



$^{31}\text{P}$  NMR (162 MHz,  $\text{CDCl}_3$ ):  $\delta$  -2.3.